



OREGON NEARSHORE SEMI-PELAGIC ROCKFISH SURVEY

**Leif K. Rasmuson PhD, Matthew T.O. Blume, Kelly A. Lawrence, Elizabeth J. Bailey,
Mark R. Terwilliger, Stephanie A. Fields, Polly S. Rankin, Anthony J. Phillips**

Submitted: September 12, 2022

Marine Fisheries Research Project
2040 SE Marine Science Drive
Newport, OR 97365
(541) 867-4741
Leif.K.Rasmuson@odfw.oregon.gov



TABLE OF CONTENTS

Nearshore Semi-Pelagic Rockfish Biology And Ecology	4
Field Work	5
Sampling Tools.....	5
Vessels.....	5
Oceanographic Sampling	5
Acoustics	5
Video	6
Hook And Line Sampling	7
Survey Design	8
Survey operations	10
Data Processing.....	11
CTD Data.....	11
Fisheries Acoustics.....	11
Echo Integration.....	13
Echo Counting	13
Video Sampling.....	14
Camera System and Calibration.....	14
Video Review	14
Hook And Line Sampling.....	16
Data Analysis.....	17
Video Sampling.....	17
Volumetric Densities-Target Strength Relationship Selection	17
Background Densities	18
Hook And Line Sampling.....	18
Fisheries Acoustics.....	19
Inclement Weather Analysis	19
Echo Integration.....	19
Echo Counting	20
Population Estimation	21
Habitat Blocking And Regions.....	21
Background Population Estimate.....	22
Design Based Estimate.....	22
Model Based	24
Results and Abundance Estimate	25
Oceangraphy	25
Video.....	26
Hook and Line.....	28
Fisheries Acoustics.....	29
Population Estimate	30
Design Based	30
Model Based	30
Conclusions	31

Recommendations	31
Acknowledgments.....	32
References	32
Tables	36
Survey Design	36
Video Sampling.....	39
Hook And Line Sampling.....	40
Fisheries Acoustics.....	40
Population Estimate	44
Design Based	44
Model Based	48
Figures.....	62
CTD Data	62
Video Sampling.....	67
Hook And Line Sampling.....	88
Fisheries Acoustics.....	106
Population Estimate	124
Design Based	124
Model Based	130
Appendix	177
1: Online Survey Map How To.....	177
2: Movement Patterns of Black Rockfish (Sebastes melanops) in Oregon Coastal Waters ...	180
Abstract.....	180
Introduction	180
Materials and methods.....	183
Results	187
Discussion.....	193
Acknowledgments.....	196
References	196
3: Patterns in vertical movements of black rockfish Sebastes melanops.....	199
Abstract.....	199
Introduction	199
Materials and Methods.....	200
Results	204
Discussion.....	211
Acknowledgements.....	213
Literature Cited	213
4: Effect of hypoxia on rockfish movements: implications for understanding the roles of temperature, toxins and site fidelity.....	216
Abstract.....	216
Introduction	216
Materials and Methods.....	218
Results	222
Discussion.....	230

Acknowledgements.....	235
Literature Cited	235
5: Habitat use and activity patterns of female Deacon Rockfish (<i>Sebastes diaconus</i>) at seasonal scales and in response to episodic hypoxia	238
Abstract.....	238
Introduction	238
Materials and methods	240
Results	246
Discussion.....	254
Acknowledgments.....	258
References	259
6: Susceptibility of five species of rockfish (<i>Sebastes spp.</i>) to different survey gears inferred from high resolution behavioral data.	264
Abstract.....	264
Introduction	264
Methods.....	266
Results	268
Discussion.....	274
Acknowledgments.....	277
References	277
7: Combined video-hydroacoustic survey of nearshore semi-pelagic rockfish in untrawlable habitats.....	281
Abstract.....	281
1. Introduction.....	281
2. Methods.....	284
3. Results	296
4. Discussion.....	303
Data availability.....	307
Acknowledgments.....	308
Literature Cited	308
Supplement.....	313
8: Influence of near bottom fish distribution on the efficacy of a combined hydroacoustic video survey.	318
Abstract.....	318
Introduction	318
Materials and Methods.....	321
Results	330
Discussion.....	339
Acknowledgments.....	343
References	343
Supplement.....	347
9: Survey Design simulations.....	357

NEARSHORE SEMI-PELAGIC ROCKFISH BIOLOGY AND ECOLOGY

Background information on the focal species of this report, Black (*Sebastes melanops*), Blue (*Sebastes mystinus*) and Deacon (*Sebastes diaconus*) Rockfishes, can be found in the most recent stock assessments for each species, available at www.pcouncil.org. Blue and Deacon Rockfish are difficult to distinguish from one another and therefore are assessed as a complex.

An understanding of each focal species' average height off bottom, and their horizontal and vertical movement in normoxic and hypoxic conditions is important for the review of methods described in this document. Background information regarding the height off bottom of these species, and therefore their availability to hydroacoustic survey gear, were previously published by Rasmuson (2021), provided in Appendix 6 of this document. The effects of hypoxia on rockfish behavior as well as studies of their movement (not in response to hypoxia) in Oregon were previously published (Parker et al. 2005, 2008, Rankin et al. 2013, Rasmuson et al. 2021a), provided in Appendices 2-5 of this document. In certain conditions it can be difficult to differentiate fish from bottom returns in acoustics, this is especially true in high relief areas (Ona & Mitson 1996, Rasmuson et al. 2022). This region is often called the near bottom dead zone. Relative height off bottom data for each species can inform its availability to acoustics, and how much (if any) of the population occurs within the near bottom dead zone.

Overall, research has shown Blue and Deacon Rockfish are located above the near bottom dead zone, making them available to hydroacoustic sampling (Rasmuson et al. 2021a). However, the species also exhibits strong diel movement, indicating surveys must occur during daylight hours. When examined individually, Black Rockfish's vertical movement is inconsistent, but when considered as a population, most are above bottom and therefore available to acoustics (Parker et al. 2008, Rasmuson 2021). This observation was supported by the results of one of our pilot studies combining our video-acoustic method with a remotely operated vehicle (ROV) to examine the extent to which near bottom fish impact video-acoustic survey data (Appendix 8, Rasmuson et al. 2022).

Oregon's oceans are known to experience periodic hypoxia. For Deacon Rockfish, hypoxia causes them to move greater distances from their home range (Rasmuson et al. 2021a). Hypoxia also causes them to remain higher in the water column regardless of time of day. Black Rockfish's response to hypoxia has not been studied as explicitly as Deacon Rockfish. However, fishermen participating in the live fish fishery report Black Rockfish must be transported at lower densities than other species, which they hypothesize is because Black Rockfish have a greater oxygen requirement.

FIELD WORK

SAMPLING TOOLS

The design and methodologies of the sampling tools introduced below are described in detail by Rasmuson et al. (2021b) and Rasmuson et al. (2022), provided in Appendix 7 and 8 of this document. These manuscripts also address the effect of the camera systems catchability, calibration of the survey method to preexisting surveys, and the impacts of the near bottom dead zone on population estimates. A video of the equipment and tools used for this survey is available [online](#).

VESSELS

The primary vessel used in the statewide survey was the RV Pacific Surveyor, a 17 m retired commercial fishing vessel converted for research purposes. The vessel had a beam of 6.7 m, a draft of 2.4 m, and equipped with a bulbous bow. The vessel was powered by a single 450 hp 855 Cummins diesel engine.

The secondary vessel, used for shallow water applications, was the RV Arima, a 4.9 m recreational fishing vessel converted for nearshore research in depths shallower than the primary vessel could achieve. The secondary vessel had a beam of 2.4 m, and a draft of 0.6 m. The vessel was powered by a 115 hp Suzuki outboard motor.

OCEANOGRAPHIC SAMPLING

Oceanographic sampling was conducted with a Seabird 19+ V2 conductivity temperature depth (CTD) sensor, equipped with a SBE 43 dissolved oxygen sensor and a EcoBB turbidity and fluorescence sensor. The CTD was deployed on a load bearing Kevlar cable using a modified electric winch.

ACOUSTICS

Acoustic data were collected aboard the RV Pacific Surveyor using two downward-facing, pole-mounted transducers (BioSonics DT-X split beam Scientific Echosounders: 38 and 201 kHz). The pole, a 15.25 cm diameter, schedule 80 steel pole, was mounted to the deck and extended 2.9 meters below the surface, which was 0.5 below the keel. The transducers' ping rates were set to 2.97 pings per second. The 38 and 201 kHz transducers had a 10° and 6.9° beam width, respectively. The 38 kHz transducer was operated with a pulse duration of 1 ms and the 201 kHz transducer was operated with a pulse duration of 0.3 ms. See **Table 10** for transducer settings and geometries.

Due to the small size of the RV Arima, only the 201 kHz transducer was used. The transducer was pole mounted and extended 0.8 m below the water, which was 0.2 m below the keel. The ping rate was 5 pings per second and the pulse duration was 0.3 ms.

Tungsten sphere calibrations were attempted on the primary vessel while moored at the dock and while at sea following the methods of Demer et al. (2015).

Behavioral studies of Black, Blue, and Deacon Rockfishes have shown that at least a component of each species' population exhibit diel migratory behavior and reside directly on the bottom at night, therefore acoustic data were collected from one hour after sunrise to one hour before sunset.

VIDEO

Video was collected using the Benthically Anchored Suspended Stereo Camera (BASSCam) versions 1.0 and 2.0. BASSCam 2.0 was built as a scaled down version of 1.0, to be used specifically for operations on the RV Arima in shallow waters.

Both BASSCams were trapezoidal in shape, and positively buoyant via non-compressible trawl floats. BASSCam had a center fin designed to orient it to the prevailing current. The camera system utilized a stereo pair of GoPro Hero4 Black Edition cameras facing forward from the center of the camera frame. A third GoPro camera, located between and slightly below, the paired stereo cameras was angled downward **Figure 6**. All cameras were operated at 30 frames per second. For both BASSCam 1.0 and 2.0, the forward cameras had a horizontal and vertical field of view were 67.4° and 39.3°, respectively. While both BASSCams had the same model of downward-facing cameras, the waterproof housings were different. BASSCam 1.0's downward camera had a horizontal and vertical field of view of 94.4° and 55°, respectively; and BASSCam 2.0's downward camera had a horizontal and vertical field of view of 65.2° and 38°, respectively. On BASSCam 1.0, the downward-facing camera is angled at 22° below the horizontal plane, and on BASSCam 2.0 the downward-facing camera is angled at 43° below the horizontal plane. The left forward-facing camera was used to count fish above the near bottom dead zone (fish available to acoustics sampling) and the downward-facing camera was used to count fish that may occur within the near bottom dead zone (see [Fisheries Acoustics](#)). Both BASSCams were equipped with a StarOddi Tilt sensor to determine how the camera system was oriented during deployments.

To maximize the ability to accurately measure fish, stereo cameras should be placed as far apart as possible, while still maintaining a shared field of view. BASSCam 1.0 had a base separation of 39.5 cm and BASSCam 2.0 had a separation of 32.7 cm. Both stereo camera pairs were angled inward slightly to create the overlap necessary for length measurements (BASS 1.0

left and right stereo cameras: -7.5° and 8°, and BASSCam 2.0 left and right stereo cameras: -7.12° and 6.1°).

While deployed, BASSCams was suspended two meters above an anchor resting on the seafloor, a leader connecting the bottom of the camera frame to the anchor. Another attachment point on the top of the frame was connected to a surface float with a small diameter, torque-resistant line. This design minimized drag, allowing the camera to remain as vertical as possible.

Video deployment locations were selected *in situ* by the scientist monitoring the acoustic data in real-time. When a fish school was observed on the echogram, a mark was made in the navigation software and the skipper of the vessel was informed that a camera drop was desired. The captain navigated the boat to the marked location and the science crew prepared the BASSCam for deployment. Cameras were turned on and synchronized with a clapper board. The skipper used their best knowledge of water current and wind conditions to work with the navigation computer operator to determine the best location to drop the camera so that it drifted into the school of fish identified on the acoustics. If the camera did not deploy as planned, a second drop was completed.

During our pilot study, we found two-minute deployments were sufficient for collecting accurate count and length data (Rasmuson, unpublished data). At the beginning of this survey, deployments were two minutes, measured from the time the camera's anchor reached the seafloor to the time the camera was pulled off the bottom. However, by day seven of the statewide survey, it was apparent that fish behavior was not congruent with our pilot study. While previous behavioral response to the BASSCam was either no reaction or a brief avoidance, *in-situ* video review during the first week of the statewide survey revealed a strong startle response paired with slow or zero return to the BASSCam deployment location. Scientists hypothesized fish were responding to the markedly low ambient light and oxygen conditions present on the north coast during this sampling period, and therefore, beginning on the eighth day of the survey, deployment time was increased to four minutes to increase the likelihood of observing, counting, and measuring fish from underwater video. Behavioral responses returned to those observed during the pilot study after leaving the regions of hypoxia.

HOOK AND LINE SAMPLING

Hook and line sampling gear and methods were based on the National Oceanic and Atmospheric Administration (NOAA) Southern California Bight Hook and Line Survey (Harms et al. 2008, 2010). Hook and line sampling was attempted twice a day, at approximately 1000 and 1400 hrs, when acoustic fish school observations occurred. If no schools were observed, no

hook and line sampling was conducted. When a school was identified, a point was made in the navigation software and a 100 m radius drawn around the point, this was referred to as a fishing station. The captain was allowed to explore within the fishing station to identify where he wanted to start/end each fishing drift. Four drifts were conducted at each fishing station. Four anglers were randomly assigned a location on the starboard gunnel of the boat. The same anglers were used for the entire day. Two anglers fished with a gangion consisting of 5 red shrimp flies (modeled after Harms et al. 2010), and the other two anglers fished with a gangion consisting of 6 Sabiki (herring) flies **Figure 28**. Both flies had barbed “J” hooks, size 5/0 on the shrimp flies and size 1/0 on the Sabiki files. Both gear types had an 18” breakaway leader between the bottom of the gangion and the lead sinker. The captain decided the size of lead to be used, between 6-24 oz, based on wind/drift speed. The same lead size was used for all four drifts. The location of the gear on the gunnel was randomized. After the first two drifts, the anglers switched to the other gear type.

Each drift began when the captain told the fishers to deploy their gear. Each drift lasted 5 minutes before fishers were told to retrieve their gear; however, they were allowed to retrieve their gear earlier if desired (e.g., if they caught fish). Using stopwatches with four timers, each angler marked the amount of time that it took for them to reach the bottom, the time of the first bite, the time they began to reel up, and the time their rig reached the surface. In the event something did not happen (e.g., they never got a bite), NA was recorded. If a time was not recorded correctly, it was coded as 999.

When gear reached the surface, individual fish were placed into a partitioned crate, specific to each fisher and drift, where each partition was associated with the hook number. If a fish popped off a hook, the fish was placed into the best guess partition and noted as such. Broken hooks were also recorded. Following each fishing station, fish were weighed and measured individually. All rockfish had their otoliths extracted for later ageing.

SURVEY DESIGN

The methods and tools used in the survey have been applied to a variety of species but were adapted for this survey with intention of providing an abundance estimate for Black Rockfish. The survey design was initially predicated around two assumptions 1) Black Rockfish primarily reside on rocky reef habitats and 2) most Black Rockfish occur inside of the 80 m contour. Therefore we designed our survey using the best available habitat data for Oregon’s nearshore ocean, Surficial Geologic Habitat Map Version 4.0 (SGHv4) for Oregon, provided by the Goldfinger Laboratory at Oregon State University (Goldfinger et al. 2014). While this dataset is the best available data, the quality and resolution within it are variable due to the variety of data sources informing habitat classification. Multibeam mapping surveys have been conducted

on several rocky reefs throughout Oregon waters but were not comprehensive at the time of our statewide survey or this report. For example, a large rocky reef off the Rogue River has not been mapped, so available data were based on combining interpolations of NOAA bathymetry charts with satellite observations of rocks or kelp.

The SGHv4 Map defines primary and secondary lithology types by the relative abundance of bottom types present in each polygon, such as primarily rock with secondary lithology consisting of sand. The map also distinguishes between a homogeneous mixture (such as *sandy mud*) and a heterogeneous mix of lithology types (such as *gravel and rock*, where *gravel* is the primary lithology and *rock* the secondary). Map creators concatenated primary, secondary, and mixed lithology classifications into one field referred to as 'Lith3'. By basing our survey design on the Lith3 layer, we were able to account for either lithology mixtures or mixes containing "Hard" habitat when creating our survey transects. We defined "Hard" habitat as any region containing either rock, boulder, cobble, or gravel in any concentration. Remaining regions that did not contain those lithology types were classified as "Soft". The various lithology classes from Lith3 that were categorized into soft/hard groupings for the purposes of our study design were:

Soft: Mud, muddy sand, sand, sand/mud, sand/shell, sandy mud, sand mud, and shell.

Hard: Boulder, cobble, cobble mix, cobble/gravel, gravel, gravel mix, gravel/rock, gravelly mud, gravelly sand, rock, rock mix, rock/boulder, rock/gravel, rock/sand, rock/shell, sand/boulder, sand/gravel, sand/rock, sandy gravel, and shell/gravel.

See pages 152 – 154 in Goldfinger et al. 2014 for a detailed description of how each lithology class was created and defined.

Based on our pilot studies, we determined a zig-zag survey design with evenly spaced transects would maximize data collection, while preserving data quality. To minimize the impact of vessel motion from ocean swell on acoustic data, east-west transects, or zigs, were transited from the offshore end of the transect towards the nearshore. Zags were transited from onshore to offshore while transiting to the next zig. Video and hook and line sampling only occurred on zigs except in marine reserves and protected areas, where fishing occurred anywhere within the reserve/protected area. This design allowed us to 1) use multiple analytical methods to generate abundance estimates (design based and model based) and 2) allow for habitat mapping by collecting acoustic data while transiting to the next transect on the zags.

The survey was a systematic sampling layout with parallel transects. Parallel (perpendicular to the north south axis) transects were evenly spaced from the Washington border to the California border, with a random transect start. To create the random start, a randomly placed point was placed in a region bounded by the Washington border to a distance of 1 km south,

which determined the latitude of the first east-to-west transect. From there, moving south, “full” transects were spaced every 15 km extending from the 80 m contour to the 0 m contour, and “rock” transects spaced every 1 km where “Hard” habitat existed (defined above). The length of each rock transect was equal to the east-to west length of the hard habitat plus a 0.5 km buffer applied around the hard habitat.

Areas far from shore that contained reef features ≤ 80 m (such as Stonewall Bank) were excluded. In the event hard habitat was patchy, rock transects created were continuous from the outer most patch of hard habitat to the inner most patch.

SURVEY OPERATIONS

An [Online Map](#) of our survey has been provided to visualize the extent of the survey transects and their relation to each other as well as the SGHv4 habitat layer. Additionally, it shows vessel tracks from pass 1 and pass 2 and locations of CTD casts, video drops, fishing stations, and locations of in-situ acoustic fish schools that fishing and video events were based on. A description of how to use the map is provided in **Appendix 1: Online Survey Map How To**.

The survey began on August 1, 2021, at the mouth of the Columbia River and progressed southwards. Transects were systematically sampled southward until September 9th (Cape Blanco), at which point transects were sampled in a somewhat random order. This change allowed the vessel to continue to operate as much as possible in response to inclement weather encountered at this point, and for the remainder of the survey. The survey was completed on October 9, 2021. Secondary vessel (RV Arima) operations were conducted on September 11 and October 7-9, 2021.

The north coast, from the Columbia River to approximately Heceta Head (August 1-August 26), was characterized by low oxygen conditions that appeared to affect fish behavior. In response, additional funds were added to the contract and rocky reefs in the section of the survey from Three Arch Rocks to Waldport were resampled on October 17 through November 29, 2021. Hereafter we call this pass 2, and data collected from August 1-October 9, pass 1. During pass 2, winter conditions were present, causing sampling days to be more infrequent than pass 1. Extension of our survey timeline caused it to overlap with the survey vessels preparation for Dungeness crab season, therefore, to ensure pass 2 was completed, only CTD and acoustic sampling (no video or hook and line) were conducted during the last three days of pass 2 (beginning on November 21st).

For every full transect, CTD casts were conducted at water depths of 80, 60, 40, and 20 meters, and a final cast conducted at the shallowest end of the transect. Additional CTD casts were conducted haphazardly throughout the survey to inform speed of sound calculations for

acoustic data. Also, whenever the vessel transited past the nearshore Ocean Observatories Initiative buoy (OOI), a CTD cast was conducted to ground truth our sensors.

DATA PROCESSING

All analyses were performed using R version 4.2.1 “Funny-Looking Kid”. Versions of individual packages are listed at the point they were used. Acoustics were processed using Echoview 12.1 and some spatial analyses were conducted in ArcGIS Desktop versions 10.6 and 10.8.2, and ArcGIS Pro 3.0.0.

CTD DATA

CTD data were filtered and aligned using SBE Data Processing software and exported to R. They were then loop edited and filtered using the OCE package. Six CTD casts were adjacent to the Ocean Observing Initiative’s nearshore buoy (<https://dataexplorer.oceanobservatories.org/#ooi/array/CE/subsite/CE01ISSM/node/CE01ISSM-RI/data>). CTD cast data collected at depths of 7 and 25 m were plotted over the timeseries from July-December 2021.

Near bottom oceanographic conditions plots and cross-shelf contour plots were generated using the OCE package.

Although CTD casts were not conducted on every acoustic transect, we predicted the speed of sound in the water at the midpoint of each transect using a simple generalized additive model (GAM) in the mgcv package in R (Wood 2006). This was done by extracting speed of sound data from each CTD cast at 5 m depth. The GAM was developed using speed of sound as our dependent variable, and interaction between latitude and longitude using a tensor spline as our explanatory variables. Data were modeled with a normal distribution and identity link. Models were fit for pass 1 and pass 2 independently. The model was then used to predict the speed of sound in water at the midpoint of each transect. Predicted speed of sound values were included in acoustic calibration files (described below) and applied to corresponding acoustic data within the Echoview software package. The same modeling method was applied to near bottom oxygen data to predict oxygen concentrations at each 50 m midpoint along every transect. Based on the numerical predictions generated, we categorized data into normoxia (>2.5 mg/L) and hypoxia (<2.5 mg/L) which were used as an input for our sdmTMB model of fish abundance (see [Model Based](#)).

FISHERIES ACOUSTICS

During dockside calibration of both transducers using the standard tungsten sphere method, before and after survey operations, there was not sufficient depth in the marina to get the sphere far enough below the transducer face. At-sea calibration attempts also failed due to

poor ocean conditions that did not allow the calibration sphere to remain in the beam of the transducer. In all instances, resulting calibrations were unsatisfactory and not applied to the acoustic data. Alternatively, based on guidance from Biosonics, factory-based calibrations conducted by the manufacturer both before and after the survey were used. Receiver sensitivity data from these calibrations were fit with a linear regression. Predicted receiver sensitivity values for each frequency on each survey day were applied to corresponding acoustic data within the Echoview software package.

A near bottom exclusion zone is a prescribed height off the bottom that is excluded because it contains the near bottom dead zone (Ona & Mitson 1996, Kotwicki et al. 2013). In our previous work, we elected to define this near bottom exclusion zone as the area from the bottom and extending upwards to 1 m above the bottom. For the purposes of this survey, methods used to process acoustic data depended on which “zone” the acoustic data occurred in, above or below the exclusion zone. The different zones, relative to exclusion zone, that were used to inform acoustic data analysis are depicted in **Figure 53**.

Acoustic data were processed following the methods of Rasmuson et al. (2021b & 2022: **Appendices 7 & 8**) but were adapted to account for the addition of a 38 kHz transducer to the primary survey vessel, as well as the addition of the secondary vessel. Each transect was processed separately in Echoview. Where acoustic data for a transect was collected by both vessels, data were analyzed independently for each vessel. Upon loading the BioSonics dt4 files into Echoview, any data collected before and after completion of the transect were coded as ‘no data’. Acoustic data from any sampling activity (video drop, CTD and fishing stations) were also coded as ‘no data’. This step effectively excluded any erroneous data from subsequent processing.

In Echoview, data in the nearfield exclusion zone, within 0.5 m of the transducer face, were excluded from further analysis. Within each echogram, the seafloor (referred to as the bottom herein) was identified using the Max S_v Bottom line identifier in the 38 kHz transducer data (201 kHz on RV Arima). The detection variables used were: start depth of 5 m, stop depth of 1000 m and a minimum S_v of -70 re 1m^2 . A backstep was applied with a discrimination level of -50 dB and a backstep range of 0 m. Following bottom detection, the Max S_v Bottom line was reviewed and edited as needed. Finally, a second exclusion zone, the near bottom acoustic exclusion zone, was defined as 1 m above the edited bottom line.

After defining the bottom, data from the 38 kHz and 201 kHz transducers were corrected following Ryan et al. (2015), and processed using a S_v threshold of -70 dB re 1m^2 . Data were corrected using a series of algorithms within Echoview: first the Dunford Motion Correction algorithm; followed by the attenuated signal removal; impulse noise removal; and finally, background noise removal. Settings for each algorithm are presented in **Table 11**.

ECHO INTEGRATION

Following the correction steps described above, the Echoview school detection algorithm was used to identify schools in the 201 kHz acoustic backscattering data. Detection was applied to the 201 kHz data because school edges are sharper and more defined than in the 38 kHz data. This resulted in better fits from the school detection algorithm settings, described in **Table 12**. All data was then median smoothed on a 3 sample by 3 ping window. This step prevented the school detection algorithm from over identifying zooplankton communities as fish schools. School detection was run on each transect twice: first, excluding data within 1 m of the bottom (near bottom exclusion zone); and second by including data occurring both above and within exclusion zone. When all data was included, data within 0-1 m of the bottom was corrected by applying the dead zone estimation algorithm, which averaged school data within 1-2 m off bottom and extrapolated it into the 0-1 m schools.

Following school detection, all schools (above and below 1 m), were visually assessed in both the 201 and 38 kHz echograms. Incorrect detections were deleted, and school edges corrected as needed. A mask was applied to the entire transect to ensure that the nautical area scattering coefficient (NASC) values were informed by fish school data only. Masked data was exported for a single NASC value per transect as well as for each 50 m along-transect bin. For the RV Arima these steps were all completed using the 201 kHz transducer.

ECHO COUNTING

After fish school detection was complete, the next step was to define regions of single targets (individual fish). First, target strength data were masked in the 201 kHz echogram using both the Sawada and ratio of multiple echoes indices. Regions where the Sawada index values were < 0.1 and the ratio of multiple echoes value was < 0.7 were used for single target analysis. Single target identification settings are presented in **Table 12**. Due to an abundance of zooplankton present in the data, rather than detect single targets for the entire echogram, which results in errant data, the target strength echogram was reviewed and regions with noticeable echo returns attributable to single fish were defined manually. After defining all potential single target regions, the Echoview fish tracking algorithm was applied to identify fish tracks within each of the predefined regions. Fish tracks being the algorithms correction for when a single target appeared as multiple fish over several pings. Fish tracks were then edited by a reviewer and exported. No single targets detection was conducted within the near bottom exclusion zone (0-1 m).

VIDEO SAMPLING

CAMERA SYSTEM AND CALIBRATION

Two BASSCams were used to capture underwater video during the survey; BASSCam 1.0 was used while sampling from the primary survey vessel, and the smaller BASSCam 2.0 was used while sampling from the secondary survey vessel. Both systems used GoPro Hero4 Black Edition cameras for the two forward-looking stereo cameras (see [Video](#)). Precise stereo video calibration is necessary to obtain accurate fish length measurements and can be obtained through either two-dimensional or three-dimensional calibration methods. There is strong evidence to suggest that 3D calibration methods not only require less frequent calibrations but also result in higher measurement accuracy and precision. Due to the prolonged timeframe of a statewide survey, and the importance of length measurement accuracy to the biomass estimate, each of our systems were calibrated with specific stereo camera pairs using a 3D calibration cube. This calibration footage was then processed using CAL software (SeaGIS™ Pty Ltd; Victoria, Aus), and the resulting calibration file was applied to corresponding field data. Our 3D calibration method was informed by training from the software manufacturer and previous research that utilized the same methodology for rockfish species in the eastern Pacific (Denney et al. 2017, Knight et al. 2018, Rasmuson et al. 2021b). Knight et al. 2018 (Appendix B) describes, in detail, the three-step process of conducting a 3D calibration. To summarize:

1. A 3D calibration cube is used in a swimming pool to capture calibration footage with each stereo camera pair/BASSCam combination.
2. Calibration footage is processed in CAL software to produce a custom calibration file for each camera pair/BASSCam combination.
3. Each calibration is checked for accuracy and precision in EventMeasure photogrammetry software by taking multiple measurements of the scale bar (objects of known length) in every portion of the field-of-view and at varying distances from the cameras.

VIDEO REVIEW

Species counts generated from underwater video are commonly generated using the MaxN review method, which produces a conservative relative abundance estimate by counting the maximum number of each species in one frame of each video deployment (Ellis & DeMartini 1995, Watson et al. 2005, Bacheler & Shertzer 2014). However, as described in Rasmuson et al. 2021b, the MeanCount approach (Schobernd et al. 2014) was shown to not only generate similar species proportions as the MaxN approach, but is also more efficient in terms of review time (see online supplement of Rasmuson et al. 2021b, recreated here in **Appendix 7**). Because

this survey targeted semi-pelagic species known to form large schools, the MeanCount approach was used to review all videos from both camera systems collected during the statewide survey.

All videos were reviewed by one technician using EventMeasure photogrammetry software (developed by SeaGIS). Video review typically included four minutes of “bottom time”, beginning from the time the camera reached the bottom, to the time it was pulled up. In instances where bottom time was longer than four minutes, the entire bottom time was reviewed, up to six minutes. Fish were counted in the left forward-facing stereo camera and the downward-facing camera only. To conduct a MeanCount review, the number of fish for each species was recorded at five second intervals. The camera recorded at 30 frames per second, so five seconds was equivalent to 150 frames, this made it so the number of frames counted was dependent on the length of the bottom time. For example, for a four-minute video: $\frac{(4 \text{ min} * 60 \text{ s})}{5 \text{ s}}$ = 48, the reviewer would review 48 frames, where the first frame was randomly selected from the first 150 frames. If a fish was not identifiable in any of the selected frames, the reviewer was able to play the video forward or backwards to attempt an identification in the original frame. For each species group, count from each frame was summed and divided by the number of frames counted, resulting in a single MeanCount for each drop and species group:

$$MeanCount_{g,d} = \frac{\sum_{i=1}^{nf_d} FishN_{g,d,i}}{nf_d}$$

Equation 1

Where $MeanCount_{g,d}$ is the average of the count (FishN) of each species group of rockfish (g), in each drop (d) for each frame (i). nf_d denotes the total number of frames enumerated on each drop. The MeanCount calculation includes zeros from frames where no fish were observed. All species were identified to the lowest taxonomic unit possible. Due to the frequent poor visibility in Oregon waters, Blue and Deacon Rockfishes were often difficult to differentiate in underwater video footage and so these two species were combined into a single species group. These two species are assessed and managed as a complex.

In addition to counts, fish measurements were also generated within the photogrammetry software, but only when the entire fish was observed in both the left and right forward-looking cameras. Using a random number generator, the reviewer selected five frames with fish present and attempted to measure every fish. If the fish was not measurable in the original frame, the reviewer was able to play the video forward or backwards to attempt a measurement in any frame. The photogrammetry software allows the application of filters to increase the possibility of identifying a fish to species or performing an accurate length measurement **Figure 7**. To maximize accuracy in length measurements, the reviewer attempted

to find the frame in which each fish was closest to the cameras, the middle of the field of view, and as parallel to the cameras as possible. At the time of each measurement, the software calculates the length measurement, as well as the precision and root mean square error (RMS) values; allowing the reviewer to repeat a measurement if either value or the length measurement were not satisfactory. Precision values reflect the physical geometry of the camera system (e.g., the base separation, or the degree at which the cameras are facing inward); as well as the properties of the measurement (e.g., distance to or angle of the fish relative to the camera). Therefore, high precision values are relative to each camera system and may indicate to the reviewer when the accuracy of a measurement may be improved; say for example by finding a frame where the fish is closer to the cameras. BASSCam measurements are generally conducted on fish within 4 meters of the stereo cameras **Figure 8**. While an ideal RMS value is 0, indicating perfect intersection of all points in the measured length, values <10 mm were considered satisfactory and therefore did not merit re-measuring. RMS values >10 mm prompted the reviewer to re-measure, and values >20 mm prompted the reviewer to check the synchronization of the cameras and/or that they were using the correct calibration file. Only measurements with RMS values lower than 20 mm were retained for inclusion in analysis but most length measurements had an RMS value near or below 10 mm **Figure 9**. Determination of when length values were too high or low were based on the reviewer's knowledge of reported maximum length of each species.

HOOK AND LINE SAMPLING

Ages were obtained from all otoliths collected during the survey following methods approved by the Committee of Age Reading Experts (Committee of Age-Reading Experts 2006), an affiliate of the Technical Subcommittee of the Canada-U.S. Groundfish Committee. Initially, the left sagittal otolith was submerged in tap water in a black-backed petri dish and the surface was examined under reflected light using a binocular dissecting microscope paired with a fiber optic light source. Analyzing the otolith surface under such conditions enhanced the dark translucent zones and allowed for a better understanding of otolith topography and growth mark location prior to subsequent analyses. The widely accepted method for production aging of groundfish is the break-and-burn method (Committee of Age-Reading Experts 2006). The right sagitta was broken through the core in the transverse plane using a scalpel, lightly burned over an alcohol lamp, and lightly coated in mineral oil to accentuate growth marks. Annuli were counted and an age was determined using the same microscope and lighting used to examine the otolith surface. An age was assigned to each fish by first counting annuli from the otolith nucleus to the proximal margin of the dorsal lobe and then corroborating that age by counting annuli on a similar path on the ventral lobe. After all otoliths were aged, a 20% random subsample each of Black Rockfish, Deacon Rockfish, and all other species was selected for a second read to determine within-reader precision in terms of absolute percent error (APE) (Beamish &

Fournier 1981). If the two ages on these subsamples did not match, a final age was assigned to each otolith after a third read.

DATA ANALYSIS

Much of the data were plotted to examine trends and not all are discussed in this section or in the results, rather we focused on more extensive analyses that contributed directly to the abundance and population estimates.

In multiple sections below we compare distributions of fish lengths. Due to the large discrepancy in sample sizes often present in our data, we elected to compare kernel density estimate (KDE) probability density functions of raw and standardized length data to approximate the length-frequency differences between sampling methods or regions. This novel use of KDE, described by Langlois et al. (2012), was specifically designed to address the bias toward larger fish present in hook and line fishing when compared to underwater stereo video data. For the raw data, both location (expected value-measured as the mean or median) and shape (variation around the location-measured as skewness or kurtosis) are compared. When standardized, only shape is compared. Standardization acts to somewhat remove size selectivity of different gears. Standardization of the lengths is done using the following formula $y = \frac{x - \text{median}}{\text{standard deviation}}$. This formula was applied to each dataset independently. This method is based on a comparison to a null model with multiple permutations. In all instances, 1,000 bootstraps were used. Bandwidth selection was automated by the algorithm.

VIDEO SAMPLING

VOLUMETRIC DENSITIES-TARGET STRENGTH RELATIONSHIP SELECTION

Following the methods described in Rasmuson et al. (2021b) which built on methods of Williams (2018), we compared the volumetric density of fish counted in video to acoustic data from individual schools to determine which target strength-to-length relationship to use for echo integration. Schools identified in the acoustics that had a corresponding BASSCam drop that occurred within 10 m of the center of the school were used for this analysis. For each school observed by the BASSCam, the number of rockfish counted in the left stereo camera were turned into volumetric density by calculating the volume of water viewed by the BASSCam's forward camera (based on camera field of view and height off bottom) and dividing that by the number of fish counted.

Acoustic fish school data (NASC) was turned into fish density using the average length of fish observed by the BASSCam in the associated school. The conversion of NASC to abundance was done with multiple published target strength to length relationships (see [Echo Integration](#)

below for a description of the mathematics). Rasmuson et al. 2021b applied this method after comparing multiple methods and determined densities derived from averaging the b_{20} values from Kang and Hwang (2003) and Hwang (2015) generated the most similar densities between the acoustics and the video. However, the analysis in Rasmuson et al. 2021b was conducted using a 201 kHz transducer, so we repeated the analysis for a 38 kHz transducer using b_{20} values specific to 38 kHz transducers (Foote 1987, Gauthier 2002, Kang & Hwang 2003, Hwang 2015). Like our previous work, we averaged the b_{20} values from Kang & Hwang 2003 and Hwang 2015. Densities of the acoustics were compared to the densities from the video using a one-way ANOVA.

BACKGROUND DENSITIES

We used fish counts from the BASSCam’s downward-facing camera to generate an areal density of each species/species group within the exclusion zone that are not associated with acoustic data (fish schools or single targets). Drops within 35 m of a fish school or single targets were excluded. We then used the counts from the drops conducted at distances > 35 m to derive a density of fish. To do so, we calculate the amount of seafloor observed by the downward-facing camera on each drop, based on camera field of view and height off bottom, then divided by the number of fish we counted. The density was calculated for each species/species group and we refer to it as the background density.

HOOK AND LINE SAMPLING

A length weight curve was developed from the data by fitting a linear regression to log transformed length and log transformed weight data using the *lm* package in R. Length and age data were fit with a von Bertalanffy curve using a nonlinear least squares as described by Ogle et al (2017). Growth was modeled as follows:

$$L_t = L_\infty [1 - e^{-K(t)}] + \varepsilon$$

Equation 2

Where L_t is the total length (cm) at age t , L_∞ is the asymptotic length, and K is the rate at which the asymptotic length is approached. We elected to set t_0 to 0 due to the paucity of small fish in the Black Rockfish samples. Curves were fit using length and age data from fish caught on hook and line in this study for Blue/Deacon Rockfish and for Black Rockfish. For Black Rockfish data from the 2021 recreational and commercial fisheries were also included due to the lack of small fish. However, the points shown on the curve are only from this study.

FISHERIES ACOUSTICS

The different zones, relative to exclusion zone, that were used to inform acoustic data analysis are depicted in **Figure 53**.

INCLEMENT WEATHER ANALYSIS

We followed Jech et al. (2021) and calculated the percentage of pings that were attenuated in both the 38 and 201 kHz transducers. Percentages were calculated in 50 m, along transect, bins and were compared to weather conditions as reported by the on-vessel scientists.

ECHO INTEGRATION

Backscattering cross-section data were calculated in 1 cm bins, and scaled for relative abundance of each species/species group, following methods of Robertis et al. (2014). Backscattering cross-section data (σ_{bs}) were calculated using the standard target strength to length equation given as:

$$TS=20\log_{10}(L)-b_{20}$$

Equation 3

where TS is the fish target strength, L is the fish length in cm, and b_{20} is a species-specific constant. Specifically, we used:

$$TS_{38 \text{ kHz}}=20\log_{10}(L)-67.7$$

Equation 4

$$TS_{201 \text{ kHz}}=20\log_{10}(L)-71.9$$

Equation 5

Where the b_{20} constant for the 38 kHz transducer (Equation 3) came from Hwang (2015) and the 201 kHz transducer relationship (Equation 4) came from Rasmuson et al. (2021b). Data from the 38 kHz transducer was used for echo integration on all transects conducted on the primary research vessel (RV Pacific Surveyor). For all transects conducted on the secondary research vessel (RV Arima) 201 kHz transducer data was used. Length data from the entire survey (for each pass individually) was obtained from stereo measurements of fish observed by both BASSCams (both survey vessels). Backscattering cross-section of each length was calculated as:

$$\sigma_{bs,L} = 10^{\left(\frac{TS_{L,f}}{10}\right)}$$

Equation 6

Where $\sigma_{bs,L}$ is the backscattering cross-section for length (L), and TS is the target strength at length (L) for the specified frequency (f). Following the vessel-based determination of when to

use each target strength length relationship, mean back scattering cross-section was calculated as:

$$\overline{\sigma_{bs}} = \sum_{L,g} (P_{L,g} * \sigma_{bs,L})$$

Equation 7

Where $\overline{\sigma_{bs}}$ is the mean back scattering coefficient, $P_{L,g}$ is the proportion of a group of rockfish (g) at length (L) and $\sigma_{bs,L}$ is the back scattering cross-section at length L . The proportion of each species group by length ($P_{L,g}$) was calculated as

$$P_{L,g} = \frac{NCamFish_{g,L}}{\sum NCamFish_g}$$

Equation 8

Where $NCamFish_{g,L}$ is the number of fish for a given species group (g) at length (L) observed by the BASSCam's forward-facing stereo cameras, and $\sum NCamFish_g$ is the sum of all fish counted in species group g by the forward camera. Video data from all drops (per pass) were used in the calculation and not separated based on region or habitat. Mean back scattering cross-section was converted to number of fish using

$$Eldens_{L,g,t} = \left(\left(\frac{NASC_t}{4\pi\overline{\sigma_{bs}}} \right) * P_g \right) * \left(\frac{1}{3.43 * 10^6} \right)$$

Equation 9

Where $Eldens_{L,g,t}$ is the density of fish in a length bin L for each species group (g) in number of fish per meter square on given transect (t). $NASC_t$ is the nautical areal scattering coefficient provided as an output from the acoustic software for transect (t), and P_g is calculated as the number of fish counted in group g divided by the sum of all counted fish.

To determine the density of fish within the near bottom exclusion zone, we subtracted the NASC value of the full water column echo integration from the dataset that excluded the near bottom region. As a reminder, the near bottom exclusion zone data was generated by averaging school data from above the exclusion zone into the exclusion zone. The resulting value was used in place of $NASC_t$ in equation 9. Proportions used in calculating P_g were informed by the BASSCam's downward-facing camera counts rather than the forward-facing cameras in equation 9. However, lengths used in equations 4-8 were determined from the forward-facing camera since the downward-facing camera was not a stereo system.

ECHO COUNTING

For single target regions analyzed by echo counting, we follow the protocol for identifying single targets outlined in Tschersich (2015). All single target detection and analysis was

performed with the 201 kHz data regardless of research vessel. Echoes within these regions were identified using the Echoview single target identification algorithm described by (Soule 1997, Ona 1999) which differentiates single fish signals from multiple fish signals. However, because multiple detections are often made of the same fish, a fish tracking algorithm (Balk & Lindem 2000, ICES 2000), was also applied to detect where groups of single targets were in fact a single fish **Table 12**. Following Tschersich (2015), fish density was computed from individual fish tracks using:

$$ECdens_t = \frac{1}{l_t} \sum_{f=1}^{f_n} \left(\frac{1}{2 \tan(\theta) * z_n} \right)$$

Equation 10

Where $ECdens$ is the summed density (number of fish per m^2) of all single fish tracks on a specific transect (denoted by t), l is the length of the transect in meters, θ is half of the full angle beam width of the transducer (3.45° in this case), and z is the depth, in meters, of each individual fish track (denoted by f) from the face of the transducer.

POPULATION ESTIMATION

HABITAT BLOCKING AND REGIONS

Habitat classifications that ultimately informed population estimates were summarized in two ways. The classifications defined from the SGHv4 dataset were grouped into either two habitat types (Hard & Soft: see [Survey Design](#)) or three habitat types (Hard, Soft, and Gravel: see below).

Soft: Mud, muddy sand, sand/mud, sand/shell, sandy mud, sand, sand mud and shell.

Gravel: Gravel, gravel mix, gravel/rock, gravelly mud, gravelly sand, sand/gravel, shell/gravel, and sandy gravel.

Hard: Boulder, cobble, cobble mix, cobble/gravel, rock, rock mix, rock/boulder, rock/gravel, rock/sand, rock/shell, sand/boulder, and sand/rock.

When grouped into only two habitat types, gravel, was included in the hard class based on the literature's suggestion that gravel habitats are utilized by Black Rockfish. However, during the survey, few schools of fish were observed when collecting data over habitat defined as gravel. As such the three-habitat type model allowed us to estimate densities on these gravel habitats separately from soft and hard habitats.

When performing design-based analyses, transect level habitat was initially defined based on whether the transects were full or rock transects. Then, full transects were further broken up based on habitat type (Soft, Gravel, or Hard), and the NASC value associated with each habitat type extracted separately. Rock transects were defined as gravel or rock based on which habitat was the predominate habitat of the transect.

Most of Oregon's nearshore rocky reefs are in the northern and southern portions of the state, separated by a large expanse of soft habitat in the middle. To account for this, we divided the state into three regions: north (Washington border to Heceta Head), central (Heceta Head to Coos Bay Bar) and south (Coos Bay Bar to California border).

Areas for expansion were made by summing polygon areas from the SGHv4 layer into their corresponding 2 and 3 habitat types in each of the three regions. These were then turned into a total state area by summing the regions.

BACKGROUND POPULATION ESTIMATE

Abundance of Black and Blue/Deacon Rockfishes, in each habitat type, in each region was calculated using densities derived from BASSCam drops that occurred at distances > 35 m from fish schools or single targets observed in the acoustics (i.e., areas above the exclusion zone where fish were observed on video but not on acoustics, see [Background Densities](#)). To determine how much of each region was not associated with fish schools or single targets, we first buffered identified fish schools and single targets with a 35 m buffer. We then calculated, by habitat type, what percentage of each transect did not contain any schools or single targets. Transect percentages were averaged in each region by habitat type. We then multiplied each percentage by the total area of the habitat type (for both two and three-habitat groups) in each region, and then multiplied by the densities from the [BASSCam](#) to generate a total background abundance for each region.

DESIGN BASED ESTIMATE

BASSCam data (MeanCount and Lengths) from all video drops were combined to determine the ratio of each species abundance relative to total fish abundance, as well as to generate a distribution of lengths for each species. Species specific ratios of abundance were generated for each 1 cm size bin and used to convert the hydroacoustic data into a survey-level density estimate of Black and Blue/Deacon Rockfishes. These density estimates were generated independently for the echo counting and echo integration data and further divided for each habitat grouping (two and three habitat groups), as well as for each region grouping (statewide and three region categories). Data were calculated separately for pass 1 and pass 2.

Average (above exclusion zone) echo integration density of each rockfish species group for each habitat was calculated as the total density of each species group at each transect averaged by the total number of transects sampled:

$$\overline{EIdens}_{g,h,r} = \frac{\sum_i EIdens_{g,h,r}}{n_{t,h,r}}$$

Equation 11

$$EIvar_{g,h,r} = \frac{\sum (EIdens_{g,t,h,r} - \overline{EIdens}_{g,h,r})^2}{T_{h,r} - 1}$$

Equation 12

$$EIstdev_{g,h,r} = \sqrt{EIvar_{g,h,r}}$$

Equation 13

Where $\overline{EIdens}_{g,h,r}$ is the average echo integration density in number of fish per m² of each species group of rockfish (*g*) for each habitat type (*h*) in region (*r*) at transect (*t*). $n_{t,h,r}$ is the number of transects in each region and habitat type. $EIvar_{g,h,r}$ is the variance of the average echo integration density for each group of rockfish for each habitat type where (*t*) is the total number of transects at habitat type (*h*) in region (*r*). $EIstdev_{g,h,r}$ is the standard deviation of average echo integration density for each species group of rockfish for each habitat group in each region. These averages were calculated for each region independently and for the state as a whole. Equations 11-13 were also used to calculate the density of fish in the near bottom exclusion zone using just the NASC corrected for the exclusion zone.

Average (above exclusion zone) echo counting density and standard deviation was calculated as:

$$\overline{ECdens}_{g,h,r} = \frac{\sum ECdens_{t,g,h,r}}{T_{h,r}}$$

Equation 14

$$ECvar_{g,h,r} = \frac{\sum (ECdens_{t,h,r} - \overline{ECdens}_{g,h,r})^2}{T_{h,r} - 1}$$

Equation 15

$$ECstdev_{g,h,r} = \sqrt{ECvar_{g,h,r}}$$

Equation 16

Where $\overline{ECdens}_{g,h,r}$ is the average echo counting density in number of fish per m² of each species group of rockfish (g) for each habitat type (h) in region (r) at transect (t). T is the total number of transects at habitat type (h) in region (r). $ECvar_{g,h,r}$ is the variance of the echo counting density for each rockfish group (g) at habitat type (h) in region (r), and transect (t). $ECstdev_{g,h,r}$ is the standard deviation of echo counting density for each rockfish group (g) at habitat type (h) in region (r).

Echo counting and echo integration densities were turned into regional abundances by multiplying each density (echo integration and echo counting) by the total survey area (m²) of each region. As a reminder, regions were north, central, south, and statewide. Abundance from echo integration and echo counting for each region was aggregated by summing the abundances. Standard deviation of the aggregation was calculated as:

$$AbundSD_{g,r} = \sqrt{\sum_h ECvar_{g,h,r} * A_{r,h}^2 + \sum_h EIVar_{g,h,r} * A_{r,h}^2}$$

Equation 17

Where A is the area of habitat (h) in region (r). Abundances were calculated for the north, central, south, and statewide regions as well as a statewide-combined summation which summed the values from the north, central and southern regions. These summations were applied to the data above the exclusion zone and within the exclusion zone, though there was no echo counting within the exclusion zone, only echo integration.

Biomass was calculated by multiplying the estimated abundance for each region (including the statewide-combined) by the proportion of fish in each size class (1 cm bins) for each species group. The number in each size class was converted to weight using the length weight relationships obtained from the hook and line data **Figure 41**.

MODEL BASED

The model-based estimate was developed using the sdmTMB package in R (Anderson et al. 2022). NASC values were extracted in 50 m along transect bins from the above exclusion zone acoustics. These data were then converted into densities of Black or Blue/Deacon Rockfish using Equation 9. Models were developed for Black and Blue/Deacon Rockfishes independently. Models were fit using a delta gamma distribution with a logit link for the binomial model and a log link for the gamma model. The model included a spatial random effect but no temporal component was included as a random effect. The INLA mesh was designed using a coastline barrier. The full model was:

$$Density_m^2 = s(Depth, k = 5) + s(Hour\ of\ Day, k = 5) + Substrate\ Category + Oxygen\ Category$$

Equation 18

Where $Density_m^2$ is the density of fish in each 50 m along transect bin, $Depth$ is the average depth of that 50 m bin (fit with a smoothing function and restricted to 5 knots), $Hour\ of\ Day$ is the hour of the day (fit with a smoothing function and restricted to 5 knots), $Substrate\ Category$ is the three habitat categories (hard, soft, gravel) and $Oxygen\ Category$ is whether that cell was normoxic or hypoxic. For this estimate, habitat type was assigned based on the predominate habitat in each 50 m along transect bin. For this variable we used predicted oxygen values at 50 m midpoints along each transect (see [CTD Data](#)) binned into hypoxic (values < 2.5 mg/L) and normoxic (>2.5 mg/L). Spatial autocorrelation was included in the model. For each species group, a model was run for pass 1, pass 2 and with pass as a random effect.

Best fit models were selected using AIC. Residuals were simulated for each of the two model parts independently using the maximum likelihood estimator Markov chain Monte Carlo (MCMC) flag in the “residuals” function and examined visually as a histogram. It is worth noting that, although each species was modeled independently, because the data were derived from the same acoustic data, the model fits (especially for the binomial model) are similar between the species.

To generate an abundance estimate, habitat and depth data from the entire survey area (Washington to California 0-80 m) was gridded into 50 x 50 m bins. Average depth and primary habitat type (hard, gravel or soft) was extracted for each 50x50 m bin from the best available digital elevation model (DEM) and SGHv4, respectively. We assumed all observations occurred in normoxic conditions and at noon (if oxygen and time of day variables were in the best fit model). Using these data as a prediction data set allowed us to spatial random fields throughout our survey area. We used the `get_index` function to calculate total abundance.

RESULTS AND ABUNDANCE ESTIMATE

An [Online Map](#) of our survey has been provided to visualize the extent of the survey transects and their relation to each other as well as the SGHv4 habitat layer. Additionally, it shows vessel tracks from pass 1 and pass 2 and locations of CTD casts, video drops, fishing stations, and locations of in-situ acoustic fish schools that fishing and video events were based on. A description of how to use the map is provided in **Appendix 1: Online Survey Map How To**.

OCEANOGRAPHY

Overall, conditions were upwelling favorable during pass 1 (August 1 – October 9) and then became downwelling favorable during pass 2 (October 17 – November 29) **Figure 1**. Upwelling

strength decreased from north to the south. Data from our CTD was in agreement with data from the Ocean Observing Initiatives buoy located near Yaquina Head **Figure 2**. Of highest importance to this study was the verified observation that oxygen conditions were low near the seafloor. Water temperatures were warmer in the south, accompanied with higher turbidity and greater oxygen concentrations **Figure 3**. When sampled a second time on pass 2, conditions in the north were warmer and more oxygen rich **Figure 4**. Although chlorophyll levels were lower during the second pass, the water was more turbid, likely due to winter storms **Figure 5**.

VIDEO

In total, there were 567 video drops, 496 of which occurred during pass 1 and 71 occurred during pass 2 **Table 3**. Pass 1 video drops consisted of 258 drops in the north region, 4 drops in the central region, and 234 drops in the southern region **Table 2**. No fish were observed on the four drops in the central region **Table 5**. Black Rockfish were observed on 129 video drops, Blue/Deacon on 91 and all Non-Focal Semi-Pelagic Species (Canary, Puget Sound, Widow, and Yellowtail Rockfishes) were observed on 79 drops. The juvenile rockfish species group, composed of two categories (1. Unidentified Black/Blue/Deacon Juvenile Rockfish; and 2. Unidentified Juvenile Rockfish), was observed on 68 drops (BBD Juvenile Rockfish n=32 and UNID Juvenile Rockfish n=36). The final rockfish species group, the Demersal Rockfish species group, counted 12 demersal species from 32 video drops.

Of the thirty-three species or species groups that were observed from underwater video, Blue/Deacon Rockfish were the most prevalent (TotalCount n=16,803, MeanCount n=312), followed by Black Rockfish (TotalCount n=13,555, MeanCount n=265), **Table 5**. Where TotalCount is the sum of all fish counted from every frame and MeanCount is the sum of the averages of each video. The majority of Black Rockfish counted were in the north region, while the opposite was true for Blue/Deacon Rockfish **Figure 18**. Total Count, for the Juvenile, Non-Focal Semi-Pelagic and Demersal species groups were 4,680, 4,290 and 1,147, respectively **Figure 11A & Figure 12A**. Most Juvenile Rockfish were seen in the north region on pass 2, while a majority of both Non-Focal Semi-Pelagic and Demersal Rockfish were seen on pass 1 **Figure 12**. TotalCount and MeanCount values include the number of fish seen in the forward-looking and downward-looking cameras.

On average, a higher number of semi-pelagic species were counted in the forward-looking cameras, whereas a higher number of demersal species were counted in the downward-looking camera **Figure 19**. This relationship was strongest for Blue/Deacon Rockfish, which are consistently seen more frequently in the forward camera; and the relationship was weakest for species in the Non-Focal Semi-Pelagic group, where the MeanCount was relatively equal in the forward and downward cameras. These findings were verified by looking at the proportion of

each species group seen in the forward-looking cameras **Figure 20**. Proportions varied based on the species/species group and region, but in general the proportion of Black, Demersal, and Non-Focal Semi-Pelagic Rockfish counted in the forward vs. downward-looking camera was about equal **Figure 21**; however, for Blue/Deacon Rockfish there was a significantly higher proportion seen in the forward-looking camera.

Because accurate length measurements from underwater video are more difficult to achieve than species identification, the number of measurements was far lower than the number of fish counted for each species **Figure 12A vs. 12B**. Fish were measured in 63% of video drops where fish were counted in the forward camera (seen in left camera on 158 drops, and measured in 116). On average, Blue/Deacon Rockfish length (mean: 28.7 ± 6.3 cm) was lower than Black Rockfish (mean: 39.9 ± 5.9 cm). Each species' average length was roughly equal in the north and south regions **Figure 23**. However, statistical comparison of the length-distributions in each region, using the Kernel Density Estimate (KDE) method, showed the slight differences in average length were significant in some cases. Mean length of Black Rockfish was slightly lower in the southern region, illustrated by the KDE probability function lying outside of the null model area, indicating there was significant difference between the location (expected value-measured as the mean or median) and shape (variation around the location-measured as skewness or kurtosis) of the length-frequency data for the raw data **Figure 25**. However, once data were standardized to test the shape of the distribution only, the difference in the shape of the length-frequency KDEs was no longer significant. KDE tests between regions for Blue/Deacon Rockfish were significant on both raw and standardized data indicating significant differences in both the location and shape of the length frequency data. This is likely due to the bimodal distribution of Blue/Deacon Rockfish lengths in the north region. Both Demersal and Non-Focal Semi-Pelagic species groups showed slightly higher mean lengths in the north region. While Black Rockfish show similar size distributions in the north and south regions, Blue/Deacon Rockfish length data were slightly bimodal in the north region only.

When compared to our survey's hook-and-line data, length distributions of both Black and Blue/Deacon Rockfishes match up well, with video capturing a slightly larger number of small (<30 cm) Black Rockfish than hook-and-line **Figure 43**. However, the KDE analysis reveals that differences were significant in the raw data only; when standardized the shape of the length frequency showed no significant difference, indicating that size selectivity of video and hook and line were similar for both species **Figure 46**.

When compared to recreational and commercial fishing data from the same year (2021), fish lengths from our video and hook-and-line data show a more complete size distribution than either fishery-dependent dataset, especially in the lower size classes for Blue/Deacon Rockfish (<20 cm) **Figure 26 and Figure 47**. For both species, the largest size classes captured by the

recreational and commercial fleets were also captured by our survey hook-and-line and video data.

Background densities were derived from fish counts from the downward-facing camera from drops greater than 50 m from acoustically observed fish schools (see [Background Densities](#)). Average densities of Black and Blue/Deacon Rockfishes were higher in areas classified as hard substrate than in areas classified as gravel substrate. Within hard habitat, background densities were higher for Blue/Deacon Rockfish than Black Rockfish **Figure 27**.

HOOK AND LINE

Forty-eight fishing stations were conducted in pass 1 and 7 in pass 2 **Table 3**. A total of 869 fish were caught with Blue/Deacon Rockfish being the most prevalent followed by Black Rockfish **Table 5**. Most drifts were less than 0.5 km long and occurred on the north south axis **Figure 29**. While most species showed relatively similar catches between the north and south, Blue/Deacon catch was distinctly higher in the south region **Figure 37**. Female Blue/Deacon Rockfish were larger than the males whereas length distributions were similar between sexes for all other species **Figure 36 & Figure 37**. As expected, most Blue/Deacon were caught on Sabiki rigs whereas Black Rockfish were caught on shrimp flies **Figure 39 & Figure 40**. Overall, Blue/Deacon Rockfish captured by hook and line showed a wider distribution of lengths and ages as compared to Black Rockfish, which showed a dearth of small, young fish **Figure 41 & Figure 42**.

KDE analysis of raw Black Rockfish length-frequency data found fish in the northern region had a smaller mean length than the south region. However, once this data was standardized, to test for shape alone, no significant difference was found, indicating that differences in the two regions are based on location of the curve **Figure 45**. Blue/Deacon Rockfish however, showed significant differences in length-frequency data between the two regions, though patterns were weak. The same analysis was repeated with gear type, comparing length data collected coast-wide from hook and line to coast-wide stereo video lengths **Figure 46**. For both Black and Blue/Deacon Rockfish the raw data showed significant differences between the length-frequency data, however there was no difference following standardization. KDE tests of the hook and line data were also conducted with the combined 2021 recreational and commercial fleet data for Black and Blue/Deacon Rockfish and significant differences were found in all iterations of the tests except for test of shape only for Black Rockfish, where no significant difference was found between the fishery dependent and fishery-independent datasets **Figure 47**.

FISHERIES ACOUSTICS

The different zones, relative to exclusion zone, that were used to inform acoustic data analysis are depicted in **Figure 53**.

Although Oregon is well known for its windy conditions, the pitch and roll of the vessel remained relatively low throughout the survey **Figure 48 & Figure 49**. Analysis of varying attenuated signal percentage cutoffs showed cutoffs of 5% or greater resulted in minimal loss of data **Table 13**. Wind speeds > 10 knots were associated with an increase in percentages of attenuated signal **Figure 51** but even still the percentage of attenuated cells was very low. Further, because wind speeds remained relatively low during data collection, resulting in a low number of data points being affected by signal attenuation, we elected to not exclude transects based on attenuation alone. Rather, the attenuated signal operator was used to remove individual pings that were attenuated.

There was no statistical difference in the volumetric densities observed by the BASSCam when compared to the six acoustic volumetric densities calculated using different target strength to length models **Figure 52**. We elected to use the model from Hwang (2015) because this model is based on *Sebastes inermis*, the most phylogenetically similar species to the Northeast Pacific Ocean's Black and Blue/Deacon Rockfishes.

Apart from the soft habitat along the central Oregon coast, fish schools were observed throughout the survey area **Figure 57**. Fish were infrequently observed on the deeper ends of the "full" transects, likely because full transects extended to the 80 m contour which was typically soft habitat. NASC (Nautical area scattering coefficient) values for each transect were highest when associated with rocky reefs, the highest values were associated with reefs well-known to anglers along the Oregon coast **Figure 61**. The majority of transects had NASC values less than 1,000 but maximum values > 10,000 did occur **Figure 63**.

Fish tracks (single fish not associated with a school) were present throughout the survey region, with notably more observed in the northern region **Figure 67**. This is potentially, due to increased scattering of fish in response to hypoxic conditions on the north coast during pass 1. However, during the development of the population model we unexpectedly found densities of schools to be greater during hypoxia, so it may just be a regional difference.

After conversion to density, we observed most rockfish were detected inside of fish schools regardless of habitat model or region **Figure 70, Figure 71, Figure 72, Figure 73**. Modeling gravel habitat independently from the rocky hard bottom demonstrated that there were greater densities of rockfish on the gravel habitat than the soft habitat but much less than the hard habitat **Figure 72 & Figure 73**.

POPULATION ESTIMATE

DESIGN BASED

The above exclusion zone abundance estimates did not differ dramatically between the two and three habitat type models **Table 15, Figure 74, Figure 75**. There were however noticeable differences that occurred when deriving abundance estimates from a single statewide density versus summing up the regional densities. Overall, more fish were observed above than within the exclusion zone **Table 16, Figure 74, Figure 75**. CV estimates were lower in the above exclusion zone than within the exclusion zone. Lowest abundances were observed in the background areas **Table 17, Figure 74, Figure 75**, suggesting most fish were available to the acoustics, and of the fish not directly available, the majority were directly below schools that were available to the acoustics.

The biomass estimates for the two-habitat Black Rockfish model were very similar (12,741 mt statewide and; 13,680 mt regional statewide) to the unfished age 3+ biomass estimate from the 2015 Black Rockfish stock assessment (11,611 mt) (Cope et al. 2015). Estimates were even closer when compared to the 3-habitat model (11,372 mt statewide and; 11,445 mt regional statewide). It is worth noting these estimates do not include fish within the exclusion zone or those in the background zone.

Comparison of the biomass estimates for the two-habitat Blue/Deacon Rockfish model were much higher in our survey (6,920 mt statewide and; 7,430 mt regional statewide) than the reported unfished age 0+ biomass from the 2017 stock assessment (2,199 mt) (Dick et al. 2017). Estimates were closer when compared to the 3-habitat model (6,176 mt statewide and; 6,216 mt regional statewide). As with the Black Rockfish estimates, these numbers do not include fish within the exclusion zone or those in the background zone.

MODEL BASED

For both Blue/Deacon and Black Rockfish, our best fit models for 'pass 1' and 'pass as a random effect' data included depth, hour of the day, oxygen category and habitat type **Table 18, Table 19, Table 21, Table 22, Table 25, Table 26, Table 28, Table 29**. The next best fit model (and not a large difference in delta AIC) did not include oxygen in the model. Trends were the same regardless if data were only from pass 1 or if pass was modeled as a random effect **Figure 82, Figure 83, Figure 89, Figure 90, Figure 103, Figure 104, Figure 110, Figure 111**. Both probability of detection and density were higher in hard habitat than in gravel habitat. More fish were detected at a depth of 40 m and the density declined with depth. Detection decreased as the day progressed, but density rose till 10 am and then fluctuated but remained higher than the morning. Probability of detection was higher in normoxic waters, but densities were higher in

hypoxic waters. Maps of the estimates closely tracked with the location of reefs and where Black and Blue/Deacon Rockfish are known to reside **Figure 84, Figure 85, Figure 86, Figure 87, Figure 91, Figure 92, Figure 93, Figure 94, Figure 98, Figure 99, Figure 100, Figure 101, Figure 105, Figure 106, Figure 107, Figure 108**. The random effects captured an anomalous high-density event in deeper sandy waters around Waldport. The population estimates for the model-based estimates were higher than the design-based estimates but not dramatically higher **Table 24 vs. Table 31**. The model-based CVs were lower than the design-based except for in the central region which is likely due to the predominantly soft habitat in that region.

We present the models developed using pass 2 data in this manuscript **Table 23 & Table 30** for the purpose of comprehensiveness of the report. However, estimates and the associated CVs from pass 2 models are very high and we do not consider these models as useful or viable.

CONCLUSIONS

This work builds on our preliminary work described in Rasmuson et al. (2021b, 2022) and expands it to a regional survey. In general, we hypothesize that the methods described here provide an accurate estimate of the population abundance of Black and Blue/Deacon Rockfishes. Further, the methods provide direct population abundance estimates (combined with uncertainty) which allows us to provide an estimate of population scale. It is worth noting that for Black and Blue/Deacon Rockfishes, estuaries are not considered and for Blue/Deacon Rockfish, the waters of Stonewall Bank are not considered. Despite this, we conclude that a majority of habitat was surveyed, and abundance estimates provided. The use of sdmTMB allowed us to consider the effects of hypoxia directly in the model. The spatial estimates tracked well with known locations of Black and Blue/Deacon Rockfish and the model greatly reduced the CV of our population estimates.

RECOMMENDATIONS

1. Repeat the survey in future years. Conduct supplemental surveys within estuaries and at Stonewall Bank.
2. Continue to develop methods for at-sea calibration.
3. Continue to develop species specific target strength to length relationships.
 - a. Work to develop models from X-Rays of fish swim bladders is ongoing.
4. Develop methods to better utilize data from both the 38 and 201 kHz transducers.
5. For model-based estimates, consider developing models which include the near bottom exclusion zone after an expansion was done. And explore development of single target models.

- Determine if acoustic data collected on zags would improve the estimates and CVs derived from the design-based model.

ACKNOWLEDGMENTS

Captain Dave DeBelloy and the crew of the CPFV Enterprise were instrumental in the design of this survey method and conducting the pilot studies that informed the statewide survey. Captain Al Pazar and the crew of the RV Pacific Surveyor were key to implementation of the survey at a statewide level. Funding for initial research and support staff was provided by the Saltonstall-Kennedy grant foundation. Primary funds for the statewide survey were contributed by the Oregon Department of Fish and Wildlife's Restoration and Enhancement Board. Dr. David Sampson, Dr. Aaron Berger, and Keith Bosley all contributed greatly to survey design and logistics discussions. Dr. Kresimir Williams, Dr. Dezhang Chu, and Dr. Sandy Parker helped immensely with the acoustic analysis and design. Dr. Sean Anderson and Dr. Eric Ward helped with guidance on the use and implementation of sdmTMB. Finally, we thank the Marine Resources Program for providing numerous talented at-sea crew members, and one expert video review technician.

REFERENCES

- Anderson S, Ward EJ, English P, Barnett LAK (2022) SdmTMB: an R package for fast, flexible, and user-friendly generalized linear mixed effects models with spatial and spatiotemporal random fields. bioRxiv.
- Bacheler NM, Shertzer KW (2014) Estimating relative abundance and species richness from video surveys of reef fishes. *Fish Bull* 113:15–26.
- Balk H, Lindem T (2000) Improved fish detection in data from split-beam sonar. *Aquat Living Resour* 13:297–303.
- Beamish RJ, Fournier DA (1981) A method for comparing the precision of a set of age determinations. *Can J Fish Aquat Sci* 38:982–983.
- Committee of Age-Reading Experts (2006) Manual on generalized age determination procedures for groundfish.
- Cope JM, Sampson D, Stephens A, Key M, Mirick PP, Stachura M, Tsou S, Weyland P, Berger A, Buell T, Councill E, Dick EJ, Fenske KH, Monk M, Rodomsky BT (2015) Assessments of California, Oregon and Washington Stocks of Black Rockfish (*Sebastes melanops*) in 2015. 402.
- Demer D, Berger L, Bernasconia M, Bethke E, Boswell K, Chu D, Domokos R, Dunford AJ, Fassler S, Gauthier S, Hufnagle LC, Jech JM, Bouffant N, Lebourges-Dhaussy A, Lurton X, Macaulay GJ, Perrot Y, Ryan T, Parker Stetter SL, Stienessen S, Weber TC, Williamson NJ (2015) Calibration of acoustic instruments.

- Denney C, Fields R, Gleason M, Starr R (2017) Development of New Methods for Quantifying Fish Density Using Underwater Stereo-video Tools. *J Vis Exp*.
- Dick EJ, Berger AM, Bizzarro J, Bosley K, Cope J, Field J, Gilbert-Horvath L, Grunloh N, Ivens-Duran M, Miller R, Privtera-Johnson K, Rodomsky BT (2017) The combined status of Blue and Deacon Rockfishes in U.S. waters off California and Oregon in 2017. Pacific Fishery Management Council.
- Ellis D, DeMartini E (1995) Evaluation of a video camera technique for indexing abundances of juvenile pink snapper *Pristipomoides filamentosus*, and other Hawaiian insular shelf fishes. *Fish Bull* 93:67–77.
- Foote KG (1987) Fish target strengths for use in echo integrator surveys. *J Acoust Soc Am* 82:981–987.
- Gauthier S (2002) In situ target strength studies on Atlantic redfish (*Sebastes* spp.). *ICES J Mar Sci* 59:805–815.
- Goldfinger C, Henkel S, Romsos C, Havron B (2014) Benthic habitat characterization offshore the Pacific Northwest volume 1: evaluation of continental shelf geology. US Dep Inter Bur Ocean Energy Manag Pac Outer Cont Shelf Reg OCS Study BOEM 2014-662 Camarillo Calif.
- Harms JH, Benante J, Barnhart RM (2008) The 2004-2007 hook and line survey of shelf rockfish in the southern California bight: Estimates of distribution, abundance and length composition.
- Harms JH, Wallace JR, Stewart IJ (2010) Analysis of fishery-independent hook and line-based data for use in the stock assessment of bocaccio rockfish (*Sebastes paucispinis*). *Fish Res* 106:298–309.
- Hwang B (2015) Morphological Properties and Target Strength Characteristics for dark banded rockfish (*Sebastes inermis*). *J Korean Soc Fish Technol* 51:120–127.
- ICES (2000) Report on Echo Trace Classification.
- Jech JM, Schaber M, Cox MJ, Escobar-Flores P, Gastauer S, Haris K, Horne JK, Jarvis T, Ladroit Y, O’Driscoll R, Pedersen G, Pena M, Ryan T, Sakinan S, Thomas R, Viehman H, Wall C, Whitton T (2021) Collecting quality echosounder data in inclement weather. *ICES Coop Res Rep*.
- Kang D, Hwang D (2003) Ex situ target strength of rockfish (*Sebastes schlegeli*) and red sea bream (*Pagrus major*) in the Northwest Pacific. *ICES J Mar Sci* 60:538–543.
- Knight A, Watson J, Dixon J, Aylesworth L, Don C, Fox D (2018) A stereo video system for monitoring Oregon’s Marine Reserves: Construcion, testing, and pilot study of a convertible stereo system for lander and SCUBA surveys.
- Kotwicki S, De Robertis A, Ianelli JN, Punt AE, Horne JK (2013) Combining bottom trawl and acoustic data to model acoustic dead zone correction and bottom trawl efficiency parameters for semipelagic species. *Can J Fish Aquat Sci* 70:208–219.

- Langlois TJ, Fitzpatrick BR, Fairclough DV, Wakefield CB, Hesp SA, McLean DL, Harvey ES, Meeuwig JJ (2012) Similarities between Line Fishing and Baited Stereo-Video Estimations of Length-Frequency: Novel Application of Kernel Density Estimates. *PLoS ONE* 7:e45973.
- Ogle DH, Brenden TO, McCormick JL (2017) Growth estimation: Growth models and statistical inference. In: *Age and growth of fishes: Principles and techniques*. Quist MC, Isermann DA (eds) American Fisheries Society, p 265–359
- Ona E (1999) Methodology for target strength measurements. *ICES Coop Res Rep* 235:59.
- Ona E, Mitson RB (1996) Acoustic sampling and signal processing near the seabed: the deadzone revisited. *ICES J Mar Sci* 53:677–690.
- Parker S, Olson J, Rankin P, Malvitch J (2008) Patterns in vertical movements of black rockfish *Sebastes melanops*. *Aquat Biol* 2:57–65.
- Parker SJ, Rankin PS, Olson J, Hannah R (2005) Movement patterns of Black Rockfish (*Sebastes melanops*) in Oregon coastal waters. In: *Biology, Assessment, and Management of North Pacific Rockfishes*. Lowell Wakefield Fisheries Symposium,
- Rankin P, Hannah R, Blume M (2013) Effect of hypoxia on rockfish movements: implications for understanding the roles of temperature, toxins and site fidelity. *Mar Ecol Prog Ser* 492:223–234.
- Rasmuson L (2021) Susceptibility of five species of rockfish (*Sebastes* spp.) to different survey gears inferred from high resolution behavioral data. Oregon Department of Fish and Wildlife, Salem.
- Rasmuson LK, Blume MTO, Rankin PS (2021a) Habitat use and activity patterns of female Deacon Rockfish (*Sebastes diaconus*) at seasonal scales and in response to episodic hypoxia. *Environ Biol Fishes* 104:535–553.
- Rasmuson LK, Fields SA, Blume MTO, Lawrence KA, Rankin PS (2021b) Combined video–hydroacoustic survey of nearshore semi-pelagic rockfish in untrawlable habitats. *ICES J Mar Sci:fsab*245.
- Rasmuson LK, Marion SR, Fields SA, Blume MTO, Lawrence KA, Rankin PS (2022) Influence of near bottom fish distribution on the efficacy of a combined hydroacoustic video survey. *ICES J Mar Sci:fsac*138.
- Robertis AD, McKelvey D, Taylor K, Honkalehto T (2014) Development of Acoustic-Trawl Survey Methods to Estimate the Abundance of age-0 Walleye Pollock in the Eastern Bering Sea Shelf During the BeringArctic Subarctic Integrated Survey (BASIS). 55.
- Ryan TE, Downie RA, Kloser RJ, Keith G (2015) Reducing bias due to noise and attenuation in open-ocean echo integration data. *ICES J Mar Sci J Cons* 72:2482–2493.
- Schobernd ZH, Bacheler NM, Conn PB, Trenkel V (2014) Examining the utility of alternative video monitoring metrics for indexing reef fish abundance. *Can J Fish Aquat Sci* 71:464–471.

- Soule M (1997) Performance of a new phase algorithm for discriminating between single and overlapping echoes in a split-beam echosounder. *ICES J Mar Sci* 54:934–938.
- Watson DL, Harvey ES, Anderson MJ, Kendrick GA (2005) A comparison of temperate reef fish assemblages recorded by three underwater stereo-video techniques. *Mar Biol* 148:415–425.
- Williams K, Rooper CN, De Robertis A, Levine M, Towler R (2018) A method for computing volumetric fish density using stereo cameras. *J Exp Mar Biol Ecol* 508:21–26.
- Wood S (2006) *Generalized additive models: An introduction with R*. CRC Press, Boca Raton, FL.

TABLES

SURVEY DESIGN

Table 1. Original best guesses for effort allocation for survey design.

<i>Event</i>	<i>Time Break Down</i>	<i>Total Time (hrs)</i>
Full Transects	346 km @ 7 km/h	49.4
Rock Transects	1,491 km @ 7 km/h	213
Video Drops	550 drops @ 15 min per drop	137.5
Fishing Stations	100 Stations at 1 hour per station	100

Table 2. Number of each type of sampling event that occurred in each region.

<i>Gear</i>	Number of Events			
	<i>North</i>	<i>Central</i>	<i>South</i>	<i>Total</i>
CTD Casts	115	25	141	281
Video Drops	329	4	234	567
Fishing Stations	36	—	19	55

Table 3. Number of each type of sampling event that occurred during pass 1 and pass 2. All of pass 2 occurred in the north portion of the survey area.

<i>Gear</i>	Number of Events		
	<i>Pass 1</i>	<i>Pass 2</i>	<i>Total</i>
CTD Casts	229	52	281
Video Drops	496	71	567
Fishing Stations	48	7	55

Table 4. Total numbers (pass 1 and pass 2 combined) of each species or species group of fish observed in the BASSCam or using hook and line sampling. Note: BASSCam counts include both forward and downward-facing camera counts.

<i>Common Name</i>	<i>Scientific Name</i>	<i>Species Group</i>	<i>Video</i>	<i>Hook and Line</i>
Yellowtail Rockfish	<i>Sebastes flavidus</i>	Non-Focal Semipelagic	520	62
Black Rockfish	<i>Sebastes melanops</i>	Black Rockfish	13,555	119
Blue/Deacon Rockfish	<i>Sebastes mystinus/diaconus</i>	Blue/Deacon Rockfish	16,803	572
Rosethorn Rockfish	<i>Sebastes helvomaculatus</i>	Demersal Rockfish	50	1
Canary Rockfish	<i>Sebastes pinniger</i>	Non-Focal Semipelagic	3685	61
Widow Rockfish	<i>Sebastes entomelas</i>	Non-Focal Semipelagic	23	14
Sanddab	<i>Citharichthys spp.</i>	Non-Swimbladder	0	4
Lingcod	<i>Ophiodon elongatus</i>	Non-Swimbladder	192	12
Chillipepper Rockfish	<i>Sebastes goodei</i>	Demersal Rockfish	0	1
Yelloweye Rockfish	<i>Sebastes ruberrimus</i>	Demersal Rockfish	361	4
Kelp Greenling	<i>Hexagrammos decagrammus</i>	Non-Swimbladder	120	2
Puget Sound Rockfish	<i>Sebastes emphaeus</i>	Non-Focal Semipelagic	62	1
Copper Rockfish	<i>Sebastes caurinus</i>	Demersal Rockfish	107	4
Quillback Rockfish	<i>Sebastes maliger</i>	Demersal Rockfish	359	9
Brown Rockfish	<i>Sebastes auriculatus</i>	Demersal Rockfish	0	1
Greenstriped Rockfish	<i>Sebastes elongatus</i>	Demersal Rockfish	0	1
Rosy Rockfish	<i>Sebastes rosaceus</i>	Demersal Rockfish	2	1

Table 5. Total count of each species or species group of fish observed in the BASSCam or using hook and line sampling north and south of 43.5 °N.

Common Name	Scientific Name	Species Group	North		Central		South	
			Video	Hook and Line	Video	Hook and Line	Video	Hook and Line
Yellowtail Rockfish	<i>S. flavidus</i>	Non-Focal Semipelagic	442	28	—	—	78	34
Black Rockfish	<i>S. melanops</i>	Black Rockfish	8462	69	—	—	5093	50
Blue/Deacon Rockfish	<i>S. mystinus/diaconus</i>	Blue/Deacon Rockfish	7377	162	—	—	9426	410
Rosethorn Rockfish	<i>S. helvomaculatus</i>	Demersal Rockfish	—	—	—	—	50	1
Canary Rockfish	<i>S. pinniger</i>	Non-Focal Semipelagic	1550	34	—	—	2135	27
Widow Rockfish	<i>S. entomelas</i>	Non-Focal Semipelagic	15	—	—	—	8	14
Sanddab	<i>Citharichthys spp.</i>	Non-Swimbladder	—	4	—	—	0	—
Lingcod	<i>Ophiodon elongatus</i>	Non-Swimbladder	143	5	—	—	49	7
Chillipepper Rockfish	<i>S. goodei</i>	Demersal Rockfish	—	—	—	—	0	1
Yelloweye Rockfish	<i>S. ruberrimus</i>	Demersal Rockfish	166	1	—	—	195	3
Kelp Greenling	<i>Hexagrammos decagrammus</i>	Non-Swimbladder	65	1	—	—	55	1
Puget Sound Rockfish	<i>S. emphaeus</i>	Non-Focal Semipelagic	36	1	—	—	26	—
Copper Rockfish	<i>S. caurinus</i>	Demersal Rockfish	9	—	—	—	98	4
Quillback Rockfish	<i>S. maliger</i>	Demersal Rockfish	249	2	—	—	110	7
Brown Rockfish	<i>S. auriculatus</i>	Demersal Rockfish	—	1	—	—	0	—
Greenstriped Rockfish	<i>S. elongatus</i>	Demersal Rockfish	—	—	—	—	0	1
Rosy Rockfish	<i>S. rosaceus</i>	Demersal Rockfish	1	—	—	—	1	1

Table 6. Total numbers of each species or species group of fish observed in the BASSCam or using hook and line sampling in pass 1 and pass 2.

Common Name	Scientific Name	Species Group	Pass 1		Pass 2	
			Video	Hook and Line	Video	Hook and Line
Yellowtail Rockfish	<i>Sebastes flavidus</i>	Non-Focal Semipelagic	498	58	22	4
Black Rockfish	<i>Sebastes melanops</i>	Black Rockfish	7959	71	5596	48
Blue/Deacon Rockfish	<i>Sebastes mystinus/diaconus</i>	Blue/Deacon Rockfish	10384	435	6419	137
Rosethorn Rockfish	<i>Sebastes helvomaculatus</i>	Demersal Rockfish	50	1	0	—
Canary Rockfish	<i>Sebastes pinniger</i>	Non-Focal Semipelagic	3612	52	73	9
Widow Rockfish	<i>Sebastes entomelas</i>	Non-Focal Semipelagic	23	14	0	—
Sanddab	<i>Citharichthys spp.</i>	Non-Swimbladder	0	4	0	—
Lingcod	<i>Ophiodon elongatus</i>	Non-Swimbladder	103	11	89	1
Chillipepper Rockfish	<i>Sebastes goodei</i>	Demersal Rockfish	0	1	0	—
Yelloweye Rockfish	<i>Sebastes ruberrimus</i>	Demersal Rockfish	305	3	56	1
Kelp Greenling	<i>Hexagrammos decagrammus</i>	Non-Swimbladder	59	2	61	—
Puget Sound Rockfish	<i>Sebastes emphaeus</i>	Non-Focal Semipelagic	62	1	0	—
Copper Rockfish	<i>Sebastes caurinus</i>	Demersal Rockfish	98	4	9	—
Quillback Rockfish	<i>Sebastes maliger</i>	Demersal Rockfish	247	9	112	—
Brown Rockfish	<i>Sebastes auriculatus</i>	Demersal Rockfish	0	1	0	—
Greenstriped Rockfish	<i>Sebastes elongatus</i>	Demersal Rockfish	0	1	0	—
Rosy Rockfish	<i>Sebastes rosaceus</i>	Demersal Rockfish	2	1	0	—

VIDEO SAMPLING

Table 7. Total numbers of each species or species group of fish observed in the BassCam in pass 1 and pass 2. Species also observed in hook and line sampling highlighted in grey.

Common Name	Scientific Name	Species Group	Fish Counted	Lengths Measured	Percent Measured	Average Length (mm)	SD
Black Rockfish	<i>S. melanops</i>	Black Rockfish	13,555	418	3.1	399.2	58.8
Blue or Deacon Rockfish	<i>S. mystinus or diaconus</i>	Blue/Deacon Rockfish	16,803	678	4.0	287.2	64.6
Juvenile Black, Blue, Deacon	<i>S. melanops, mystinus or diaconus, Juvenile</i>	Juvenile	2,920	85	2.9	108.9	39.1
Juvenile Rockfish	<i>Sebastes sp., Juvenile</i>	Juvenile	1,760	14	0.8	154.7	51.6
Adult Rockfish	<i>Sebastes sp., Adult</i>	UNID	387	NA	—	—	—
Canary Rockfish	<i>S. pinniger</i>	Non-Focal Semi-Pelagic	3685	72	2.0	351.6	63.1
China Rockfish	<i>S. nebulosus</i>	Demersal	122	7	5.7	329.4	24.3
Copper Rockfish	<i>S. caurinus</i>	Demersal	107	1	0.9	359.8	NA
Puget Sound Rockfish	<i>S. emphaeus</i>	Non-Focal Semi-Pelagic	62	14	22.6	172.6	12.7
Quillback Rockfish	<i>S. maliger</i>	Demersal	359	3	0.8	510.2	60.1
Rosy Rockfish	<i>S. rosaceus</i>	Demersal	2	0	0	—	—
Rosethorn Rockfish	<i>S. helvomaculatus</i>	Demersal	50	4	8.0	296.3	32.5
Shortbelly Rockfish	<i>S. jordani</i>	Demersal	0	0	—	—	—
Splitnose Rockfish	<i>S. diploproa</i>	Demersal	22	0	0	—	—
Stripetail Rockfish	<i>S. saxicola</i>	Demersal	1	0	0	—	—
Tiger Rockfish	<i>S. nigrocinctus</i>	Demersal	13	0	0	—	—
Vermilion Rockfish	<i>S. miniatus</i>	Demersal	110	1	0.9	709.7	NA
Widow Rockfish	<i>S. entomelas</i>	Non-Focal Semi-Pelagic	23	2	8.7	280.6	82.0
Yelloweye Rockfish	<i>S. ruberrimus</i>	Demersal	361	17	4.7	454.0	99.8
Yellowtail Rockfish	<i>S. flavidus</i>	Non-Focal Semi-Pelagic	520	9	1.7	407.0	95.1
Cabezon	<i>Scorpaenichthys marmoratus</i>	Other	80	0	0	—	—
Pile Surfperch	<i>Rhacochilus vacca</i>	Other	6	0	0	—	—
Striped Surfperch	<i>Embiotoca lateralis</i>	Other	6	0	0	—	—
Kelp Greenling	<i>Hexagrammos decagrammus</i>	Other	120	3	2.5	289.9	80.4
Painted Greenling	<i>Oxyilebius pictus</i>	Other	1	0	0.0	—	—
Lingcod	<i>Ophiodon elongatus</i>	Other	192	5	2.6	665.9	182.9
Northern Ronquil	<i>Ronquilus jordani</i>	Other	20	0	0.0	—	—
Spotted Ratfish	<i>Hydrolagus colliei</i>	Other	61	4	6.6	457.5	134.0
Sculpin	<i>Cottidae sp.</i>	UNID	3	NA	—	—	—
Flatfish	<i>Pleuronectiformes sp.</i>	UNID	133	NA	—	—	—
Forage Fish	NA	UNID	4,140	NA	—	—	—
Fish	NA	UNID	8	NA	—	—	—
Eelpout or gunnel or ronquil or cusk eel or poacher or threadfin sculpin	<i>Zoarcidae Pholidae Bathymasteridae Ophidiidae or Agonopsis sp.</i>	UNID	29	NA	—	—	—

HOOK AND LINE SAMPLING

Table 8. Number of length measurements and average lengths from data derived from the hook-and-line and video components of the statewide survey (HnL and Video), as well as from the 2021 Oregon recreational and commercial fishing fleets (Recreational and Commercial).

<i>Method</i>	<i>Common Name</i>	<i>Scientific Name</i>	<i>Number Measured</i>	<i>Average Length (mm)</i>	<i>SD</i>
HnL	Black	<i>S. melanops</i>	119	40.9	0.42
Video	Black	<i>S. melanops</i>	418	39.9	0.59
Recreational	Black	<i>S. melanops</i>	9321	39.5	0.44
Commercial	Black	<i>S. melanops</i>	3212	39.4	0.40
HnL	Blue/Deacon	<i>S. mystinus or diaconus</i>	572	29.0	0.67
Video	Blue/Deacon	<i>S. mystinus or diaconus</i>	678	28.6	0.63
Recreational	Blue/Deacon	<i>S. mystinus or diaconus</i>	2895	32.4	0.37
Commercial	Blue/Deacon	<i>S. mystinus or diaconus</i>	604	34.1	0.34

FISHERIES ACOUSTICS

Table 9. ANOVA results comparing the different target strength to length models.

	<i>Degrees of Freedom</i>	<i>Sum of Squares</i>	<i>Mean Sum of Squares</i>	<i>F-Value</i>	<i>p-value</i>
Method	5	0.82	0.1633	0.178	0.97
Residuals	54	49.44	0.9156		

Table 10. Transducer settings and parameters for the 38 and 201 kHz transducers when co-located on RV Pacific Surveyor and for the 201 kHz located only on RV Arima

Vessel: RV Pacific Surveyor		Ping Rate: 2.97 pings per second
<i>Transducer</i>	<i>Variable</i>	<i>System Setting</i>
DT-X 38	Frequency (kHz)	38
	Pulse length (ms)	1
	Post Processing Sv Threshold	-70
	2-way beam angle (dB re 1 steradian)	-17.6206
	3 dB beamwidth (along)	10
	3 dB beamwidth (athwart)	10
	Major axis angle offset (along)	-0.1
	Min axis angle offset (athwart)	0.13
DT-X 201	Frequency (kHz)	201
	Pulse length (ms)	0.3
	Post Processing Sv Threshold	-70
	2-way beam angle (dB re 1 steradian)	-20.843618
	3 dB beamwidth (along)	6.9
	3 dB beamwidth (athwart)	6.9
	Major axis angle offset (along)	-0.26
	Min axis angle offset (athwart)	0.02
Vessel: RV Arima		Ping Rate: 5.0 pings per second
<i>Transducer</i>	<i>Variable</i>	<i>System Setting</i>
DT-X 201	Frequency (kHz)	201
	Pulse length (ms)	0.3
	Post Processing Sv Threshold	-70
	2-way beam angle (dB re 1 steradian)	-20.843618
	3 dB beamwidth (along)	6.9
	3 dB beamwidth (athwart)	6.9
	Major axis angle offset (along)	-0.26

Table 11. Correction settings used by Echoview to reduce bias in the acoustic data.

<u>Motion Correction</u>		
<i>Parameter</i>	<i>38 kHz</i>	<i>201 kHz</i>
Separation cut-off 3DB beam angle factor	1	1
Current 3 dB beam angle (degrees)	10	6.9
Maximum separation angle (degrees)	10	6.9
Maximum correction (factor)	5	5.03
Maximum correction (dB)	6.99	7.02
<u>Attenuated Signal Removal</u>		
<i>Parameter</i>	<i>38 kHz</i>	<i>201 kHz</i>
Context window size	31	31
Percentile	50	50
Threshold (dB)	7	10
Replacement	No Data	No Data
<u>Impulse Noise Removal</u>		
<i>Parameter</i>	<i>38 kHz</i>	<i>201 kHz</i>
Exclude below threshold (dB at 1m)	-170	-170
Vertical window units	Samples	Samples
Vertical window size (samples)	5	5
Horizontal size (pings)	5	5
Threshold (dB re 1m ²)	10	10
Noise sample replacement value	Mean	Mean
<u>Background Noise Removal</u>		
<i>Parameter</i>	<i>38 kHz</i>	<i>201 kHz</i>
Horizontal extent (pings)	20	20
Vertical units	Samples	Samples
Vertical extent (samples)	5	5
Vertical overlap (%)	0	0
Maximum noise (dB)	-125	-125
Minimum SNR	10	10

Table 12. School detection, single target detection and fish tracking algorithm parameters used by Echoview to process the data.

<u>School Detection</u>	
<i>Parameter</i>	<i>Value</i>
Minimum school length	5.00 m
Minimum school height	2.00 m
Minimum candidate length	3.00 m
Maximum vertical linking distance	5.00 m
Maximum horizontal linking distance	2.00 m
<u>Single Target Detection</u>	
<i>Parameter</i>	<i>Value</i>
Compensates target strength threshold	-60.00 dB
Pulse length determination level	6.00 dB
Minimum normalized pulse length	0.30
Maximum normalized pulse length	2.00
Maximum beam compensation	12.00 dB
Maximum standard deviation exclusion of minor axis angles	4.00 degrees
Maximum standard deviation exclusion of major axis angles	4.00 degrees
<u>Fish Tracking (collected for 4d data)</u>	
<i>Parameter</i>	<i>Value</i>
Alpha major axis	0.800
Alpha minor axis	0.800
Alpha range	0.800
Beta major axis	0.100
Beta minor axis	0.100
Beta range	0.100
Target gate major axis exclusion distance	1.00 m
Target gate minor axis exclusion distance	1.00 m
Target gate range exclusion distance	0.20 m
Target gate major axis missed ping expansion	50.00 %
Target gate minor axis missed ping expansion	50.00 %
Target gate range missed ping expansion	100.00 %

Table 13. Percentage of total number cells attenuated for different percentage cutoffs.

<i>Attenuation Cutoff</i>	<i>Frequency</i>	<i>Percentage Cells Attenuated</i>
1	201	6.4
1	38	15.8
5	201	2.9
5	38	2.4
10	201	1.2
10	38	0.8
20	201	0.1
20	38	0.1

POPULATION ESTIMATE

DESIGN BASED

Table 14. Habitat areas (square meters) for different habitat types for the two and three habitat models for each region individually and for the whole state combined.

<i>Habitat Model</i>	<i>Region</i>	<i>Habitat Type</i>	<i>Area (m²)</i>
Two Habitat	North	Hard	144,924,331
Two Habitat	North	Soft	2,837,244,002
Two Habitat	Central	Hard	795,138
Two Habitat	Central	Soft	749,488,129
Two Habitat	South	Hard	273,536,003
Two Habitat	South	Soft	1,107,643,781
Two Habitat	Statewide	Hard	419,255,471
Two Habitat	Statewide	Soft	4,694,375,912
Three Habitat	North	Gravel	61,802,493
Three Habitat	North	Hard	83,121,838
Three Habitat	North	Soft	2,837,244,002
Three Habitat	Central	Gravel	0
Three Habitat	Central	Hard	593,475
Three Habitat	Central	Soft	749,488,129
Three Habitat	South	Gravel	53,040,709
Three Habitat	South	Hard	220,495,294
Three Habitat	South	Soft	1,107,643,781
Three Habitat	Statewide	Gravel	115,044,864
Three Habitat	Statewide	Hard	304,210,607
Three Habitat	Statewide	Soft	4,694,375,912

Table 15. Abundance estimates for Black and Blue/Deacon Rockfish for the design-based extrapolation above the exclusion zone. Statewide abundance: calculated from average statewide density and total habitat area for the survey area. Statewide-combined: summed the abundances in each of the three regions. There data include both single targets and fish schools observed at heights off bottom >1 m. Two habitat denotes allocation to soft or hard substrate and three habitat denotes allocation to soft, gravel or hard substrate.

Pass	Habitat Model	Region	<u>Black Rockfish</u>					<u>Blue/Deacon Rockfish</u>				
			Count (# Fish)	Count SD	Biomass (MT)	Biomass SD	CV	Count (# Fish)	Count SD	Biomass (MT)	Biomass SD	CV
1	Two Habitat	North	3,774,088	2,998,280	3,788.6	3,009.8	79	4,732,392	3,759,593	2,057.7	1,634.7	79
1	Two Habitat	Central	322	176	0.3	0.2	55	403	221	0.2	0.1	55
1	Two Habitat	South	9,853,650	7,144,593	9,891.7	7,172.2	73	12,355,655	8,958,724	5,372.3	3,895.3	73
1	Two Habitat	Statewide	12,692,513	9,719,994	12,741.5	9,757.5	77	15,915,352	12,188,061	6,920.1	5,299.4	77
1	Two Habitat	Statewide-Combined Regions	13,628,060	7,748,219	13,680.6	7,778.1	57	17,088,450	9,715,620	7,430.2	4,224.4	57
1	Three Habitat	North	3,204,904	2,003,839	3,217.3	2,011.6	63	4,018,682	2,512,647	1,747.3	1,092.5	63
1	Three Habitat	Central	360	161	0.4	0.2	45	452	202	0.2	0.1	45
1	Three Habitat	South	8,196,634	5,854,201	8,228.2	5,876.8	71	10,277,896	7,340,679	4,468.9	3,191.8	71
1	Three Habitat	Statewide	11,328,416	7,689,553	11,372.1	7,719.2	68	14,204,889	9,642,058	6,176.4	4,192.4	68
1	Three Habitat	Statewide-Combined Regions	11,401,898	6,187,652	11,445.9	6,211.5	54	14,297,029	7,758,799	6,216.4	3,373.6	54
2	Two Habitat	North	2,991,218	1,485,526	3,002.8	1,491.3	50	14,618,916	7,260,181	6,356.4	3,156.8	50
2	Two Habitat	Statewide	8,653,374	4,297,518	8,686.7	4,314.1	50	5,053,331	2,509,632	2,197.2	1,091.2	50
2	Two Habitat	Statewide-Combined Regions	2,991,218	1,485,526	3,002.8	1,491.3	50	5,053,331	2,509,632	2,197.2	1,091.2	50
2	Three Habitat	North	2,302,305	882,350	2,311.2	885.8	38	3,889,489	1,490,633	1,691.2	648.1	38
2	Three Habitat	Statewide	7,545,735	3,225,344	7,574.8	3,237.8	43	12,747,684	5,448,861	5,542.8	2,369.2	43
2	Three Habitat	Statewide-Combined Regions	2,302,305	882,350	2,311.2	885.8	38	3,889,489	1,490,633	1,691.2	648.1	38

Table 16. Abundance estimates for Black and Blue/Deacon Rockfish for the design-based extrapolation within the exclusion zone. Statewide- was calculated using an average statewide density and the total habitat area for the state. Statewide-combined: summed up the abundances in each of the three regions. These data only include fish schools within 1 m of the bottom. Two habitat denotes allocation to soft or hard substrate and three habitat denotes allocation to soft, gravel or hard substrate.

<i>Pass</i>	<i>Habitat Model</i>	<i>Region</i>	Black Rockfish					Blue/Deacon Rockfish				
			<i>Count (# Fish)</i>	<i>Count SD</i>	<i>Biomass (MT)</i>	<i>Biomass SD</i>	<i>CV</i>	<i>Count (# Fish)</i>	<i>Count SD</i>	<i>Biomass (MT)</i>	<i>Biomass SD</i>	<i>CV</i>
1	Two Habitat	North	721,844	723,081	724.6	725.9	100	681,586	682,754	296.4	296.9	100
1	Two Habitat	Central	58	55	0.1	0.1	95	54	52	0.0	0.0	95
1	Two Habitat	South	2,869,853	3,049,897	2,880.9	3,061.7	106	2,709,798	2,879,800	1,178.2	1,252.2	106
1	Two Habitat	Statewide	3,071,192	3,504,474	3,083.0	3,518.0	114	2,899,908	3,309,025	1,260.9	1,438.8	114
1	Two Habitat	Statewide-Combined Regions	3,591,755	3,134,441	3,605.6	3,146.5	87	3,391,438	2,959,629	1,474.6	1,286.9	87
1	Three Habitat	North	613,510	475,659	615.9	477.5	78	579,293	449,131	251.9	195.3	78
1	Three Habitat	Central	64	50	0.1	0.1	77	61	47	0.0	0.0	77
1	Three Habitat	South	2,592,681	2,510,224	2,602.7	2,519.9	97	2,448,084	2,370,225	1,064.4	1,030.6	97
1	Three Habitat	Statewide	2,796,378	2,761,482	2,807.2	2,772.1	99	2,640,420	2,607,471	1,148.1	1,133.7	99
1	Three Habitat	Statewide-Combined Regions	3,206,255	2,554,892	3,218.6	2,564.7	80	3,027,438	2,412,403	1,316.3	1,048.9	80
2	Two Habitat	North	1,255,616	1,481,093	1,260.5	1,486.8	118	987,590	1,164,936	429.4	506.5	118
2	Two Habitat	Statewide	3,632,404	4,284,692	3,646.4	4,301.2	118	341,381	402,684	148.4	175.1	118
2	Two Habitat	Statewide-Combined Regions	1,255,616	1,481,093	1,260.5	1,486.8	118	341,381	402,684	148.4	175.1	118
2	Three Habitat	North	900,179	882,354	903.7	885.8	98	244,744	239,897	106.4	104.3	98
2	Three Habitat	Statewide	3,054,591	3,224,848	3,066.4	3,237.3	106	830,492	876,782	361.1	381.2	106
2	Three Habitat	Statewide-Combined Regions	900,179	882,354	903.7	885.8	98	244,744	239,897	106.4	104.3	98

Table 17. Abundance estimates for Black and Blue/Deacon Rockfish for the design-based extrapolation in background areas. Statewide- was calculated using an average statewide density and the total habitat area for the state. Statewide-combined: summed up the abundances in each of the three regions. Background areas are areas of a reef (as defined from the acoustics) that are not associated with any fish (schools or single targets). Density data is derived from BASSCam drops that occurred away from observations of fish schools and single targets. Two habitat denotes allocation to soft or hard substrate and three habitat denotes allocation to soft, gravel or hard substrate. Background densities were not calculated for pass 2 due to the lack of non-school or single target associated BASSCam drops.

<i>Pass</i>	<i>Habitat Model</i>	<i>Region</i>	<u>Black Rockfish</u>					<u>Blue/Deacon Rockfish</u>				
			<i>Count (# Fish)</i>	<i>Count SD</i>	<i>Biomass (MT)</i>	<i>Biomass SD</i>	<i>CV</i>	<i>Count (# Fish)</i>	<i>Count SD</i>	<i>Biomass (MT)</i>	<i>Biomass SD</i>	<i>CV</i>
1	Two Habitat	North	172,027	219,964	172.69	220.81	128	492,953	909,232	214.34	395.34	184
1	Two Habitat	Central	944	1,207	0.95	1.21	128	2,705	4,989	1.18	2.17	184
1	Two Habitat	South	324,690	415,169	325.94	416.77	128	930,419	1,716,121	404.55	746.18	184
1	Two Habitat	Statewide	497,661	636,341	499.58	638.79	128	1,426,077	2,630,341	620.07	1,143.69	184
1	Two Habitat	Statewide-Combined Regions	497,661	469,842	499.58	471.65	94	1,426,077	1,942,112	620.07	844.44	136
1	Three Habitat	North	101,183	126,249	101.57	126.74	125	282,735	521,493	122.93	226.75	184
1	Three Habitat	Central	713	901	0.72	0.90	126	2,019	3,723	0.88	1.62	184
1	Three Habitat	South	263,890	334,689	264.91	335.98	127	750,004	1,383,352	326.11	601.49	184
1	Three Habitat	Statewide	365,786	461,810	367.20	463.59	126	1,034,757	1,908,568	449.92	829.86	184
1	Three Habitat	Statewide-Combined Regions	365,786	357,710	367.20	359.09	98	1,034,757	1,478,388	449.92	642.81	143

MODEL BASED

BLACK

Table 18. Model selection for Black Rockfish species distribution model developed in sdmTMB for pass 1. Best fit models are bold.

<i>Model Formula</i>	<i>ΔAIC</i>
s(Depth) + s(Hour of Day) + Substrate Category + Oxygen Category	0
s(Depth) + s(Hour of Day) + Substrate Category	2.8
s(Depth) + Substrate Category + Oxygen Category	103.1
s(Depth) + s(Hour of Day) + Oxygen Category	4869.5
s(Hour of Day) + Substrate Category + Oxygen Category	547.2
s(Depth) + Oxygen Category	4955.9
s(Depth) + s(Hour)	4888.7
s(Depth) + Substrate Category	105.6
s(Hour of Day) + Substrate Category	565.6
s(Hour of Day) + Oxygen Category	5698.6
Substrate Category + Oxygen Category	642.7
Oxygen Category	5795.1
Substrate Category	660.7
s(Depth)	4976.4
s(Hour of Day)	5763.4
~1	5859.9

Table 19. Model selection for Black Rockfish species distribution model developed in sdmTMB with pass as a random effect. Best fit models are bold.

<i>Model Formula</i>	<i>ΔAIC</i>
s(Depth) + s(Hour of Day) + Substrate Category + Oxygen Category	0
s(Depth) + s(Hour of Day) + Substrate Category	5.0
s(Depth) + Substrate Category + Oxygen Category	119.8
s(Depth) + s(Hour of Day) + Oxygen Category	6155.5
s(Hour of Day) + Substrate Category + Oxygen Category	353.3
s(Depth) + Oxygen Category	6247.0
s(Depth) + s(Hour)	6193.0
s(Depth) + Substrate Category	124.7
s(Hour of Day) + Substrate Category	381.3
s(Hour of Day) + Oxygen Category	6857.4
Substrate Category + Oxygen Category	473.3
Oxygen Category	6963.5
Substrate Category	500.6
s(Depth)	6285.1
s(Hour of Day)	6927.7
~1	7032.5

Table 20. Model selection for Black Rockfish species distribution model developed in sdmTMB for pass 2. Best fit models are bold.

<i>Model Formula</i>	<i>ΔAIC</i>
s(Depth) + s(Hour of Day) + Substrate Category + Oxygen Category	0.918872
s(Depth) + s(Hour of Day) + Substrate Category	0
s(Depth) + Substrate Category + Oxygen Category	55.95865
s(Depth) + s(Hour of Day) + Oxygen Category	1220.753
s(Hour of Day) + Substrate Category + Oxygen Category	120.3541
	1338.674
s(Depth) + Oxygen Category	1224.542
s(Depth) + s(Hour)	55.4872
s(Depth) + Substrate Category	121.1804
s(Hour of Day) + Substrate Category	1409.9
s(Hour of Day) + Oxygen Category	176.5051
Substrate Category + Oxygen Category	1499.446
	177.4237
Oxygen Category	1344.747
Substrate Category	1420.32
s(Depth)	1513.144
s(Hour of Day)	0.918872
~1	

Table 21. Summary of best fit Black Rockfish model developed using sdmTMB for pass 1.

```

Spatial model fit by ML ['sdmTMB']
Formula: density_m2 ~ s(Depth, k = 5) + s(HR, k = 5) + Substrate + O2 + 0
Family: delta_gamma(link1 = 'logit', link2 = 'log')

Delta/hurdle model 1: -----
Family: binomial(link = 'logit')
                coef.est coef.se
Substrate: gravel      -3.58      2.30
Substrate: hard        -3.12      2.30
Substrate: soft        -3.99      2.30
O2: Normoxic           0.16      0.16
sDepth                 3.08      0.89
sHR                    -1.40      0.14

Smooth terms:
                Std. Dev.
sds(Depth)      3.09
sds(HR)         0.00

Matern range: 56.68
Spatial SD:    52.81

Delta/hurdle model 2: -----
Family: Gamma(link = 'log')
                Coef.est coef.se
Substrate: gravel      -2.47      0.26
Substrate: hard        -1.95      0.22
Substrate: soft        -2.71      0.22
O2: Normoxic          -0.43      0.18
sDepth                -1.86      1.27
sHR                   3.32      1.14

Smooth terms:
                Std. Dev.
sds(Depth)      1.63
sds(HR)         2.84

Dispersion parameter: 0.41
Matern range:        4.65
Spatial SD:         0.90
ML criterion at convergence: 599.674
    
```

Table 22. Summary of best fit Black Rockfish model developed using sdmTMB with pass as a random effect. Spatial model fit by ML ['sdmTMB']

```

Formula: density_m2 ~ s(Depth, k = 5) + s(HR, k = 5) + Substrate + O2 + 0
Family: delta_gamma(link1 = 'logit', link2 = 'log')

Delta/hurdle model 1: -----
Family: binomial(link = 'logit')
                coef.est coef.se
Substrate: gravel      -5.56      2.17
Substrate: hard        -5.00      2.17
Substrate: soft        -5.93      2.17
O2: Normoxic           0.37      0.13
sDepth                 0.49      0.76
sHR                    -1.44      0.60

Smooth terms:
                Std. Dev.
sds(Depth)       2.01
sds(HR)          1.11

Random intercepts:
                Std. Dev.
Pass             0.05

Matern range:    62.12
Spatial SD:     53.98

Delta/hurdle model 2: -----
Family: Gamma(link = 'log')
                Coef.est coef.se
Substrate: gravel      -2.45      0.26
Substrate: hard        -2.24      0.24
Substrate: soft        -7.67      0.23
O2: Normoxic           -0.11      0.15
sDepth                 -3.96      0.48
sHR                     4.19      1.04

Smooth terms:
                Std. Dev.
sds(Depth)           0.00
sds(HR)              3.74

Random intercepts:
                Std. Dev.
Pass                 0.1

Dispersion parameter: 0.39
Matern range:         5.16
Spatial SD:           1.03

ML criterion at convergence: -16447.685

```

Table 23. Summary of best fit Black Rockfish model developed using sdmTMB for pass 2. Spatial model fit by ML sdmTMB.

```

Formula: density_m2 ~ s(Depth, k = 5) + s(HR, k = 5) + Substrate + O2 + 0
Family: delta_gamma(link1 = 'logit', link2 = 'log')

Delta/hurdle model 1: -----
Family: binomial(link = 'logit')
              coef.est      coef.se
Substrate: gravel      -4.45         2.21
Substrate: hard        -3.52         2.21
Substrate: soft        -4.72         2.21
sDepth                 27.47         2.88
sHR                    -6.77         1.60

Smooth terms:
              Std. Dev.
sds(Depth)    4.94
sds(HR)       3.16

Matern range:  14.70
Spatial SD:    9.64

Delta/hurdle model 2: -----
Family: Gamma(link = 'log')
              Coef.est coef.se
Substrate: gravel      -1.44         0.68
Substrate: hard        -1.41         0.68
Substrate: soft        -7.42         0.67
sDepth                 4.54         3.66
sHR                    -2.30         1.05

Smooth terms:
              Std. Dev.
sds(Depth)    2.43
sds(HR)       0.70

Dispersion parameter:  0.39
Matern range:         3.14
Spatial SD:           2.07

ML criterion at convergence: -1494.855

```

Table 24. Population estimates for Black Rockfish from the best fit sdmTMB models developed for pass 1, pass 2 and with pass as a random effect (RE)

<i>Pass</i>	<i>Region</i>	Black Rockfish				<i>CV</i>
		<i>Count (# Fish)</i>	<i>Count SD</i>	<i>Biomass (MT)</i>	<i>Biomass SD</i>	
1	North	5,634,690	428,964	5,656.4	430.6	8
1	Central	25,656	60,193	25.8	60.4	235
1	South	14,079,245	1,100,146	14,133.5	1,104.4	8
1	Statewide	19,739,591	1,334,337	19,815.7	1,339.5	7
RE	North	5,420,209	398,471	5,441.1	400.0	7
RE	Central	9,357	5,911	9.4	5.9	63
RE	South	15,941,146	1,289,539	16,002.6	1,294.5	8
RE	Statewide	21,370,713	1,492,082	21,453.1	1,497.8	7
2	North	198,761,406	651,527,082	199,528.0	654,040.0	328
2	Statewide	218,982,833	570,314,052	219,827.5	572,513.8	260

BLUE/DEACON

Table 25. Model selection for Blue/Deacon Rockfish species distribution model developed in sdmTMB for pass 1. Best fit models are bold.

<i>Model Formula</i>	<i>ΔAIC</i>
s(Depth) + s(Hour of Day) + Substrate Category + Oxygen Category	0
s(Depth) + s(Hour of Day) + Substrate Category	2.7
s(Depth) + Substrate Category + Oxygen Category	103.1
s(Depth) + s(Hour of Day) + Oxygen Category	4869.5
s(Hour of Day) + Substrate Category + Oxygen Category	547.2
s(Depth) + Oxygen Category	4955.9
s(Depth) + s(Hour)	5267.3
s(Depth) + Substrate Category	105.6
s(Hour of Day) + Substrate Category	565.6
s(Hour of Day) + Oxygen Category	5698.6
Substrate Category + Oxygen Category	642.7
Oxygen Category	5795.1
Substrate Category	660.7
s(Depth)	4975.8
s(Hour of Day)	5761.6
~1	5857.9

Table 26. Model selection for Blue/Deacon Rockfish species distribution model developed in sdmTMB with pass as a random effect. Best fit models are bold.

<i>Model Formula</i>	<i>ΔAIC</i>
s(Depth) + s(Hour of Day) + Substrate Category + Oxygen Category	0
s(Depth) + s(Hour of Day) + Substrate Category	4.9
s(Depth) + Substrate Category + Oxygen Category	120.1
s(Depth) + s(Hour of Day) + Oxygen Category	6156.0
s(Hour of Day) + Substrate Category + Oxygen Category	353.3
s(Depth) + Oxygen Category	6247.5
s(Depth) + s(Hour)	6195.7
s(Depth) + Substrate Category	124.9
s(Hour of Day) + Substrate Category	381.2
s(Hour of Day) + Oxygen Category	6934.2
Substrate Category + Oxygen Category	473.5
Oxygen Category	6965.0
Substrate Category	6287.9
s(Depth)	6127.3
s(Hour of Day)	6924.8
~1	7034.9

Table 27. Model selection for Blue/Deacon Rockfish species distribution model developed in sdmTMB for pass 2. Best fit models are bold.

<i>Model Formula</i>	<i>ΔAIC</i>
s(Depth) + s(Hour of Day) + Substrate Category + Oxygen Category	0.918872
s(Depth) + s(Hour of Day) + Substrate Category	0
s(Depth) + Substrate Category + Oxygen Category	55.95865
s(Depth) + s(Hour of Day) + Oxygen Category	289.2458
s(Hour of Day) + Substrate Category + Oxygen Category	120.3541
s(Depth) + Oxygen Category	352.8231
s(Depth) + s(Hour)	291.1734
s(Depth) + Substrate Category	55.4872
s(Hour of Day) + Substrate Category	121.1804
s(Hour of Day) + Oxygen Category	397.1203
Substrate Category + Oxygen Category	176.5051
Oxygen Category	457.4162
Substrate Category	177.4237
s(Depth)	357.5049
s(Hour of Day)	406.3051
~1	471.0591

Table 28. Summary of best fit Blue/Deacon Rockfish model developed using sdmTMB for pass 1. Spatial model fit by ML ['sdmTMB']

Spatial model fit by ML ['sdmTMB']
 Formula: density_m2 ~ s(Depth, k = 5) + s(HR, k = 5) + Substrate + O2 + 0
 Family: delta_gamma(link1 = 'logit', link2 = 'log')

Delta/hurdle model 1: -----
 Family: binomial(link = 'logit')

	coef.est	coef.se
Substrate: gravel	-3.58	2.30
Substrate: hard	-3.12	2.30
Substrate: soft	-3.99	2.30
O2: Normoxic	0.16	0.16
sDepth	3.08	0.89
sHR	-1.40	0.14

Smooth terms:

	Std. Dev.
sds(Depth)	3.09
sds(HR)	0.00

Matern range: 56.68
 Spatial SD: 52.81

Delta/hurdle model 2: -----
 Family: Gamma(link = 'log')

	Coef.est	coef.se
Substrate: gravel	-2.47	0.26
Substrate: hard	-1.95	0.22
Substrate: soft	-2.71	0.22
O2: Normoxic	-0.43	0.18
sDepth	-1.86	1.27
sHR	3.32	1.14

Smooth terms:

	Std. Dev.
sds(Depth)	1.63
sds(HR)	2.84

Dispersion parameter: 0.41
 Matern range: 4.65
 Spatial SD: 0.90

ML criterion at convergence: -13771.065

Table 29. Summary of best fit Blue/Deacon Rockfish model developed using sdmTMB with pass as a random effect. Spatial model fit by ML ['sdmTMB']

```

Formula: density_m2 ~ s(Depth, k = 5) + s(HR, k = 5) + Substrate + O2 + 0
Family: delta_gamma(link1 = 'logit', link2 = 'log')

Delta/hurdle model 1: -----
Family: binomial(link = 'logit')
                coef.est coef.se
Substrate: gravel      -5.56      2.17
Substrate: hard        -5.00      2.17
Substrate: soft        -5.93      2.17
O2: Normoxic           0.37      0.13
sDepth                 0.49      0.76
sHR                    -1.44      0.60

Smooth terms:
                Std. Dev.
sds(Depth)       2.01
sds(HR)          1.11

Random intercepts:
                Std. Dev.
Pass            0.05

Matern range:    62.16
Spatial SD:     53.98

Delta/hurdle model 2: -----
Family: Gamma(link = 'log')
                Coef.est coef.se
Substrate: gravel      -2.06      0.24
Substrate: hard        -1.85      0.22
Substrate: soft        -7.27      0.21
O2: Normoxic           -0.10      0.15
sDepth                 -3.95      0.48
sHR                     4.17      1.04

Smooth terms:
                Std. Dev.
sds(Depth)           0.00
sds(HR)              3.76

Random intercepts:
                Std. Dev.
Pass                 0.0

Dispersion parameter: 0.39
Matern range:        5.09
Spatial SD:          1.03
ML criterion at convergence: -14095.212

```

Table 30. Summary of best fit Blue/Deacon Rockfish model developed using sdmTMB for pass 2. Spatial model fit by ML ['sdmTMB']

Formula: $\text{density_m2} \sim s(\text{Depth}, k = 5) + s(\text{HR}, k = 5) + \text{Substrate} + \text{O2} + 0$
 Family: $\text{delta_gamma}(\text{link1} = \text{'logit'}, \text{link2} = \text{'log'})$

Delta/hurdle model 1: -----
 Family: $\text{binomial}(\text{link} = \text{'logit'})$

	coef.est	coef.se
Substrate: gravel	-4.45	2.21
Substrate: hard	-3.52	2.21
Substrate: soft	-4.72	2.21
sDepth	27.47	2.88
sHR	-6.77	1.60

Smooth terms:

	Std. Dev.
sds(Depth)	4.94
sds(HR)	3.16

Matern range: 14.70
 Spatial SD: 9.64

Delta/hurdle model 2: -----
 Family: $\text{Gamma}(\text{link} = \text{'log'})$

	Coef.est	coef.se
Substrate: gravel	-0.95	0.68
Substrate: hard	-0.91	0.68
Substrate: soft	-2.32	0.67
sDepth	4.54	3.66
sHR	-2.30	1.05

Smooth terms:

	Std. Dev.
sds(Depth)	2.43
sds(HR)	0.70

Dispersion parameter: 0.39
 Matern range: 3.14
 Spatial SD: 2.07

ML criterion at convergence: 2206.394

Table 31. Population estimates for Blue/Deacon Rockfish from the best fit sdmTMB models developed for pass 1, pass 2 and with pass as a random effect (RE)

Blue/Deacon Rockfish						
<i>Pass</i>	<i>Region</i>	<i>Count (# Fish)</i>	<i>Count SD</i>	<i>Biomass (MT)</i>	<i>Biomass SD</i>	<i>CV</i>
1	North	7,829,911	596,085	3,404.5	259.2	8
1	Central	35,651	83,644	15.5	36.4	235
1	South	19,564,382	1,528,752	8,506.7	664.7	8
1	Statewide	27,429,944	1,854,181	11,926.7	806.2	7
RE	North	7,767,929	523,376	3,377.5	227.6	7
RE	Central	13,293	8,415	5.8	3.7	63
RE	South	22,662,241	1,721,403	9,853.7	748.5	8
RE	Statewide	30,443,463	1,998,782	13,237.0	869.1	7
2	North	31,923,595,115	111,052,592,725	13,880,568.5	48,286,325.8	348
2	Statewide	32,003,276,089	110,576,002,082	13,915,214.2	48,079,101.4	346

FIGURES

CTD DATA

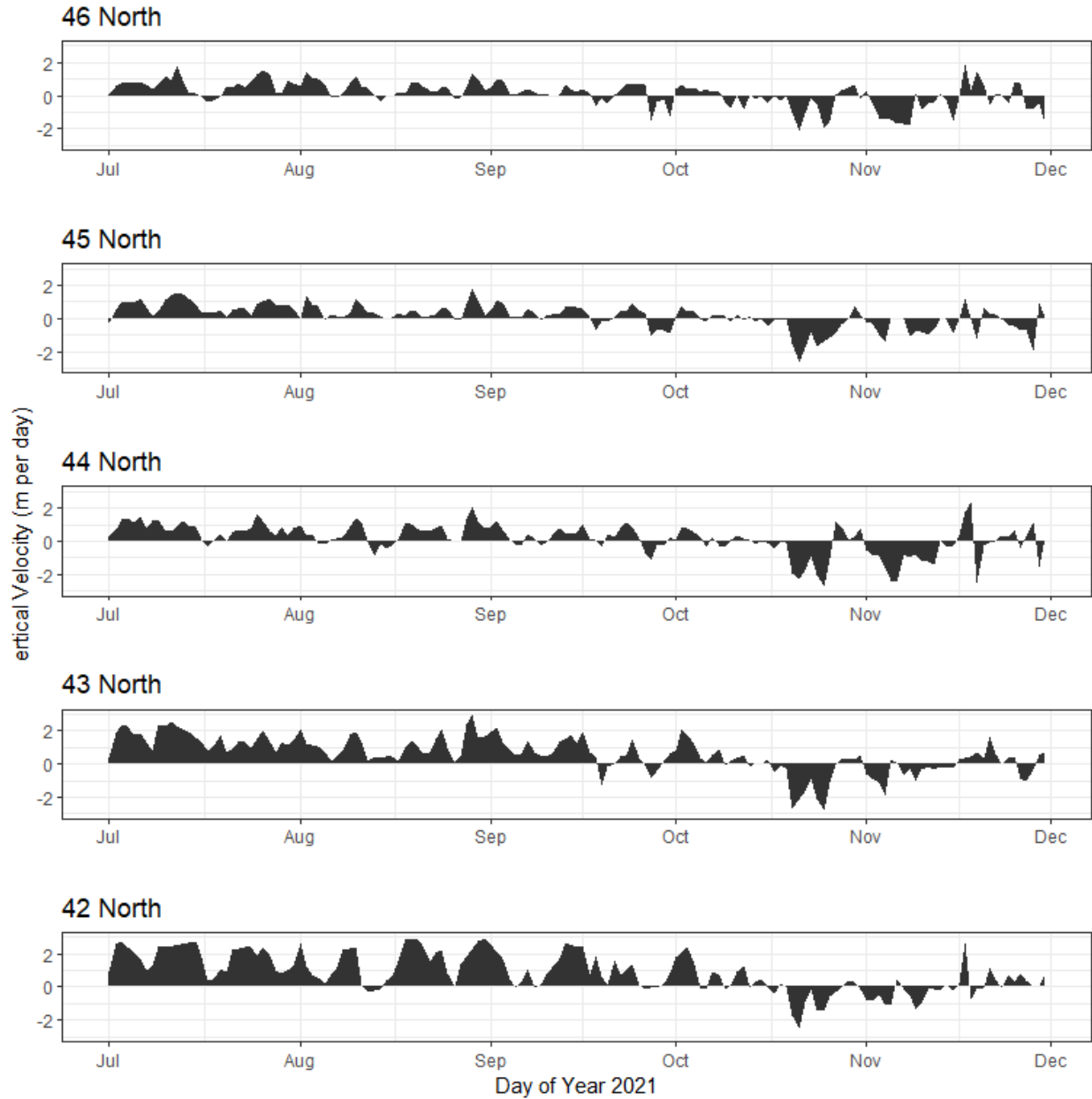


Figure 1. CUTI upwelling index conditions from July 1 to November 30 of 2021 for all latitudes surveyed. Positive values denote vertical movement of water upwards towards the surface of the ocean and negative values denote negative movement of the water towards the seafloor.

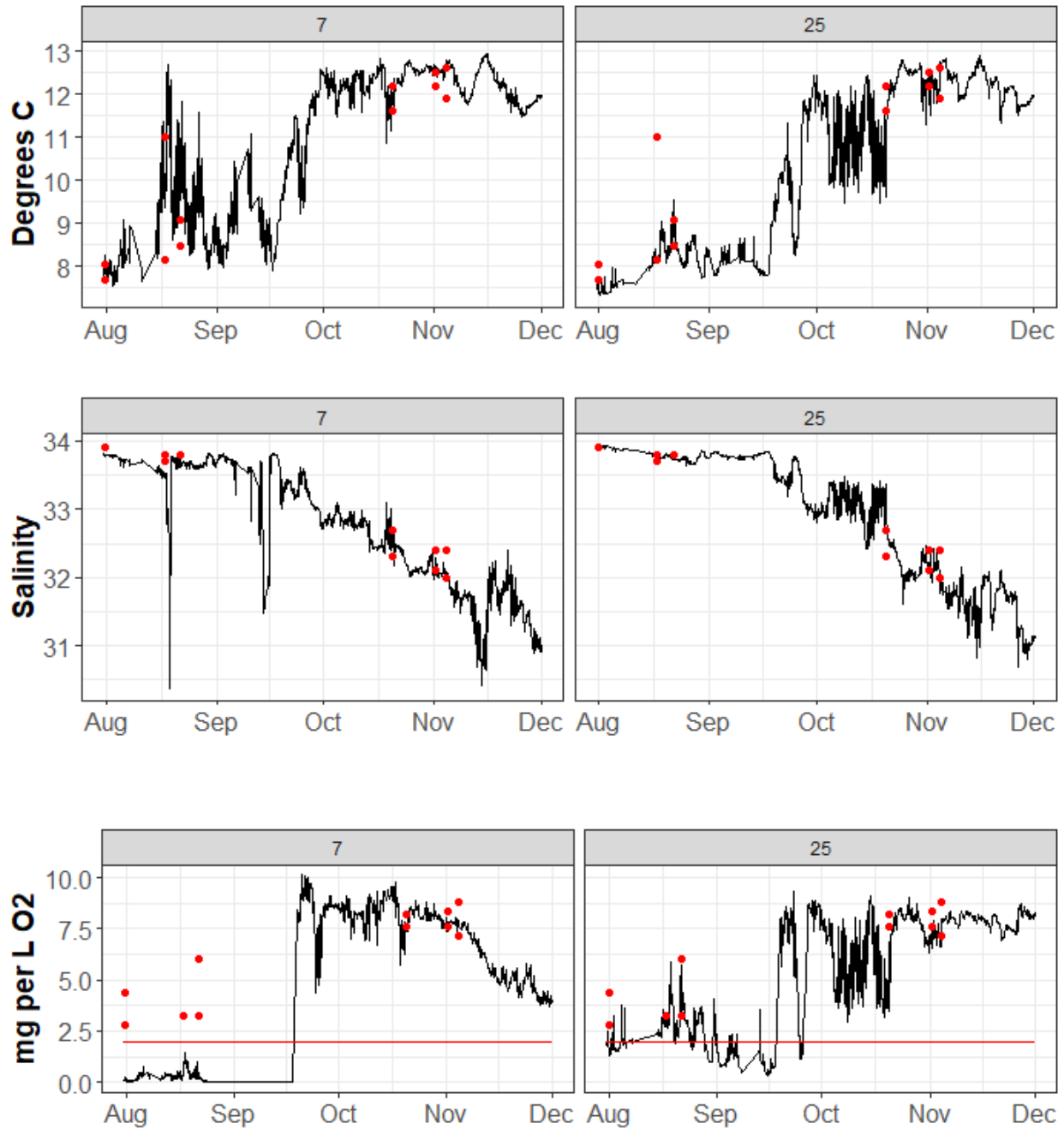


Figure 2. Time series of hydrographic observations from the Ocean Observing Initiative's nearshore mooring at 7 and 25 m waters depth (black line) with red dots denoting discrete observations collected by the survey vessel with our shipboard CTD near the mooring. The horizontal red line in the lower row of plots represents the hypoxia line. Values below that line are considered hypoxic.

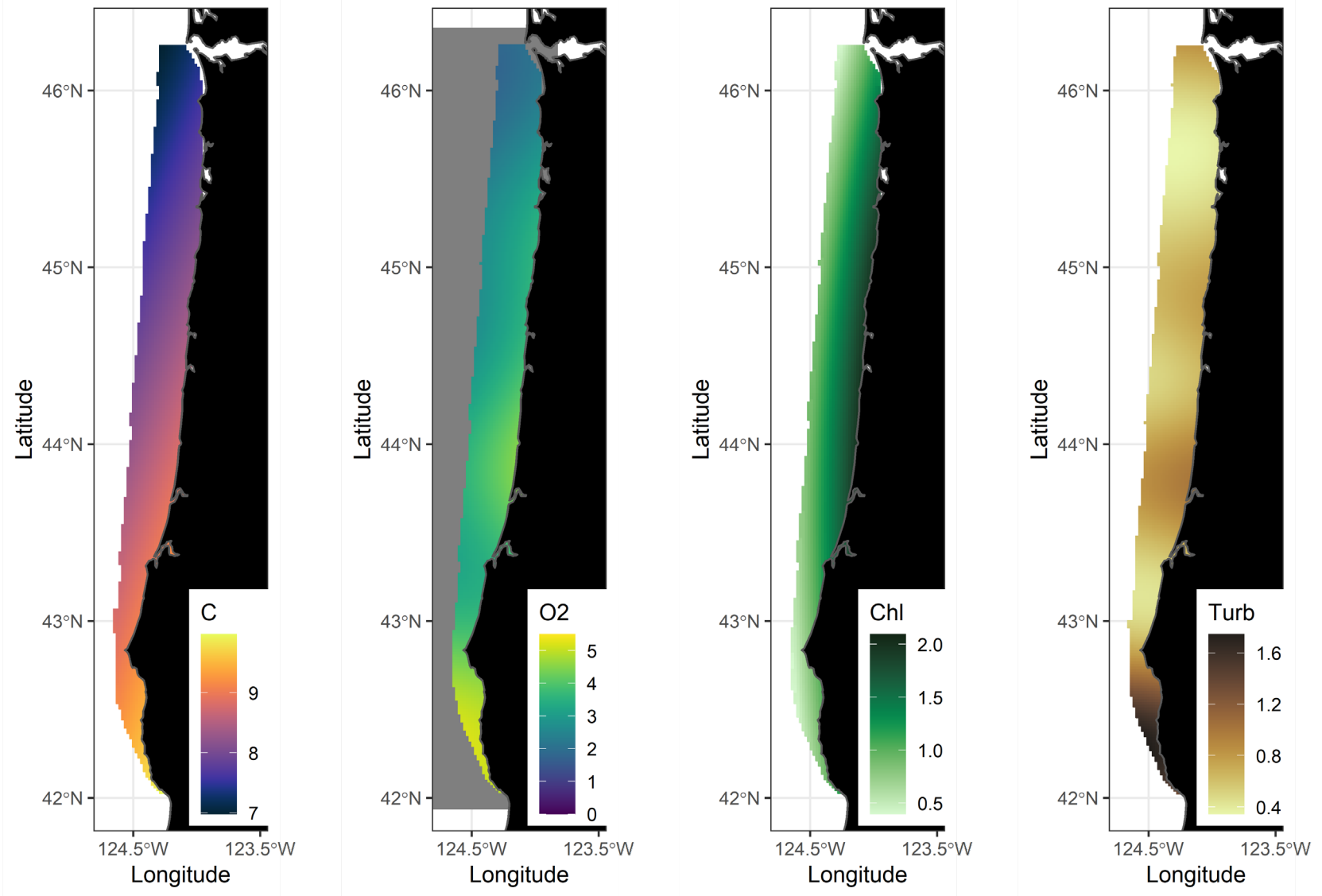


Figure 3. Statewide near bottom temperature, oxygen, chlorophyll, and turbidity conditions during the survey.

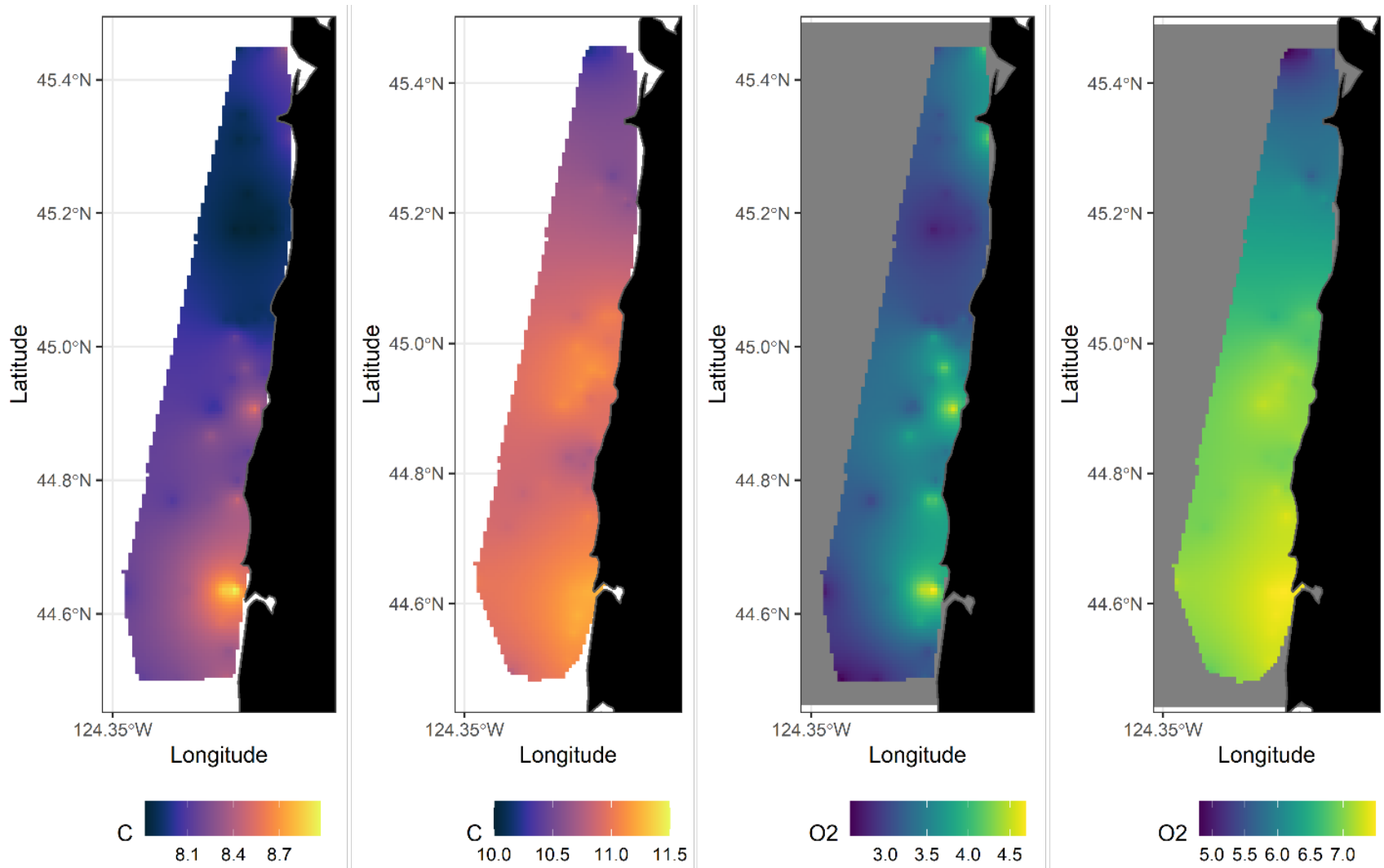


Figure 4. Near bottom temperature (purple/pink plots) and oxygen (blue/yellow plots) conditions during the first pass (left) and second pass (right)

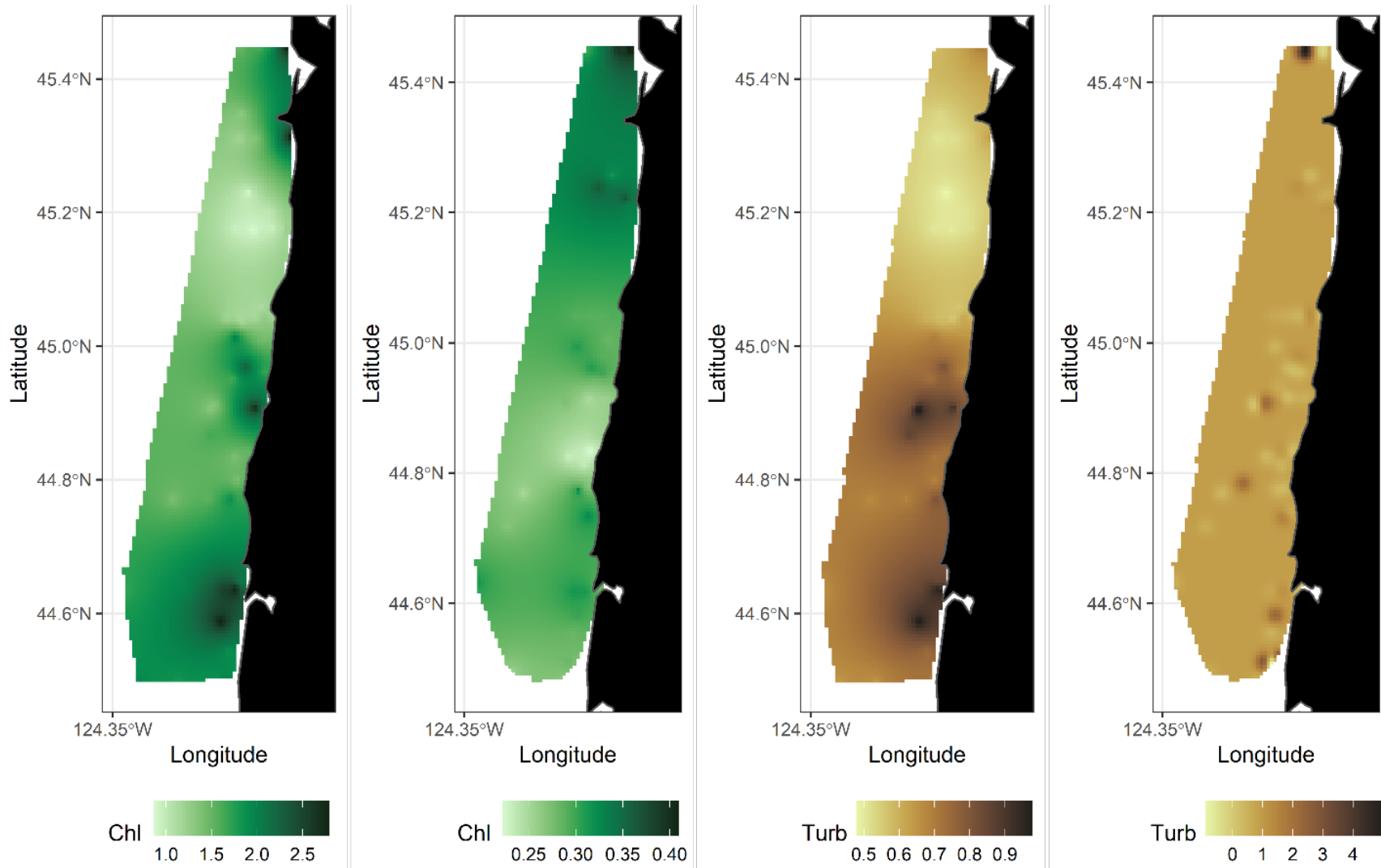
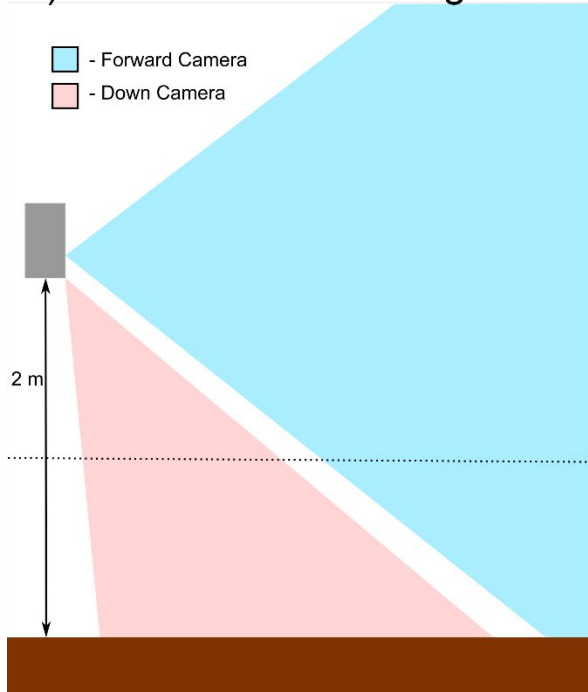


Figure 5. Near bottom chlorophyll (green plots) and turbidity (brown plots) conditions during the first pass (left) and second pass (right).

VIDEO SAMPLING

A) BASSCam View Diagram



B) BASSCam Example

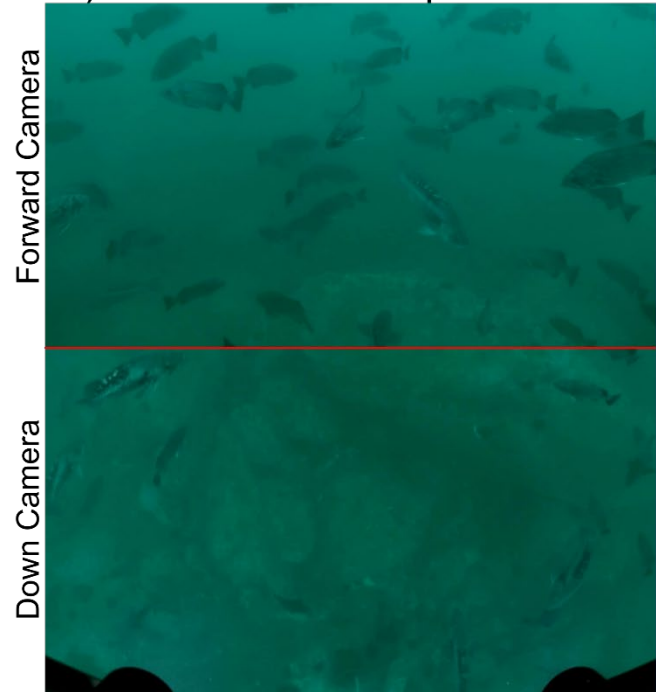


Figure 6. Diagram of viewed areas by the forward and down cameras on the BASSCam (A) and an example of a fish school being viewed by the BASSCam 1.0 (B). Note the diagram (A) is not to scale.



Figure 7. Example of applying a filter to increase ability to identify fish to species and/or take accurate length measurements

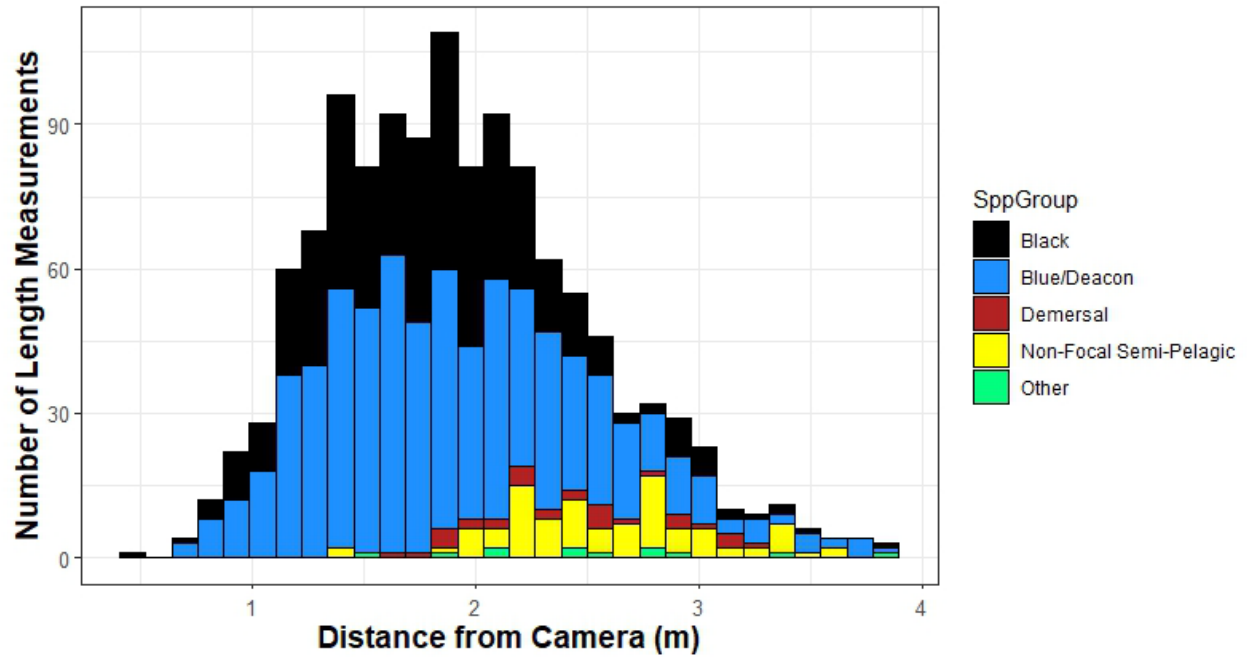


Figure 8. Relationship between distance of a fish from the camera to frequency of measurements. Video reviewer will follow fish through frames to find the frame where there is the highest chance for measurement accuracy.

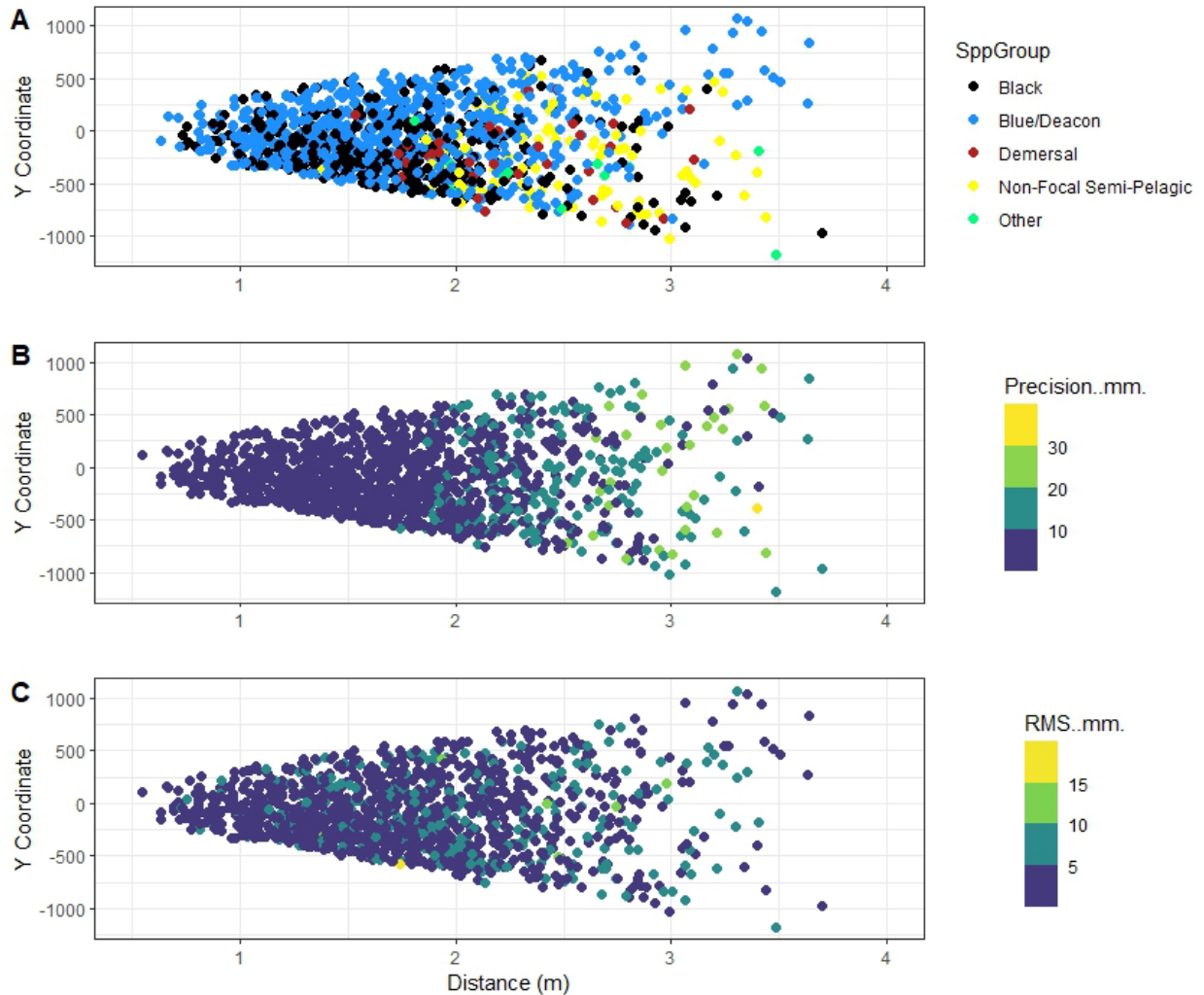


Figure 9. The location of the midpoint of the Y coordinate of the length measurements (A) for five species groups. Here length measurements were limited to < 4 meters due to water clarity. Precision of a length measurement (B) is estimated by the photogrammetry software based on the stereo camera properties, configuration, and three-dimensional orientation. RMS values reported in (C) are the worst of the two RMS values calculated for each length measurement. RMS values > 20 mm are not acceptable.

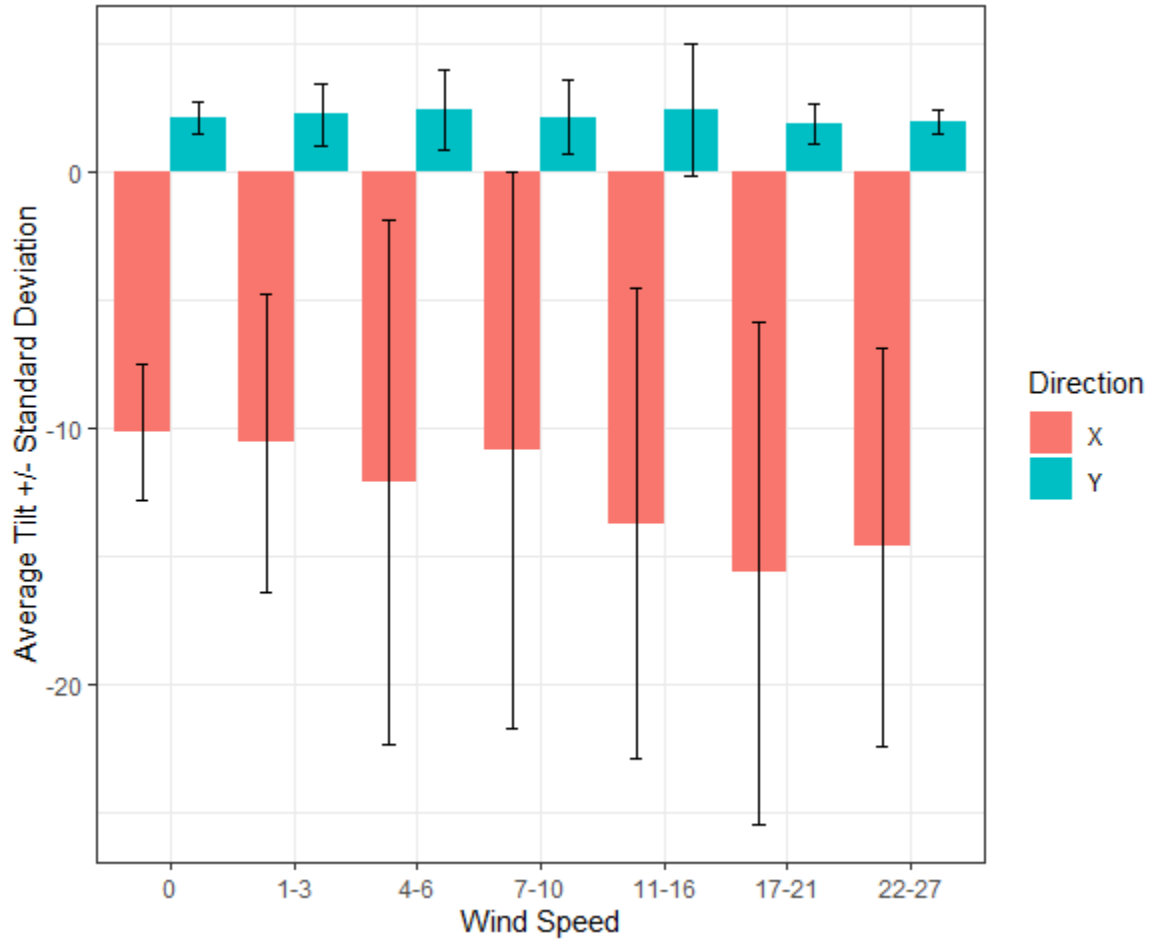


Figure 10. Orientation of BASSCam relative to wind speed. Y denotes tilting side to side and X values denote tilting either forward (negative values) or backwards (positive values).

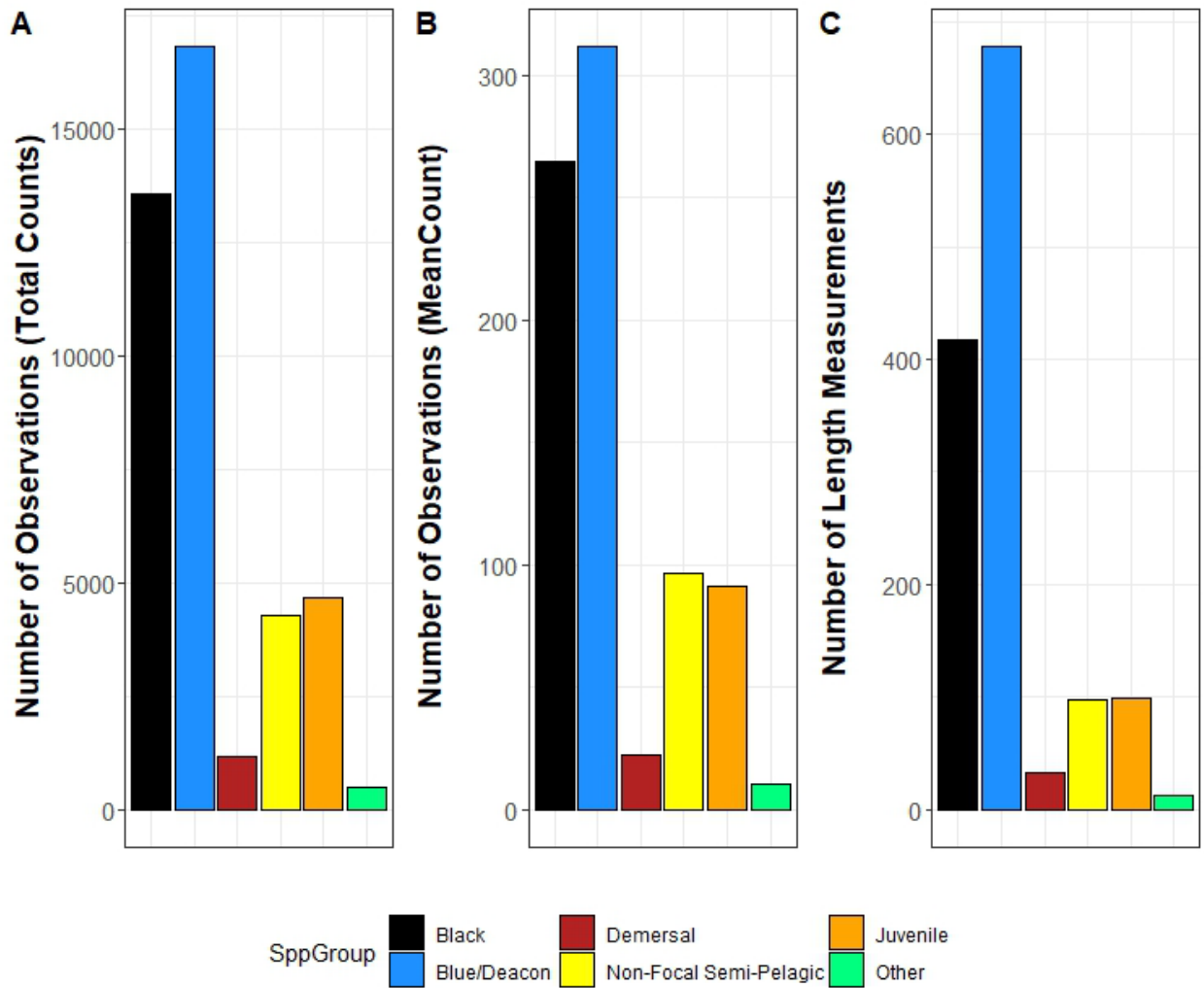


Figure 11. Total number of fish counted on video (A), sum of MeanCount (B), and number of fish measured (C) from underwater video drops conducted during the entire survey duration (entire coast and both pass 1 and pass 2). TotalCount and MeanCount include forward and downward-looking cameras.

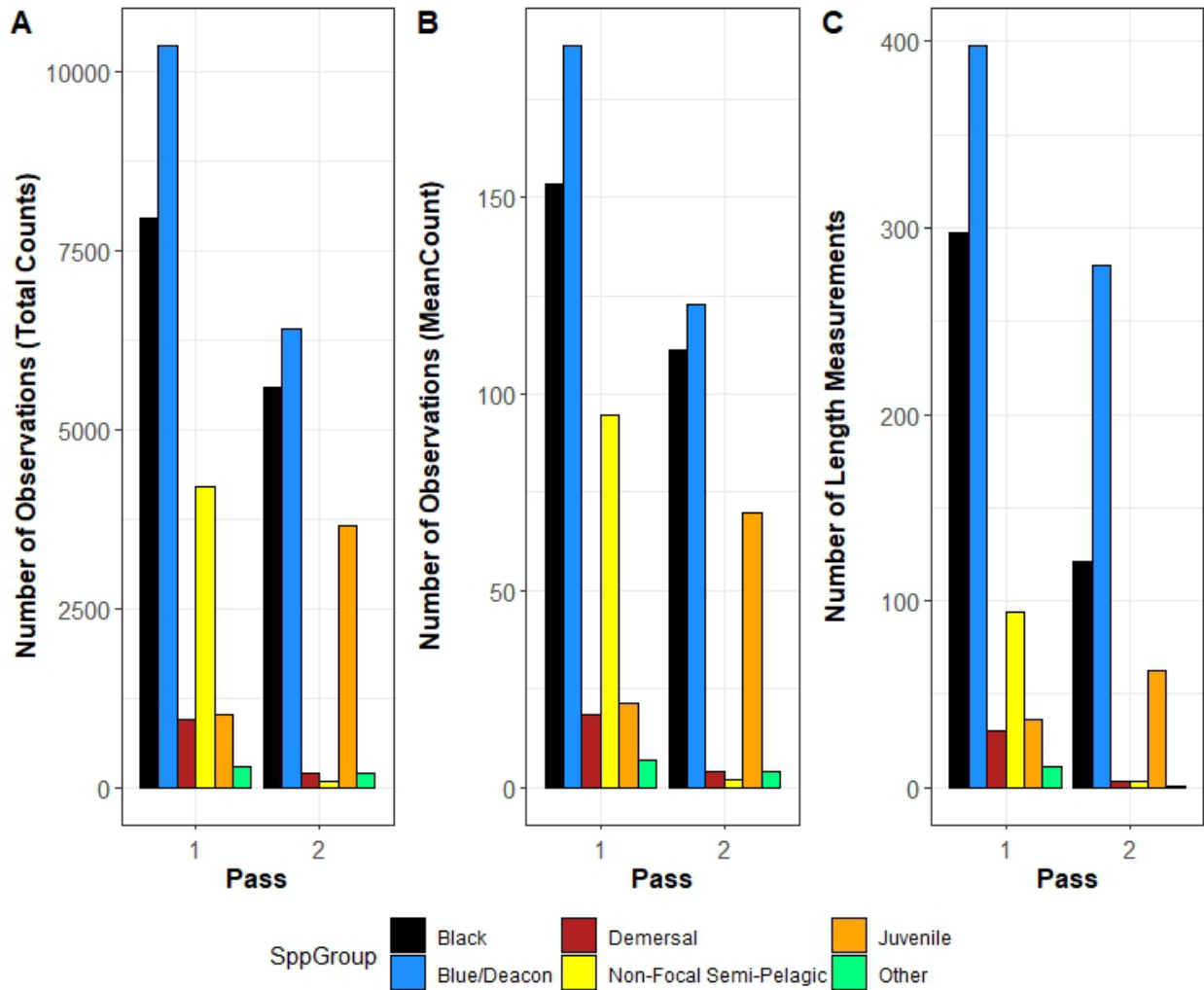


Figure 12. Total number of fish counted on video (A), sum of MeanCount (B), and number of fish measured (C) from underwater video drops conducted in all regions (pass 1) and for just the repeated portion of the north coast (pass 2). TotalCount and MeanCount include forward and downward-looking cameras.

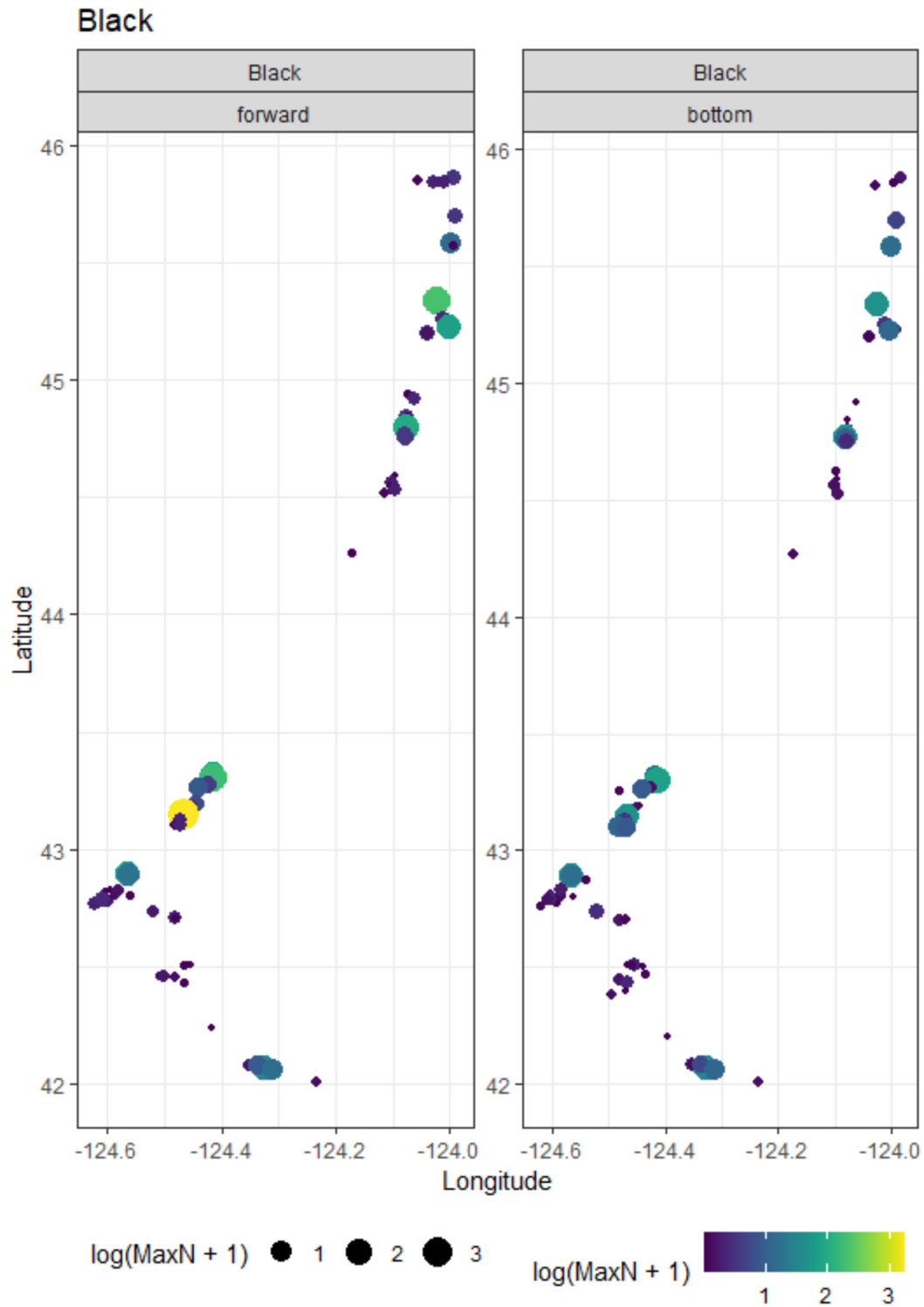


Figure 13. Video drop locations where Black Rockfish were observed on pass 1 in the forward and bottom camera and the logged count.

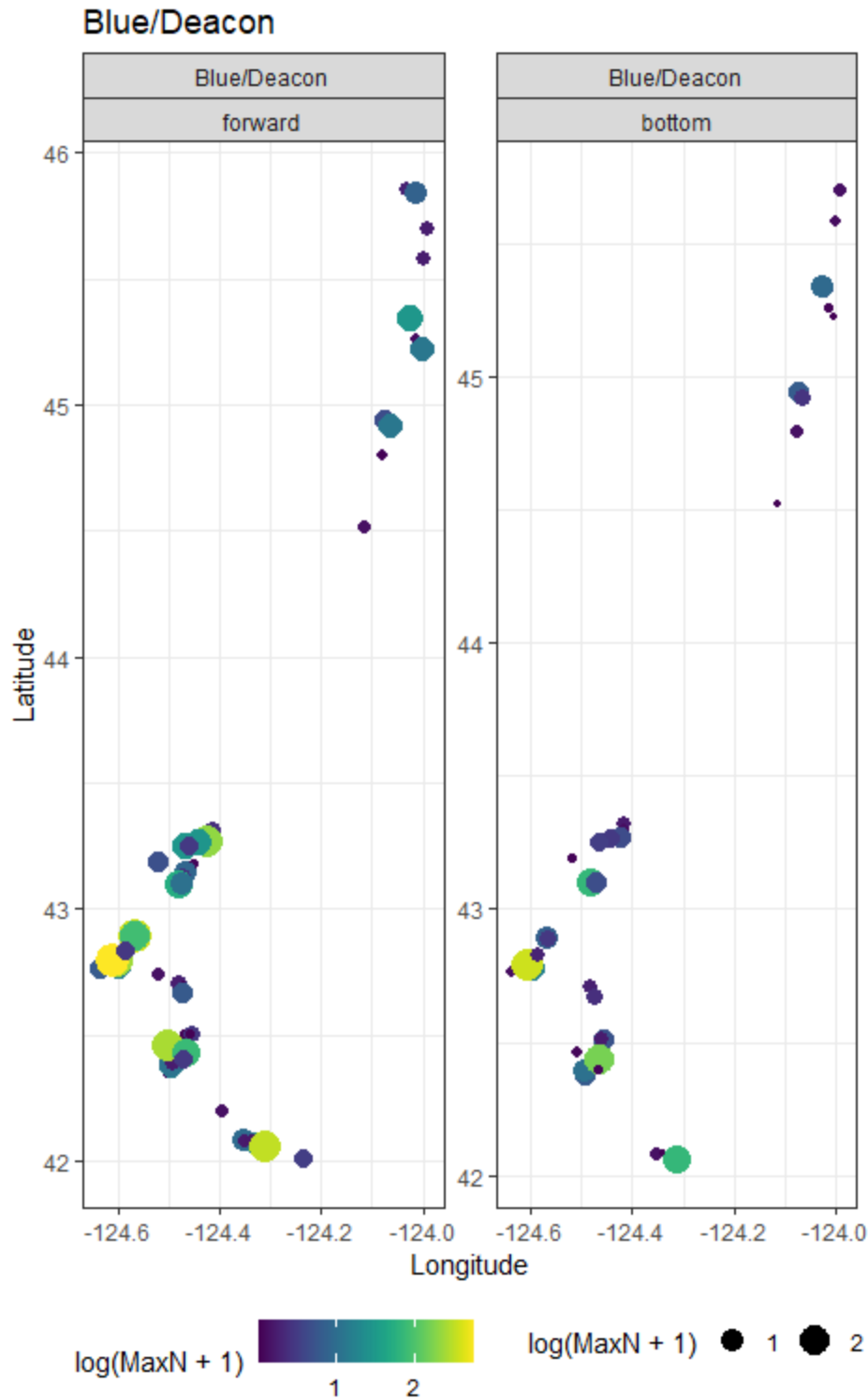


Figure 14. Video drop locations where Blue/Deacon Rockfish were observed on pass 1 in the forward and bottom camera and the logged count.

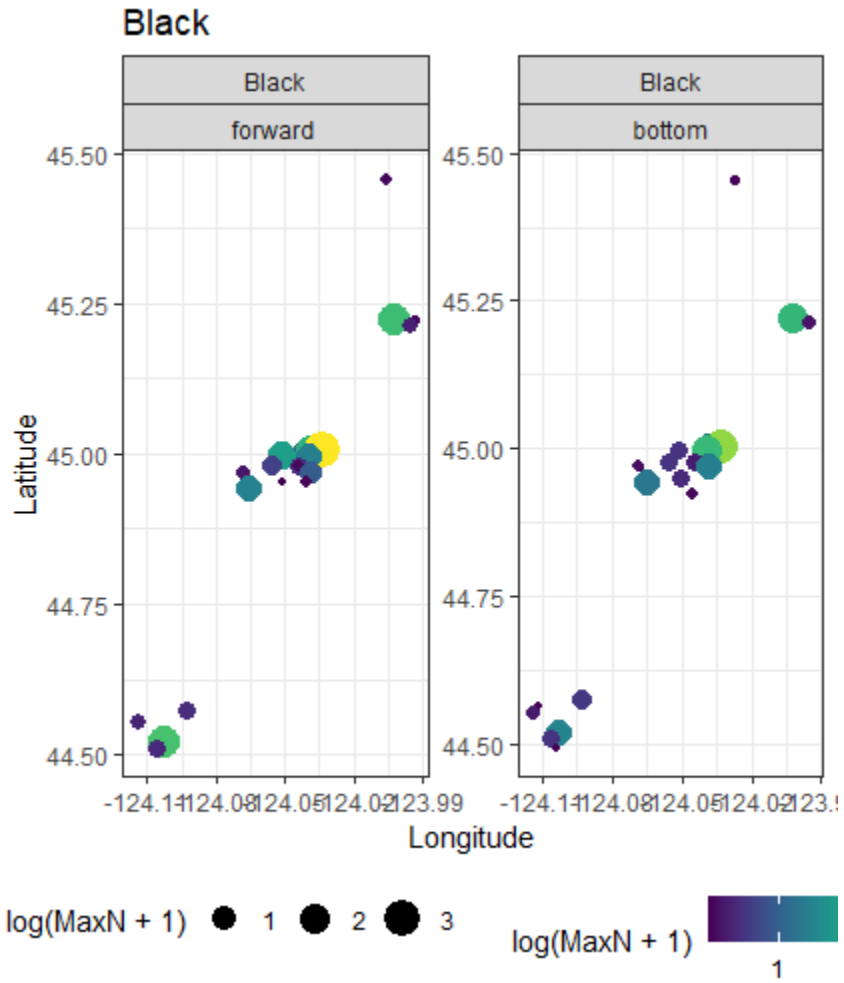


Figure 15. Video drop locations where Black Rockfish were observed on pass 2 in the forward and bottom camera and the logged count.

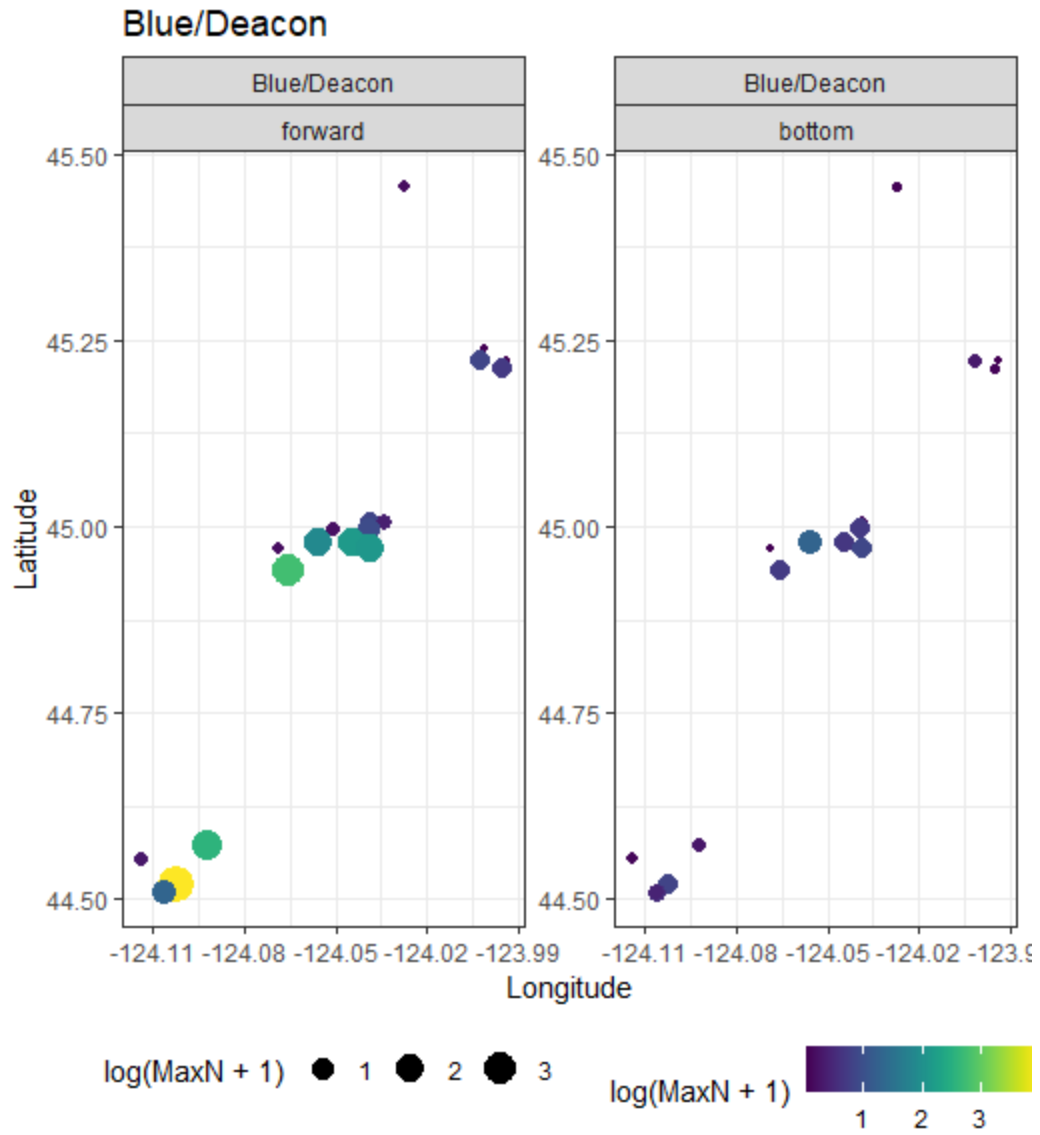


Figure 16. Video drop locations where Blue/Deacon Rockfish were observed on pass 2 in the forward and bottom camera and the logged count.

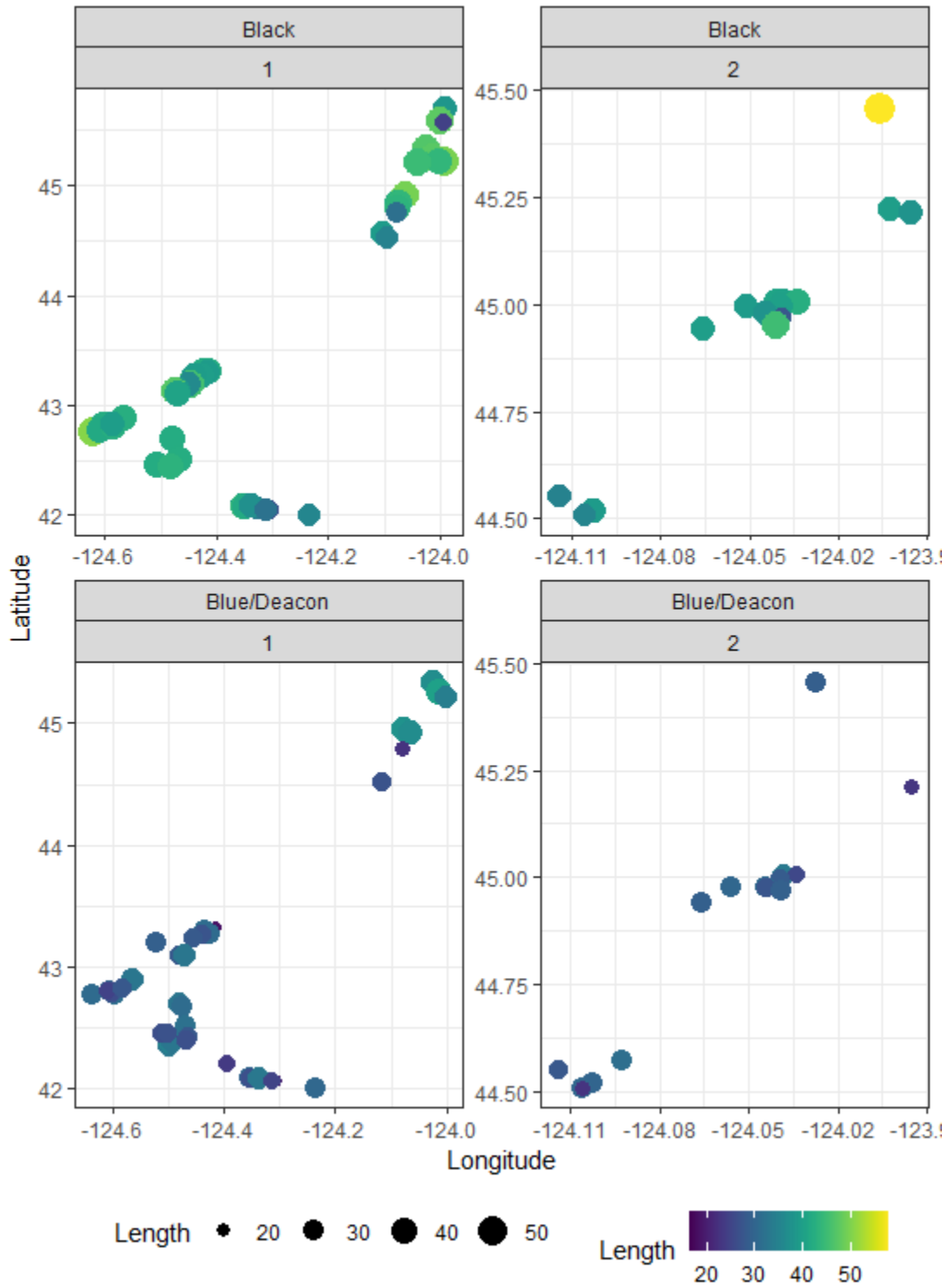


Figure 17. Video drop locations and average size of Black(top) and Blue/Deacon (bottom) for pass 1 (left and pass 2(right).

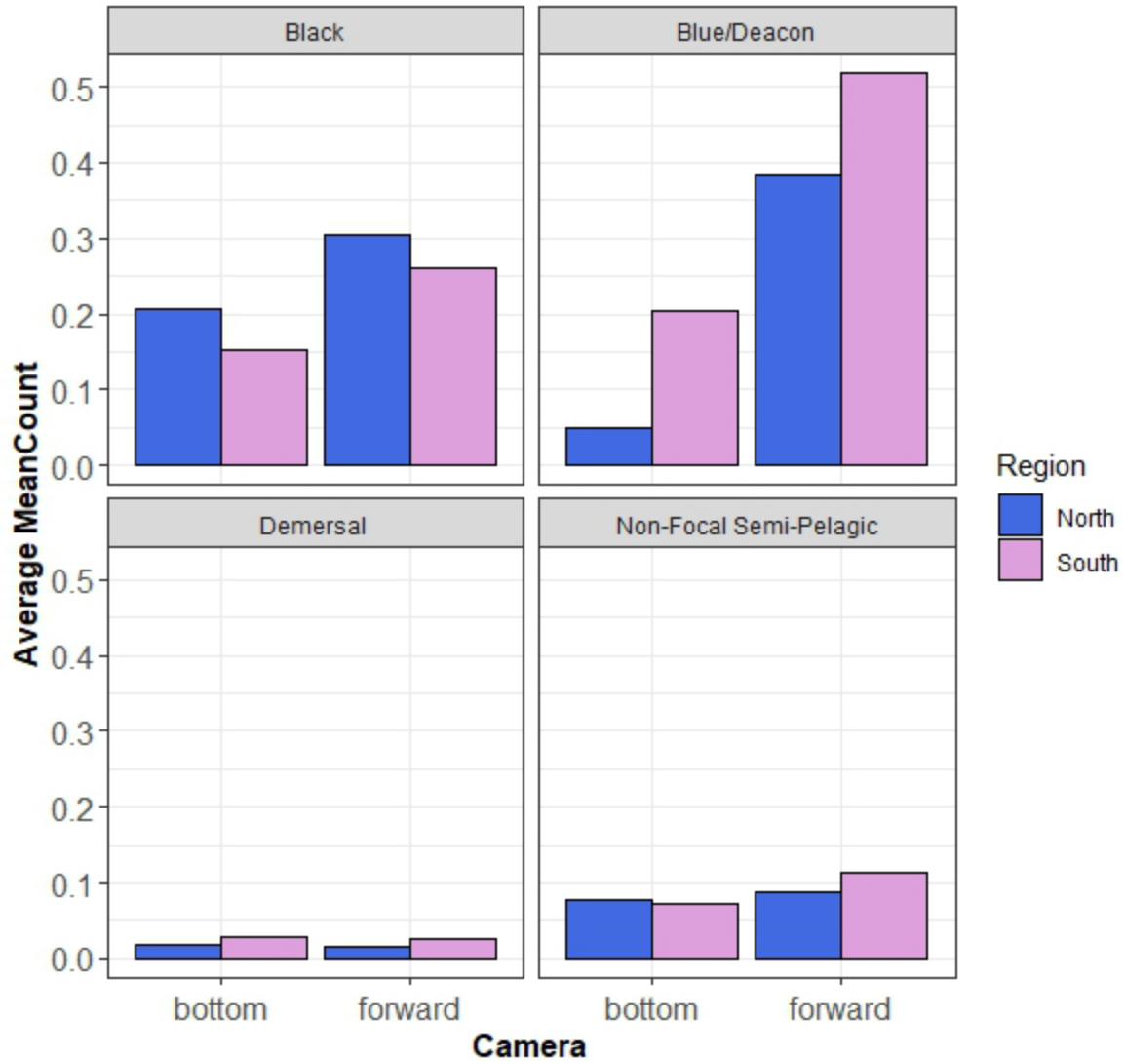


Figure 18. Average MeanCount of four main species groups. Averages were generated for each species group by summing the MeanCount from each drop. Averages are grouped into the two regions where fish were observed, and by the camera they were observed in.

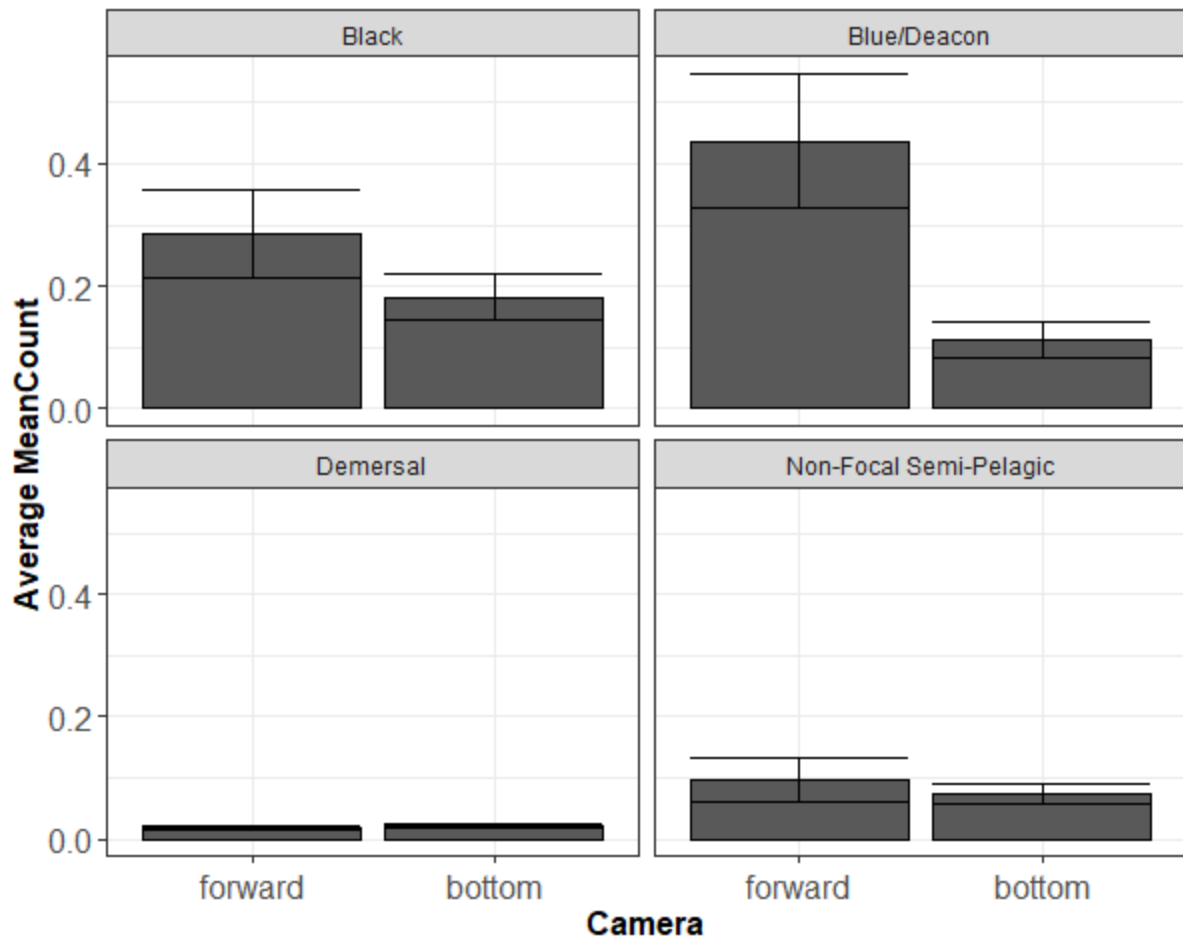


Figure 19. Average MeanCount of four main species groups summed across all video drops. Averages were generated for each species group by summing the MeanCount from each drop. Counts are grouped into the two regions where fish were observed, and by the camera they were observed in.

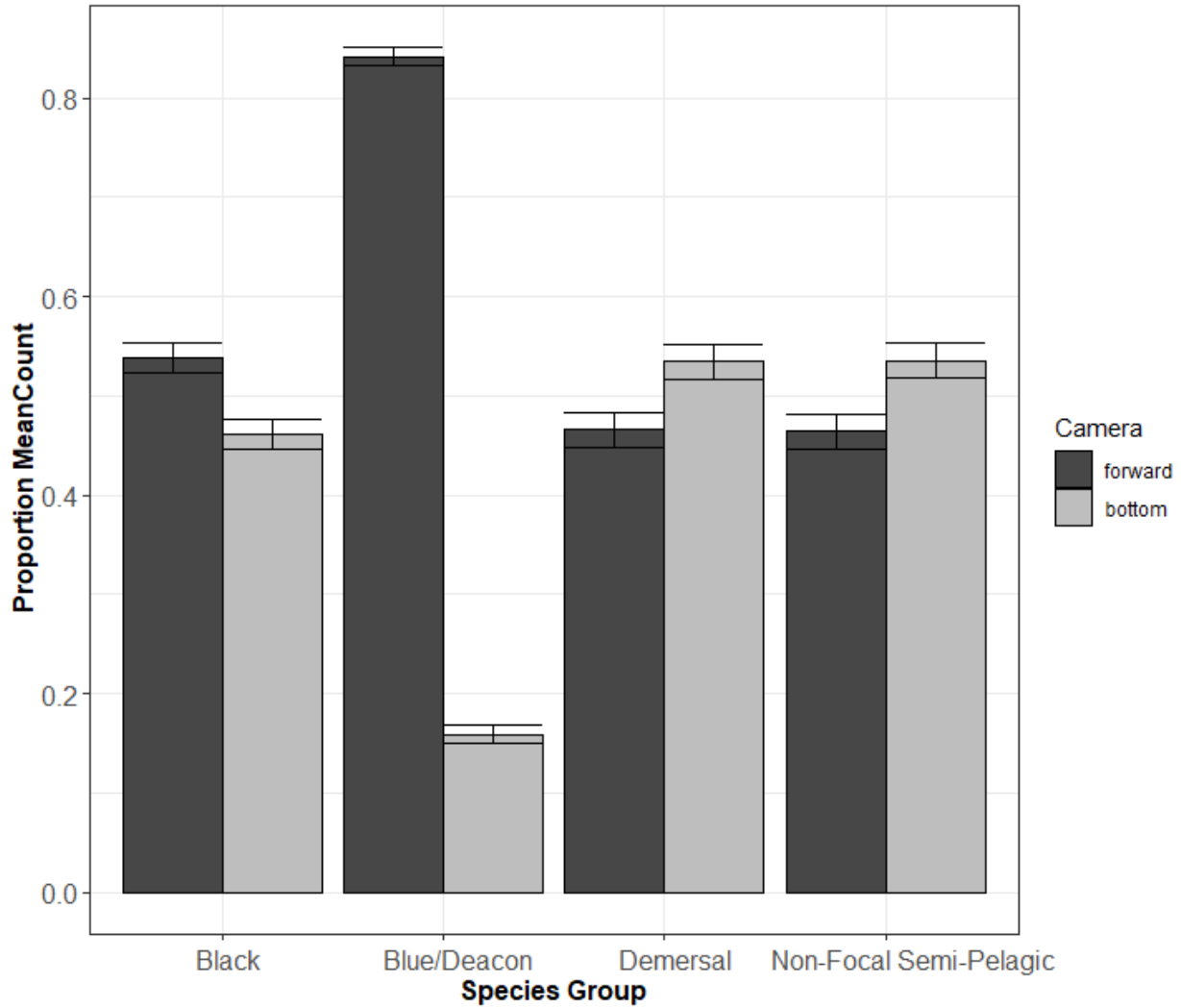


Figure 20. Average proportion (+/- SE) of each species group seen in the forward and downward facing cameras. Forward indicates fish were counted in the left forward-facing stereo camera, and bottom indicates fish were counted in the downward-facing camera. MeanCount of the bottom was corrected for the difference in the field-of-view between the forward and downward-looking cameras as well as for the percentage of the counts within the near bottom exclusion zone (Rasmuson et al. 2022).

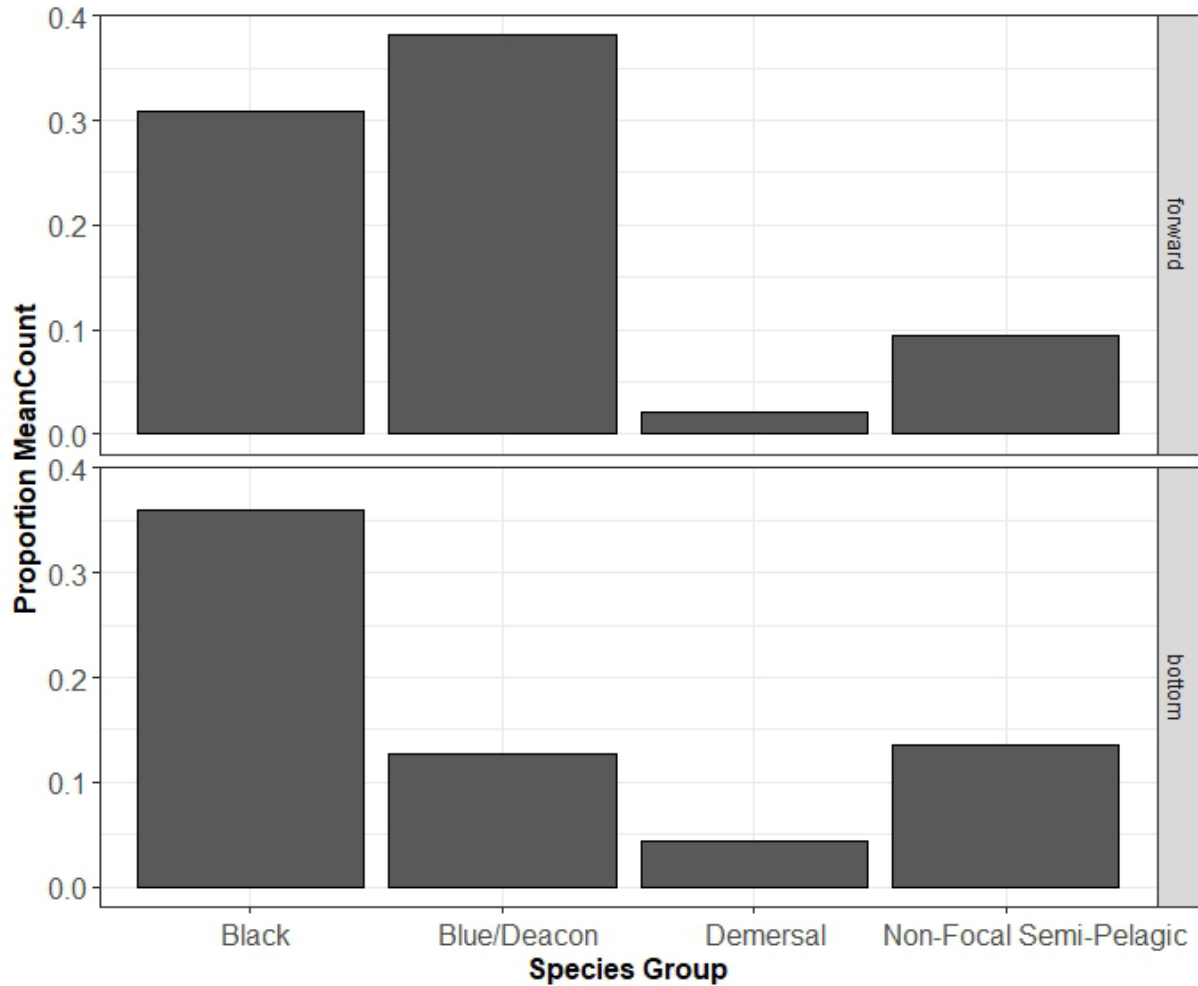


Figure 21. Average proportion each species group to the sum of MeanCount for all four species groups. Forward indicates fish were counted in the left forward-facing stereo camera, and bottom indicates fish were counted in the downward-facing camera. MeanCount of the bottom was corrected for the difference in the field-of-view between the forward and downward-looking cameras as well as for the percentage of the counts within the near bottom exclusion zone (Rasmuson et al. 2022).

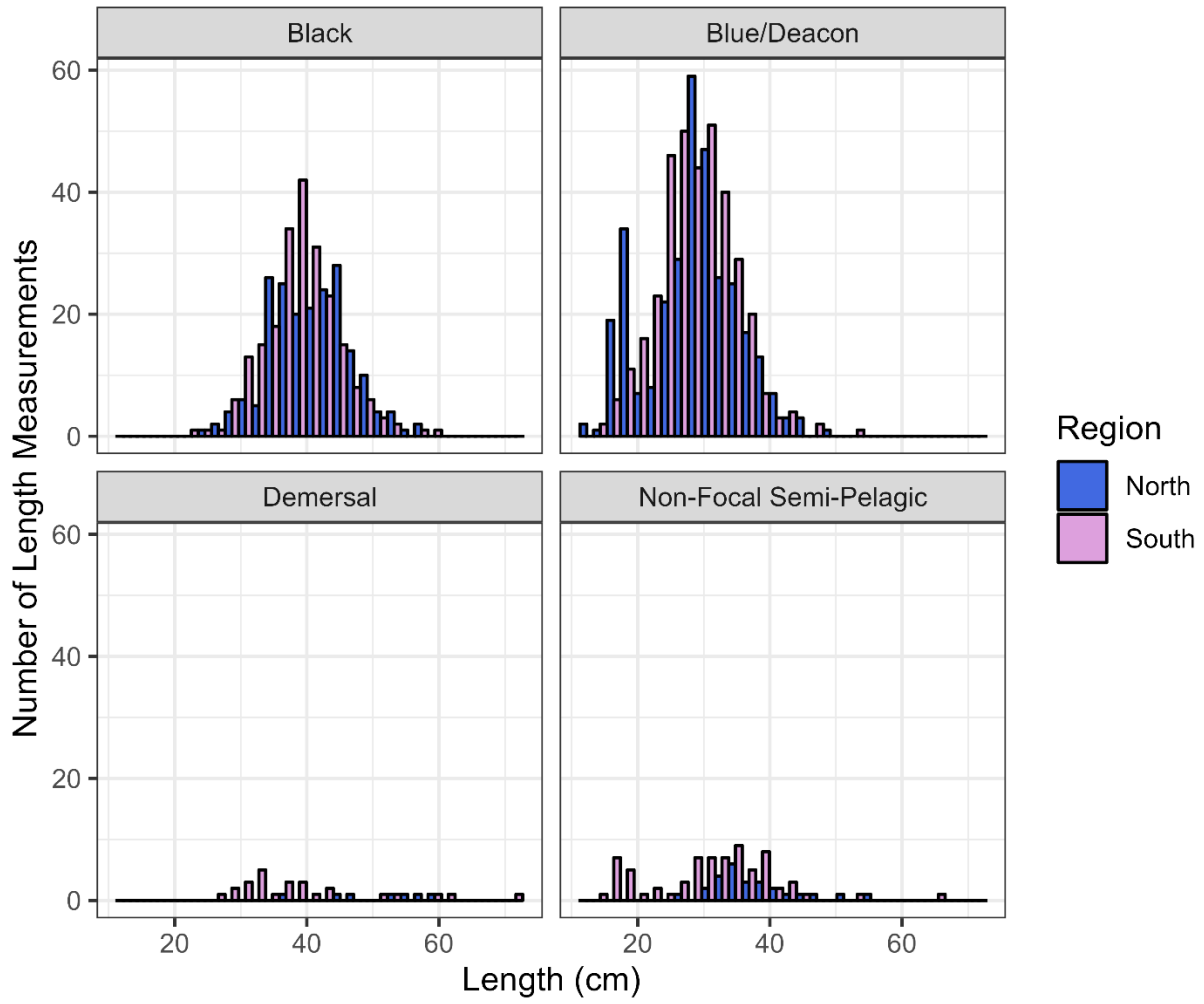


Figure 22. Length distribution of fish measured in both regions fish were present.

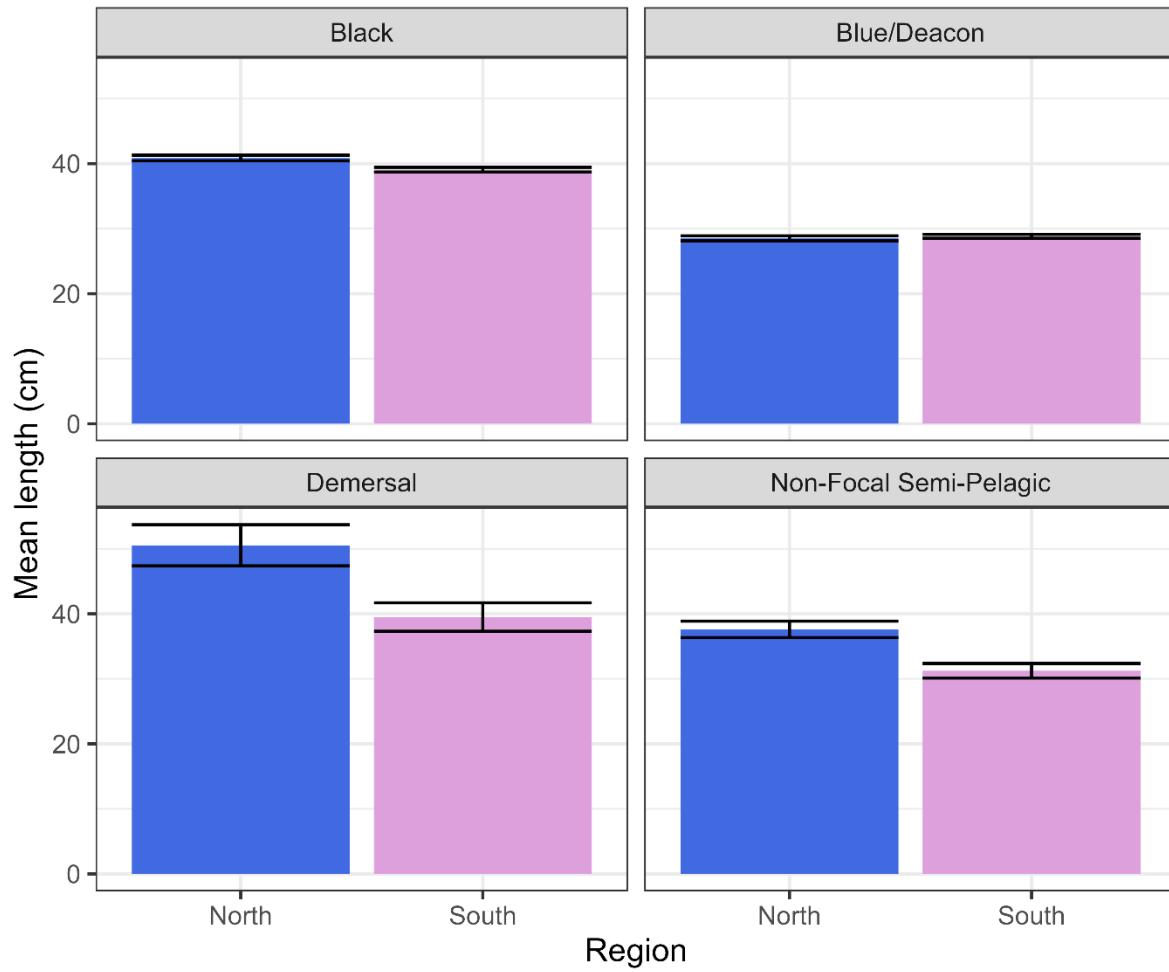


Figure 23. Average length (+/- SE) for four main species groups for each region fish were observed on video.

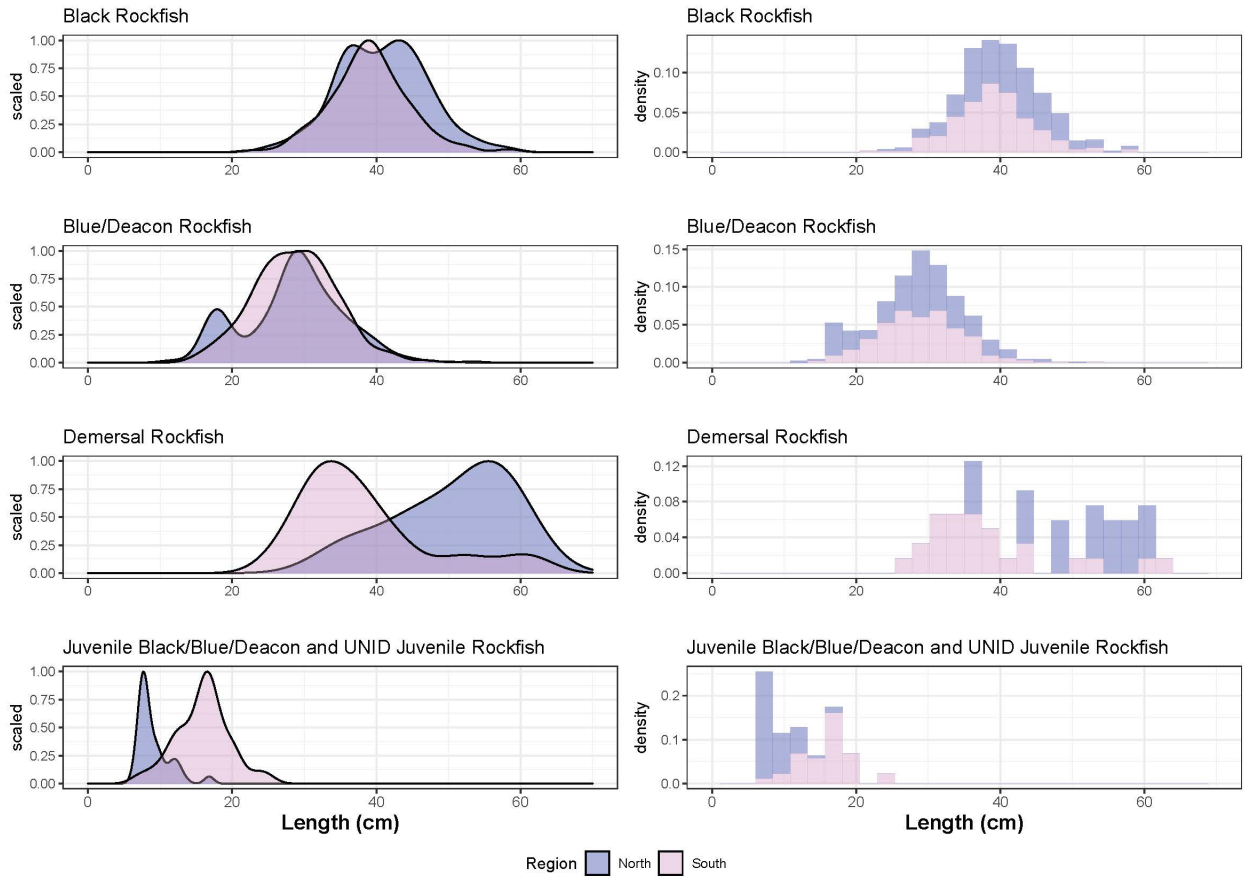


Figure 24. Length scaled density distributions for both regions (left) and density histogram (right) for video length data in both regions fish were observed.

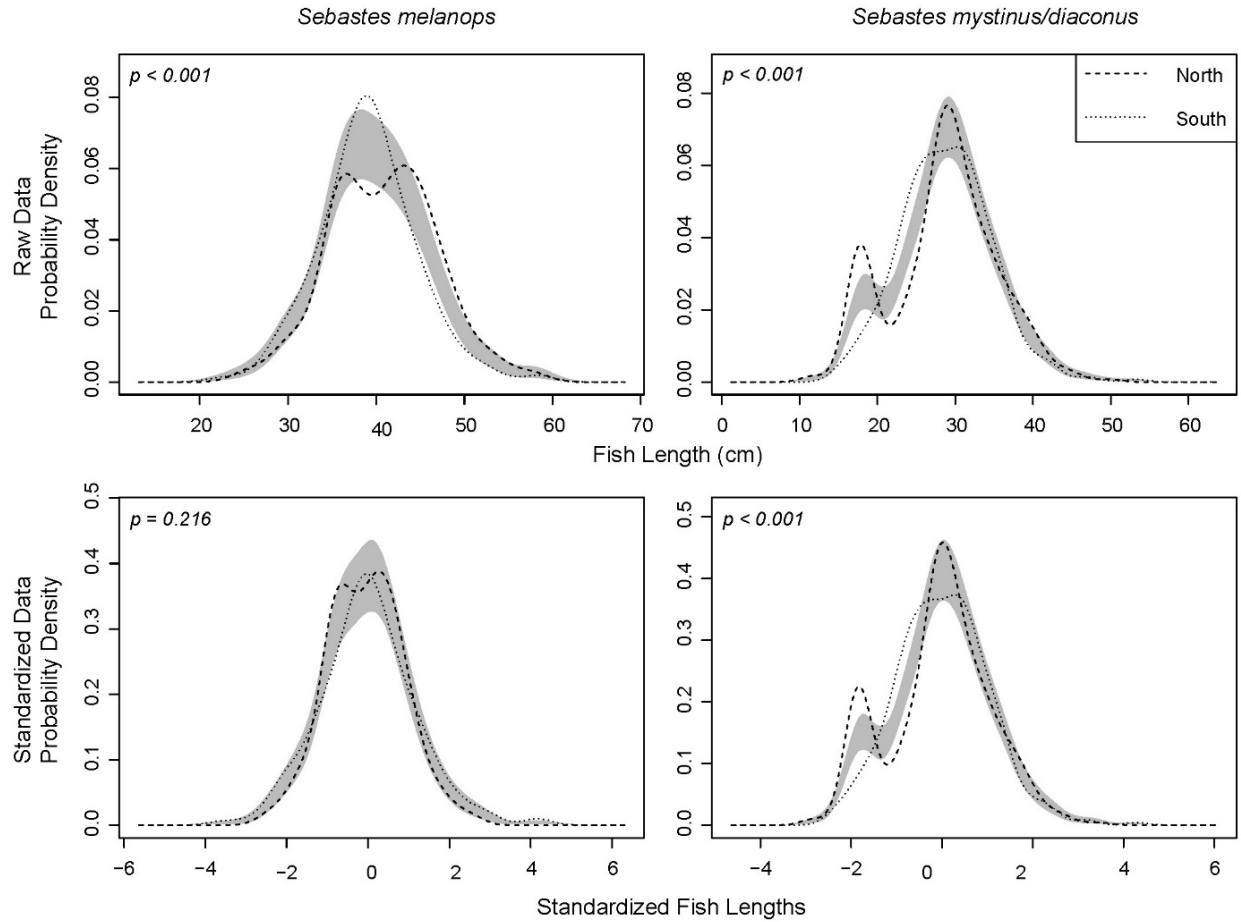


Figure 25. Kernel density estimate (KDE) probability density functions used to compare length-frequency data between the North and South regions for Black and Blue/Deacon Rockfish. The grey area extends one standard error above and below the null model (no difference in KDEs for each dataset), signaling significant differences in length-frequency distributions when the dotted or dashed lines fall outside of this area. Permutation tests of the area between the two probability density functions provided significance values (p). Length-frequency data was standardized (bottom row) to analyze the shape of the distribution in comparison to the location and shape distribution (top row). All KDE probability density function analysis methods were adapted from Langlois et al. (2012).

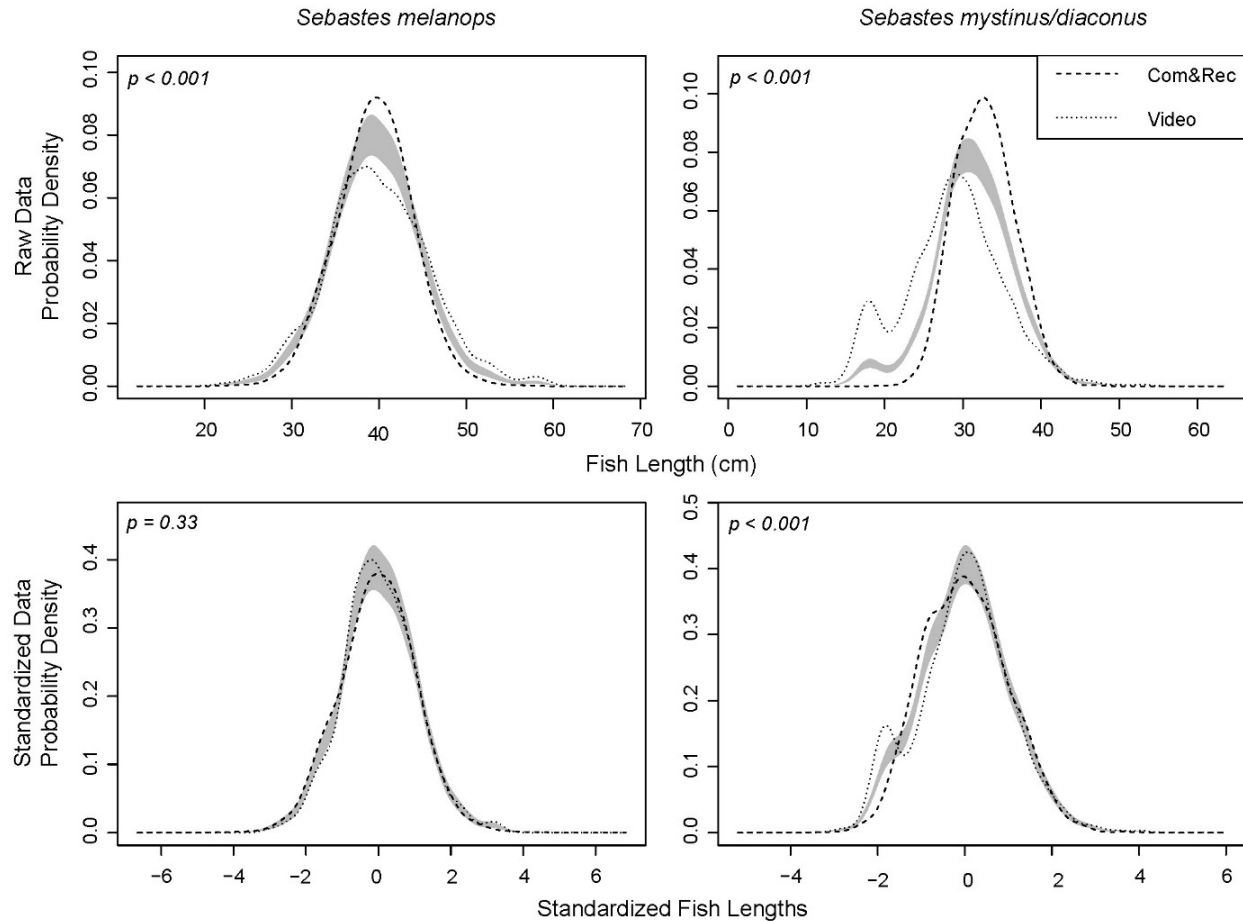


Figure 26. Kernel density estimate (KDE) probability density functions used to compare length-frequency data between the 2021 commercial and recreational fishing fleet data (Com&Rec) and our stereo video (Video) data for Black and Blue/Deacon Rockfish. The grey area extends one standard error above and below the null model (no difference in KDEs for each dataset), signaling significant differences in the length-frequency distributions when the dotted or dashed lines fall outside of this area. Permutation tests of the area between the two probability density functions provided significance values (p). Length-frequency data was standardized (bottom row) to analyze the shape of the distribution in comparison to the location and shape distribution (top row). All KDE probability density function analysis methods were adapted from Langlois et al. 2012.

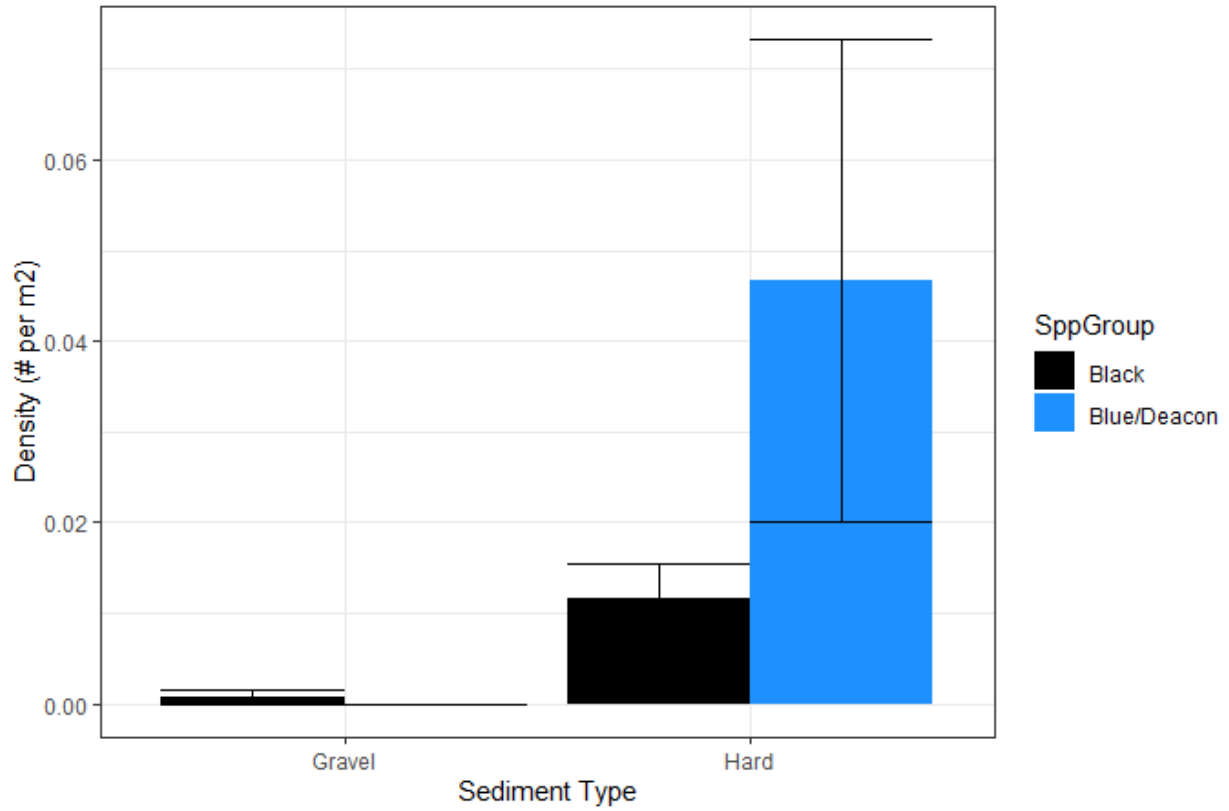


Figure 27. Average background density of Black and Blue/Deacon Rockfish observed in the downward-facing camera from drops greater than 50 m from acoustically observed fish schools.

HOOK AND LINE SAMPLING

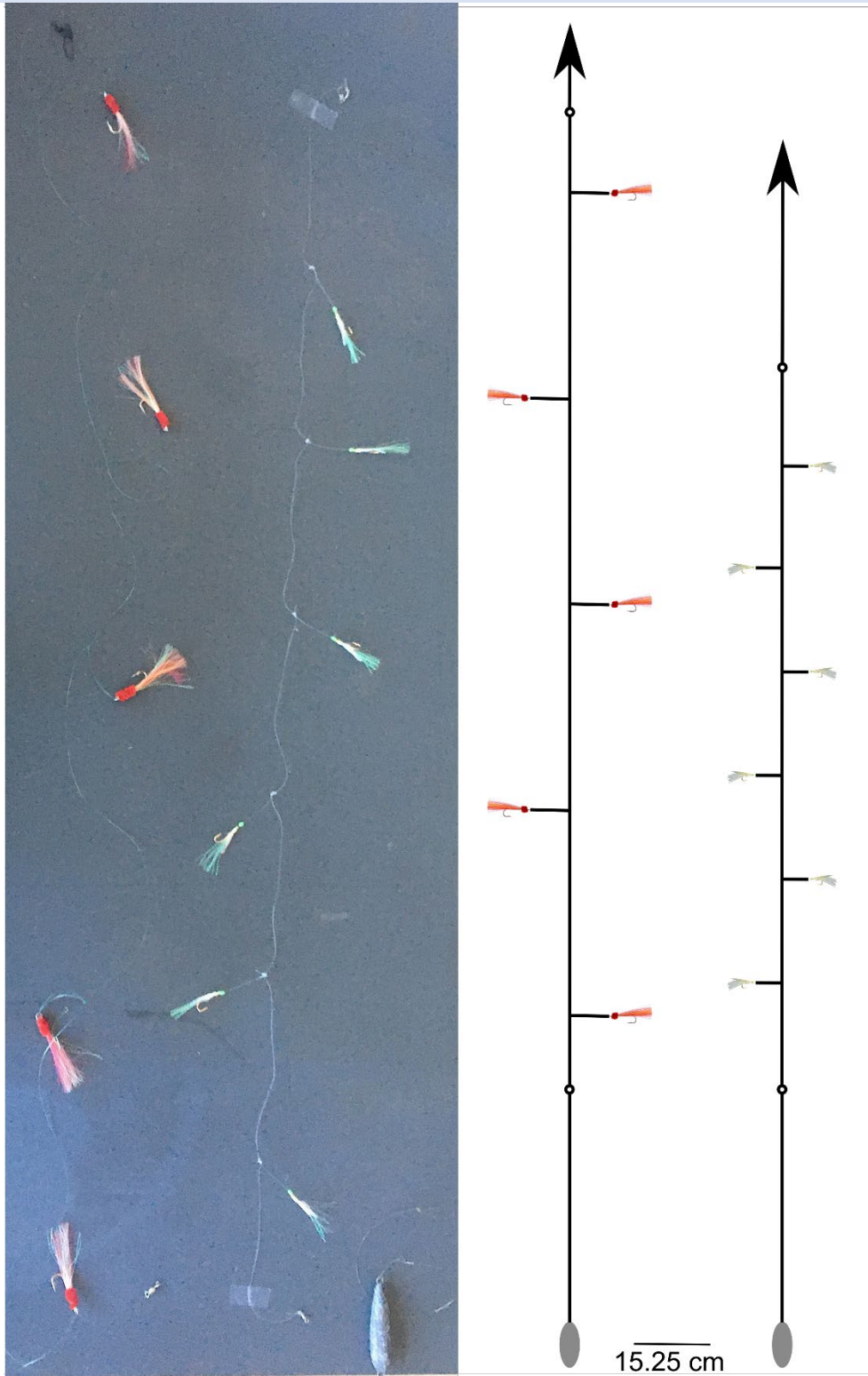


Figure 28. Photograph of hook and line sampling gear used for sampling (left) and schematics of hook locations on gangions (right).

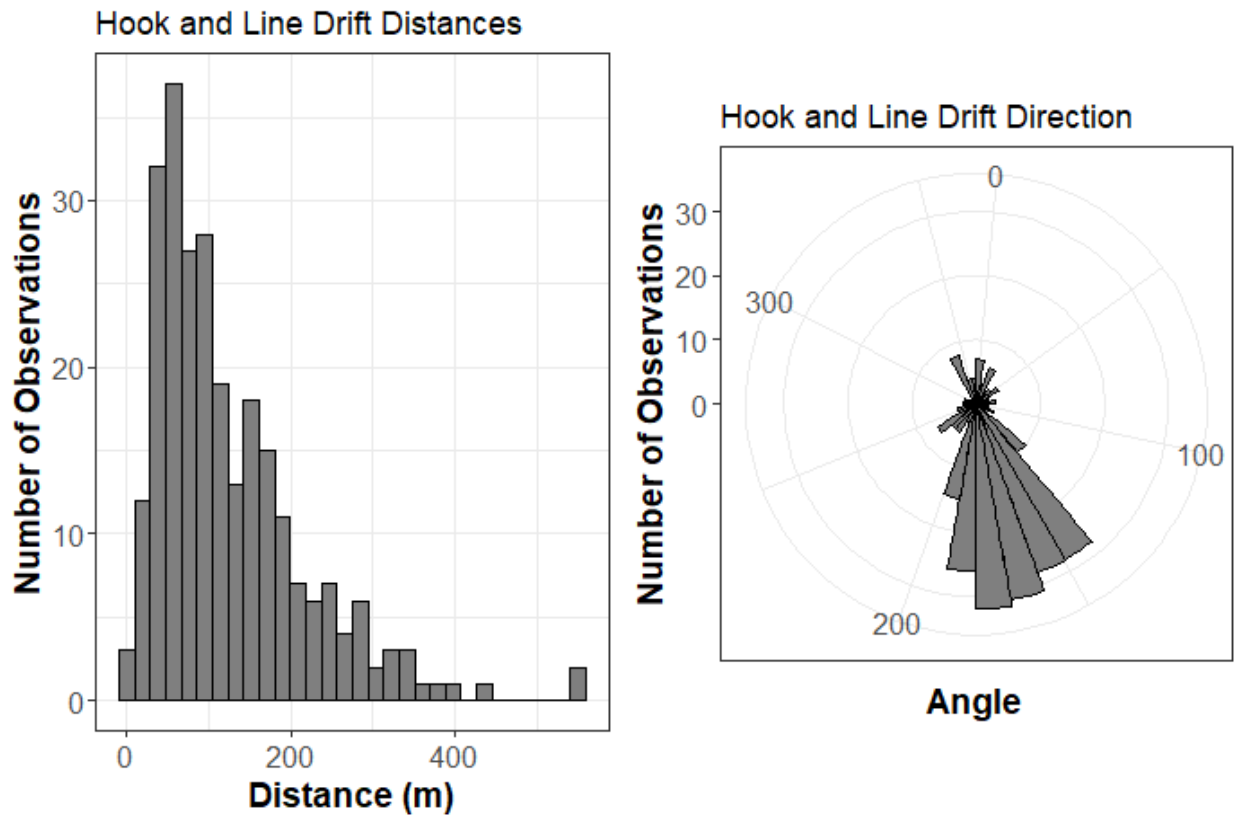


Figure 29. Distribution of drift distances for each fishing drift and the distribution of drift angles. 0 denotes northward advection and 180 southwards.

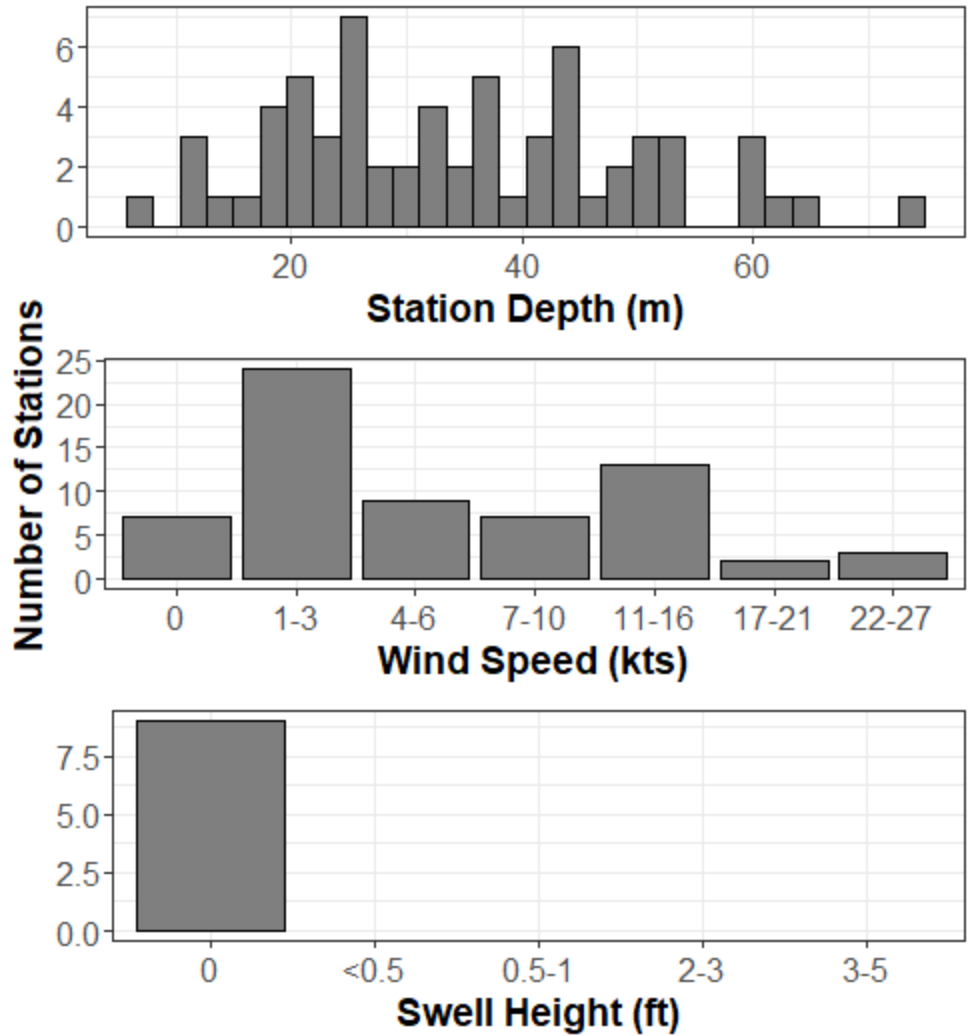


Figure 30. Distribution of station depths, wind speed and swell heights for each fishing station.

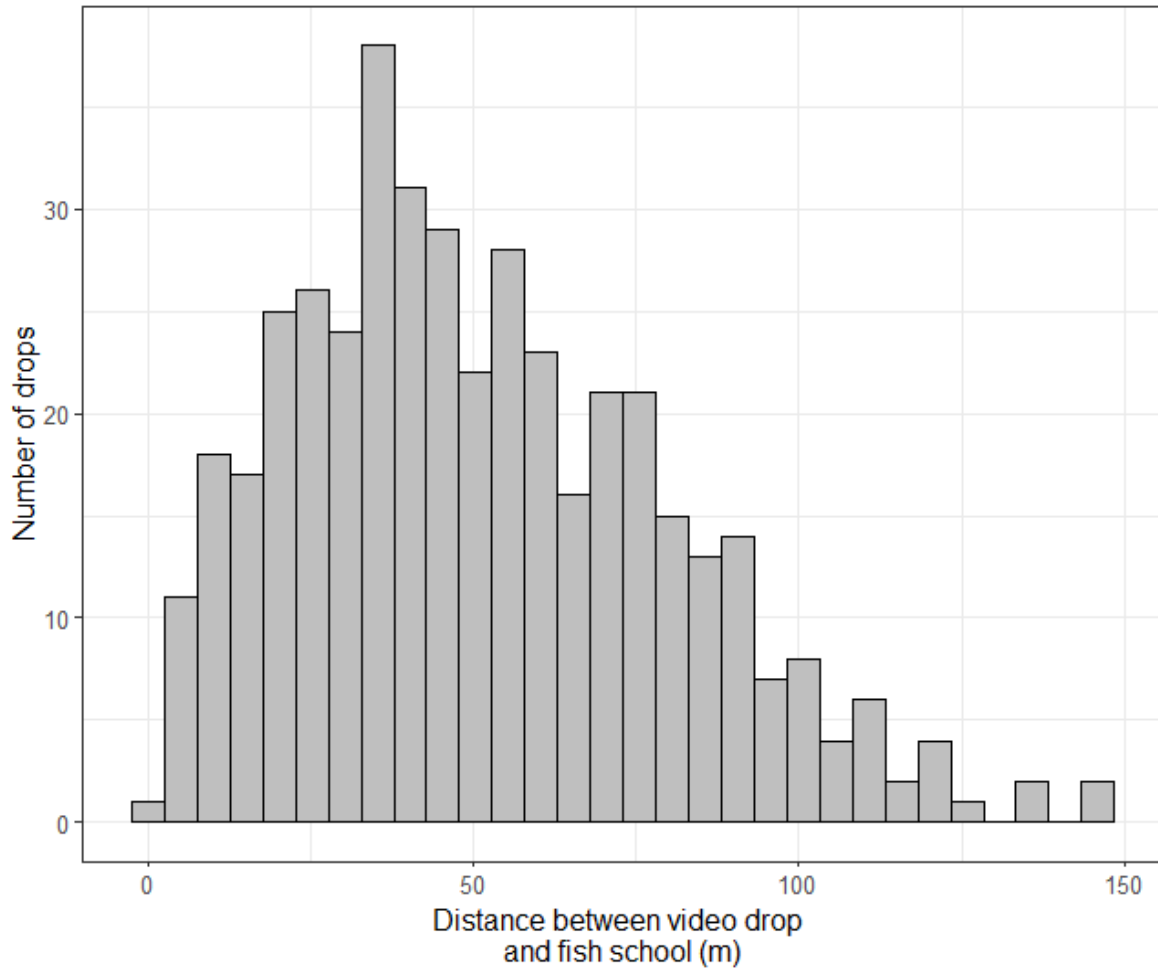


Figure 31. Histogram of distances from video drops to the schools identified on the acoustics.

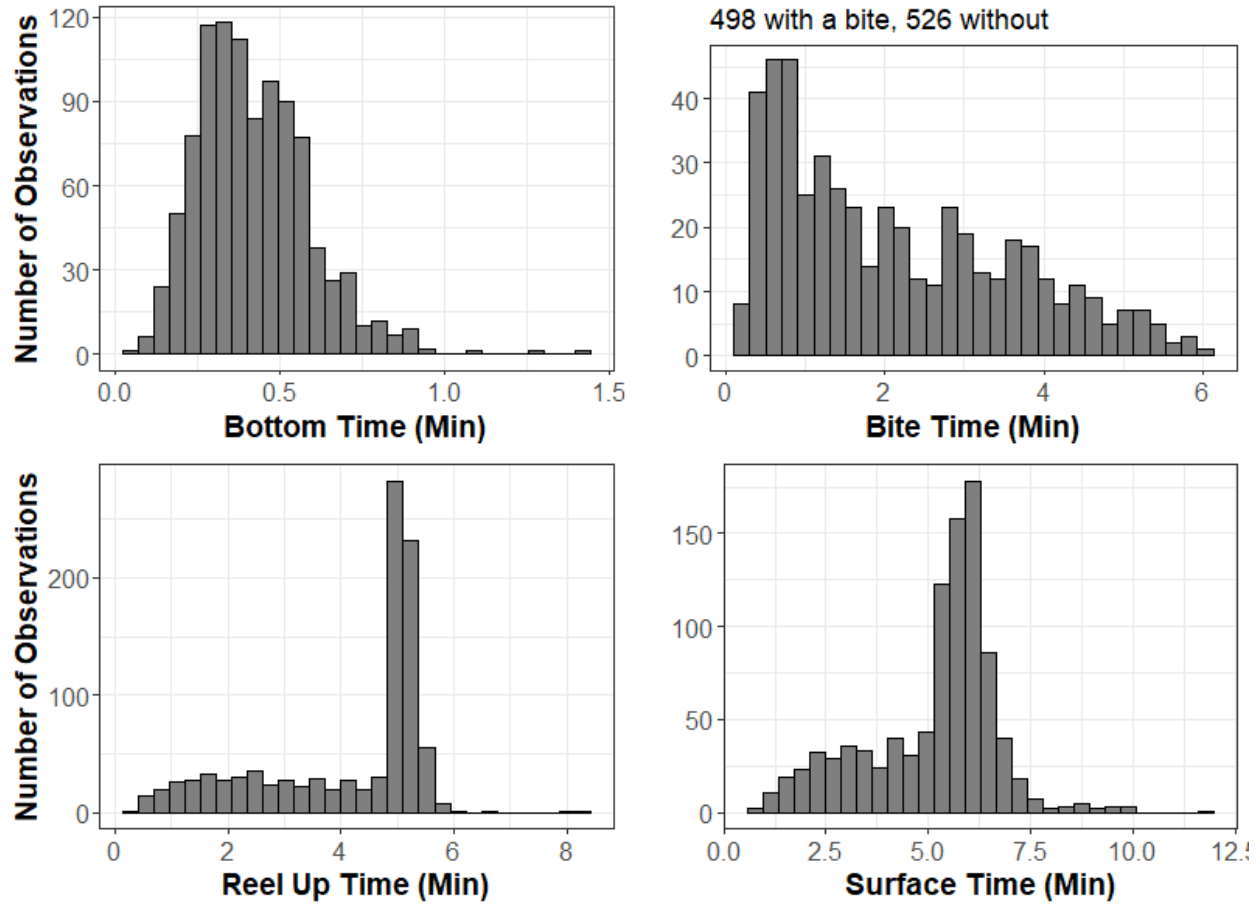


Figure 32. Distribution of time for different events to occur during each fishing drift. For bite time, 498 drifts had a bite and 526 did not receive a bite.

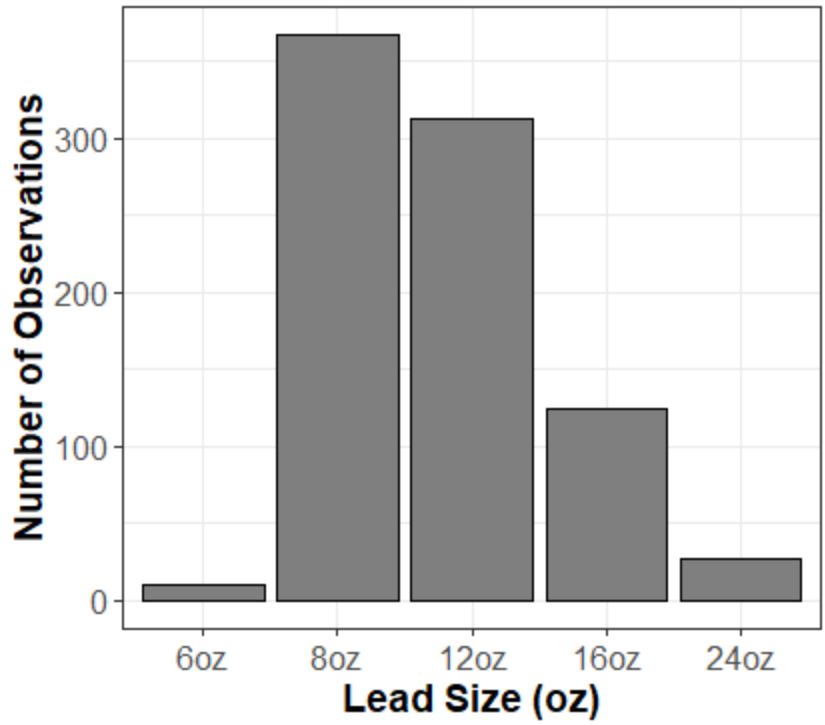


Figure 33. Number of stations fished with each lead size.

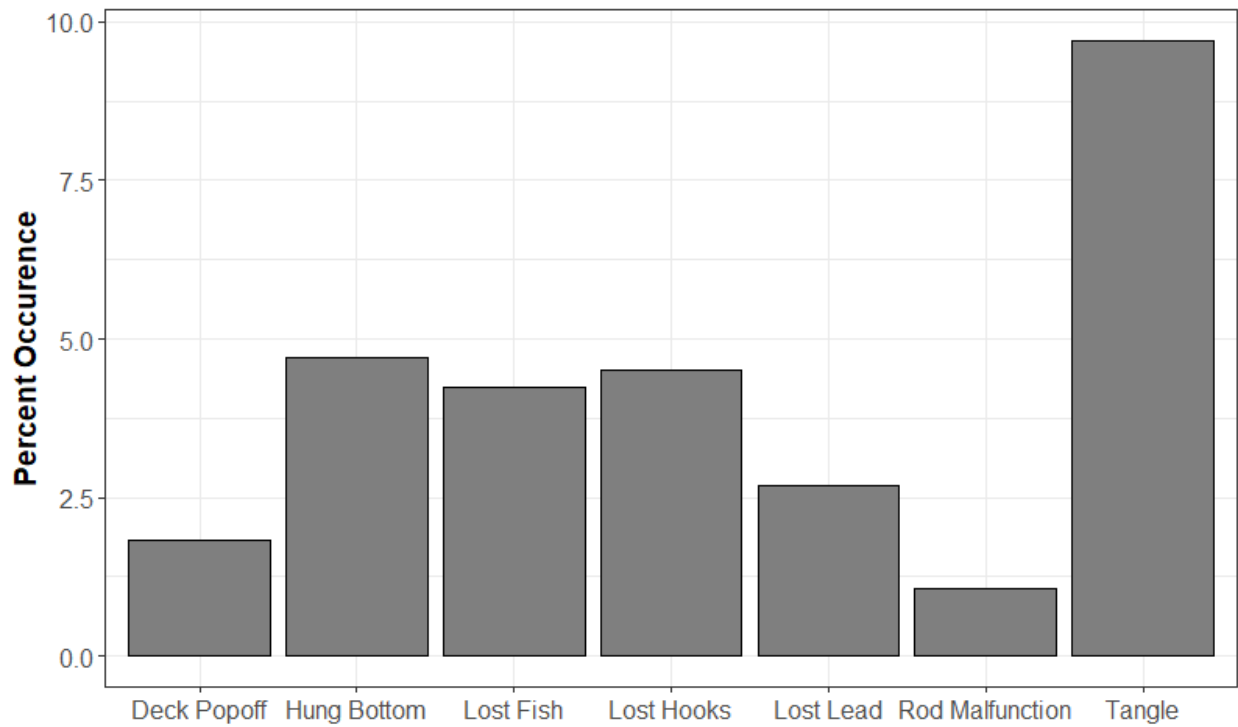


Figure 34. Percent of drifts that resulted in a comment code.

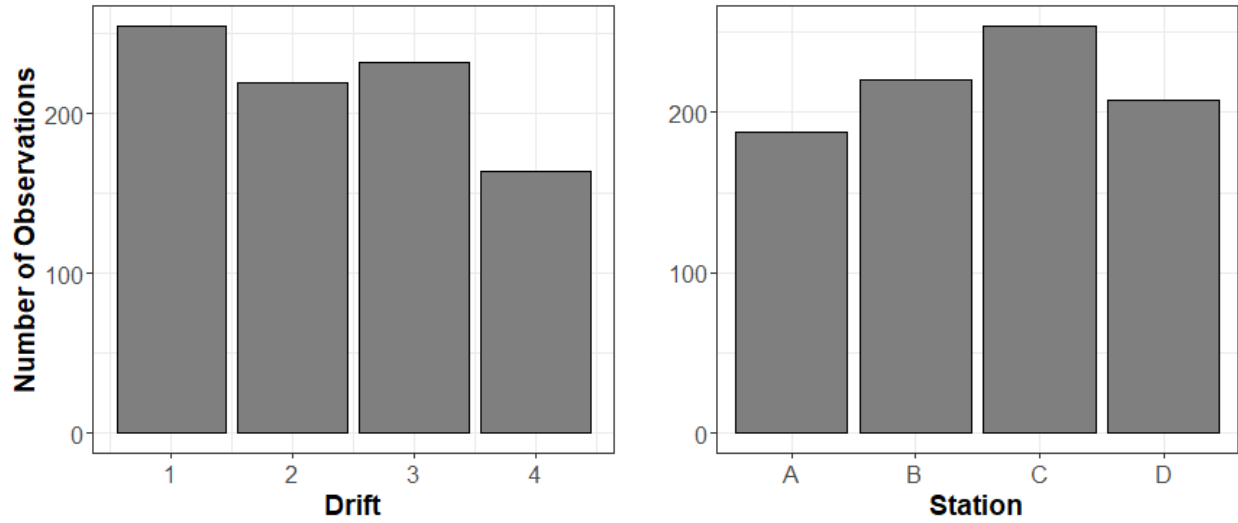


Figure 35. Number of fish caught during each drift and at each station.

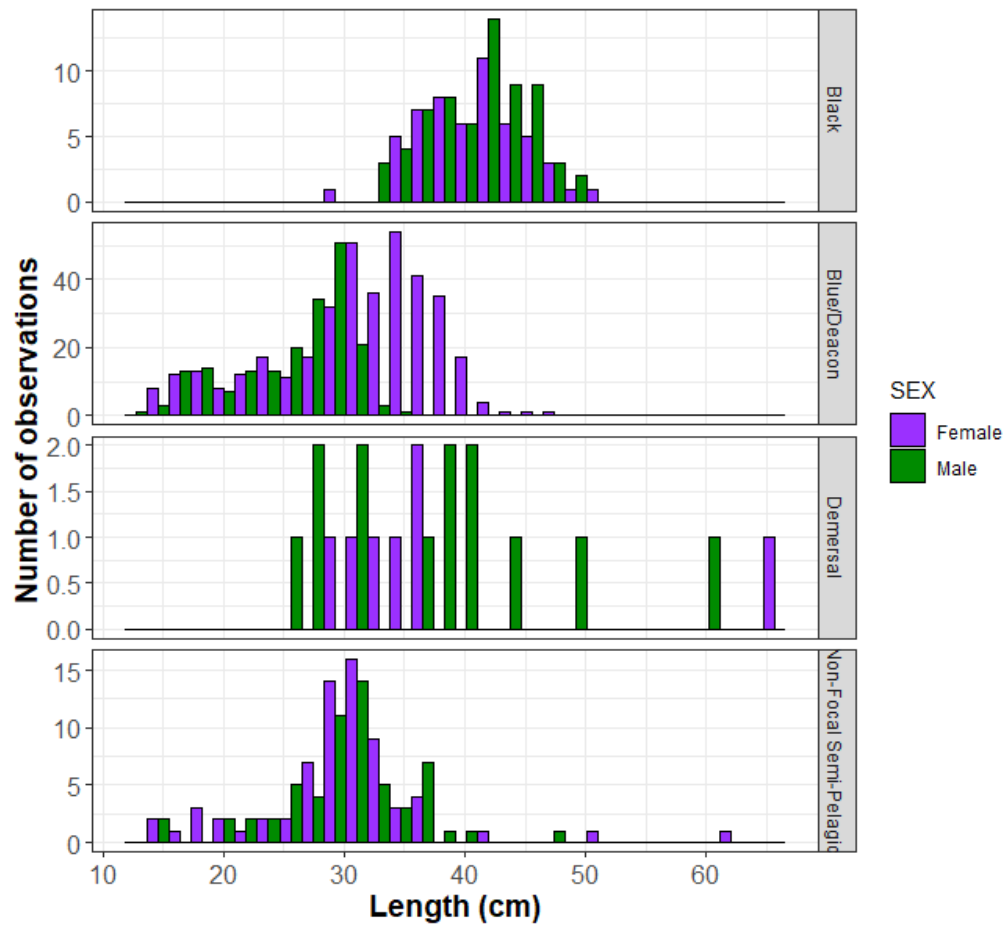


Figure 36. Length distribution of each sex of each species group caught in the hook and line portion of the survey.

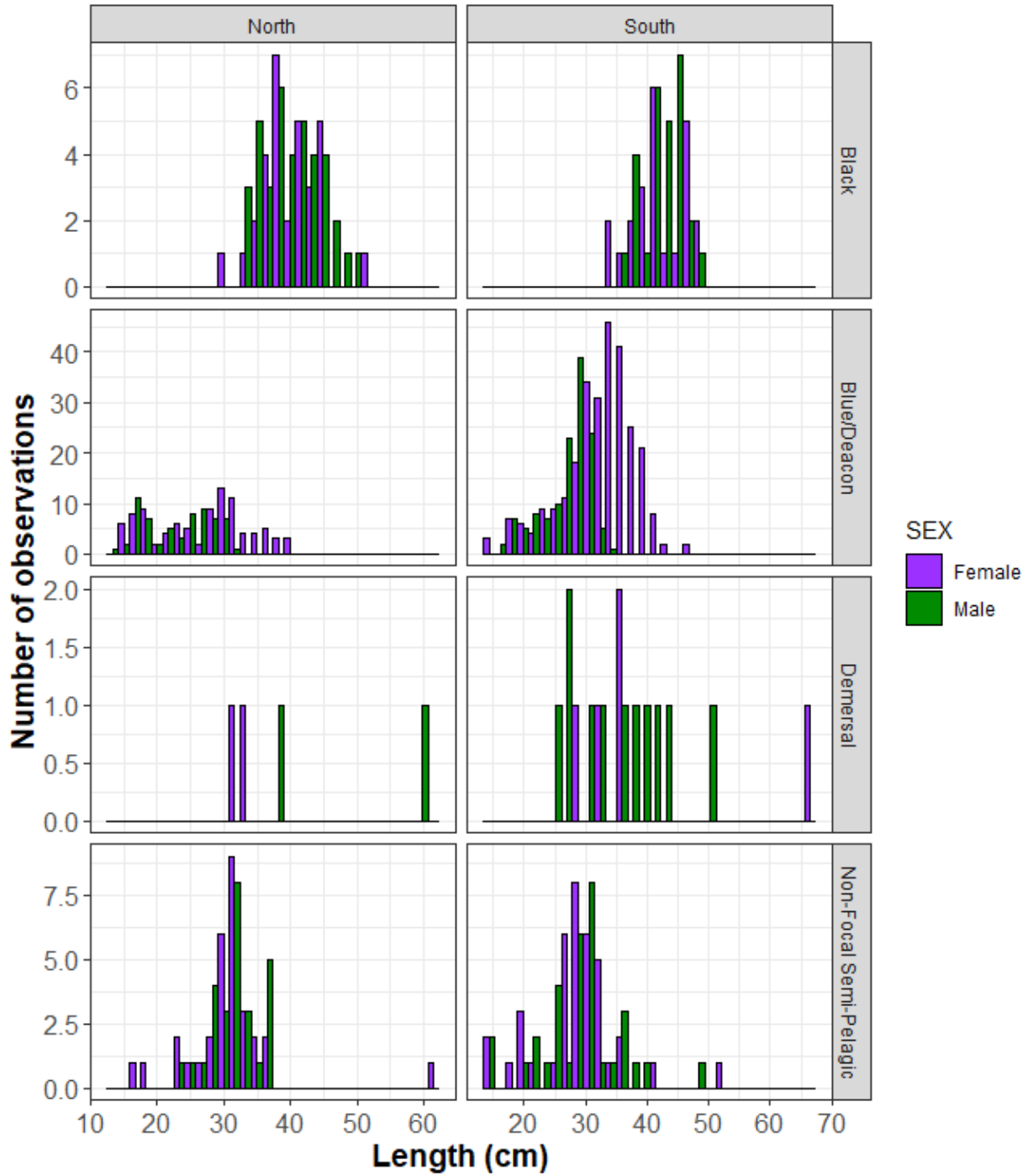


Figure 37. Length distribution of each sex of each species group caught in the hook and line portion of the survey in the northern and southern regions. No stations were conducted in the central region, so no data are depicted.

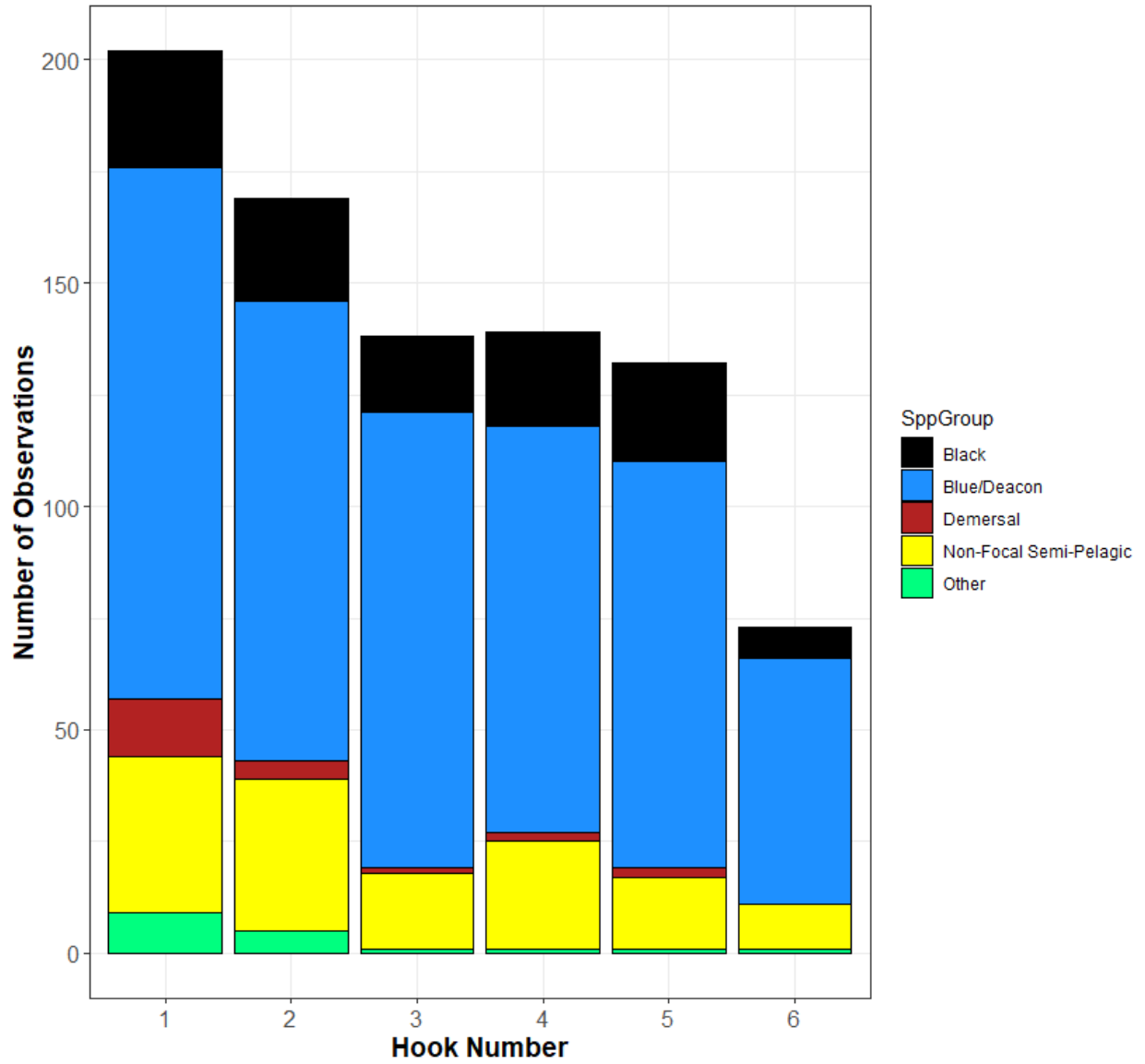


Figure 38. Number of fish caught by hook and by species group.

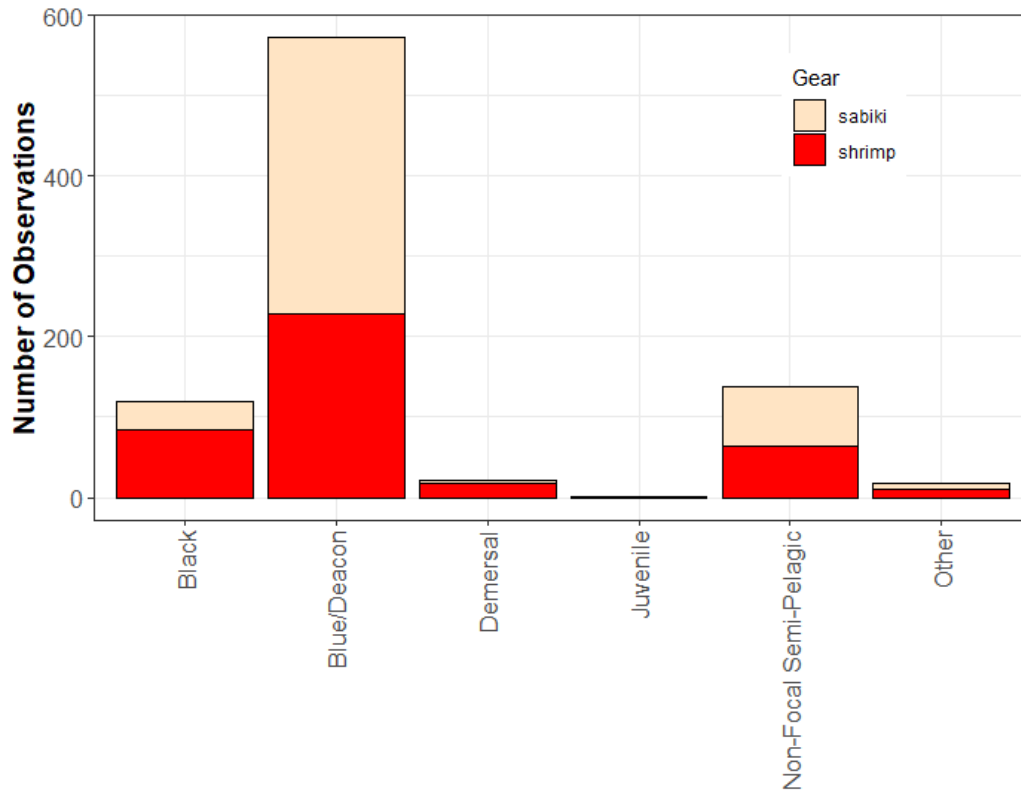


Figure 39. Number of fish caught using Sabiki and Shrimp-Fly gear during the survey.

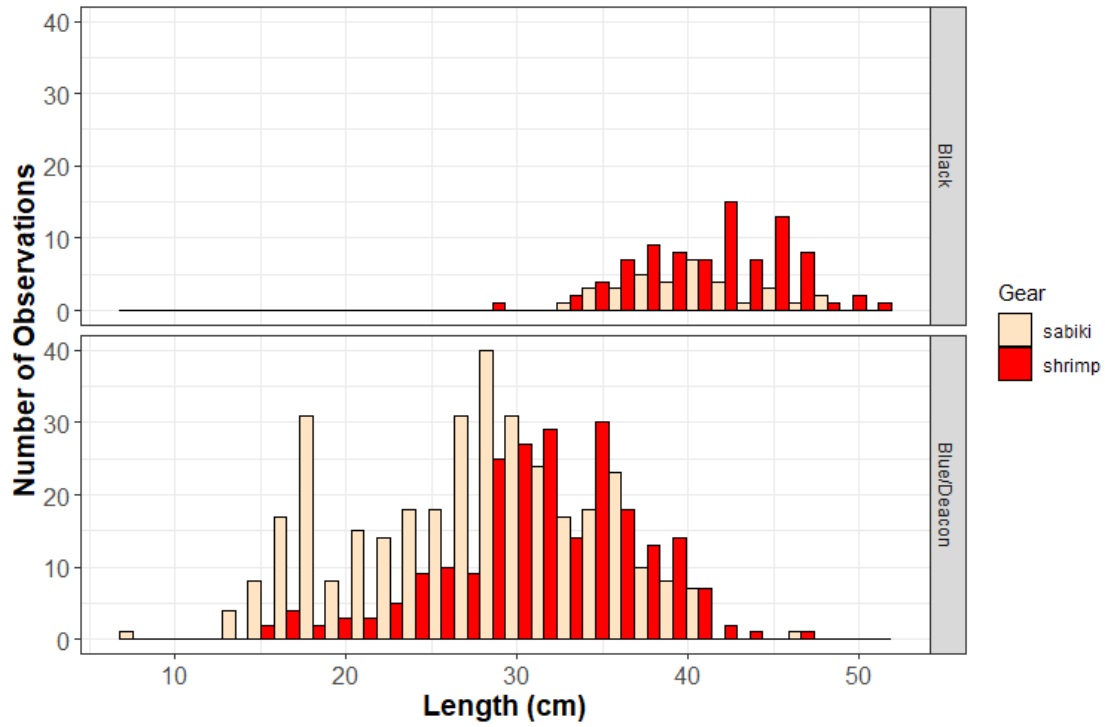


Figure 40. Length distributions of Black and Blue/Deacon Rockfish caught with Sabiki and Shrimp-Fly gear during the survey.

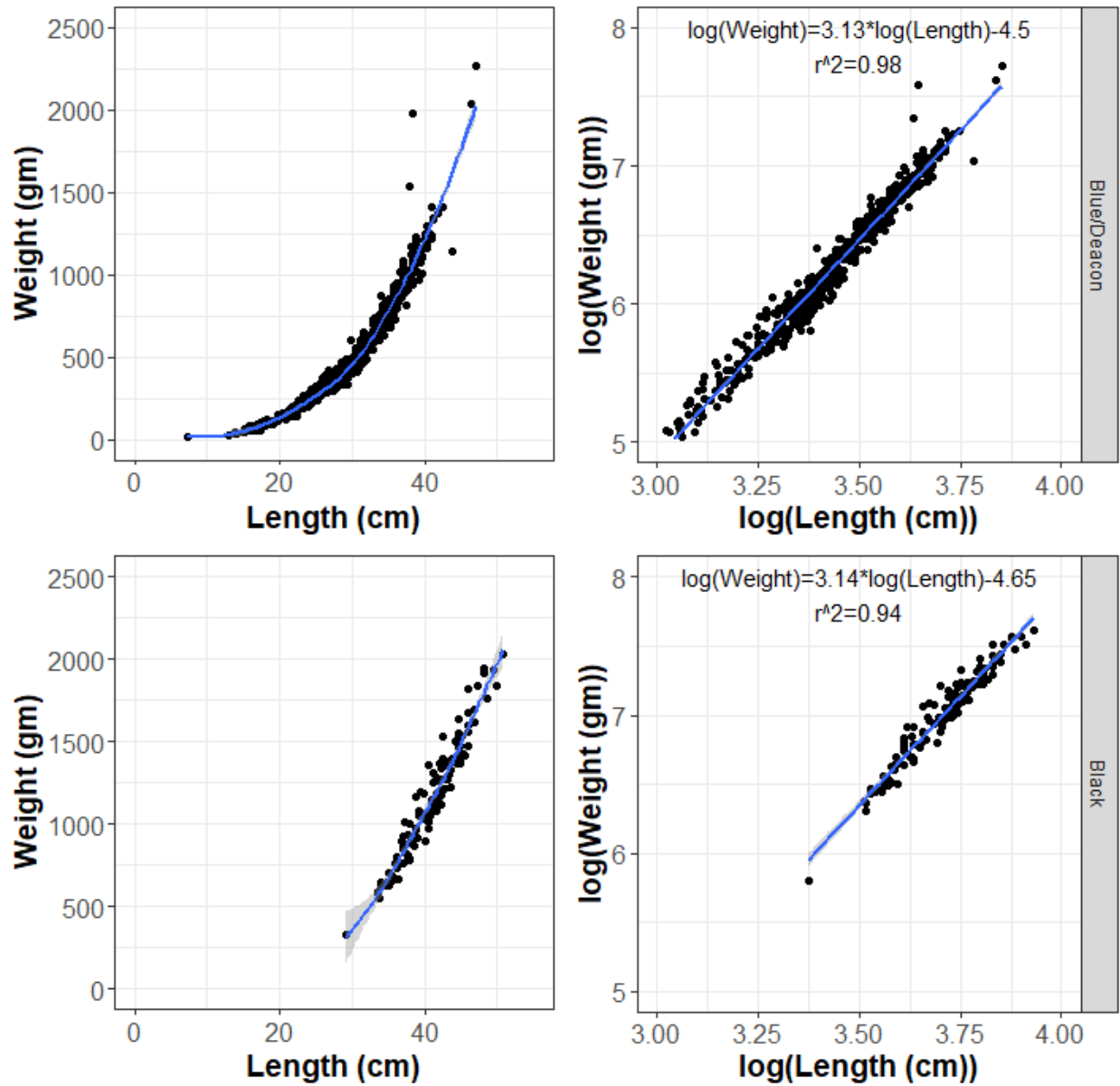


Figure 41. Length weight relationships of Blue/Deacon and Black Rockfish caught during the hook and line portion of the survey.

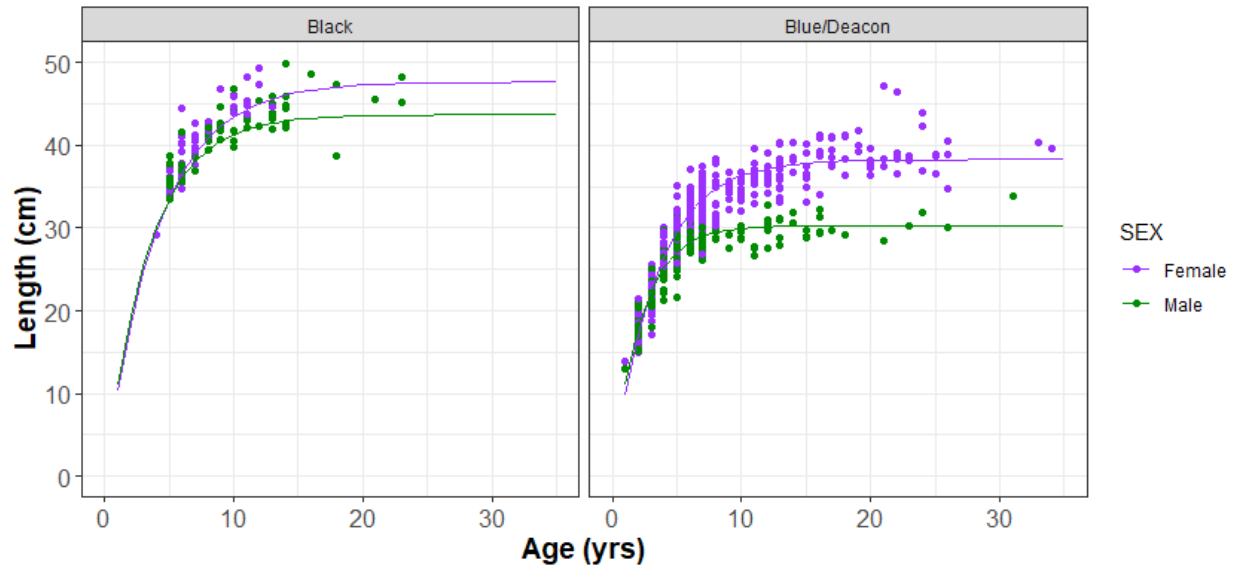


Figure 42. Relationship between length and age for Black and Blue/Deacon Rockfish captured as part of the hook and line components of this survey. Curves for Black Rockfish were fit using 2021 data from the recreational and commercial fleet due to low sample sizes. Black Female: $L_{\infty}=47.6584$, $k=0.2428$; Black Male: $L_{\infty}=43.7041$, $k=0.2905$; Blue/Deacon Female: $L_{\infty}=38.287$, $k=0.296$; Blue/Deacon Male: $L_{\infty}=30.2969$, $k=0.4488$

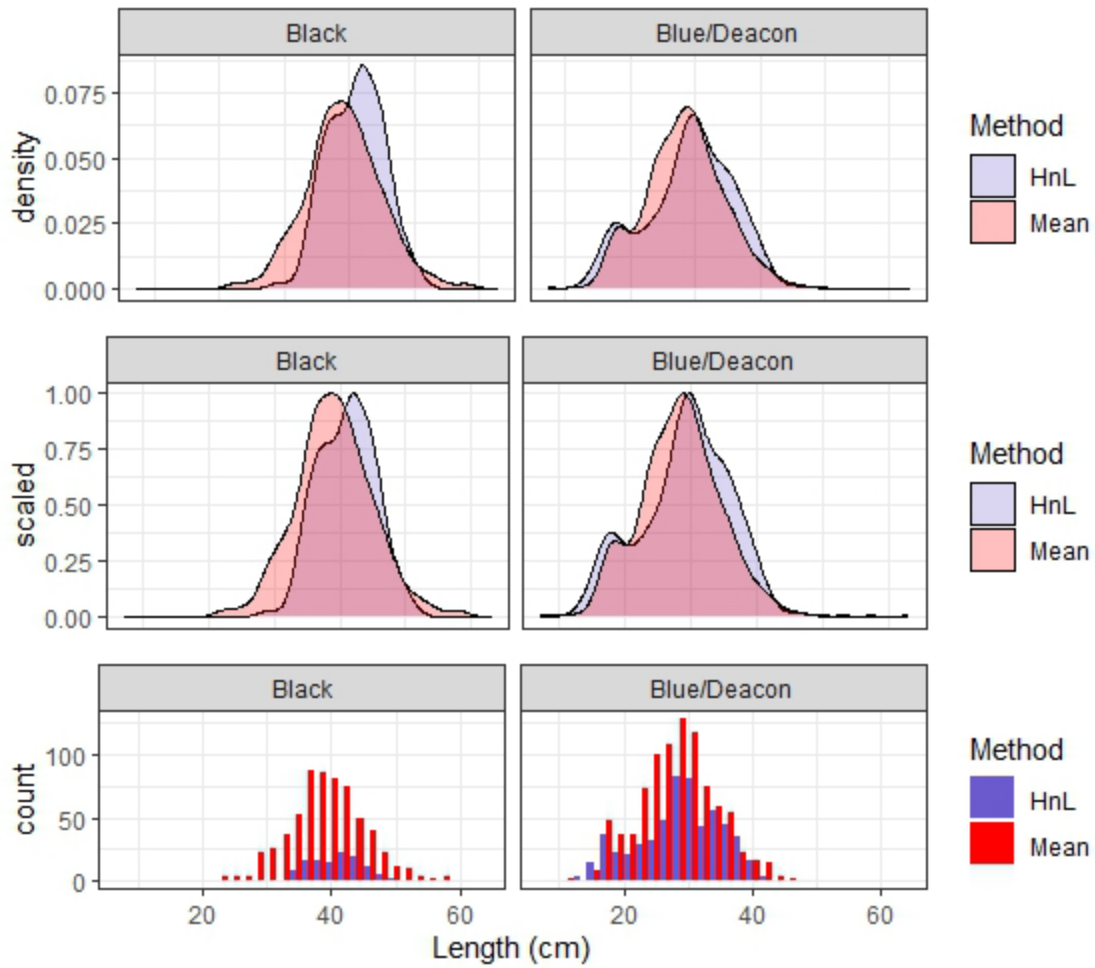


Figure 43. Length distribution by density and scaled density distributions and count of lengths for the survey hook-and-line catch data (purple) and the underwater video MeanCount data (red).

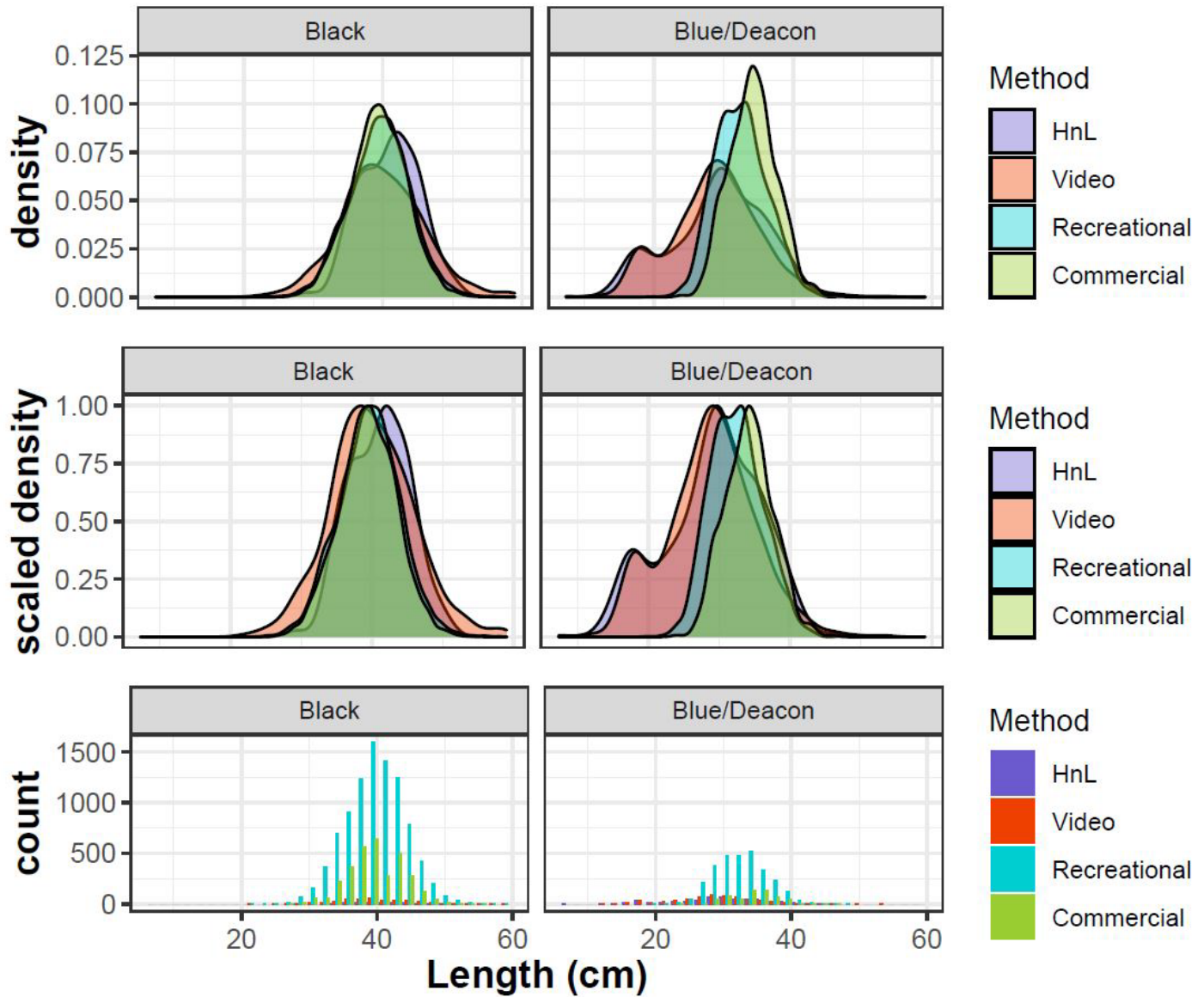


Figure 44. Length distribution of length data derived from the hook-and-line and video components of the statewide survey (HnL and Video respectively), as well as from the 2021 Oregon recreational and commercial fishing fleets (excluding recreational fishing data from Winchester Bay – Central coast).

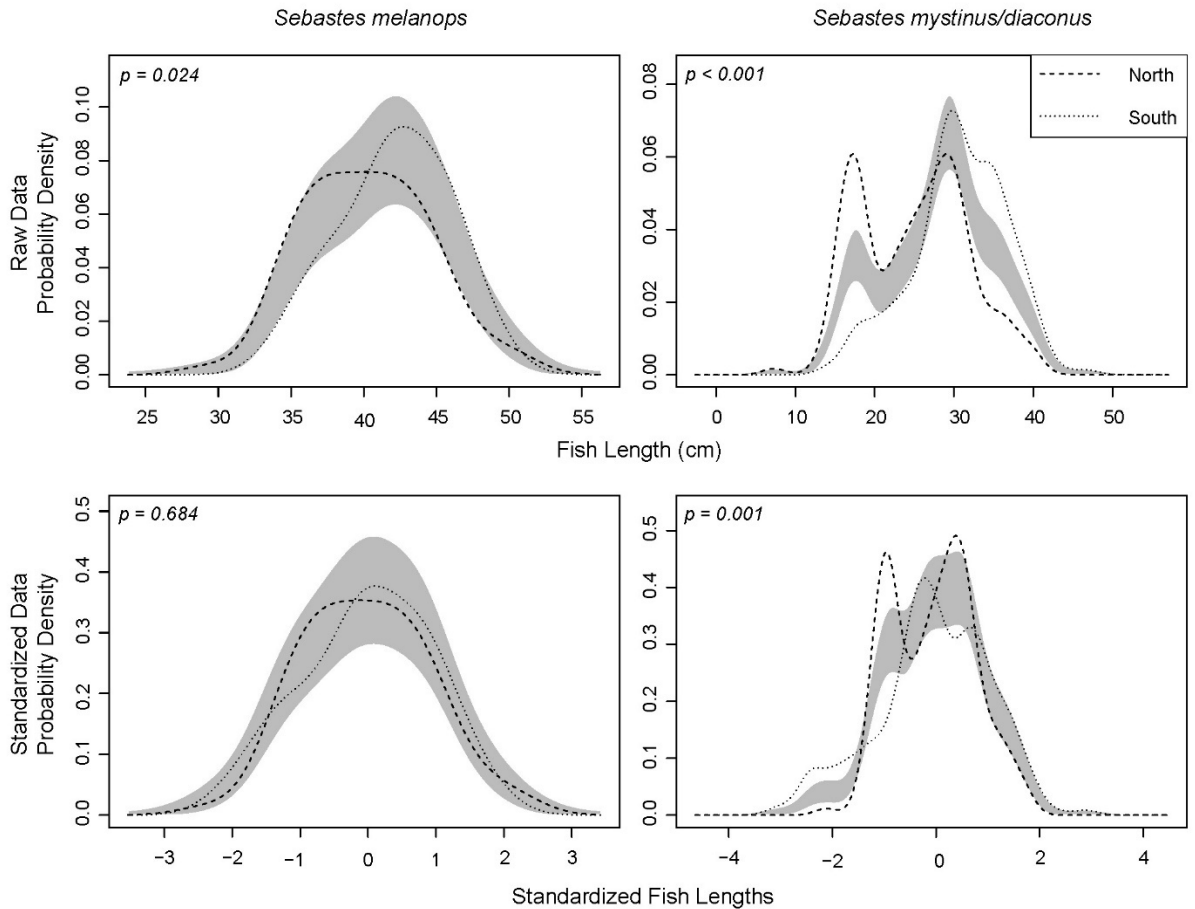


Figure 45. Kernel density estimate (KDE) probability density functions used to compare hook and line length-frequency data between the north and south regions for Black and Blue/Deacon Rockfish. The grey area extends one standard error above and below the null model (no difference in KDEs for each dataset), signaling significant differences in the length-frequency distributions when the dotted or dashed lines fall outside of this area. Permutation tests of the area between the two probability density functions provided significance values (p). Length-frequency data was standardized (bottom row) to analyze the shape of the distribution in comparison to the location and shape distribution (top row). KDE probability density functions were adapted from Langlois et al. 2012.

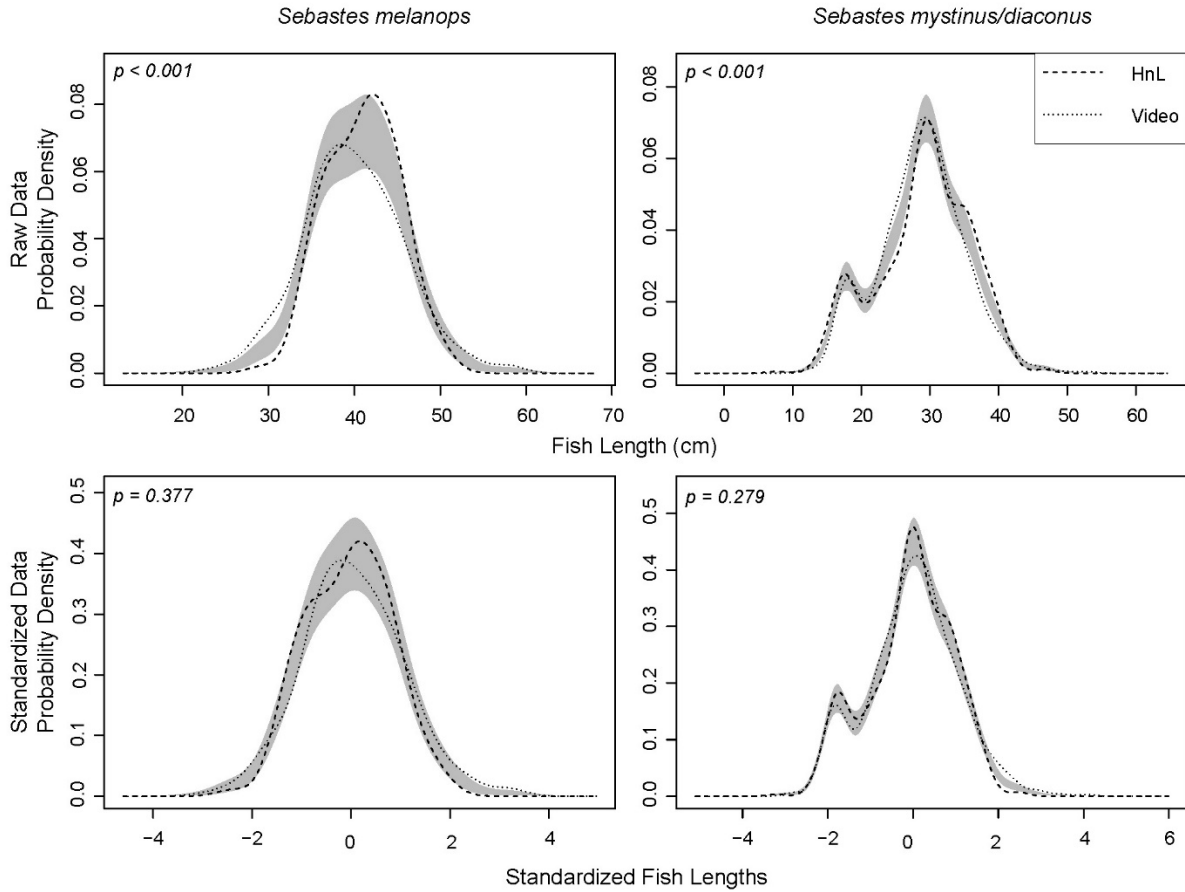


Figure 46. Kernel density estimate (KDE) probability density functions used to compare length-frequency data between our hook and line (HnL) and stereo video (Video) datasets for Black and Blue/Deacon Rockfish. The grey area extends one standard error above and below the null model (no difference in KDEs for each dataset), signaling significant differences in the length-frequency distributions when the dotted or dashed lines fall outside of this area. Permutation tests of the area between the two probability density functions provided significance values (p). Length-frequency data was standardized (bottom row) to analyze the shape of the distribution in comparison to the location and shape distribution (top row). All KDE probability density function analysis methods were adapted from Langlois et al. 2012.

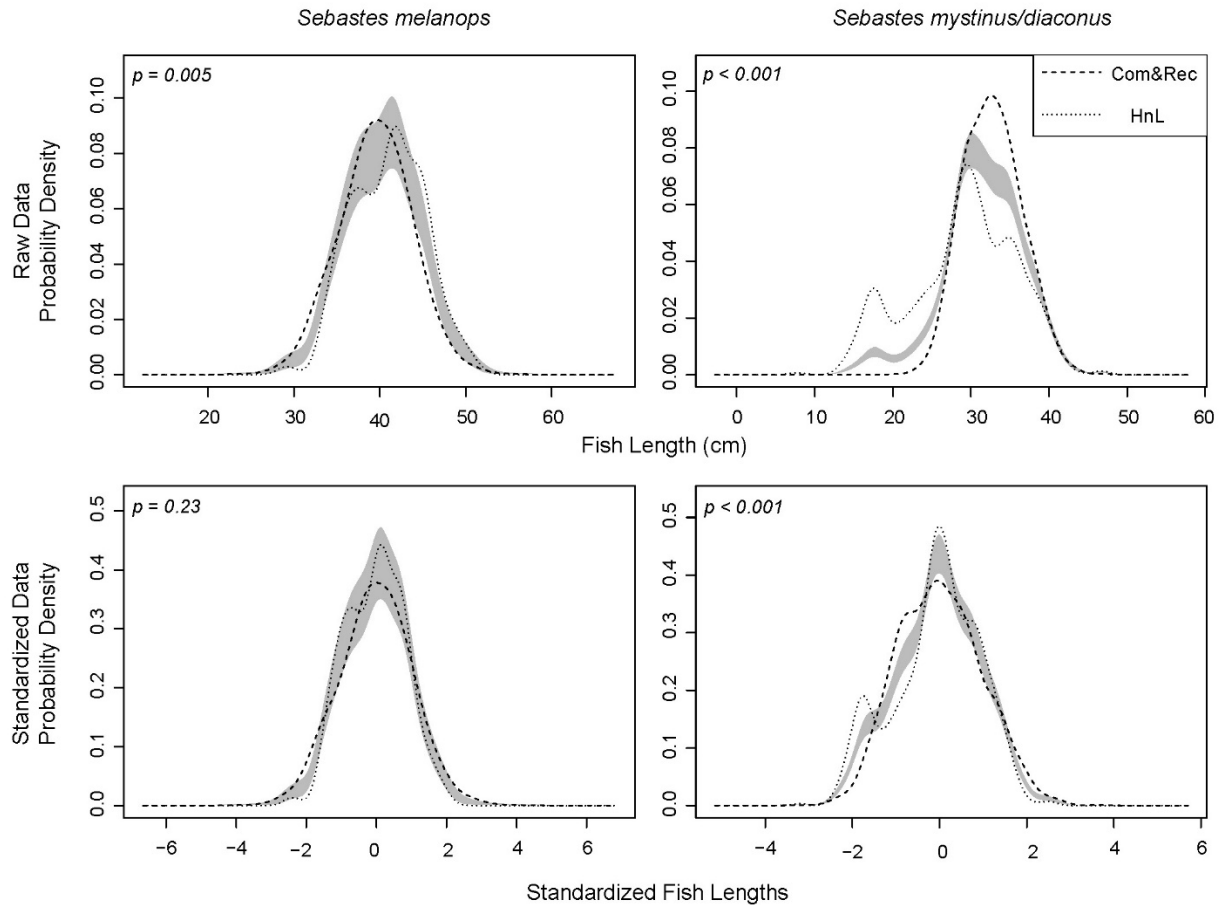


Figure 47. Kernel density estimate (KDE) probability density functions used to compare length-frequency data between the 2021 commercial and recreational fishing fleet data (Com&Rec) and our hook and line (HnL) data for Black and Blue/Deacon Rockfish. The grey area extends one standard error above and below the null model (no difference in KDEs for each dataset), signaling significant differences in the length-frequency distributions when the dotted or dashed lines fall outside of this area. Permutation tests of the area between the two probability density functions provided significance values (p). Length-frequency data was standardized (bottom row) to analyze the shape of the distribution in comparison to the location and shape distribution (top row). All KDE probability density function analysis methods were adapted from Langlois et al. 2012.

FISHERIES ACOUSTICS

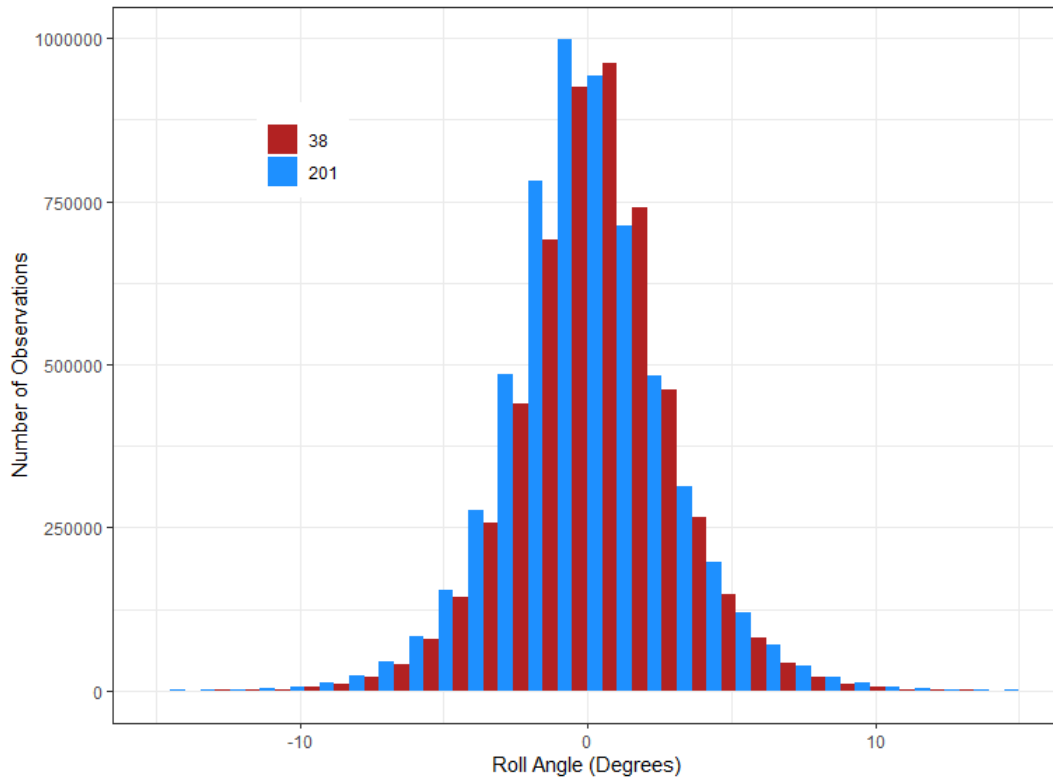


Figure 48. Distribution of transducer roll for 38 and 201 kHz transducer.

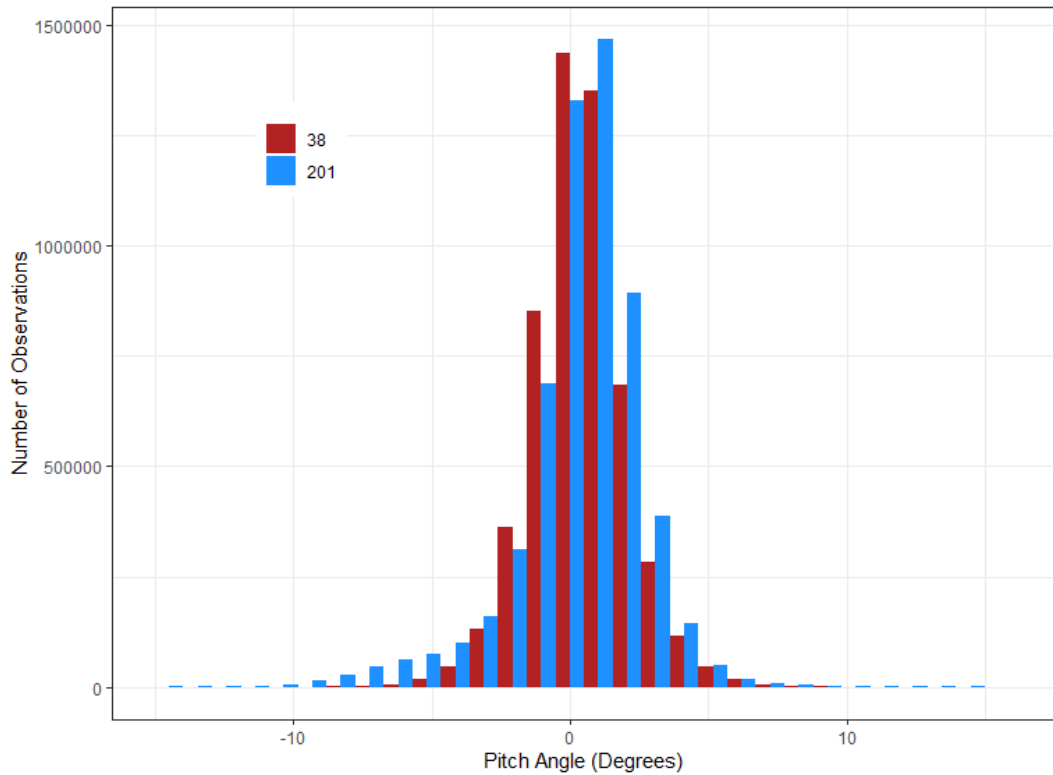


Figure 49. Distribution of transducer pitch for 38 and 201 kHz transducer.

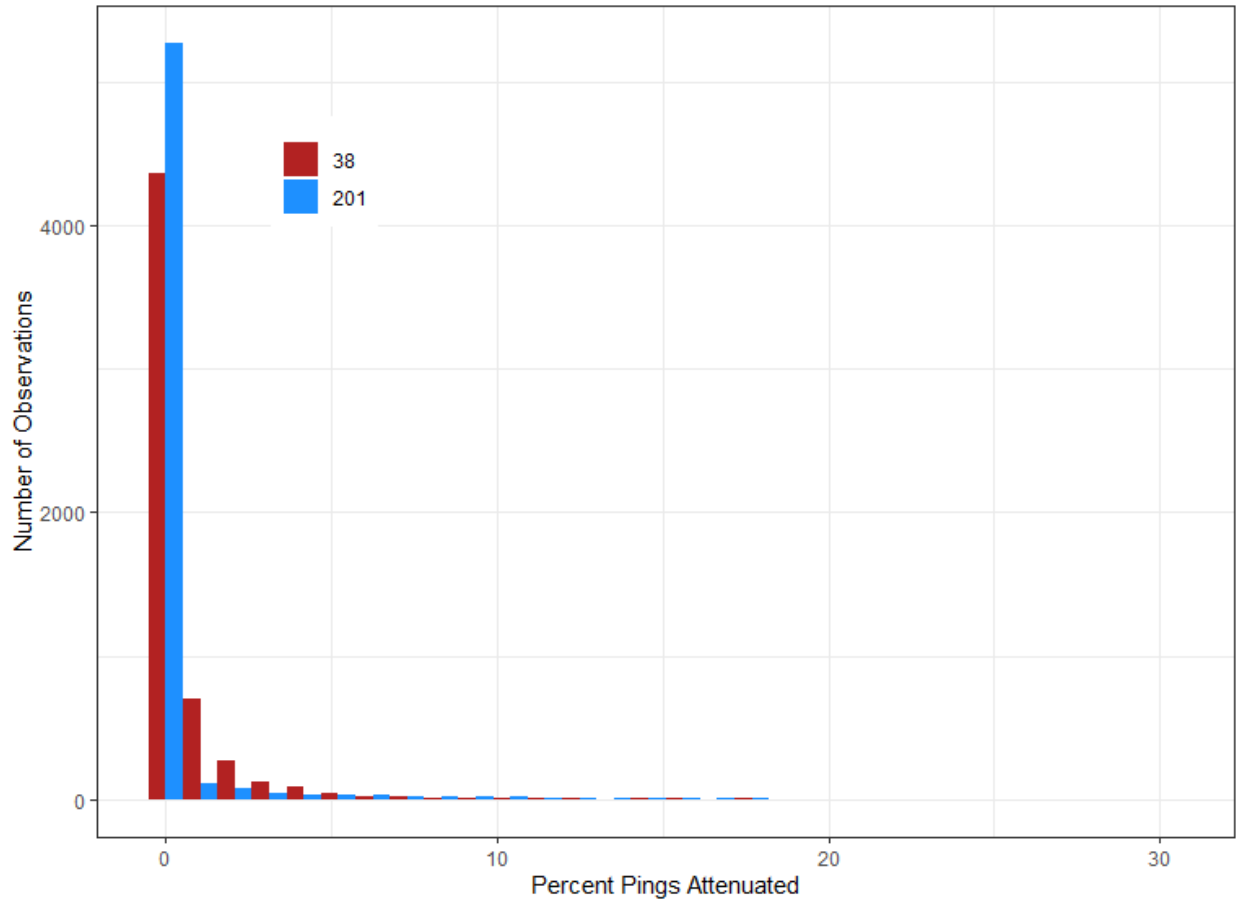


Figure 50. Distribution of percentage of pings in 50 m bins that are attenuated.

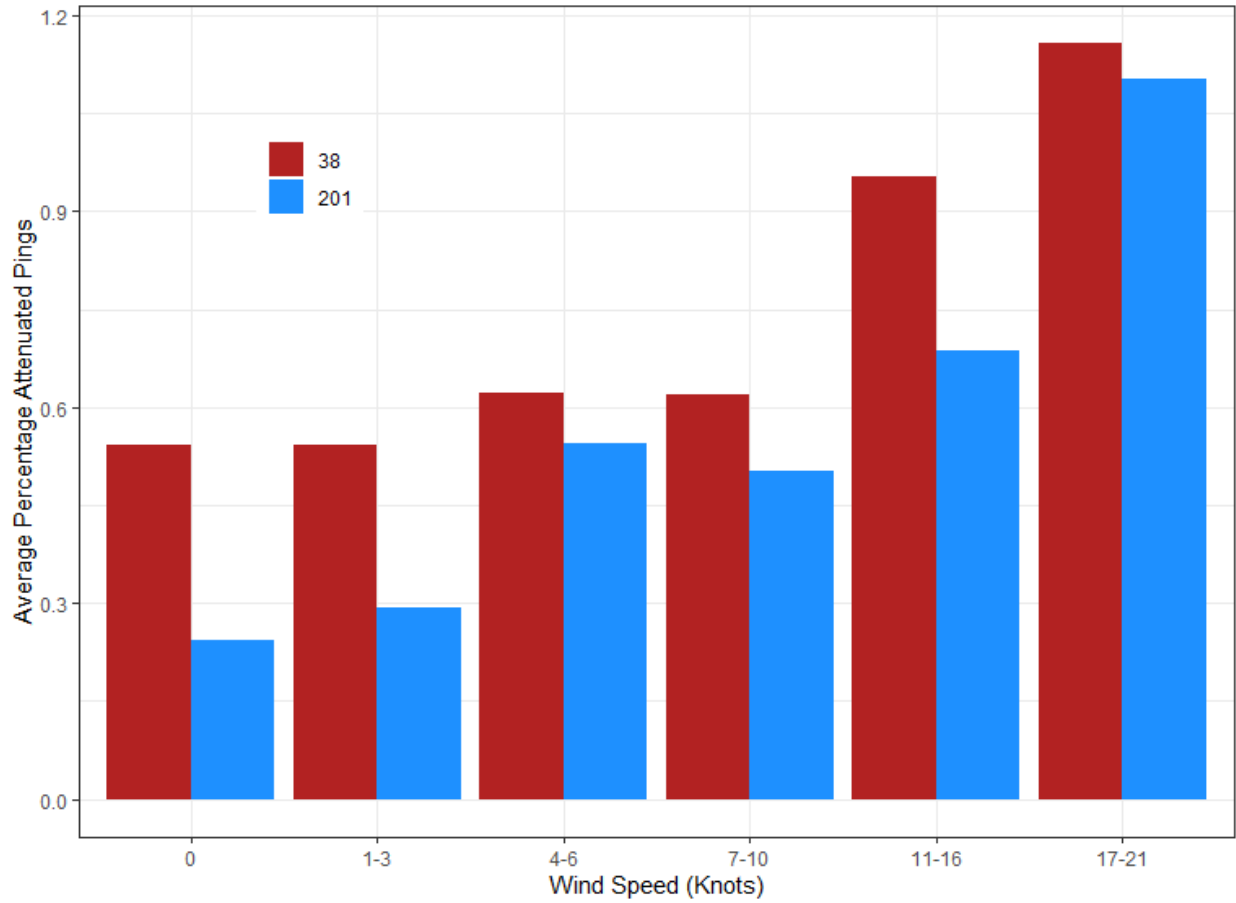


Figure 51. Average percentage of attenuation by wind speed.

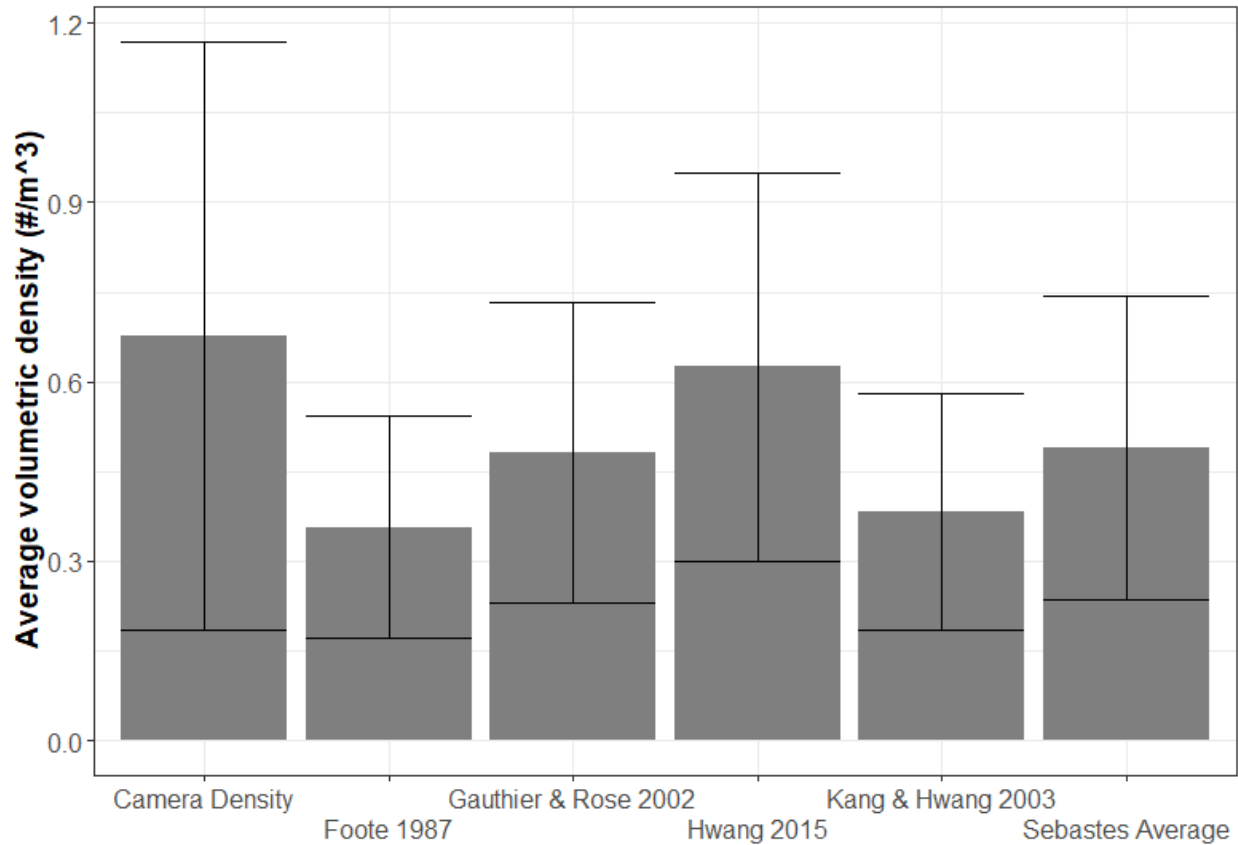


Figure 52. Volumetric densities (number of fish per m³) generated from the BASSCam and schools of fish identified in the acoustics. Acoustics were converted from backscattering values to densities using length data from the closest video deployment to that school. Only camera deployments occurring within 10 m of fish schools are reported here. No models were statistically different from one another.

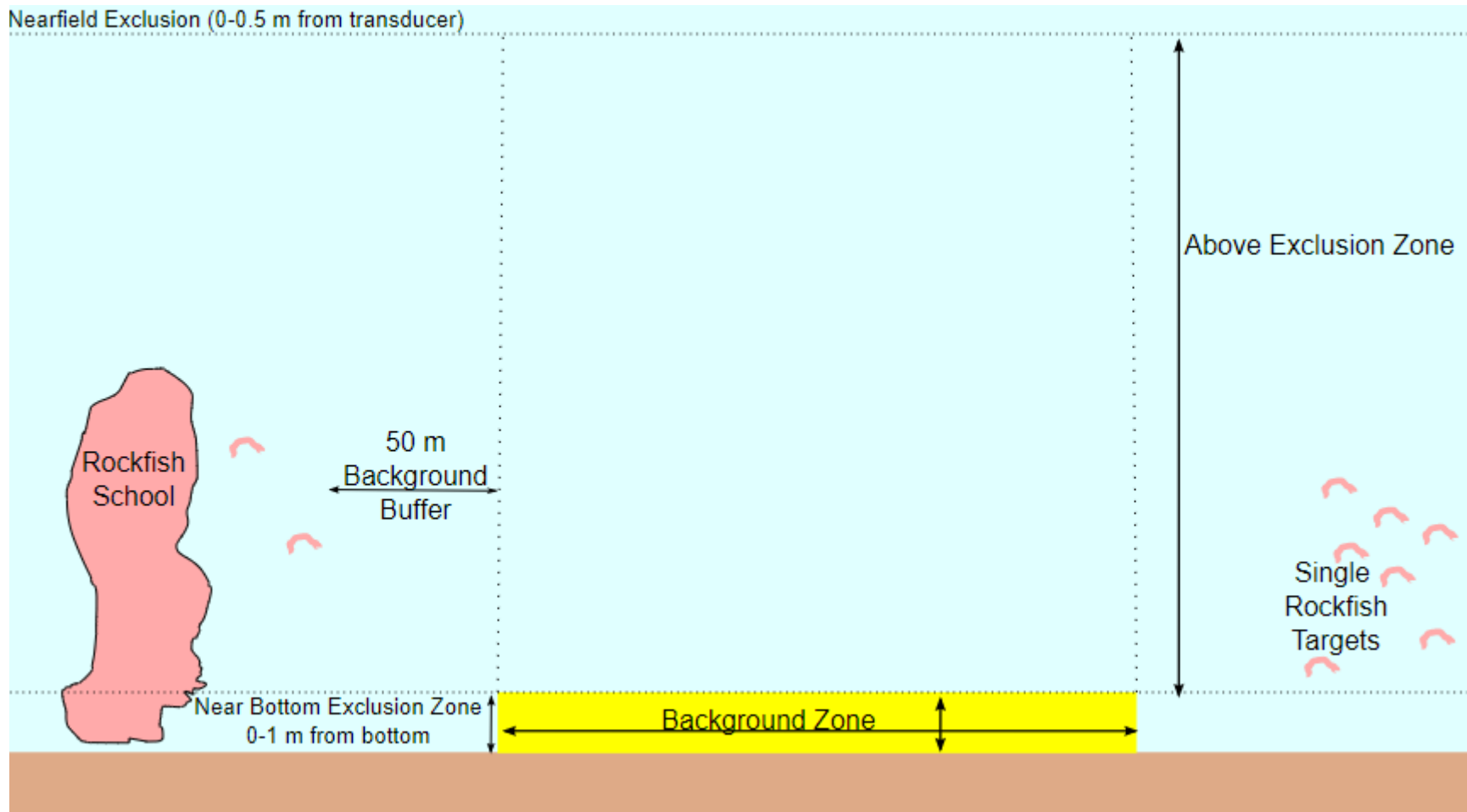


Figure 53. Schematic of how the echogram was apportioned for analysis. Three primary analytical zones were considered: above exclusion zone, within exclusion zone and background zone. The dashed lines above the background zone are for reference. Figure not to scale.

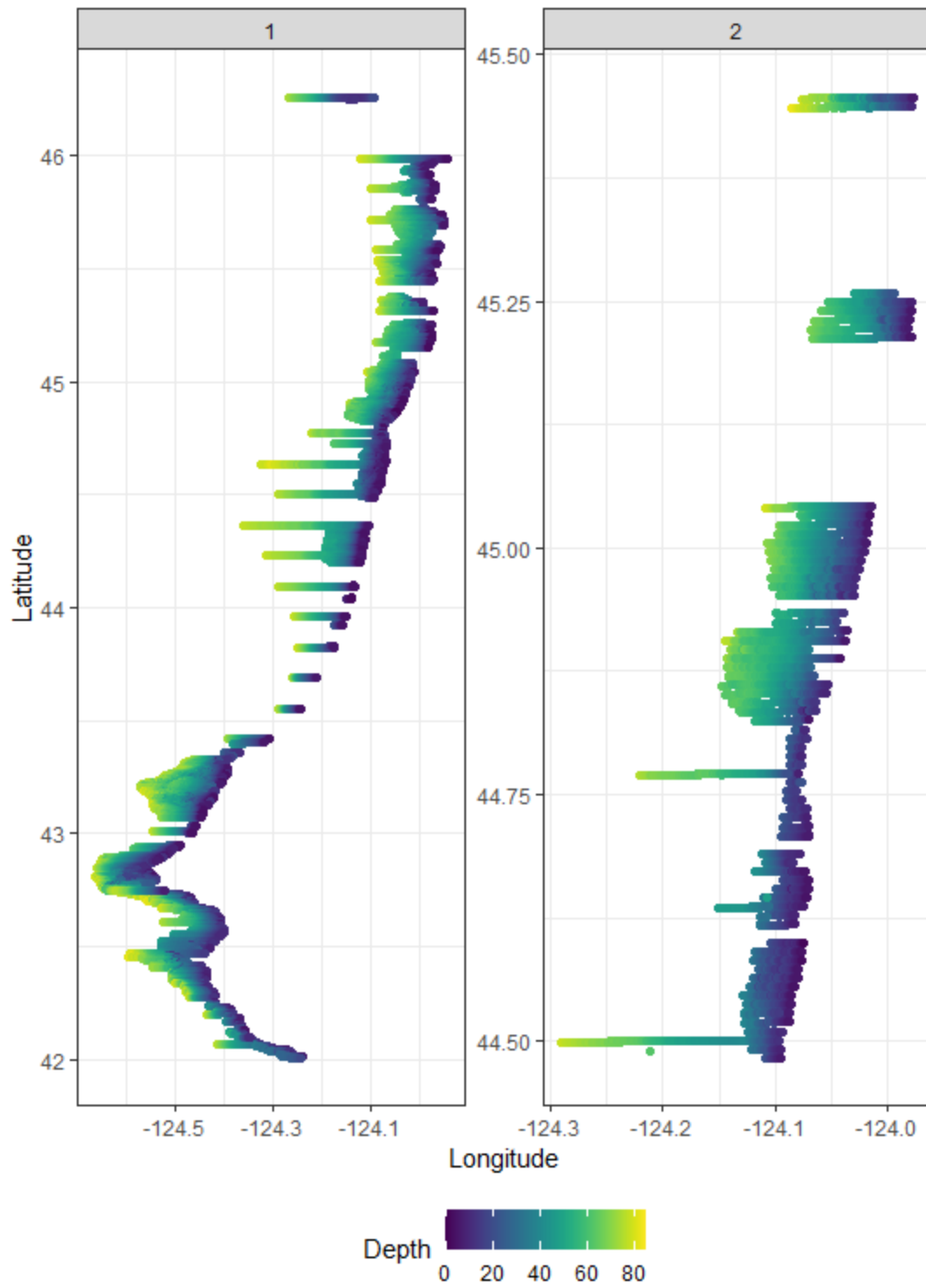


Figure 54. Bottom depth observed while conducting the acoustic transects.

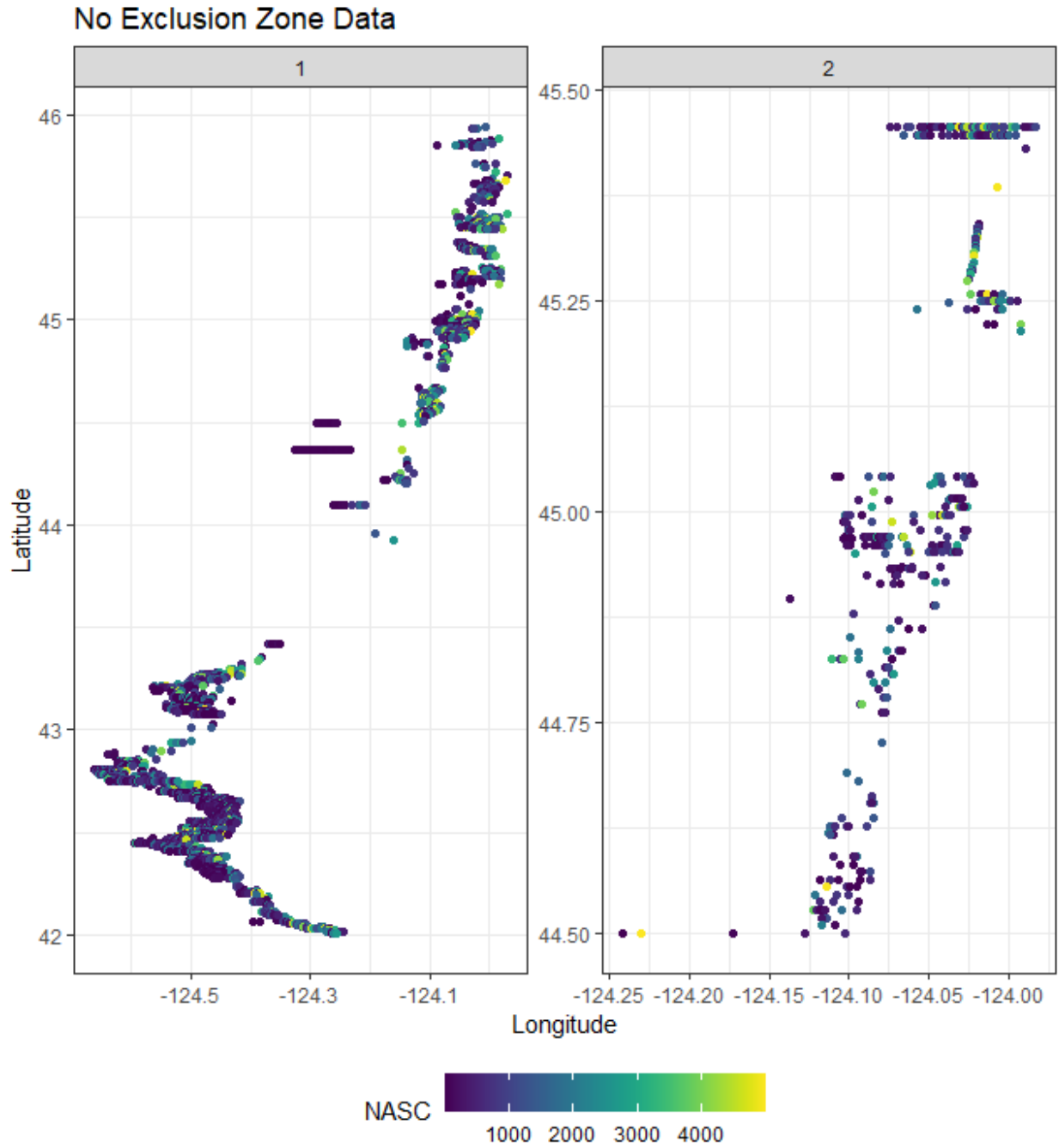


Figure 55. NASC values for each of the individual schools identified by the school detection algorithm during pass 1 and pass 2 above the exclusion zone.

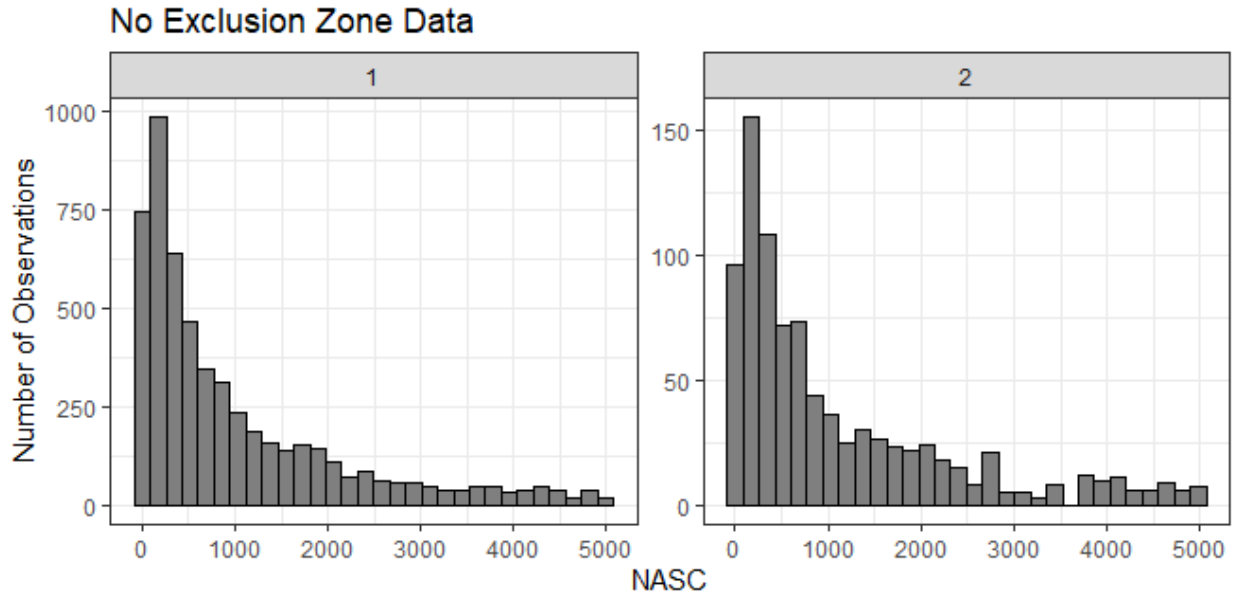


Figure 56. Histograms of NASC values for each observed school during pass 1 and pass 2 above the exclusion zone.

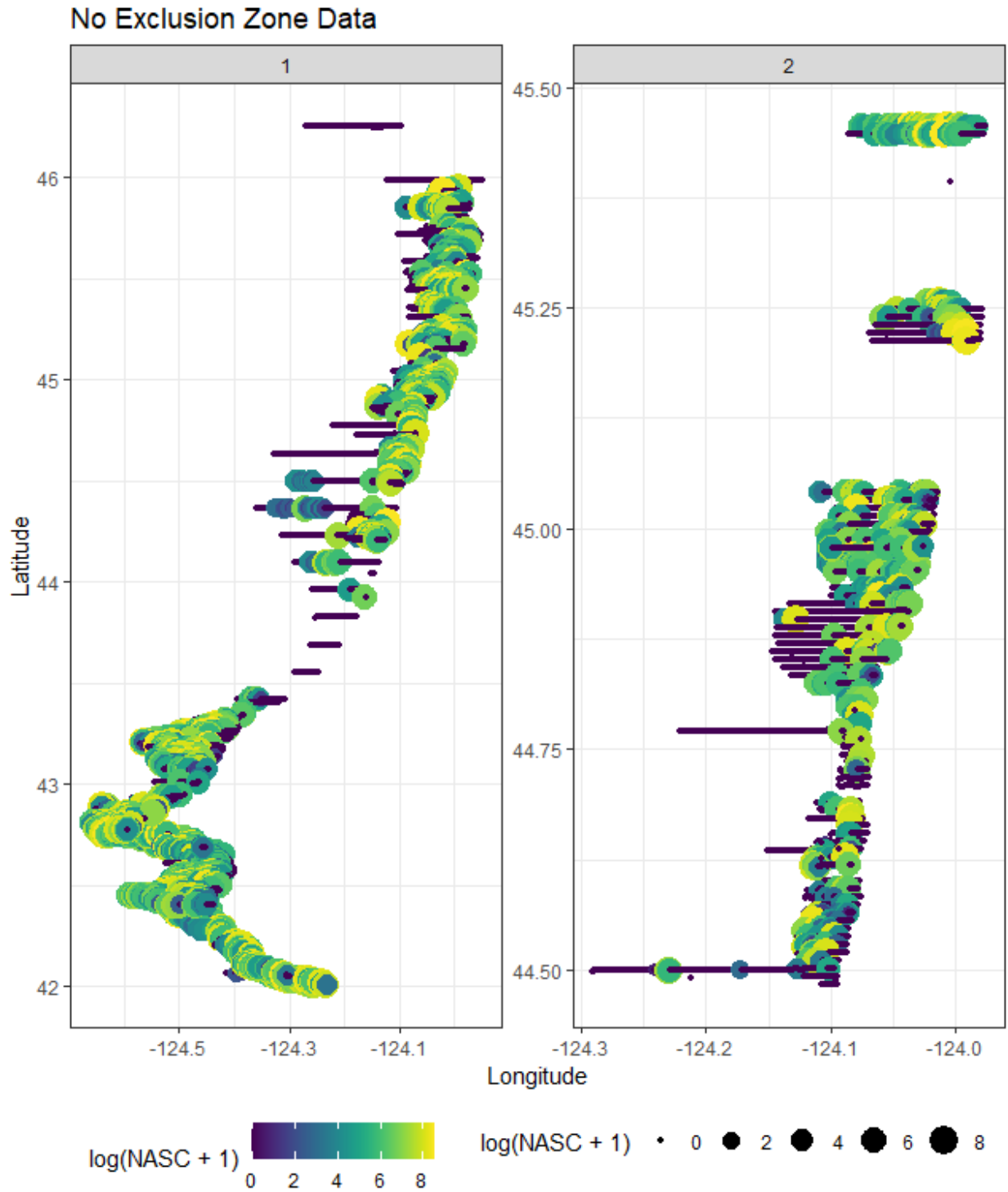


Figure 57. Map of log transformed NASC values in 50 m along transect bins for pass 1 and pass 2 above the exclusion zone.

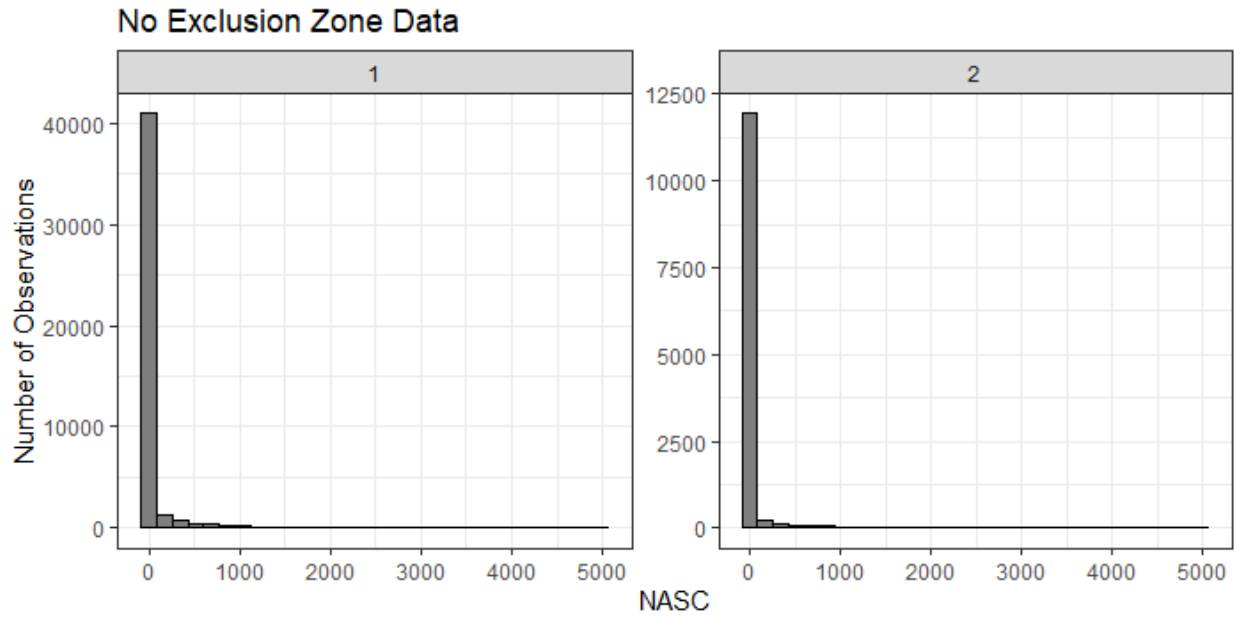


Figure 58. Histogram of NASC values for the 50 m along transect bins above the exclusion zone for pass 1 and pass 2.

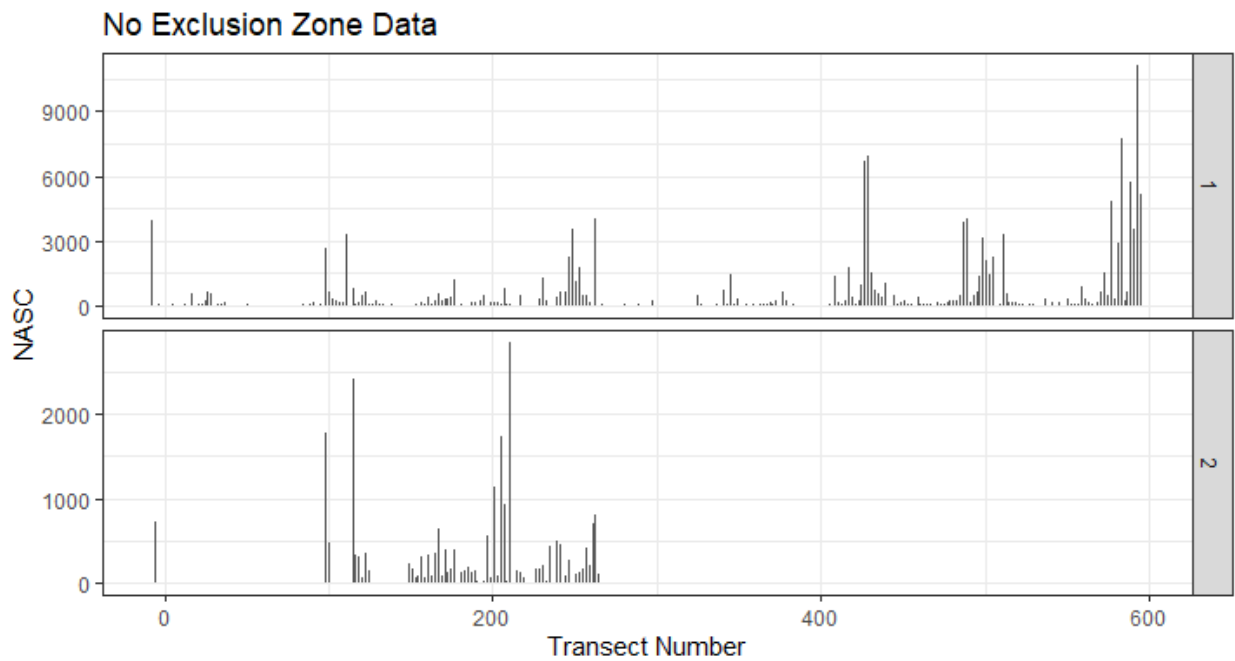


Figure 59. NASC values for each transect for pass 1 and pass 2 above the exclusion zone.

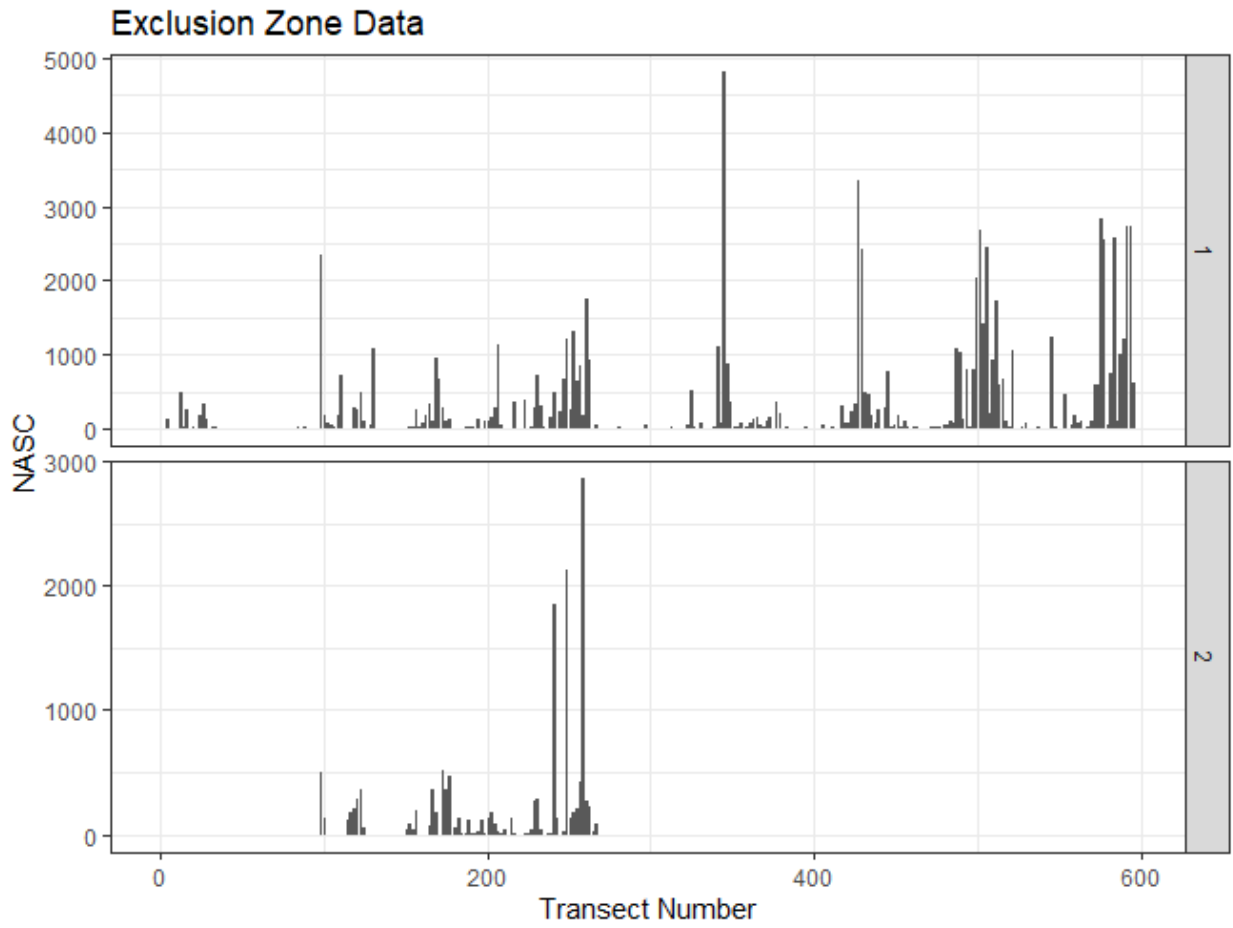


Figure 60. NASC values for each transect for pass 1 and pass 2 within the exclusion zone.

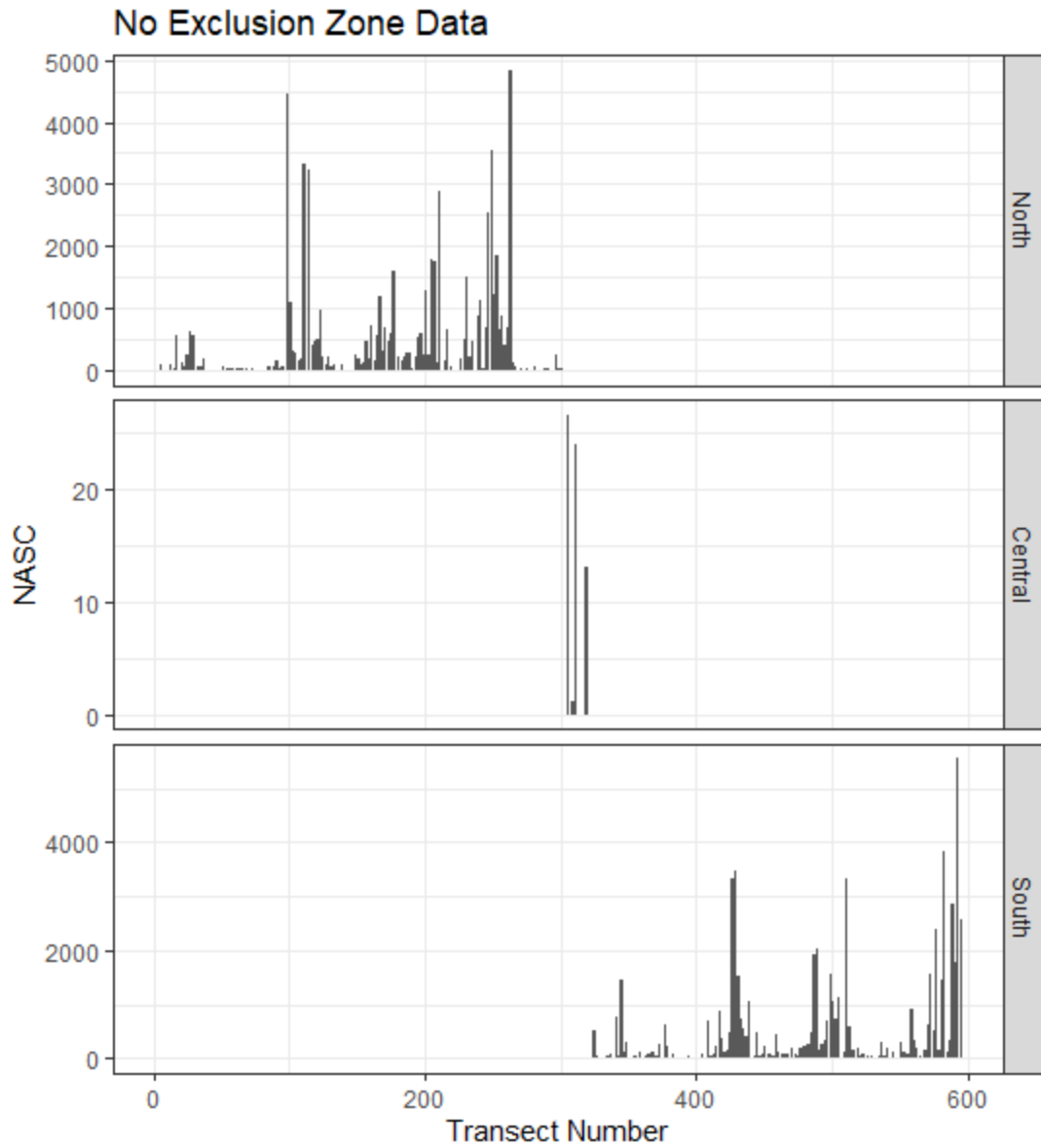


Figure 61. NASC values above the exclusion zone for each transect individually (pass 1) separated by survey region.

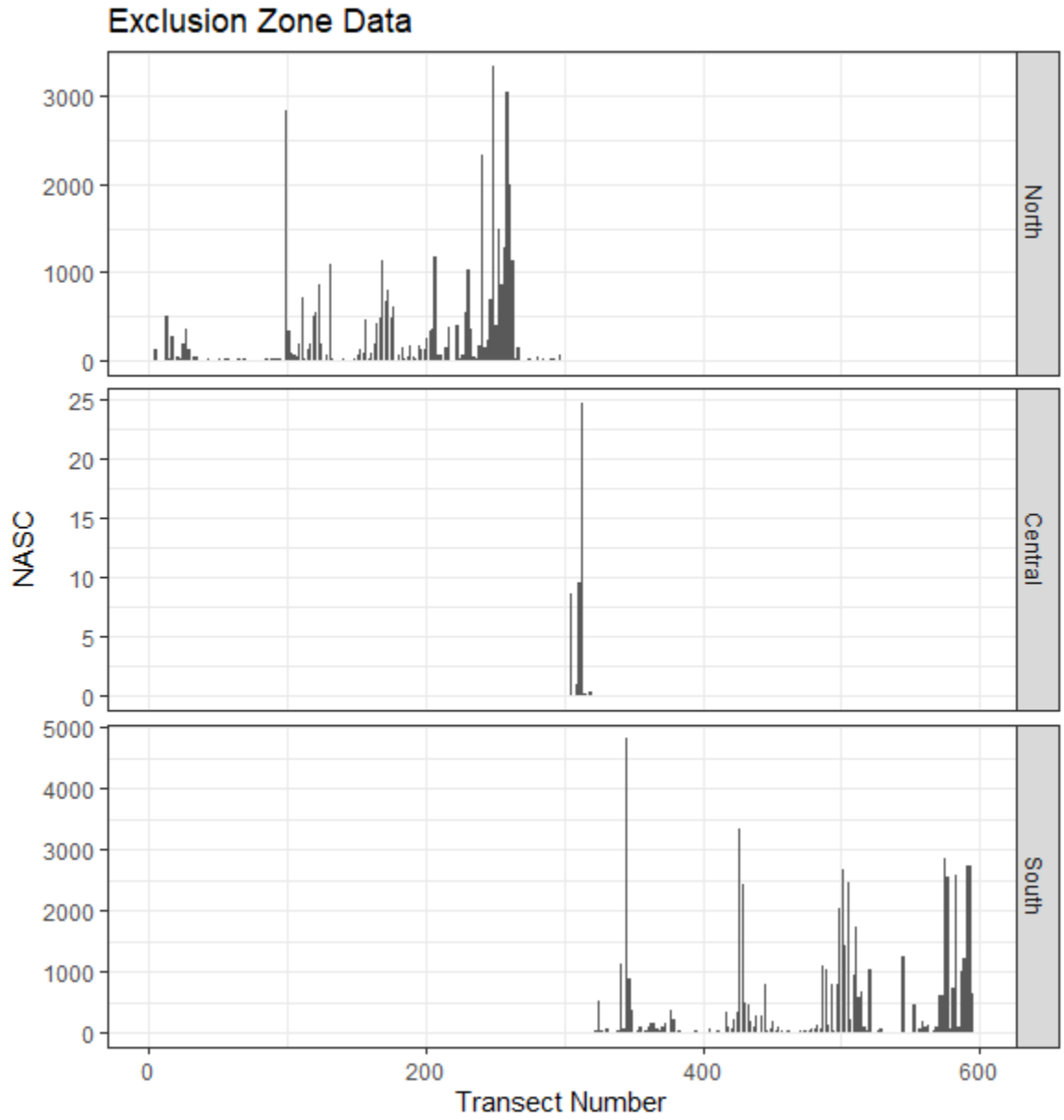


Figure 62. NASC values within the exclusion zone for each transect individually (pass 1) separated by survey region.

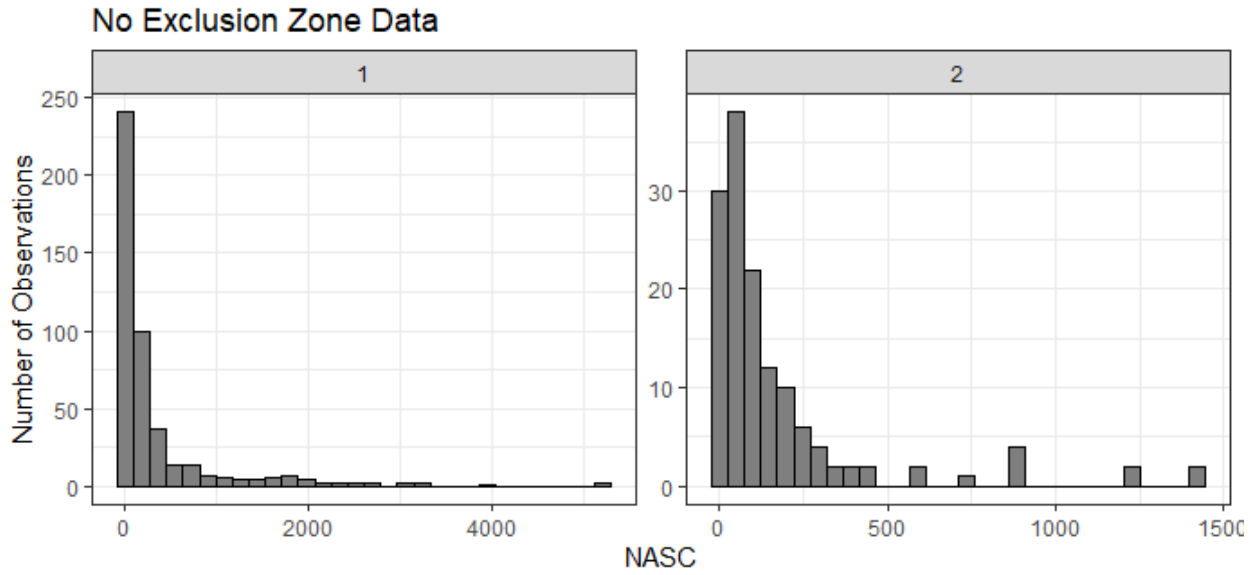


Figure 63. Histogram of NASC values for each transect for pass 1 and pass 2 above the exclusion zone.

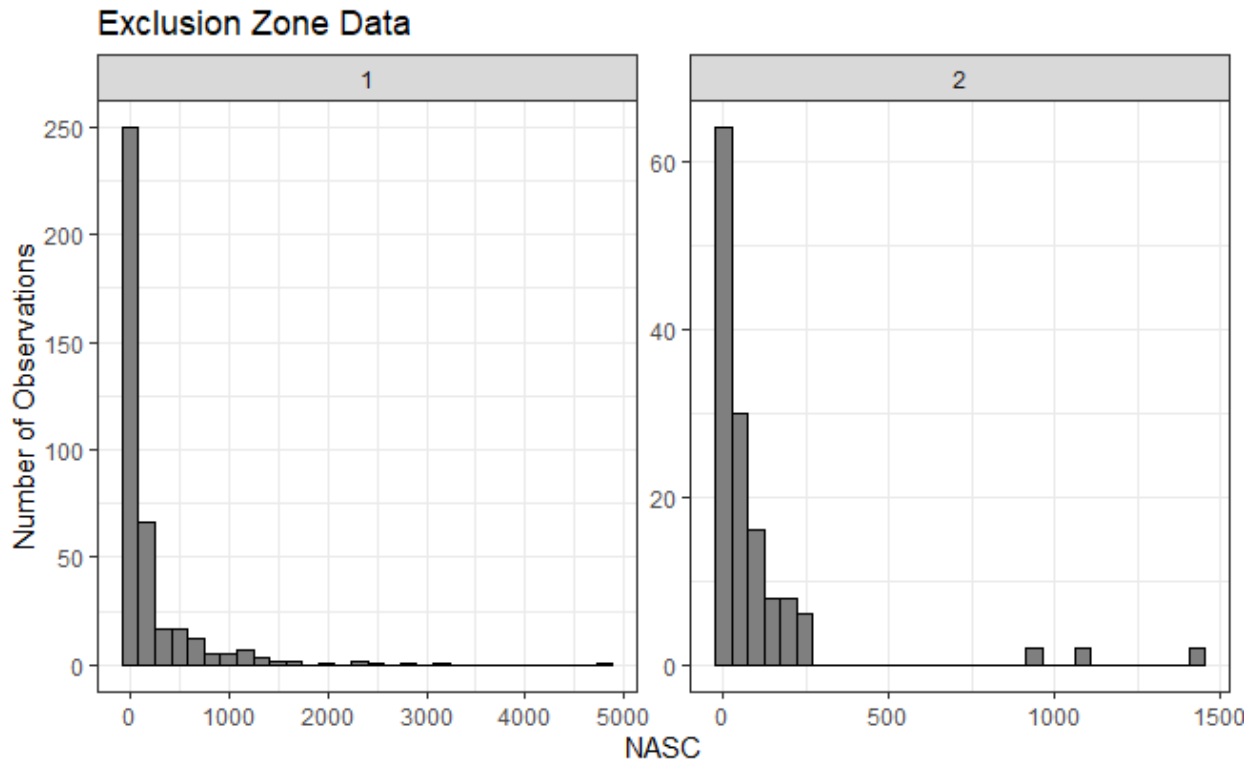


Figure 64. Histogram of NASC values for each transect for pass 1 and pass 2 within the exclusion zone.

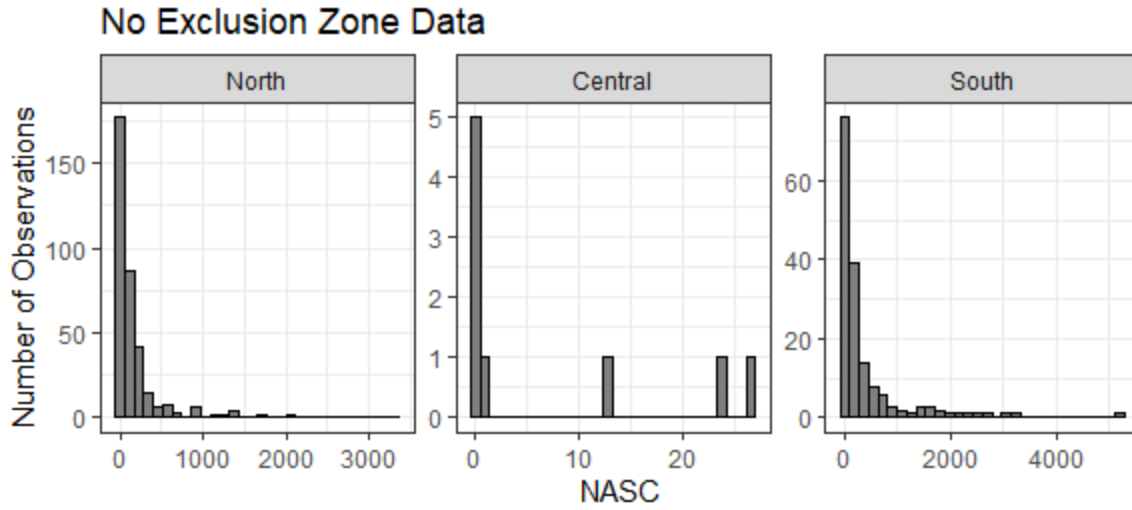


Figure 65. Histogram of NASC values for each transect for pass 1 above the exclusion zone by survey region.

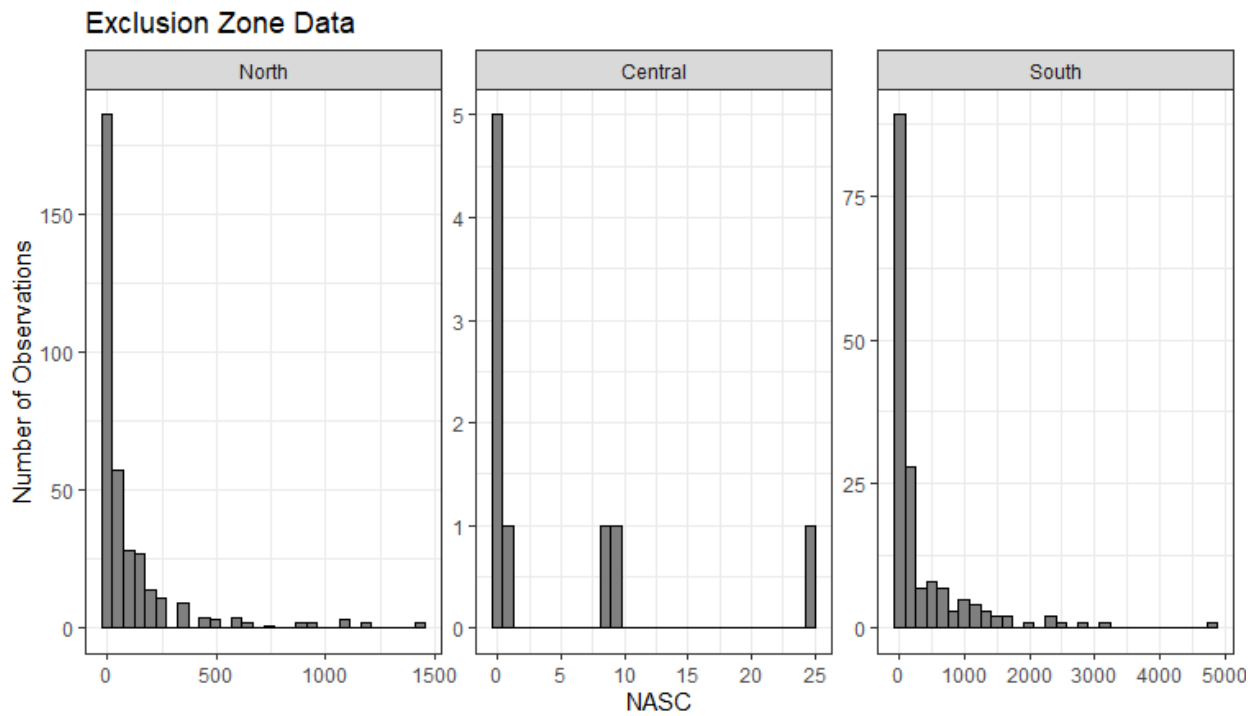


Figure 66. Histogram of NASC values for each transect for pass 1 within the exclusion zone by survey region.

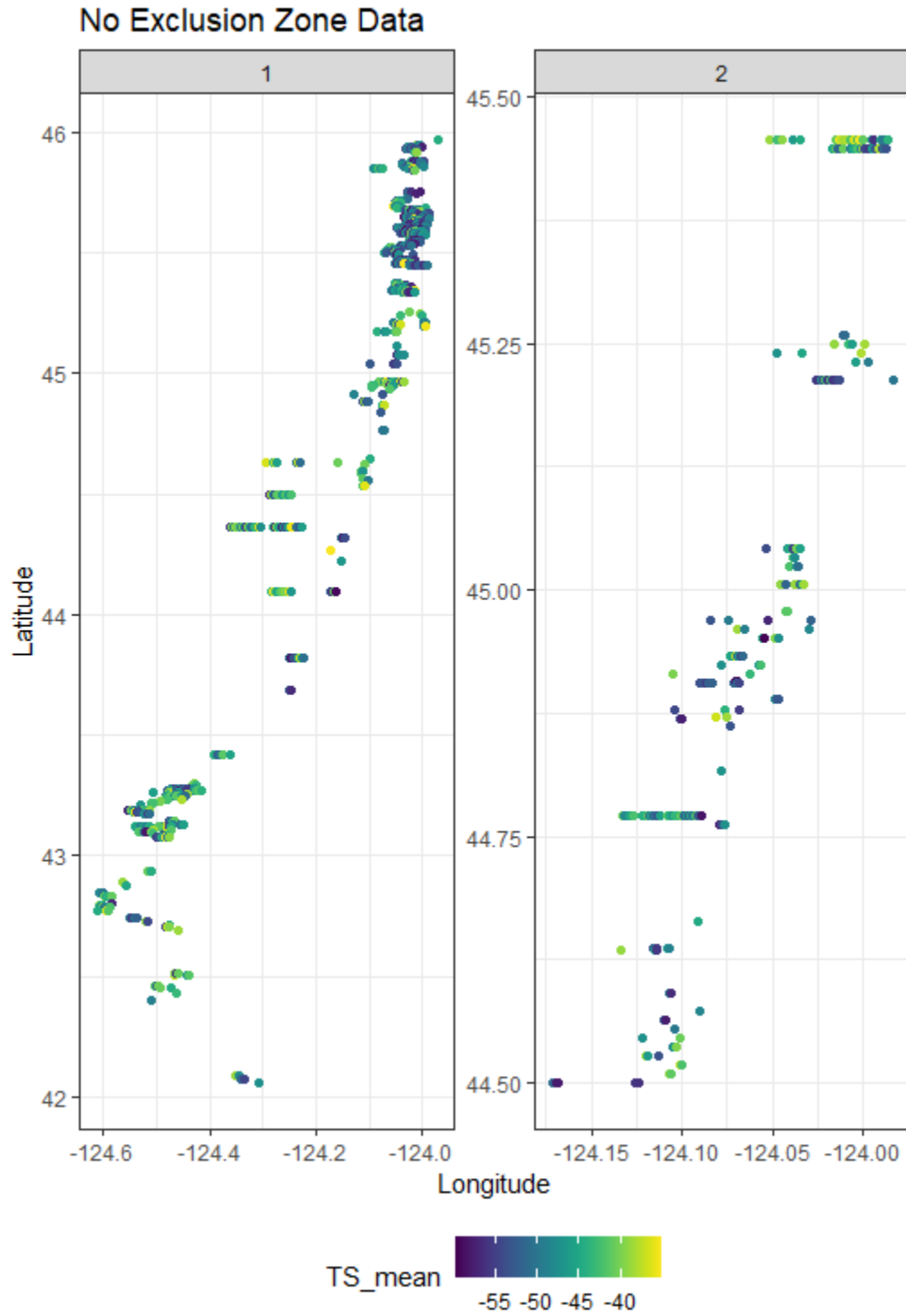


Figure 67. Locations of fish tracks identified during pass 1 and pass 2 above the exclusion zone.

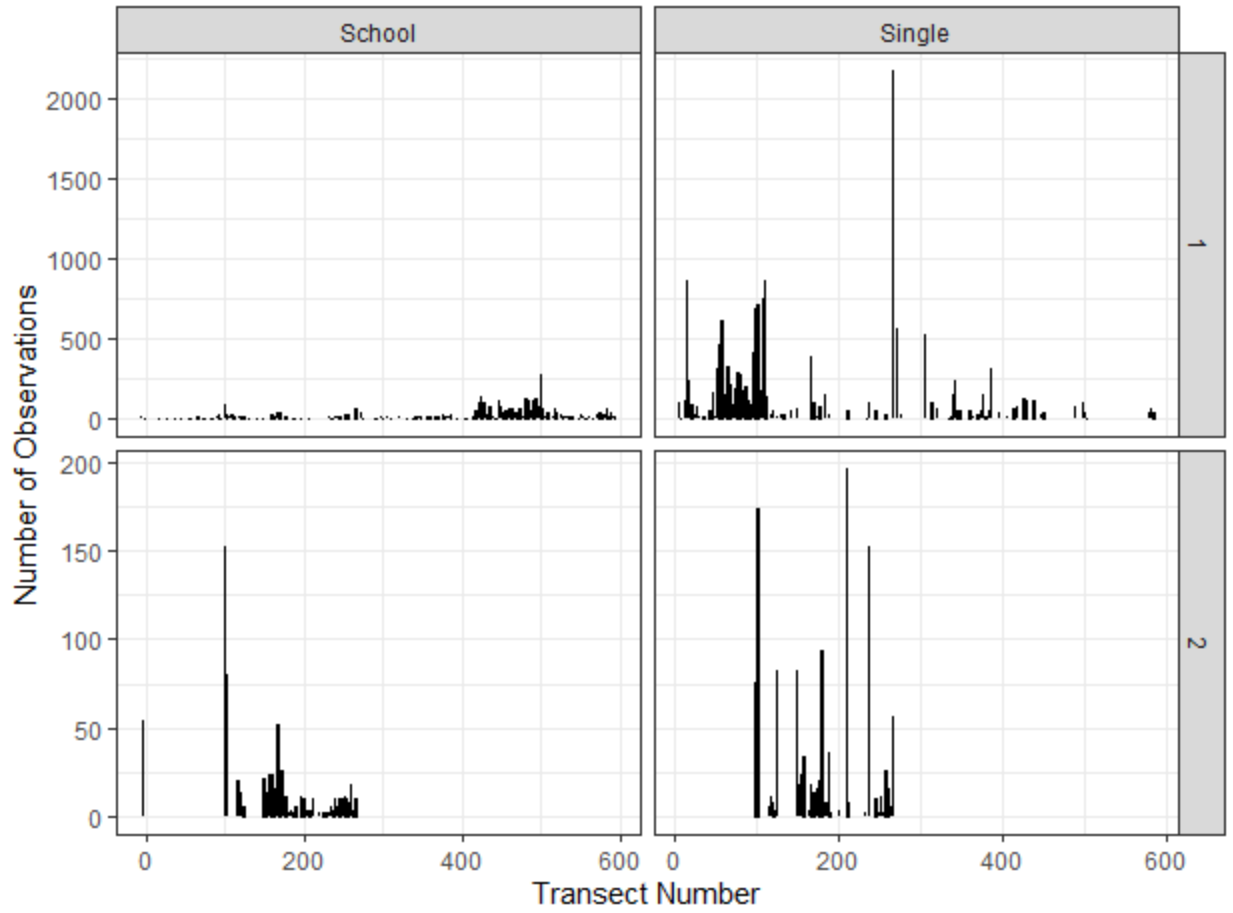


Figure 68. Number of fish schools and fish tracks identified by transect number and pass above the exclusion zone.

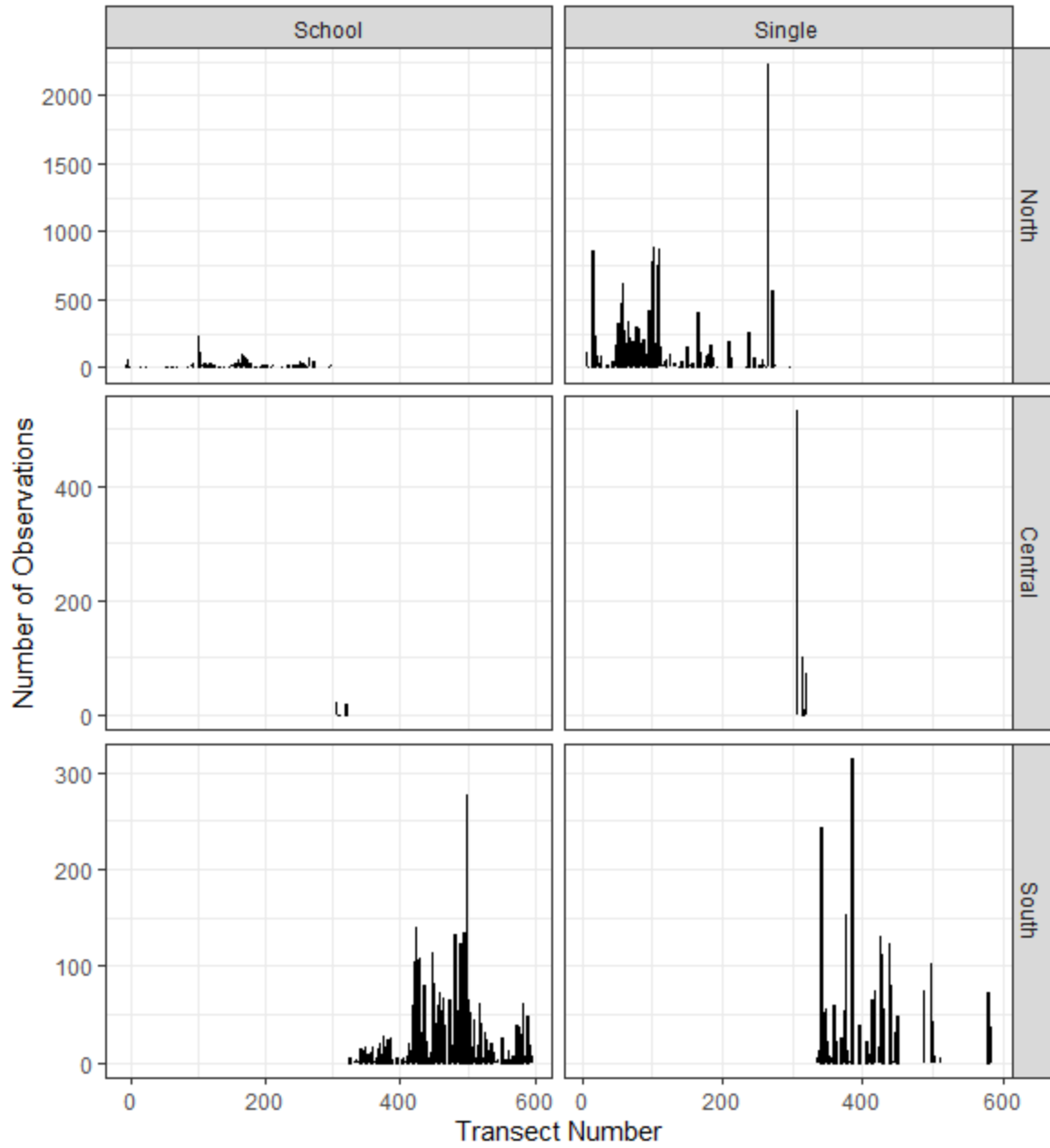


Figure 69. Number of fish school and fish tracks identified above the exclusion zone by region for each transect.

POPULATION ESTIMATE

DESIGN BASED

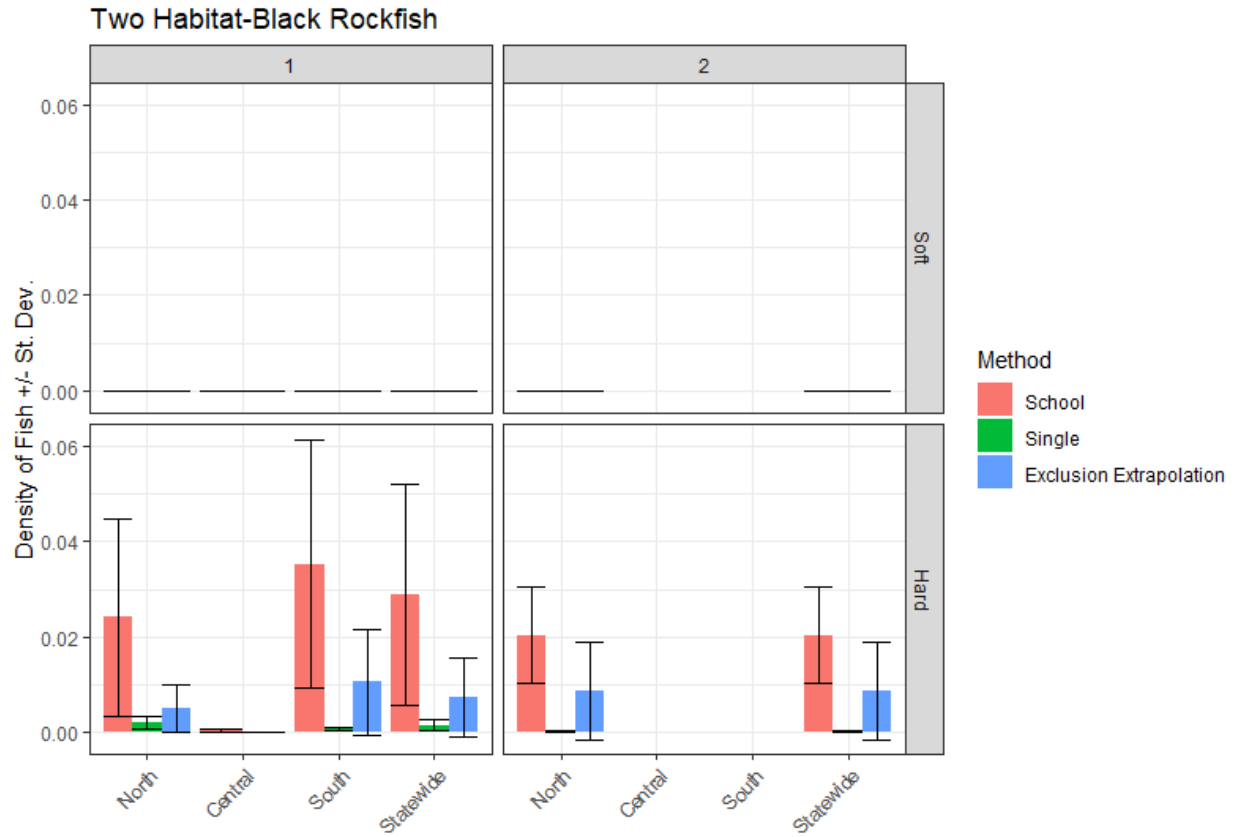


Figure 70. Density of Black Rockfish in the two-habitat model for pass 1 and pass 2 as detected in schools, as single targets and for the extrapolation of schools into the near bottom exclusion zone.

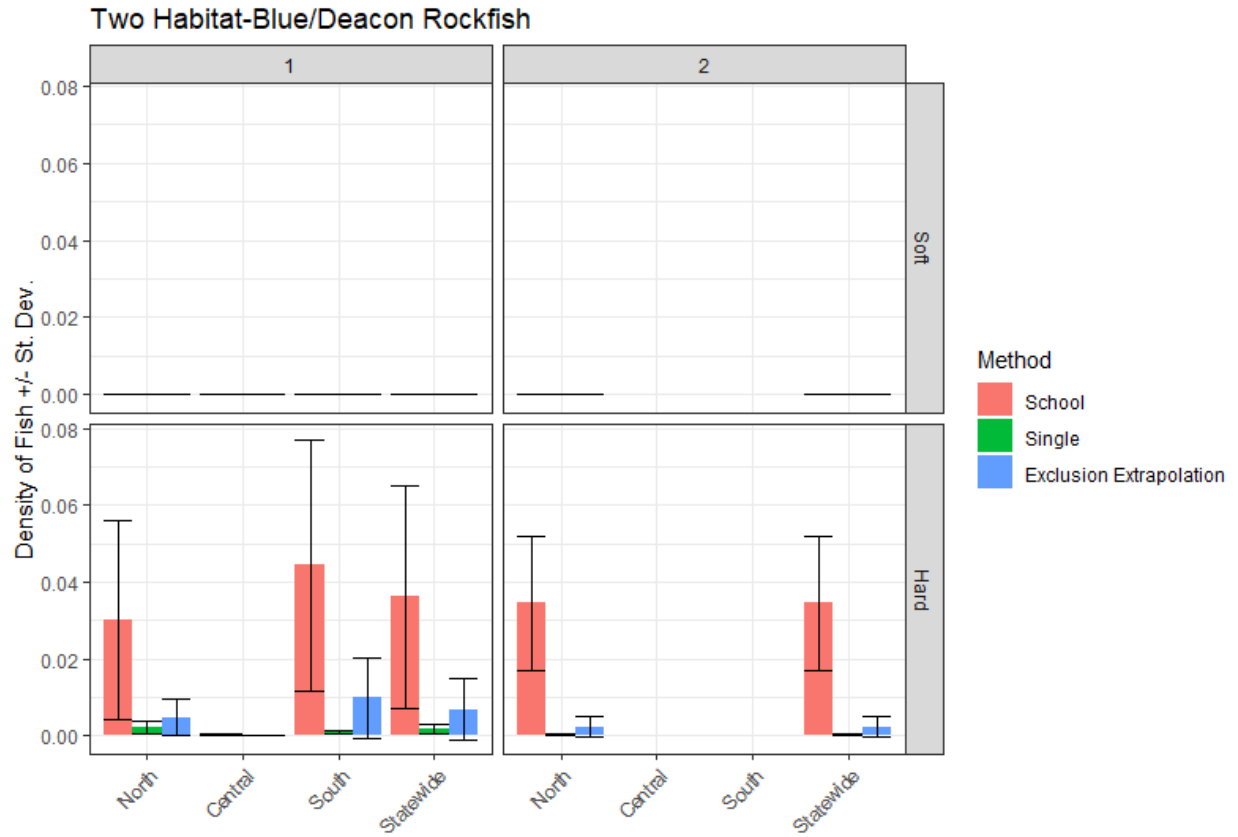


Figure 71. Density of Blue/Deacon Rockfish in the two-habitat model for pass 1 and pass 2 as detected in schools, as single targets and for the extrapolation of schools into the near bottom exclusion zone.

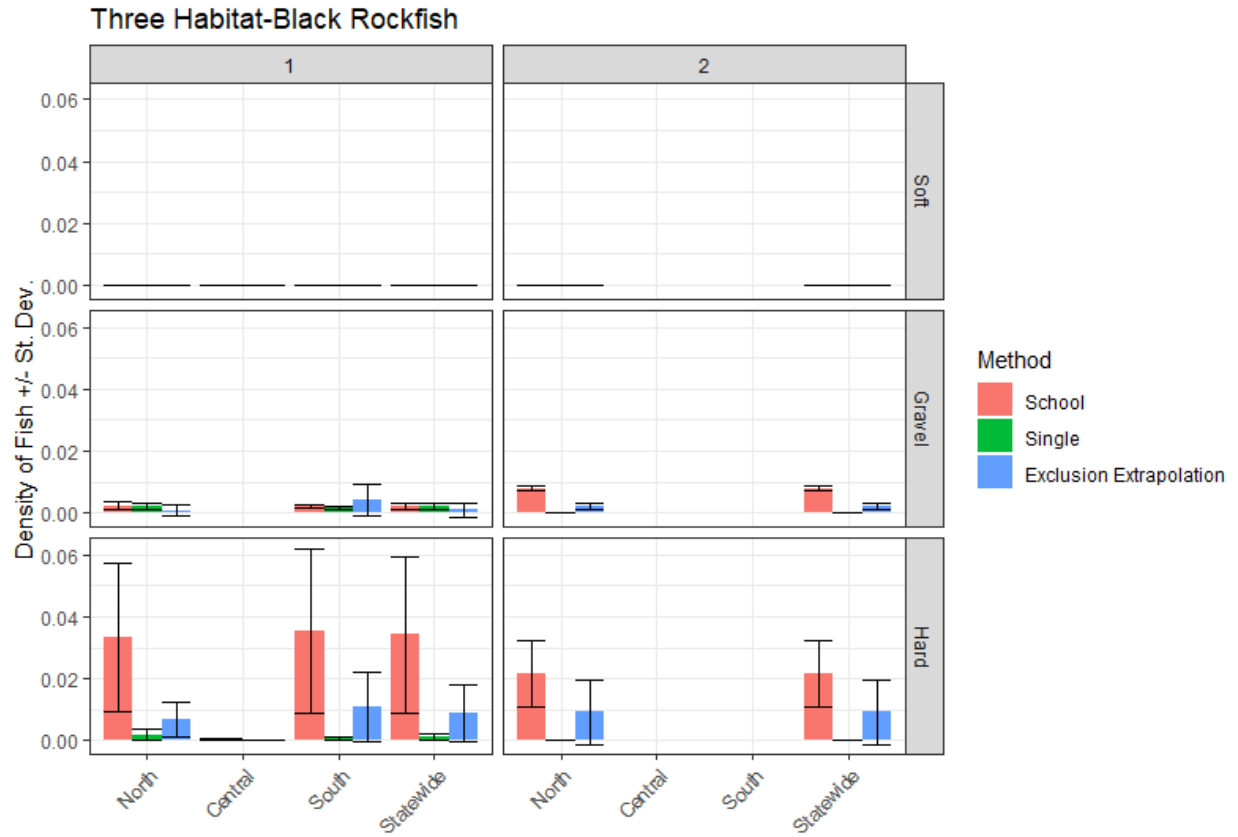


Figure 72. Density of Black Rockfish in the three-habitat model for pass 1 and pass 2 as detected in schools, as single targets and for the extrapolation of schools into the near bottom exclusion zone.

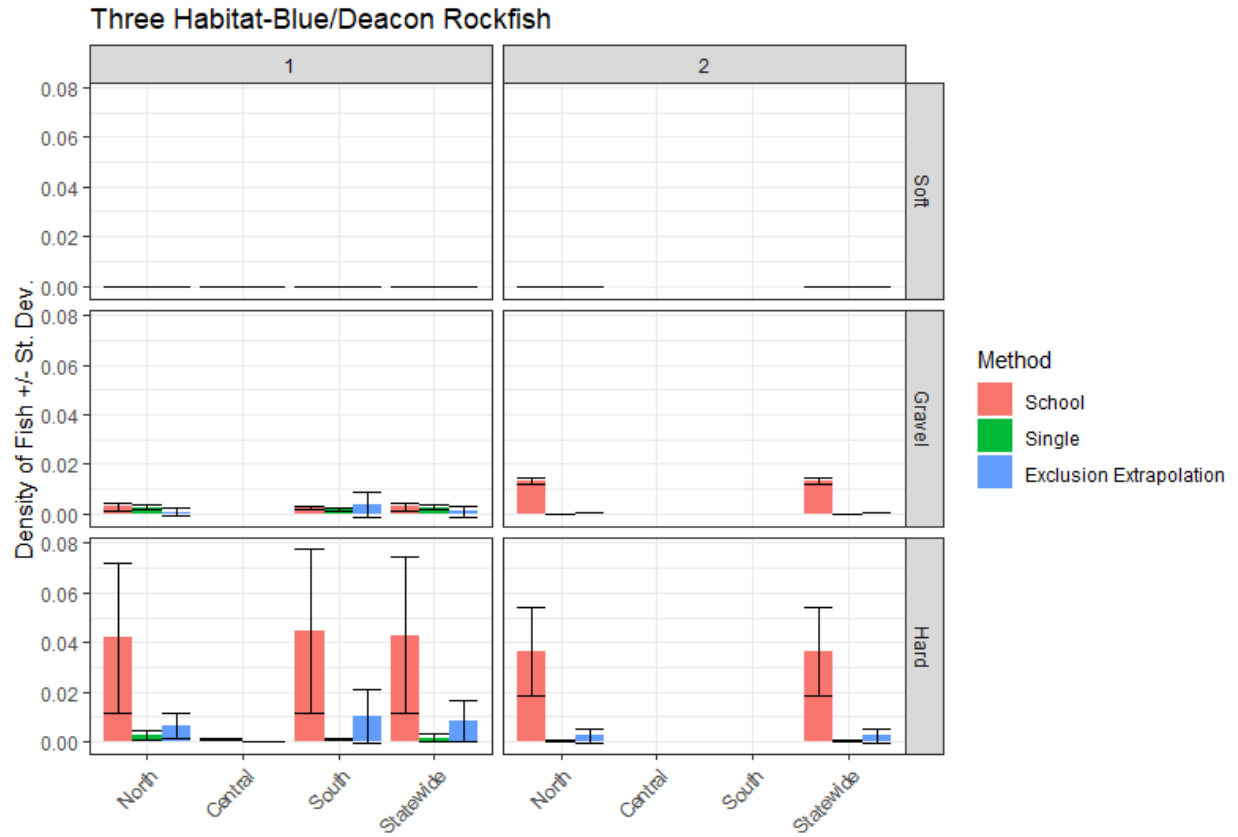


Figure 73. Density of Blue/Deacon Rockfish in the three-habitat model for pass 1 and pass 2 as detected in schools, as single targets and for the extrapolation of schools into the near bottom exclusion zone.

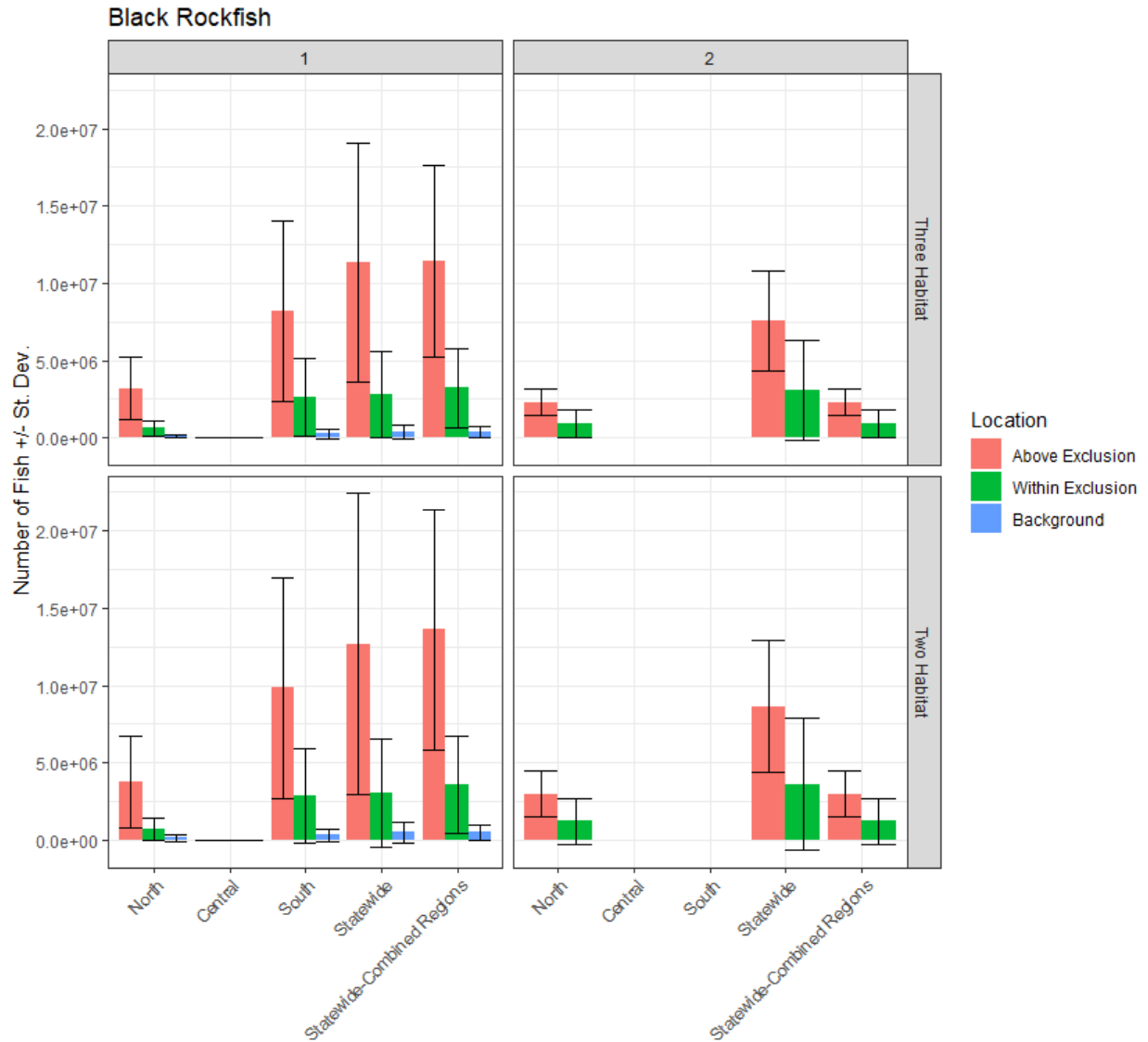


Figure 74. Number of Black Rockfish above the exclusion zone, within the exclusion zone and in the background regions for the two and three habitat methods observed during pass 1 and pass 2 in each region. Statewide- was calculated using an average statewide density and the total habitat area for the state. Statewide-combined: summed up the abundances in each of the three regions. Above exclusion zone includes single targets and fish schools observed at heights off bottom >1 m. Within exclusion zone only include fish schools within 1 m of the bottom. Background areas are areas of a reef (as defined from the acoustics) that are not associated with any fish (schools or single targets). Density data is derived from BASSCam drops that occurred away from observations of fish schools and single targets. Two habitat denotes allocation to soft or hard substrate and three habitat denotes allocation to soft, gravel or hard substrate.

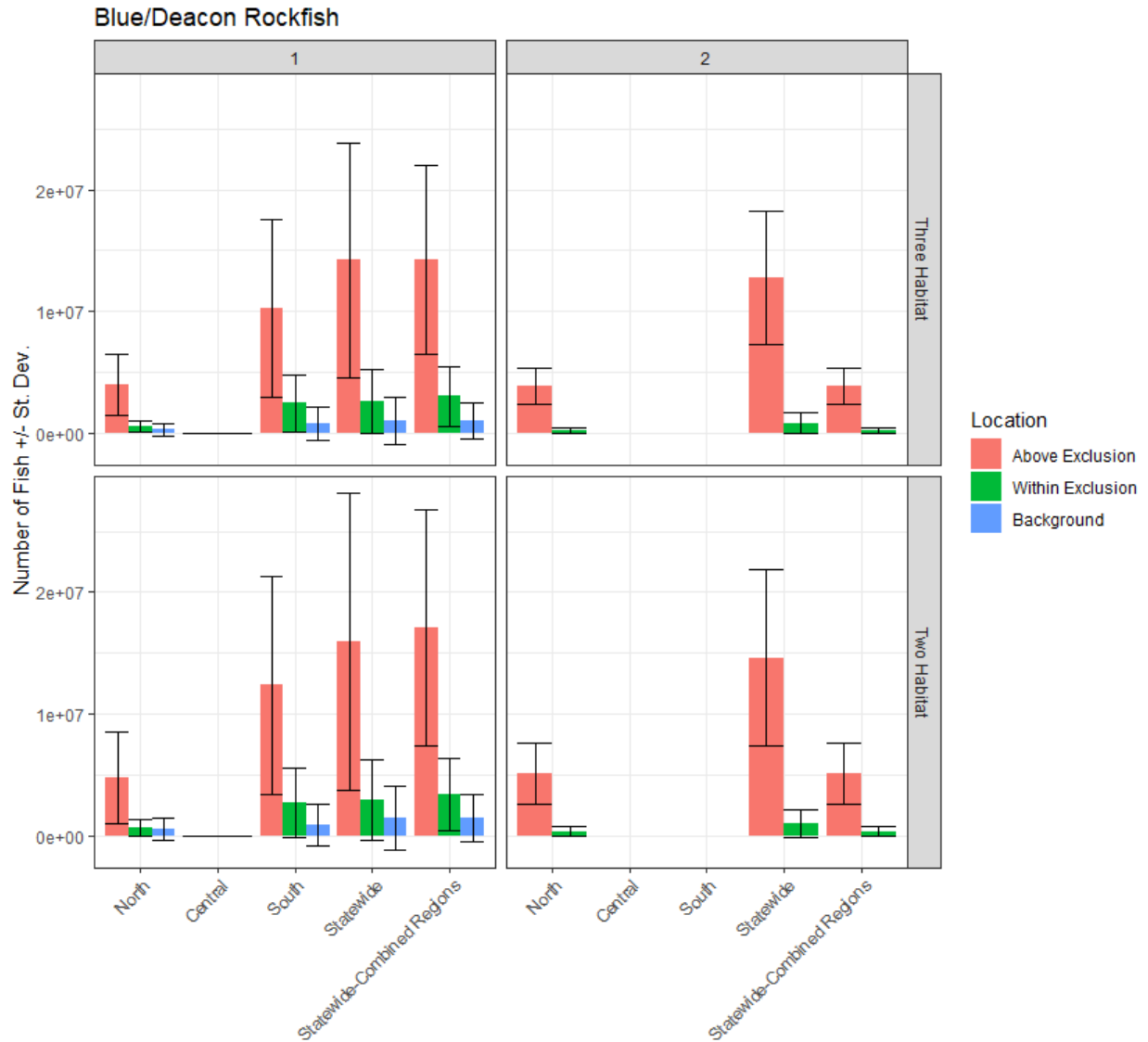


Figure 75. Number of Blue/Deacon Rockfish above the exclusion zone, within the exclusion zone and in the background regions for the two and three habitat methods observed during pass 1 and pass 2 in each region. Statewide- was calculated using an average statewide density and the total habitat area for the state. Statewide-combined: summed up the abundances in each of the three regions. Above exclusion zone includes single targets and fish schools observed at heights off bottom >1 m. Within exclusion zone only include fish schools within 1 m of the bottom. Background areas are areas of a reef (as defined from the acoustics) that are not associated with any fish (schools or single targets). Density data is derived from BASSCam drops that occurred away from observations of fish schools and single targets. Two habitat denotes allocation to soft or hard substrate and three habitat denotes allocation to soft, gravel or hard substrate.

MODEL BASED

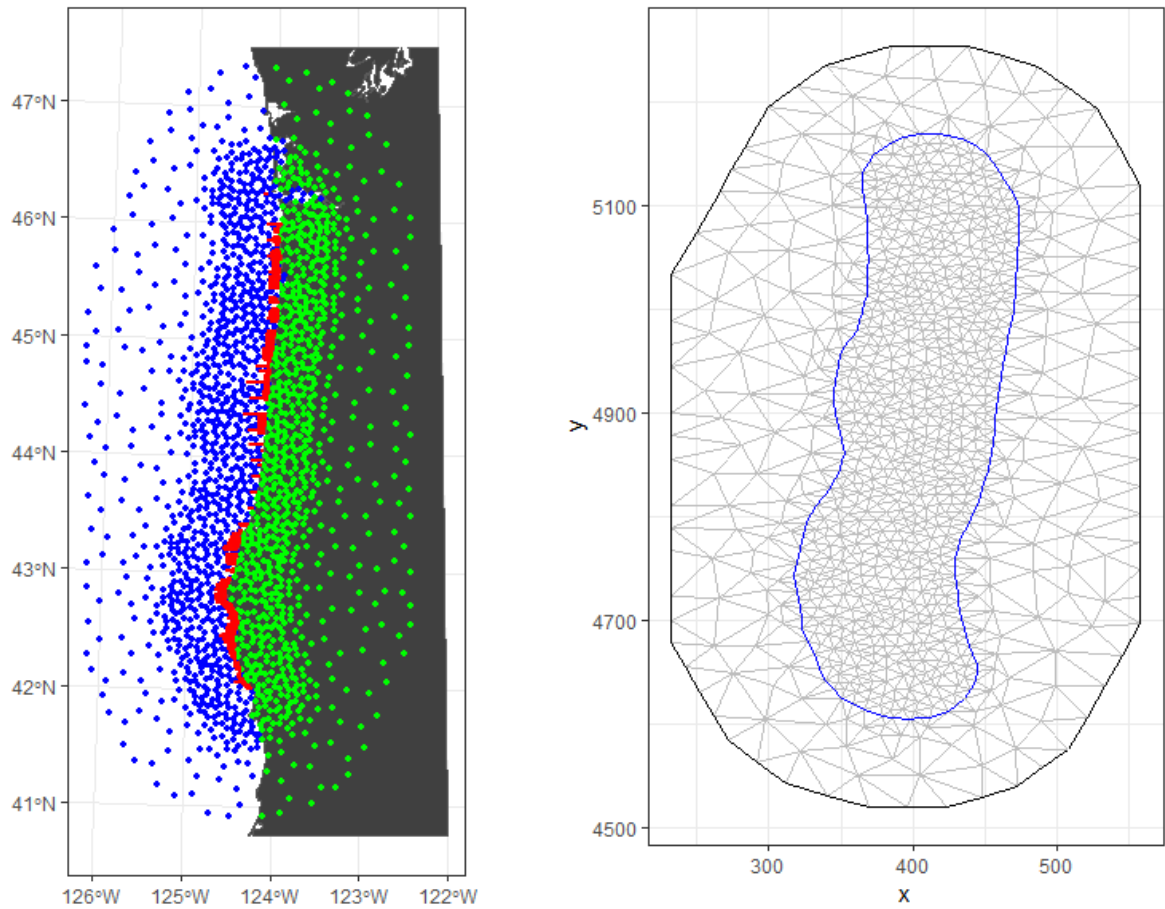


Figure 76. INLA mesh used to develop the spatiotemporal model for Black and Blue/Deacon Rockfish for the pass 1 and with pass as random effect models. On the left, blue dots denote knots that were included in the analysis and green dots denote knots that were excluded due to being on land. The red dots are the survey locations. The figure on the right depicts the resolution of the interior and exterior mesh used prior to barrier exclusion.

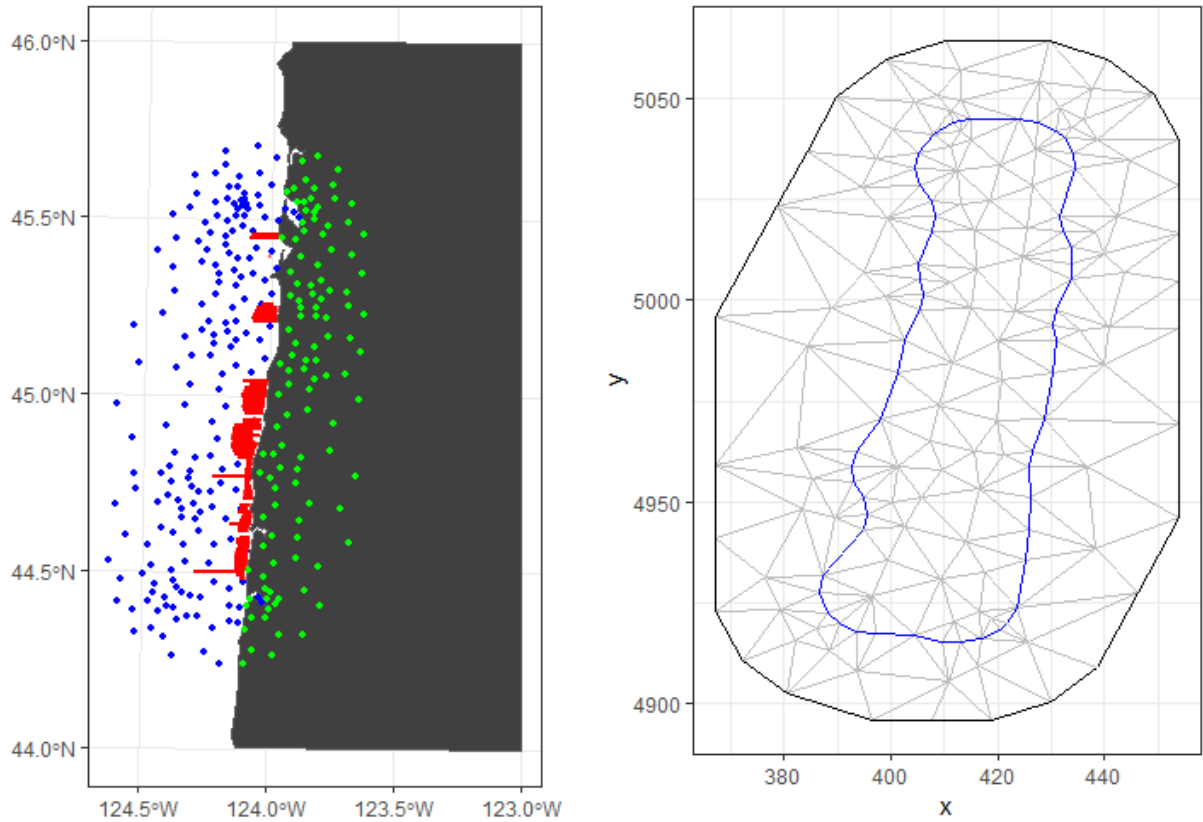


Figure 77. INLA mesh used to develop the spatiotemporal model for Black and Blue/Deacon Rockfish for the pass 2 models. On the left, blue dots denote knots that were included in the analysis and green dots denote knots that were excluded due to being on land. The red dots are the survey locations. The figure on the right depicts the resolution of the interior and exterior mesh used prior to barrier exclusion.

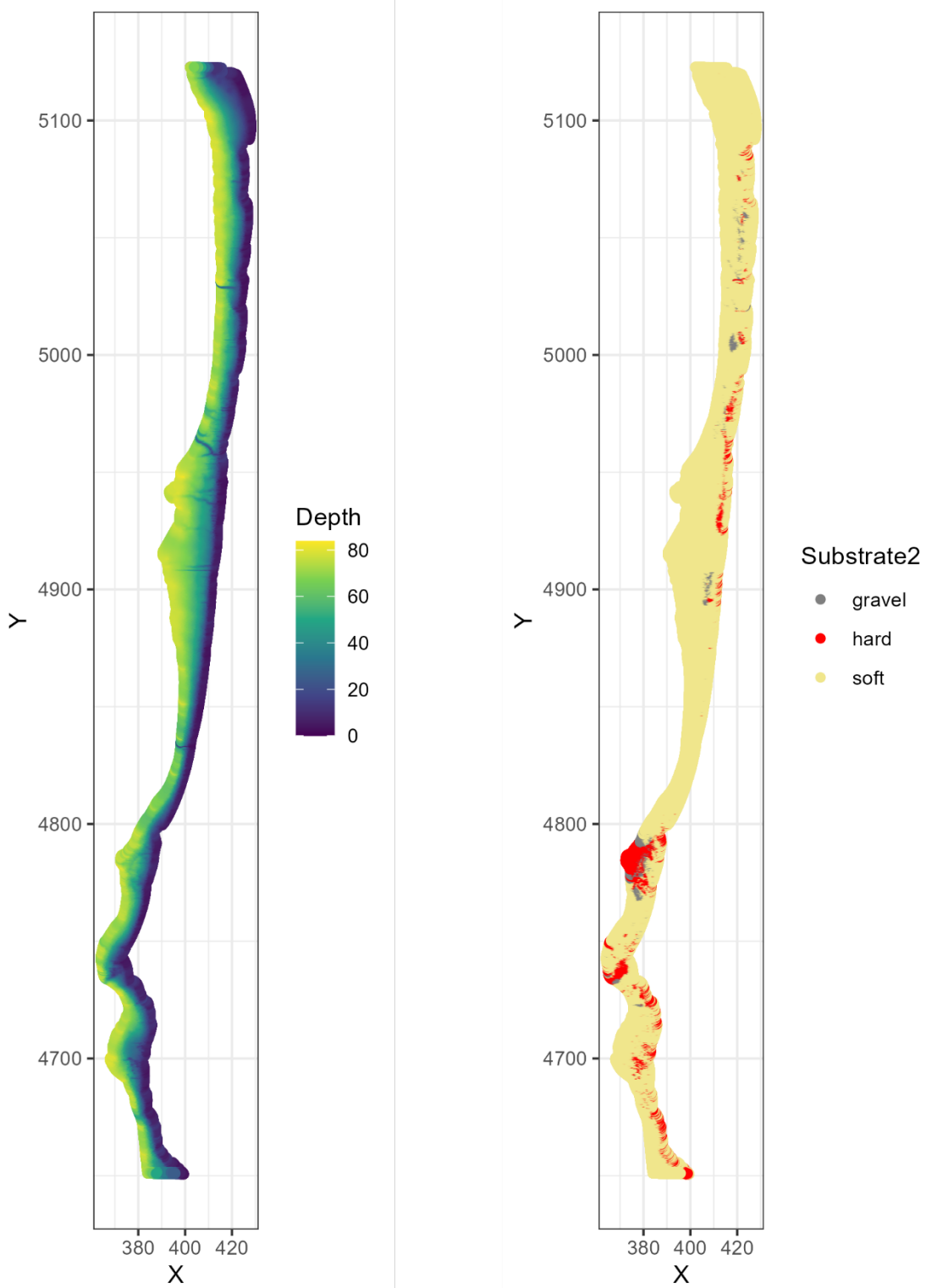


Figure 78. Depth and primary habitat for each 50 x 50 m cell used to predict fish populations with the best fit sdmTMB models.

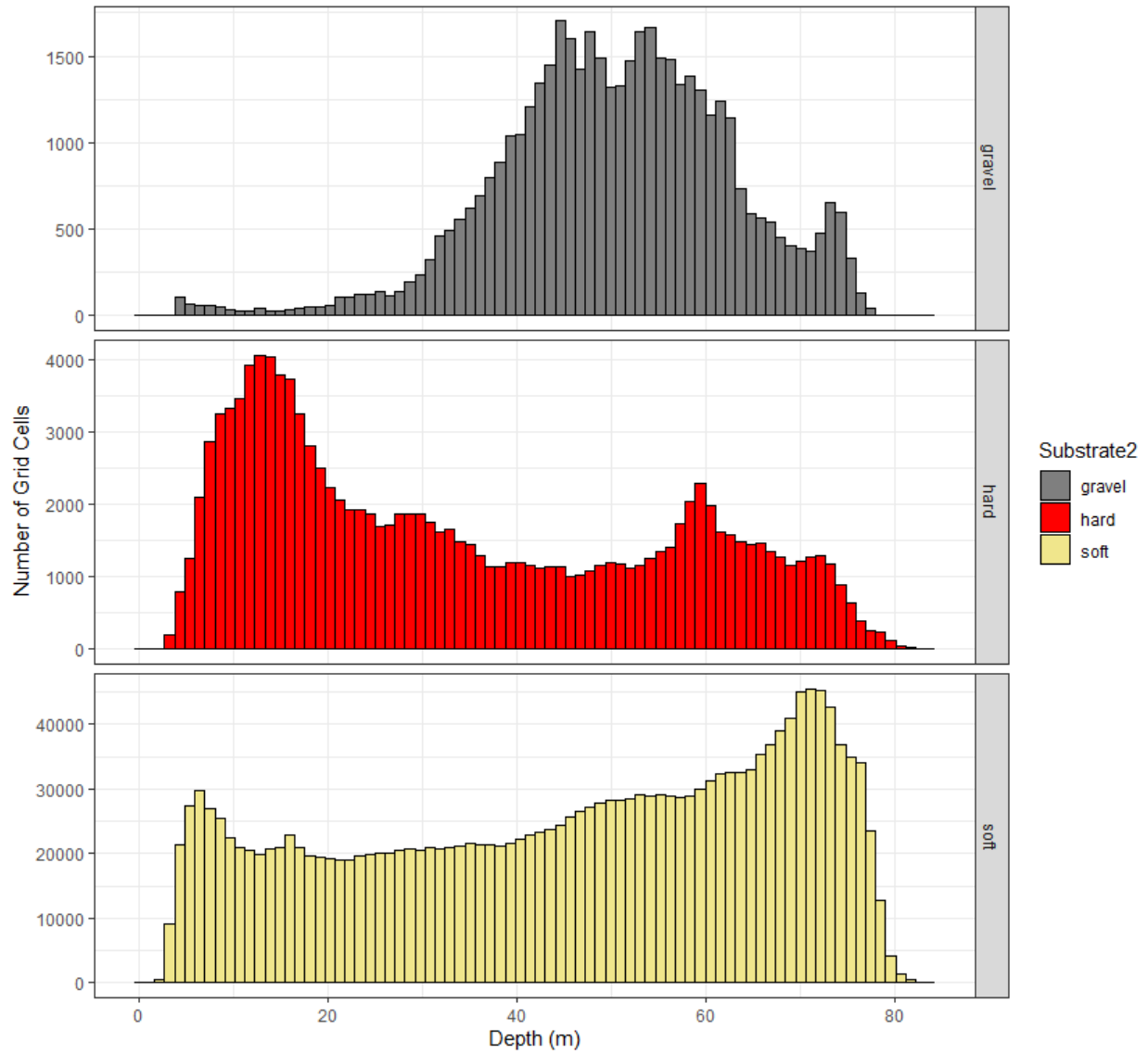


Figure 79. Histogram of how many grid cells were observed in each habitat type by depth.

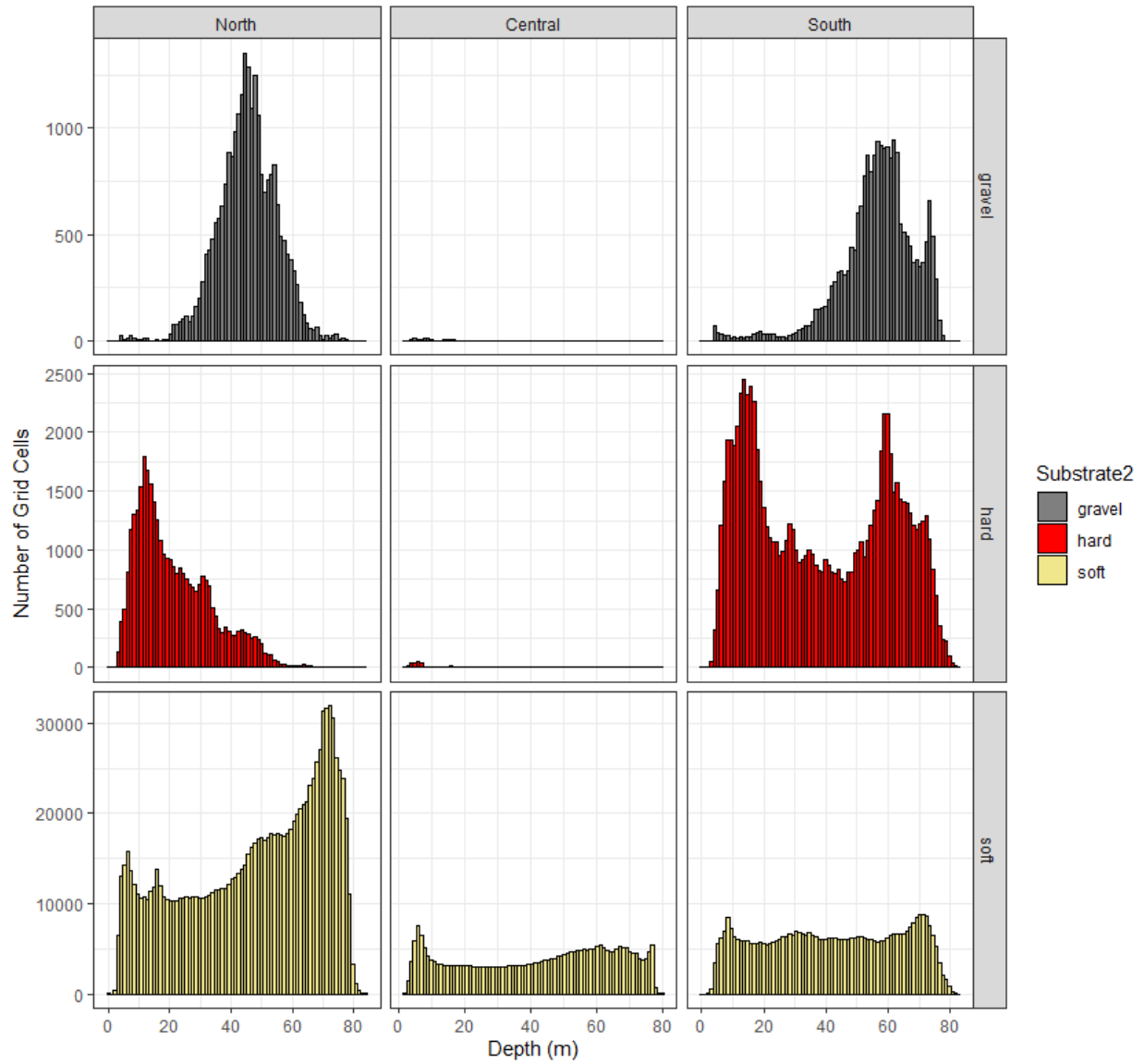


Figure 80. Histogram of how many grid cells were observed in each habitat type by depth in each region.

BLACK

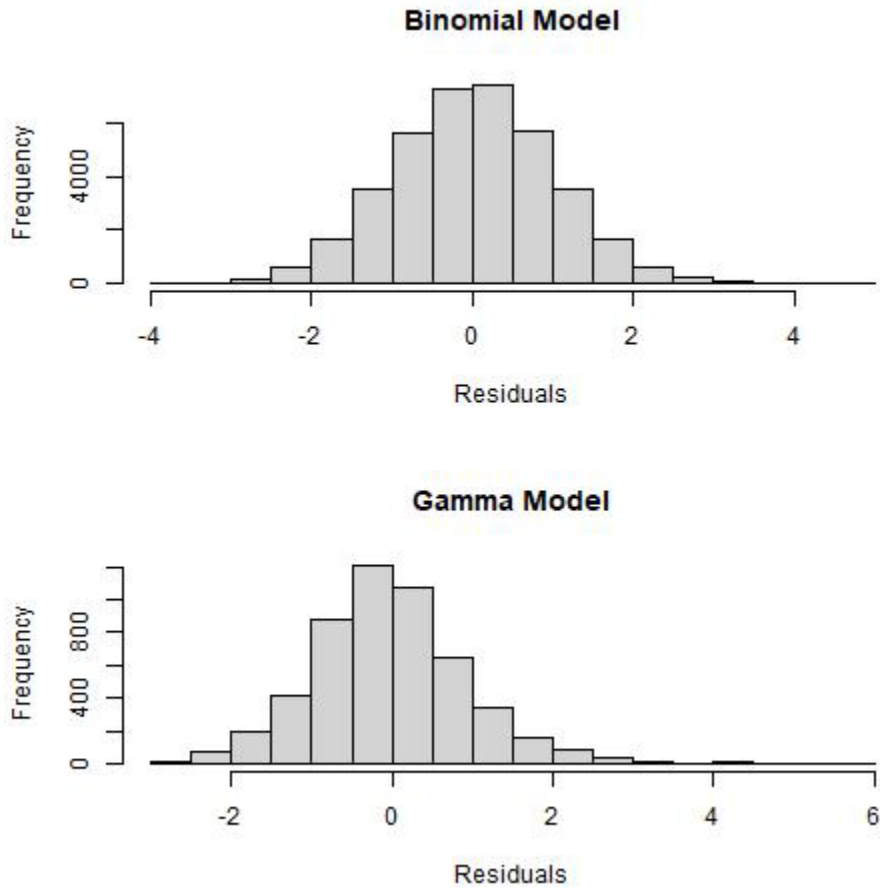


Figure 81. MCMC derived residuals for the best-fit Black model for the binomial component of the model (upper) and the gamma component of the model (lower) for pass 1.

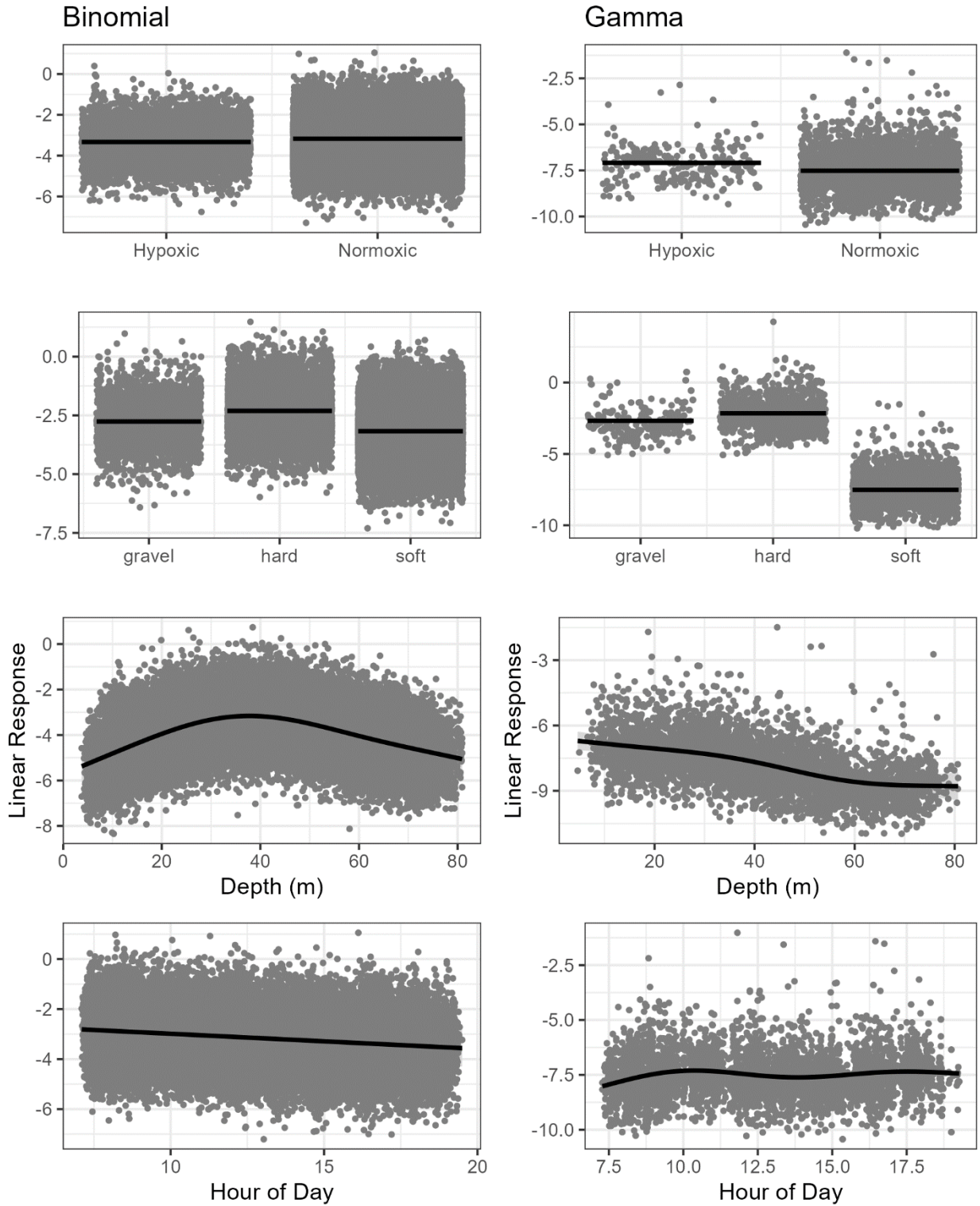


Figure 82. Linear response of each variable for the Black Rockfish model, plots on the left are for the binomial model which was modeled using a logit link and plots on the right are for positive data only and modeled using a gamma model with a log link for pass 1.

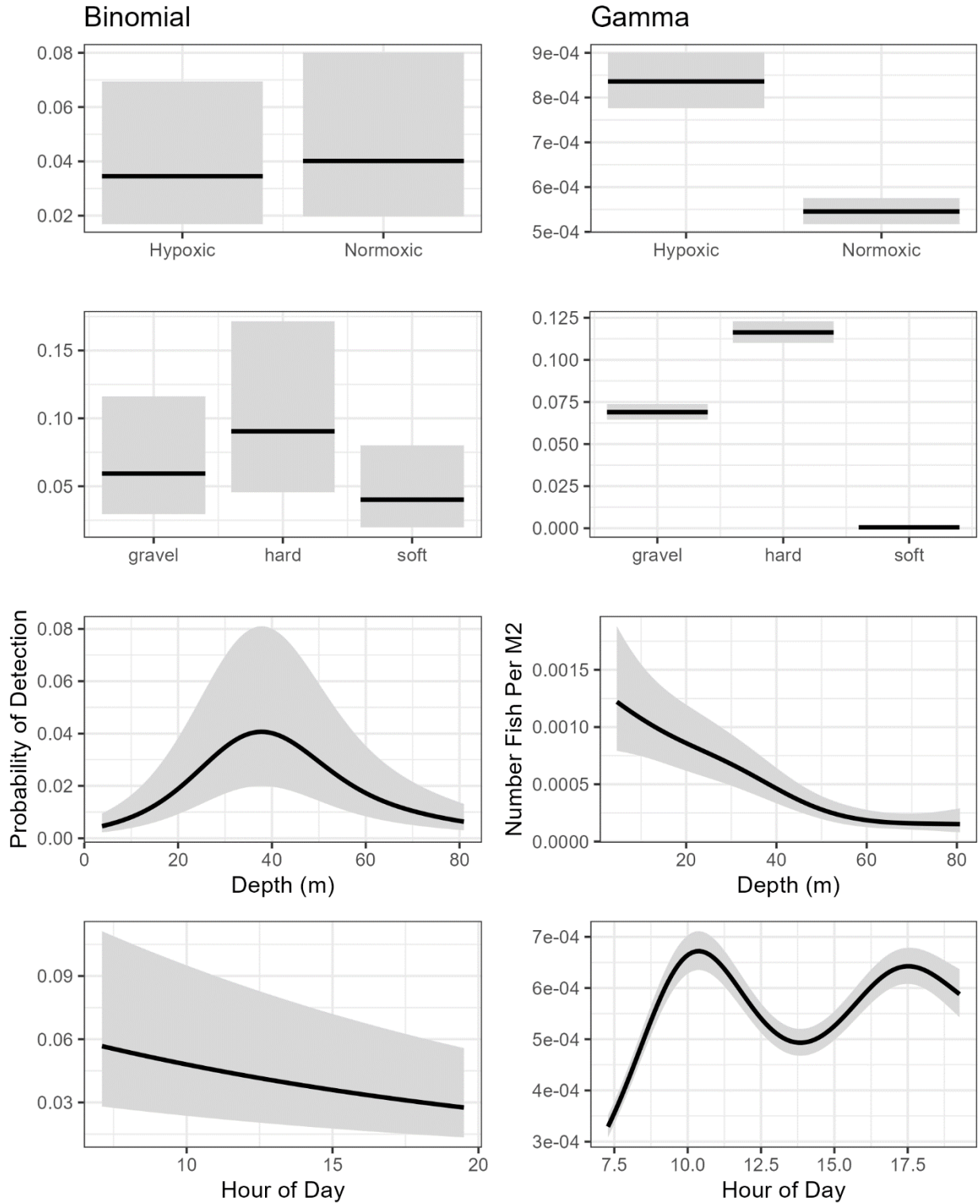


Figure 83. Affect of explanatory variables on the density for the Black Rockfish model, plots on the left are for the binomial model which was modeled using a logit link and plots on the right are for positive data only and modeled using a gamma model with a log link for pass 1.

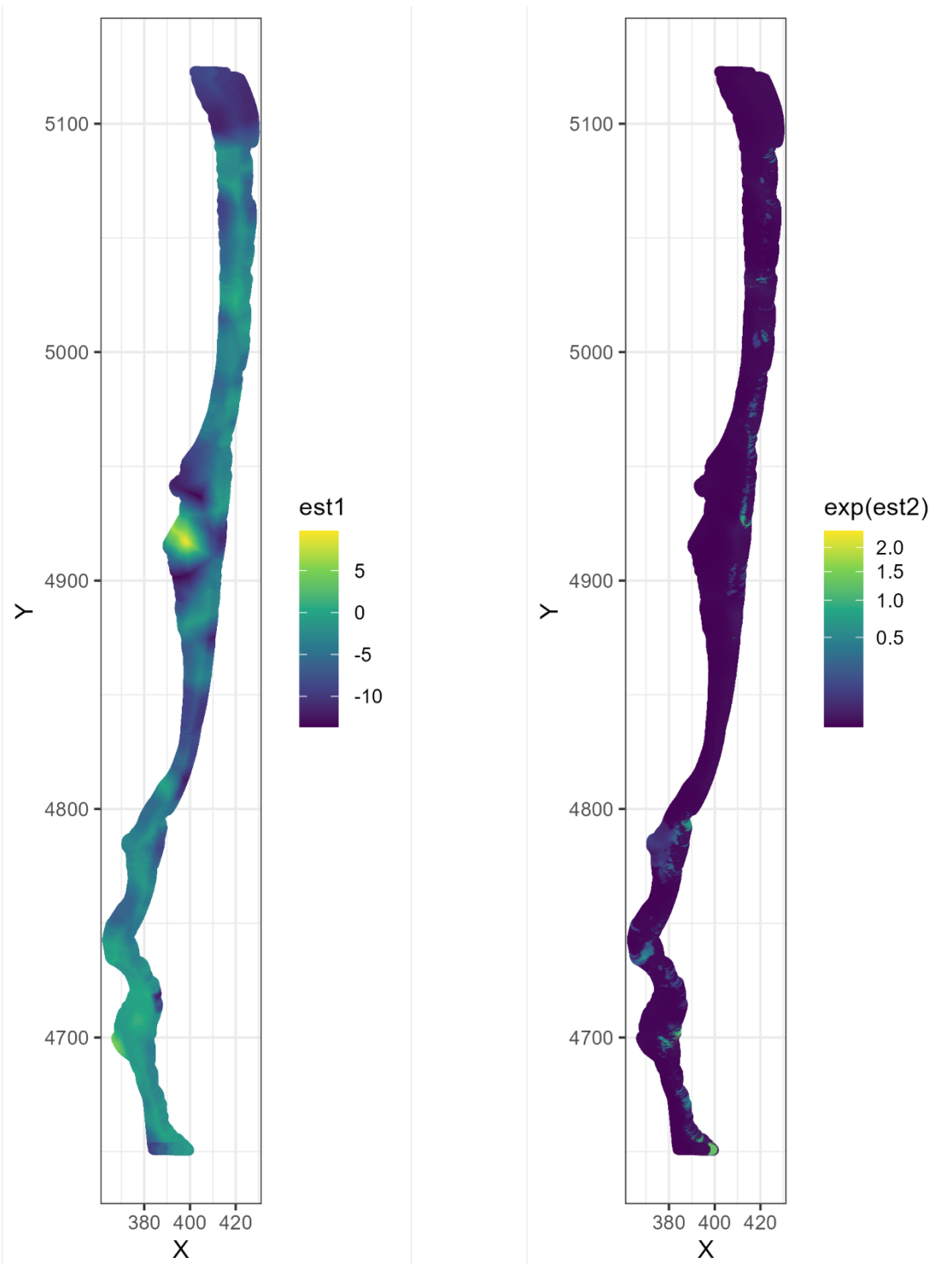


Figure 84. Predicted spatial estimates (including random effects) for the binomial (left) and gamma (right) models for Black Rockfish for pass 1.

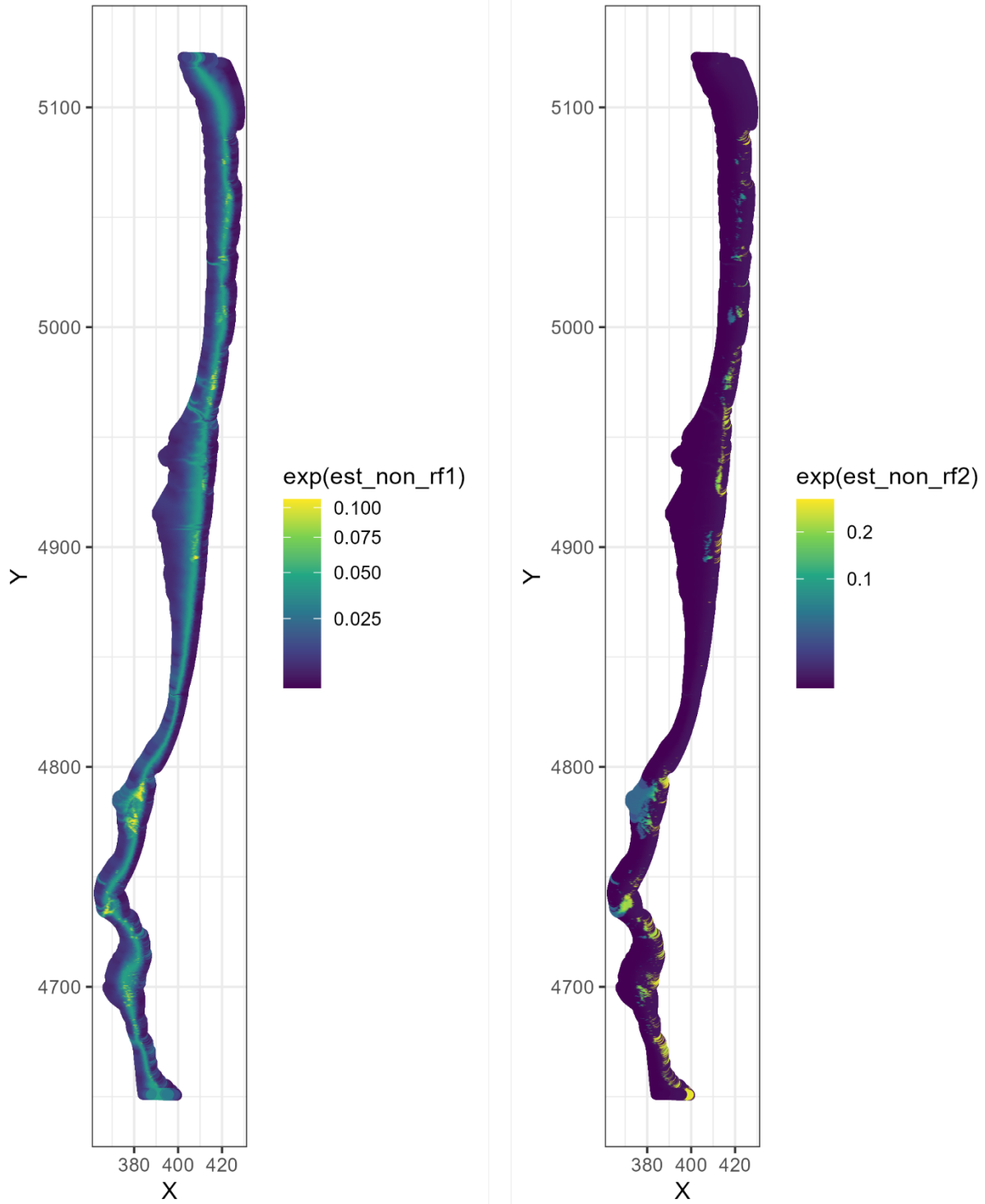


Figure 85. Predicted spatial estimates (not including random effects) for the binomial (left) and gamma (right) models for Black Rockfish for pass 1.

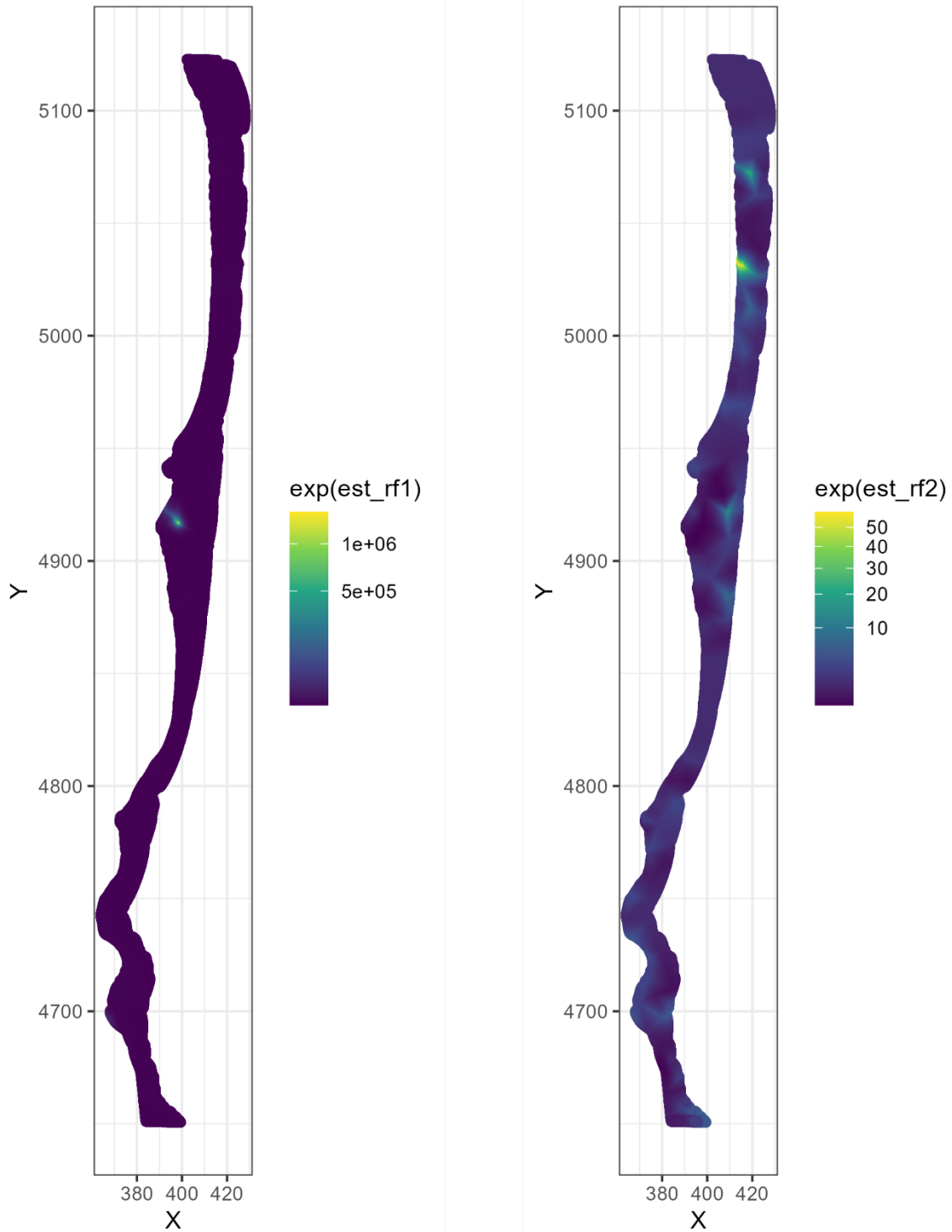


Figure 86. Predicted spatial estimates (just random effects) for the binomial (left) and gamma (right) models for Black Rockfish for pass 1.

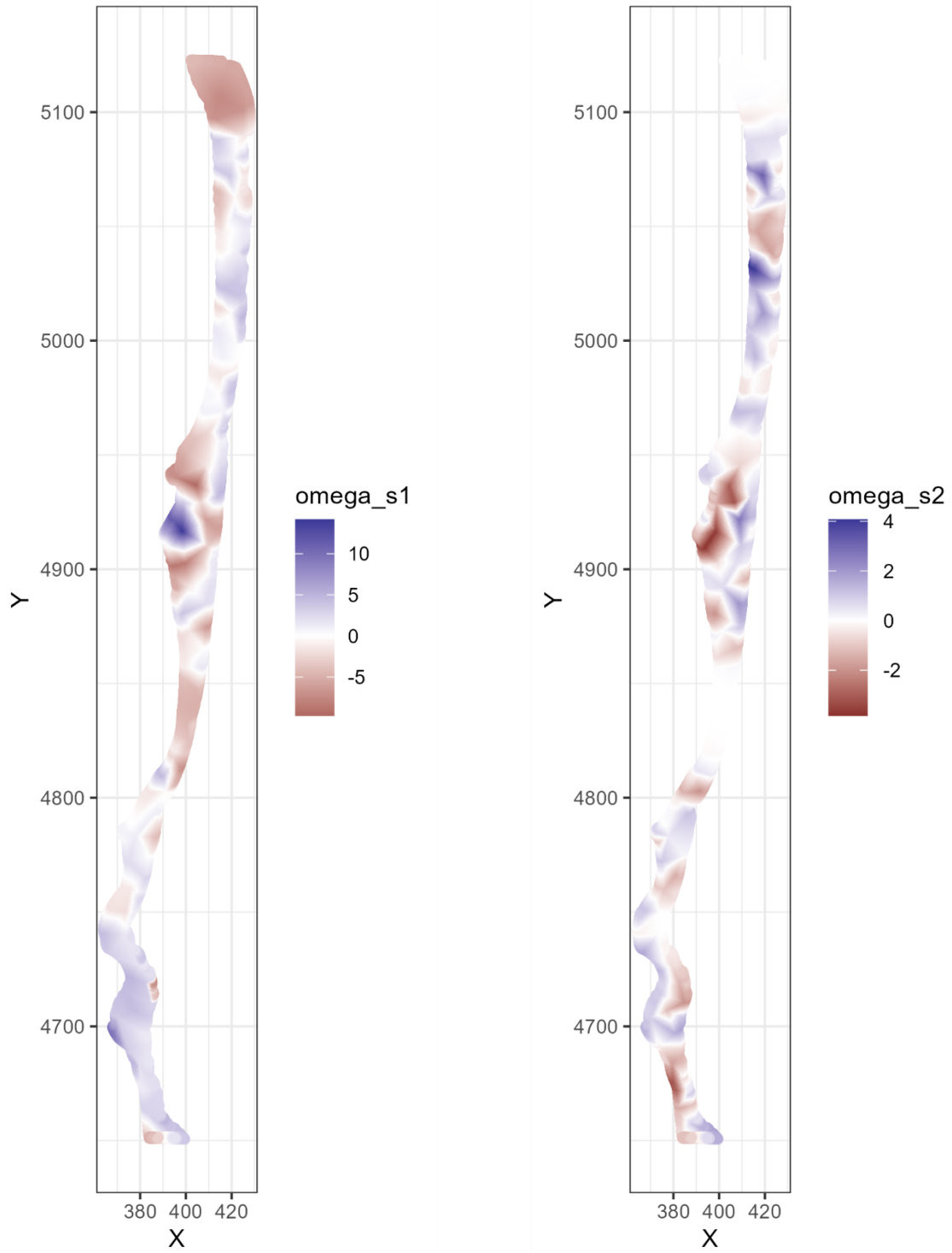


Figure 87. Predicted spatial random fields for the binomial (left) and gamma (right) models for Black Rockfish for pass 1.

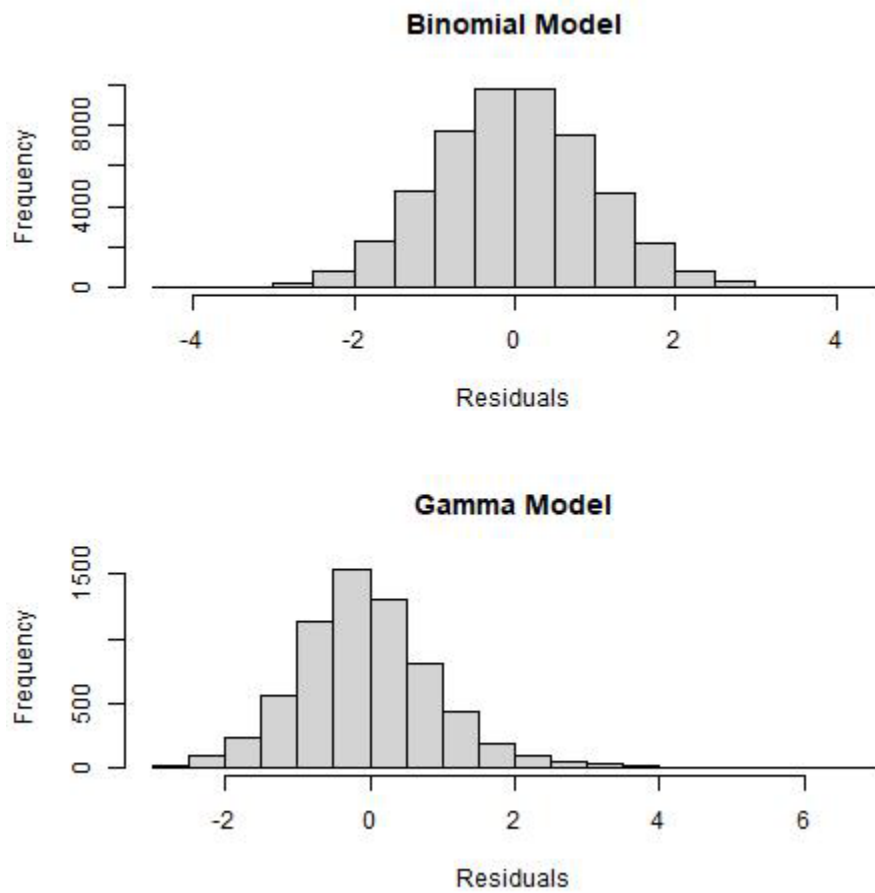


Figure 88. MCMC derived residuals for the best-fit Black Rockfish model for both the binomial (upper) and gamma (lower) components of the model, with pass as a random effect.

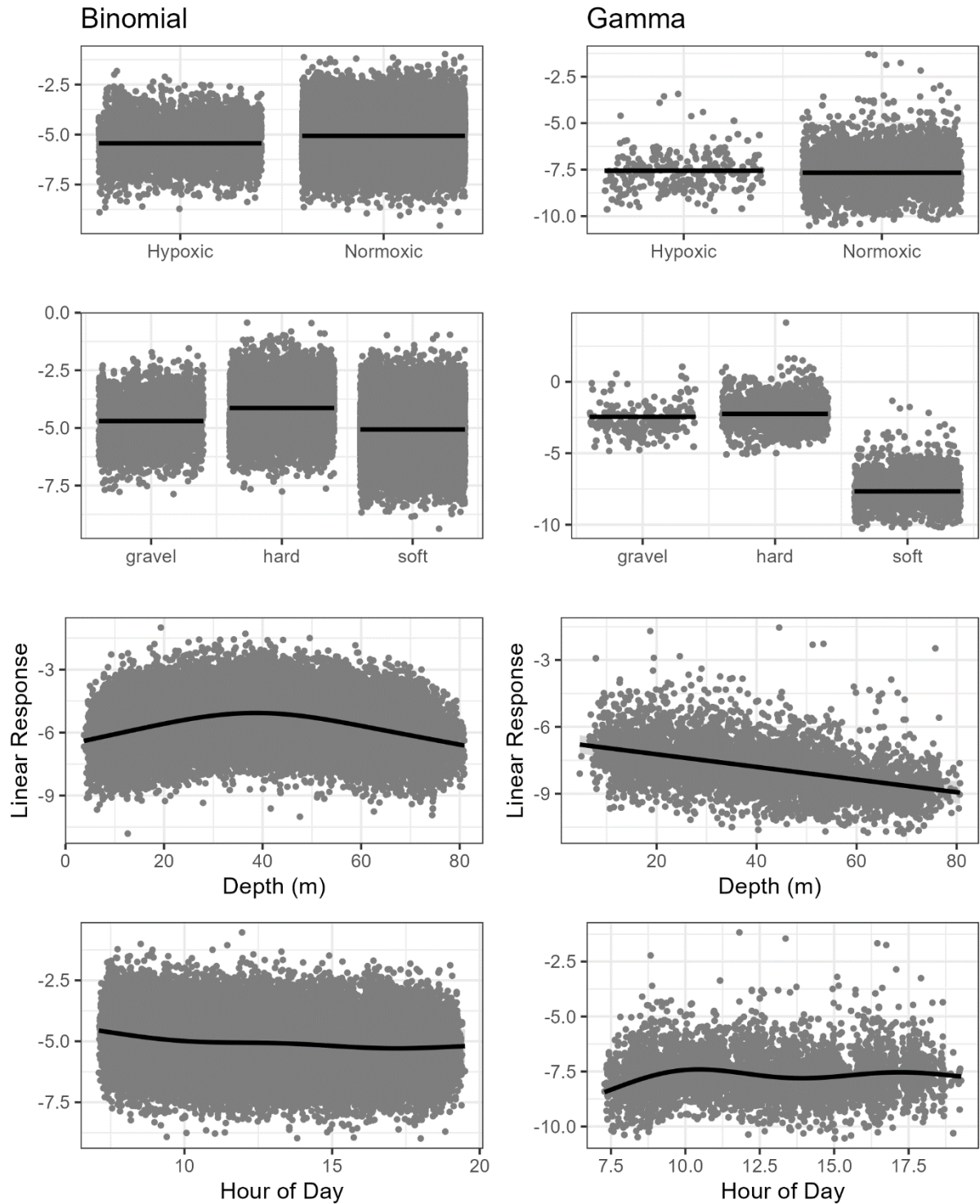


Figure 89. Linear response of each variable for the Black Rockfish model, plots on the left are for the binomial model which was modeled using a logit link and plots on the right are for positive data only and modeled using a gamma model with a log link with pass as a random effect.

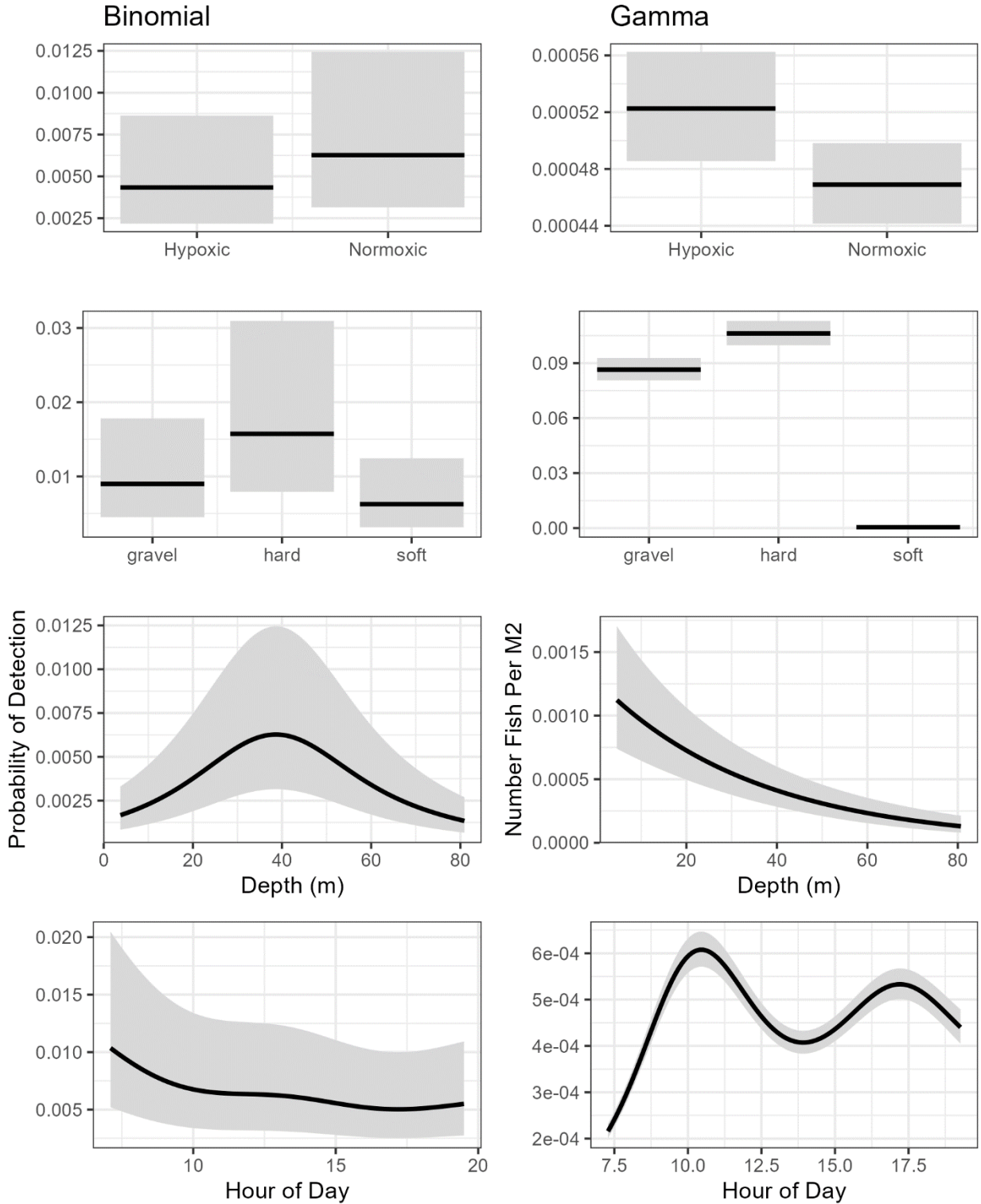


Figure 90. Affect of explanatory variables on the density for the Black Rockfish model, plots on the left are for the binomial model which was modeled using a logit link and plots on the right are for positive data only and modeled using a gamma model with a log link with pass as a random effect.

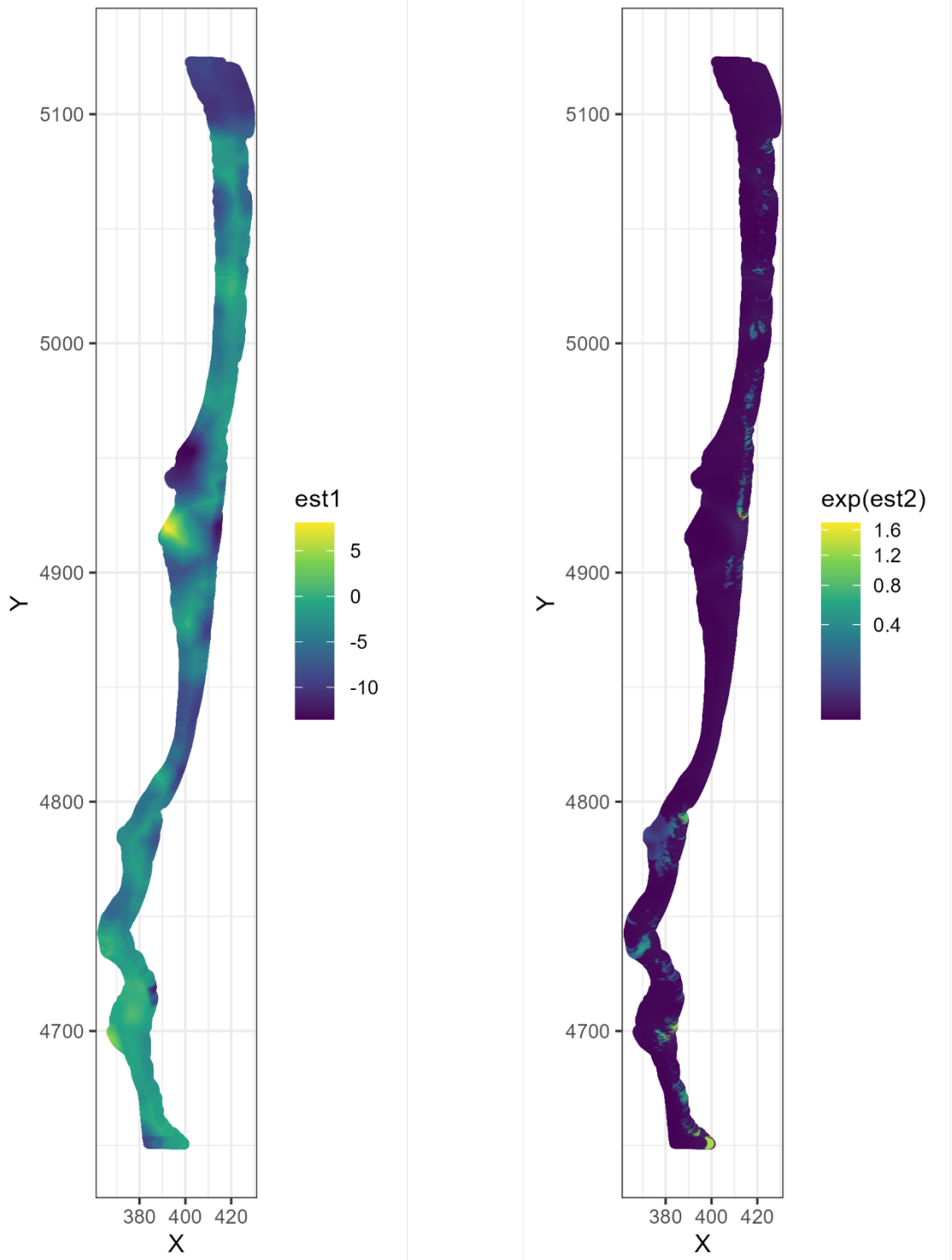


Figure 91. Predicted spatial estimates (including random effects) for the binomial (left) and gamma (right) models for Black Rockfish with pass as a random effect.

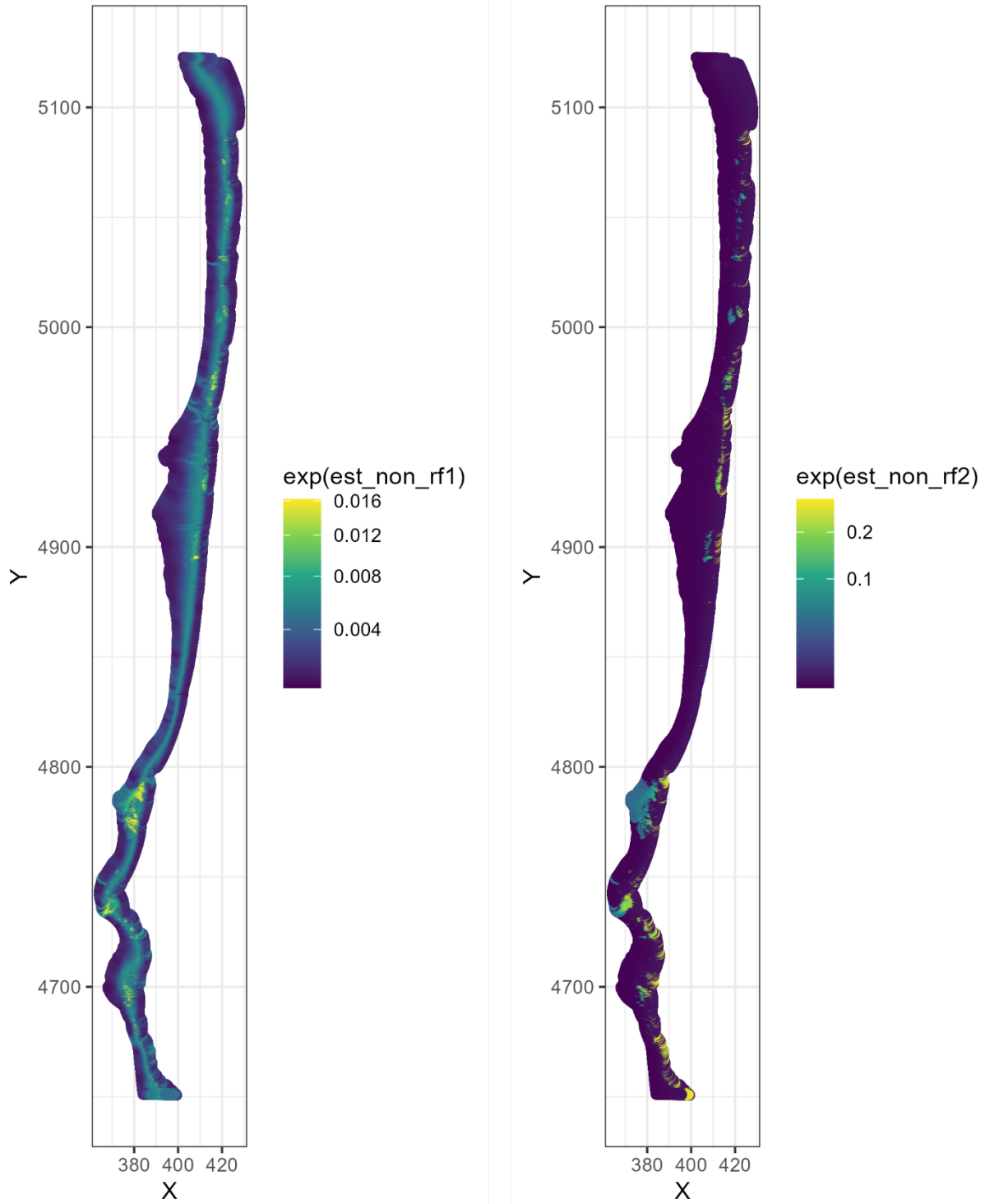


Figure 92. Predicted spatial estimates (not including random effects) for the binomial (left) and gamma (right) models for Black Rockfish with pass as a random effect.

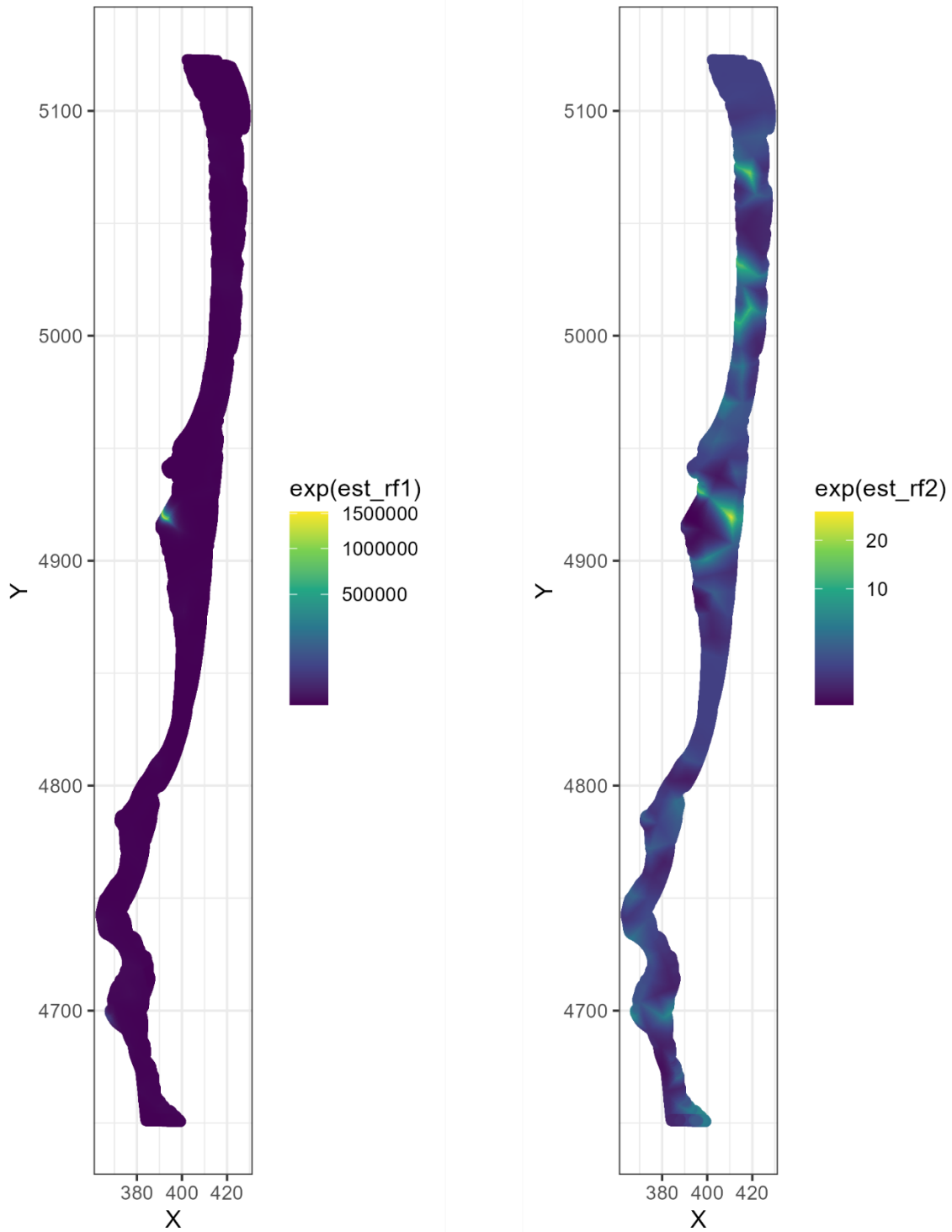


Figure 93. Predicted spatial estimates (just random effects) for the binomial (left) and gamma (right) models for Black Rockfish with pass as a random effect.

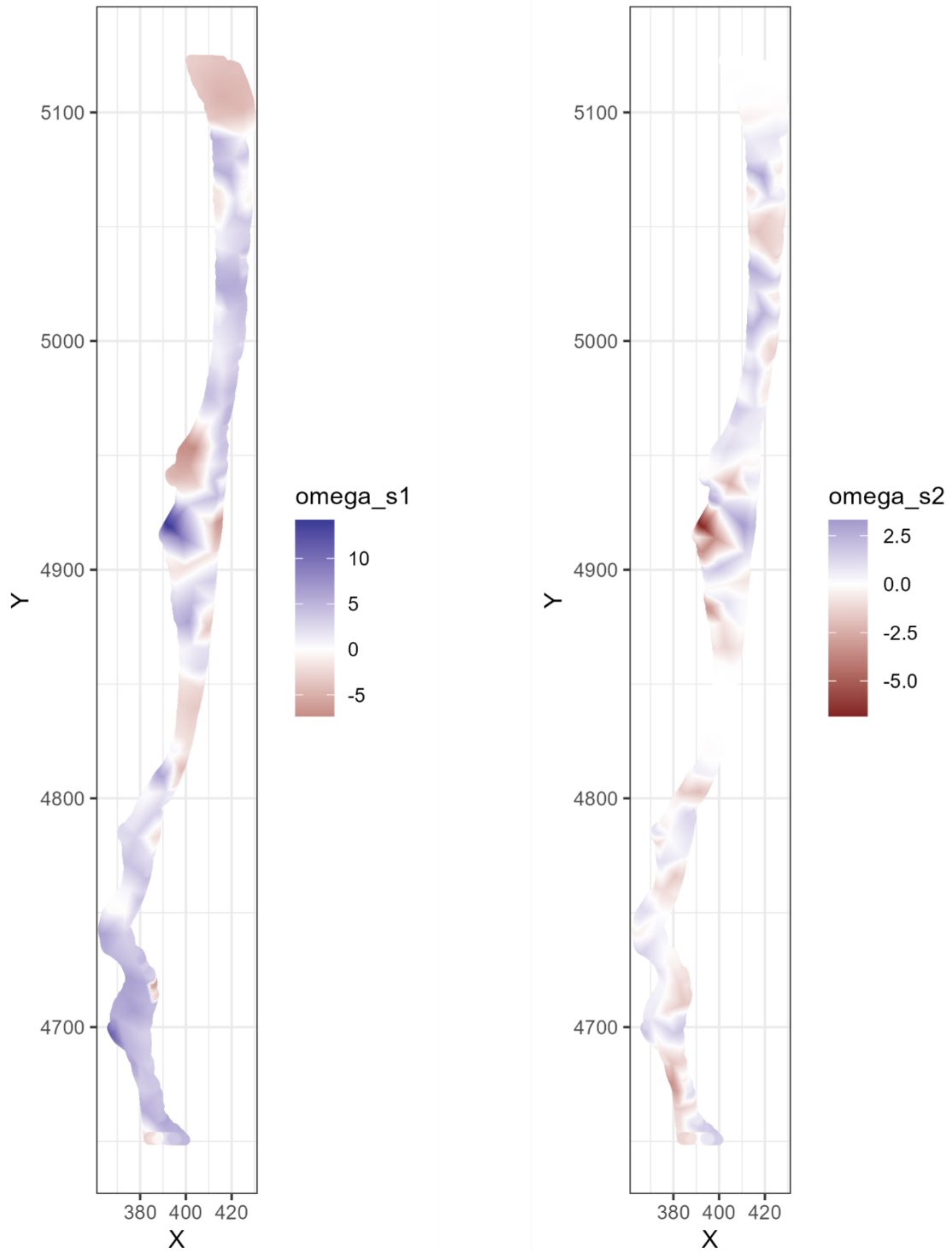


Figure 94. Predicted spatial random fields for the binomial (left) and gamma (right) models for Black Rockfish with pass as a random effect.

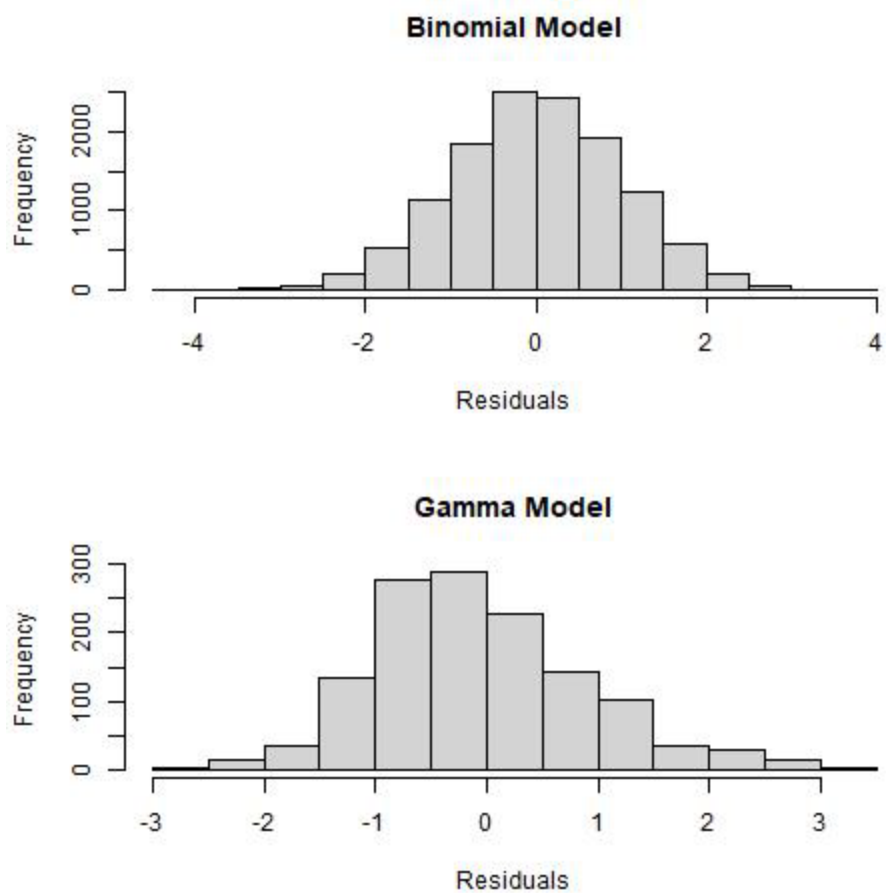


Figure 95. MCMC derived residuals for the best-fit Black Rockfish model for both the binomial (upper) and gamma (lower) components of the model, for pass 2.

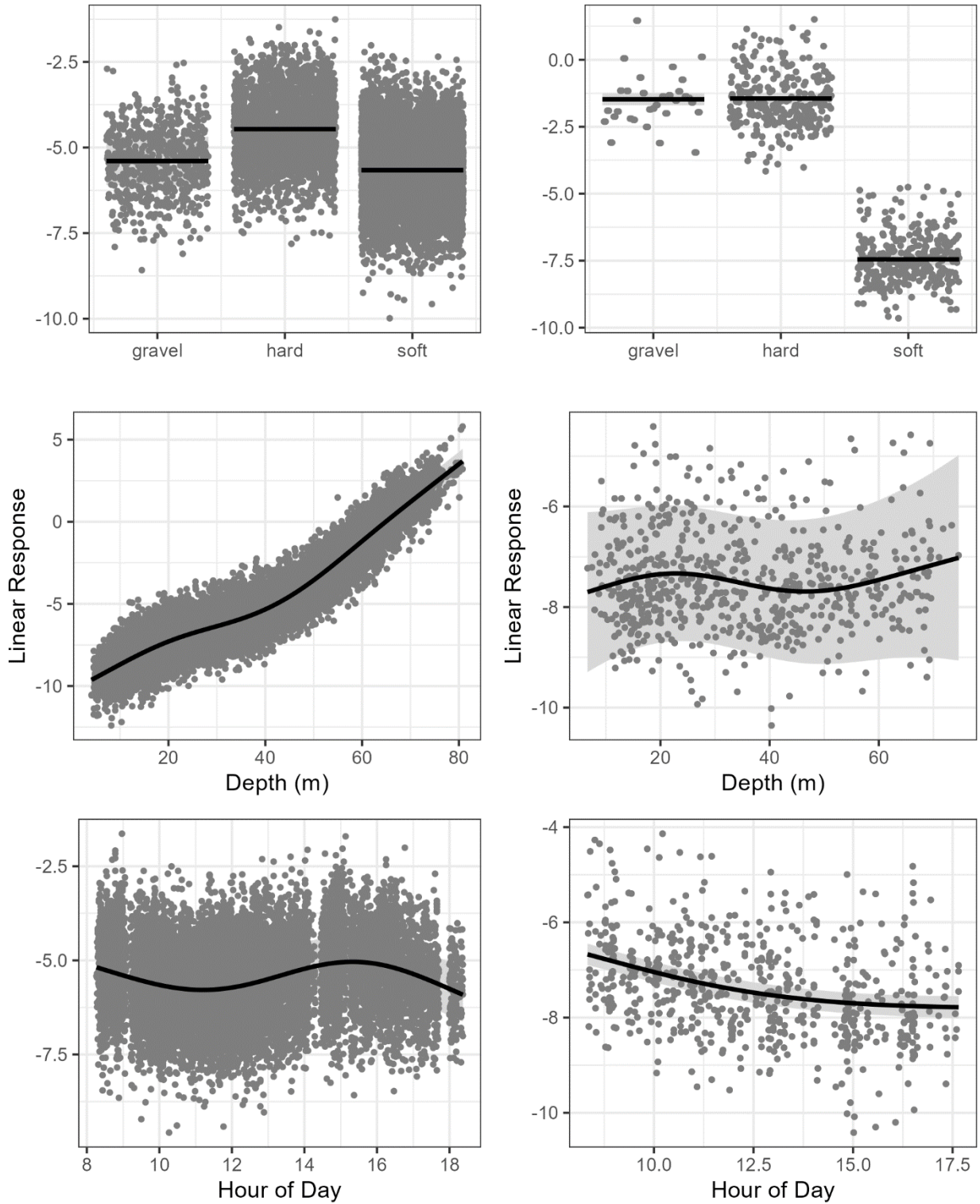


Figure 96. Linear response of each variable for the Black Rockfish model, plots on the left are for the binomial model which was modeled using a logit link and plots on the right are for positive data only and modeled using a gamma model with a log link pass 2.

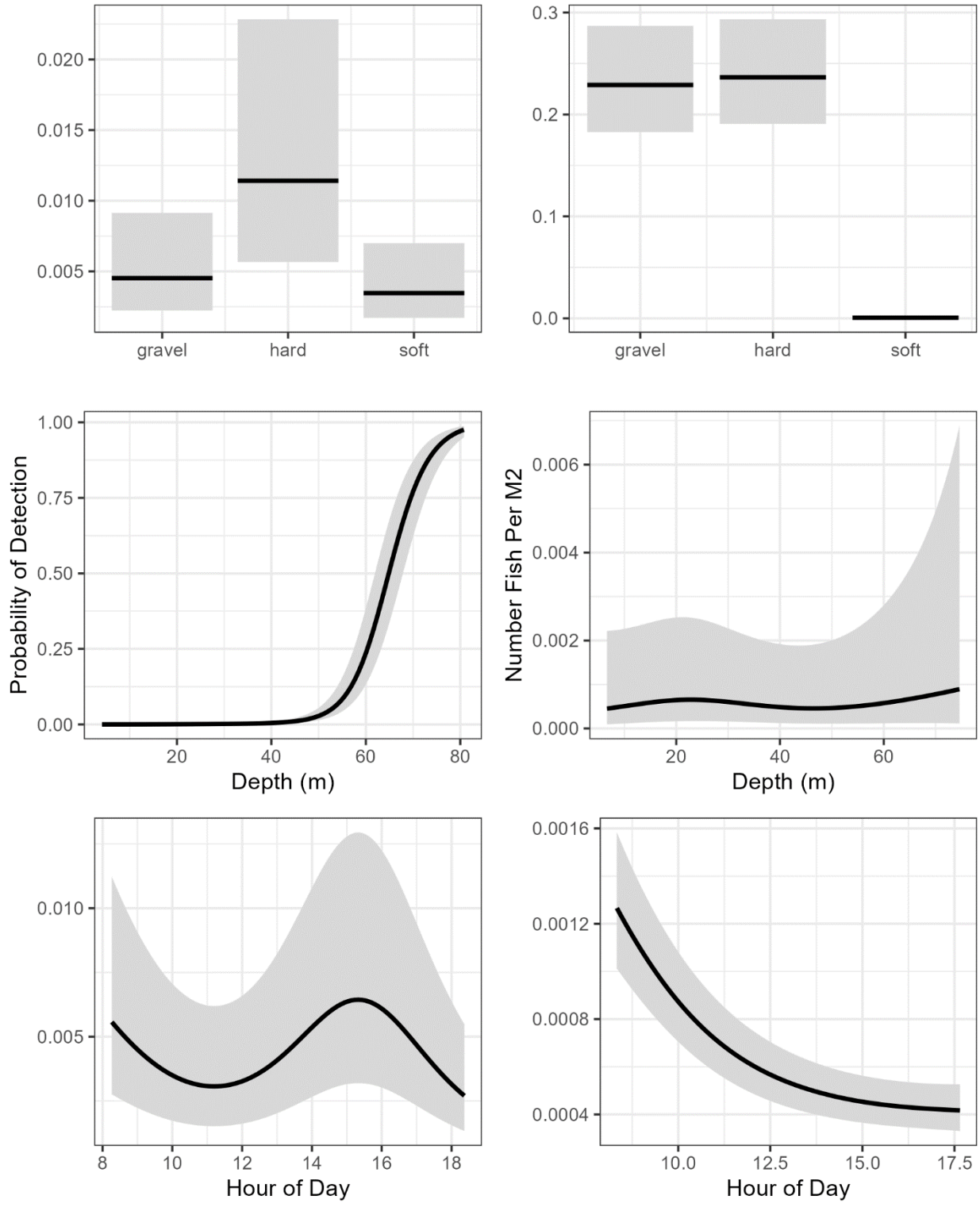


Figure 97. Affect of explanatory variables on the density for the Black Rockfish model, plots on the left are for the binomial model which was modeled using a logit link and plots on the right are for positive data only and modeled using a gamma model with a log link pass 2.

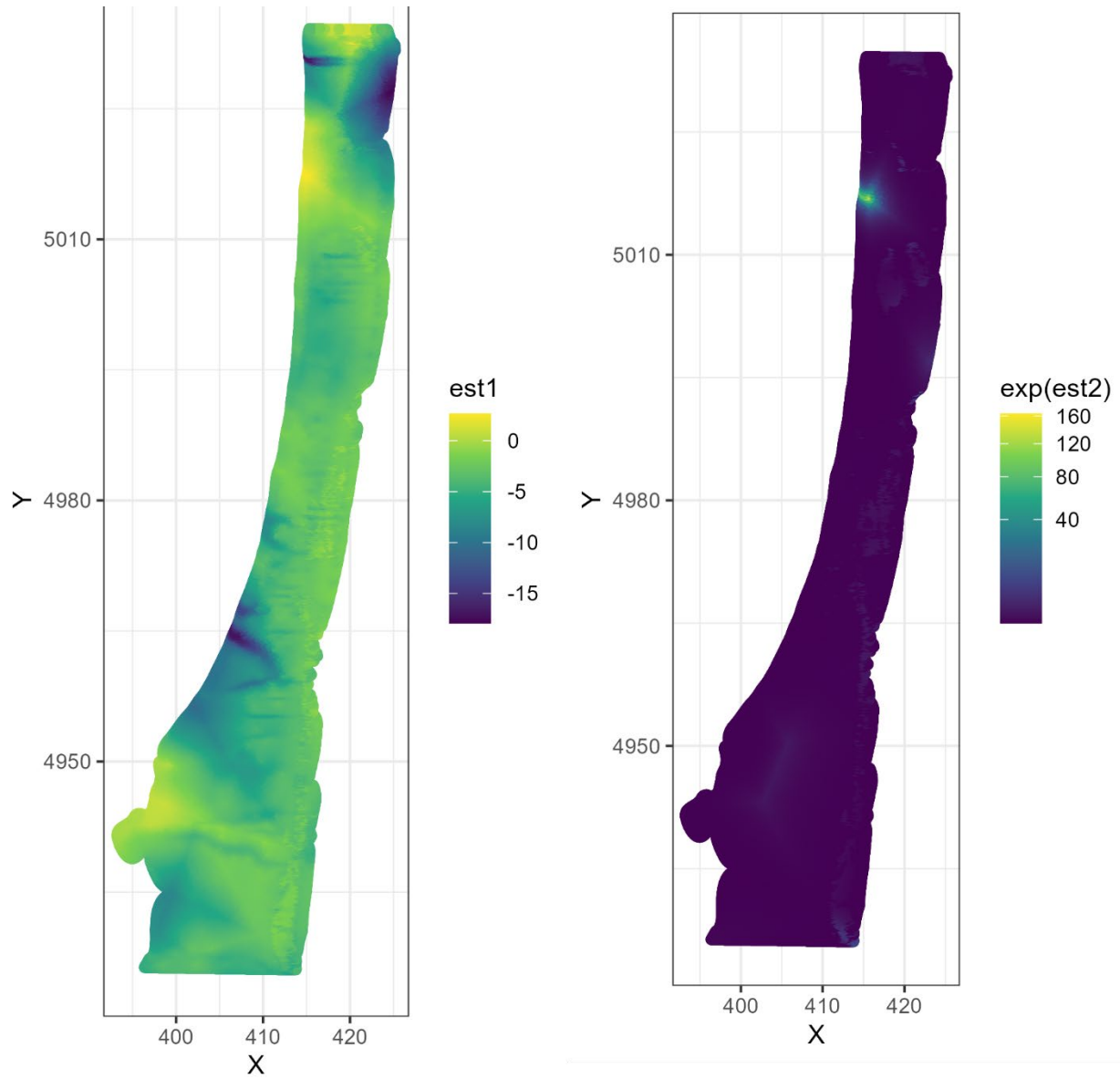


Figure 98. Predicted spatial estimates (including random effects) for the binomial (left) and gamma (right) models for Black Rockfish pass 2.

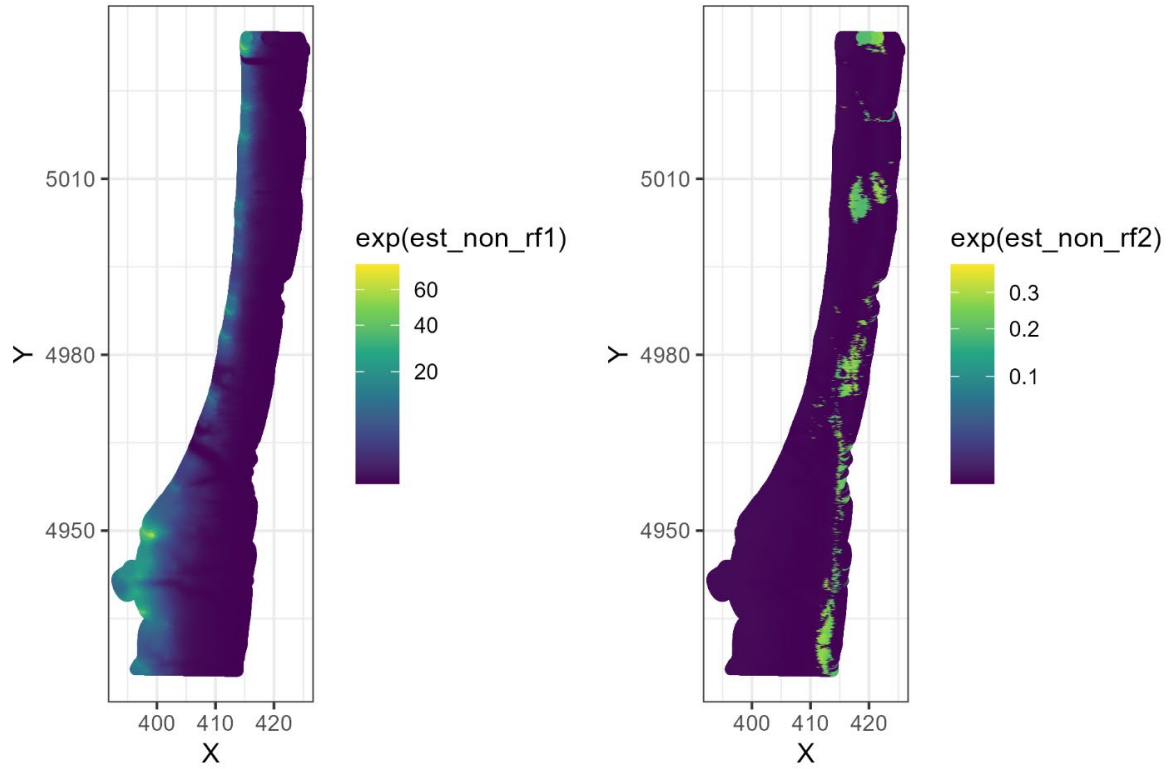


Figure 99. Predicted spatial estimates (not including random effects) for the binomial (left) and gamma (right) models for Black Rockfish pass 2.

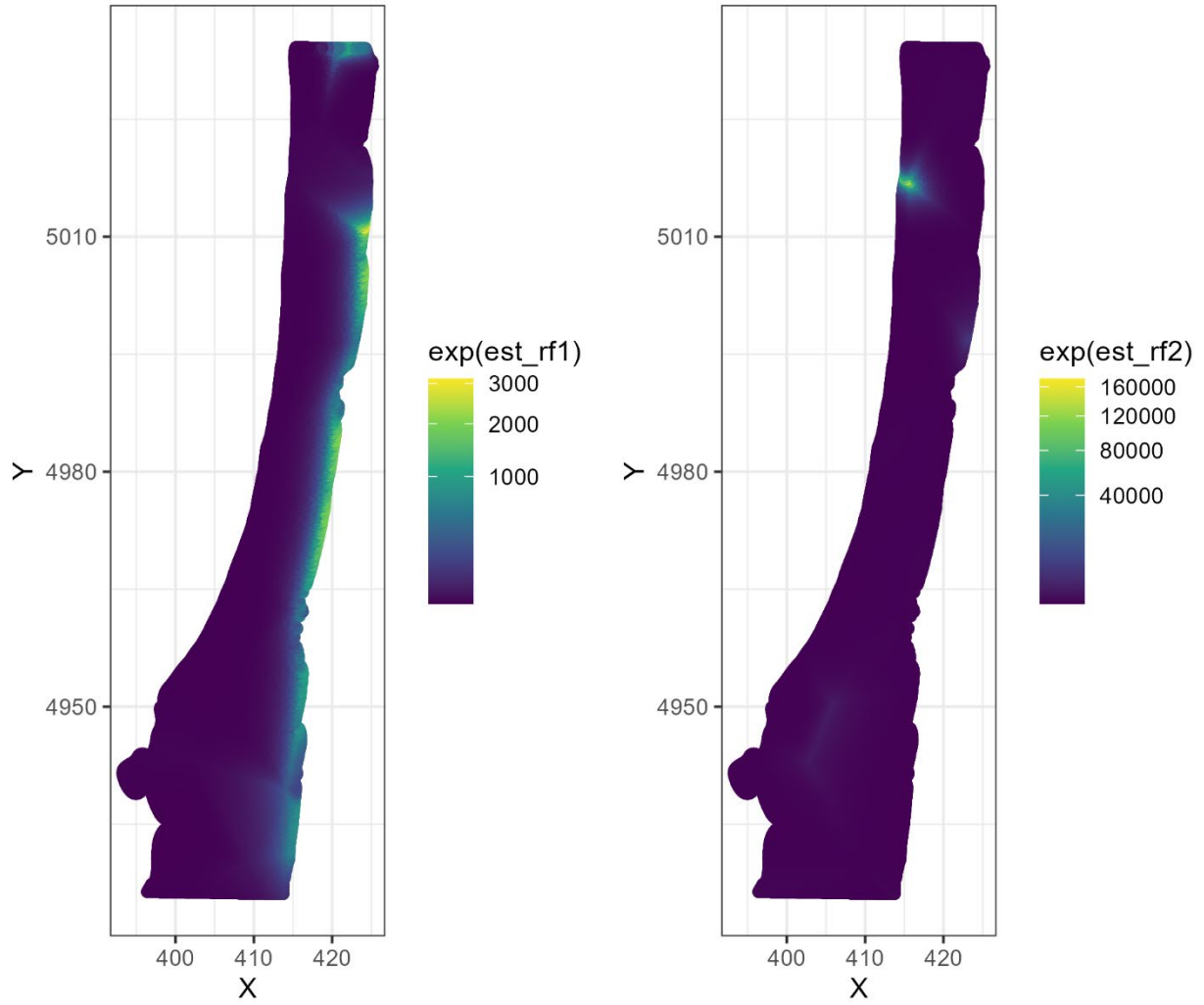


Figure 100. Predicted spatial estimates (just random effects) for the binomial (left) and gamma (right) models for Black Rockfish pass 2.

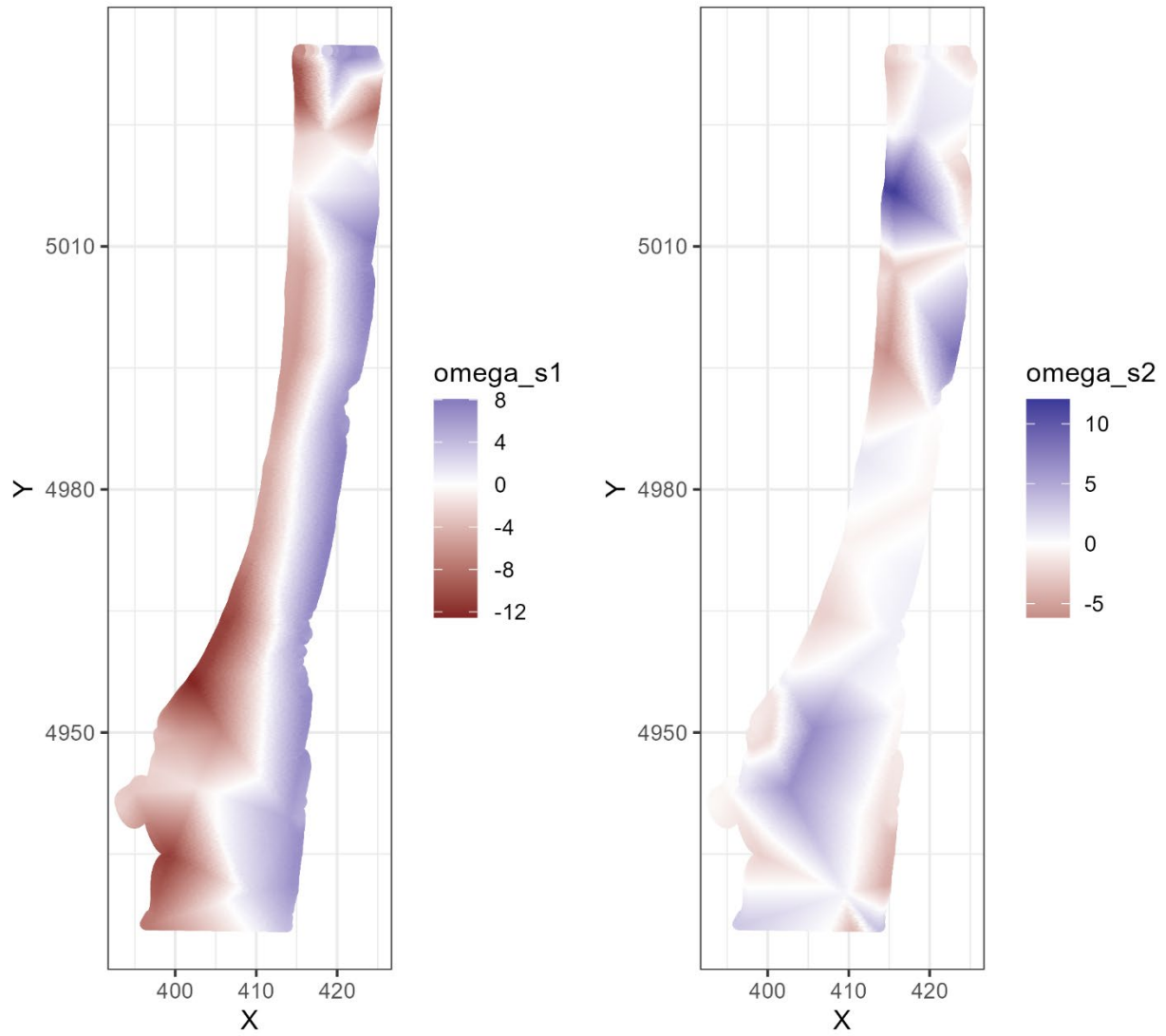


Figure 101. Predicted spatial random fields for the binomial (left) and gamma (right) models for Black Rockfish pass 2.

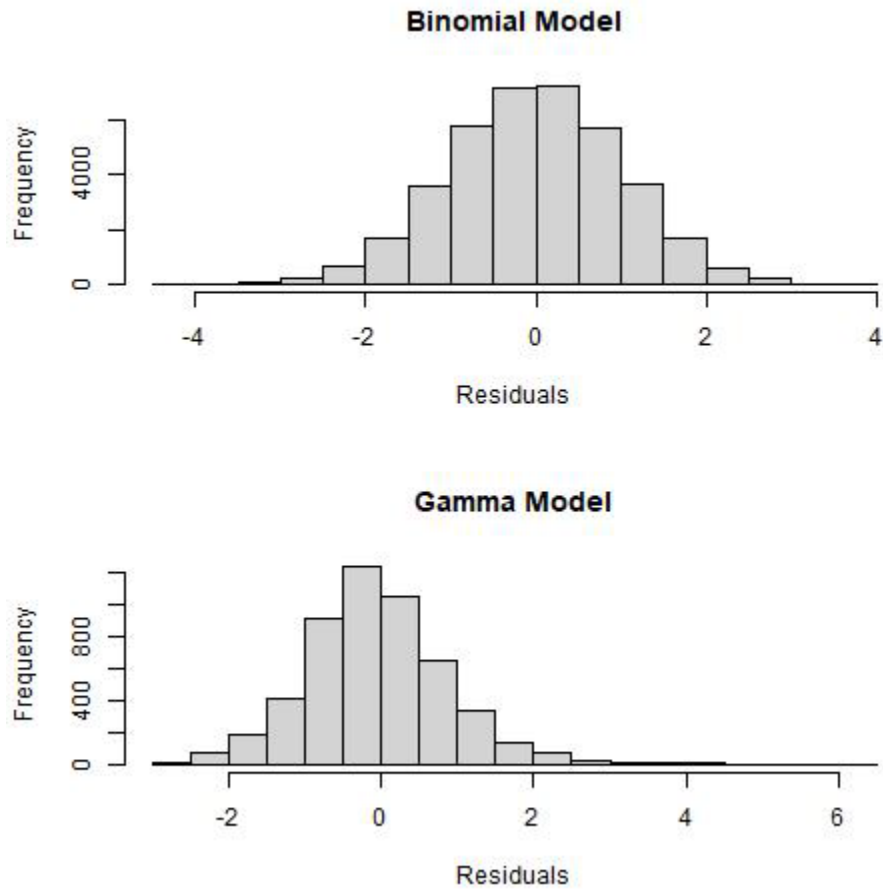


Figure 102. MCMC derived residuals for the best-fit Blue/Deacon Rockfish model for both the binomial (upper) and gamma (lower) components of the model for pass 1.

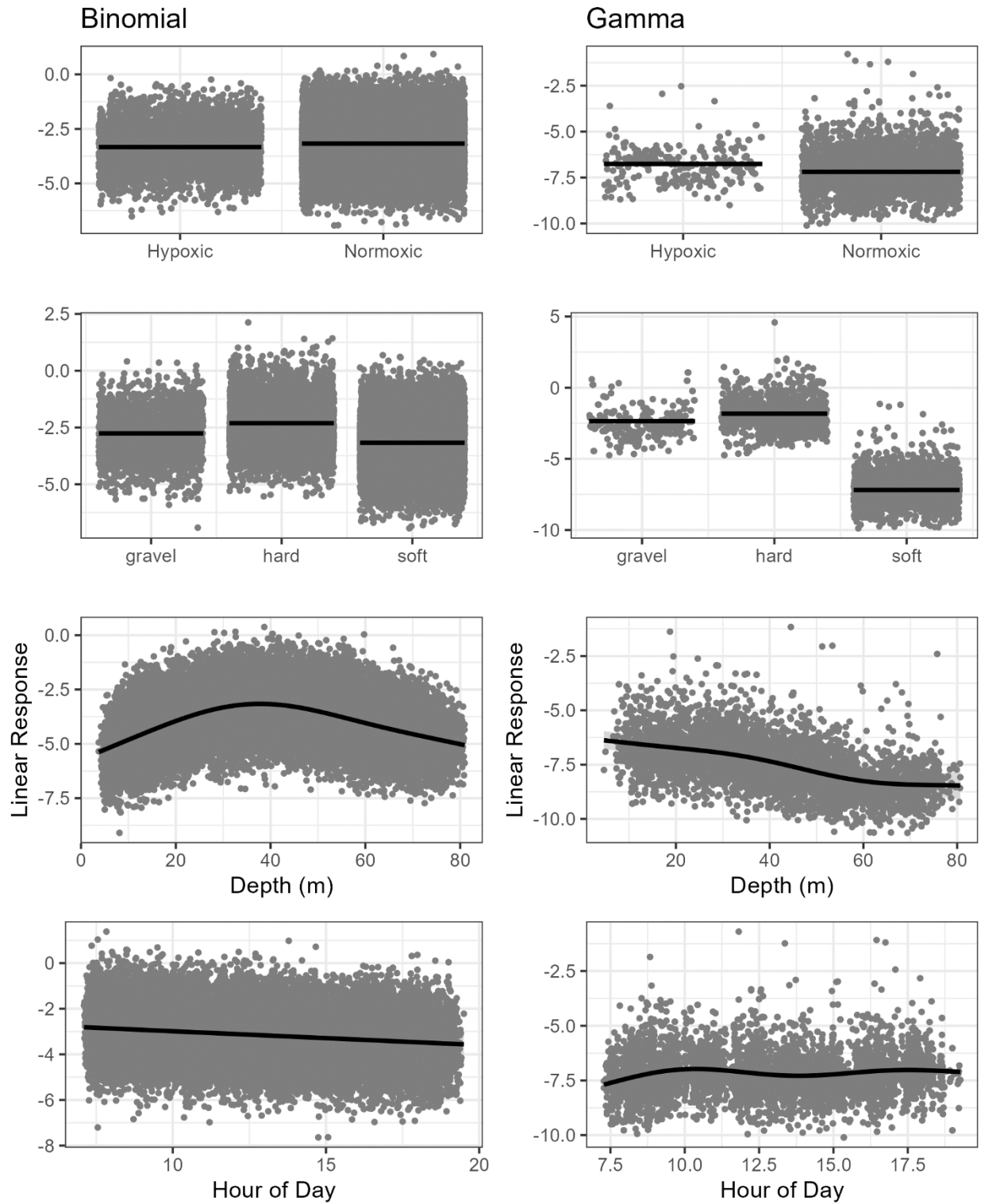


Figure 103. Linear response of each variable for the Blue/Deacon Rockfish model, plots on the left are for the binomial model which was modeled using a logit link and plots on the right are for positive data only and modeled using a gamma model with a log link for pass 1.

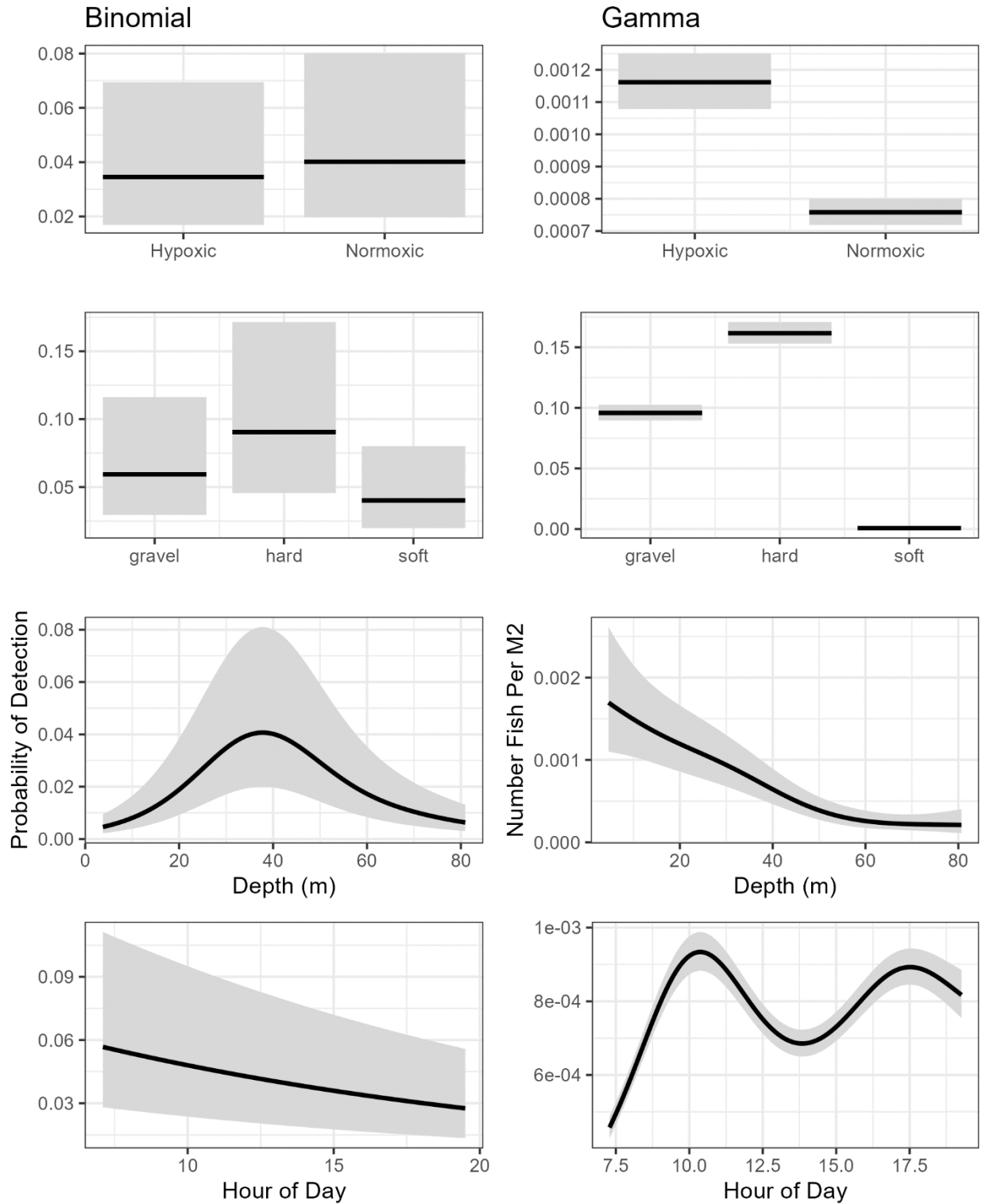


Figure 104. Affect of explanatory variables on the density for the Blue/Deacon Rockfish model, plots on the left are for the binomial model which was modeled using a logit link and plots on the right are for positive data only and modeled using a gamma model with a log link for pass 1.

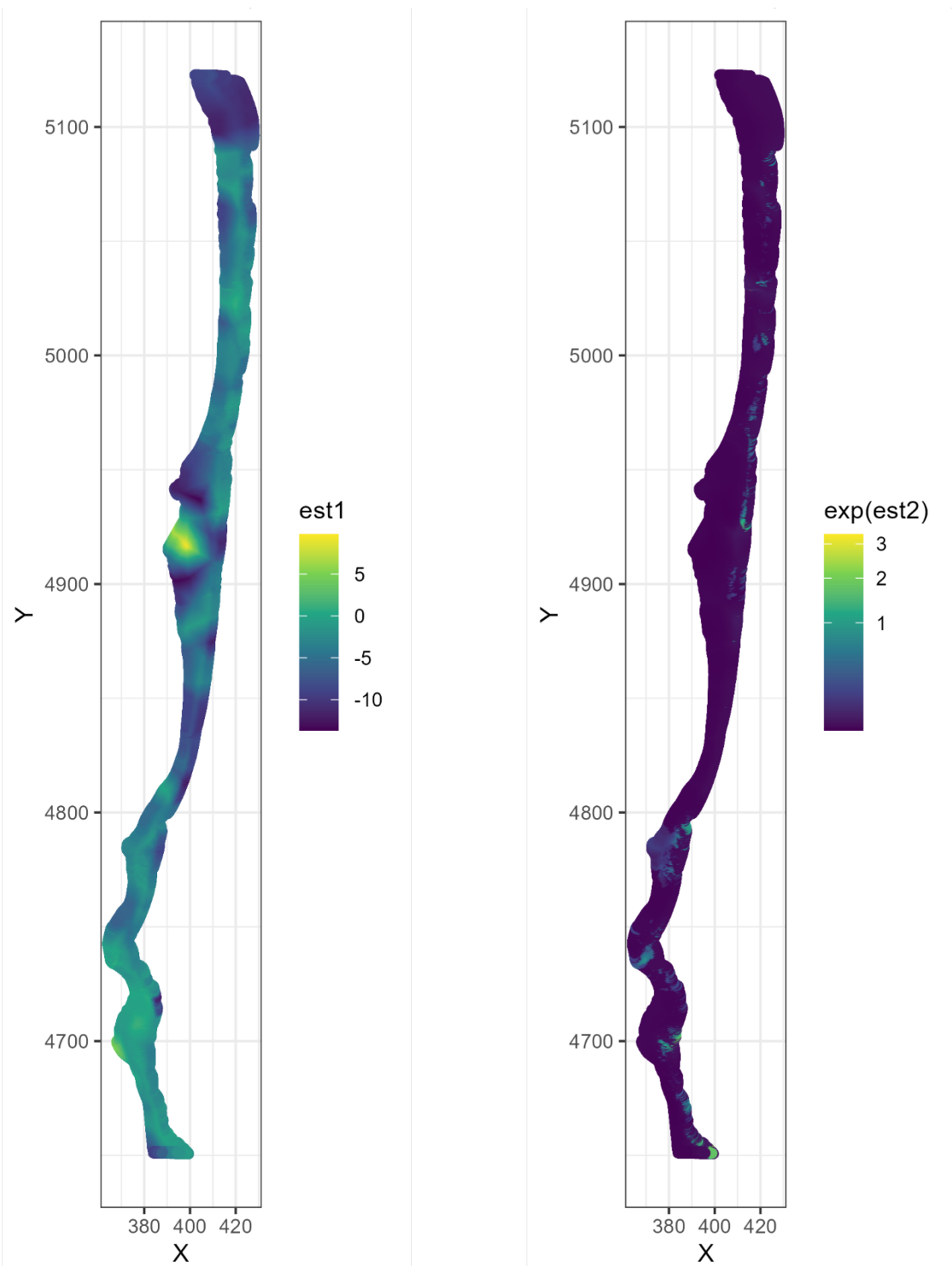


Figure 105. Predicted spatial estimates (including random effects) for the binomial (left) and gamma (right) models for Blue/Deacon Rockfish for pass 1.

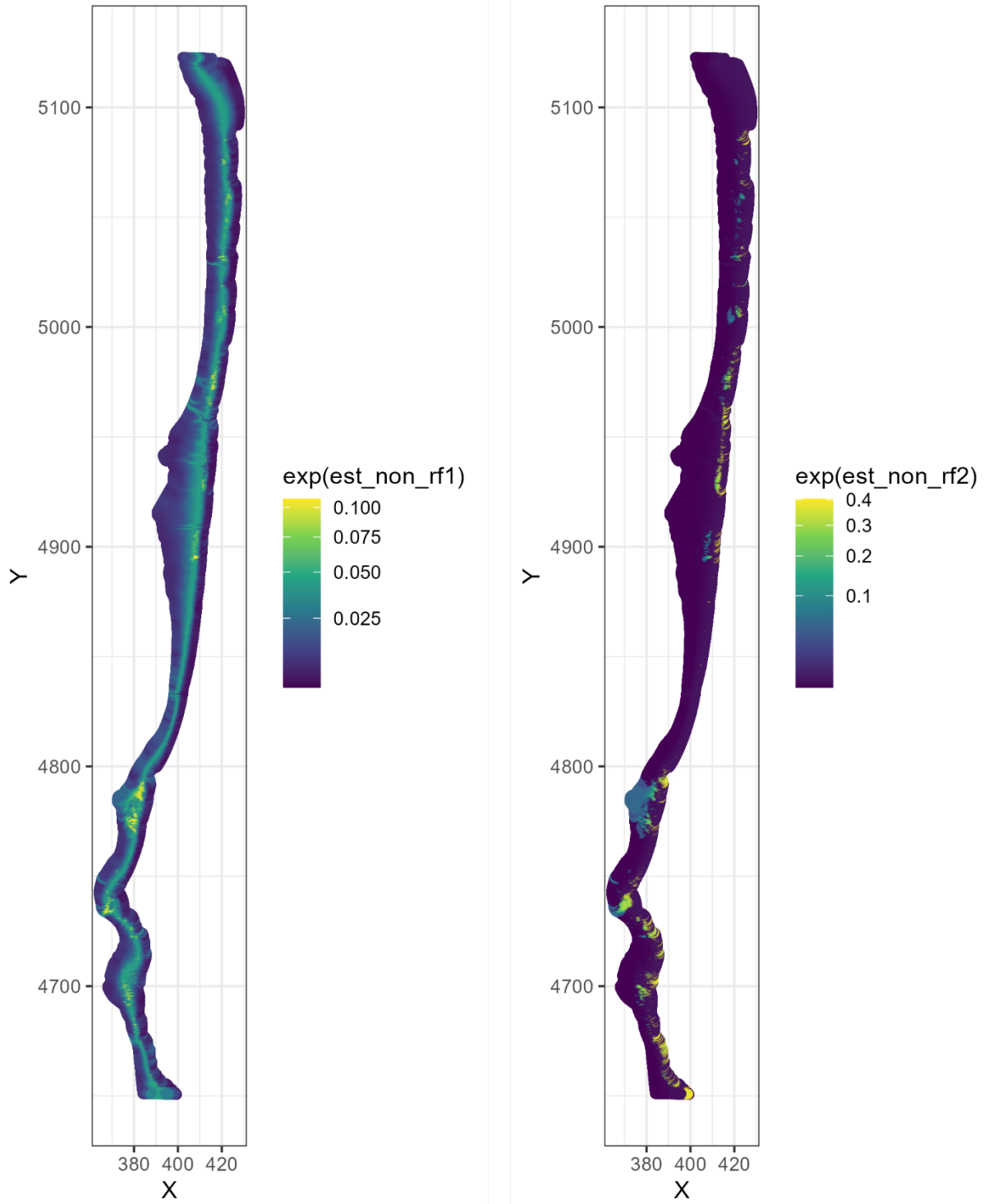


Figure 106. Predicted spatial estimates (not including random effects) for the binomial (left) and gamma (right) models for Blue/Deacon Rockfish for pass 1.

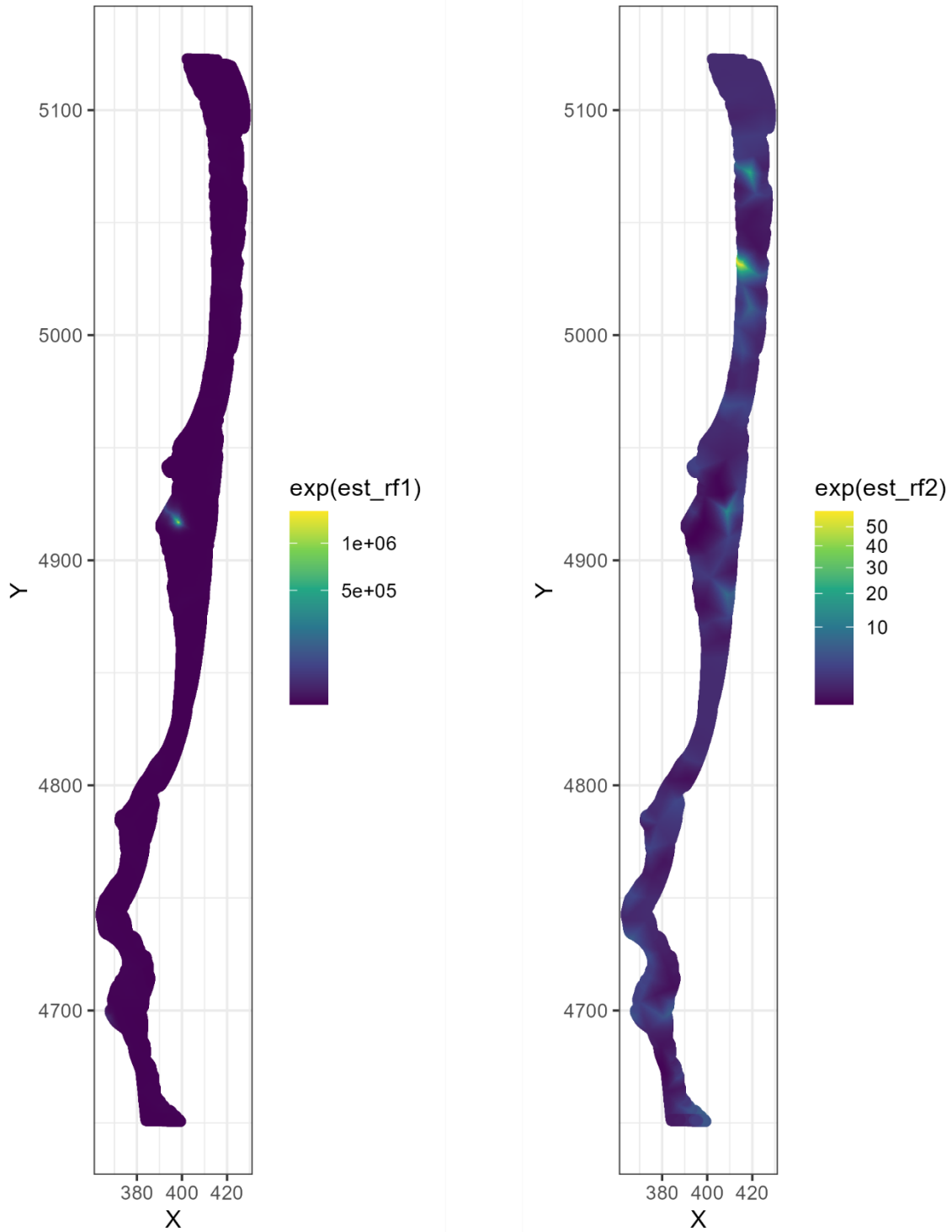


Figure 107. Predicted spatial estimates (just random effects) for the binomial (left) and gamma (right) models for Blue/Deacon Rockfish for pass 1.

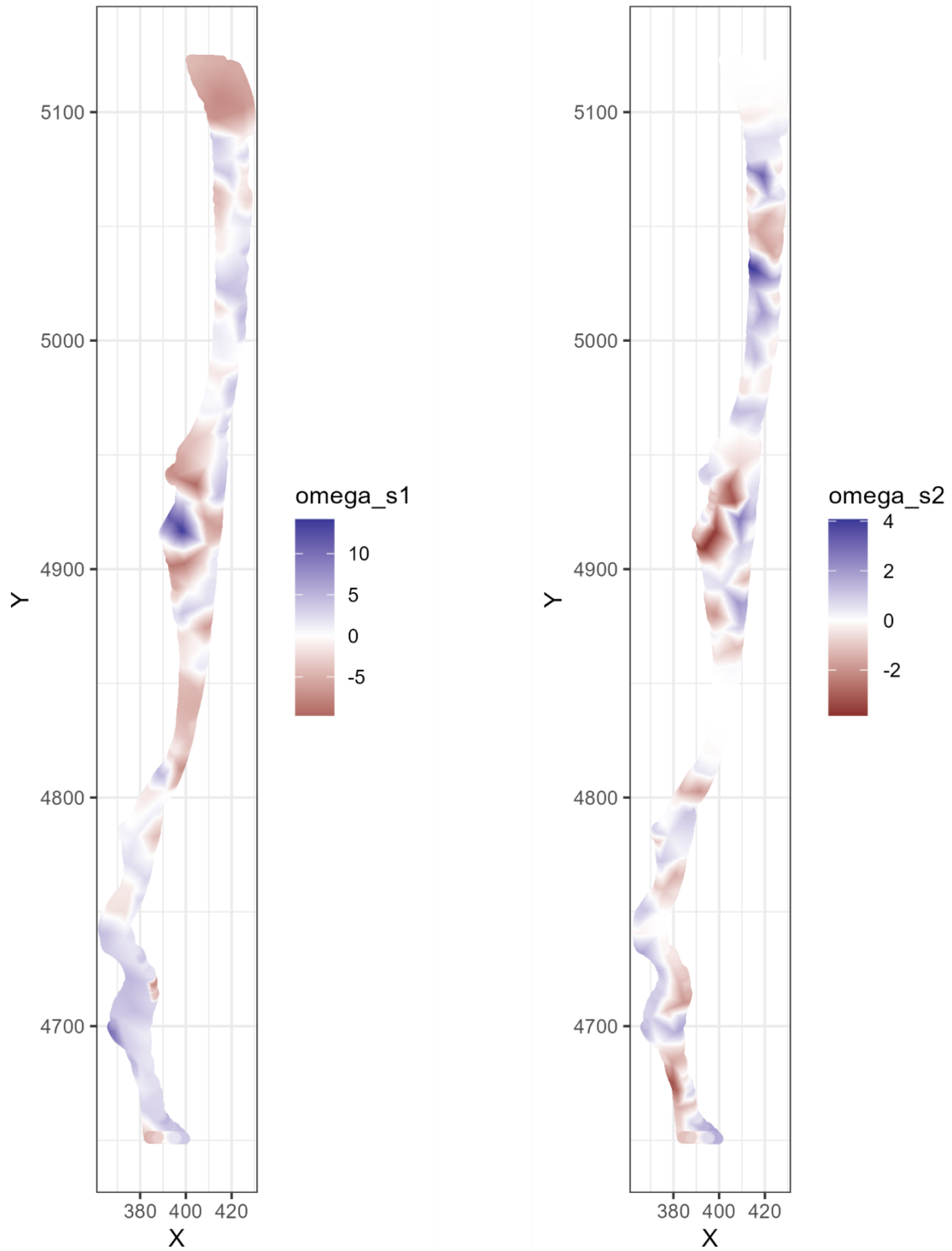


Figure 108. Predicted spatial random fields for the binomial (left) and gamma (right) models for Blue/Deacon Rockfish for pass 1.

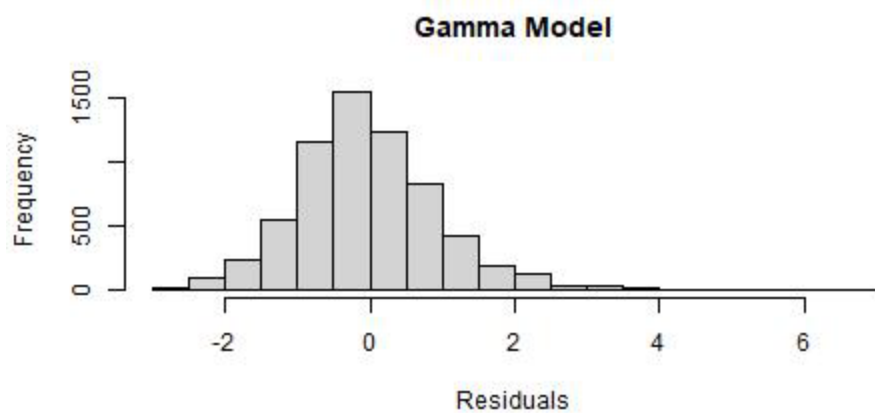
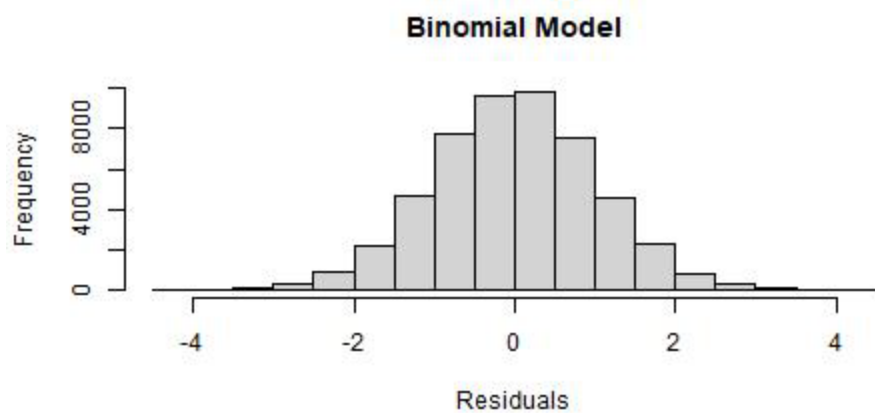


Figure 109. MCMC derived residuals for the best-fit Blue/Deacon Rockfish model for both the binomial (upper) and gamma (lower) components of the model, with pass as a random effect.

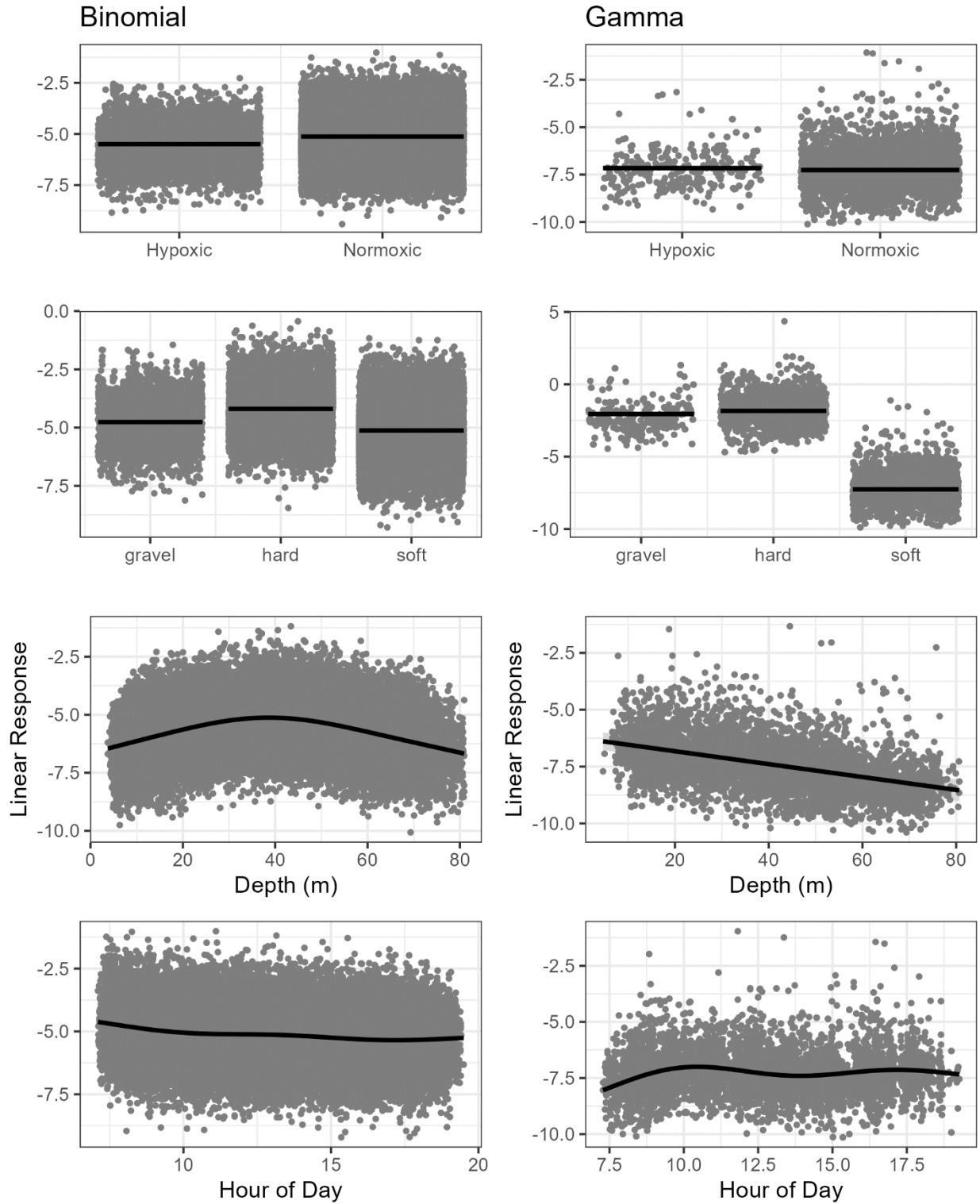


Figure 110. Linear response of each variable for the Blue/Deacon Rockfish model, plots on the left are for the binomial model which was modeled using a logit link and plots on the right are for positive data only and modeled using a gamma model with a log link with pass as a random effect.

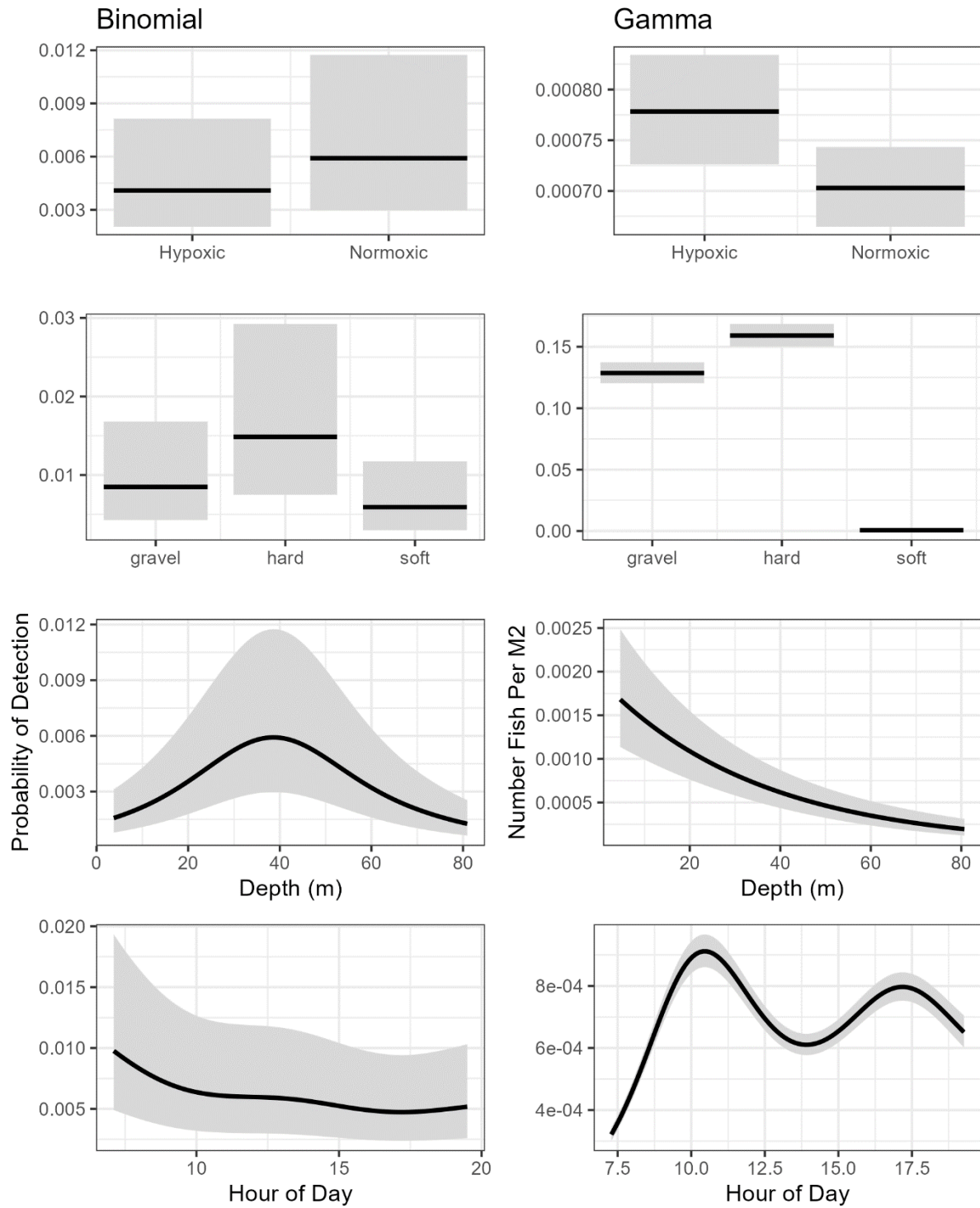


Figure 111. Affect of explanatory variables on the density for the Blue/Deacon Rockfish model, plots on the left are for the binomial model which was modeled using a logit link and plots on the right are for positive data only and modeled using a gamma model with a log link with pass as a random effect.

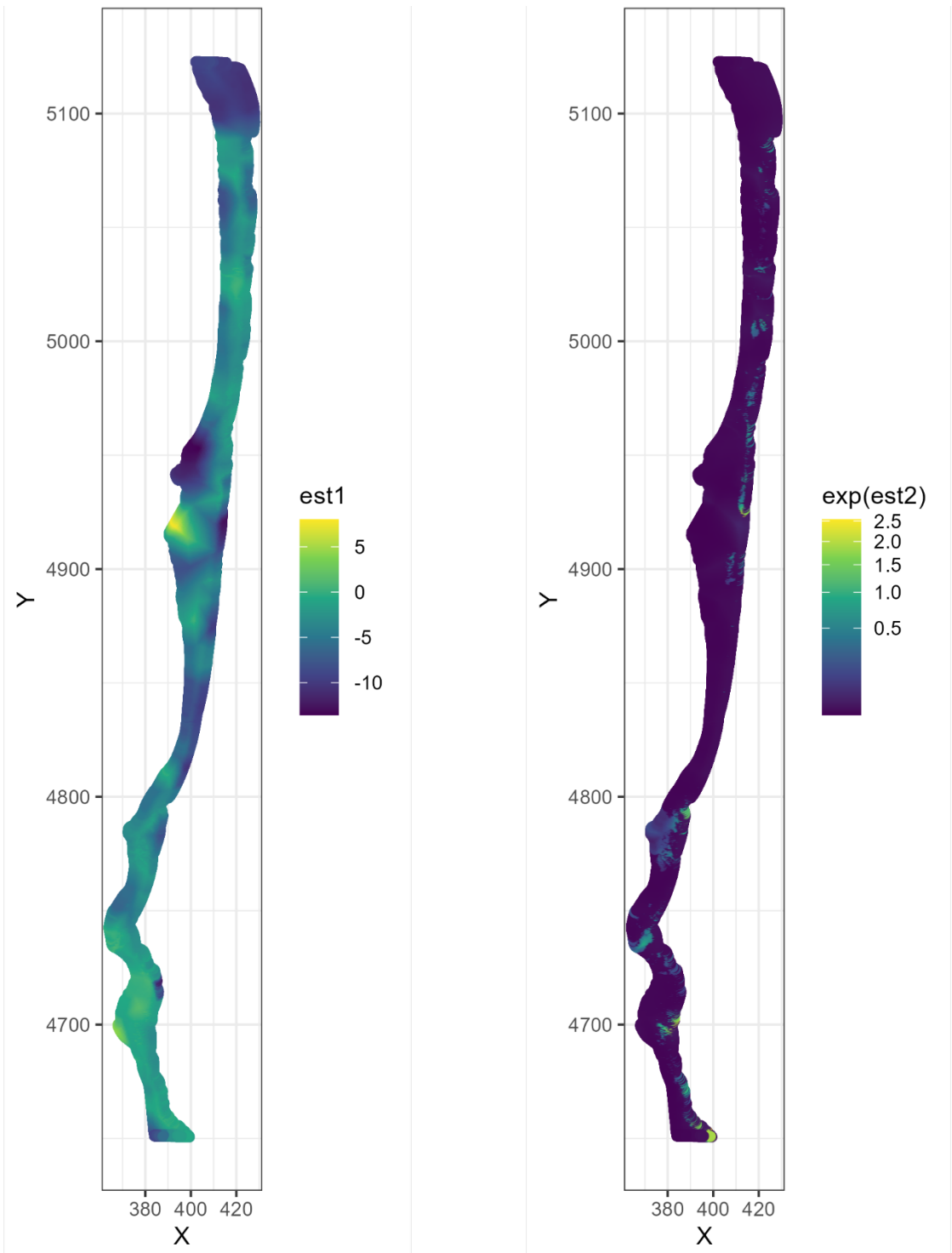


Figure 112. Predicted spatial estimates (including random effects) for the binomial (left) and gamma (right) models for Blue/Deacon Rockfish with pass as a random effect.

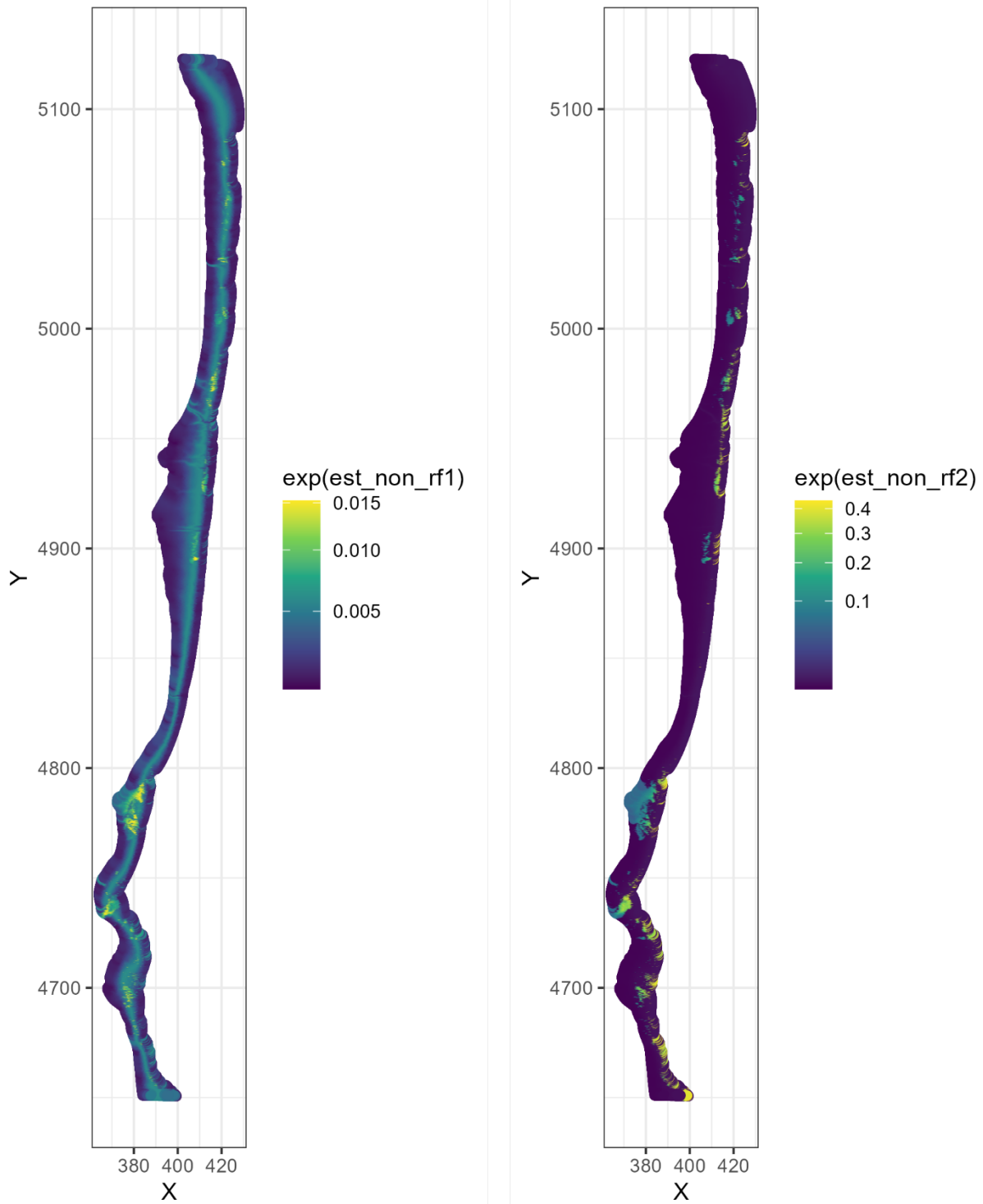


Figure 113. Predicted spatial estimates (not including random effects) for the binomial (left) and gamma (right) models for Blue/Deacon Rockfish with pass as a random effect.

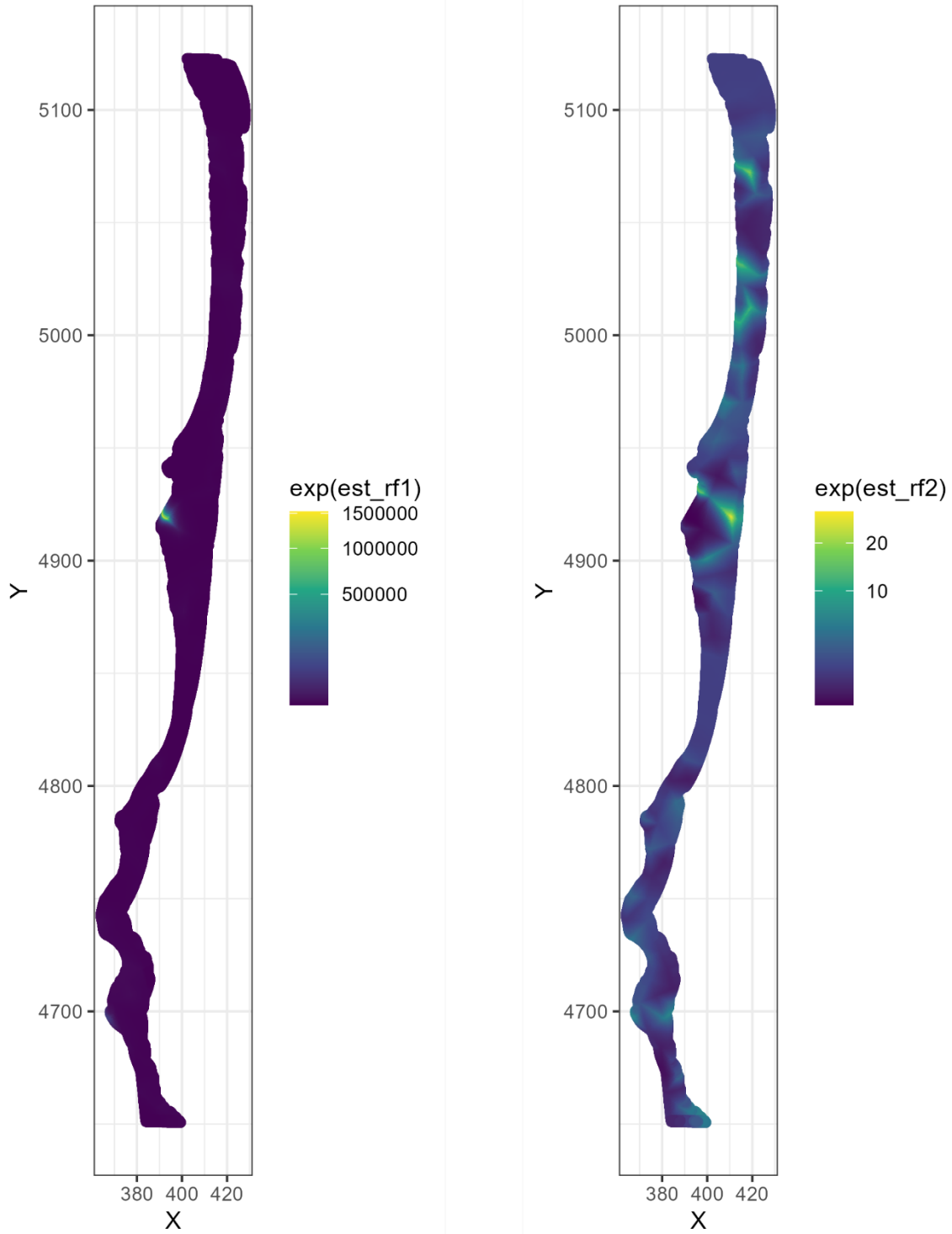


Figure 114. Predicted spatial estimates (just random effects) for the binomial (left) and gamma (right) models for Blue/Deacon Rockfish with pass as a random effect.

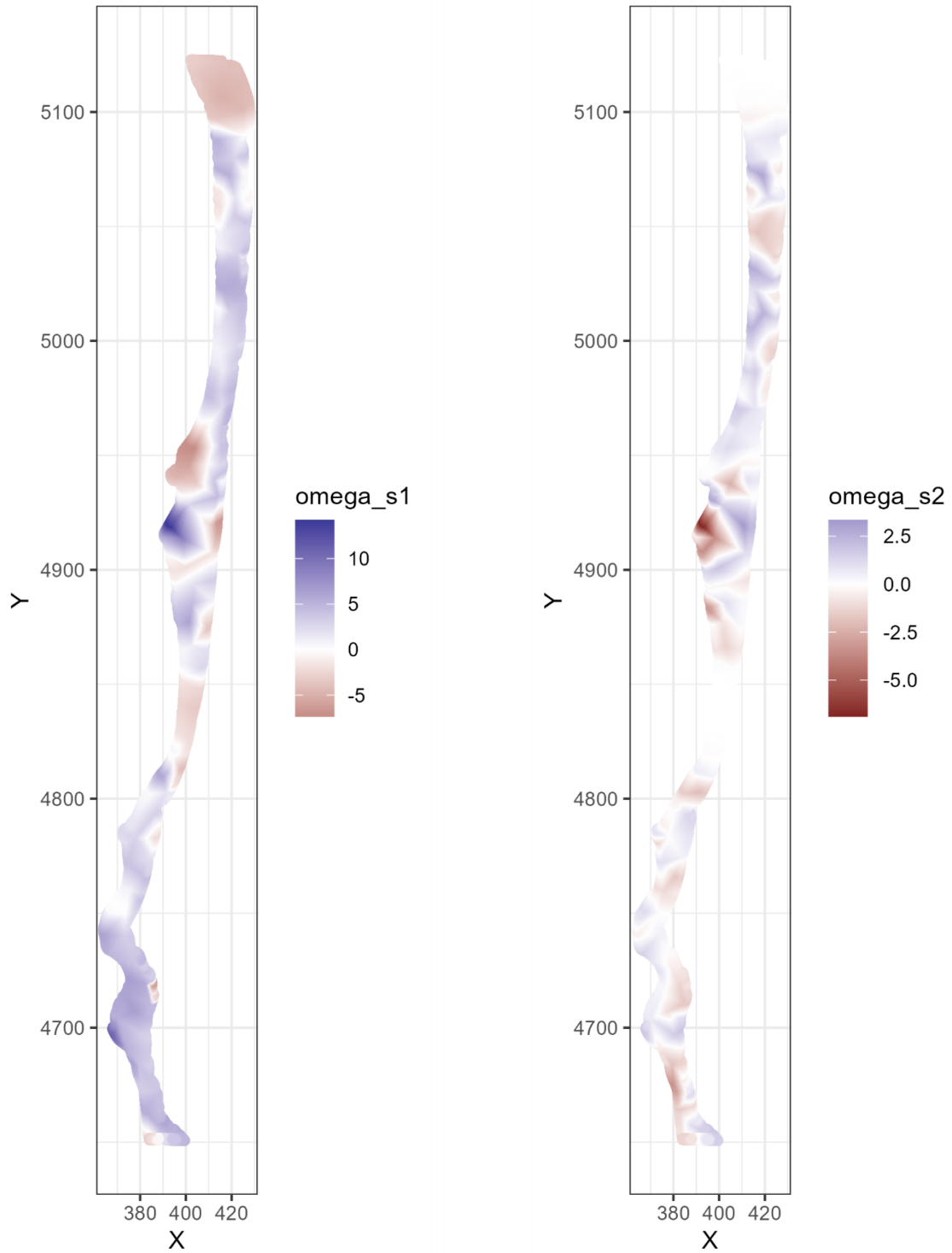


Figure 115. Predicted spatial random fields for the binomial (left) and gamma (right) models for Blue/Deacon Rockfish with pass as a random effect.

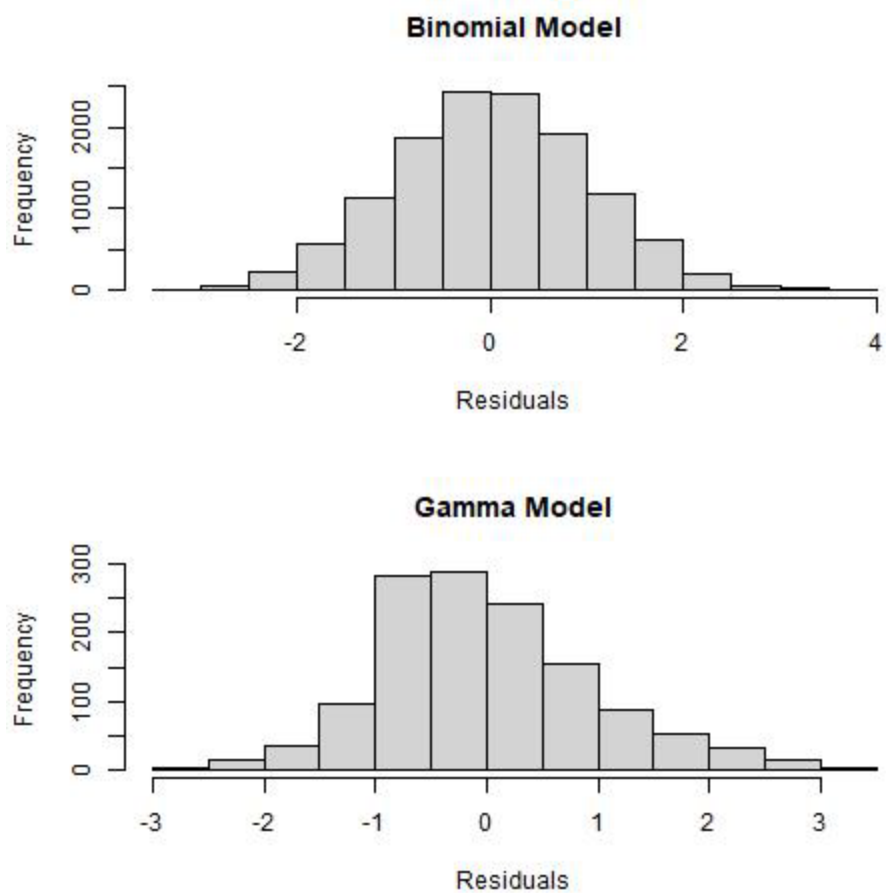


Figure 116. MCMC derived residuals for the best-fit Blue/Deacon Rockfish model for both the binomial (upper) and gamma (lower) components of the model for pass 2.

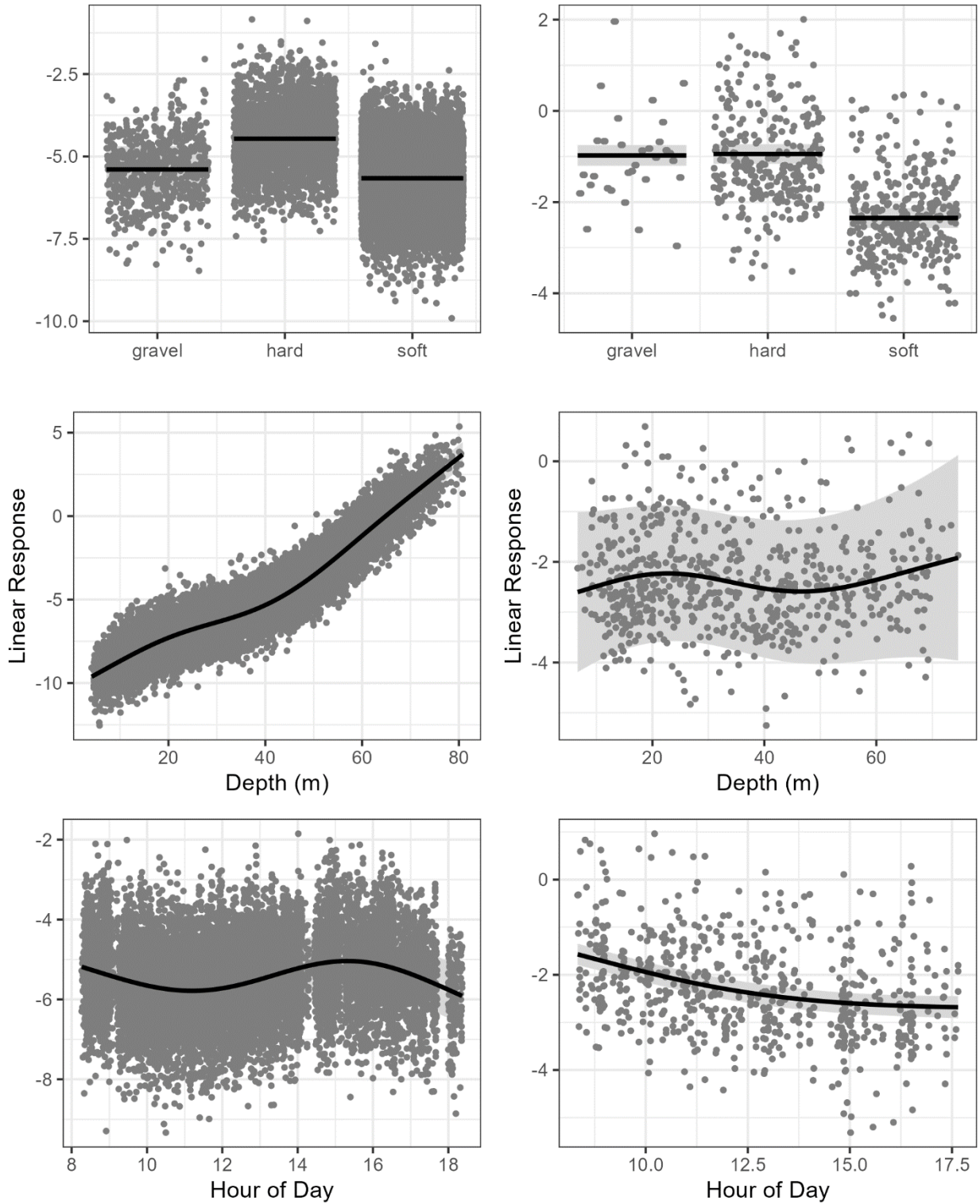


Figure 117. Linear response of each variable for the Blue/Deacon Rockfish model, plots on the left are for the binomial model which was modeled using a logit link and plots on the right are for positive data only and modeled using a gamma model with a log link pass 2.

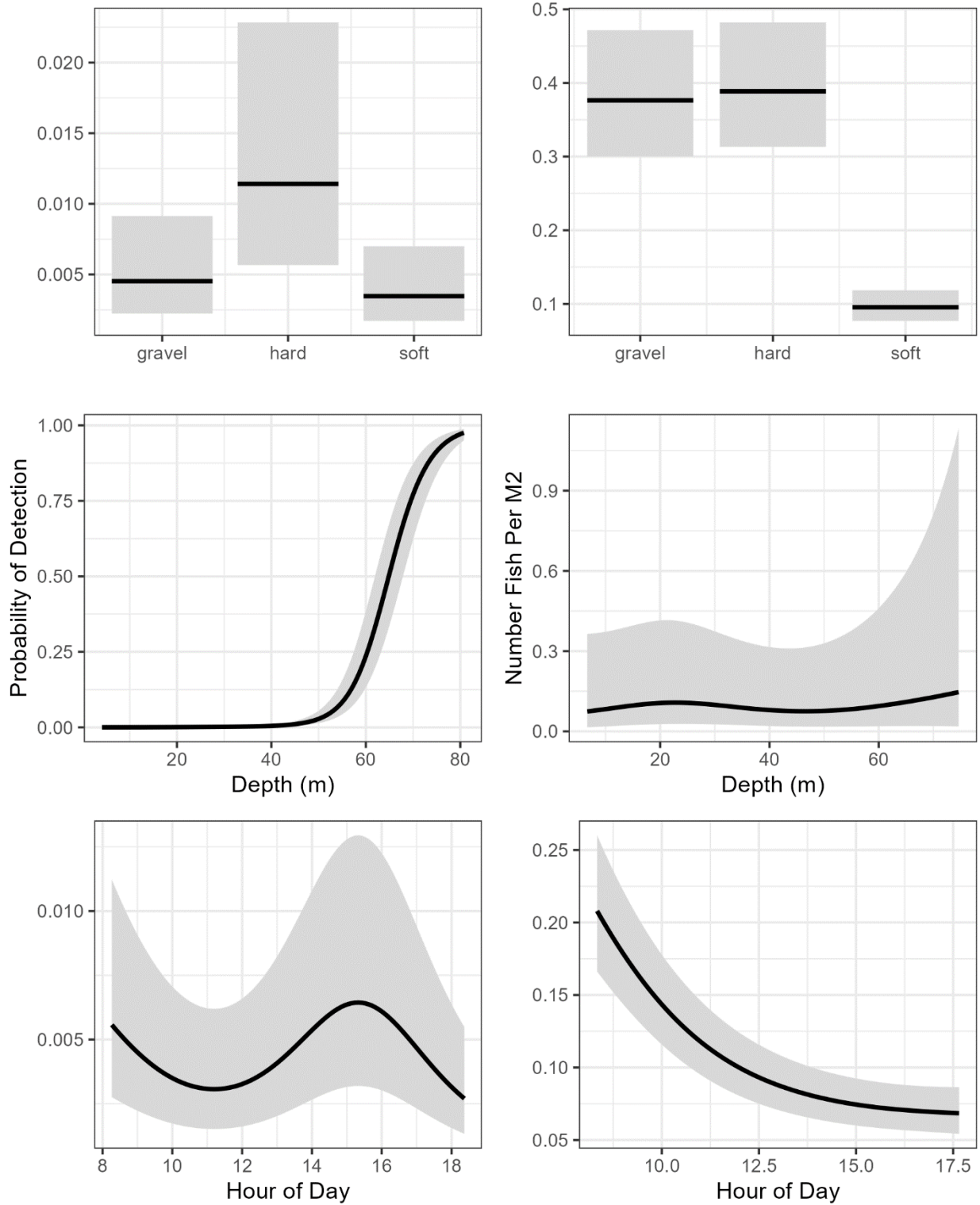


Figure 118. Affect of explanatory variables on the density for the Blue/Deacon Rockfish model, plots on the left are for the binomial model which was modeled using a logit link and plots on the right are for positive data only and modeled using a gamma model with a log link pass 2.

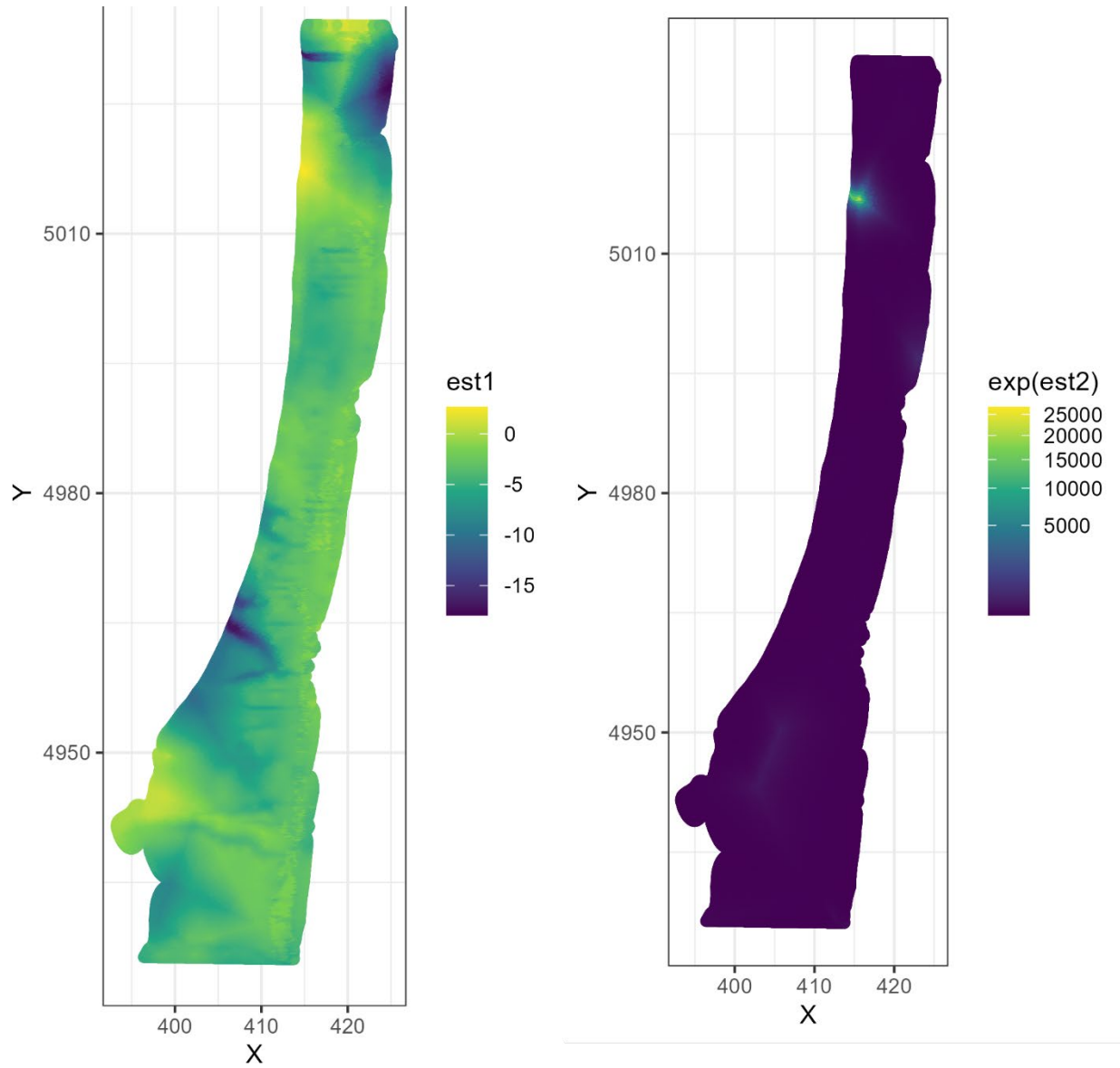


Figure 119. Predicted spatial estimates (including random effects) for the binomial (left) and gamma (right) models for Blue/Deacon Rockfish pass 2.

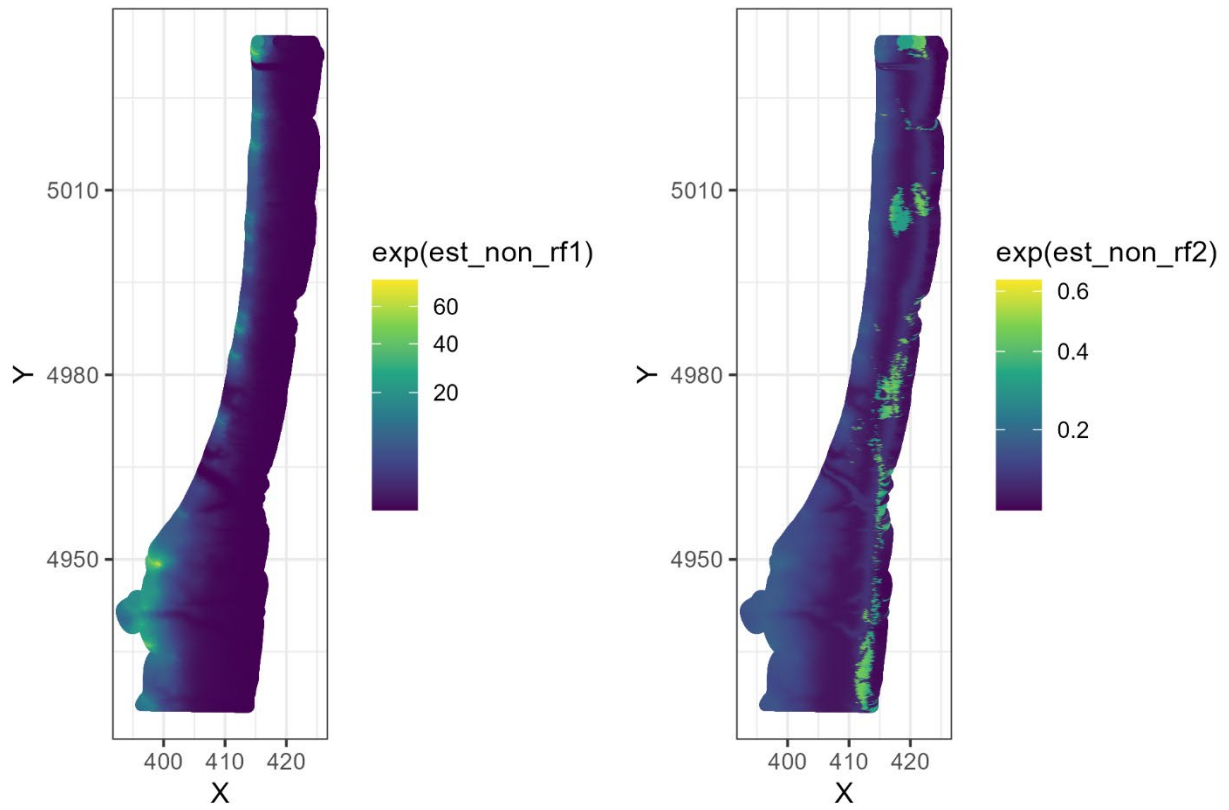


Figure 120. Predicted spatial estimates (not including random effects) for the binomial (left) and gamma (right) models for Blue/Deacon Rockfish pass 2.

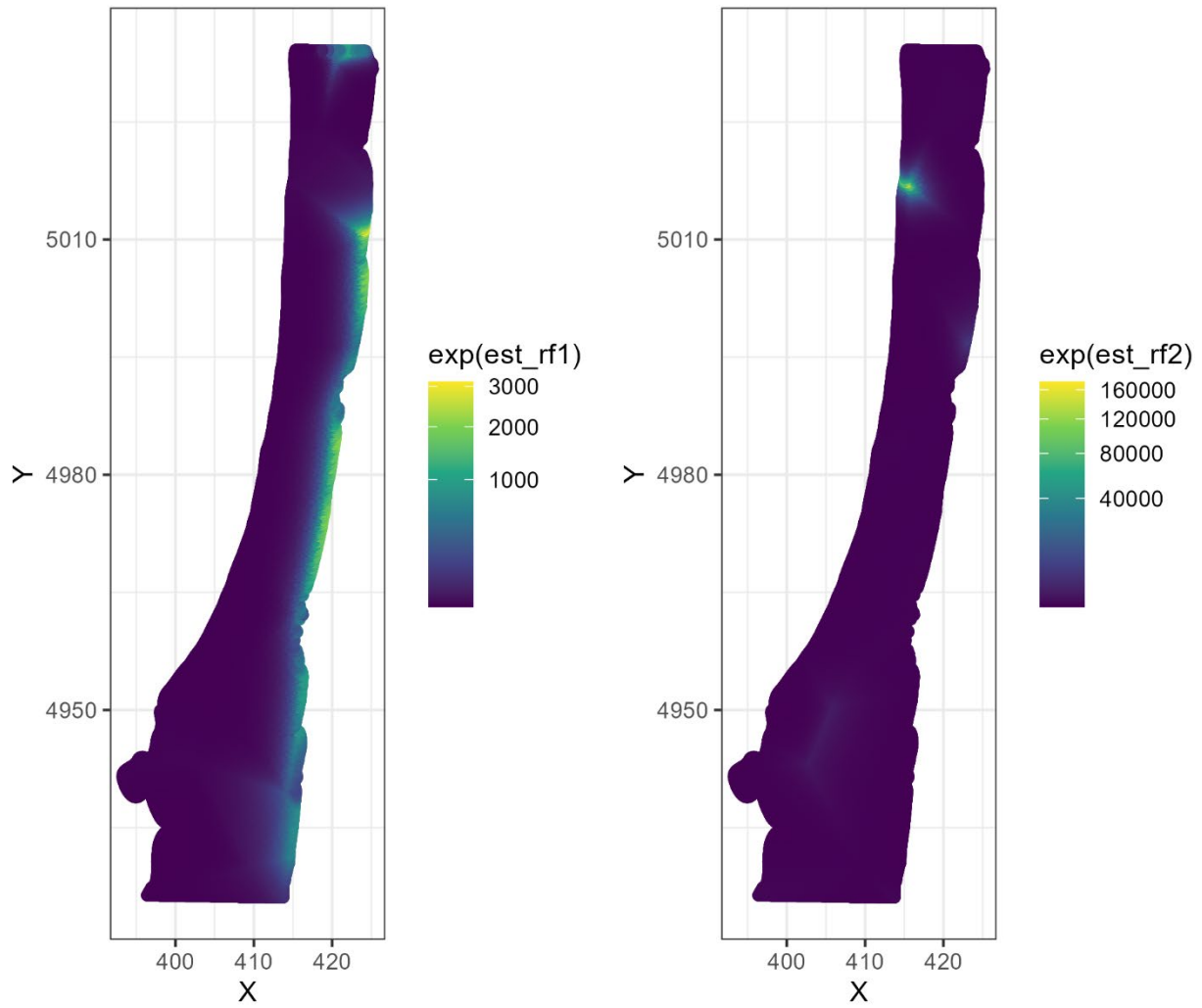


Figure 121. Predicted spatial estimates (just random effects) for the binomial (left) and gamma (right) models for Blue/Deacon Rockfish pass 2.

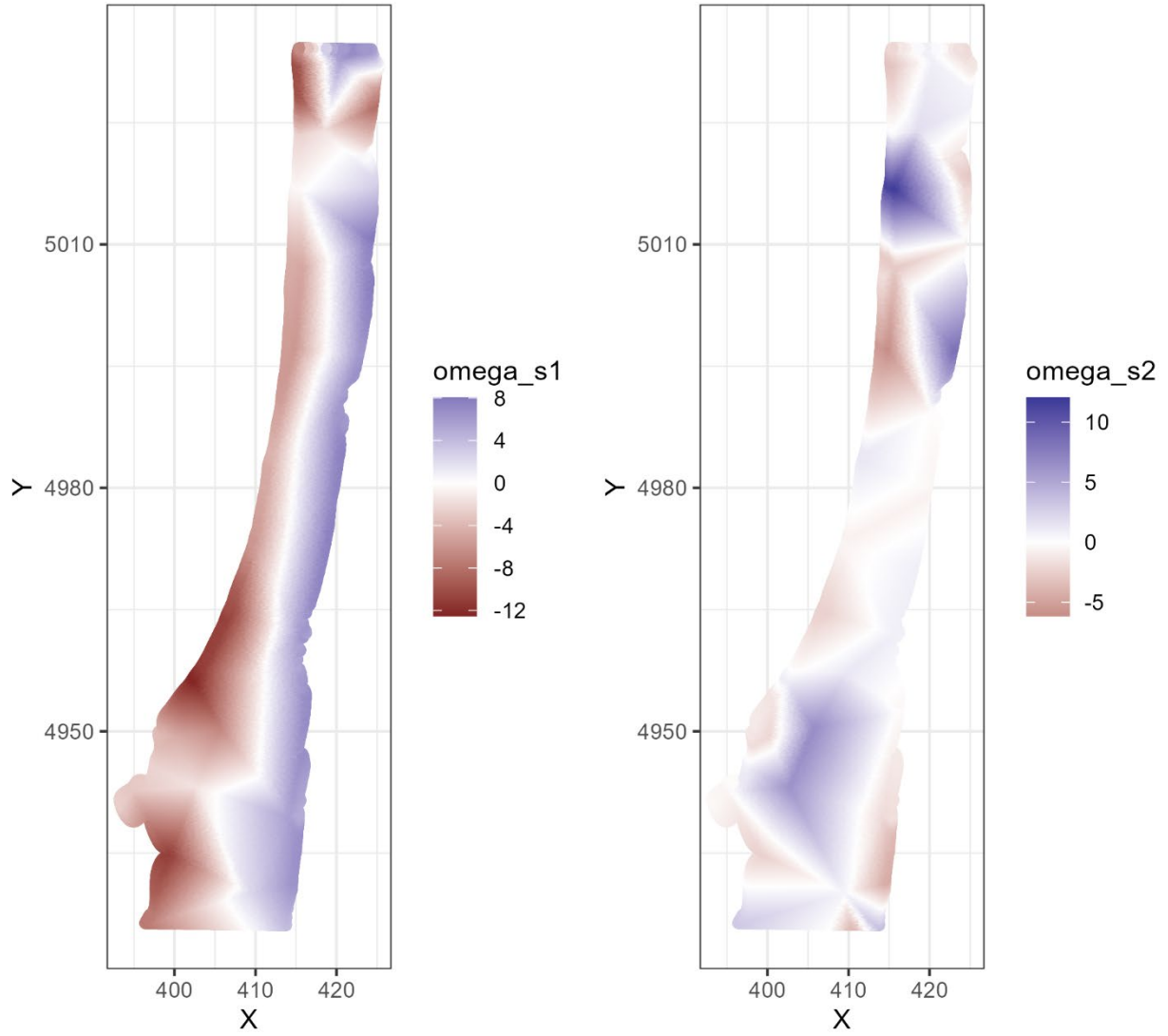


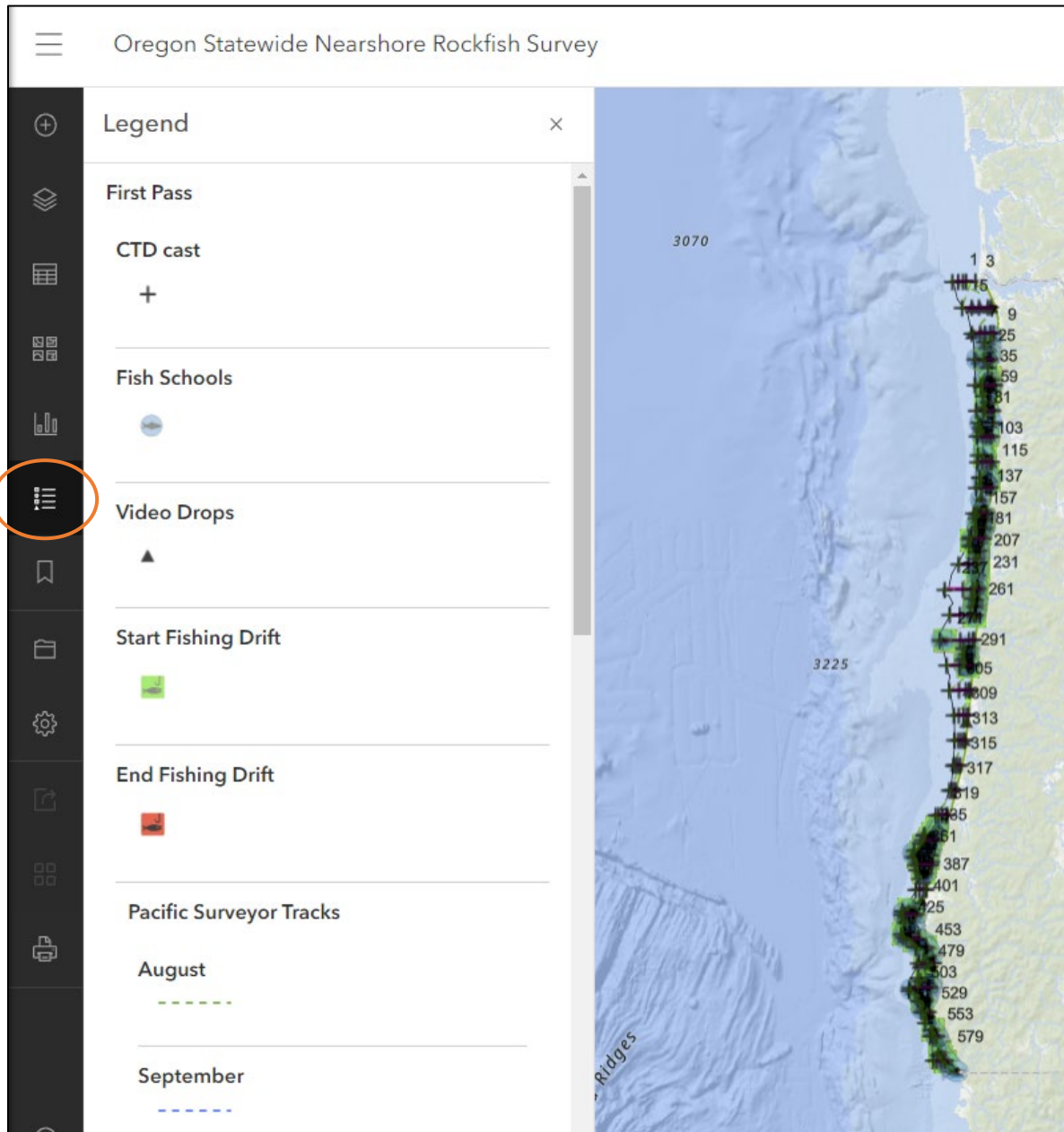
Figure 122. Predicted spatial random fields for the binomial (left) and gamma (right) models for Blue/Deacon Rockfish pass 2.

APPENDIX

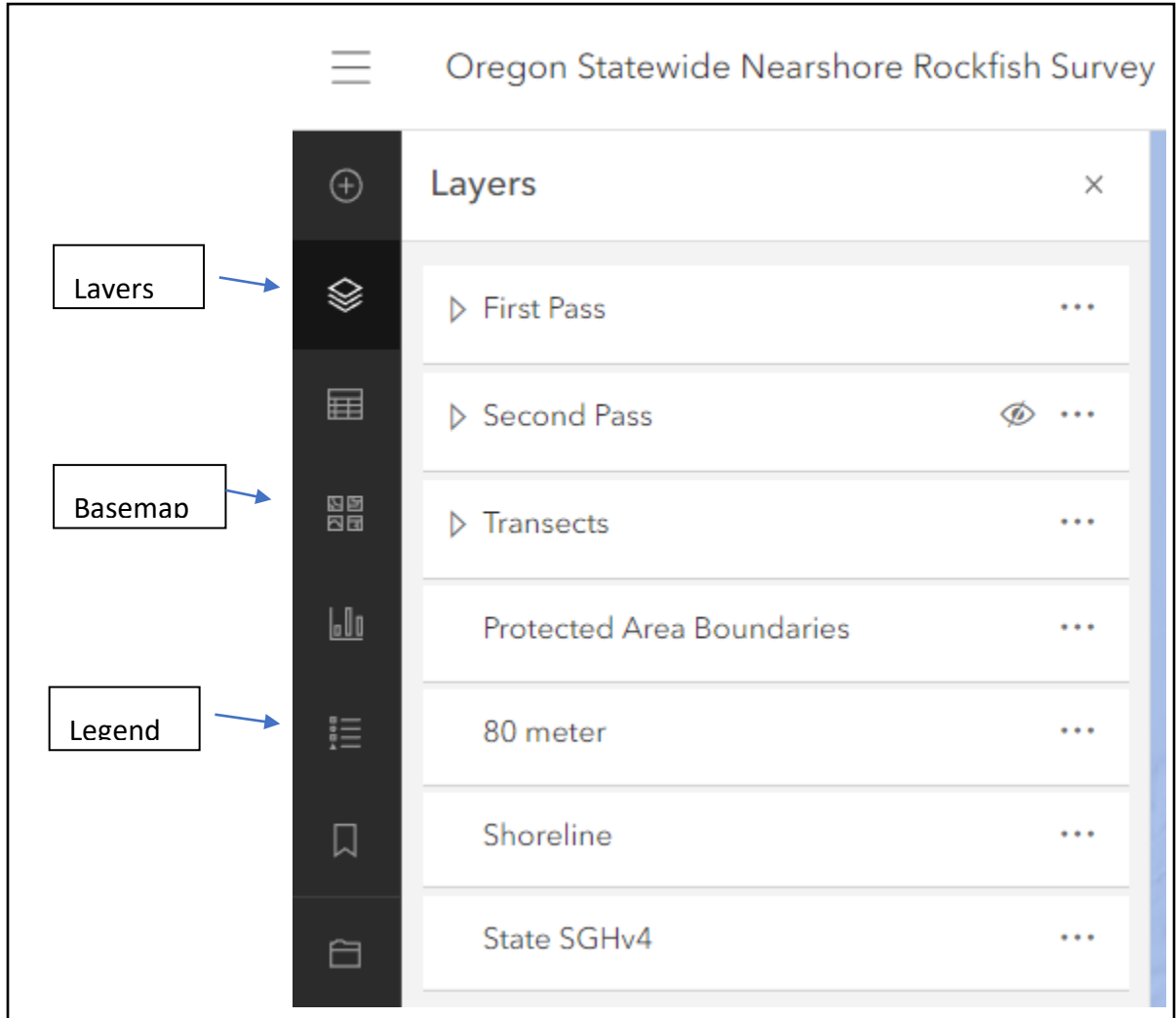
1: ONLINE SURVEY MAP HOW TO

Hyperlink to the online map is here: [Nearshore Rockfish Survey](#)

Legend: Clicking on the Legend tab shows symbology for feature layers that have been selected in the layers tab.



Layers:



Features (Layers) have been grouped into:

1. Data collection was done in two "Passes" First Pass includes August, September, and October. Second Pass consists of October and November. Features have been grouped by pass and consist of:






- a. Waypoints: CTD casts, Fish Schools, Video Drops, Start Fishing Drifts, End Fishing Drifts, and Ship Tracks separated by months.

CTD cast	Fish Schools	Video Drops	Start Fishing Drift	End Fishing Drift	Pacific Surveyor Tracks
b. +	Transects	are the	planned	transects	for the entire coast, ID is the numeric
		transect	number, Full	Transect is 80 meters to shore, Rock	Transect is focused




over rock and gravel, Zags are the transiting transects not included in our survey results.

ID	Full Transect	Rock Transect	Zags
●	—	—	- - - -

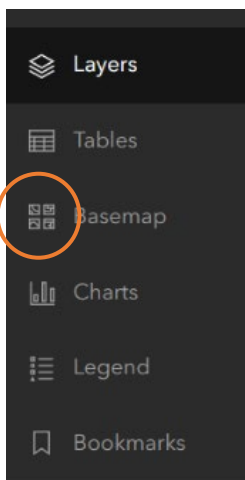
2. Other Features include Protected Area Boundaries; Marine Reserves, Marine Protected Area, Seabird Protection Area, the 80 meter contour, coastal shoreline, and SGHv4 Habitat layer (Surficial Geologic Habitat). *SGHv4 was filtered to 0-80 meters and only show Hard and Gravel habitat. Soft habitat is the remaining area inside 0-80 meters.

 Marine Reserve	80 meter —	 Hard
 Marine Protected Area	Shoreline —	 Gravel
 Seabird Protection Area		

a. Turning ON/OFF layers:

- Select “Layers” tab to turn ON/OFF layers.
- Click on  to expand the layer options available.
- Click on the eye  to show/ Hide  layer.

3. Basemap: Clicking the Basemap tab, you can select different base maps.



2: MOVEMENT PATTERNS OF BLACK ROCKFISH (SEBASTES MELANOPS) IN OREGON COASTAL WATERS

Steven J. Parker, Polly S. Rankin, Jean M. Olson, and Robert W. Hannah

Recreated from

<https://aquadocs.org/bitstream/handle/1834/18366/akuw05002.pdf?sequence=1#page=49> for simplicity.

ABSTRACT

We studied the movement patterns of black rockfish (*Sebastes melanops*) in Oregon coastal waters to estimate home range over daily to annual time scales, determine if females relocate during the reproductive season, and evaluate the influence of environmental variation on movement. We moored 18 acoustic receivers in a 3 × 5 km array south of Newport, Oregon, at depths from 9 to 40 m. We then surgically implanted 42 black rockfish (34-48 cm total length [TL]) with coded, pressure transmitters having an approximate lifespan of 6 months. Fish were tagged in August (n = 6), September (n = 13), October (n = 7), and February (n = 8 depth and 8 non-depth). Fish were temporarily absent from the monitored area for short periods (usually <7 days) indicating limited travel outside the monitored area. Seven fish left the area permanently. During one full year of monitoring, home ranges were relatively small (55±9 ha) and did not vary seasonally. Absences of females >39 cm (likely mature) from the array were longer in duration than for mature males, especially during the reproductive season (November, January, and February), but both sexes had the longest absences during April through July. These data indicate that black rockfish in open coastal waters live in a very restricted area for long periods as adults, but may relocate periodically. A small home range could make them susceptible to local depletion from targeted fishing, but also make them good candidates for protection using marine reserves.

INTRODUCTION

Understanding movement patterns and behavior is fundamental to understanding the ecology of a species. Defining an area of normal activity or home range and determining home range size stability is critical in developing strategies to manage local populations (Vincent and Sadovy 1998). In the nearshore environment along the northeast Pacific coast (<50 m depth), black rockfish (*Sebastes melanops*) are the primary target of the recreational groundfish fishery. Managers need to know the scale of daily, seasonal, and annual movements of these fish to define population boundaries and interpret catch statistics. Fisheries scientists must also know mixing rates to validate experiment assumptions (e.g., mark-recapture studies) and to understand if variable catch rates are the result of fish movement among local reefs or the

result of changes in behavior. Some earlier tagging studies have been conducted using external visual tags, providing location information for only two points in time (Coombs 1979, Gowan 1983, Mathews and Barker 1983, Culver 1987). Even with a multiyear design, both location points often occur during the seasonal fishing months, providing no information on locations at other times. For example, lower catch rates for female rockfish during the reproductive season have led to speculation that they may move to deeper water to release larvae in areas favorable for larval retention (Welch 1995; Worton and Rosenkranz 2003; Farron Wallace, Washington Department of Fish and Wildlife, pers. comm.). Managers also need to understand the scale and timing of movements if they are to use closed areas or marine protected areas (MPAs) as conservation tools to limit the impact of fishing on local populations (Kramer and Chapman 1999, Parker et al. 2000).

High resolution, medium- and long-term movement studies of rockfishes in temperate environments are challenging to conduct. The experimental design needed to monitor fish locations frequently and for relatively long periods in the marine environment requires the use of remote sensing. The tool of choice is often acoustic telemetry, which is expensive and requires an intensive monitoring and data management effort (Arnold and Dewar 2001). Weather restricts access to nearshore environments along the exposed Pacific coast year-round, but especially in winter months when storms generate strong wind and wave action (>7 m). In addition to logistical challenges, most rockfish suffer barotrauma when captured due to the expansion of gas in their physoclastic swim bladder (Parker et al. 2006). This trauma makes choosing an individual likely to survive capture more risky, makes surgical tagging more difficult, and requires additional studies to conclude that the barotrauma has no significant impact on subsequent movement behavior. Few acoustic telemetry studies of rockfish exist for these reasons. These telemetry studies have typically addressed only a few of these constraints, often by facing great logistical hurdles (Matthews 1990; Pearcy 1992; Starr et al. 2000, 2002). Our study used receiver moorings specifically designed to withstand wave and current action for long periods, yet be periodically retrievable by boat. We also removed excess swim bladder gas at the surface and used surgical implantation of transmitters.

Our objectives were to document annual, seasonal, and diel movement patterns of black rockfish, estimate home range size under different environmental conditions, and evaluate female movement during the reproductive season off the Oregon coast. Understanding black rockfish movement patterns with high resolution on both short and long time scales will provide fundamental information necessary to define local population characteristics, movement patterns and pathways, make habitat associations, and aid in the design of MPAs.

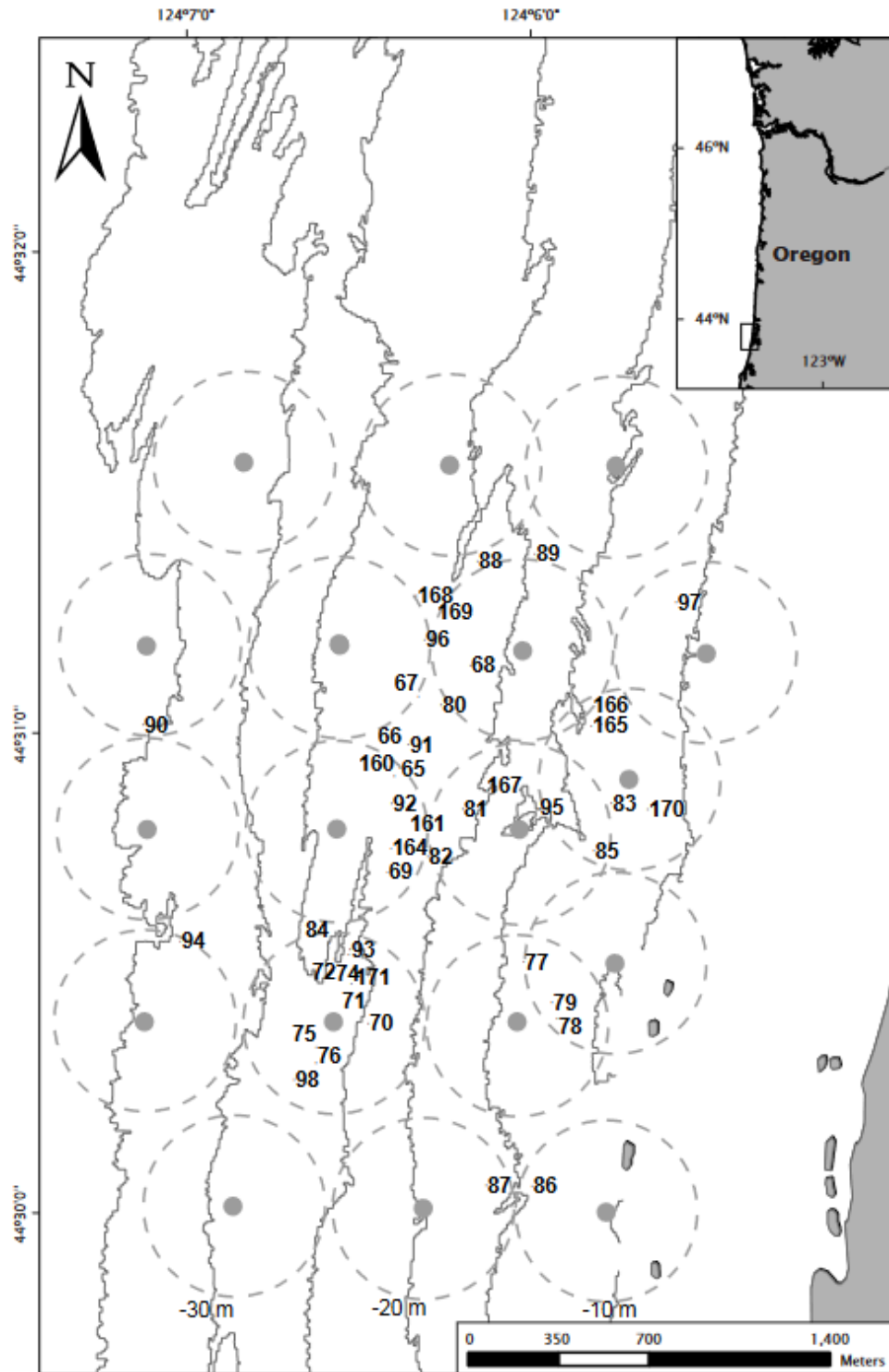


Figure 1. Map of study area showing locations of 18 acoustic receivers off Seal Rock, Oregon, and 5 m bathymetric contours. Dashed circles show expected detection range from range tests. Initial locations of released fish are shown by tag ID number. Inset shows study area location on Oregon coast. ID 84 is a moored positive-control tag.

MATERIALS AND METHODS

STUDY AREA AND ACOUSTIC ARRAY

This study was conducted in the Pacific Ocean near Newport, Oregon, at depths of 9-40 m, within an area normally fished by the recreational groundfish fishery (Fig. 1). We monitored the study site using a rectangular array of 18 VR2 69-kHz omni-directional acoustic receivers (Vemco Ltd., Nova Scotia, Canada) designed to monitor for transmitters in a 1,500 hectare area. The receivers were individually anchored on single buoy lines according to manufacturer specifications, approximately 5 m off bottom. The receivers recorded tag code, receiver number, date, time, and depth of the transmitter (for depth transmitters) at a known location. Range testing showed a normal detection range of 350-500 m radius, and receivers were spaced 700 m apart to allow tags to be detected by more than one receiver. Some receivers were moved slightly to avoid shielding by observed bathymetric features. If during the study, a receiver was lost, it was replaced as soon as possible. We also moored a tag within the array for 27 days to provide an indication of horizontal positioning accuracy and precision.

TAGGING

Fish were captured by barbless hook and line fishing throughout the study area using typical recreational fishing gear periodically from August 2004 through February 2005. We attempted to catch and tag fish throughout the monitored area to minimize transmission interference from multiple tags in the same area and to gather data on fish living at different depths. Coded acoustic V-13 HP transmitters (69 kHz, pressure sensitive [0-50 m] 155 dB output, 13 × 42 mm) were programmed to transmit at a random period of between 30-90 seconds, giving an expected battery life of 6 months (Vemco Ltd.). Black rockfish (34-48 cm TL) were vented to release excess pressure from the expanded swim bladder using an 18 gauge hypodermic needle. No anesthesia was used. Length and sex (based on external genitalia) were recorded. Only fish with few visible barotrauma symptoms were tagged (Parker et al. in press), except for ID 67. After venting, the fish was held ventral side up in a tagging cradle so that its gills were partially immersed in oxygenated seawater. Several scales were then removed on the midline, anterior to the anus. A 2 cm incision was made and a disinfected tag was inserted into the peritoneal cavity. The incision was closed with 2 to 3 sutures using PDS II 3-0 monofilament absorbable suture thread (Ethicon, New Jersey), and a small smear of Neosporin® ointment was applied to the wound as a temporary barrier to water and bacteria. The fish was allowed to recover briefly in a darkened tank until oriented, and was then released at the surface at the location of capture.

ANALYSIS

Periodically, when weather allowed, we downloaded data from the receivers and replaced any missing receivers. Data files from each receiver were appended to a master file, and any non-project or spurious transmitter codes were removed. Fish were assumed to be alive if some evidence of vertical movement beyond a continuous tidal rhythm was apparent in the depth data (tidal range ≈ 3 m, tag precision < 0.5 m). Environmental observations at the time of each transmitter detection were added (e.g., photoperiod, tide stage, wave height) from standard tables, formulas, or acquired from Oregon State University (hmsc.oregonstate.edu/weather), or the NOAA National Weather Service (ndbc.noaa.gov).

Periods of absence were determined for each tag, and the mean number of days absent was analyzed by month and sex using ANOVA of log-transformed data. The analysis of seasonal absences was restricted to fish that were likely to be mature based on the size at maturity relationship (Bobko and Berkeley 2004). We also examined periods just prior to and following

Table 1. Summary data of black rockfish tagged and released off Seal Rock, Oregon, from August 4, 2004, through August 16, 2005.

Fish ID ^a	Date range	Fork length (cm)	Sex	Duration (days)	Number of 2 h blocks	Number of absences >1 d	Linearity index	Home range MCP (ha)
65D	08/04-04/19	36	M	259	1448	33	0.004	37
66D	08/04-04/11	42	F	251	1498	23	0.002	39
67D	08/04-07/09	40	M	340	3148	5	0.002	14
68D	08/04-06/03	40	M	304	2904	7	0.008	59
69D	09/21-08/16	45	M	330	2253	26	0.004	89
70D	09/21-08/16	43	M	330	2961	12	0.001	88
71D	09/21-08/01	42	M	315	2470	9	0.003	18
72D	09/21-05/21	41	F	243	1909	6	0.002	130
74D	09/21-07/12	43	M	295	2216	15	0.003	9
75D	09/21-07/13	41	M	296	3176	3	0.001	13
76D	09/21-03/31	46	F	192	1523	5	0.006	3
77D	09/21-05/29	45	F	251	822	40	0.022	21
78D	09/21-08/16	39	M	330	2392	30	0.001	89
79D	09/21-03/28	36	M	189	988	27	0.003	7
80D	09/23-10/06	38	F	14	16	1	NA	NA
81D	09/23-07/12	34	M	293	432	38	0.012	271
82D	09/23-07/25	34	M	306	725	64	0.001	33
83D	10/04-07/16	39	M	286	2634	3	0.008	36
85D	10/04-08/15	40	F	316	827	28	0.005	59
86D	10/04-07/22	35	F	292	1981	4	0.003	18
87D	10/04-01/30	40	F	119	269	17	0.006	2
88D	10/04-08/16	40	F	317	1087	53	0.008	57
89D	10/04-08/08	46	F	309	1902	30	0.001	49
90D	10/04-08/16	45	F	317	2563	19	0.001	53
91C	02/15-08/16	38	F	183	1836	0	0.009	94
92C	02/15-05/07	38	F	82	336	6	0.217	28
93C	02/24-03/18	48	F	23	135	3	0.012	108
94C	02/24-08/16	36	F	174	1839	0	0.001	15
95C	02/15-08/16	36	M	183	1969	0	0.002	16
96C	02/25-08/16	38	M	173	1708	0	0.001	16

^aThe letter after each tag number indicates if the tag was a depth transmitter or a simple coded transmitter.

Date range is from date tagged to last day ID was detected. Duration is the total number of days ID was detected during the study. Number of 2 h blocks is the total number of 2 h average positions for each tag. Linearity index is a measure of site fidelity with little site fidelity approaching one, and strong site fidelity approaching zero. MCP is minimum convex polygon home range area.

Table 1. (Continued.)

Fish ID ^a	Date range	Fork length (cm)	Sex	Duration (days)	Number of 2 h blocks	Number of absences >1 d	Linearity index	Home range MCP (ha)
97C	02/25-08/16	38	M	173	1650	1	0.072	60
98C	02/25-07/08	36	M	134	39	6	0.228	15
160D	08/04-12/19	41	F	138	1268	5	0.004	35
161D	08/04-12/16	40	M	135	1202	4	0.000	54
164D	02/15-08/16	37	M	183	1384	16	0.004	121
165D	02/24-08/16	38	M	174	1542	2	0.003	30
166D	02/24-05/13	37	F	79	810	0	0.003	40
167D	02/15-07/02	38	F	138	215	6	0.035	232
168D	02/25-08/16	37	F	173	1757	1	0.002	17
169D	02/25-08/16	38	F	173	1117	2	0.004	33
170D	02/15-08/16	35	M	183	1092	12	0.003	26
171D	02/25-08/16	44	M	173	704	13	0.001	117
Mean		39.6		218.29		15.5	0.017	55
SEM		0.6		132.66		2.5	0.008	9

absences to determine if the fish was likely outside the array, or was not detected due to other factors (e.g., storms, loss of receiver).

Fish locations were interpolated within the receiver array as described by Simpfendorfer et al. (2002). Briefly, to calculate a mean location for a given period, the numbers of detections from multiple receivers with known locations were used as weighting factors to generate a mean position for that period. Fish positions were plotted using GIS (ArcGIS 9.1 or ArcView 3.3, ESRI, Redlands, California). We used the 5% outlier removal method from the Animal Movement Analysis Extension (Hooge and Eichenlaub 2000) to remove the effect of sample size on home range size and to remove spurious locations (Schoener 1981). This method yields a more conservative estimate of home range size given the bias in position densities determined when only two receivers detected a tag during a period, resulting in positions along a straight line between the receivers (Simpfendorfer et al. 2002).

A maximum home range for any given period was determined using the minimum convex polygon (MCP) function from ArcGIS (Beyer 2004). We calculated a site fidelity index as the ratio of distance between the first and last positions, and the total distance moved, where 1 equals a straight line (no fidelity) and a value close to zero implies strong site fidelity. Home range sizes were compared statistically with a paired t-test (diel comparisons). The relationship between fish size and home range size for each sex was examined with linear regression and a student's t-test.

RESULTS

Forty-two black rockfish were tagged and released within the array on seven different days within a seven-month period (August 2004 to February 2005) (Table 1, Fig. 1). Fish were tagged in August (n = 6), September (n = 13), October (n = 7), and February (n = 8 depth and 8 non-depth transmitters). From the appearance of external genitalia, we determined that 20 of these fish were females (one was equivocal). Based on length at maturity curves, it is likely that only 11 females were reproductively mature (>39 cm) (Bobko and Berkeley 2004). Total surgical time (removal from water to recovery chamber) was less than 10 minutes and total time from capture to release was less than 18 minutes.

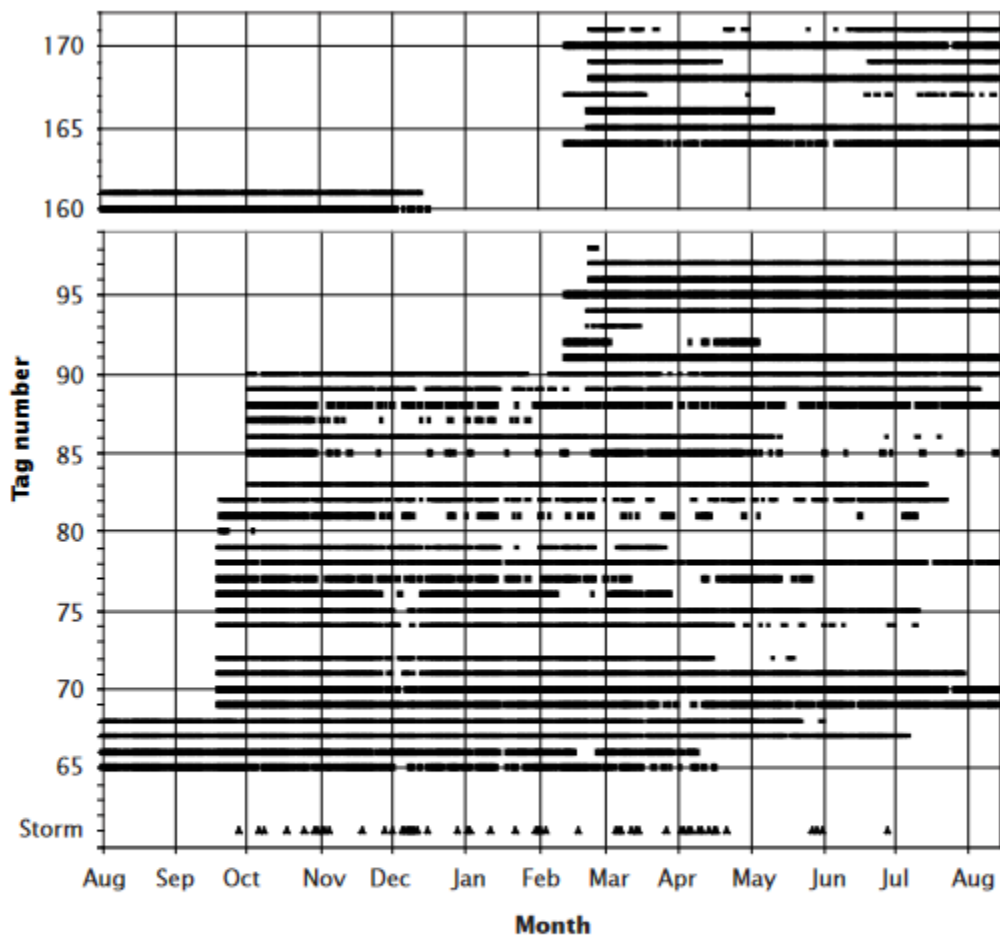


Figure 2. Presence-absence diagram showing which tags were detected in the array each day between August 4, 2004, and August 16, 2005. Days when mean overall wave height was >4.5 m are indicated by filled triangles on the line labeled “Storm”.

We recorded more than 2.4 million detections between August 4, 2004, and August 16, 2005. Fish locations were interpolated based on all observations occurring within a 2 hour period. This period was determined by comparing the number of detections per receiver for periods from 1 to 6 hours for each tag (Simpfendorfer et al. 2002). Longer periods utilize more detections when generating a position estimate. However, if the animal is moving, longer periods can yield a less accurate position. The moored tag indicated that the position averaging method was accurate to within 227 m of the known location.

We observed no evidence in the pressure data or horizontal position patterns to suggest that any fish had died within the array. However, a number of fish (7 of 42) left the array and did not return during the sixmonth period that the transmitter was expected to be functional (Fig. 2). Most of these fish left between March and May (IDs 80, 87, 92, 93, 98, 166, 167). The loss of a receiver was not correlated with any fish leaving the array for the duration of the study. The fates of these individuals are unknown, but include leaving the area volitionally (relocation), capture in the recreational fishery, tag malfunction, or predation by an animal that subsequently left the area. Although transmitters were expected to last six months, most lasted 10 months and some provided information for up to 340 days (Table 1).

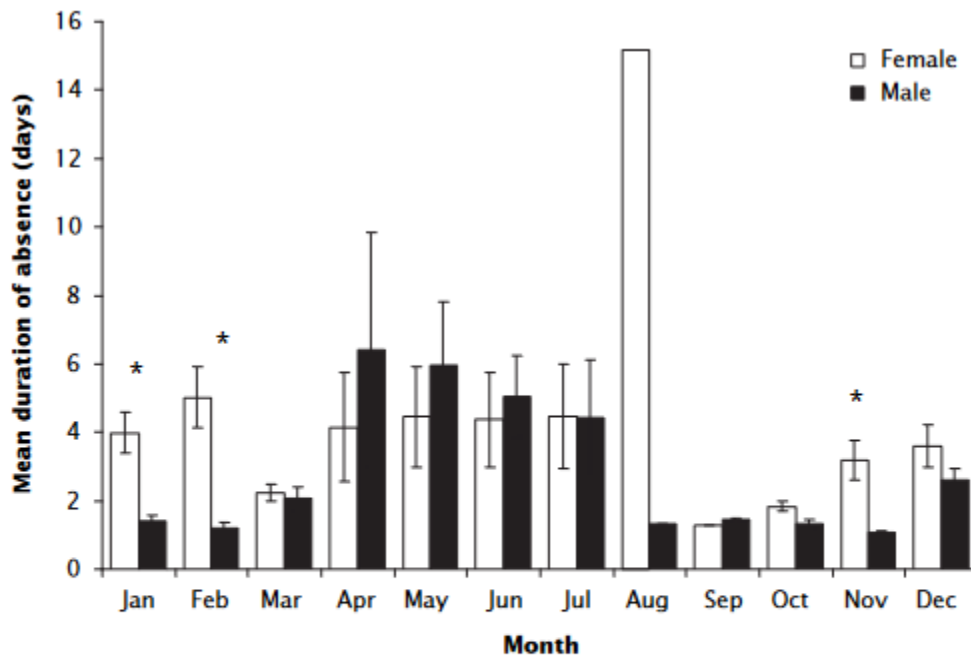


Figure 3. Mean number of consecutive days a tag was not detected within the array for males and females of reproductive size (>39 cm) for each month. Error bars are \pm standard error of the mean. Months with significant differences between sexes are indicated with *. Note: N=1 for August females, males, and September females.

The distribution of cumulative days without detection ($n = 575$ absences > 1 day) shows that for all fish combined, the median number of days absent was only 2.00, and 90% of the absences were less than 7.78 days duration. This indicates that if fish left the array, they did not range far and were usually detected again within a few days. Multiple long absences outside the monitored area were observed, some lasting more than one month, and one lasting almost four months. The fact that many fish left the array for extended periods but returned to the same sub-area within the array suggests some ability to home to a specific area. There was an overall pattern of fish temporarily leaving the array area for longer periods from April through July (Fig. 3). Females of reproductive size (>39 cm) were absent from the array for longer periods than mature males overall ($F = 6.458$, $df = 1$, $P = 0.012$) and the duration of absences varied by month ($F = 2.73$, $df = 11$, $P = 0.002$). Within a month females were absent for longer periods than males during the reproductive months; October, November through February ($P < 0.05$), though not in December ($P = 0.186$).

Some recorded absences were due to acoustic noise from storm events. Several brief periods with few detections were correlated with storm events having combined seas of more than 4.5 m (Fig. 2). We were not able to discern differences between lack of detection due to movement or due to storm events, except that storm events typically affected many fish simultaneously, and that the fish were usually detected in the area soon after the storm passed (Fig. 2, see early December). Furthermore, storms were relatively short in duration and did not impact detection for more than a few days.

For the fish that remained in the study area, horizontal movements were typically restricted to a small area. Fish had an average home range for the entire period of 55 ± 9 ha ($n = 41$), ranging from 2 to 271 ha (Table 1, Fig. 4). One fish (ID 80) was only detected at a single receiver for a short period, so a home range could not be determined. The site fidelity index was low (0.017 ± 0.008) indicating overall nondirected movement. There were a few instances of fish spending considerable time along the edge of the array, potentially biasing home range size because the scale of movement outside the monitored area is unknown (e.g., IDs 86 and 97 in Table 1). However, mean home range of fish with locations completely within the array was not significantly different from the home ranges of fish with many locations along an edge of the array ($P = 0.819$). We detected no relationship between fish length and overall home range size for either sex (females: $df = 18$, $P = 0.917$; males: $df = 21$, $P = 0.768$). There was no difference in overall home range size between sexes ($df = 39$, $P = 0.952$).

The 12 month period examined in this study did not exhibit the typical seasonal cycle in environmental conditions with long periods dominated by upwelling or downwelling conditions (Hickey 1989). The typical seasonal pattern in the study area shows upwelling beginning in May and continuing through September. 2005 was atypical in that the upwelling did not begin until

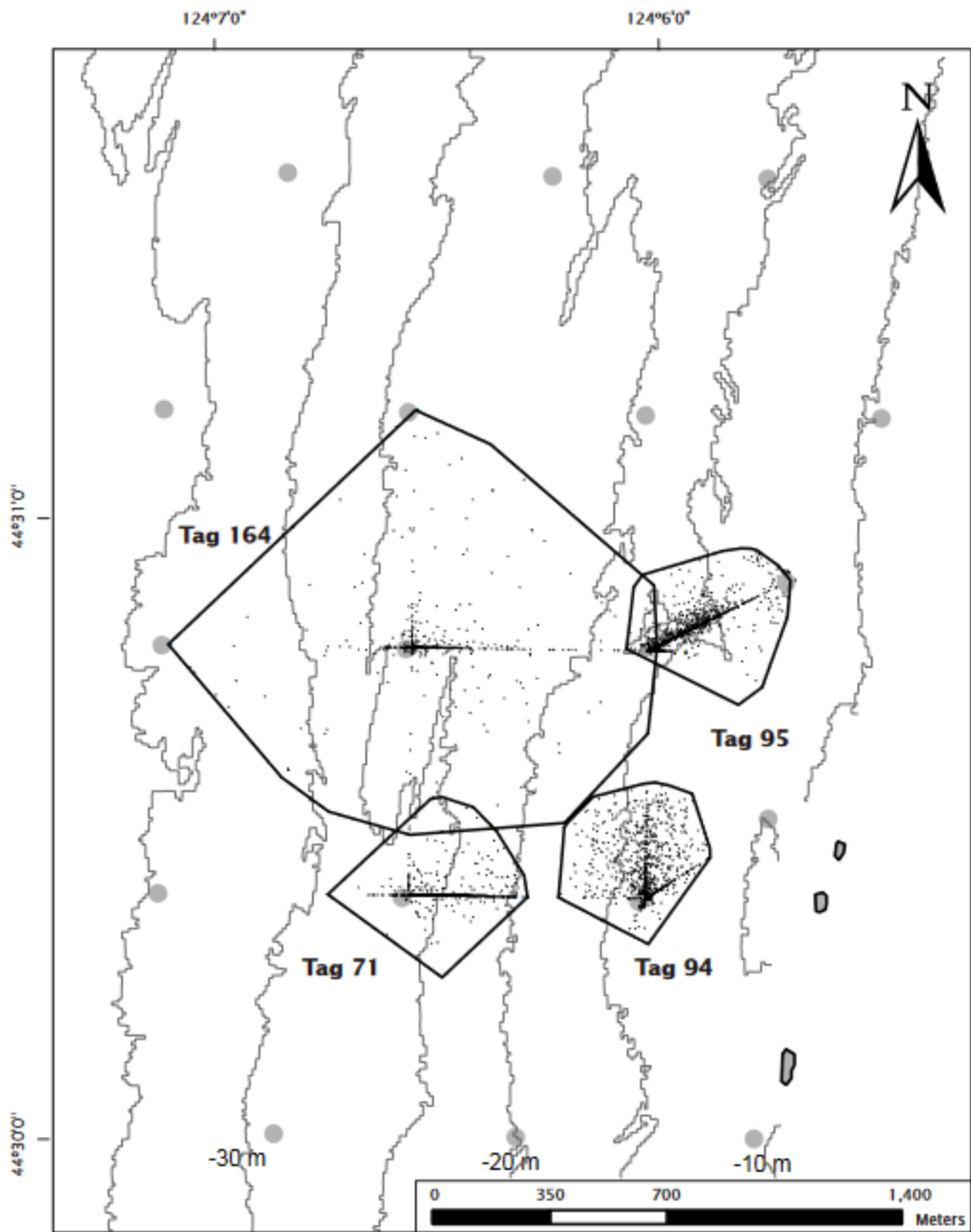


Figure 4. Examples of overall minimum convex polygons (MCPs) for black rockfish off Seal Rock, Oregon, showing small (IDs 71, 94, 95), and large (ID 164) home range sizes and the corresponding distribution of locations for each ID.

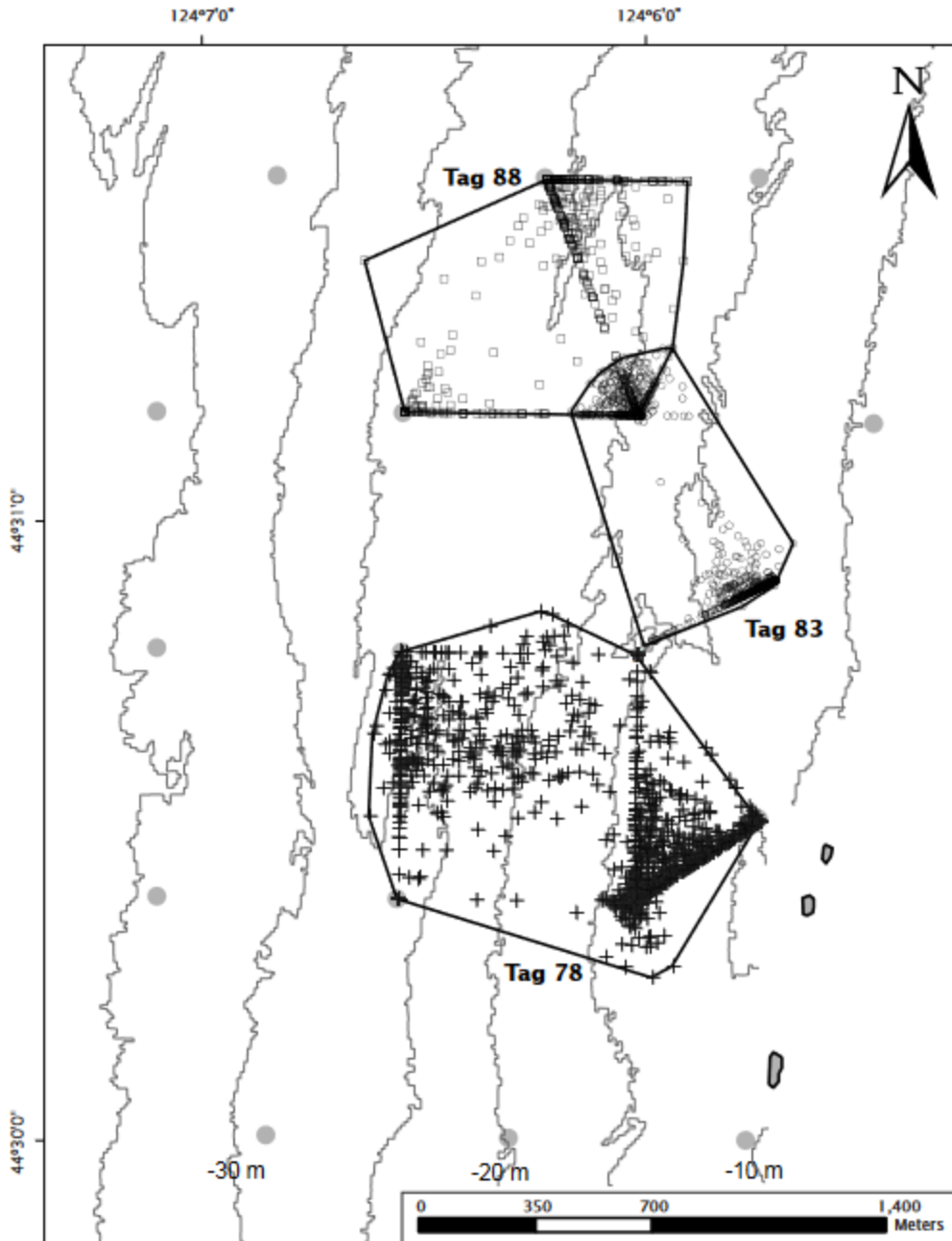


Figure 5. Examples of discrete relocations of activity areas for three black rockfish from August 2004 through August 2005. IDs 78, 83, and 88 showed repetitive movements between their two respective areas, with stays lasting several days to several months at each site.

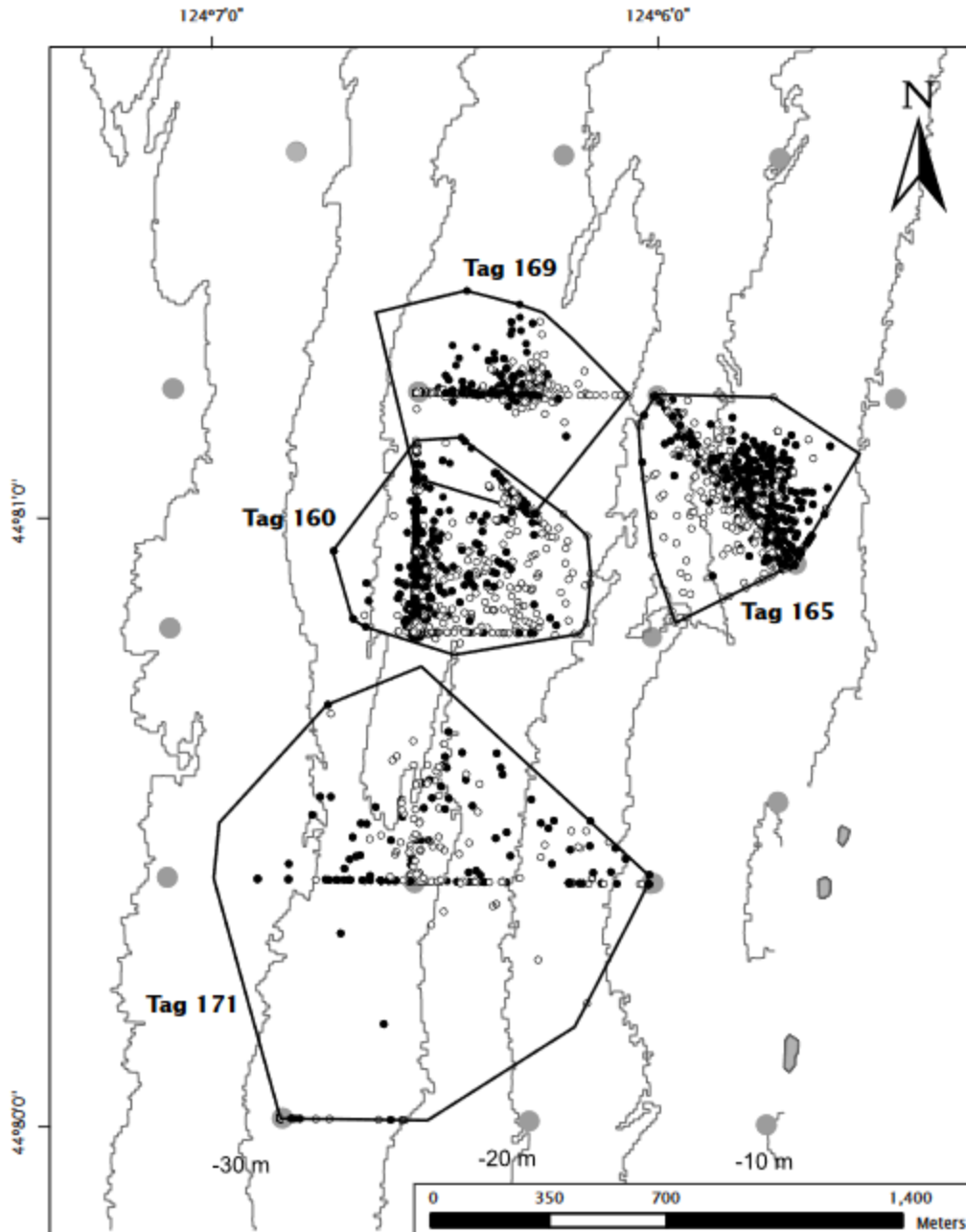


Figure 6. Examples of segregation in location during day (white circles) and night (black circles) for four fish (IDs 160, 165, 169, 171).

the end of June and then became stronger than normal. Downwelling was weaker than normal throughout the study period as well. We observed no difference in home range size associated with periods of upwelling, downwelling, or transition using the monthly upwelling index at 45°N, 125°W (www.pfeg.noaa.gov/products/las.html), ($F = 0.520$, $df = 3$, $P = 0.670$). We recorded a distinct shift in location within the array for 11 individuals during the study. These

shifts occurred on various dates and although discrete, they were not large distances (<1 km). Several fish showed repeated shifts between two sites approximately 1 km apart (Fig. 5). These relocations lasted various periods, from a few days to several months and occurred in different directions. We did not find any evidence of fish movement away from the surf zone during storm events, even though the shallow region of the array was only 9 m deep and sometimes subjected to waves more than 6 m. These repetitive relocations also suggest the ability to home over short distances. Some examples of individuals making short forays within the array but returning to a core area were observed, usually lasting just a few days. These infrequent movements were typically removed by the outlier removal process, but three individuals made multiple short forays resulting in the largest home range estimates (Table 1).

Diel movements were minor and usually not associated with a particular direction. However, four fish did show obvious directional and repetitive movements with a diel pattern (Fig. 6). Each fish moved in a different direction and the spatial shift did not appear to be directed to a specific bathymetric feature, but rather to a broader region covering a considerable portion of the home range.

DISCUSSION

Our array design allowed us to monitor the movements of 42 black rockfish at a high temporal resolution (minutes) spanning a full year for the group as a whole. Our study also provides detailed behavioral information on black rockfish from a previously unstudied environment; exposed rocky coastline in a temperate ocean. The low frequency and duration of absences observed indicate that the fish remained within the monitored area essentially for the entire period with a few exceptions, which were usually forays lasting less than 7 days, or some fish that left the monitored area permanently.

On average, black rockfish showed restricted daily movements and a relatively small home range size. However, the variation in home range size was large. Our ability to determine larger scale movements was limited, but presence-absence data allowed us to determine that most movements outside the array were of short duration and no evidence of mass seasonal movements north or south following prevailing currents was detected. Any underestimation of home range size due to edge effects was obscured by the large variability in movements among individuals. Small home range areas have been typical for rockfishes studied to date, although most telemetry studies have been of short duration (Matthews 1990, Starr et al. 2002).

Previous tagging studies of black rockfish using visual marks showed that the vast majority of recoveries were from the local tagging area during the same or following season, but the degree of movement was on short time scales, and the pattern of movements throughout the annual cycle could not be described (Culver 1987). Our results suggest that most adult black

rockfish live primarily on the same reef, and although their home ranges are large compared with some rockfish species studied in Puget Sound (Matthews 1990), they are relatively small given the dynamic environment along the open coast, especially through the winter months. If home range size was affected by ocean currents, then a more elongated north-south home range would be expected due to prevailing along-coast currents.

The size of the home range has been shown to be correlated with fish size in several tropical species, but not for rockfishes (Kramer and Chapman 1999). This relationship has been attributed to the ability of larger males to traverse larger areas, or the relative lower energy requirements for larger fish to patrol larger areas. But there is no evidence that black rockfish males actually defend a territory given their schooling nature (Hallacher 1977). The few extended absences we detected (i.e., over 1 week) suggest some ability for black rockfish to relocate a small activity area after a foray on the scale of at least several kilometers. Although Coombs (1979) displaced 50 tagged black rockfish, she did not recapture any individuals to address the possibility of homing. Studies of some other rockfish species have demonstrated homing through classic displacement techniques (Carlson and Haight 1972, Matthews 1990). Maintaining position in a small area while living semi-pelagically in a dynamic environment with strong currents, and turbid water would likely require some degree of navigation even over short distances.

We observed no distinct seasonal movement pattern or shift in distribution within an individual's home range associated with seasonal oceanographic conditions. Eleven individuals showed a distinct shift in activity centers during the study, but these were not correlated in time or direction in any discernable way. Those shifts in activity centers may be related to a home range relocation, where an individual makes a definite shift to a new location (Kramer and Chapman 1999). The most distinct seasonal movement pattern was the longer mean absence time for both sexes from April through June compared with the rest of the year, and the longer absences for females only during the winter reproductive season. Individuals may range farther during April through June as food availability changes seasonally with the start of upwelling. The absence of pregnant females in the catch during the reproductive season has generated the hypothesis that females leave their normal home range and move to an area in deeper water for gestation and parturition (Welch 1995, Worton and Rosenkranz 2003). Fisheries in the winter months are typically limited to nearshore waters close to ports. Recreational catch shows that these females are prevalent by the end of March, but not in February (Oregon Department of Fish and Wildlife, unpubl. data). An alternative hypothesis is that the females remain on the reefs but cease to actively feed, which is supported by observations of scuba-collected fish in Oregon (S. Berkeley, pers. comm.). Although not conclusive, our data suggest that females of reproductive size may leave their usual area between copulation and parturition for longer periods than males or smaller females. More

directed studies of this phenomenon are needed to show that these absences are related to reproduction and to determine where these individuals go during that period. We suspect they do not travel excessive distances because the duration of their absences was relatively short.

Marine protected areas are being considered as conservation tools to protect a portion of a population from exploitation, generate and maintain a natural age structure, or serve as a research area (Murray et al. 1999). The effectiveness of an MPA relative to these objectives depends on the temporal and spatial scale of movements of animals in and near the reserve (Kramer and Chapman 1999). The degree of exposure an individual has to exploitation outside the reserve, especially in the long term, will determine the effectiveness of any protection offered within the reserve. Other factors, such as the degree of home range relocation, or the degree to which fish density is determined by habitat type, density-dependence or environmental conditions will also affect the stability of the population inside the reserve (Chapman et al. 2005). Preference for habitat types not included in the reserve can result in fish leaving the reserve, especially if the habitat is occupied through competitive interaction. Conversely, if adult fish never leave the reserve area (no spillover), any reserve contribution to outside populations and local fisheries would be limited to export of larvae or juveniles.

Movement patterns and presence-absence data from this experiment show that although black rockfish have relatively small home ranges, these home ranges may be ephemeral and open to relocation over various distances. We observed eleven fish that shifted to a new activity center within the array, and seven fish that left the array completely, for a total of 18 fish (43%) exhibiting some type of relocation. The distance outside the array that the seven traveled is not known, but likely not more than a few kilometers given the scale of the movements within the array and information from other tagging studies. In addition to these individuals, others left the array for more than two weeks at a time. Scaling a protected area's size as a function of the home range size to achieve a specified reduction in fishing pressure still may not provide sufficient protection for a species that relocates periodically if the relocations are outside the protected area (Kramer and Chapman 1999). This is especially important in that this study monitored individual fish for more than six months. The vast majority of telemetry studies span much shorter periods, from weeks to two months, and therefore may not detect such relocations. The distances some fish moved outside the monitored area are not known and the proximal cause for the relocation is not known. Therefore, with these data it is not possible to determine a minimum reserve area that would provide a prescribed degree of protection for black rockfish. The home ranges we calculated incorporate any observed relocations, but not those leaving the monitored area. Tagging studies conducted by the Oregon Department of Fish and Wildlife and the Washington Department of Fish and Wildlife indicate that a significant portion of the population remains in the same general area for long periods, often moving less than one kilometer in two years (Oregon Department of Fish and Wildlife unpubl. data; Culver

1987). The overall pattern appears to be reef-specific dwelling with occasional relocations to nearby reefs, possibly returning to some reefs over time. This amount of mixing would allow individuals to identify and take advantage of better habitats as environment, natural mortality, and fishing pressure slowly modify the size and sex composition on nearby reefs.

Perhaps most important is the observation that black rockfish movement patterns (and scale of movement) change seasonally, and do so differently for each sex. The implications are that the design of protected areas should incorporate long-term monitoring data and that different population segments may behave differently (Chapman et al. 2005, Heupel and Simpfendorfer 2005). Therefore, caution should be used to apply our data to describe the movement patterns of black rockfish juveniles, or even black rockfish adults in different habitats. Understanding the ecology that drives movement patterns will ultimately lead to more effective protection methods.

ACKNOWLEDGMENTS

This field project required extensive fieldwork and the help of many people to deploy and maintain the array. J. Scott Malvitch managed the challenging database and tracked the status of individual fish for the entire year. We especially thank Zeb Schobernd, Troy Buell, Keith Matteson, Steve Kupillas, Jon Nottage, and Stephen Jones for their assistance in catching fish, maintaining the array, and downloading the receivers. Christopher Romsos provided GIS assistance. We also thank the fishermen and beachcombers that found and returned receivers that were lost during storm events or fishing mishaps.

REFERENCES

- Arnold, G., and H. Dewar. 2001. Electronic tags in marine fisheries research: A 30-yr perspective. In: J.R. Sibert and J.L. Nielsen (eds.), *Electronic tagging and tracking of marine fisheries*. Kluwer Academic publishers, Dordrecht, pp. 7-64.
- Beyer, H.L. 2004. Hawth's analysis tools for ArcGIS. Available at www.spatialecology.com/htools. (Accessed September 2006.)
- Bobko, S.J., and S.A. Berkeley. 2004. Maturity, ovarian cycle, fecundity, and age-specific parturition of black rockfish, *Sebastes melanops*. *Fish. Bull. U.S.* 102:418-429.
- Carlson, H.R., and R.E. Haight. 1972. Evidence for a home site and homing of adult yellowtail rockfish, *Sebastes flavidus*. *J. Fish. Res. Board Can.* 29:1011-1014.
- Chapman, D.D., E.K. Pikitch, E. Babcock, and M.S. Shivji. 2005. Marine reserve design and evaluation using automated acoustic telemetry: A case-study involving coral reef-associated sharks in the Mesoamerican Caribbean. *Mar. Tech. Soc. J.* 39:42-55.
- Coombs, C.I. 1979. Reef fishes near Depoe Bay, Oregon: Movement and the recreational fishery. M.S. thesis, Oregon State University, Corvallis. 39 pp.

- Culver, B.N. 1987. Results from tagging black rockfish (*Sebastes melanops*) off the Washington and northern Oregon coast. In: Proceedings of the International Rockfish Symposium. Alaska Sea Grant, University of Alaska Fairbanks, pp. 231-240.
- Gowan, R.E. 1983. Population dynamics and exploitation rates of rockfish (*Sebastes* spp.) in central Puget Sound, Washington. Ph.D. thesis, University of Washington, Seattle. 90 pp.
- Hallacher, L.E. 1977. Patterns in space and food used by inshore rockfishes (*Scorpaenidae*: *Sebastes*) of Carmel Bay, California. Ph.D. thesis, University of California, Berkeley. 115 pp.
- Heupel, M.R., and C.A. Simpfendorfer. 2005. Using acoustic monitoring to evaluate MPAs for shark nursery areas: The importance of long-term data. *Mar. Tech. Soc. J.* 39:10-18.
- Hickey, B.M. 1989. Patterns and processes of circulation over the Washington continental shelf and slope. In: M.R. Landry and B.M. Hickey (eds.), *Coastal oceanography of Washington and Oregon*. Elsevier Oceanography Series, New York, pp. 41-109.
- Hooge, P.N., and W.M. Eichenlaub. 2000. Animal movements extension to Arcview. Alaska Biological Center, U.S. Geological Survey, Anchorage, Alaska.
- Kramer, D.L., and M.R. Chapman. 1999. Implications of fish home range size and relocation for marine reserve function. *Environ. Biol. Fishes* 55:65-79.
- Mathews, S.B., and M.W. Barker. 1983. Movements of rockfish (*Sebastes*), tagged in northern Puget Sound. *Fish. Bull. U.S.* 82:916-922.
- Matthews, K.R. 1990. An experimental study of the habitat preferences and movement patterns of copper, quillback, and brown rockfishes (*Sebastes* spp.). *Environ. Biol. Fishes* 29:161-178.
- Murray S., R. Ambrose, J. Bohnsack, L. Botsford, M. Carr, G. Davis, P. Dayton, D. Gotshall, D. Gunderson, M. Hixon, et al. 1999. No-take reserves: Sustaining fishery populations and marine ecosystems. *J. Am. Fish. Soc.* 24(11):11-25.
- Parker, S.J., H.I. McElderry, P.S. Rankin, and R.W. Hannah. 2006. Bouyancy regulation and barotrauma in two species of nearshore rockfish. *Trans. Am. Fish. Soc.* 135:1213-1223.
- Parker, S.J., S.A. Berkeley, J.T. Golden, D.R. Gunderson, J. Heifetz, M.A. Hixon, R. Larson, B.M. Leaman, M.S. Love, J.A. Musick, et al. 2000. Management of Pacific rockfish. *J. Am. Fish. Soc.* 23:22-25. P
- earcy, W.G. 1992. Movements of acoustically tagged yellowtail rockfish *Sebastes flavidus* on Heceta Bank, Oregon. *Fish. Bull. U.S.* 90:726-735.
- Schoener, T.W. 1981. An empirically based estimate of home range. *J. Theor. Biol.* 20:281-325.
- Simpfendorfer, C.A., M.R. Heupel, and R.E. Hueter. 2002. Estimation of shortterm centers of activity from an array of omnidirectional hydrophones and its use in studying animal movements. *Can. J. Fish. Aquat. Sci.* 59:23-32.
- Starr, R.M., J.N. Heine, and K.A. Johnson. 2000. In situ techniques for tagging and tracking rockfishes. *N. Am. J. Fish. Manag.* 20:597-609.
- Starr, R.M., J.N. Heine, J.M. Felton, and G.M. Cailliet. 2002. Movements of bocaccio (*Sebastes paucispinis*) and greenspotted (*Sebastes chlorostictus*) rockfishes in a Monterey submarine canyon: Implications for the design of marine reserves. *Fish. Bull. U.S.* 100:324-337.
- Vincent, A.C.J., and Y.J. Sadovy. 1998. Reproductive ecology in the conservation and management of fishes. In: T.M. Caro (ed.), *Behavioral ecology and conservation biology*. Oxford University Press, New York, pp. 209-245.

- Welch, D.W. 1995. First offshore spawning for black rockfish, *Sebastes melanops*. *Can. Field-Nat.* 109(4):477-479.
- Worton, C.L., and G.E. Rosenkranz. 2003. Sex, age, and growth of black rockfish *Sebastes melanops* from a newly exploited population in the Gulf of Alaska, 1993-1999. *Alaska Fish. Res. Bull.* 10:14-27.

3: PATTERNS IN VERTICAL MOVEMENTS OF BLACK ROCKFISH SEBASTES MELANOPS

S. J. Parker, J. M. Olson, P. S. Rankin, J. S. Malvitch

Recreated here for simplicity from <https://www.int-res.com/abstracts/ab/v2/n1/p57-65/>.

ABSTRACT

Black rockfish *Sebastes melanops* are generally associated with benthic structure, but are also described as semi-pelagic and are frequently found near the surface. We described patterns associated with the vertical movements of 33 black rockfish using acoustic telemetry in the nearshore waters of the Northeast Pacific Ocean off Newport, Oregon (9 to 45 m depth). The fish were monitored by an array of 18 moored receivers for a 12 mo period. Black rockfish showed larger, more frequent, and more temporally structured vertical movements throughout the study period than are typically assumed for rockfishes, which may make hydroacoustic surveys difficult to design. Diel vertical movements occurred sporadically, with individuals sometimes being shallower either during day or at night, and the pattern was often maintained for more than a week. Periods of large vertical movements (multiple excursions > 5 m not in synch with diel phase) were most common during the months of October and May. The diel behavior of being shallower at night was most common during spring months and showed a slow decline in prevalence throughout the summer months. The reverse pattern (shallower depths during daylight hours) was less common overall, but most prevalent in autumn. These data show that black rockfish make extensive vertical movements, often tightly in phase with sunrise or sunset, and that several behaviors, such as diel vertical migration, may be more prevalent at certain times of the year.

INTRODUCTION

As their common name implies, rockfishes *Sebastes* spp. are typically tightly associated with benthic structure (Love et al. 2002). Exceptions exist, especially for continental shelf species such as widow rockfish *S. entomelas*, yellowtail rockfish *S. flavidus*, and chilipepper rockfish *S. goodei*, which are often captured in mid-water trawl fisheries and observed in pelagic schools (Wilkins 1986, Pearcy 1992, Stanley et al. 1999, 2000, Parker et al. 2000). The black rockfish *S. melanops* is also a semi-pelagic species, although it typically inhabits waters shallower than 55 m from central California to the Aleutian Islands (Love et al. 2002). Because rockfishes have a physoclistic swimbladder, they are subject to decompression injuries from excessive vertical movements, especially at these shallow depth scales (Parker et al. 2006). This potential for injury should limit the extent of rapid vertical excursions, especially as they approach the surface where gas volume increases by 50% between 20 and 10 m depth, and doubles in the

final 10 m. This physical constraint suggests limited or slow vertical movements, especially if approaching the surface.

There has been considerable interest in developing a hydroacoustic survey for black rockfish to take advantage of their semi-pelagic distribution (Boettner & Burton 1990, Pedersen & Boettner 1992, Alaska Department of Fish and Game unpubl. data). Significant vertical movements, especially if occurring nonrandomly and by various segments of the population, can influence availability to sonar and could bias hydroacoustic survey biomass estimates. These surveys also rely on the ability to distinguish midwater targets from the bottom echo return, which may not be possible if black rockfish spend significant time resting on the bottom, as sometimes observed in SCUBA surveys (Love et al. 2002). Conversely, because much of their range is shallower than 25 m, significant time spent within a few meters of the surface also renders black rockfish undetectable by downwardly aimed hydroacoustic devices (Krieger et al. 2001). Knowledge of the vertical distribution of black rockfish is necessary to determine whether the proportion of the population undetectable at a given time is uniform, or, if variable, to determine whether their vertical movements show predictable patterns.

As targets of both recreational and commercial fisheries, and because they live in relatively shallow water, there is significant observational information from divers and fishers on black rockfish behavior patterns, movement, and habitat associations (Leaman 1977, McElderry 1979). These observations suggest they may move to the surface relatively quickly and that they tend to be inactive and rest on or near the bottom at night, at least in shallow kelp forest habitats (Love et al. 2002). However, these observations are of very short duration and consist of groups of fish, not individuals. The goal of the present study was to characterize the vertical movements of individual black rockfish in open-coast reef habitats using acoustic telemetry. Knowledge of these patterns will aid in designing survey methods and in understanding the role of black rockfish in nearshore ecosystems. Our specific objectives were to quantify the scale, frequency, duration, stability, and population-level coherence of vertical movements on an annual time scale and to correlate environmental conditions with selected movement patterns.

MATERIALS AND METHODS

This study was conducted in the Pacific Ocean near Newport, Oregon, at depths of 9 to 40 m as part of a telemetry study of home range size (Fig. 1, Parker et al. 2007). We monitored the study site using a rectangular array of 18 VR2 69 kHz omni-directional acoustic receivers (Vemco Ltd.) arranged to monitor for transmitters in a 15 km² area. The receivers were individually anchored on single buoy lines approximately 5 m off bottom. The receivers recorded tag code, receiver number, date, time, and depth of the transmitter at a known

location. Range testing showed a normal detection range of 350 to 500 m radius, and receivers were spaced approximately 700 m apart to allow tags to be detected by >1 receiver.

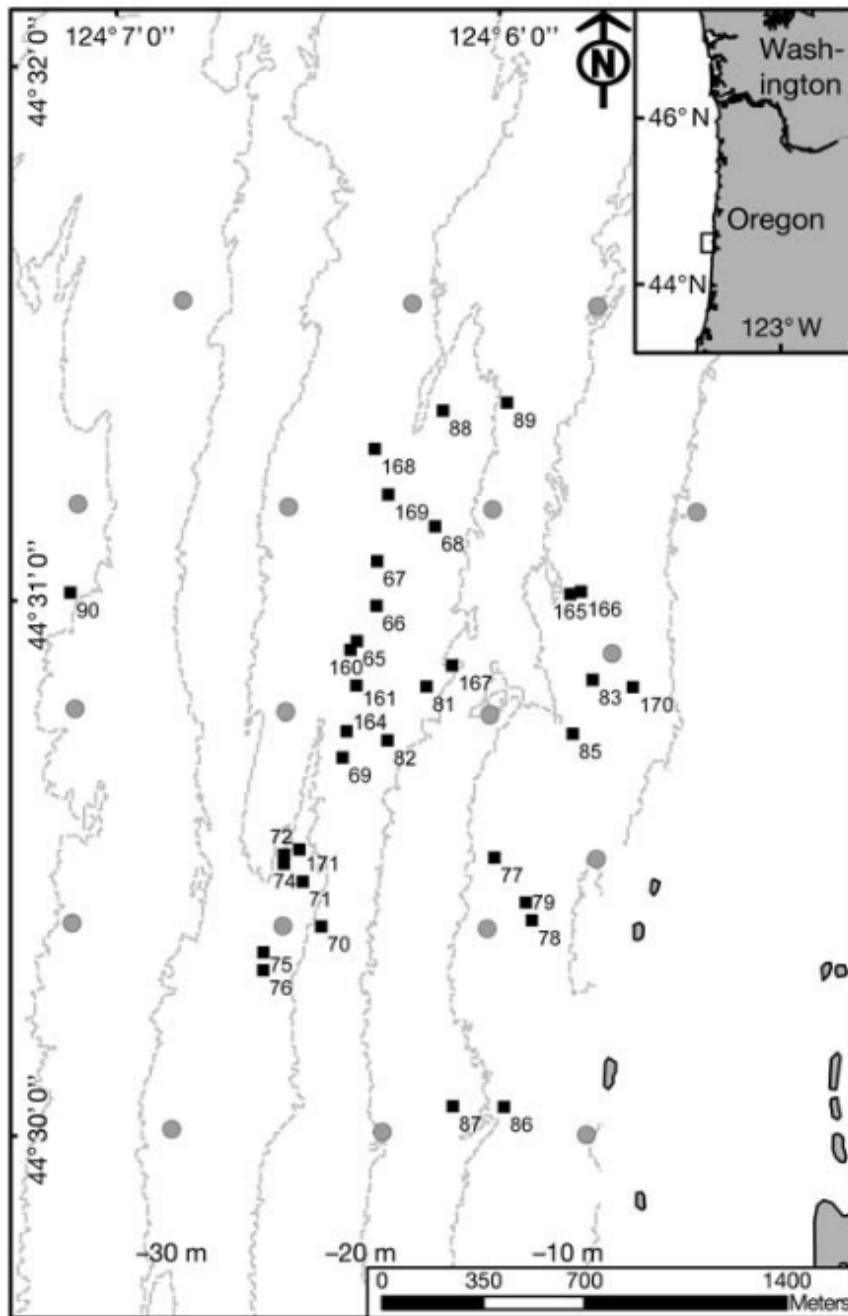


Fig. 1. Study area showing locations of 18 acoustic receivers off Seal Rock, OR, and 5 m bathymetric contours. Initial locations of released fish *Sebastes melanops* for each identification number (■); locations of acoustic receiver moorings (●); 5 m depth contours (---); inset: study area location on Oregon coast

Black rockfish *Sebastes melanops* were captured by barbless hook and line fishing throughout the study area using typical recreational fishing gear on 7 occasions from August 2004 through February 2005. Fish were tagged with surgically implanted transmitters and released at capture sites throughout the monitored area to maximize habitats studied and to minimize transmission interference from multiple tags in the same area (for details, see Parker et al. 2007). Coded acoustic V-13 HP transmitters (Vemco Ltd., 69 kHz, pressure sensitive [0 to 50 m] 155 dB output, 13 × 42 mm, vertical precision < 0.25 m) were programmed to transmit at a random period of between 30 and 90 s, with a nominal battery life of 6 mo.

Table 1. *Sebastes melanops*. Category definitions describing vertical movements occurring during each 24 h period for black rockfish off Seal Rock, OR, from August 2004 through August 2005

Abbreviation	Behavior type	Description
BT	Bottom tending	Bottom-oriented behavior which resembled a tidal pattern for most of the 24 h period
LV	Large vertical movement	Frequent vertical movements exceeding 5 m in scale throughout the 24 h period
SV	Small vertical movement	Frequent vertical movements <5 m in scale throughout the 24 h period
SN	Shallower during night	Vertical movements partitioned during the diel cycle where there was a distinct shift to a shallower depth during hours of darkness
SD	Shallower during day	Vertical movements partitioned during the diel cycle where there was a discrete shift to a shallower depth during hours of daylight
Other	Uncategorized	Days lacking enough observations to categorize behavior as any of the other behaviors

Periodically, when weather allowed, we downloaded the receivers and replaced any missing receivers. Fish were assumed to be alive on a given day if some evidence of vertical movement beyond a continuous tidal rhythm was apparent in the depth data (tidal range = ~3 m) after that day. Environmental observations at the time of each detection, including photoperiod, lunar day, tide stage, wave height, solar irradiance at Newport, cloud cover, water temperature at Seal Rock, and daily east and north upwelling, were obtained from standard tables, formulas, or acquired from Oregon State University, the NOAA National Weather Service, Pacific Fisheries Environmental Laboratory, or the US Naval Observatory (<http://hmsc.oregonstate.edu/weather/>, <http://ndbc.noaa.gov/>, <http://las.pfeg.noaa.gov> and <http://aa.usno.navy.mil/>).

Table 2. *Sebastes melanops*. Summary data of 33 black rockfish tagged and released off Seal Rock, OR, from August 4, 2004 through November 15, 2005

Fish ID	Date range (mm/dd)	Length (cm)	Gender	Duration (d)	Max. depth (m)	Min. depth (m)	Annual mean depth (m)
65	08/04-04/19	36	M	259	-28.5	0.0	-19.3
66	08/04-04/11	42	F	251	-26.4	-0.6	-11.0
67	08/04-07/09	40	M	340	-34.2	-0.3	-26.0
68	08/04-06/03	40	M	304	-44.6	0.0	-12.4
69	09/21-08/16	45	M	330	-36.4	-0.3	-21.1
70	09/21-08/16	43	M	330	-35.7	-0.6	-20.3
71	09/21-08/01	42	M	315	-33.0	-5.1	-23.0
72	09/21-05/21	41	F	243	-37.1	-1.6	-21.1
74	09/21-07/12	43	M	295	-39.6	-3.4	-27.8
75	09/21-07/13	41	M	296	-42.6	-1.2	-24.0
76	09/21-03/31	46	F	192	-35.9	-4.4	-28.0
77	09/21-05/29	45	F	251	-32.7	-0.3	-18.6
78	09/21-08/16	39	M	330	-37.8	-0.3	-11.3
79	09/21-03/28	36	M	189	-21.0	-1.3	-13.2
81	09/23-07/12	34	M	293	-31.0	-2.8	-18.9
82	09/23-07/25	34	M	306	-31.0	-1.2	-15.0
83	10/04-07/16	39	M	286	-30.2	-0.9	-15.4
85	10/04-08/15	40	F	316	-33.4	-0.6	-6.6
86	10/04-07/22	35	F	292	-28.0	-0.3	-11.1
87	10/04-01/30	40	F	119	-27.1	-0.6	-9.3
88	10/04-08/16	40	F	317	-31.1	-3.1	-14.9
89	10/04-08/08	46	F	309	-36.0	-0.6	-12.0
90	10/04-08/16	45	F	317	-44.8	-0.9	-34.2
160	08/04-12/19	41	F	138	-30.1	-0.6	-16.8
161	08/04-12/16	40	M	135	-27.0	-0.6	-12.0
164	02/15-08/16	37	M	183	-30.3	-0.6	-10.4
165	02/24-08/16	38	M	174	-21.0	0.0	-12.0
166	02/24-05/13	37	F	79	-18.8	0.0	-7.4
167	02/15-07/02	38	F	138	-25.7	-3.4	-12.1
168	02/25-08/16	37	F	173	-27.1	-0.3	-8.4
169	02/25-08/16	38	F	173	-30.6	-1.2	-15.0
170	02/15-08/16	35	M	183	-18.0	-0.3	-3.0
171	02/25-08/16	44	M	173	-36.8	-0.9	-16.2
Mean		39.6		218	-31.5	-1.2	-16.3
SEM		0.6		132	1.2	0.2	1.2

Plots of vertical movements were generated for each fish, and the movement pattern for each 24 h period was categorized to the most detailed level possible (Table 1). These daily patterns were then analyzed with respect to prevailing environmental conditions and with the movement patterns of other tagged black rockfish. Descent and ascent rates were calculated by sorting records by date, time, tag number, and receiver number, calculating the time elapsed between successive records and normalizing to a per minute standard, providing a minimum vertical movement rate. Because there were many fish simultaneously at large, we looked for coherence in daily behavior patterns among fish. Coherence in behavior patterns among fish was summarized by calculating the percentage of observed fish showing a particular behavior pattern on a given day. Daily behaviors were categorized visually based on a detailed depth trace, which also included photoperiod information. Periodicity in vertical movements was evaluated using a Lomb-Scargle periodogram to identify significant rhythms in vertical movements occurring with periods between 5 and 30 h, available as a routine in R (for details see Ruf 1999). Sample size requirements prohibited analyses searching for cycles with longer periods (weeks or months), as the data series must contain observations spanning at least 10 cycles of interest for adequate statistical power.

RESULTS

Thirty-three black rockfish *Sebastes melanops* (34 to 46 cm total length [TL]) were tagged with depth transmitters and released within the array during 7 tagging days within a 7 mo period (Table 2, Fig. 1). From the appearance of external genitalia, we determined that 15 of these fish were females. Based on length at maturity curves, it is likely that only 10 of the females were reproductively mature (>39 cm) (Bobko & Berkeley 2004).

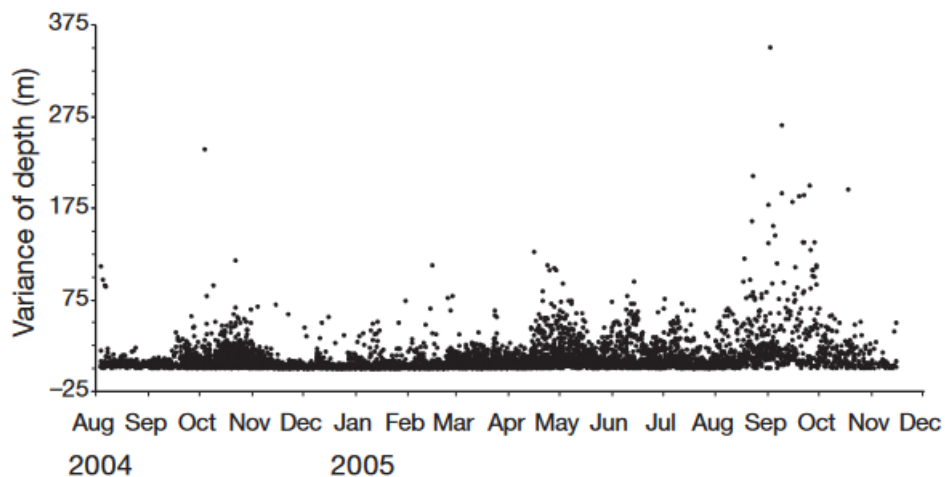


Fig. 2. *Sebastes melanops*. Daily variance in depth (m) for each fish from August 4, 2004 to November 15, 2005. Note: excludes 1 data point at 590.69 for Tag ID 171 on August 22, 2005

We recorded > 3 million detections between August 4, 2004 and November 14, 2005. We observed no evidence in the pressure data indicating that any fish had died within the array. However, 3 fish left the array and did not return during the 6 mo period that the transmitter was expected to be functional (IDs 87, 166, 167). These 3 fish still provided 79 to 138 d of information. Although nominal transmitter life was 6 mo, most lasted 10 mo and some provided information for nearly 1 yr (Table 2).

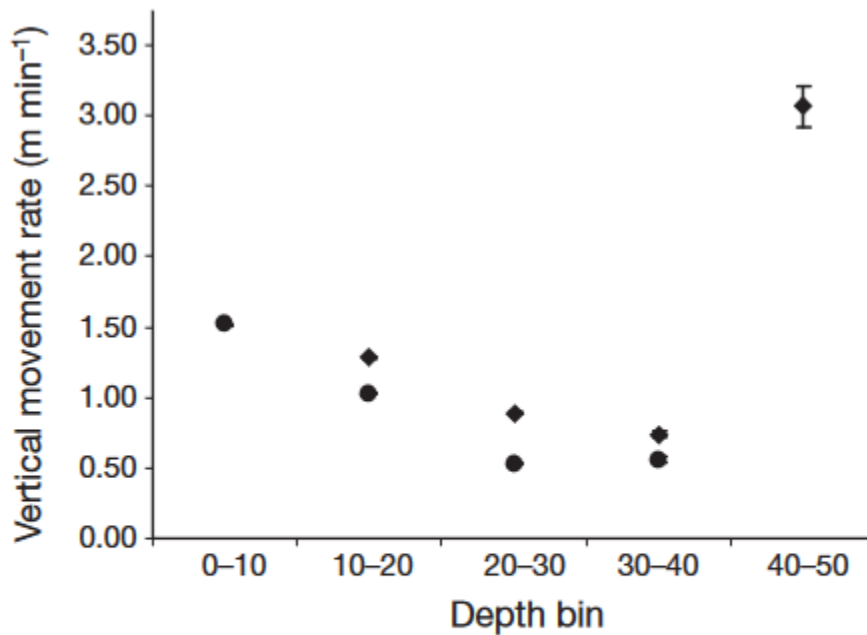


Fig. 3. *Sebastes melanops*. Mean ascent (◆) and descent (●) rates (m min⁻¹) for movements beginning at different depth ranges from 0 to 50 m. Movements near boundaries (ascents beginning at 0 to 10 m and descents beginning at 40 to 50 m) are not meaningful and therefore omitted. Error bars: SEM

The daily variance in depth for each fish plotted for the entire study period shows a pulse in range of vertical movement from September through November in 2004 and 2005, and a series of 3 short pulses during the summer months (Fig. 2). In general, vertical movements were smaller in the winter. Minimum rates of ascent and descent had identical ranges, with > 99% of the values <14 cm s⁻¹, equivalent to 8.4 m min⁻¹. The ratio of ascents to descents versus speed of the movement showed that fast movements (>15 m min⁻¹) were 10 to 50% more likely to be dives, whereas movements slower than 15 m min⁻¹ were equally likely to be descents or ascents. Vertical movement rates were different depending on starting depth (Fig. 3). The fastest ascents began at depths of 40 to 50 m (log-transformed ANOVA, $p < 0.0001$), whereas the fastest descents occurred at starting depths of 0 to 10 m (logtransformed ANOVA, $p < 0.0001$). Long

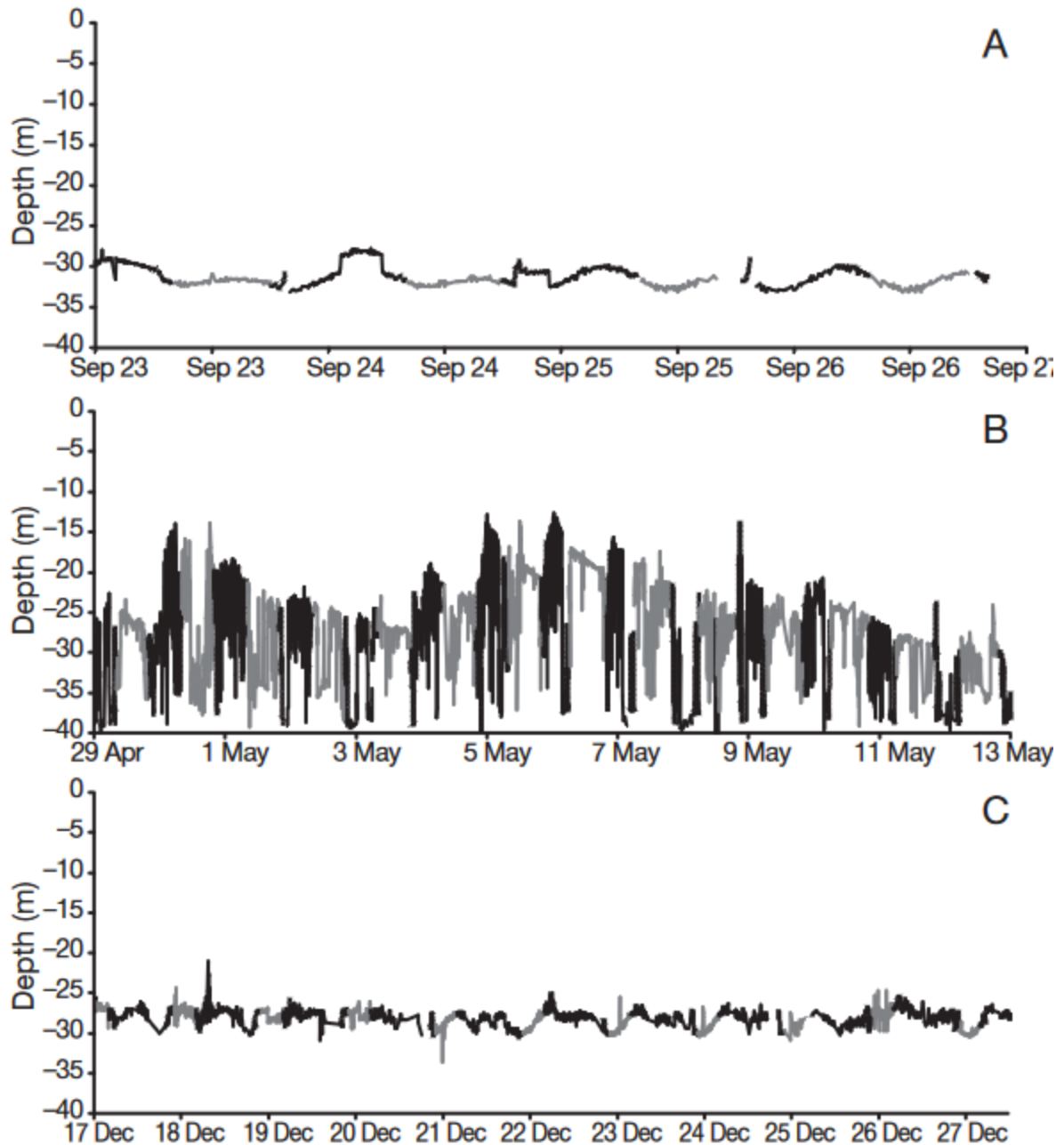


Fig. 4. *Sebastes melanops*. Examples of black rockfish behaviors observed between August 4, 2004 and November 15, 2005. Black line segments: night; grey lines: daylight; dotted lines: crepuscular periods (within 1 h of sunrise or sunset). Zero depth represents the surface. (A) Bottom tending behavior, ID76; (B) large vertical movements (>5 m), ID 90; and (C) small vertical movements (<5 m), ID 75

periods between detections were few (90% of observations were <10 min apart), bias in dive rates was negligible, and no change in pattern with depth was observed by including all the data.

We also observed multi-day periods in which the depth of a fish varied directly with the tidal cycle, indicating it was either on the bottom or maintaining a fixed position in the water column relative to the bottom. This behavior was termed bottom tending (BT) (Fig. 4A) and was displayed intermittently by most fish, with the behavior much more common among a few fish (Table 3). BT behavior was observed for up to 9 contiguous days, but typically it was observed for only a single day at a time. Common examples of BT behavior may be due to a recovery period following surgery and release. Of the 33 fish, 8 did not show BT behavior during the first 10 d. Of the 25 fish that did, 21 fish showed BT behavior for between 2 and 4 d, with most fish at 2 d. Substantial and frequent vertical movements were apparent in all individuals throughout the study. No fish showed a continuous tidal pattern in depth which would indicate that the fish had died.

Table 3. *Sebastes melanops*. Summary of percent of days showing categorized behavior types observed from black rockfish tagged and released off Seal Rock, OR, from August 4, 2004 through November 15, 2005. Max. days indicates maximum number of contiguous days an individual fish showed the particular behavior pattern. Abbreviations of behavior types: see Table 1

Fish ID	BT	SD	SN	LV	SV	Other
65	5.4	11.6	1.2	23.2	13.1	45.6
66	4.0	6.0	6.8	32.3	17.9	33.1
67	26.3	14.8	2.7	8.9	40.2	7.1
68	4.1	2.4	39.7	33.9	11.9	8.1
69	17.9	7.9	3.3	13.9	27.9	29.1
70	3.9	8.5	31.2	32.4	11.8	12.1
71	8.6	13.4	2.2	21.3	39.5	15.0
72	7.8	6.2	9.5	21.4	32.1	23.0
74	41.6	8.4	2.0	6.8	6.8	34.5
75	18.6	4.7	45.6	20.9	4.4	5.7
76	33.9	7.3	10.4	8.9	15.6	24.0
77	13.1	0.0	1.2	9.2	12.4	64.1
78	0.9	6.1	23.9	23.6	17.3	28.2
79	4.8	4.8	2.1	7.9	28.0	52.4
81	0.0	2.7	0.0	3.8	8.5	85.0
82	0.3	0.0	0.3	9.5	12.4	77.5
83	6.6	18.9	6.6	5.9	49.3	12.6
85	0.3	2.3	3.6	14.9	4.0	74.8
86	2.2	0.9	37.5	6.3	43.3	9.8
87	0.9	1.7	6.1	0.0	11.3	80.0
88	0.0	1.9	0.3	0.6	26.8	70.3
89	0.3	1.6	21.4	14.6	19.4	42.7
90	6.3	28.4	2.2	13.9	21.1	28.1
160	8.0	30.4	5.1	26.8	10.1	19.6
161	5.2	15.6	3.7	23.7	31.1	20.7
164	1.1	3.3	26.8	29.0	9.8	30.1
165	34.5	9.8	6.9	13.2	20.1	15.5
166	3.8	8.9	54.4	11.4	20.3	1.3
167	0.0	0.7	1.4	6.5	8.0	83.3
168	1.2	1.2	58.4	27.7	8.1	3.5
169	3.5	4.6	34.7	16.2	3.5	37.6
170	0.5	1.1	31.9	15.4	25.3	25.8
171	4.6	5.8	12.7	13.9	1.7	61.3
Mean	8.2	7.3	15.0	15.7	18.6	35.2
SEM	1.9	1.3	3.0	1.6	2.2	4.5
Max. days	9	19	28	21	29	73

We observed several patterns in vertical movements. At a coarse level, black rockfish were typically very active vertically (Fig. 4B), moving often between the bottom and midwater (10 to 15 m depth), and sometimes reaching the surface. These ascents and dives were often incessant and lasted for days. We classified this behavior as large vertical movements (LV) as there was no obvious finer pattern in the daily frequency, scale, or timing of the movements. All but 1 fish showed the LV pattern, with some doing so continuously up to 21 d (Table 3). There were, however, some distinct patterns in which fish slowly changed their minimum depth over several days (Fig. 4B), raising interesting questions about how they repeatedly return to the same minimum depth, even at night (Fig. 5A).

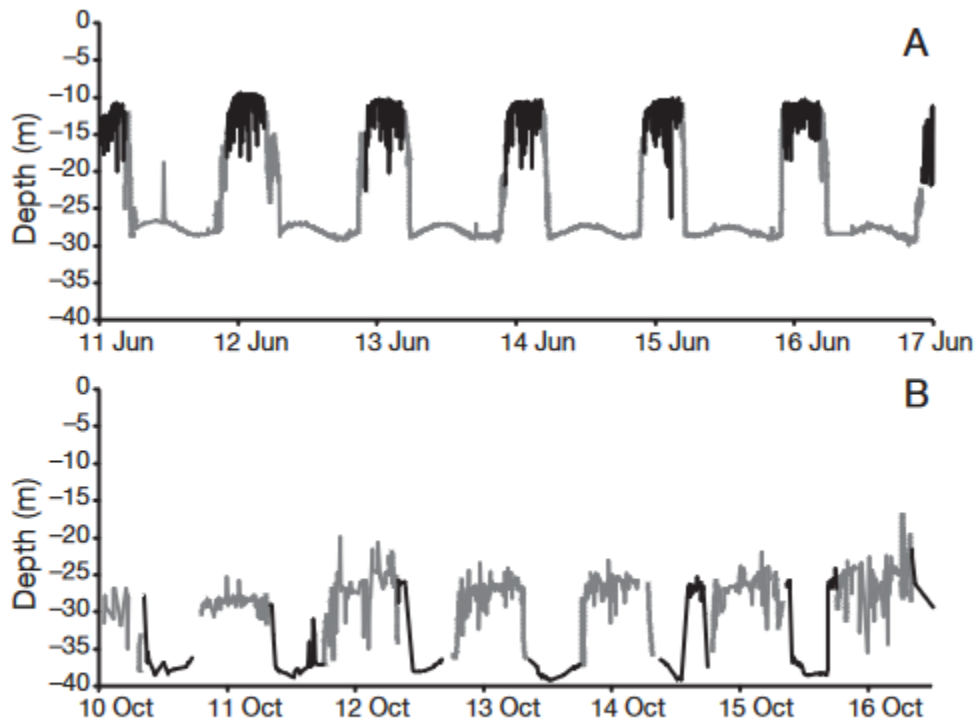


Fig. 5. *Sebastes melanops*. Examples of diel vertical migration. Black, greyscale and dotted lines as in Fig. 4. (A) Depth shallower during night phase, ID 75, and (B) depth shallower during the day phase, ID 90

At other times, fish made small vertical movements <5 m (SV), but did not remain a constant height off bottom. When this behavior occurred very close to the bottom, the depth profile showed a noisy sinusoidal trace of the tidal signal, generated when the fish's relationship to bottom was fairly constant. One fish showed this pattern for 29 continuous days (Table 3). This behavior occurred at various depths, but showed no finer scale pattern in frequency or timing (Fig. 4C).

Several, more complex, vertical movement patterns were observed. Patterns of ascending to shallower depths at night (SN) as well as patterns with regular movement to shallower depths during the day (SD) were frequently observed (Fig. 5). This pattern was defined graphically by a shift in mean depth between day and night, with a small degree of variation around that mean. The timing of the major vertical movements was often tightly correlated with sunrise and sunset, even though photoperiod phase duration changes throughout the year. But there were also examples where the daily depth change was not associated with sunrise or sunset (Fig. 5B). The deep phase of this pattern showed that the fish was tightly associated with the bottom, given the presence of a smooth tidal signal (Fig. 5). All fish showed a diel vertical movement pattern for several days at some point during the study, with 1 fish showing the behavior for 28 d continuously. The pattern was most commonly observed for a single day, but often lasted more than a week before dissolving or morphing into another behavior pattern.

The percentage of fish showing behaviors of LV, SV, SD, SN, and BT was summarized for each day. These behaviors were mutually exclusive, as each 24 h period was assigned 1 behavior. The 'other' category was used to classify days in which the number of detections was too few to describe a movement pattern for the day and includes days with no detections. Most fish showed all behaviors at some point, but did so for variable periods (Table 3). Summarizing for all fish, the behaviors categorized were split about evenly among SV, LV, and SN, with fewer observations of SD and BT behaviors, though this ignores some individuals with contrasting behavior patterns (e.g. ID 74). We note that because the 'other' category represented a significant portion of the days observed, some behaviors may be underestimated if the behavior decreased the probability of detection (e.g. acoustic transmissions may be obscured when in close proximity to complex substrate, as in BT).

The analysis shows coherence among individuals with sometimes > 60% of the observed fish performing the same behavior pattern for multiple days. In addition, although multi-day pulses in coherence are apparent, the degree of coherence changed gradually throughout the year, especially for SN, which peaked in late April and gradually declined to zero in late September (Fig. 6). SD behavior showed several pulses throughout the study period at various intervals. Short vertical movements dominated all behaviors during winter months, and large vertical movements were most prevalent from September through November (Fig. 6). A generalized pattern of more SV behavior occurred during winter months, and the largest peak in LV behavior was in September and October (Fig. 6). Only the BT behavior changed with respect to lunar phase, being much less common during new moon (transformed ANOVA, $p < 0.001$).

Periodogram analysis of 28 black rockfish with sufficient data showed that they all had a significant diel rhythm in vertical movement, with a dominant period of 23.939 ± 0.050 h ($p < 0.05$). One fish, with a low dominant period length of 23.205 h, also had an additional

significant period at 24.000 h (ID 165). Three of the fish (those with the lowest sample sizes) showed multiple significant periods near 24 h, but with slightly more variable dominant periods (23.448, 24.662, and 23.419 h). In addition to diel rhythms, 13 fish showed a significant rhythm in vertical movement, with a mean period of 12.354 ± 0.040 h ($p < 0.05$), suggesting vertical movements linked to the tidal cycle. We detected no significant correlation between the recorded environmental variables (wave height, solar irradiance at Newport, cloud cover, water temperature at Seal Rock, or daily east and north upwelling) and normalized depth, variance of depth, or any of the categorized behaviors.

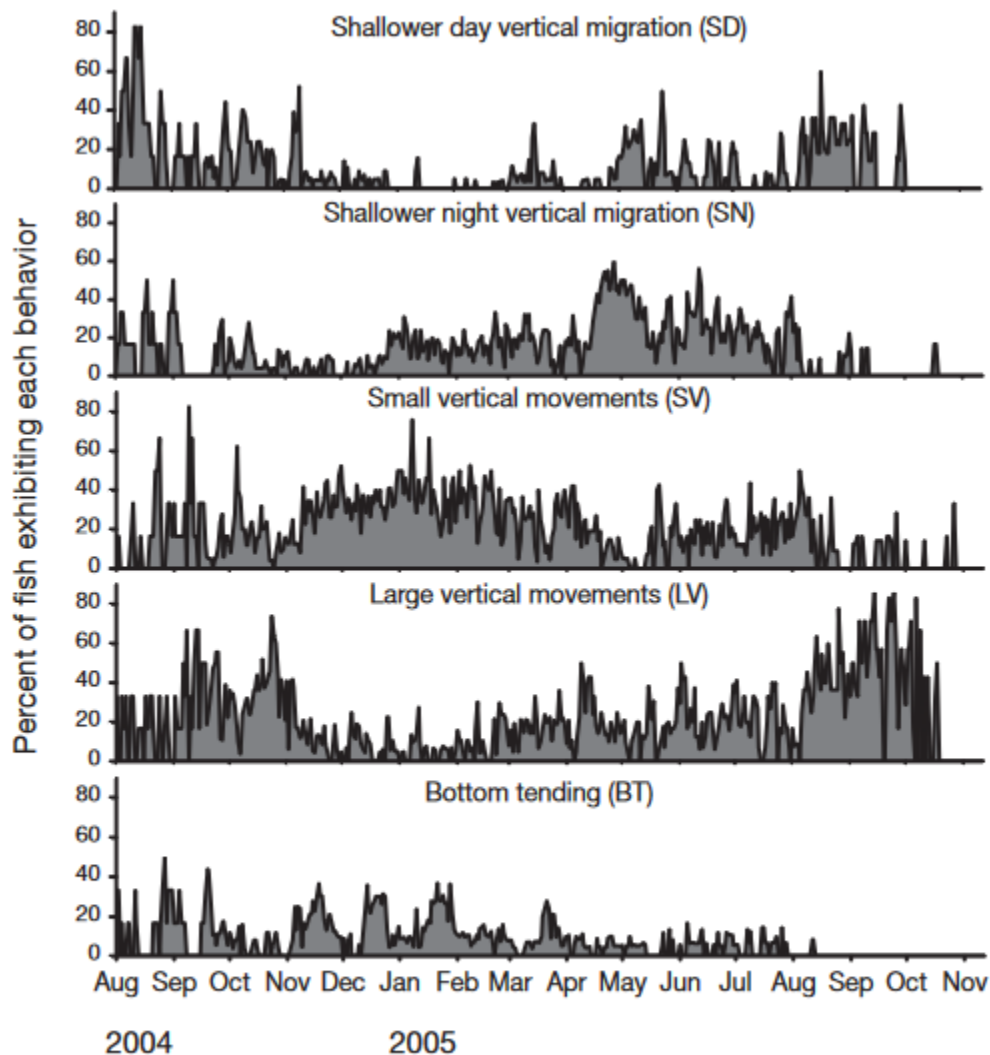


Fig. 6. *Sebastes melanops*. Behavioral coherence (the percentage of fish observed showing a particular behavior) on a daily basis for fish showing 5 categorized behaviors

DISCUSSION

Black rockfish *Sebastes melanops* showed larger, more frequent, and more temporally structured vertical movements throughout the 12 mo study period than have been reported in the literature based on video or diver observations (Leaman 1977, McElderry 1979). Direct or video observations are severely limited in duration, especially on individual fish, with the result being that movement patterns over more than a few minutes, especially at night or in variable weather, have not been observed. This behavior is surprising because black rockfish possess a closed swimbladder and live in relatively shallow water, making them especially susceptible to injury due to swimbladder gas expansion during ascents (Parker et al. 2006). McElderry (1979) showed that black rockfish swimbladders cannot expand more than approximately 60% in volume prior to rupture. In addition, hyperbaric chamber experiments resulted in rupture of swimbladders in 100% of black rockfish exposed to a 90 s, 3 ATA (absolute atmospheres) decrease in pressure followed by 2 min at surface pressure — a 300% increase in gas volume (Parker et al. 2006). Because we observed larger (> 30 m) and faster (< 2 min) movements (e.g. Fig. 4B) than those simulated in the hyperbaric chamber experiments, we conclude that black rockfish maintain their swimbladders so that neutral buoyancy occurs at a much shallower depth than the bottom. The actual volume of the black rockfish swimbladder in nature has not been determined, but black rockfish have been acclimated to neutral buoyancy at a particular depth in hyperbaric aquaria (Parker et al. 2006). Combined, this suggests that black rockfish are constantly, but slowly, acclimating to their depth at any moment. Because removing gas from the swimbladder is much faster than adding gas (Parker et al. 2006), the neutral depth of a vertically active fish will be consistently shallower than its actual depth.

The degree of vertical activity was also surprising given the relatively small horizontal movements observed in other studies (Culver 1987, Parker et al. 2007). Fish with a small home range (average of 0.55 km² from Parker et al. 2007) would not be expected to spend significant time off bottom in an environment with continuous currents sometimes exceeding 1 m s⁻¹ (Kosro 2005). Black rockfish behavior could be characterized as utilizing the vertical dimension of their habitat more than the horizontal dimension. This close association to a home site while making significant vertical movements is unusual, as most fishes with small home ranges are linked to a territory (Keenleyside 1979), patchy habitat (Matthews 1990), or are associated with midwater structures such as kelp beds (Lowe et al. 2003). It is likely that black rockfish maintain their relatively small horizontal home ranges by frequently diving to bottom for spatial reference. However, our data frequently show long periods, both during daylight and darkness, when an individual fish maintained its position while in midwater, likely in a shoal (e.g. Fig. 5A). Pitcher & Parrish (1993) described many of the evolutionary pressures that may shape shoaling behavior. While some apply to black rockfish behaviors, such as foraging efficiency, it is also possible that black rockfish maintain a geographic position while in low-visibility conditions in

midwater by remaining near conspecifics in a shoal, so that there is always a visual link back to the substrate.

The combination of unpredictable patterns in vertical movement, maintaining the swimbladder at a smaller volume than neutral, and spending significant amounts of time in close proximity to the bottom make hydroacoustic surveys of black rockfish problematic. Our data suggest that a constant or predictable portion of the population is not detectable by sonar at any time and that signal strength data will vary depending on both the depth of the individual and the recent vertical activity pattern of that individual fish.

We documented a seasonal pattern in the variability of vertical movements, suggesting that, during winter months, vertical activity is reduced and more time is spent in close proximity to the bottom. The timing of this reduction in variance is associated with an increase in wave height from winter storms, though there was a period in August and September where reduced vertical activity was observed. Inversely, the pattern could be described as pulsed periods of increased activity (fall and spring months), with a longer period of reduced vertical movement.

We recorded vertical position every 30 to 90 s; minimum vertical movement rates were almost exclusively $< 8.4 \text{ m min}^{-1}$ or 14 cm s^{-1} . Still, at 8 m min^{-1} , gas expansion would be much faster than gas removal abilities, and injury could occur. Parker et al. (2006) showed that black rockfish acclimated to 30 m showed significant barotrauma signs during a 90 s ascent to the surface, whereas these field data show minimum ascent rates of 16 m in 2 min. Most of the observations in the present study occurred at bottom depths of $< 40 \text{ m}$, where the gas expansion is most extreme. Ascent rates were fastest at deeper depths, where gas expansion was minimal, and descent rates were fastest near the surface, where gas compression is maximal, suggesting that black rockfish display the most freedom of movement in situations where problems associated with gas expansion are minimized.

At some point during the study, every fish showed a diurnal vertical migration pattern. This was most often distinguishable for only a single day at a time, but was commonly observed for 2 to 6 contiguous days by various individuals during the observation period. Our ability to detect this pattern graphically was often limited by large numbers of quick ascents and dives superimposed on the general pattern of a change in mean depth during 1 phase of the photoperiod (Fig. 4). Often a SD or SN behavior pattern faded into an LV pattern as the variance in vertical movements increased. However, the periodogram analysis showed the long-term, dominant 24 h rhythm in depth for each fish. The timing of the vertical movements in the SN or SD patterns was not always associated with sunrise or sunset, though it was usually within a few hours, indicating their movements were not a response solely to changes in light level. Our analysis also suggested a circatidal period in vertical movements for some fish. We consider this probable, but it is confounded by the amount of time that fish remained in close contact with

the bottom, which would tend to create a 12.4 h rhythm in depth as the water rose and fell above them. Countering this effect is the large amount of vertical movement observed by almost all fish throughout the entire study. When fish are off bottom, they do not regulate their depth with reference to the bottom, so any pattern in depth is volitional. As only 11 fish showed this periodicity, and it is not possible to determine when a fish was close enough to the bottom to influence its choice of depth, additional information is needed to address these possibilities.

Seasonal patterns in behavioral coherence in activity suggest that black rockfish are responding to local external stimuli as opposed to an internal rhythm or a more global environmental cue, such as photophase. Activity regulated by an internal clock would occur in the majority of individuals, and more coherence would be expected than we observed. More localized environmental information, such as patchy prey availability (e.g. schools of sand lance, ctenophores, or crab zoeae; Oregon Department of Fish and Wildlife unpubl. data) could explain a weak pattern of many fish in the study area showing the same behavior during a period lasting several days. The seasonal peaks in SN and SD behavior suggest a link to local factors that are themselves seasonal, such as the prevalence of particular prey species that are most effectively preyed upon in certain conditions.

The environmental and physiological drivers of the observed patterns in vertical movement are speculative, but the dynamic nature of the vertical movements for this rockfish species is clear. Black rockfish have developed a niche similar to semi-pelagic continental shelf species such as yellowtail and widow rockfish (Love et al. 2002), but have done so in a nearshore environment where decompression constraints and discrete habitat associations create additional pressures for behavioral adaptation.

ACKNOWLEDGEMENTS.

We thank Troy Buell, Keith Matteson, Steve Kupillas, Jon Nottage, Zeb Schobernd, Bob Hannah, and Stephen Jones for their assistance in catching fish, maintaining the array, and downloading the receivers. Christopher Romsos provided expert GIS assistance. We also thank the fishermen and beachcombers that found and returned receivers that were lost during storm events or fishing mishaps.

LITERATURE CITED

Bobko SJ, Berkeley SA (2004) Maturity, ovarian cycle, fecundity, and age-specific parturition of black rockfish, *Sebastes melanops*. *Fish Bull* 102:418–429

- Boettner JF, Burton SF (1990) Hydroacoustic stock assessment study of Washington coastal black rockfish of Washington State. Tech. Report 108, Wash. Dept. of Fisheries, Olympia, WA
- Culver BN (1987) Results from tagging black rockfish (*Sebastes melanops*) off the Washington and northern Oregon coast. In: Proceedings of the international rockfish symposium, Anchorage, Alaska. University of Alaska Sea Grant Report No. 87.2, Fairbanks, AK, p 231–240
- Keenleyside MHA (1979) Diversity and adaptation in fish behavior. Springer-Verlag, Berlin
- Kosro PM (2005) On the spatial structure of coastal circulation off Newport, Oregon, during spring and summer 2001 in a region of varying shelf width. *J Geophys Res* 110:C10S06
- Krieger K, Heifetz J, Ito D (2001) Rockfish assessed acoustically and compared to bottom-trawl catch rates. *Alsk Fish Res Bull* 8:71–77
- Leaman BM (1977) The diel activities of the black rockfish (*Sebastes melanops* Girard) and beds of *Macrocystis integrifolia* Bory in Barkley Sound, BC, Canada. *J Phycol* 13(Suppl 1):39
- Love MS, Yoklavich M, Thorsteinson L (2002) The rockfishes of the Northeast Pacific. University of California Press, Berkeley, CA
- Lowe CG, Topping DT, Cartamil DP, Papastamatiou YP (2003) Movement patterns, home range, and habitat utilization of adult kelp bass *Paralabrax clathratus* in a temperate no take marine reserve. *Mar Ecol Prog Ser* 256:205–216
- Matthews KR (1990) An experimental study of the habitat preferences and movement patterns of copper, quillback, and brown rockfishes (*Sebastes* spp.). *Environ Biol Fishes* 29:161–178
- McElderry HI (1979) A comparative study of the movement habits and their relationship to buoyancy compensation in two species of shallow reef rockfish (*Pices*, *Scorpaenidae*). MS thesis, University of Victoria
- Parker SJ, Berkeley SA, Golden JT, Gunderson DR and others (2000) Management of Pacific rockfish. *Fisheries* 23:22–25
- Parker SJ, McElderry HI, Rankin PS, Hannah RW (2006) Buoyancy regulation and barotrauma in two species of nearshore rockfish. *Trans Am Fish Soc* 135:1213–1223
- Parker SJ, Rankin PS, Olson JM, Hannah RW (2007) Movement patterns of black rockfish (*Sebastes melanops*) in Oregon coastal waters. In: Heifetz J, DiCosimo J, Gharrett AJ, Love MS, O'Connell VM, Stanley RD (eds) *Biology, assessment, and management of North Pacific rockfishes*. Alaska Sea Grant, University of Alaska, Fairbanks, AK, p 39–57
- Pearcy WG (1992) Movements of acoustically tagged yellowtail rockfish *Sebastes flavidus* on Heceta Bank, Oregon. *Fish Bull* 90:726–735
- Pedersen MG, Boettner JF (1992) Application of hydroacoustic technology to marine fishery management in Washington State. *Fish Res* 14:209–219
- Pitcher TJ, Parrish JK (1993) Functions of shoaling behavior in teleosts. In: Pitcher TJ (ed) *Behavior of teleost fishes*. Chapman and Hall, New York
- Ruf T (1999) The Lomb-Scargle

periodogram in biological rhythm research: analysis of incomplete and unequally spaced time series. *Biol Rhythm Res* 30:178–201

Stanley RR, Keiser R, Leaman BM, Cooke KD (1999) Diel vertical migration by yellowtail rockfish, *Sebastes flavidus*, and its impact on acoustic biomass estimation. *Fish Bull* 97:320 – 331

Stanley RD, Kieser R, Cooke KD, Surry AM, Mose B (2000) Estimation of a widow rockfish (*Sebastes entomelas*) shoal off British Columbia, Canada, as a joint exercise between stock assessment staff and the fishing industry. *ICES J Mar Sci* 57:1035–1049

Wilkins ME (1986) Development and evaluation of methodologies for assessing and monitoring the abundance of widow rockfish, *Sebastes entomelas*. *Fish Bull* 84: 287 – 310

4: EFFECT OF HYPOXIA ON ROCKFISH MOVEMENTS: IMPLICATIONS FOR UNDERSTANDING THE ROLES OF TEMPERATURE, TOXINS AND SITE FIDELITY

Polly S. Rankin, Robert W. Hannah, Matthew T. O. Blume

Recreated from <https://www.int-res.com/abstracts/meps/v492/p223-234/> for simplicity.

ABSTRACT

We used a high-resolution acoustic telemetry array to study the effect of seasonal hypoxia (defined as dissolved oxygen concentration [DO] < 2 mg l⁻¹) on the movements of quillback rockfish *Sebastes maliger* and copper rockfish *S. caurinus* at Cape Perpetua Reef, Oregon, USA. Over 18 weeks in summer 2010, a period with both normoxic and hypoxic conditions at the reef, both species showed high site fidelity. Home range was variable within species, was much larger than previously shown, and was influenced by foray and relocation behavior. Several quillback rockfish forayed well off of the reef into sand and gravel areas. Foray departure time was synchronous among individuals and related to time of day (sunset). Hypoxic conditions reduced home range for copper rockfish by 33%, but home range was variable for quillback rockfish, with no change in foray behavior. We propose that the origin, chemistry, and temperature of the hypoxic water mass and the species' innate behavioral tendencies must be considered, along with DO, in determining the effects of hypoxia on fish.

INTRODUCTION

Evaluating species' ecology within an ecosystem exposed to complex and dynamic environmental conditions requires a comprehensive understanding of both the species' natural history and the conditions to which it may be responding. Changing ocean conditions illustrate this challenge and may affect species' movements and fitness in broad- and fine scale ways. One environmental phenomenon which can influence the health and distribution of marine life is a change in oxygen availability. Episodes of decreasing oxygen concentration in marine waters have been reported worldwide and are caused by a variety of antropogenic and natural conditions (Gray et al. 2002, Grantham et al. 2004, Newton 2008). Hypoxia — defined here as dissolved oxygen concentration (DO) <1.4 ml l⁻¹ or < 2 mg l⁻¹ —is found naturally in the oxygen minimum zone (OMZ) where its marine residents are evolutionarily adapted to a low oxygen environment (Vetter & Lynn 1997).

Large-scale hypoxic water masses exist naturally in the deeper marine waters of the US Pacific Northwest (Grantham et al. 2004, Connolly et al. 2010). In the summer, strong NW winds create upwelling which can advect this cold, high-nutrient water mass inshore into the shallower (< 70 m) waters of the inner continental shelf. As the nutrients become available within the photic

zone, plankton populations flourish, contributing to the high primary productivity of the area (Pauly & Christensen 1995). However, the cycle of intense productivity, decomposition and oxygen consumption can further reduce oxygen levels. If NW winds continue in strength and duration, this increasingly hypoxic water mass may move into nearshore areas and even enter bays and estuaries where the marine life may not be adapted to low oxygen conditions (Grantham et al. 2004, Brown & Power 2011, Roegner et al. 2011).

There is strong historical (1950 to 1975) evidence of episodic, seasonally occurring hypoxia in Pacific NW coastal waters (Brown & Power 2011). Since 2002, areas of seasonal hypoxia have been well documented in the nearshore waters of Oregon (Chan et al. 2008). The movement of hypoxic water masses is influenced by bathymetry, as well as other oceanographic conditions, and certain locales off the Oregon coast have been repeatedly exposed to low oxygen water (Grantham et al. 2004). One area, a small, isolated rocky reef located 5 km southwest of Cape Perpetua, Oregon (see Fig. 1), has been exposed to several known hypoxic events since 2002, but in 2006 an episode of severe hypoxia ($DO < 0.5 \text{ ml l}^{-1}$, $< 0.7 \text{ mg l}^{-1}$) occurred (Chan et al. 2008). This reef had been surveyed in prior years with a video equipped remotely operated vehicle (ROV) and showed a diverse community of mobile and encrusting invertebrates, as well as many species of fishes including various rockfishes *Sebastes* spp., lingcod *Ophiodon elongatus* and kelp greenling *Hexagrammos decagrammus* (Weeks et al. 2005). When this video survey was repeated in August 2006 (after the severe hypoxia event), mortality of many forms of invertebrates was observed. Rockfishes, which had previously dominated the fish fauna at the reef, were absent (Chan et al. 2008). Rockfishes were subsequently observed during each annual ROV survey of the Cape Perpetua reef from 2007 to 2009 (M. Donnellan pers. comm.).

Rockfishes comprise a large (102 species), diverse group of long-lived, late-maturing fishes, with many species exhibiting substantial niche overlap in nearshore areas (Love et al. 2002). Recent findings using acoustic telemetry have shown considerable variability in behavior and site fidelity among and within the rockfishes of the NE Pacific (Lowe et al. 2009, Tolimieri et al. 2009, Hannah & Rankin 2011). However, these species' responses to changes in environmental conditions, such as hypoxia, are not well known and have only recently been reported for a few areas (Palsson et al. 2008). Oxygen tolerances for NE Pacific rockfishes have not been established, and experimental results for many other types of fishes indicate varying thresholds (Nakanishi & Itazawa 1974, Gray et al. 2002, Vaquer-Sunyer & Duarte 2008).

Changes in oxygen availability can significantly influence behavior in fish, with laboratory experiments showing fish sensing and avoiding areas of low oxygen (Herbert et al. 2011). However, little research has been conducted with reef-dwelling, refuge-seeking fishes, nor with fishes that may be strongly territorial, have strong site fidelity, or small home ranges. These behavioral traits may lead to hiding or remaining within an area as conditions deteriorate,

particularly if there is no nearby safe habitat (Palsson et al. 2008, Herbert et al. 2011), making fish particularly vulnerable to deteriorating water quality. These fishes may subsequently incur greater harm than other, more mobile fishes.

High site fidelity, small home ranges and a strong affinity for substrate have been documented for several species of reef-dwelling, nearshore rockfish, increasing their potential vulnerability to detrimental environmental conditions (Lowe et al. 2009, Tolimieri et al. 2009, Hannah & Rankin 2011). Knowledge of their physical and behavioral responses to environmental stress is critical to a basic understanding of their ecology. We report here on our use of acoustic telemetry in a high-resolution positioning system (VPS) to study the behavior and movements of 2 species of rockfishes inhabiting Cape Perpetua Reef. The area encompassing the Cape Perpetua Reef was recently designated as a marine reserve site (Oregon Ocean Information www.oregonocean.info), with rockfishes being a taxon of interest. The primary study objective was to determine the home range, site fidelity, and movement patterns for these species living on this type of low-relief reef, during the summer, when seasonal hypoxia can develop. An additional objective was to observe and describe any changes in movement behavior in response to changing oceanographic conditions.

MATERIALS AND METHODS

Cape Perpetua Reef is located 5 km southwest of Cape Perpetua, Oregon (Fig. 1) and ranges in depth from 47 to 53 m (Fox et al. 2004). The reef is small, approximately 0.07 km², and consists of rock patches with low vertical relief within a large expanse of gravel and coarse sand. Rock patches are variable, and range in size from 1 m³ boulders to 1.6 ha benches (Fox et al. 2004). Our study focused primarily on 2 species of nearshore rockfish — quillback *Sebastes maliger* and copper rockfish *S. caurinus*. These demersal species are relatively abundant at Cape Perpetua Reef (Weeks et al. 2005), allowing us to increase sample size by species to better capture variability in individual behavior. We also opportunistically tagged a single brown rockfish *S. auriculatus*, a demersal species which is rarely captured in Oregon, but is commonly encountered in Hood Canal, Washington — another area of recurring hypoxia in the Pacific Northwest (Newton 2008, Palsson et al. 2008).

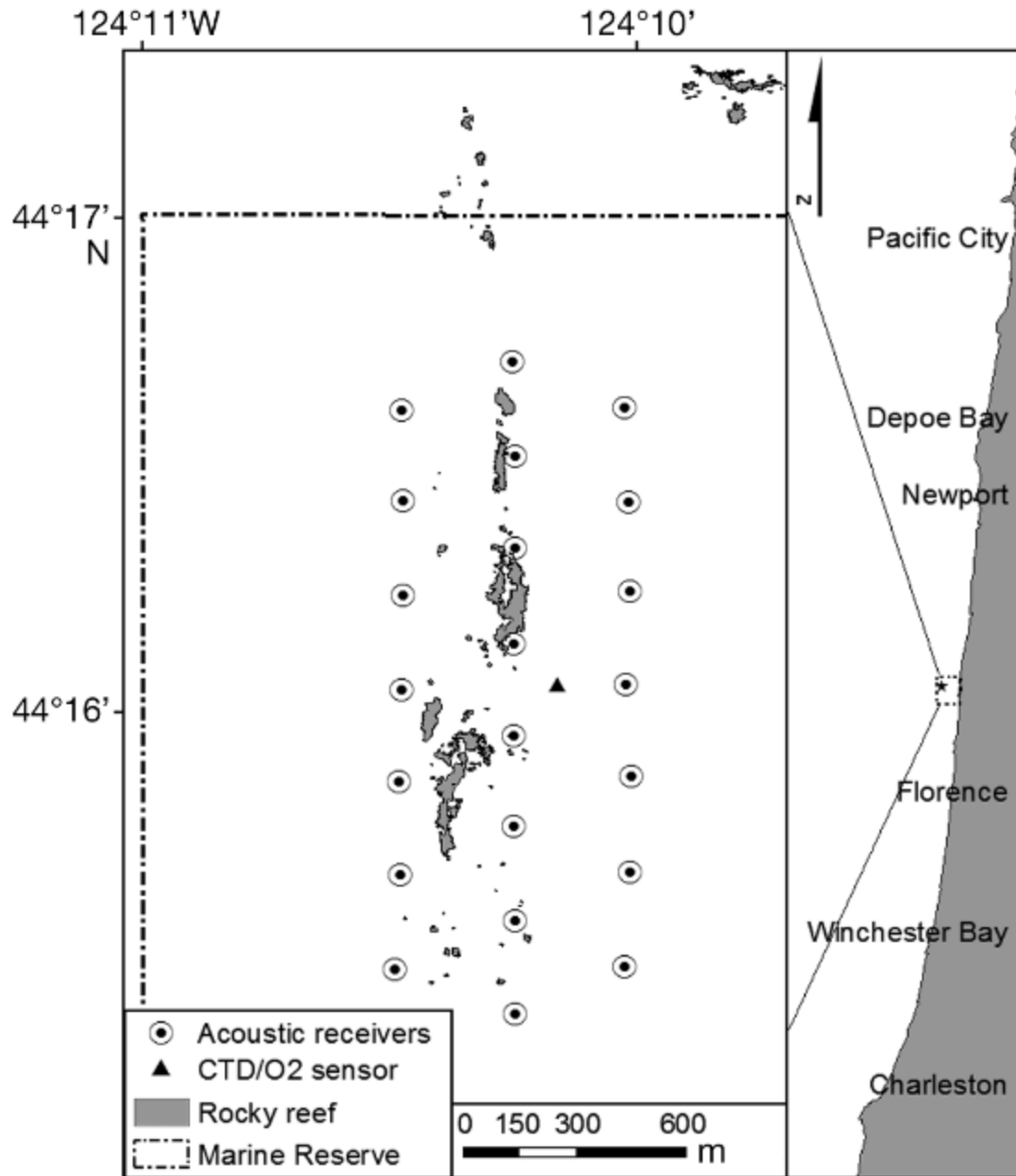


Fig. 1. Study area showing rocky reef, location of acoustic receivers and CTD/O₂ sensor, and marine reserve boundary line

Rockfish were captured in May 2010, using recreational hook-and-line fishing gear. Each fish was evaluated for barotrauma, measured for length (cm, total length), and vented using an 18-gauge hypodermic needle inserted through the body wall to remove excess gas from the swim bladder. Fish were surgically tagged as per methods outlined in Parker et al. (2007). Implanted

tags were Vemco V13-P coded acoustic transmitters (69 kHz, 158 dB power output, 13 × 45 mm, pressure-sensing 100 m, accuracy ± 5 m, resolution 0.44 m) which transmit a unique identification number and the depth of the tagged fish. All tags were tested prior to deployment. After tagging, fish were immediately returned to depth in a videoequipped underwater release cage (Hannah & Matteson 2007) at the point of original capture, as per methods outlined in Hannah & Rankin (2011).

To track tagged fish, we used a Vemco VPS positioning system, which utilized moored VR2W single-channel acoustic receivers (Vemco) in a grid, in combination with moored ‘synctag’ transmitters. With precise position information on receiver and synctag locations, environmental parameters (to determine the speed of sound in water) and synchronized clocks within all receivers, very precise fish location information can be obtained for each individual (Andrews et al. 2011). The receiver grid was designed based on range-testing in the area which showed 350 m spacing to be optimal for maximizing acoustic reception. This spacing generally allowed tagged fish to be detected by 3 or more receivers for accurate position triangulation. Downloaded detection data was sent to Vemco for data processing. For each download, Vemco provided a fish ID code, the time of detection, precise position information (latitude and longitude), depth (m), and an estimate of horizontal position error (HPE) for each triangulated position.

Our VPS system used a grid of 22 receivers with collocated V16 synctags (random delay 700 to 1100 s) and was deployed from 13 April through 21 September 2010, encompassing an area of roughly 1.4 km² (Fig. 1). Three additional V16 synctag transmitters were separately moored within the grid. These ‘reference tags’ were left in place throughout the study period, without being brought to the surface, to provide a stable locational ‘fix’ for the rest of the array, which had to be pulled and redeployed monthly to download telemetry data.

We recorded conductivity, temperature, depth and DO at our study site using a Sea-Bird SBE16plus V2, equipped with an SBE43 oxygen sensor (Sea-Bird Electronics). The unit was moored within the acoustic receiver array from 28 May through 21 September 2010. It was positioned 1 m off the bottom and was programmed to sample every 15 min.

DATA ANALYSIS

To allow for a recovery period following tagging, we disregarded the first 48 h of fish locations for all analyses. We estimated home range for each tagged fish as the 95% kernel utilization distribution (KUD) from all remaining locations for the complete study duration, using the program Ade habitat HR, as implemented in R (Calenge 2006). We defined core area similarly, but based on the 50% KUD. To estimate the use of space for shorter time periods or subsets of the data, we also used the 95% KUD, but use the term ‘activity space’ to avoid confusion with

home range or core area. To examine how activity space changed in relation to the diel cycle, we

Table 1. *Sebastes maliger*, *S. auriculatus*, *S. caurinus*. Kernel utilization density (KUD, m²) for Pacific rockfish by species and tag ID. 95% KUD = home range; 50% KUD = core area. Normoxia KUD (mean DO = 5.9 mg l⁻¹) spanned 11 d (30 May to 9 June 2010). Hypoxia KUD (mean DO = 1.8 mg l⁻¹) spanned 11 d (9 July to 19 July 2010). Forays were defined as beginning 100 m beyond the calculated center of the activity space. Relocations were defined as 2 or more distinct activity spaces, persisting for more than 1 wk

Rockfish species/ tag ID	Fish length (cm)	KUD (m ²)		95 % KUD (m ²)		Forays (n)	Relocations (n)
		95 %	50 %	Normoxia	Hypoxia		
<i>S. caurinus</i>							
100	40	8017	1221	9996	7156	–	–
103	44	2774	320	2286	2224	–	–
104	42	1966	269	2538	1007	–	–
249	47	2866	434	3903	2459	–	–
252	46	13834	2873	3485	1699	–	6
254	39	2637	350	3306	1656	–	–
255	46	1874	275	2074	1584	–	–
256	34	3283	579	3567	2972	2	–
Mean KUD	–	4656	790	3894	2595	–	–
<i>S. maliger</i>							
101	42	2175	240	2034	2033	–	–
102	45	3274	447	2149	23624	20	–
105	41	2231	278	2279	1870	5	–
223	36	2877	483	3046	2930	–	–
225	40	1232	190	1211	899	–	–
227	43	24164	1263	2711	4835	34	–
250	40	1645	185	1779	851	4	–
251	38	2932	588	2916	2890	–	–
253	36	7493	1671	10057	7949	–	–
Mean KUD	–	5336	594	3131	5320	–	–
<i>S. auriculatus</i>							
226	42	3272	501	979	904	–	1

divided all positional fixes into either day, night or the crepuscular period, which was defined as from 1 h before to 1 h after either sunrise or sunset. Sunrise and sunset at the study site were determined from tables provided by the United States Naval Observatory (<http://aa.usno.navy.mil/data/>). We evaluated site fidelity by analyzing how frequently tagged animals made

'relocations' or 'forays'. A relocation was defined as a tagged specimen with a spatial distribution encompassing 2 or more distinct activity spaces that were each persistent for more than 1 wk. In contrast, we defined a foray as a movement of at least 100 m away from the calculated center of activity that lasted for more than 1 h, consisted of a pattern of sequential movements (in time and space) as opposed to just a single positional fix, and ended in a return to a spot within 100 m of the activity center. We estimated the duration of each foray based on when the tagged fish left and returned to a location less than 100 m from its center of activity. We also calculated the maximum distance of the foray based on the positional fix that was most distant from the center of activity. In some instances, this was considered a minimum estimate because the tagged fish completely left the study area and then later returned. The maximum foray distances are also approximations because the accuracy of position data using VPS is influenced by the tagged fish's position relative to the receivers.

To quantify how hypoxia influenced movements of these demersal rockfish, we examined how fish locations and movements changed as the oxygen concentration reached levels generally considered 'hypoxic'. To make a quantitative comparison of the effect of oxygen concentrations on space use, we selected 2 equal time periods (11 d each), one encompassing the lowest continuous oxygen concentrations encountered during the study and a second period of much higher (non-hypoxic) oxygen levels. We then compared, by species, the 95% KUD for these 2 equal time periods using a paired t-test (Sokal & Rohlf 1981).

RESULTS

FISH TAGGING AND RECEIVER ARRAY

We tagged 8 copper, 9 quillback and 1 brown rockfish between 06 May and 16 May 2010 (Table 1). The time from capture until release at depth ranged from 3 to 12 min (average = 7 min). All fish survived the tagging process, remained in the study area, and were consistently detected for the 18 wk of the 2010 array deployment (13 April to 21 September). The VPS acoustic receiver array remained in place and functioned well throughout the study. Due to the depth of the array (50 m), an error minimization algorithm was applied to the calculated receiver positions which served to calibrate the system. Transmission propagation times for syntags were somewhat variable, likely due to changing environmental conditions. The precision of the system was estimated at about ± 15 m (Vemco VPS Results Report). The high resolution data generated by the VPS system allowed us to differentiate a variety of movement patterns, including relocation, habitat utilization, foray behavior away from the reefs and daily activity patterns. The CTD/O₂ sensor acquired pressure, temperature, salinity and oxygen data from a depth of 50 m from the date of deployment until 31 July. The unit was recalibrated by the manufacturer at the end of the study and there was no significant sensor drift.

DEVELOPMENT OF SEASONAL HYPOXIA

As the upwelling season progressed, hypoxia developed at 50 m of water depth in the study area. Early in the study period, southerly winds generated downwelling conditions off Cape Perpetua which resulted in seafloor DO ranging from 3.9 to 8.9 mg l⁻¹ and a temperature range of 8.9 to 12.9°C at the study site (Fig. 1). By 15 June, NW winds had produced strong coastal upwelling, and the resulting oceanographic conditions reduced seafloor DO to 1.6–3.2 mg l⁻¹ and the temperature to 6.8–8.2°C for the rest of the sensor sampling period (Fig. 2). Oxygen saturation levels ranged from 42 to 102% during the initial downwelling period and dropped to 17–34% during the subsequent upwelling. A period of hypoxia (DO range = 1.62–1.97 mg l⁻¹) began on 7 July and lasted until 25 July when DO rose to > 2 mg l⁻¹ (average = 2.5 mg l⁻¹) for 6 d. Seafloor water temperature remained cold, and averaged 7°C during the hypoxic period (Fig. 2). DO levels < 3 mg l⁻¹ continued to be present off Cape Perpetua at 70 m depth for the remainder of the study period (Adams et al. in press).

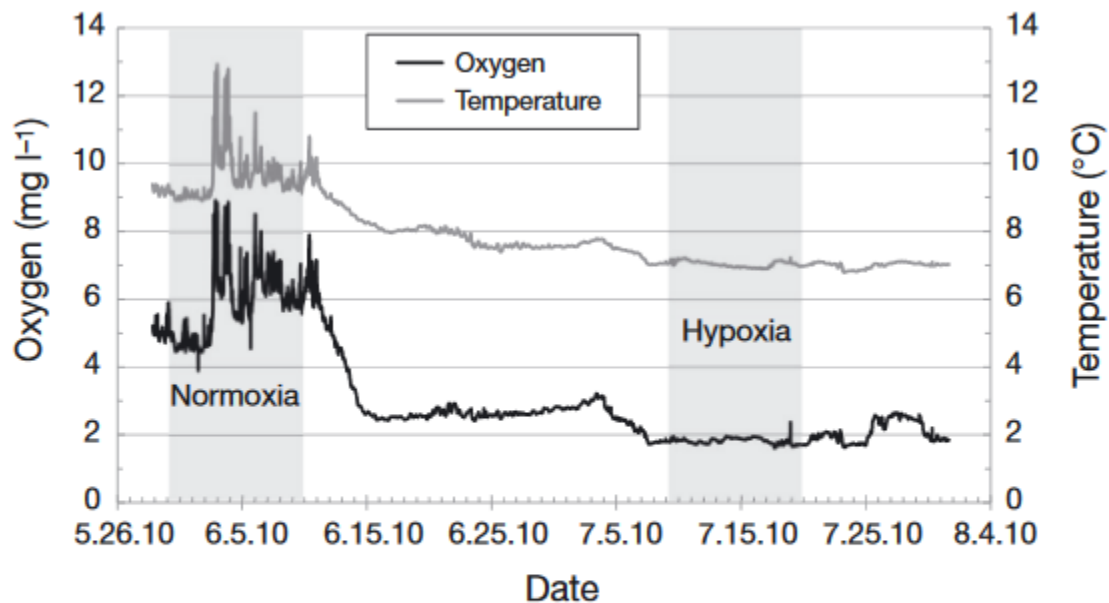


Fig. 2. Oxygen and temperature at the study site at 50 m water depth from 28 May to 31 July 2010. The 11 d comparison periods chosen were 30 May to 9 June 2010 for normoxia conditions (average DO = 5.9 mg l⁻¹), and 9 July to 19 July 2010 for hypoxia conditions (average DO = 1.8 mg l⁻¹). Dates are mm.dd.yy

SITE FIDELITY AND HOME RANGE

All of the tagged fish maintained high site fidelity to the reef area throughout a wide range of oceanographic conditions for the duration of the study, including a prolonged period of low oxygen, and a period of hypoxia (Figs. 2 & 3). Home range was variable among individual fish

and was influenced by foray behavior (excursions away from the reef) and by some individual's use of multiple, distinct core areas (Table 1, Fig. 3). Home ranges for 8 of 9 quillback rockfish ranged from 1232 to 7493 m², but forays conducted by quillback 227 resulted in a very large home range of 24 164 m² (Table 1, Fig. 3a). The home range of quillback 227 was comprised of 2 separate areas; however, this fish did not actually have a 'center of activity' in the western area. It simply passed through this area repeatedly as it traveled away from and back to its center of activity, located in the eastern area of the reef (Table 1, Fig. 4). Home ranges for 7 of the 8 copper rockfish ranged from 1874 to 8016 m², but copper 252 relocated alternately to 1 of 2 distinct areas 6 times throughout the study, generating a larger home range of 13 833 m² (Table 1, Fig. 3b). The single brown rockfish had a home range of 3272 m², comprised of 2 distinct areas (Table 1, Fig. 3a).

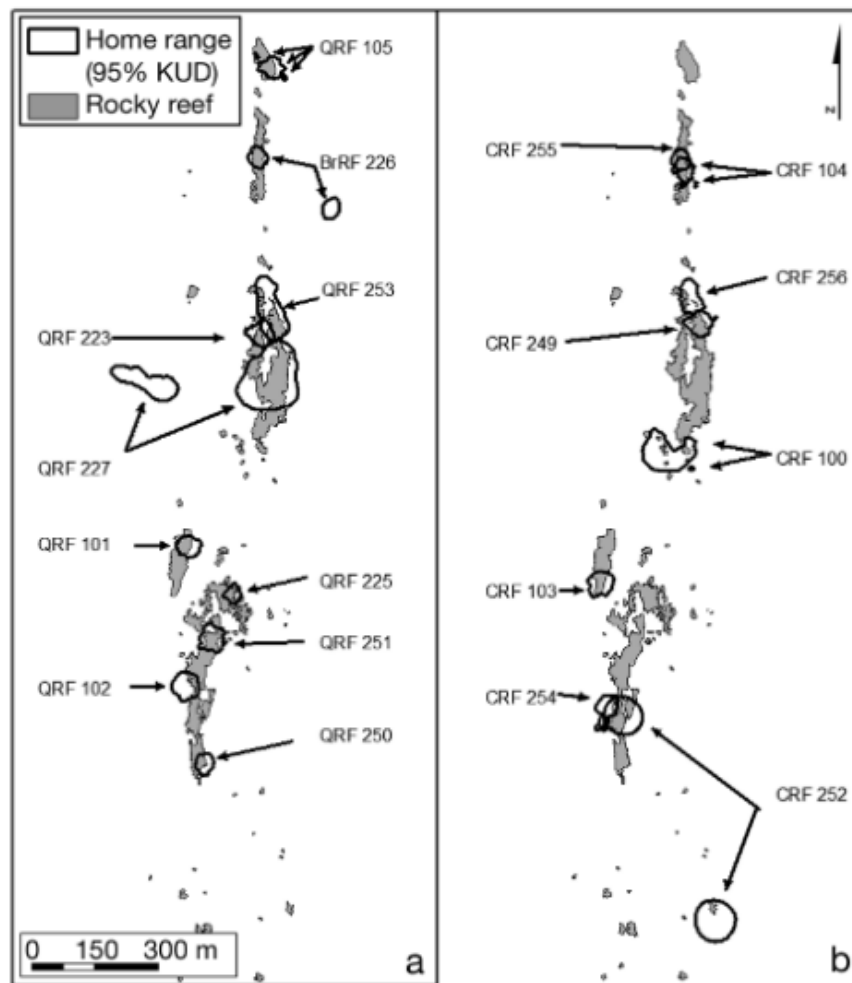


Fig. 3. *Sebastes maliger*, *S. auriculatus*, *S. caurinus*. 95% KUD (black line) and rocky reef for (a) quillback rockfish (QRF) and brown rockfish (BrRF) and (b) copper rockfish (CRF). KUD: kernel utilization density

HABITAT UTILIZATION AND MOVEMENT PATTERNS

RELOCATION

Copper 252 repeatedly (6 times) moved between 2 activity centers, located, located 535 m apart (Fig.3b). The time interval between relocations ranged from 9 to 39 d. Once initiated, relocations were direct and rapid, with the fish leaving one area, swimming directly towards the other area and arriving (on average) in about 1 h. Brown 226 relocated only once during the study to a new activity center 211 m away from the original area (Fig. 3a). The fish's path was indirect and meandering, and the time to relocate (6 h) was much longer than for copper 252.

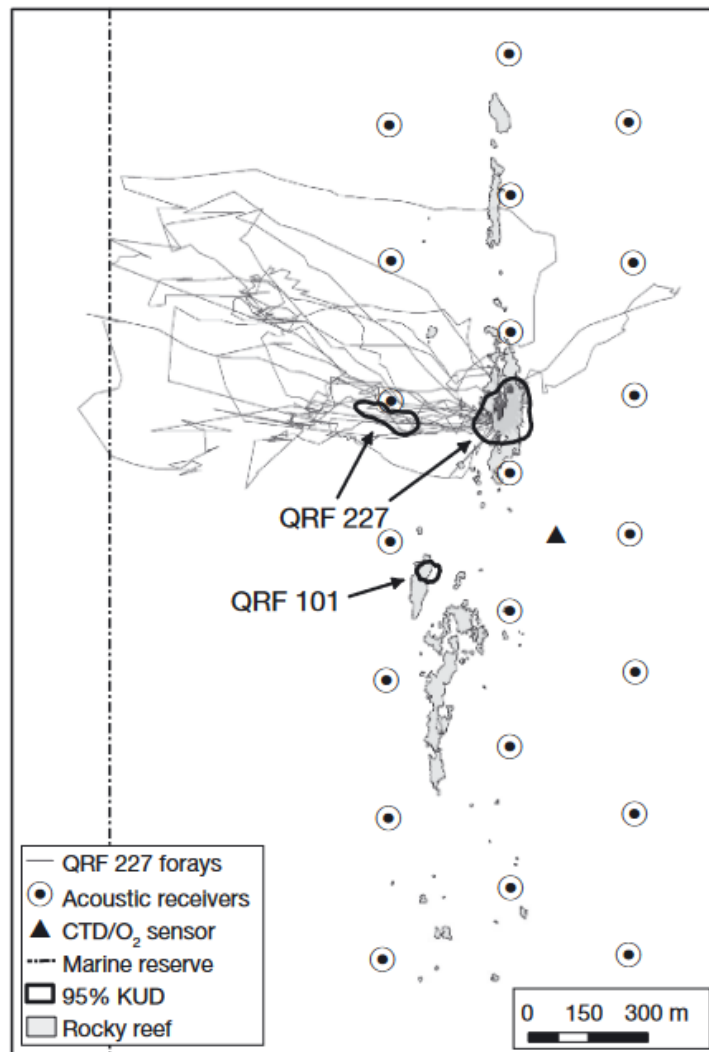


Fig. 4. *Sebastes maliger*. Foray tracks (grey line) for quillback rockfish 227 (QRF 227) for September 2010, and 95% KUD (solid outline) for QRF 227 and comparison fish QRF 101

HABITAT UTILIZATION AND FORAY BEHAVIOR

Most tagged fish remained within the rocky reef area; however, quillback 227 and quillback 102 conducted repeated, extensive nightly forays well beyond the reefs to the west, in an area comprised of large expanses of sand interspersed with gravel patches (Goldfinger et al. 2012). Foraging quillback rockfish generally completed a roughly elliptical route, returning to the reefs close to their center of activity. Rarely, fish returned to the reefs well away from their center of activity, but once within the reef area, they traveled directly home.

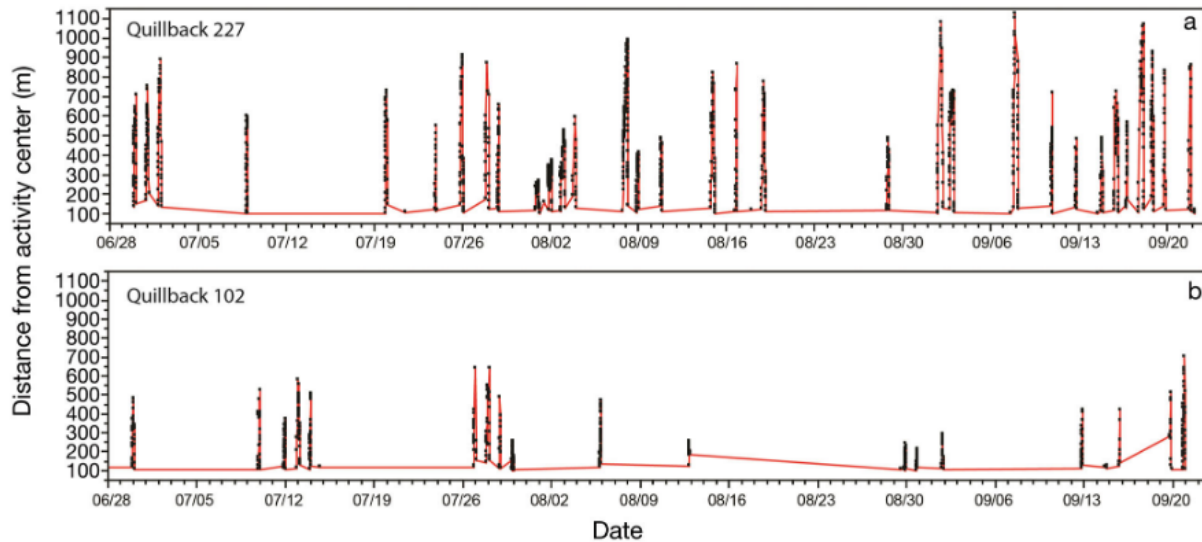


Fig. 5. *Sebastes maliger*. Foray date and foray distance from activity center for (a) quillback 227 and (b) quillback 102. Dates are mm/dd. Black dots are individual detections. Red line indicates the time series of detections

Five fish exhibited foray behavior: 4 of 9 quillback rockfish and 1 of 8 copper rockfish. Variability among individuals' foray behavior was evident in many aspects of the fish's travel: frequency, distance, duration and direction. Quillback 227 had the highest frequency of forays ($n = 34$) (Fig. 4), followed by quillback 102 ($n = 20$), quillback 105 ($n = 5$), quillback 250 ($n = 4$), and copper 256 ($n = 2$) (Table 1). Forays ranged from 105 m to 1124 m from the designated activity center (Fig. 5) and lasted from 30 min to 12.5 h (Fig. 6). The maximum measurable path travelled was over 3000 m, but at times quillback 227 appeared to have moved completely out of acoustic range west of the array (>1 km), returning into range some hours later, suggesting a longer path than measured (Fig. 4). In contrast, quillback 105 had 5 forays, all less than 200 m from its activity center and traveled to the east, southeast or south. The only copper to foray was copper 256. This fish had 2 forays (Table 1), both to a rock patch 120 m to the north.

Intriguingly, some movement patterns were repeated within individuals, and on several occasions the timing of the patterns was synchronous among individuals and related to time of day. For example, most (31 of 34) of quillback 227's forays were west of the reef area (Fig. 4)

and occurred close to sunset (Fig. 7). Quillback 102 also exhibited this behavior, travelling exclusively

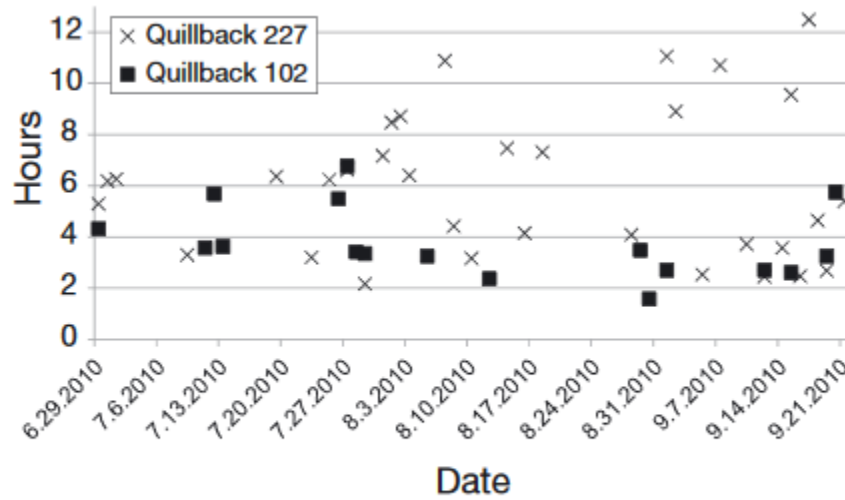


Fig. 6. *Sebastes maliger*. Foray date and foray duration for quillback 227 and quillback 102. Dates are mm.dd.yy

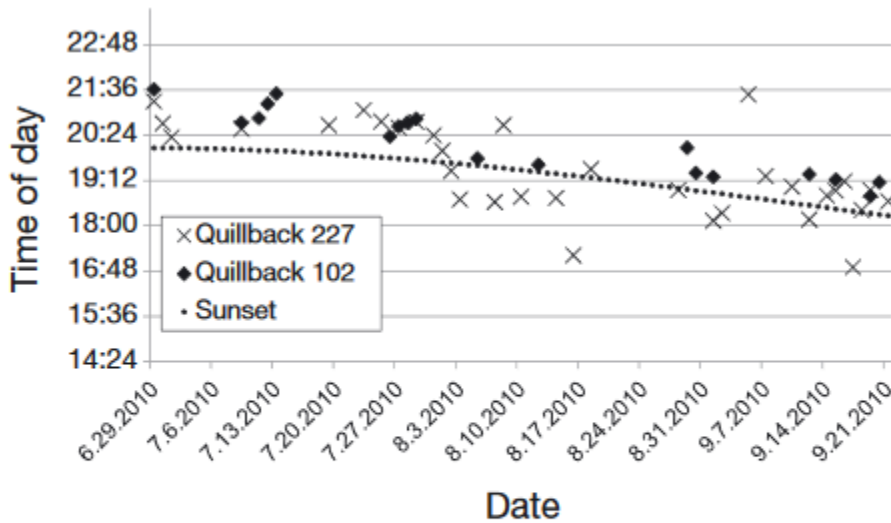


Fig. 7. *Sebastes maliger*. Foray date and time of departure from activity center for quillback 227 and quillback 102, showing synchrony of timing between rockfish and relationship to time of sunset. Dates are mm.dd.yy

to the west of the study site and leaving the core area within 1.5 h of sunset (Fig. 7). Although core areas for these 2 fish were separated by 738 m (Fig. 3a), on 8 occasions their foray departure times were within minutes of each other (Figs. 5 & 7). Synchronous foray timing was

a prevalent aspect of foray behavior. In total, 53 of 65 rockfish foray departure times were within 1.5 h of sunset.

DAILY ACTIVITY PATTERNS

We found little difference in the activity space used by tagged fish during day, night and crepuscular periods for all but 2 fish (Fig. 8) — quillbacks 227 and 102. The frequent nighttime foray behavior exhibited by these fish resulted in markedly larger home ranges at night (both fish) and during the crepuscular period (quillback 227) (Fig. 8b).

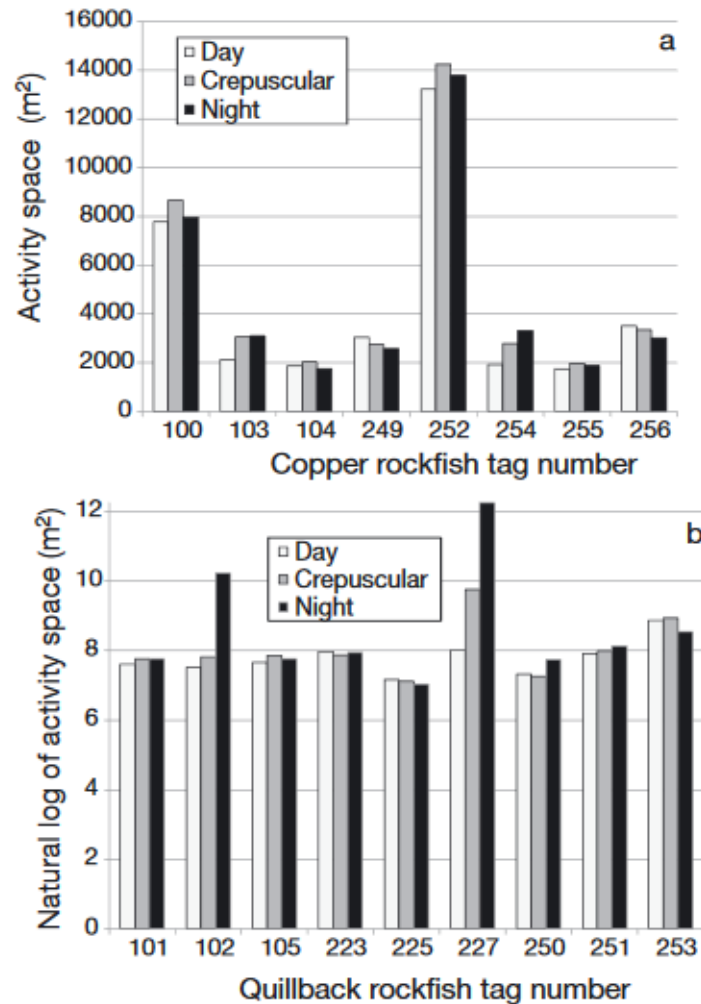


Fig. 8. *Sebastes caurinus*, *Sebastes maliger*. Activity space (95% KUD, m²) compared by day, crepuscular and nighttime periods for each (a) copper rockfish and (b) quillback rockfish. Forays by quillback rockfish 102 and quillback rockfish 227 resulted in larger nighttime activity spaces for both fish and a larger crepuscular activity space for quillback rockfish 227 (note log scale for quillback rockfish)

COMPARISON OF HYPOXIC AND NORMOXIC CONDITIONS

Although all fish remained in the study area and within their previously established home ranges during the hypoxic period, the hypoxic water mass did influence the size of the activity space used by most fish. For copper rockfish, the 95% KUD was 33% smaller during the hypoxic period ($p < 0.01$; Fig. 9a). The response of quillback rockfish to the onset of hypoxia was more variable (Table 1). Seven quillback averaged a 14% reduction in 95% KUD during the hypoxic period, and quillback 253 reduced its very large (>10 000 m²) activity space by 21%. In contrast, quillbacks 102 and 227 increased their 95% KUDs 1099% and 178%, respectively during the hypoxic period due to foray behavior (Table 1, Fig. 9b). The single brown rockfish showed a small (<1%) reduction in 95% KUD during the hypoxic period.

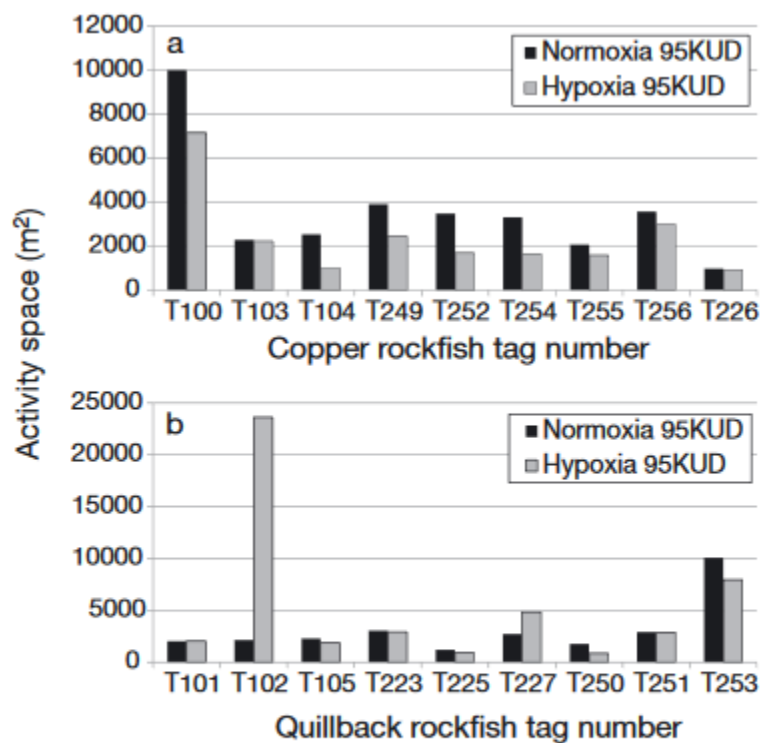


Fig. 9. *Sebastes caurinus*, *Sebastes maliger*. Comparison of activity space (95% KUD, m²) for normoxia and hypoxia periods for each (a) copper rockfish and (b) quillback rockfish

Other than the effect on the size of the activity space, the onset of hypoxia had little effect on fish movement. Copper 252 and brown 226 each utilized 2 distinct home ranges throughout the varied environmental conditions of the study period (Table 1, Figs. 3a,b), but relocations did not appear to be initiated by the change in temperature and oxygen concentration. Copper 252 relocated during the normoxic period before upwelling (22 May), again 39 and 66 d later in periods of low oxygen (DO range = 2.6 to 2.8 mg l⁻¹, O₂ saturation = 26 to 29%), but not during

the hypoxic period. Brown 226 relocated 211 m from its previous home on 22 August, well after (44 d) the hypoxic period.

Foray behavior was evaluated in relation to the presence of hypoxic water and did not appear to be initiated by changes in DO. One foray was observed during the initial downwelling (normoxic) phase of the study, and forays were observed with equal frequency during the low-oxygen and hypoxic periods.

DISCUSSION

By combining a VPS system with a larger sample size of tagged animals from each of 2 rockfish species occupying the same reef area, our study provided high-resolution data on fish movements that showed both between- and within-species variation in the use of space and the response to hypoxia. The precision of the system and a high frequency of tag transmission allowed the description of both intraseasonal variation and variation among individual fish in the use of areas away from the rocky reefs. The on-site moored CTD/O₂ sensor allowed us to relate changes in water chemistry to fish behavior, providing a very complete picture of how these species of rockfish use the reef and surrounding areas as conditions changed over time.

Mean home range sizes for copper and quillback rockfish in our study were larger than those previously described by Tolimieri et al. (2009) for a summer study in Puget Sound, Washington. The larger sample sizes in our study revealed substantial behavioral variability within species. Home ranges were 3.6 times larger for quillback rockfish (mean = 5336 m² vs. 1463 m²; our study vs. Tolimieri et al. 2009, respectively) and 1.9 times larger for copper rockfish (mean = 4656 m² vs. 2448 m²), due primarily to foray behavior and relocations of a few fish. Our findings support previous work showing that habitat type and habitat quality influence the scale of movement with larger home ranges being associated with lower relief habitat for rockfishes (Matthews 1990). However, the scale of movements for quillback rockfish in our study is far larger than previously reported.

Relocation to a different activity center by copper 252 supports previous findings for 2 copper rockfish studied at Siletz Reef, Oregon, showing fish moving repeatedly between 2 primary locations (Hannah & Rankin 2011). Lowe et al. (2009) reported highly variable detectability rates and low site fidelity for copper rockfish (detected < 30% of days at liberty), and one specimen was shown to move between 2 oil platforms. The relocations exhibited by copper 252 and the brown rockfish provide an interesting contrast in relocation behavior. The copper rockfish's quick (1 h), direct and repeated relocation to 1 of 2 core areas suggests knowledge of the habitat and recollection of a suitable home. The 6 h of meandering behavior leading to the brown rockfish's new home suggests the fish was investigating or foraging in the area, versus travelling directly to a known location.

The quillback rockfish foray behavior described in this study is also novel. Our study is not the first report of foray-like behavior, as Tolimieri et al. (2009) described 'wandering' for 1 of 5 quillbacks tracked in Puget Sound. In that study, wandering was defined as 'extensive movements that occur only during a particular portion of the day, but which are not substantial enough to result in a core area seen only nocturnally or diurnally.' Our study differs in that the movements revealed were repeated and extensive enough to result in substantially larger activity space at night and/or in the crepuscular period. Our findings also conflict with the contention by Love et al. (2002) that quillback rockfish are likely 'inactive at night'. Four of our quillback rockfish were also shown to consistently utilize open sand and gravel areas, spending considerable time off the reef in this open area with a combined total of 64 forays, ranging as far as 1000 m off the reef, and sometimes traveling more than 3 km in transit. One fish was off the reef for over 12 h. These fish would seem to be in a remarkably vulnerable position in terms of lack of suitable refuge from predators. The ecological advantage of such potentially risky behavior suggests a substantial gain in fitness. Reproductive maturity data support neither mating nor parturition for quillback rockfish off Oregon during our study period (Hannah & Blume 2011). The timing and repeated nature of this behavior, with the majority of forays commencing at sunset, strongly suggests foraging upon nocturnally active benthic prey such as the smooth bay shrimp *Lissocrangon stylirostris* (Wakefield 1984, Marin Jarrin & Shanks 2008) and Dungeness crab *Metacarcinus magister*. Prey transitioning into or out of the sand, such as sand lance *Ammodytes hexapterus* (Love 2011), or vertically migrating pelagic invertebrates (Murie 1995) may also be potential prey. Juvenile fish are another known food item for quillback rockfish (Murie 1995), and have been shown to reside within rippled scour depression habitat, defined in part as depressions in the seabed comprised of sediments coarser than the surrounding area (Hallenbeck et al. 2012). Multibeam and sidescan sonar data from the foray areas show gravel beds recessed up to 0.5 m below the surrounding sand, which may similarly provide juvenile fish habitat and prey for quillback rockfish in an otherwise featureless area (Goldfinger et al. 2012).

Although hypoxia was present for an extended time period in our study, the tagged fishes' minimal response to these conditions would seem to indicate that low oxygen levels are well-tolerated by these species. In contrast, tolerance was not indicated in the 2002 hypoxia event ($DO < 2.24 \text{ mg l}^{-1}$) at Cape Perpetua Reef, where Oregon Department of Fish and Wildlife (ODFW) ROV video footage at this same site showed numerous dead sculpins (family Cottidae; ODFW unpubl. data) and no visible rockfish (Grantham et al. 2004). A likely scenario for this difference is that DO may have reached much lower levels at the reef proper in 2002. Our results are also contrary to other published studies, the most relevant of which is Palsson et al. (2008) who reported on hundreds of copper rockfish monitored in Hood Canal during seasonally-occurring hypoxia from 2001 to 2006. In that study, copper rockfish made dramatic,

definitive changes in their behavior and distribution with the onset of hypoxia, moving towards the shore and into shallow water, moving to new reef areas, and forming dense schools in shallow water. Over time, these fish became physically compromised, showed weight loss, lethargy and scale loss. Another significant study which also conflicts with our findings is that of Vaquer-Sunyer & Duarte (2008). The authors reviewed 872 publications to conduct a comparative analysis of experimentally derived oxygen thresholds for 4 taxa, including fish. They found that the conventional definition of DO = 2 mg l⁻¹ was actually well below the lethal and sublethal oxygen thresholds for fish, which exhibited sublethal responses to DO levels as high as 4.8 mg l⁻¹.

Our fishes' minimal response to these low oxygen concentrations suggests other factors must be considered in understanding the effects of hypoxia on fish in the wild. We propose these factors include origin of the source water mass, its physical and chemical properties, and the species' innate behavioral tendencies within their specific habitat.

The source water for hypoxia at Cape Perpetua differs from hypoxic water in other areas. In many coastal waters, eutrophication and resulting hypoxia can be caused by anthropogenic addition of nitrogen and phosphate, conditions not applicable to our source water (Gray et al. 2002). In coastal Oregon, summertime NW wind advects deep (> 600 m) naturally oxygen-poor waters onto the lower shelf and into the photic zone (Wheeler et al. 2003, Grantham et al. 2004). This source water is characterized by lower temperatures (e.g. 7°C) and higher salinity than wintertime nearshore waters. Although the oxygen concentration is reduced further through primary production processes and respiration (Wheeler et al. 2003), temperature remains low. In contrast, summertime hypoxia in Hood Canal is formed by a combination of factors which include intrusion of low-oxygen ocean water, but is confounded by stratification of fresh and saltwater, creating a barrier to mixing. Bathymetry limits flushing in the system and contributes to mid-level hypoxic water moving towards the surface (Newton 2008). Resulting temperatures in Hood Canal were considerably warmer in rockfish habitat, between 9 and 11°C below 7 m depth, while surface waters (< 3 m depth) were over 14°C (Palsson et al. 2008). The lower metabolic rate of a fish species residing in the colder temperatures of its natural temperature range (e.g. Cape Perpetua), versus the upper range of temperature tolerance (e.g. Hood Canal) could better enable fish to withstand the physiological challenge of hypoxia, as oxygen demand is lowered (Kim et al. 1995, Graham 2005).

An additional factor that contributes to a fish's fitness and respiratory capacity includes exposure to the toxic byproducts of decaying organic matter, which may be concentrated in near-bottom environments (Gray et al. 2002). Low doses of these compounds can be lethal to many species of fish and invertebrates (Gray et al. 2002). Bacteria residing in sediment generate hydrogen sulfide (H₂S) in the absence of oxygen, and ammonia is formed by

mineralization of organic nitrogen as organic matter decays. The 2006 ODFW ROV video footage at Cape Perpetua showed decomposition of crabs and sessile benthic organisms and the presence of bacterial mats during a time of severe hypoxia ($DO < 0.5 \text{ mg l}^{-1}$), when (as in 2002) no rockfish were visible (Chan et al. 2008). Although no testing was conducted to detect the presence of these compounds, it is reasonable to expect that they were present. The level of decomposition would further reduce oxygen concentration in the immediate area. Diaz & Rosenberg (1995) note that the effects of hypoxia and H_2S are difficult to separate and may be, at a minimum, additive for fauna not evolutionarily adapted to tolerate them. Video observations at Cape Perpetua during our 2010 study showed no evidence of dead or dying benthic fauna, nor bacterial mats, suggesting physiological challenges from ammonia or hydrogen sulfide compounds were not present at high concentrations.

Fishes' innate behavior and specific habitat may also influence any tendency to avoid low oxygen conditions. Although the quillback forays reveal this species is not as tightly associated with rocky habitat as previously thought, both species demonstrated very high site fidelity during hypoxia in an area with no other nearby reefs. One interesting aspect of hypoxia avoidance behavior of copper rockfish was observed in Hood Canal with fish moving 170 m horizontally to another hypoxic reef area, versus 39 m to a shallow reef with higher oxygen concentration (Palsson et al. 2008). One explanation for this behavior was that the route to the shallow reef was over non-consolidated substrate, suggesting the fishes' behavioral affinity for rocky habitat may compete with their physiological need for oxygen (Palsson et al. 2008). Cape Perpetua fish may also have strong behavioral incentive to remain associated with their isolated reef, as rocky habitat is very limited in the area. Evaluating hypoxia in light of species' site fidelity could greatly assist in spatial management for certain species. For instance, 2 rockfish species classified as overfished in Oregon vary greatly in their site fidelity tendencies: canary rockfish *Sebastes pinniger* are highly mobile, show very low site fidelity and a high range of vertical movement (up to 27 m), while yelloweye rockfish *S. ruberimus* may remain in one small area near the bottom (3 to 7 m vertical range) for many months or even years (Hannah & Rankin 2011). Although both these fish are found in association with rocky habitat, the difference in their tendencies is not subtle. The study showed most acoustically tagged canary rockfish were semi-pelagic, and left the reef area entirely and rapidly; one moving over 13 km in a 14 h period (Hannah & Rankin 2011). Exposure to hypoxia for these fish could have very different effects based on site fidelity alone, with the behavioral tendency for canary rockfish to simply leave the same area in which a yelloweye would remain. Utilizing knowledge of site fidelity and/or other behavioral tendencies, such as refuge-seeking, in addition to hypoxia tolerance could greatly enhance our understanding of these species ecology and responses to changing oceanographic conditions.

Although our study animals showed remarkable tolerance to hypoxia, some physical and ecological effects can still be expected. The reduced movements by the copper rockfish could interfere with foraging opportunities or could be caused by a decrease in prey availability. Reproductive success may be influenced as well. Hopkins et al. (1995) used oxygen consumption rates to determine metabolic rates of yellowtail rockfish *Sebastes flavidus*. They found that females incubating larvae had an 82 to 101% higher metabolic rate than spent females and males (Hopkins et al. 1995). This study also calculated the maternal nutrient contribution to the embryo. Results show that yellowtail rockfish had lower embryonic energy requirements than other rockfish species (3.4% for yellowtail, 11.5% for copper and 69.2% for black rockfish *S. melanops*) (Dygert & Gunderson 1991, Hopkins et al. 1995). These data suggest gestational metabolic demands for rockfish species could compromise incubating larvae in areas of low oxygen availability.

The broader ecological impacts of hypoxia are not insignificant for rockfish stocks. For instance, McClatchie et al. (2010) predicted significant habitat loss (18%) for *Sebastes* spp. in the Southern California Bight if the trend of shoaling of hypoxic waters does not reverse. Recurring hypoxia may fundamentally change the characteristics of a mature reef which include high levels of species diversity, abundance, biomass and larger body sizes of the associated fauna — all factors contributing to increasing reproductive opportunities and reproductive fitness of a stock (PISCO 2007). At Cape Perpetua, many species of fishes and invertebrates did not survive hypoxia in 2002 (Weeks et al. 2005). Although some rockfish returned to Cape Perpetua Reef in subsequent months and years, their abundance was reduced (Weeks et al. 2005) and the reef continues to be exposed to periodic seasonal hypoxia (PISCO hypoxia updates 2012: www.piscoweb.org/research/science-by-discipline/coastal-oceanography/hypoxia/hypoxia-updates). Although these conditions may degrade reef maturity, it is possible our fish may have an ecological advantage in the lack of competition with species which may not be as tolerant of hypoxia, particularly if prey is a limiting resource. In light of this, our quillback's potentially prey-seeking forays into open sand and gravel beds may support recharacterization of fish habitat for this species.

Although our study period encompassed a wide range of oxygen concentrations on the reef, severe hypoxia was not observed in the area in 2010, so we were not able to monitor fish movements during this greater physiological challenge; nor did we conduct the study during wintertime, when other studies have reported a seasonal component of habitat use for these species (Matthews 1990, Tolimieri et al. 2009, Hannah & Rankin 2011). It is possible that a study that captured anoxic conditions would reveal additional broad-scale movements for these and other species at Cape Perpetua.

The variability of behaviors described here and in other studies reiterates the complexity of evaluating fishes' responses to changing environmental conditions. Interacting factors including the origin, chemistry, and temperature of the hypoxic water mass and the species' innate behavioral tendencies must be considered — along with dissolved oxygen — in determining the effects of hypoxia on fish.

ACKNOWLEDGEMENTS.

We thank Captain D. Edwards, S. Jones, R. Easton, D. W. Wagman and T. Frierson for assistance in the field. M. Donnellan and B. Miller provided ROV footage. We also thank D. Fox, D. Erickson and K. Andrews for providing comments on the manuscript. Funding was provided in part by an Oregon Department of Fish and Wildlife grant from the US Fish and Wildlife Service State Wildlife Grant Program (grant #OR T-22-C-1 N-01).

LITERATURE CITED

- Adams KA, Barth JA, Chan F (2013) Temporal variability of near-bottom dissolved oxygen during upwelling off central Oregon. *J Geophys Res* (in press), doi:10.1002/jgrc. 20361
- Andrews KS, Tolimieri N, Williams GD, Samhouri JF, Harvey CJ, Levin PS (2011) Comparison of fine-scale acoustic monitoring systems using home range size of a demersal fish. *Mar Biol* 158:2377–2387
- Brown CB, Power JH (2011) Historic and recent patterns of dissolved oxygen in the Yaquina Estuary (Oregon, USA): importance of anthropogenic activities and oceanic conditions. *Estuar Coast Shelf Sci* 92:446–455
- Calenge C (2006) The package 'adehabitat' for the R software: a tool for the analysis of space and habitat use by animals. *Ecol Model* 197:516–519
- Chan F, Barth JA, Lubchenco J, Kirincich A, Weeks H, Peterson WT, Menge BA (2008) Emergence of anoxia in the California Current Large Marine Ecosystem. *Science* 319:920
- Connolly TP, Hickey BM, Geier SL, Cochlan WP (2010) Processes influencing seasonal hypoxia in the northern California Current System. *J Geophys Res* 115:C03021, doi:10.1029/2009JC005283
- Diaz RJ, Rosenberg R (1995) Marine benthic hypoxia: a review of its ecological effects and the behavioural responses of benthic macrofauna. *Oceanogr Mar Biol Annu Rev* 33:245–303
- Dygert PH, Gunderson DR (1991) Energy utilization by embryos during gestation in viviparous copper rockfish, *Sebastes caurinus*. *Environ Biol Fishes* 30:165–171
- Fox D, Merems A, Amend M, Weeks H, Romsos C, Appy M (2004) Comparison of two nearshore rocky reef areas: a high-use recreational fishing reef vs. an unfished reef. Oregon Department of Fish and Wildlife, Final Report for US Fish and Wildlife Service, Wildlife Conservation and Restoration Program, Newport, OR
- Graham JB (2005) Aquatic and aerial respiration. In: Perry SF, Tufts BL (eds) *Fish respiration*. Academic Press, New York, NY, p 85–117

- Goldfinger C, Romsos C, Erhardt ME, Hairston-Porter R, Kane T, Lockett D (2012) Oregon state waters multibeam mapping project: final report. Oregon State University active tectonics and seafloor mapping laboratory publication 2012-1. Corvallis, OR
- Grantham BA, Chan F, Nielsen KJ, Fox DS and others (2004) Upwelling-driven nearshore hypoxia signals ecosystem and oceanographic changes in the northeast Pacific. *Nature* 429:749–754
- Gray JS, Wu RS, Or YY (2002) Effects of hypoxia and organic enrichment on the coastal marine environment. *Mar Ecol Prog Ser* 238:249–279
- Hallenbeck TR, Kvitek RG, Lindholm J (2012) Rippled scour depressions add ecologically significant heterogeneity to soft sediment habitats on the continental shelf. *Mar Ecol Prog Ser* 468:119–133
- Hannah RW, Blume MTO (2011) Maturity of female quillback (*Sebastes maliger*) and china rockfish (*S. nebulosus*) from Oregon waters based on histological evaluation of ovaries. Oregon Department of Fish & Wildlife, Information Report Series, Newport, OR
- Hannah RW, Matteson KM (2007) Behavior of nine species of Pacific rockfish after hook-and-line capture, recompression, and release. *Trans Am Fish Soc* 136:24–33
- Hannah RW, Rankin PS (2011) Site fidelity and movement of eight species of Pacific rockfish at a high-relief rocky reef on the Oregon coast. *N Am J Fish Manag* 31:483–494
- Herbert NA, Skjaeraasen JE, Nilsen T, Salvanes AGV, Steffensen JF (2011) The hypoxia avoidance behavior of juvenile Atlantic cod (*Gadus morhua* L.) depends on the provision and pressure level of an O₂ refuge. *Mar Biol* 158:737–746
- Hopkins TD, Eldridge MB, Cech JJ (1995) Metabolic costs of viviparity in yellowtail rockfish, *Sebastes flavidus*. *Environ Biol Fishes* 43:77–84
- Kim IN, Chang YJ, Kwon JY (1995) The patterns of oxygen consumption in six species of marine fish. *J Korean Fish Soc* 28:373–381
- Love M (2011) Certainly more than you want to know about the fishes of the Pacific Coast. Really Big Press, Santa Barbara, CA
- Love MS, Yoklavich M, Thorsteinson L (2002) The rockfishes of the northeast Pacific. University of California Press, Berkeley, CA
- Lowe CG, Anthony KM, Jarvis, ET, Bellquist LF, Love MS (2009) Site fidelity and movement patterns of groundfish associated with offshore petroleum platforms in the Santa Barbara Channel. *Mar Coast Fish* 1:71–89
- Marin Jarrin JR, Shanks AL (2008) Ecology of a population of *Lissocrangon stylirostris* (Caridea: Crangonidae), with notes on the occurrence and biology of its parasite, *Argeia pugettensis* (Isopoda: Bopyridae). *J Crustac Biol* 28:613–621
- Matthews KR (1990) An experimental study of the habitat preferences and movement patterns of copper, quillback and brown rockfishes (*Sebastes* spp.). *Environ Biol Fishes* 29:161–178
- McClatchie S, Goericke R, Cosgrove R, Auad G, Vetter R (2010) Oxygen in the Southern California Bight: multidecadal trends and implications for demersal fisheries. *Geophys Res Lett* 37:L19602, doi:10.1029/2010GL044497
- Murie DJ (1995) Comparative feeding ecology of two sympatric rockfish congeners, *Sebastes caurinus* (copper rockfish) and *S. maliger* (quillback rockfish). *Mar Biol* 124:341–353
- Nakanishi T, Itazawa Y (1974) Effects of hypoxia on the breathing rate, heart rate and rate of oxygen consumption in fishes. *Rep Fish Res Lab Kyushu Univ* 2:41–52
- Newton J (2008) HCDOP IAM study preliminary results. www.hoodcanal.washington.edu

- Palsson WA, Pacunski RE, Parra TR, Beam J (2008) The effects of hypoxia on marine fish populations in southern Hood Canal, Washington. *Am Fish Soc Symp* 64: 255–280
- Parker SJ, Rankin PS, Olson JM, Hannah RW (2007) Movement patterns of black rockfish (*Sebastes melanops*) in Oregon coast waters. In: Heifetz J, DiCosimo J, Gharrett AJ, Love MS, O’Connell VM, Stanley RD (eds) *Biology, assessment, and management of North Pacific rockfishes*. Alaska Sea Grant College Program AK-SG-7-01, Fairbanks, AK, p 39–58
- PISCO (Partnership for Interdisciplinary Studies of Coastal Oceans) (2007) *The science of marine reserves*, 2nd edn (US version). PISCO, Corvallis, OR
- Pauly D, Christensen V (1995) Primary production required to sustain global fisheries. *Nature* 374:255–257
- Roegner GC, Needoba JA, Babtista AM (2011) Coastal upwelling supplies oxygen-depleted water to the Columbia River estuary. *PLoS ONE* 6:e18672
- Sokal RR, Rohlf FJ (1981) *Biometry*, 2nd edn. WH Freeman, New York, NY
- Tolimieri N, Andrews K, Williams G, Katz S, Levin PS (2009) Home range size and patterns of space use by lingcod, copper rockfish and quillback rockfish in relation to diel and tidal cycles. *Mar Ecol Prog Ser* 380:229–243
- Vaquer-Sunyer R, Duarte CM (2008) Thresholds of hypoxia for marine biodiversity. *Proc Natl Acad Sci USA* 105: 15452–15457
- Vetter RD, Lynn EA (1997) Bathymetric demography, enzyme activity patterns, and bioenergetics of deep-living scorpaenid fishes (genera *Sebastes* and *Sebastolobus*): paradigms revisited. *Mar Ecol Prog Ser* 155:173–188
- Wakefield WW (1984) Feeding relationships within assemblages of nearshore and mid-continental shelf benthic fishes off Oregon. MS thesis, Oregon State University, Corvallis, OR
- Weeks H, Merems A, Miller W (2005) 2004 Nearshore rocky reef habitat and fish survey, and multi-year summary. Final report for 2004-05, Oregon Department of Fish and Wildlife, Newport, OR
- Wheeler PA, Huyer A, Leischbein F (2003) Cold halocline, increased nutrients and higher chlorophyll off Oregon in 2002. *Geophys Res Lett* 30:8021, doi:10.1029/2003 GL017395

5: HABITAT USE AND ACTIVITY PATTERNS OF FEMALE DEACON ROCKFISH (*SEBASTES DIACONUS*) AT SEASONAL SCALES AND IN RESPONSE TO EPISODIC HYPOXIA

Leif K. Rasmuson & Mathew T. O. Blume & Polly S. Rankin

Recreated from <https://doi.org/10.1007/s10641-021-01092-w> for simplicity.

ABSTRACT

We combined a high-resolution acoustic telemetry array with presence/absence receivers to conduct a preliminary study of the seasonal movements, activity patterns, and habitat associations of the newly described Deacon Rockfish (*Sebastes diaconus*). Eleven mature female Deacon Rockfish were tagged and monitored during an 11-month period, at a nearshore rocky reef off Seal Rock, Oregon, USA, an area of recurring seasonal hypoxia (defined as dissolved oxygen concentration [DO] < 2 mg l⁻¹). Two tags were detected leaving the study area by day 35, indicating predation or emigration. Three tags became inactive within the array, indicating tag loss or fish death. Six “resident” fish inhabited the array for 246–326 days. Resident fish exhibited high site fidelity, small home ranges (mean 95% KDE = 4907 m²), and consistent activity patterns for the duration of the summertime high-resolution array (5 months), except during seasonal hypoxia. Resident fish were strongly diurnal in summer, with high levels of daytime activity above the bottom in relatively rugose habitat, followed by nighttime rest periods in deeper, less rugose habitat. During summertime hypoxia, resident fish exhibited less daytime activity during daytime hours with no rest periods at night, inhabited shallower water depths, and moved well away from their core activity areas on long, erratic forays. During the winter, diel patterns were less evident with higher activity levels at night (than in the summer) and lower activity levels in the day (than in the summer). We propose that some Deacon Rockfish continuously inhabit nearshore reefs throughout the year, but that daily/seasonal movement patterns, seasonally occurring hypoxia, and prey preferences for planktonic organisms influence relocation.

INTRODUCTION

The spatiotemporal scales of movement patterns for marine fishes are highly variable (Pittman and McAlpine 2003), with tunas and other large pelagics making migrations on the order of thousands of kilometers (Galuardi et al. 2010; Kraus et al. 2011) and other organisms remaining relatively sedentary in a singular spot (Bryars et al. 2012; Buston 2004). The temporal scales over which these movements occur vary widely from ontogenetic movements such as salmon and eels (Hansen et al. 1993; van Ginneken et al. 2005) to daily vertical migrations in sand lances and lanternfish (Engelhard et al. 2008; Dypvik et al. 2012). Fish movements vary

within the same genera leading to niche partitioning (Sbragaglia et al. 2019). Movement can even differ within the same species resulting in distinct behavioral differences (e.g., for size, sex differences, reproductive behavior, etc.; Bell and Sih 2007; Barnett et al. 2011). Understanding intraspecies behavioral plasticity, especially within a habitat occupied by multiple species, is ecologically necessary to understanding re- source allocation (Leggett 1977; Hays et al. 2016). Further, in the event that the species are caught in fisheries, understanding the movement dynamics, especially in mixed stock fisheries, is essential for sustainable management (Peer and Miller 2014; Ogburn et al. 2017).

Oregon's nearshore recreational fisheries primarily target schooling rockfish inhabiting nearshore rocky reefs. These schools are predominantly composed of Black Rockfish (*Sebastes melanops*), Blue Rockfish (*Sebastes mystinus*), and the newly described cryptic species Deacon Rockfish (*Sebastes diaconus*) (Frable et al. 2015). Although much is known about the movements of Black Rockfish, Blue and Deacon Rockfish have only recently been recognized as separate species, and little is known about their movements in Oregon (Parker et al. 2007; Parker et al. 2008).

In contrast to Black Rockfish, which are consistently captured throughout the year off the central Oregon coast, Deacon Rockfish are often nearly or completely absent from summer catches for weeks or months, causing fishers and managers alike to suspect seasonal and/ or ontogenetic migration away from nearshore reefs (Dick et al. 2017; C Heath, pers. comm). An alternative to the seasonal and/or ontogenetic migration hypothesis is that catchability varies seasonally, and Deacon Rockfish remain at nearshore reefs throughout the year. Whether or not Deacon Rockfish migrate has distinct ecological implications, which in turn affect how to manage fisheries for this species. In addition to seasonal movements, some rockfish are hypothesized to exhibit diel shifts in their behavior. Black Rockfish have been shown to make large vertical movements associated with sunrise and sunset (Parker et al. 2008) whereas Copper Rockfish (*Sebastes caurinus*) and Quillback Rockfish (*Sebastes maliger*) exhibited home range movements associated with tidal flow in the Puget Sound (Tolimieri et al. 2009). A complete understanding of the inter- and intra-reef movement of Deacon Rockfish on daily and monthly timescales is important for fisheries management (Crossin et al. 2017). Specifically, managers increasingly seek non-lethal, spatially extensive surveys, making knowledge of seasonal fish locations essential to survey design (Berger et al. 2015; Berger et al. 2017).

Periodic variability in the abiotic environment of a fish can also impact its health and behavior in complex ways, altering normal activity and movements (Gray et al. 2002; Grantham et al. 2004). Oregon coastal waters are subject to seasonal hypoxia (dissolved oxygen [DO] < 2 mg l⁻¹) in the upwelling favorable summer months, the varied effects of which have been documented for other species of rockfish, but not for Deacon Rockfish (Diaz and Rosenberg

1995; Hopkins et al. 1995; Rankin et al. 2013). Responses to hypoxia can lead to fish dispersal or fish concentration, but have also been shown to affect home range, site fidelity, and refuge-seeking behavior in Rockfish (Pihl et al. 1991; Rankin et al. 2013). Changes in environmental conditions can result in fish remaining within an area, but cause fish to be behaviorally or physically “unavailable” to fishery capture or survey, or alternatively may make fish more susceptible to capture in a fishery (Hannah and Blume 2016; Stanley et al. 1999). As managers often use catch rates as a proxy for fish abundance, knowing the level of environmental influence on fish behavior is essential.

Investigating the movements of Deacon Rockfish over time, and throughout a range of environmental conditions, can provide much-needed data on their natural history, responses to changing environmental conditions, and can inform survey design. Determining the scale of movements for initial study design can be challenging for Rockfish as movements for reef inhabitants may range from high site fidelity over periods of months or years for some species (*S. melanops*, *S. maliger*) to the wide-ranging Canary Rockfish (*Sebastes pinniger*) (Parker et al. 2007; Hannah and Rankin 2011). Acoustic telemetry is an effective tool for establishing baseline movements and behavior of tagged fish, while providing scale of movements to inform the design of more comprehensive investigations. The goal of this study was to use high-resolution acoustic telemetry combined with simple presence/ absence data to track Deacon Rockfish over a one-year period to: (1) provide preliminary scales of movement, (2) describe daily and seasonal patterns of behavior and use of habitat, and (3) examine the relative influence of seasonal hypoxia on movements, behavior patterns, and habitat usage.

MATERIALS AND METHODS

STUDY SITE AND ARRAY

The Seal Rocks study area, on the central Oregon coast, encompassed 11.84 km² (2.86 km × 4.14 km) of nearshore rocky reef. The study area was comprised of bedrock benches, boulders, and rocky pinnacles for which 2 × 2 m multibeam resolution and side scan bathymetry data was available (Fig. 1). The primary habitat was variably rugose with swaths of smaller, complex secondary habitat in between. Specifically, our study area included an isolated rocky reef ranging in depth from 12 to 26 m that could be surrounded by a perimeter of receivers in low-relief habitat, to detect fish traveling beyond the reef. Results of a 15-day range testing study (conducted in the most rugose, high-relief area of the reef) provided worst-case detection statistics through a range of swell and wind conditions. The results suggested an optimal receiver spacing of 250 m (see online supplement for more information).

Based on these findings, and in consideration of habitat, ocean conditions, and potential range

of travel for fish, we used two different acoustic telemetry array designs to maximize tag detections during both summer and winter periods (Andrews et al. 2011). The high-resolution summer array (May–September, 2016) included an inner grid of VPS (VEMCO Positioning System) receivers, surrounded by an outer perimeter fence of receivers used to detect any fish leaving the area (Fig. 1). The inner grid encompassed a 2.23-km² reef area to acquire fine-scale movements and habitat association, and was comprised of 21 VR2W receivers with co-located V16 coded synchronization tags (synctags, V16T-4L and V16-4L) moored at 250 m spacing to allow tag transmissions to be detected by multiple receivers. Also moored were two permanent, centrally located V16 reference tags (VEMCO, Nova Scotia, Canada). Synctags are acoustic transmitters used for time synchronization that allow calculation of triangulated positions for each fish (VEMCO, Nova Scotia, Canada). This system can provide accurate (5–15 m) position information but only for a relatively small number of tagged fish, due to the high density of synctag transmissions (VEMCO, Nova Scotia, Canada). Acoustic receivers and synctags were positioned 3 and 4 m off bottom, respectively. The 18-receiver perimeter fence was 9.74 km long, positioned 1200 m outside of the VPS array, and surrounded the north, west, and south side of the array (excluding the shallow shoreline side). Perimeter fence moorings were placed 500 m apart for presence/absence detection by a single receiver, in depths ranging from 12 to 39 m.

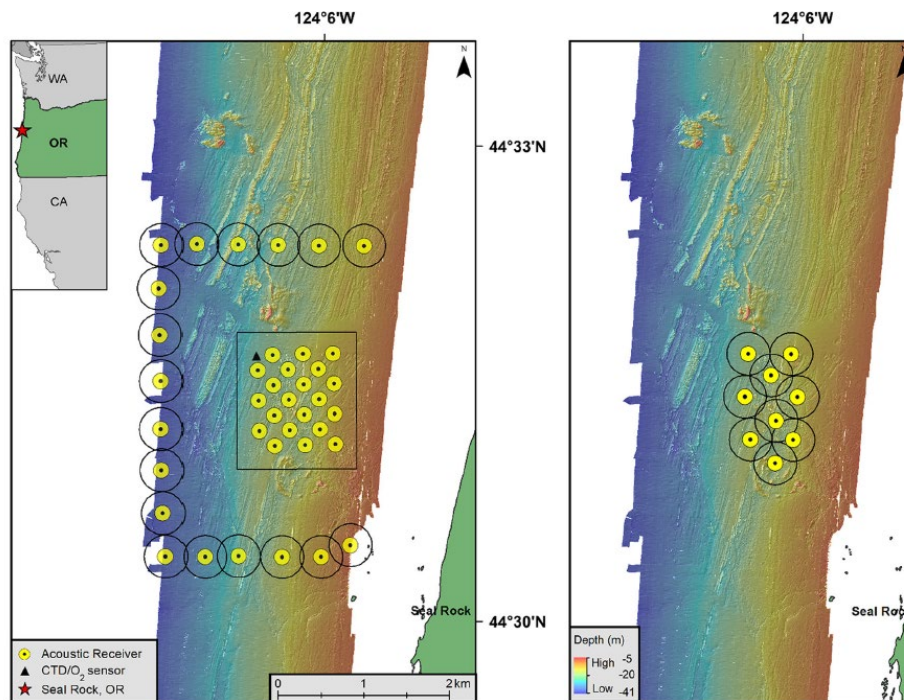


Fig. 1 Study area off Seal Rock, Oregon, showing bathymetry and locations of moored receivers and CTD. Left panel is the summertime high-resolution VPS (VEMCO Positioning System) acoustic receiver array with co-located synctags (square box indicates VPS area of acoustic detection) with the perimeter receiver “fence.” Right panel is the non-VPS winter array used for

presence/absence-only detection. Black circles indicate 250 m detection range for receivers used for presence/absence detection. Inset is the Washington, Oregon, and Northern California coastlines. Star in Oregon is the Seal Rocks study area. Triangle indicates the position of the moored CTD with oxygen sensor

A Sea-Bird SBE16plusV2 CTD, equipped with a SBE43 oxygen sensor, was moored in 27 m of water depth at the NW corner of the VPS array, to record conductivity, temperature, depth, and dissolved oxygen (Fig. 1; Sea-Bird Electronics, Bellevue, WA, USA). The CTD was positioned 1 m off bottom and sampled once every 60 min, during the summer months. The CTD was downloaded and serviced approximately bimonthly and was removed for winter.

Ocean conditions in Oregon during winter months (October–March) are typified by large, energetic storms that generate considerable acoustic noise. This noise greatly increases tag detection interference, particularly in shallow water. Thus, for the winter array, we removed all co-located synctags to increase the detection probability of fish tags. This low-resolution winter array had 9 receivers spaced 350 m apart covering an acoustic detection area of approximately 2.08 km² to acquire presence/absence-only data for fish within the reef area (Fig. 1). All acoustic receivers for both arrays (summer and winter) were downloaded and serviced bimonthly on average.

The acoustic receivers for the VPS grid and perimeter fence were deployed on 5/10/16 and 5/11/16, and the Sea-Bird SBE16plus V2 was deployed on 5/17/16 (Fig. 1). These instruments were removed on 9/30/16 and replaced with the simple 9-receiver presence/absence winter array (Fig. 1). The winter array was downloaded on 11/16/16, 1/29/17 and removed on 4/18/17. Both winter and summer arrays performed well, providing good coverage throughout the 11-month period. One receiver in the summer VPS grid failed to download on 5/31/16 and was replaced and one receiver was found missing upon the final pull of the winter grid.

ACOUSTIC TAGS AND FISH HANDLING

Fish were tagged with V13AP coded acoustic transmitters (69 kHz, 153 dB, 13 × 42 mm, pressure sensing to 136 m) which transmit a unique tag ID to the receiver. The tags also transmit the tags depth (m) and acceleration rate (m s⁻²) which is used as a measure of activity (VEMCO, Nova Scotia, Canada). To maximize detections, we chose to use the larger V13 tag (weight = 6.5 g in water) which provided long battery life (365 days) at a high sampling rate (random delay 60–180 s); therefore, we elected to tag larger fish (fork length > 32 cm) to reduce the effect of tag weight.

Due to concerns with species identification of this cryptic species, Oregon Department of Fish and Wildlife Marine Fisheries Research staff were trained with known samples to visually differentiate between Deacon and Blue Rockfish. Further, species identification of tagged fish was visually confirmed by Dr. Wolfe Wagman, coauthor of the Deacon Rockfish Frible et al. (2015) species description.

Deacon Rockfish can suffer fatal injuries from barotrauma when captured from depths >28 m (Hannah et al. 2008; Hannah et al. 2012). Further, imprudent surface handling results in reduced submergence success of released fish (Hannah et al. 2008). To mitigate these effects, the following techniques were used to capture and handle fish chosen for tagging:

1. To compensate for the weight of the acoustic tag, we selected fish >32 cm total length which, for Deacon Rockfish, only include sexually mature females (Hannah et al. 2015).
2. Fish were captured using hook and line gear with small terminal tackle (Sabiki rigs), in water depths less than 26 m. Following Rankin et al. (2016), fish were immediately recompressed in drum-type cages and held at depth for 24 h to ensure survival and to resolve barotrauma before tagging. Studies have shown that many rockfish species, including Deacon Rockfish, do not experience barotrauma a second time upon returning to the surface within 24–48 h of initial recompression. Therefore, they can be handled at surface pressure during that time without further gas expansion injury (Hannah et al. 2012; Rankin et al. 2016).
3. Fish were tagged externally as per Hannah and Rankin 2011, in order to decrease surgical trauma and to increase tag detection in the array (Dance et al. 2016).
4. Fish were released into a floating bottomless sea pen after tagging, to descend under their own power (Hannah et al. 2008).

DATA ANALYSIS

OCEANOGRAPHIC DATA

To examine how fish behavior changed during periods of hypoxia and normoxia, we used our CTD to identify periods of normoxia and periods hypoxia. Dissolved oxygen (DO) levels are strongly influenced by water temperature. Therefore, we minimized temperature as a confounding factor by identifying and selecting time periods of hypoxia and normoxia with similar temperature ranges and means. Following Diaz and Rosenberg (1995), the hypoxic period was defined by a mean dissolved oxygen <2 mg l⁻¹ and the normoxia period by a mean dissolved oxygen ≥2 mg l⁻¹. Differences in oxygen and temperature during these two time periods were compared using a Welch's two sample *t* test. Based on examination of the CTDs dissolved oxygen data, we designated two 11-day time periods: one normoxia period and one hypoxia period. These periods definitions were used to subset the acoustic telemetry data to be used in a focused analysis of how home range, site fidelity, activity, and depths differed between hypoxia and normoxia periods.

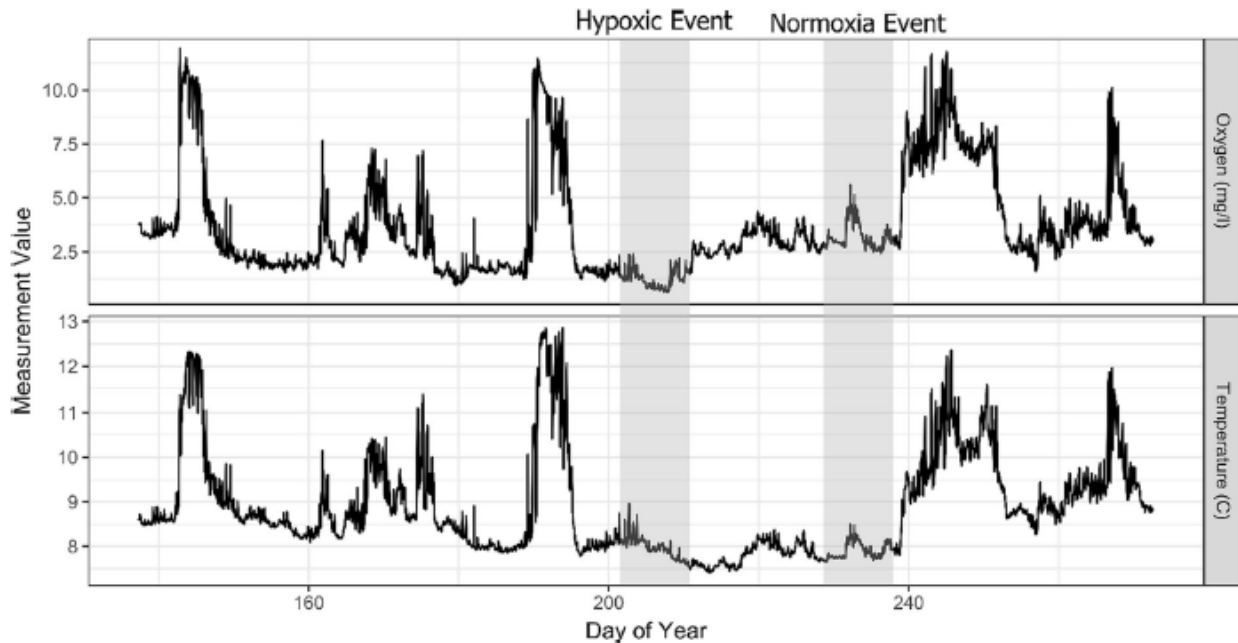


Fig. 2 Mean daily dissolved oxygen and temperature for the Seal Rocks study area from 5/17/16 through 9/30/16. Two 11-day comparison periods are indicated by gray shading: Hypoxia (DO range 0.63–2.40 mg l⁻¹, mean DO = 1.4 mg l⁻¹, mean T = 7.91 °C) from 7/20/16–7/30/16; Normoxia (DO range 2.43–5.60 mg l⁻¹, mean DO = 3.19 mg l⁻¹, mean T = 7.90 °C) from 8/16/16–8/26/16.

Oxygen levels during hypoxia and normoxia differed significantly from one another ($t(478) = -40.14$, $p < 0.001$). Temperature was also significantly different during the two periods ($t(478) = 3.58$, $p < 0.001$); however, the mean temperature difference between the two time periods was only 0.01 °C, indicating conditions were highly static

RESIDENCY AND HABITAT USAGE

Acoustic tag transmissions from tagged semi-pelagic fishes (such as Deacon Rockfish) are highly detectable, generating hundreds of validated detections per day in most conditions. However, during high ambient noise events, such as high wind and swell generated by storms, detection rates are reduced; therefore, we used a minimum of six validated detections per day to establish residence. Six validated detections allowed us to determine whether a tag was on the sea floor or on a live fish, as indicated by variation in transmitted depth and/ or activity level. Residence time was defined as the number of days live fish (active tags) were detected during the 11-month study period.

We first examined how the core area and home range differed between tagged fish. Spatial analyses were only conducted during summer months when we had high-resolution position data from the VPS array (May–September). Position data used for home range and space utilization analyses was filtered for <21 m HPE (horizontal position error), defined as “a relative, unitless estimate of how sensitive a calculated position is to errors in its inputs”, and is the estimated precision of the system for this array and the conditions (VEMCO, Nova Scotia, Canada). Initial analyses filtering HPE data to values as low as 3 m demonstrated that the only effect on our data was to reduce our sample sizes and therefore we elected to only filter data to a value of 21 m. We estimated the home range and core areas for each tagged fish residing

within the array, where home range was defined as the 95% kernel density estimator (KDE) and the core area was defined as the 50% KDE. KDEs were calculated using the program Geospatial Modeling Environment (GME, version 0.7.4.0) implemented in R (Beyer 2015; R Core Team 2018). Areas were estimated using the tool “isopleths” c(0.95,0.5) in GME.

We next examined how home ranges and core areas differed between daytime and nighttime. Daytime and nighttime were defined as daily 5-h periods in the middle of the day or night. These time periods were chosen to remove potential crepuscular or transition behaviors from the analyses. For analysis of both the home range and core area data, we estimated a maximum distance from the calculated center of the core area using “genpointinpoly” in GME. We also examined the foray behavior of each fish in their core area and home range. Forays were defined as a series of movements, which were sequential in time and space, at least 100 m away from the calculated center of activity, and lasting for more than 1 h (Rankin et al. 2013). Following a similar study, in Rankin et al. 2013, foray distances were calculated from individual detections, and foray duration was estimated based on the time a tagged fish left and returned to a location less than 100 m from its center of activity. These analyses of home range and core areas were then repeated with telemetry data subset to only include the hypoxia and normoxia periods defined in the “Oceanographic data” section.

To determine if fish utilize habitats of different rugosity during day and night, underlying bathymetric data from high-resolution Digital Elevation Model (DEM) layers were extracted from each tagged fish’s daytime and nighttime core area position data. Geomorphology analysis was conducted using the Vector Ruggedness Modeling (VRM) tool in the Benthic Terrain Modeler (BTM) implemented in ArcGIS 10.3 (Hobson 1972; Sappington et al. 2007; ESRI 2015). Vector ruggedness provides a metric for how rugose a reef is; specifically, higher values denote more rugose reef. From the underlying DEM raster, a (2 m × 2 m) VRM layer was created using BTM geomorphology tool, and neighborhood size (1) was chosen at the smallest resolution.

DAILY AND SEASONAL BEHAVIOR

Analysis of within day and seasonal patterns of accelerometer and depth data were conducted using generalized additive mixed effects models (GAMMs) using the mgcv package in R version 3.5.1, Feather Spray (Wood 2004; Wood 2011). Spatial and temporal autocorrelation were tested for using the DHARMA package (Hartig 2020). Only data from resident fish were utilized in these analyses. Data were first explored following the protocols established by Zuur et al. (2010). Four models were developed. Two models (one for activity, one for depth) were developed to assess how fish behavior changed over the course of our entire study, and two models were developed to compare activity and depth during the periods we defined as hypoxic and normoxic. These data for the second set of models are a subset of the larger seasonal dataset but were analyzed separately so as to have an approximately equal number of observations for each

category of oxygen level (see the “[Oceanographic data](#)” section).

For both sets of models, fish activity was log transformed to reduce spread and allow models to be developed using a normal distribution. Depth did not require a transformation and was modeled using a normal distribution. For all models, all observations recorded by the receivers were included, in other words potentially up to 1440 observations per fish per day. However, the randomized ping rates of the tags and the high potential for every ping to not be received by a receiver reduced the number of daily observations per tag. For the first set of models (comparing activity and depth over the duration of the study), the variables included in the model were hour of the day (continuous), and month of the year (categorical). An interaction between hour of the day and month of the year was also examined. For the second set of models (comparing activity and behavior during hypoxic and normoxic periods), the variables included in the model were (1) hour of the day (continuous) and (2) oxygen level (categorical). An interaction between hour of the day and oxygen level was also examined.

In both sets of models, continuous variables were modeled using a cyclic cubic regression spline to account for the cyclic nature of hour of the day. A cyclic cubic regression spline requires that the best fit line start and stop at the same point on the y-axis. With hour of the day, this is important because a large behavioral shift from, for example, 23:59 to 00:01, is ecologically unrealistic. Regardless of model, we included the tag ID of each individual fish as a random effect in the model to account for intra-tag variability (Pinheiro and Bates 2000). We also included a first-order autoregressive correlation structure (AR1) to account for temporal autocorrelation between successive observations (Zuur et al. 2009). No evidence of spatial autocorrelation was found. Model selection was conducted by comparing Akaike Information Criterion (AIC) values for all possible model formulations (Burnham and Anderson 2004). The model structure with the lowest AIC value was deemed the best-fit model.

RESULTS

OCEANOGRAPHY

Periodic multiday hypoxic conditions were detected in the Seal Rocks array throughout the summer season (Fig. 2). The dates assigned for the 11-day comparison periods were: (a) hypoxia; July 20–30 (DO range 0.63–2.40 mg l⁻¹, mean DO = 1.4 mg l⁻¹, mean T = 7.91 °C), (b) normoxia; August 16–26 (DO range 2.43– 5.60 mg l⁻¹, mean DO = 3.19 mg l⁻¹, mean T = 7.90 °C). (Fig. 2). Oxygen levels during hypoxia and normoxia differed significantly from one another ($t(478) = -40.14, p < 0.001$). Temperature was also significantly different during the two periods ($t(478) = 3.58, p < 0.001$). However, the mean temperature difference between the two time periods was only 0.01 °C, indicating conditions were highly static.

Table 1 Summary information and status of 11 tagged Deacon Rockfish. Fish status indicates area of final detection and classification of fish: fence (detected on fence), inactive (tag inactive), resident (in VPS array), and traveler (moved beyond fence). Residence time was defined as the number of days live fish (active tags) were detected during the 11-month study period. Home foray

is the distance between the position of release of tagged fish to a location less than 100 m from the calculated center of activity. Home foray duration is the time elapsed between the time of release of a tagged fish to a location <100 m from the calculated center of activity

Fish ID	Total length (cm)	Residence time (day)	Home foray distance (m)	Home foray duration (hh:mm)	Status	Predation/mortality * Departure** (date)
TD01	33	13	1896	2:36	Fence/inactive	05/31/2016*
TD02	35	323	581	14:58	Resident	
TD03	33	246	556	18:35	Resident/traveler	01/18/2017**
TD04	34	312	659	10:22	Resident	
TD05	41	27	1598	16:11	Traveler	06/14/2016**
TD06	35	306	311	26:46	Resident	
TD07	36	37	341	11:20	Fence/inactive	07/06/2016*
TD08	39	35	382	21:00	Traveler	06/20/2016**
TD09	39	326	311	22:09	Resident	
TD10	40	322	404	8:00	Resident	
TD11	33	112	589	21:44	Resident/inactive	07/08/2016*

FISH

Eleven female Deacon Rockfish were tagged on 5/17/ 2016. Fish ranged from 33 to 41 cm total length. Based on length weight relationships, the tag weighed from 0.62–1.19% of fish body weight (unpublished data). Prior to release, tagged fish were alert, active, free of barotrauma signs, and were able to descend without assistance (Table 1).

RESIDENCY AND HABITAT USAGE

After release, all 11 fish returned to the location of capture within 27 h (home foray, Table 1). One fish was detected in the grid for 112 days, before showing evidence of predation. Four fish had residence times between 13 and 37 days before leaving the array; two were located within the fence area, but were inactive, indicating tag loss, predation, or mortality. The other two fish were detected leaving the perimeter area via the north fence, and designated as “traveler” (Table 1, Fig. 1). Six fish “residents” remained in the grid and were consistently detected for 246–326 days (Table 1).

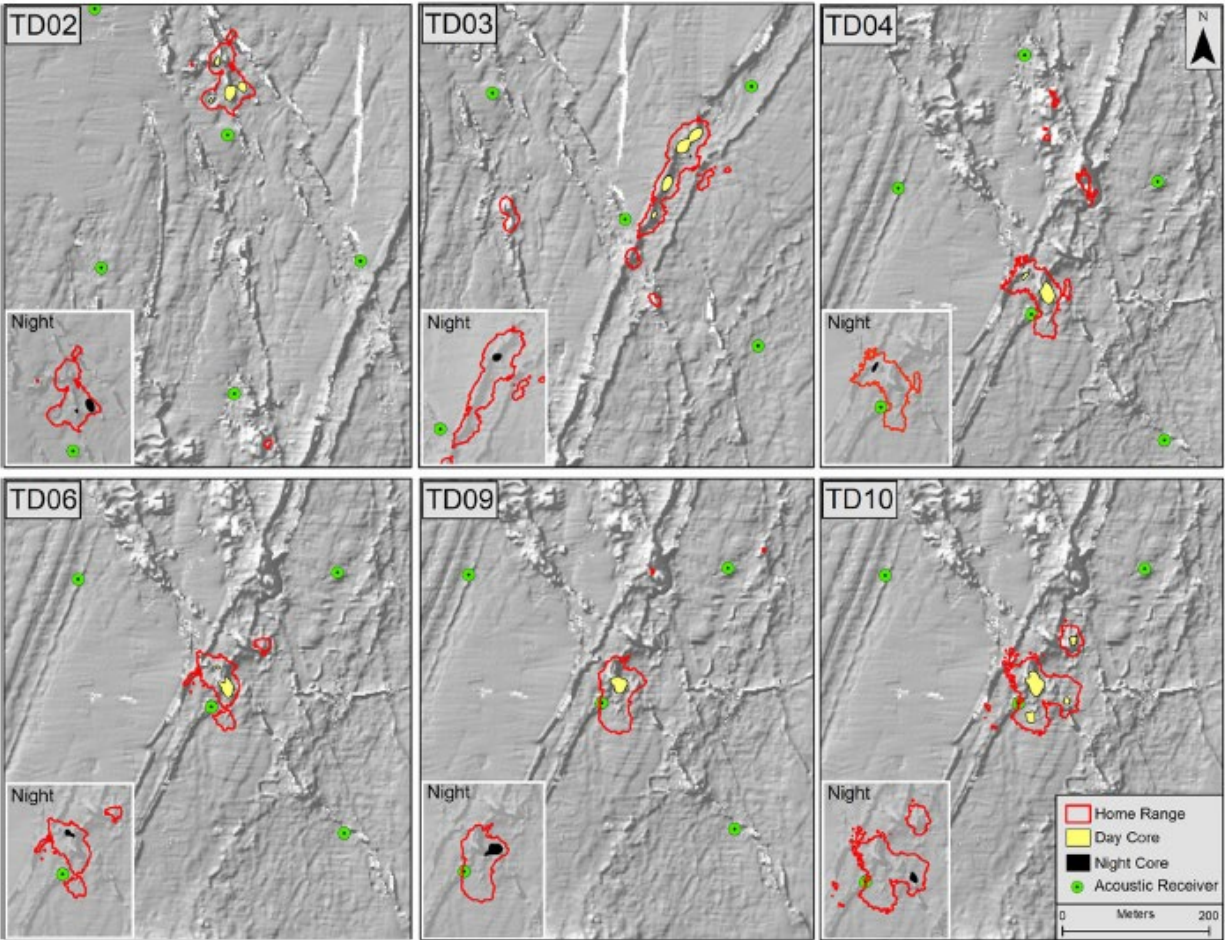


Fig. 3 Comparison of home range, daytime and nighttime core areas for resident Deacon Rockfish. Areas are within the VPS array and overlay multibeam bathymetry. Date range 5/19/16 through 9/30/16. Main panels: Home Range Area (KDE 95%, red outline) and Daytime Core Activity Area (KDE 50%, yellow

fill). Inset panels are of the home range area, at the same scale for Nighttime Core Activity Area (KDE 50%, black fill). Fish inhabit different and smaller core areas during the nighttime, than in the daytime. Four fish had overlapping home ranges (TD04, TD06, TD09, TD10)

The 19 weeks of high-resolution VPS data showed the six resident fish had high site fidelity and small home ranges ranging in area from 3511 to 6875 m² (mean 95% KDE = 4907 m²; Table 2, Fig. 3). These home ranges correspond to circles with a radius of approximately 33–47 m. Core areas ranged from 324 to 756 m² (mean 50% KDE = 477 m²; Table 2, Fig. 3). These core areas correspond to circles with a radius of approximately 10–16 m. Mean nighttime home range and core area size were 50 and 25% smaller than day- time home range and core area size, respectively (Table 2, Fig. 3). With the exception of fish TD03, which was undetected after day 246, five resident fish continued to be active and detected in the winter grid for 306–323 days (Table 1). Four resident fish (TD04, TD06, TD09, and TD10) consistently utilized an overlapping home range area (Fig. 3).

Table 2 Home range, core activity area, and foray summaries for resident Deacon Rockfish. Home range is the 95% Kernel Density Estimator (KDE) and core area is the 50% KDE. Forays were

defined as a series of movements, which were sequential in time and space, at least 100 m away from the calculated center of activity, and lasting for more than 1 h (Rankin et al. 2013)

Resident fish ID	Home range/core area/day/night						Normoxia		Hypoxia		Hypoxia foray		
	Home range (m ²)	Core area (m ²)	Home range day (m ²)	Core area day (m ²)	Home range night (m ²)	Core area night (m ²)	Home range (m ²)	Core area (m ²)	Home range (m ²)	Core area (m ²)	Foray distance (m)	Distance from center (m)	Duration (hh:mm)
TD02	3715	324	3692	499	1949	162	3487	531	11,171	1339	1726	807	27:37
TD03	6530	480	7122	810	3087	112	5125	962	10,928	1328	923	299	87:48
TD04	4546	352	4762	473	870	67	5392	610	6860	714	1081	425	55:25
TD06	3511	427	2922	373	1282	95	5016	868	3480	368	981	135	57:26
TD09	4264	526	3550	374	5551	290	4830	974	6852	260	2985	312	29:10
TD10	6875	756	6945	875	1862	123	8597	1460	3682	367	1246	253	23:04
Mean	4907	477	4832	567	2434	141	5408	901	7162	729	1490	372	46:45

All six resident fish showed a substantial change in behavior during the hypoxic period, resulting in both larger and smaller core areas used. Foray behavior was exhibited by all six resident fish during the hypoxia period only. Forays ranged in duration from 23 to 88 h and from 923 to 2985 m traveled (Table 2, Fig. 4). The farthest distance from the calculated center of the core was 807 m for TD02 (Table 2, Fig. 4).

Resident fish used more rugose habitat during day- time period than at night, although the differences were much lower for fish TD03 than for other fish (Fig. 5). Further, fish utilized significantly more rugose habitat during the day, night, or in total as compared to the average habitat rugosity for the area encompassed by the array (Fig. 5).

DAILY AND SEASONAL BEHAVIOR

The best-fit models for both activity and depth included all variables and their interaction plus the addition of the random effect of fish tag (Table 3). For activity, the model explained 21.8% of the variability in the data, and for depth, the model explained 58% of the variability in the data (Table S1). During the summer months of May–September, resident fish showed a trend of higher diurnal activity for 8–12 h a day in shallower depths versus lower activity levels in deeper waters at night (Table 3, Figs. 6 and 7). This day/night trend became less evident in October, and was not evident from November through March, during which time there were no major differences in average activity level or depth readings between day and night (Figs. 6 and 7).

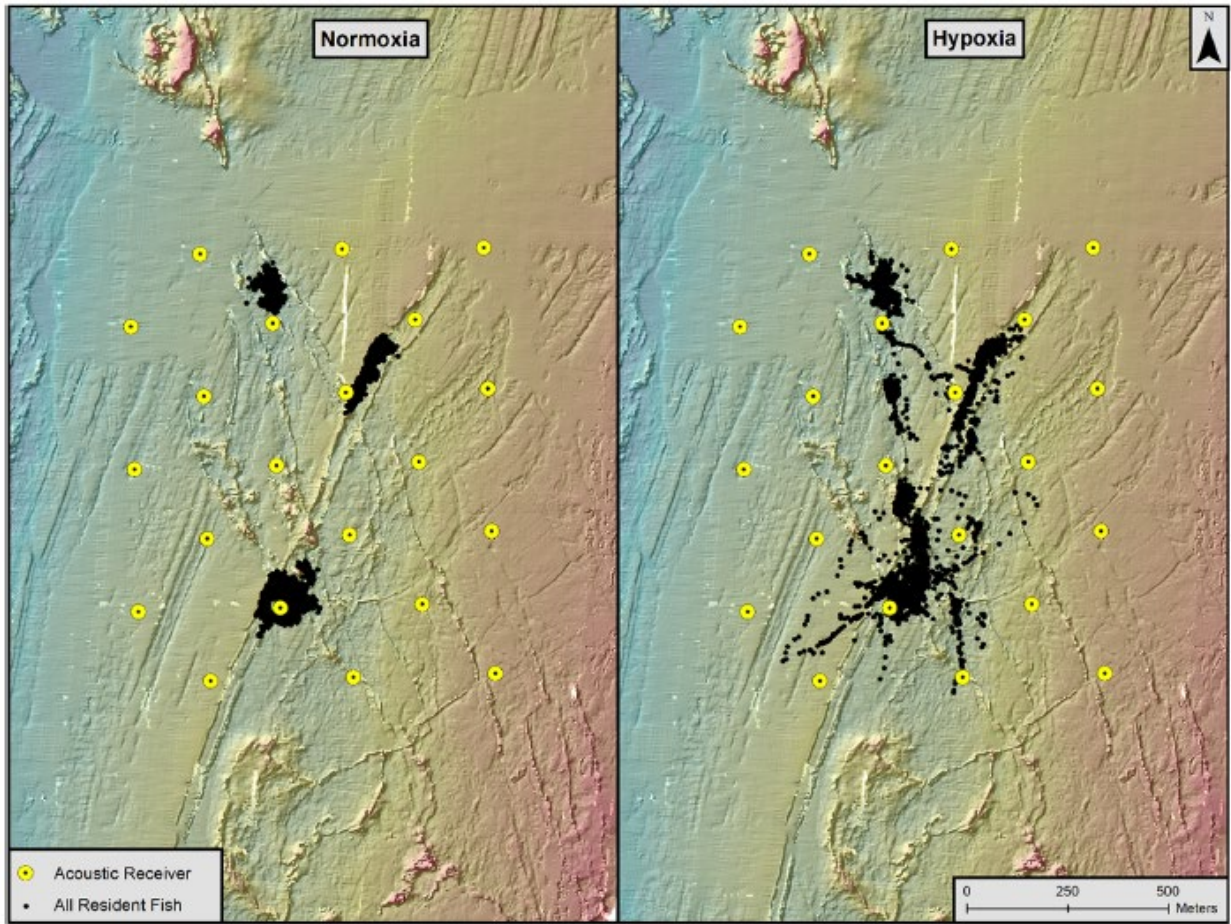


Fig. 4 Combined resident fish positions in VPS array area for two comparison periods: Normoxia and Hypoxia. Data included both daytime and nighttime for the two 11-day periods. Forays away from the core center were only observed during the hypoxic period

Table 3 Summary of model selection for fish acceleration (proxy for activity level) and depth occupied. Model selection for activity level (left) and depth occupied (right) includes the entire year's dataset (upper) and the shorter dataset comparing oxygen level (lower)

A) Seasonal model		
Model structure	Acceleration: $n=190,595$	Depth: $n=380,889$
	ΔAIC	ΔAIC
s(Hr x Month)+Month+re(Fish)	0	0
s(Hr x Month)+Month	1156	274,935
s(Hr)+Month+re(Fish)	11,894	19,545
s(Hr)+Month	13,085	287,202
s(Hr x Month)+re(Fish)	17,320	64,143
s(Hr x Month)	19,524	313,897
s(Hr)+re(Fish)	31,763	82,271
s(Hr)	33,844	326,280
Month+re(Fish)	23,783	33,659
Month	25,103	291,683
re(Fish)	44,461	94,205
1	46,721	330,311
B) Hypoxia and normoxia model		
Model structure	Acceleration: $n=11,097$	Depth: $n=22,299$
	ΔAIC	ΔAIC
s(Hr x Oxygen)+Oxygen+re(Fish)	0	0
s(Hr x Oxygen)+Oxygen	980	4588
s(Hr)+Oxygen+re(Fish)	519	1671
s(Hr)+Oxygen	1688	6135
s(Hr x Oxygen)+re(Fish)	2303	1297
s(Hr x Oxygen)	570	6318
s(Hr)+re(Fish)	1688	2560
s(Hr)	1057	7424
Oxygen+re(Fish)	2303	5915
Oxygen	1774	9348
re(Fish)	2495	5296
1	3473	10,006

Bold denotes the most parsimonious model

s variable was modeled as a cyclic spline, *re* variable modeled as a random effect, *Hr* hour of the day, *Month* month of the year, *Oxygen* Categorical definition of oxygen concentration, *Fish* fish tag ID

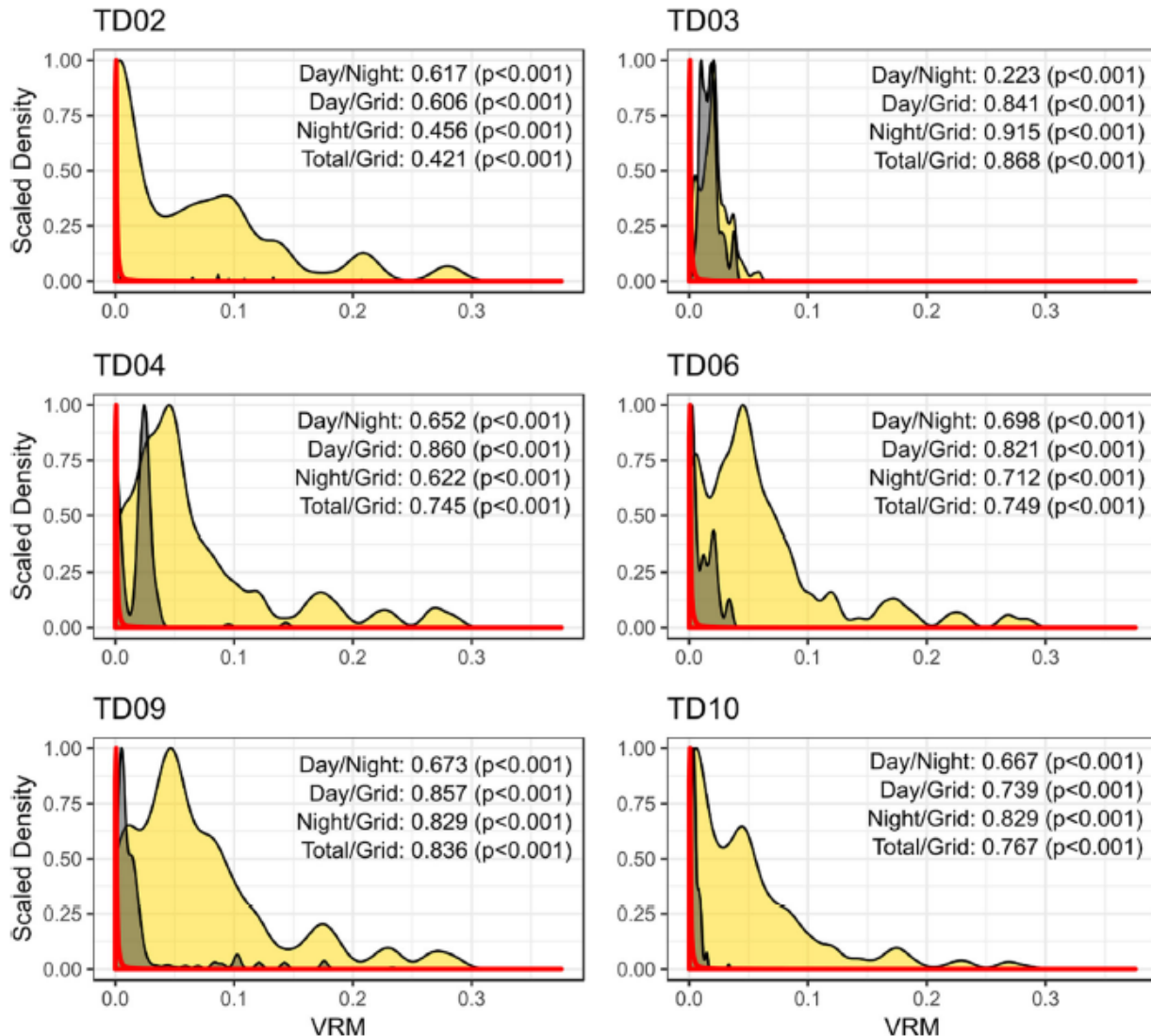


Fig. 5 Vector Ruggedness Measure (VRM) comparing resident Deacon Rockfish area usage to the VPS array area. Resident Deacon Rockfish daytime VRM (yellow), nighttime VRM (gray), and the entire VPS acoustic array area (red). Text denotes results of Kolmogorov-Smirnov tests comparing Deacon Rockfish usage between time periods and to the grid VRM values. Day-Daytime

usage, Night- Nighttime usage, VRM metric for the VPS array, Total-Usage of the tag during day and night combined. Most resident fish used more rugose habitat during the daytime period than during the nighttime period. All resident fish used more rugose habitat during the day, night, or in total compared to the average habitat rugosity for the area encompassed by the array

The best-fit models describing how both activity and depth varied between hypoxic and normoxic events included all variables and their interactions (Table 3). For activity, the model explained 27.2% of the variability in the data (Table S2). For depth, the model explained 36.3% of the variability in the data (Table S2). During normoxia, fish increased activity and moved to shallower depths during sunrise hours and decreased activity and descended to deeper depths at sunset (Fig. 8). This was in contrast to hypoxia conditions during which activity levels remained relatively stable, and changes in occupied depth over the course of the day were drastically reduced (Fig. 8).

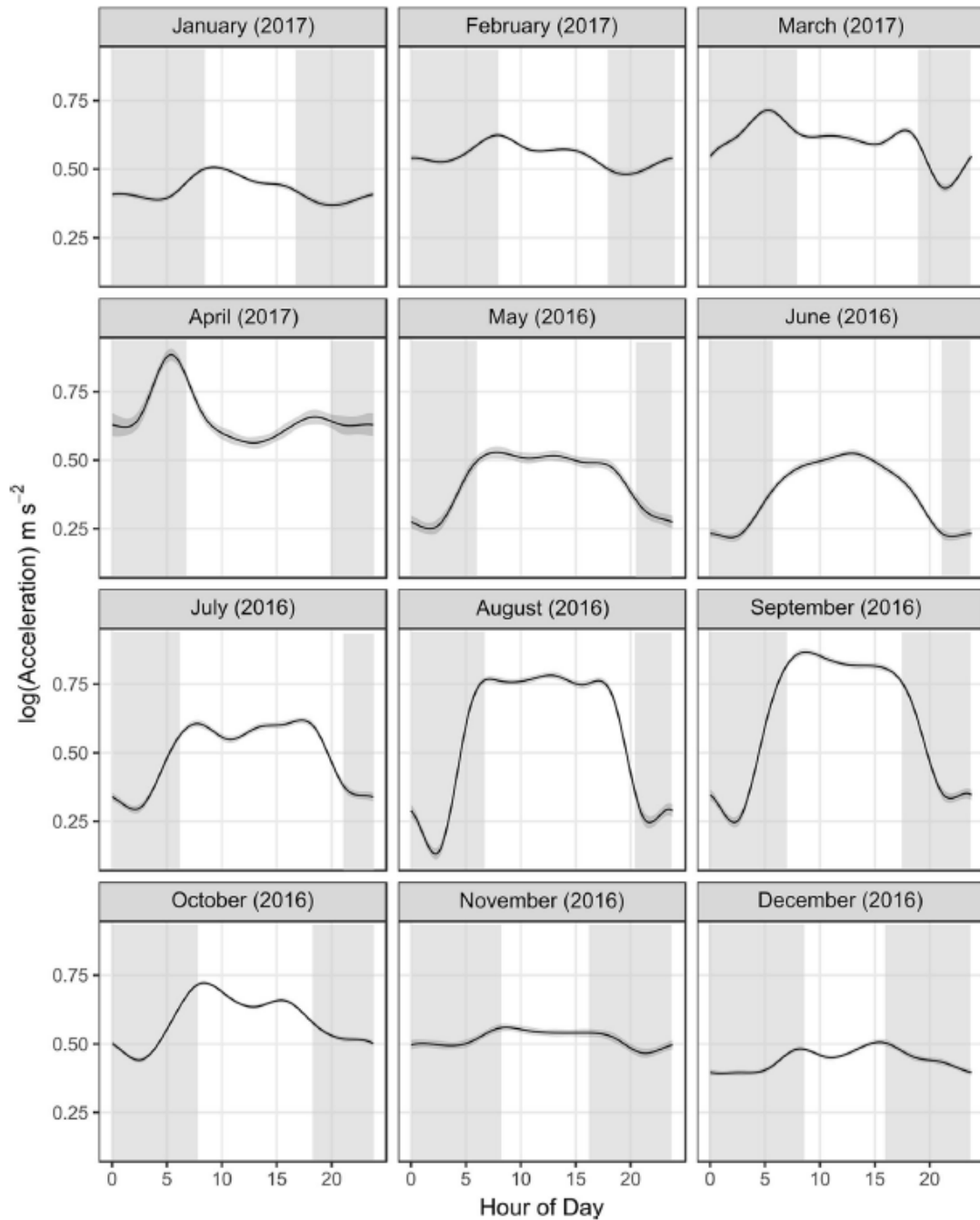


Fig. 6 Relative effect of month of the year on daily activity level of resident Deacon Rockfish. The black line within the gray shading (95% CI) is the smoothed response. Vertical gray bars denote the hours after sunset and before sunrise. Fish exhibited a

strong diurnal pattern of activity in the summer months, with relatively high levels of activity in the daytime and lower levels during the nighttime

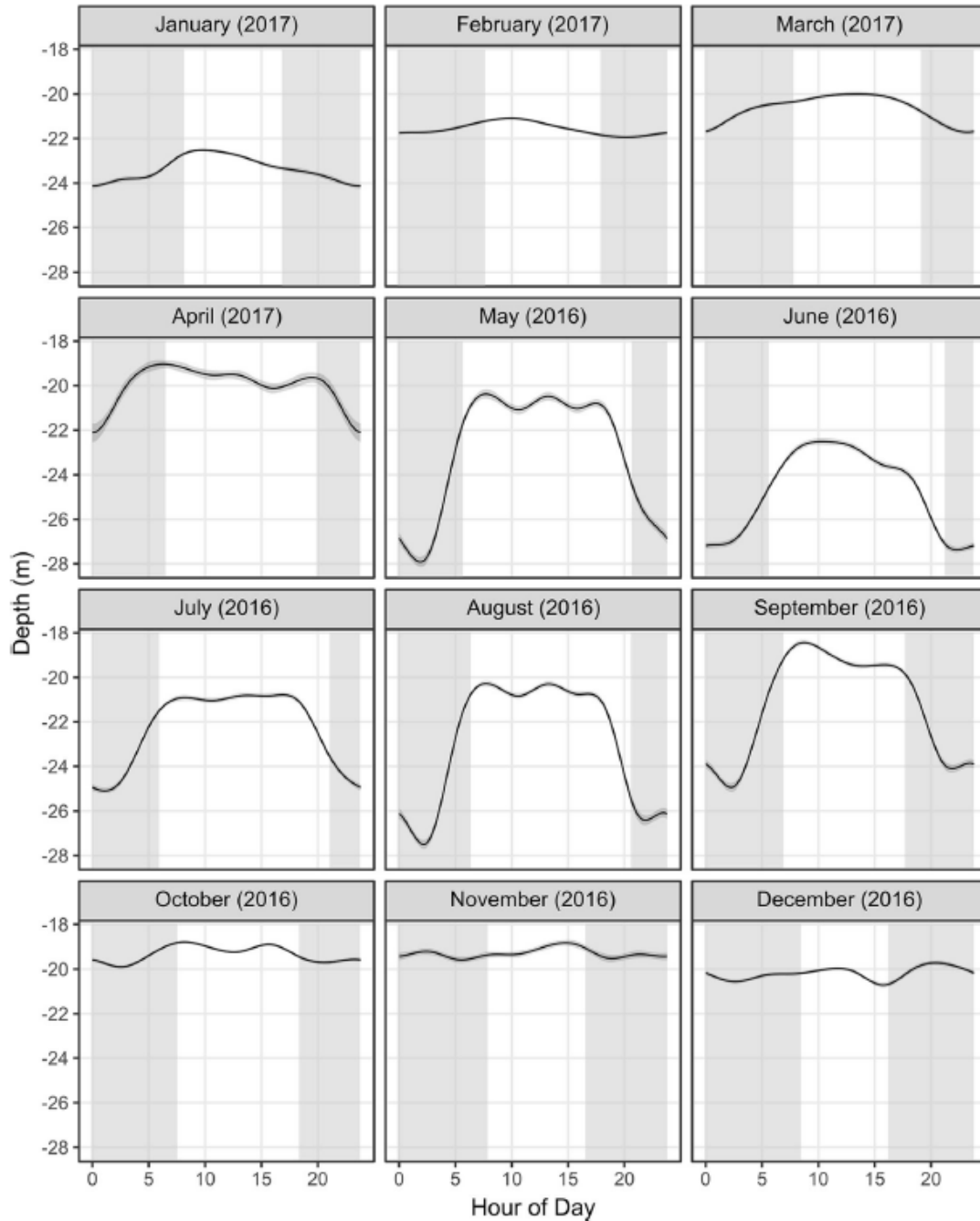


Fig. 7 Relative effect of month of the year on daily depth level occupied by resident Deacon Rockfish. The black line within the gray shading (95% CI) is the smoothed response. Vertical gray

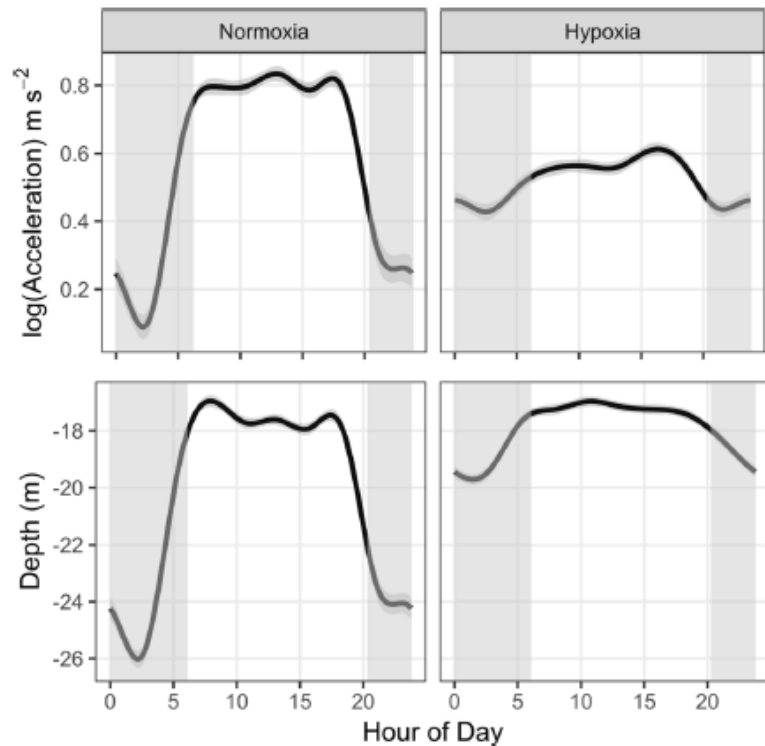
bars denote the hours after sunset and before sunrise. Fish occupied relatively deeper water depths during the nighttime in the summer months, than in the winter months

DISCUSSION

Overall, in our study, there is strong evidence of site residency for female Deacon Rockfish. The resident Deacon Rockfish displayed high site fidelity having relatively small core areas during the day, and even smaller core areas during the night. Activity and location in the water column displayed a strong diel cycle that shifted seasonally with more static activity levels and depth

usage during winter months. Hypoxic events altered daily behavior and depth occupancy as well as the way in which fish utilized the reef. Although we found strong evidence of residency, the three travelers detected leaving the array may indicate response to an environmental cue, a shift in core area beyond the scope of the array, and/or emigration from the nearshore reef area.

Fig. 8 Relative effect of oxygen concentration on activity level and depth usage for resident Deacon Rockfish. Activity (log acceleration (m s^{-2})) (upper panel) and depth (m) (lower panel) throughout a 24-h day for two 11-day time periods of normoxia and hypoxia. The black line within the gray shading (95% CI) is the smoothed response. Vertical gray bars denote the hours after sunset and before sunrise. During normoxia, fish exhibited a diurnal pattern of residing in deeper water during the nighttime with reduced activity. During hypoxia, resident fish remained at shallower depths and exhibited continuous activity with daytime activity lower than normoxic periods and nighttime levels higher than normoxic periods



High long-term survival and consistently high detection of resident fish during our 11-month study indicate that some Deacon Rockfish do not exhibit a seasonal migration away from nearshore reefs. This finding is supported by a concurrent study where researchers were able to collect Deacon Rockfish using hook and line gear, with small terminal tackle, throughout a 12-month period (Vaux et al. 2019). Further, underwater video observations in these areas routinely observed Deacon Rockfish during summer months (Rasmuson et al. 2020). In short, our work, in combination with other studies, indicates that at least a component of Deacon Rockfish do not likely undergo a seasonal migration away from nearshore reefs. However, since our study was restricted to large female Deacon Rockfish, we cannot exclude the hypothesis of an ontogenetic migration or a seasonal migration only exhibited by male rockfish or smaller females. Multiple behavior modes have been observed in the Australasian snapper (*Pagrus auratus*) and we cannot discount that possibility here (Egli and Babcock 2004). That said, in the nearshore, Vaux et al. (2019) observed both male and female Deacon Rockfish in all size classes, throughout the year, suggesting that at least a component of the smaller males and females remain in the nearshore. Thus, if there are different behavioral

modes, it is more likely a behavioral syndrome as opposed to a sex or length based trait (Bell and Sih 2007).

Given that Deacon Rockfish appear to remain in the nearshore throughout the year, why does the recreational fishing fleet not capture them during summer months? We hypothesize the diet of Deacon Rockfish may be the answer to this question. Food items ingested by Deacon Rockfish in Vaux et al. 2019 included gelatinous zoo-plankton and small planktonic crustaceans: the colonial tunicate *Pyrosoma atlanticum*, hydrozoan *Velella velella*, ctenophore *Pleurobrachia bachei*, brachyuran zoeae/megalopae, and pelagic amphipods. Feeding on gelatinous zooplankton requires specific visual abilities which allow some species of Rockfish (e.g., Blue Rockfish) to see and feed upon very small and/or transparent prey items (Hobson and Chess 1988; Hobson et al. 1996). In the closely related planktivorous Blue Rockfish, electroretinograms demonstrated that Blue Rockfish had low sensitivity to lower light levels than more nocturnally active rockfish (Reilly and Thompson 2007). Thus, the cryptic Blue and Deacon Rockfish may have similar unique visual capabilities making them well adapted to daytime light levels and to feeding on small, clear planktonic prey (Green et al. 2014). Accordingly, we hypothesize that Deacon Rockfish may be resistant to standard fishing techniques because recreational terminal gear typically does not mimic the preferred summer prey of Deacon Rockfish. These results suggest that periods of relatively low catch of Deacon Rockfish in the recreational fishery may not be indicative of a small population size, but rather a seasonal shift in diet and/or behavior. Furthermore, this dietary shift may provide some resistance to overfishing (under current effort levels), for which the high site fidelity and small home ranges of Deacon Rockfish might otherwise make them vulnerable (Patrick et al. 2010).

Although methods for calculating home range vary between studies, mean home ranges were considerably smaller for resident Deacon Rockfish (0.0049 km²) than other semi-pelagic species like Blue Rockfish in kelp habitat off Central California (0.23 km²) (Green et al. 2014), and Black Rockfish inhabiting the same reef complex in Oregon (0.55 km²) (Parker et al. 2007). Deacon Rockfish utilized small, consistent core areas with mean nighttime core areas being approximately 75% smaller than the daytime core area. Additionally, all fish displayed a distinct behavior trend of switching away from utilizing more rugose habitat during the day, to utilizing less rugose habitat at night. Pairing this observation with the nighttime video surveys where Deacon Rockfish have been observed laying directly on flat bedrock (Rasmuson unpublished data) indicates a shift away from more rugose habitat during the day to a flat bedrock sleeping environment. Why sleep out in the open directly on the bottom? In short, we are unsure. At night, Deacon Rockfish adopt much darker coloration so it is possible that laying near or on the bottom provides camouflage from visual predators. However, one would then wonder why lay in the open rather than in cracks like other rockfishes. Alternatively, they may stop their activity

at night because as a visual predator of clear planktonic organisms, they may be unable to see their prey. Ultimately, this remains an open question, which may be answered by further research.

Off Oregon, coastal circulation has two primary periods: the period from the fall transition to the spring transition, hereafter winter, and the period from the spring transition to the fall transition, hereafter summer (Huyer 1979; Strub and James 1988). Characteristically during the summer, conditions alternate between periods of upwelling and downwelling on the continental shelf, though in the nearshore, where this study was conducted, these effects are strongly muted (Austin and Lentz 2002). In the wintertime, the conditions are characteristically downwelling favorable and large storms systematically influence circulation. In 2016, the year our study started, the spring transition occurred on March 27 and the fall transition occurred on September 29, whereas in 2017 the spring transition occurred on April 26 (<http://damp.coas.oregonstate.edu/windstress/index.html>). It seems likely that the change from heterogeneous acceleration and depth during summer relatively to the more homogenous acceleration and depths of winter is associated with the spring and fall transitions. This likely indicates that the seasonal behaviors we observed are due to prevailing changes in circulation. Unfortunately, the rough winter storms off Oregon during precluded us from leaving our CTD mooring in the water and associating our observed behaviors with abiotic factors.

Tagged fish showed greatly reduced activity in their nighttime core areas, but this pattern was less evident during the wintertime. Some potential hypotheses for this wintertime behavior are that the fish receive less rest during storms because high wave action creates turbulence in nearshore reef areas, or that the fish change to nightly foraging activity during these months. Undoubtedly, other hypotheses exist. The seasonal pattern of high levels of daytime, off-bottom activity, followed by a definitive period of rest observed in the summer months aligns with Green et al. (2014), indicating nocturnal sheltering for Blue Rockfish off Central California. Although Deacon Rockfish had not been established as a separate species at the time of Green's study, the authors confirmed they were already visually differentiating between the two cryptic species and that tagged specimens were all Blue Rockfish (R. Starr, pers comm). The diurnal behavior of Deacon Rockfish is in contrast to Black Rockfish from the Seal Rocks Reef area, which demonstrate mixed diurnal/nocturnal movement patterns (Parker et al. 2008).

All resident Deacon Rockfish exhibited a response to hypoxic conditions, which interrupted 5 months of otherwise consistent movement patterns. The long-duration forays, well away from core activity areas, were atypical as were the depth and activity patterns for that time of year; fish were moderately active at shallower depths, with no high-level diurnal activity and no nighttime on-bottom rest. Our analyses suggest oxygen and temperature differed significantly between the hypoxic and normoxic time periods. However, on average, temperature only differed by 0.01

°C between the two time periods. Accordingly, although temperature is statistically different between the time periods, we hypothesize that the difference is not ecologically relevant, but rather, the larger difference in oxygen levels between the time periods is a better explanation for the observed behavioral shifts. Deacon Rockfish response to seasonal hypoxia differed considerably from the responses of more benthic rockfish in Oregon. For example, Copper Rockfish reduce their home ranges and activity in response to hypoxia, while Quillback Rockfish showed no change (Rankin et al. 2013).

Hypoxia may also result in increased respiration rate in fish, which is a physiological response to decreased oxygen availability. Movement patterns exhibited by resident fish suggest fish increased their baseline activity to compensate for respiratory stress, and moved beyond their core activity areas towards the surface, to seek areas with higher oxygen levels (Nakanishi and Itazawa 1974; Furse et al. 1996; Kim et al. 1995; Palsson et al. 2008). The independent and irregular forays were likely not prey-seeking behavior, as resident fish maintained a high level of site fidelity, as well as habitat and school fidelity through the rest of the summer season, during which variable upwelling/ downwelling/relaxation patterns intermittently interject pelagic planktonic prey into the system (Hobson and Chess 1988; Checkley Jr and Barth 2009). Additionally unlikely is reproductive activity, which takes place in late summer/fall with parturition in the wintertime (Hannah et al. 2015).

Although our sample size was necessarily small to accommodate the high numbers of synctag detections needed for high-resolution position data, detection numbers and position data for tagged fish was excellent, as mid-water schooling behavior of this semi-pelagic species benefits acoustic transmission. Detection rates can be problematic for more benthic rockfish in high-relief habitat, as habitat can block or distort the acoustic transmission. The high-resolution inner VPS array, combined with the perimeter fence, and fish tags equipped with accelerometer/depth sensors, provided additional certainty about the fate of fish that remained inside or left the array. A larger study in southern Oregon, using similar methods, but tagging both Deacon and Blue Rockfish inhabiting the same area, could shed light on differences in the cryptic pairs' movements in various habitats including un-fished offshore reefs, which may act as refuges for older, more fecund fish found in rockfish conservation areas in Oregon.

ACKNOWLEDGMENTS

This project would not have been possible without the early support of R.W. Hannah and D.S. Fox. We thank C.D. Good, C.T. Heath, and B.T. Rodomsky for providing fisheries data. R.C. Anderson, G. Krutzikowsky, J.S. Malvitch, and D.W. Wagman provided assistance at sea. We thank D.S. Fox, M. Sommer, and S.D. Groth for an early review of the manuscript. Our sincerest appreciation to Capt. David DeBelloy, and the crew of the CPFV Enterprise, who provided expert logistical

support and a superior vessel with which to conduct this work. This research did not receive any specific grant from funding agencies in the public, commercial, or not-for-profit sectors.

REFERENCES

- Andrews KS, Tolmieri N, Williams GD, Samhuri JF, Harvey CJ, Levin PS (2011) Comparison of fine-scale acoustic monitoring systems using home range size of a demersal fish. *Mar Biol* 158:2377–2387. <https://doi.org/10.1007/s00227-011-1724-5>
- Austin JA, Lentz SJ (2002) The inner shelf response to wind-driven upwelling and downwelling. *J Phys Oceanogr* 32: 2171–2193
- Barnett A, Abrantes KG, Stevens JD, Semmens JM (2011) Site fidelity and sex-specific migration in a mobile apex predator: implication for conservation and ecosystem dynamics. *Anim Behav* 81:1039–1048
- Bell AM, Sih A (2007) Exposure to predation generates personality in three-spined sticklebacks (*Gasterosteus aculeatus*). *Ecol Lett* 10:828–834
- Berger AM, Arnold L, Rodomsky BT (2015) Status of Kelp Greenling (*Hexagrammos decagrammus*) along the Oregon Coast in 2015 Pacific Fishery Management Council. Portland, OR: 1–207 <http://www.pco.uncil.org/groundfish/stock-assessments/>
- Berger AM, Goethel DR, Lynch PD, Quinn T, Mormede S, McKenzie J, Dunn A (2017) Space oddity: the mission for spatial integration. *Can J Fish Aquat Sci* 74(11):1698–1716. <https://doi.org/10.1139/cjfas-2017-0150>
- Beyer HL (2015) Geospatial Modelling Environment (Software Version 0.7.4.0). <http://www.spatialecology.com/gme/>
- Bryars S, Rogers P, Huvneers C, Payne N, Smith I, McDonald B (2012) Small home range in southern Australia's largest resident reef fish, the western blue groper (*Acherodus gouldii*): implications for adequacy of no-take marine protected areas. *Mar Freshw Res* 63:552–563
- Burnham KP, Anderson DR (2004) Multimodel inference: understanding AIC and BIC in model selection. *Sociol Methods Res* 33(2):261–304. <https://doi.org/10.1177/0049124104268644>
- Buston PM (2004) Territory inheritance in clownfish. *Proc R Soc Lond B Suppl* 4:252–254
- Checkley DM Jr, Barth JA (2009) Patterns and processes in the California Current System. *Prog Oceanogr* 83(1–4):49–64. <https://doi.org/10.1016/j.pocean.2009.07.028>
- Core Team R (2018) R: A language and environment for statistical computing. R Foundation for Statistical Computing, Vienna, Austria <https://www.r-project.org/>
- Crossin GT, Heupel MR, Holbrook CM, Hussey NE, Lowerre-Barbieri SK, Nguyen VM, Raby GD, Cooke SJ (2017) Acoustic telemetry and fisheries management. *Ecol Appl* 27:1031–1049
- Dance MA, Moutlon DL, Furey NB, Rooker JR (2016) Does transmitter placement or species affect detection efficiency of tagged animal in biotelemetry research? *Fish Res* 183:80–85. <https://doi.org/10.1016/j.fishres.2016.05.009>
- Diaz RJ, Rosenberg R (1995) Marine benthic hypoxia: a review of its ecological effects and the behavioural responses of benthic macrofauna. *Oceanogr Mar Biol Annu Rev* 33:245–303
- Dick EJ, Berger A, Bizzaro J, Bosley K, Cope J, Field J, Gilbert-Horvath L, Grunloh N, Ivens-Duran M, Miller R, Privitera-Johnson K, Rodomsky BT (2017) The combined status of blue and

- deacon rockfishes in U.S. waters off California and Oregon in 2017. Pacific Fishery Management Council, Portland, OR. <http://www.pcouncil.org/groundfish/stock-assessments/>
- Dypvik E, Røstad A, Kaartvedt S (2012) Seasonal variations in vertical migration of glacier lanternfish, *Benthosema glaciale*. Mar Biol 159:1673–1683
- Egli DP, Babcock RC (2004) Ultrasonic tracking reveals multiple behavioural modes of snapper (*Pagrus auratus*) in a temperate no-take marine reserve. ICES J Mar Sci 61:1137–1143
- Engelhard GH, van der Kooji J, Bell ED, Pinnegar JK, Blanchard JL, Mackinson S, Righton DA (2008) Fishing mortality versus natural predation on diurnally migrating sandeels *Ammodytes marinus*. Mar Ecol Prog Ser 369:213–227
- ESRI (2015) ArcGIS Desktop: Release 10.3 Redlands, CA: Environmental Systems Research Institute
- Frale B, Wagman DW, Frierson T, Aguilar A, Sidlauskas BL (2015) A new species of *Sebastes* (Scorpaeniformes: Sebastidae) from the northeastern Pacific, with a redescription of the Blue Rockfish, *S. mystinus* (Jordan and Gilbert, 1881). Fish Bull 113:355–377. <https://doi.org/10.7755/FB.113.4.1>
- Furse JB, Davis LJ, Bull LA (1996) Habitat use and movements of largemouth bass associated with changes in dissolved oxygen and hydrology in Kissimmee River, Florida. Proc Annu Conf Southeast Assoc Fish and Wildl Agencies 50:12–25
- Galuardi B, Royer F, Golet W, Logan J, Neilson M, Lutcavage M (2010) Complex migration routes of Atlantic Bluefin tuna (*Thunnus thynnus*) question current population structure paradigm. Can J Fish Aquat Sci 67. <https://doi.org/10.1139/F10-033>
- Grantham BA, Chan F, Nielsen KJ, Fox DS, Barth JA, Huyer A, Lubchenco J, Menge BA (2004) Upwelling-driven nearshore hypoxia signals ecosystem and oceanographic changes in the northeast Pacific. Nature 429:749–754. <https://doi.org/10.1038/nature02605>
- Gray JS, Wu RS, Or YY (2002) Effects of hypoxia and organic enrichment on the coastal marine environment. Mar Ecol Prog Ser 238:249–279. <https://doi.org/10.3354/meps238249>
- Green KM, Greenley AP, Starr RM (2014) Movements of Blue Rockfish (*Sebastes mystinus*) off central California with comparisons to similar species. PLoS One 9(6):e98976. <https://doi.org/10.1371/journal.pone.0098976>
- Hannah RW, Blume MTO (2016) Variation in the effective range of a stereo-video lander in relation to near-seafloor water clarity, ambient light and fish length. Mar Coast Fish 8:62–69. <https://doi.org/10.1080/19425120.2015.1135222>
- Hannah RW, Rankin PS (2011) Site fidelity and movement of eight species of Pacific Rockfish at a high-relief rocky reef on the Oregon coast. N Amer J of Fish Mgt 31:483–494. <https://doi.org/10.1080/02755947.2011.591239>
- Hannah RW, Parker SJ, Matteson KM (2008) Escaping the surface: the effect of capture depth on submergence success of surface-released Pacific rockfish. North Am J Fish Manage 28(3):694–700. <https://doi.org/10.1577/M06-291.1>
- Hannah RW, Rankin PS, Blume MTO (2012) Use of a novel cage system to measure post recompression survival of northeast Pacific rockfish. Mar Coast Fish 4:46–56. <https://doi.org/10.1080/19425120.2012.655849>

- Hannah RW, Wagman DW, Kautzi LA (2015) Cryptic speciation in the Blue Rockfish (*Sebastes mystinus*): age, growth and female maturity of the Blue-Sided Rockfish, a newly identified species, from Oregon waters. Oregon Dept Fish Wildl, Information Rept Ser Fish 2015(01):24
- Hansen LP, Jonsson N, Jonsson B (1993) Oceanic migration in homing Atlantic salmon. Anim Behav 45:927–941
- Hartig F (2020) DHARMA: Residual diagnostics for hierarchical (multi-level/mixed) regression models. R package version 0 (3):3.0
- Hays GC, Ferreira LC, Sequeira AMM, Meekan MG, others (2016) Key questions in marine megafauna movement ecology. Trends Ecol Evol 31:463–475
- Hobson RD (1972) Surface roughness in topography: quantitative approach. In: Chorley RJ (ed) Spatial analysis in geomorphology. Harper and Row, New York, New York, USA, pp 221–245
- Hobson ES, Chess JR (1988) Trophic relations of the blue rockfish, *Sebastes mystinus*, in a coastal upwelling system off northern California. Calif Dept Fish Game Fish Bull 86(4): 715–743
- Hobson ES, Chess JR, Howard DF (1996) Zooplankters consumed by Blue Rockfish during brief access to a current off California's Sonoma coast. Calif Dept Fish Game Fish Bull 82:87–92
- Hopkins TD, Eldridge MB, Cech JJ (1995) Metabolic costs of viviparity in yellowtail rockfish, *Sebastes flavidus*. Environ Biol Fish 43:77–84. <https://doi.org/10.1007/BF00001819>
- Huyer A, EJCS, Smith RL (1979) The spring transition in currents over the Oregon continental shelf. J Geophys Res 84:6995–7011
- Kim IN, Chang YJ, Kwon JY (1995) The patterns of oxygen consumption in six species of marine fish. J Korean Fish Soc 28:373–381
- Kraus R, Wells RJD, Rooker JR (2011) Horizontal movement of Atlantic blue marlin (*Makaira nigricans*) in the Gulf of Mexico. Mar Biol 158:699–713
- Leggett WC (1977) The ecology of fish migrations. Annu Rev Ecol Syst 8:285–308
- Nakanishi T, Itazawa Y (1974) Effects of hypoxia on the breathing rate, heart rate and rate of oxygen consumption in fishes. Rep Fish Res Lab Kyushu Univ
- Ogburn MB, Harrison A, Whoriskey FG, Cooke SJ, Flemming JEM, Torres LG (2017) Addressing challenges in the application of animal movement ecology to aquatic conservation and management. Front Mar Sci 16. <https://doi.org/10.3389/fmars.2017.00070>
- Palsson WA, Pacunski RE, Parra TR, Beam J (2008) The effects of hypoxia on marine fish populations in southern Hood Canal, Washington. Am Fish Soc Symp 64:255–280
- Parker SJ, Rankin PS, Olson JM, Hannah RW (2007) Movement patterns of black rockfish (*Sebastes melanops*) in Oregon coastal waters. In: Heifetz J, Di Cosimo J, Gharrett AJ, Love MS, O'Connell VM, Stanley RD (eds) Biology, assessment, and management of North Pacific rockfishes. Alaska Sea Grant College Program, AK-SG-7-01, pp 39–58 <https://seagrant.uaf.edu/bookstore/pubs/item.php?id=11233>
- Parker SJ, Olson JM, Rankin PS, Malvitch JS (2008) Patterns in vertical movements of black rockfish *Sebastes melanops*. Aquat Biol 2:57–65. <https://doi.org/10.3354/ab00036>
- Patrick WS, Spencer P, Link J, Cope J, Field J, Kobayashi D, Lawson P, Gedamke T, Cortes E, Ormseth O, Bigelow K, Overholtz W (2010) Using productivity and susceptibility indices to assess the vulnerability of United States fish stocks to overfishing. Fish Bull 108:305–322
- Peer AC, Miller TJ (2014) Climate change, migration phenology, and fisheries management interact with unanticipated consequences. N American J Fish Man 34:94–110

- Pihl L, Baden SP, Diaz RJ (1991) Effects of periodic hypoxia on distribution of demersal fish and crustaceans. *Mar Biol* 108: 349–360. <https://doi.org/10.1007/BF01313644>
- Pinheiro JC, Bates DM (2000) Mixed effects models in S and S-PLUS. Springer, New York, New York. <https://doi.org/10.1007/BF01313644>
- Pittman, S.J. and McAlpine, C.A. (2003) Movements of marine fish and decapod crustaceans: process, theory and application. In: *Advances in marine biology*, Vol. 44 (eds. A.J. Southward, P.A. Tyler, L.A. Fuiman and C.M. Young), Academic Press, Elsevier, London, U.K., pp. 205–294
- Rankin PS, Hannah RW, Blume MTO (2013) Effect of hypoxia on rockfish movements: implications for understanding the roles of temperature, toxins and site fidelity. *Mar Ecol Prog Ser* 492:223–234. <https://doi.org/10.3354/meps10479>
- Rankin PS, Hannah RW, Blume MTO, Miller-Morgan JT, Heidel JR (2016) Delayed effects of capture-induced barotrauma on physical condition and behavioral competency of recompressed Yelloweye Rockfish, *Sebastes ruberrimus*. *Fish Res* 186:258–268. <https://doi.org/10.1016/j.fishres.2016.09.004>
- Rasmuson LK, Lawrence KA, Krutzikowsky GK, Watson JL, Aylesworth L, Hannah RW, Rodomsky BT, Huntington B, Matteson K, Easton RR (2020) Nine years of video landers at the Oregon Department of Fish & Wildlife’s Marine Resources Program. *Oregon Dept Fish Wildl, Information Rept Ser Fish* 2020(01):
- Reilly CRL, Thompson SH (2007) Temperature effects on low-light vision in juvenile rockfish (Genus *Sebastes*) and consequences for habitat utilization. *J Comp Physiol A* 193:943–953. <https://doi.org/10.1007/s00359-007-0247-5>
- Sappington JM, Longshore KM, Thomson DB (2007) Quantifying landscape ruggedness for animal habitat analysis: a case study using Bighorn Sheep in the Mojave Desert. *J Wildl Manag* 71:1419–1426. <https://doi.org/10.2193/2005-723>
- Sbragaglia V, Nuñez JD, Dominoni D, Coco S, Fanelli E, Azzurro E, Marini S, Nogueras M, Ponti M, del Rio Fernandez J, Aguzzi J (2019) Annual rhythms of temporal niche partitioning in the Sparidae family are correlated to different environmental variables. *Scientific Reports* 9: <https://doi.org/10.1038/s41598-018-37954-0>
- Stanley RD, Kieser RK, Leaman BM, Cooke KG (1999) Diel vertical migration by yellowtail rockfish, *Sebastes flavidus*, and its impact on acoustic biomass estimation. *Fish Bull* 97: 322–331
- Strub J, James C (1988) Atmospheric conditions during the spring and fall transitions in the coastal ocean off Western United States. *J Geophys Res* 93:15561–15584
- Tolimieri N, Andrews K, Williams G, Katz S, Levin PS (2009) Home range size and patterns of space use by lingcod, copper rockfish and quillback rockfish in relation to diel and tidal cycles. *Mar Ecol Prog Ser* 380:229–243
- van Ginneken V, Antonissen E, Müller UK, Booms R, Eding E, Verreth J, van den Thillart G (2005) Eel migration to the Sargasso: remarkably high swimming efficiency and low energy costs. *J Exp Biol* 208:1329–1335
- Vaux F, Rasmuson LK, Kautzi LA, Rankin PR, Blume MTO, Lawrence KA, Bohn S, O’Malley KG (2019) Sex matters: otolith shape and genomic variation in deacon rockfish (*Sebastes diaconus*). *Ecol Evol* 9:13153–13173. <https://doi.org/10.1002/ece3.5763>

- Wood SN (2004) Stable and efficient multiple smoothing parameter estimation for generalized additive models. *J Am Stat Assoc* 99:673 – 686. <https://doi.org/10.1198/016214504000000980>
- Wood SN (2011) Fast stable restricted maximum likelihood and marginal likelihood estimation of semiparametric generalized linear models. *J R Stat Soc Ser B* 73(1):3–36. <https://doi.org/10.1111/j.1467-9868.2010.00749.x>
- Zuur AF, Ieno EN, Walker NJ, Saveliev AA, Smith GM (2009) *Mixed effects models and extensions in ecology with R*. Springer, New York, New York
- Zuur AF, Ieno EN, Elphick CS (2010) A protocol for data exploration to avoid common statistical problems. *Methods Ecol Evol* 1(1):3–14. <https://doi.org/10.1111/j.2041-210X.2009.00001.x>

6: SUSCEPTIBILITY OF FIVE SPECIES OF ROCKFISH (*SEBASTES SPP.*) TO DIFFERENT SURVEY GEARS INFERRED FROM HIGH RESOLUTION BEHAVIORAL DATA.

Previously published as an ODFW Science Bulletin Number 2021-05.

ABSTRACT

Fisheries independent surveys are an important data input for stock assessments. However, these surveys are expensive to conduct and require precise, well thought out planning to be effective. Although the amount of money allocated to a survey is often dictated by factors beyond the control of the survey development team, surveys must incorporate their understanding of the biology of the focal species or species group into the survey design. Acoustic telemetry data can provide a high-resolution dataset to answer some of these questions. In this study, we reanalyze past acoustic telemetry studies on Black Rockfish (*Sebastes melanops*), Copper Rockfish (*Sebastes caurinus*), Deacon Rockfish (*Sebastes diaconus*), Quillback Rockfish (*Sebastes maliger*) and Yelloweye Rockfish (*Sebastes ruberrimus*) in order to apply these data to future survey development. We combined the telemetry data with multibeam bathymetry data to 1) understand how the height off bottom of each species changed throughout a day and 2) simply define the habitat utilized by each species. We found, on average, Black, Deacon and Yelloweye Rockfish were all more than 1 m off bottom, whereas Copper and Quillback remained on, or near the bottom throughout the day. Deacon Rockfish were associated with the most rugose bottom, followed by Yelloweye Rockfish. Black, Copper and Quillback Rockfish all utilized low relief habitats. In general, we hypothesize that Black and Deacon Rockfish are good candidates for survey by hydroacoustics, whereas, Copper and Quillback Rockfish appear to be good candidates for survey by bottom trawl. However, our study was only conducted at a single nearshore reef and as such the results should be considered experimental and need validation. Surprisingly, due to the habitat they reside in, Yelloweye Rockfish were available to hydroacoustics, and likely not available to bottom trawl. However, Yelloweye Rockfish have variable behaviors, as reported by the original work, and as such, we are wary to suggest that hydroacoustics are an appropriate survey tool. We do, however, propose that Yelloweye Rockfish potentially contribute to backscattering values of acoustic surveys conducted for midwater rockfish, and that bottom trawls are likely not an effective survey tool for Yelloweye Rockfish.

INTRODUCTION

Groundfish on the West Coast of the continental United States are co-managed by state and federal partners through the collaborative Pacific Fisheries Management Council. One of the primary roles of the Council is to conduct stock assessments of groundfish stocks, which, in turn, are used to provide predictions of stock status. As with all models, these stock

assessments are only as good as the data going into them. In nearshore groundfish stock assessment reports, the authors routinely point out the need for fisheries independent surveys. A fisheries independent survey is a survey of the resource that is not affected or directly influenced by commercial or recreational fisheries.

On the Oregon coast, nearshore rockfish are an important component of the recreational and commercial fisheries. Of these nearshore rockfish, the semi-pelagic Black Rockfish (*Sebastes melanops*) are likely the most economically important recreational rockfish species caught (Research Group, LLC 2015). While semi-pelagic species are not as important to the nearshore commercial fleet, together with high value more colorful benthic rockfish species, they do represent an important component of the fishery. All nearshore groundfish species suffer from a lack of fisheries independent survey data (Rodomsky et al. 2020). Additionally, Yelloweye Rockfish are classified as overfished in Oregon's waters (Gertseva and Cope 2017). Their overfished status results in a reduction of catch quotas, which ultimately constrains the ability of the commercial and recreational fleets to utilize other resources.

While the need for fisheries independent surveys has been acknowledged for quite some time, the development and implementation of fisheries independent surveys is a complex process (Cope et al. 2015; Dick et al. 2017). During survey development one must balance budgetary and time constraints with constraints imparted by the biology of the focal species (Rotherham et al. 2007; Dennis et al. 2015). As survey costs continue to increase, and budgets tend to lag behind inflation, the need to create surveys that are cost effective is more important than ever. An effective way to reduce survey costs is to use technology that allows surveys to be conducted aboard smaller vessels, with fewer scientists going to sea (Meyer-Gutbrod et al. 2012). However, any decisions about survey tools must be made based on the biology of the animal (Stoner et al. 2008; DuFour et al. 2018). For example, although benthic bottom trawls are a common and effective survey tool, they are not, effective for surveying pelagic fish.

A fish's behavior, specifically it's average height above the bottom (hereafter referred to as height off bottom), strongly influences the availability of the fish to different survey gears (Arreguin-Sanchez 1996; Trenkel et al. 2004; Kotwicki et al. 2015). Nearshore rockfish are an extremely diverse group of fish and are known to occupy a large variety of heights off bottom. However, our knowledge of fish height off bottom is considered in a categorical sense (benthic, semi-pelagic etc.) and we do not have numerical values to define the height (Love et al. 2002). Just as height off bottom influences the catchability of a species, the habitat occupied by a species influences which gear types are suitable for surveying that species (Love 2006; Rooper 2010). Habitats where trawls cannot be deployed (untrawlable habitats) are a major example of this; an issue that strongly affects the ability to survey rockfish (Jagiello et al. 2003; Zimmermann 2003; Baker et al. 2019).

In this study we reanalyze high resolution acoustic telemetry studies conducted on Black Rockfish (*Sebastes melanops*), Copper Rockfish (*Sebastes caurinus*), Deacon Rockfish (*Sebastes diaconus*), Quillback Rockfish (*Sebastes maliger*) and Yelloweye Rockfish (*Sebastes ruberrimus*). For each species, we calculated the average height off bottom of that species throughout the day. We also calculated habitat metrics to assess what types of habitats each species was using.

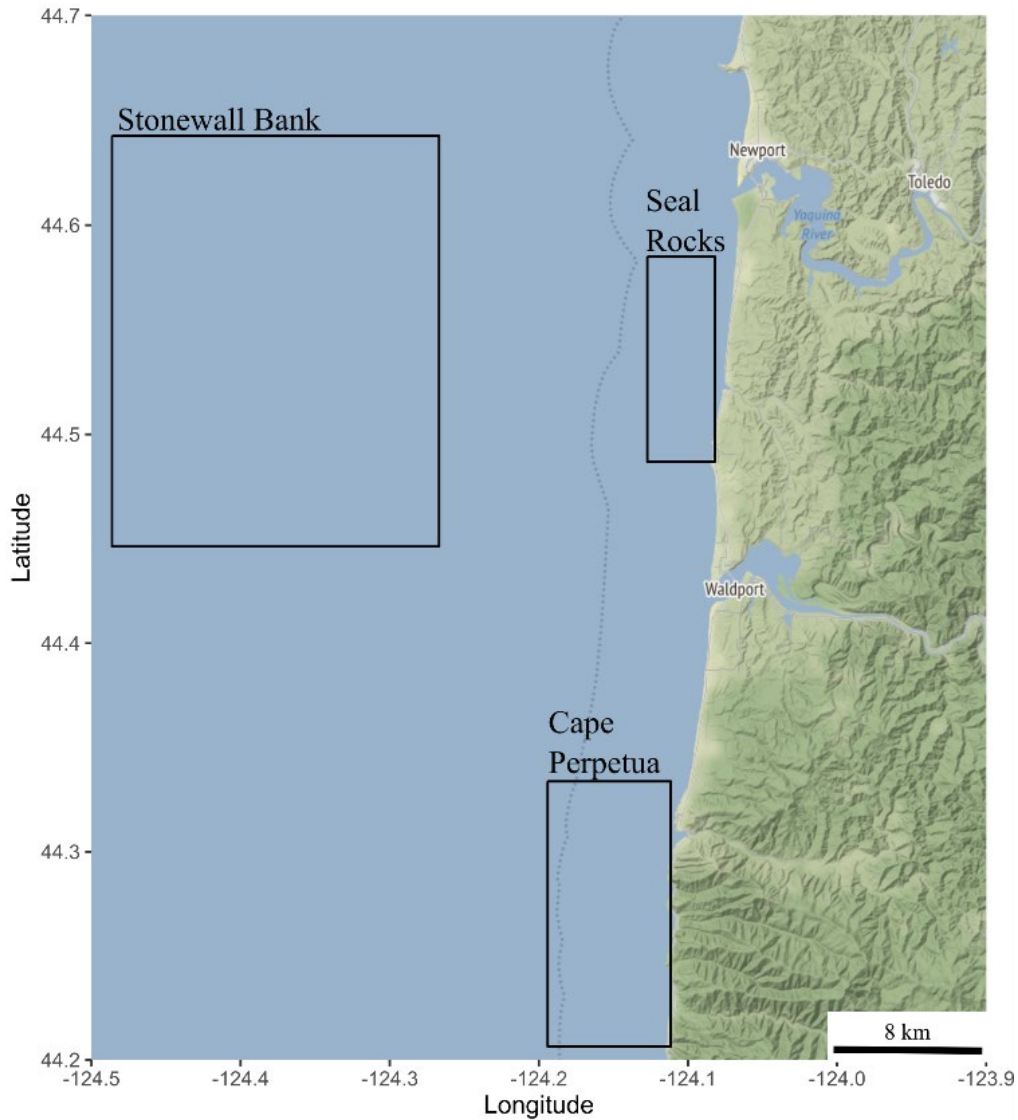


Fig. 1. Overview map of study areas. See table 1 for which fish species were tagged during each study period at each of the three reefs.

METHODS

Acoustic telemetry data were collected for five species of rockfish tagged in Oregon over a 12-year period (Table 1, Fig 1). Study areas were located on the central Oregon coast, but focal reefs differed between species. For more information on the original studies and their design,

we refer the reader back to those studies (citations available in Table 1). We utilized the acoustic telemetry data from these studies to characterize fish location (latitude, longitude) and height off bottom. All analyses and mapping were conducted in R 4.0.2 Taking Off Again (R Core Team 2020). Bathymetry data at Seal Rocks and Stonewall Bank had a 2 m resolution and data at Cape Perpetua had a 4 m resolution (Goldfinger et al. 2014).

Location records were used for all fish that had a horizontal position error (HPE) of < 25 m. These data points were then associated with raster values from multibeam bathymetry, in order to extract the bottom depth for each fish location. We then subtracted the fish's depth from the associated bathymetric depth to determine the relative height off bottom of the fish. Data were corrected for tidal signals by correcting the water column thickness for every 5 minute interval. We also calculated the slope and roughness using the Terrain function from the raster package in R (Hijmans 2020) which implements methods described by Wilson et al. (2007). For each fish location, slope and roughness were calculated using the eight neighboring (surrounding) pixels. At the scales we used to calculate them, slope and roughness are exponentially correlated with one another (Fig 2). However, both metrics are used to define untrawlable habitats in the literature and therefore both values are reported.

Height off bottom data were decimated onto a 1 minute temporal resolution for each calendar day. We then fit a generalized additive model (GAM) in the mgcv package (Wood 2006, 2011), with hour of the day as the explanatory variable, and height off bottom as the response variable. Vertical error from the tags incorporated into the model. Each species was analyzed independently. No model selection was conducted as the goal was to understand the average height off bottom throughout the day. The depth of the tag, the roughness and slope of the bottom associated with the tag location were plotted using scaled density plots to assess how habitat utilization differed between species.

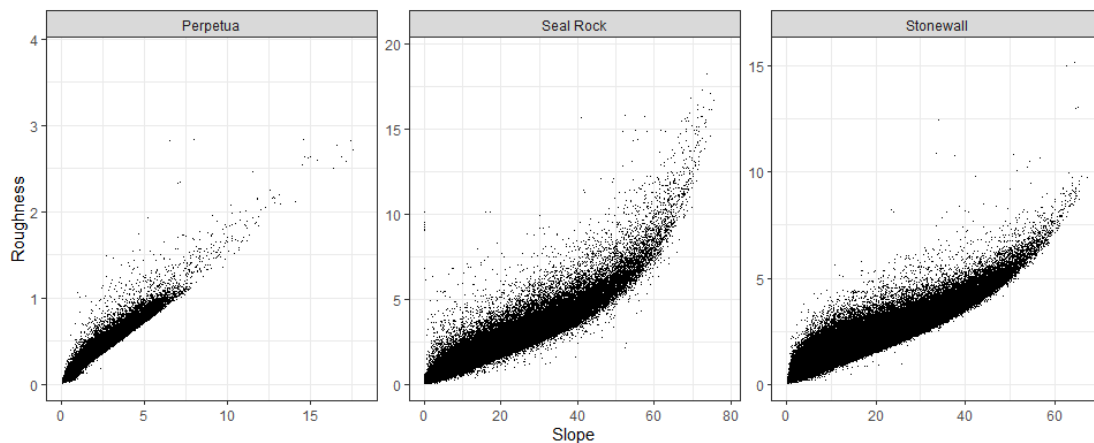


Fig. 2. Relationship between slope and roughness data calculated from the multibeam data for each reef.

Table 1. Study statistics for each of the five focal species.

Common Name	Scientific Name	Date Range	Number of Fish Tagged	Number of Observations with HPE <25	Study Reef	Reference
Black Rockfish	<i>Sebastes melanops</i>	08/2004 - 01/2005	26	1,048,575	Seal Rocks	(Parker et al. 2008)
Copper Rockfish	<i>Sebastes caurinus</i>	04/2010 - 05/2010	8	5,199	Cape Perpetua	(Rankin et al. 2013)
Deacon Rockfish	<i>Sebastes diaconus</i>	05/2016 - 09/2016	11	131,955	Seal Rocks	Rasmuson et al. 2021
Quillback Rockfish	<i>Sebastes maliger</i>	05/2010 - 05/2010	9	3,527	Cape Perpetua	(Rankin et al. 2013)
Yelloweye Rockfish	<i>Sebastes ruberrimus</i>	04/2012 - 09/2013	18	46,380	Stonewall Bank	(Rankin 2019)

RESULTS

Seal Rock's bathymetry data has an average depth of 21.6 ± 10.5 m, an average roughness estimate of 0.3 ± 0.1 , and an average slope of 3.5 ± 5.1 degrees (Fig. 3). Cape Perpetua's bathymetry data set has an average depth of 37.7 ± 12.7 m, an average roughness estimate of 0.1 ± 0.1 , and an average slope of 0.6 ± 0.5 degrees (Fig. 4). Stonewall Bank's bathymetry data has an average depth of 62.6 ± 8.9 m an average roughness estimate of 0.6 ± 0.5 and an average slope of 5.9 ± 5.3 degrees (Fig.5).

Black Rockfish and Deacon Rockfish occupied a broader depth range than the other species (Fig. 6). Both Quillback and Copper Rockfish activity was concentrated over a very fine depth range, and Yelloweye occupied a broad depth range, with some individuals even ascending to the surface. For Deacon Rockfish, the depth range equated to an average height off bottom of 5 m during the day and 1 m at night (Fig.7). Black Rockfish remained at an average depth of 3.75 m off bottom. Quillback and Coper Rockfish remained, on average, 0.01 m off bottom. Yelloweye were, on average, 2 m off bottom regardless of time of day.

Deacon Rockfish were associated with the most rugose habitat and habitat with the greatest slope (Fig. 8-9). At Seal Rocks Reef, Black Rockfish occupied far less rugose habitat than Deacon Rockfish. At Cape Perpetua, Quillback was associated with steeper bottoms than Copper Rockfish, but the roughness of the habitat used by the two species was similar. Yelloweye Rockfish used the second most sloped bottom after Deacon's but the roughness of this habitat was not as variable as that of Deacon's preferred habitat.

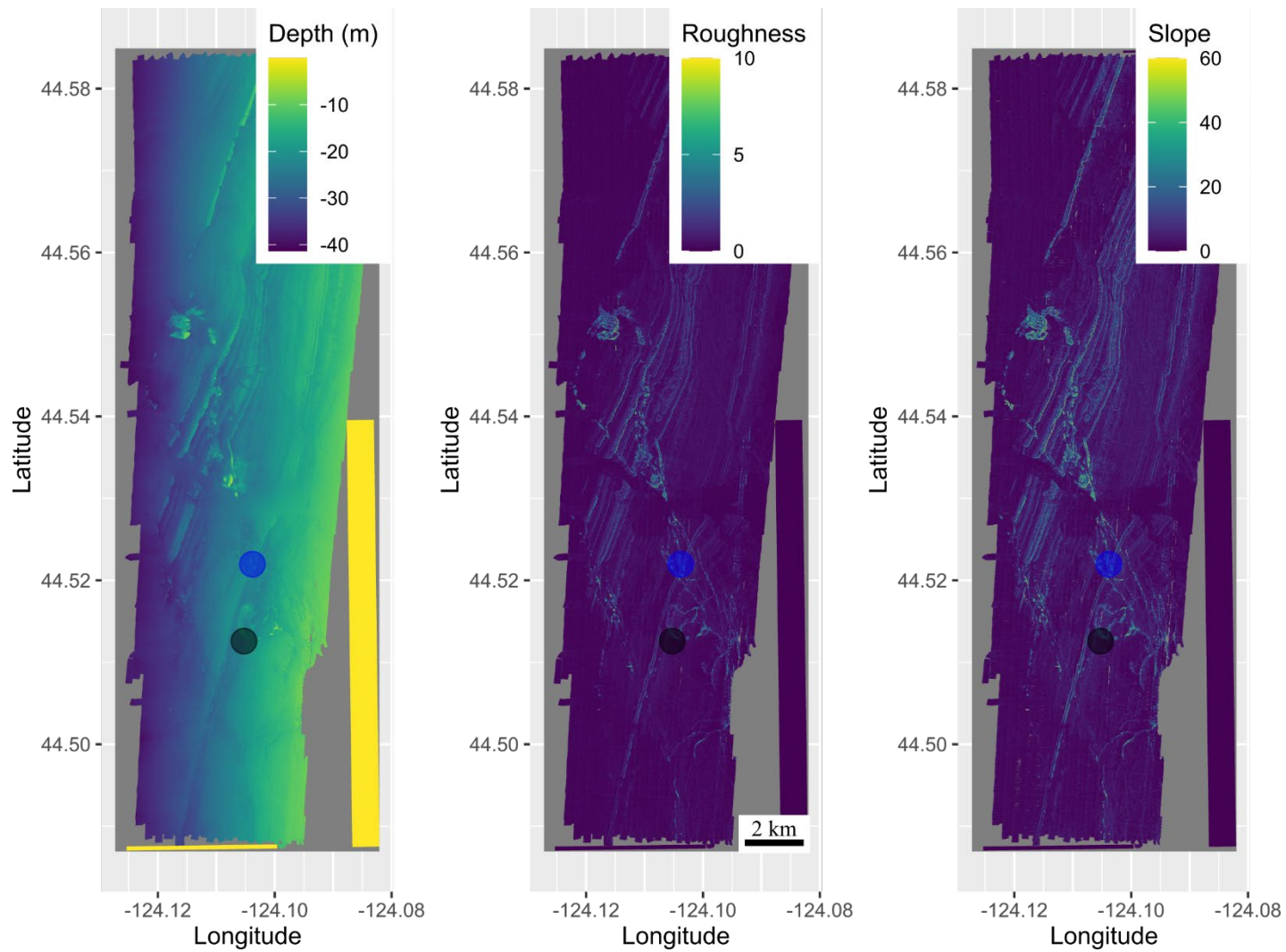


Fig. 3. Depth, rugosity and slope profiles for Seal Rocks Reef. The blue dot denotes the average location Deacon Rockfish were detected and the gray dot denotes the average location Black Rockfish were detected. Bathymetry data were provided by Goldfinger et al. (2014) and converted to rugosity and slope using the Terrain function in R (Wilson et al. 2007; Hijmans 2020).

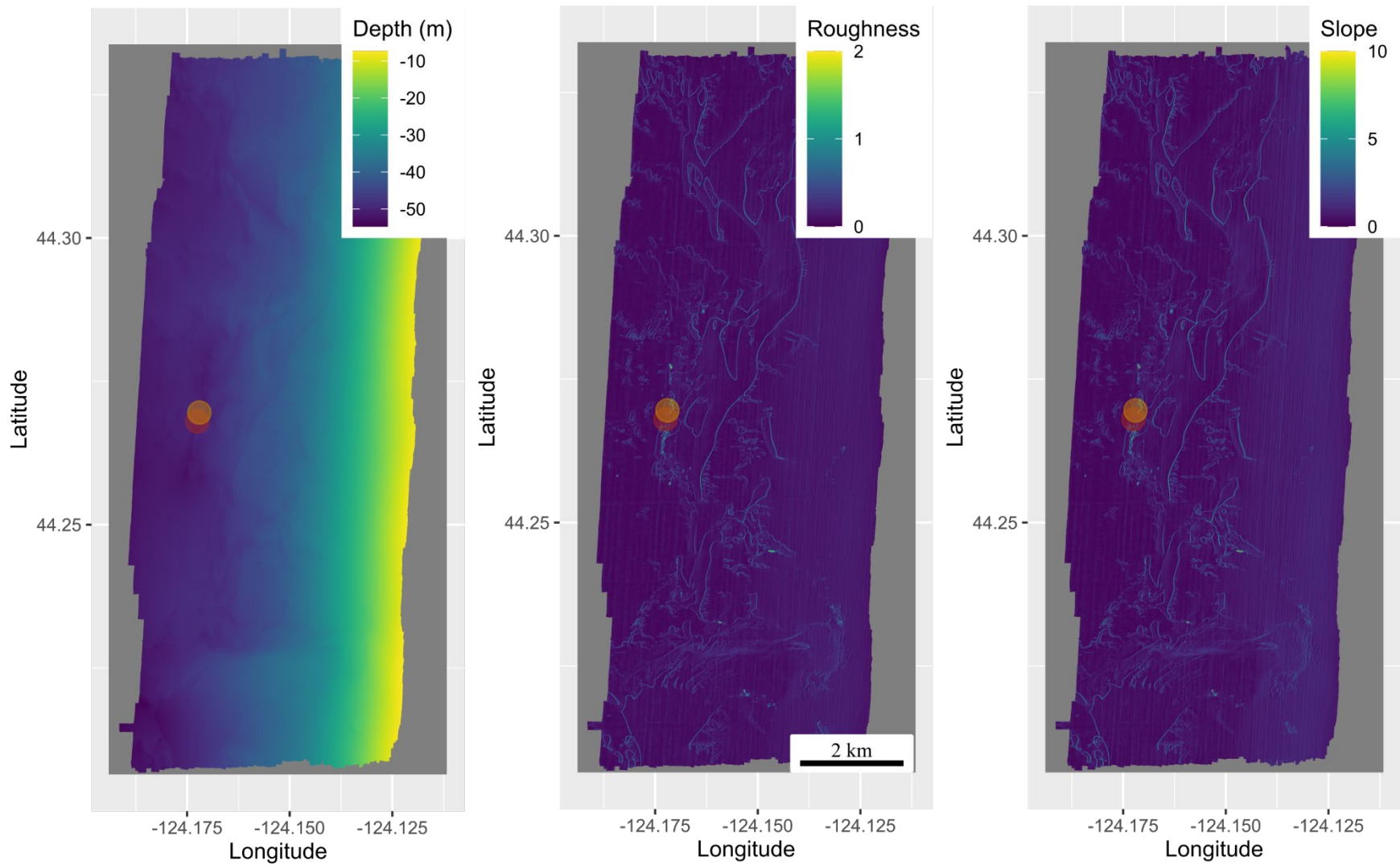


Fig. 4. Depth, rugosity and slope profiles for Cape Perpetua. The orange dot denotes the average location Copper Rockfish were detected and the brown dot denotes the average location Quillback Rockfish were detected. Bathymetry data were provided by Goldfinger et al. (2014) and converted to rugosity and slope using the Terrain function in R (Wilson et al. 2007; Hijmans 2020).

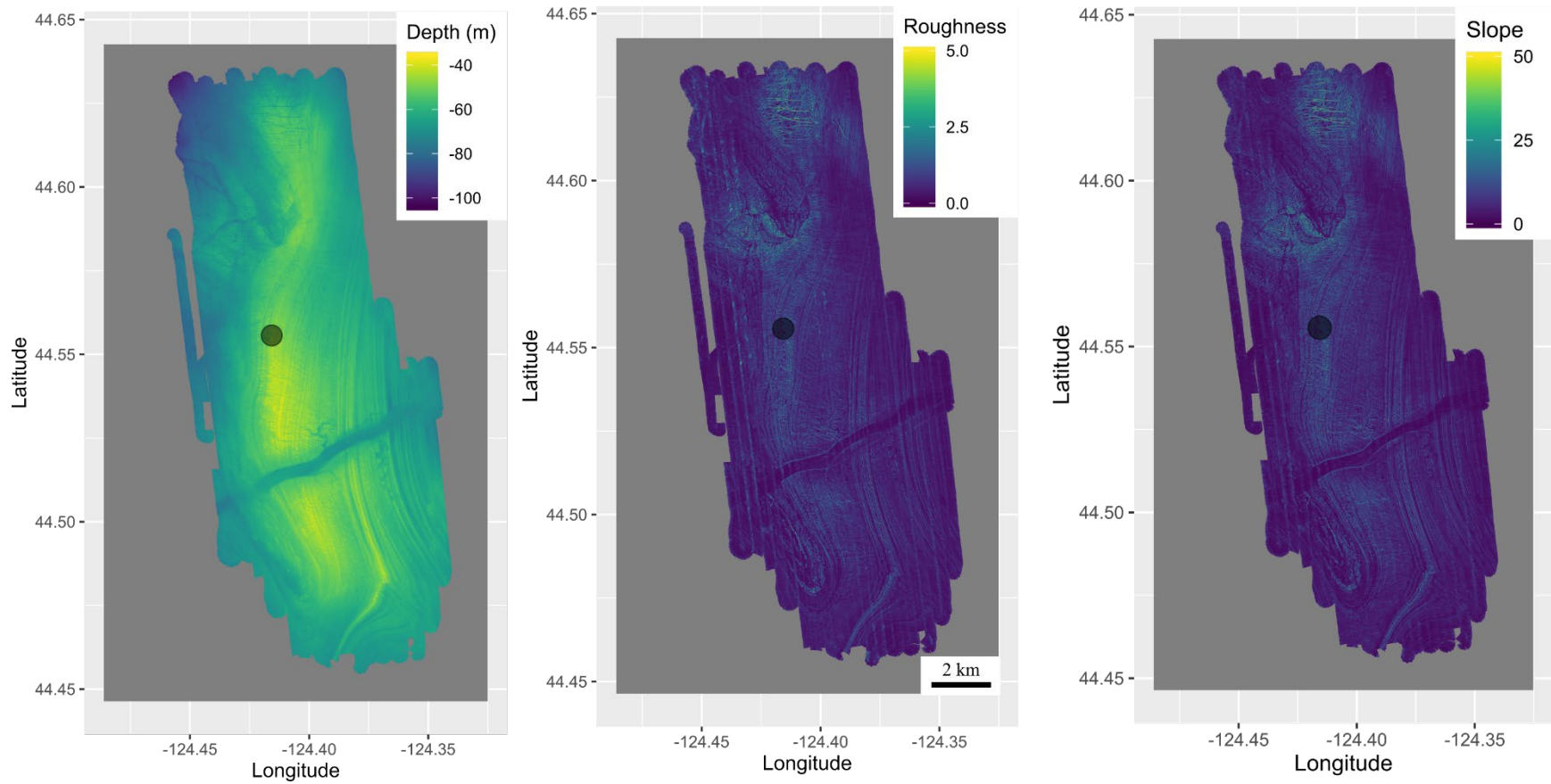


Fig. 5. Depth, rugosity and slope profiles for Stonewall Bank. The gray dot denotes the average location Yelloweye Rockfish were detected. Bathymetry data were provided by Goldfinger et al. (2014) and converted to rugosity and slope using the terrain function in R (Wilson et al. 2007; Hijmans 2020).

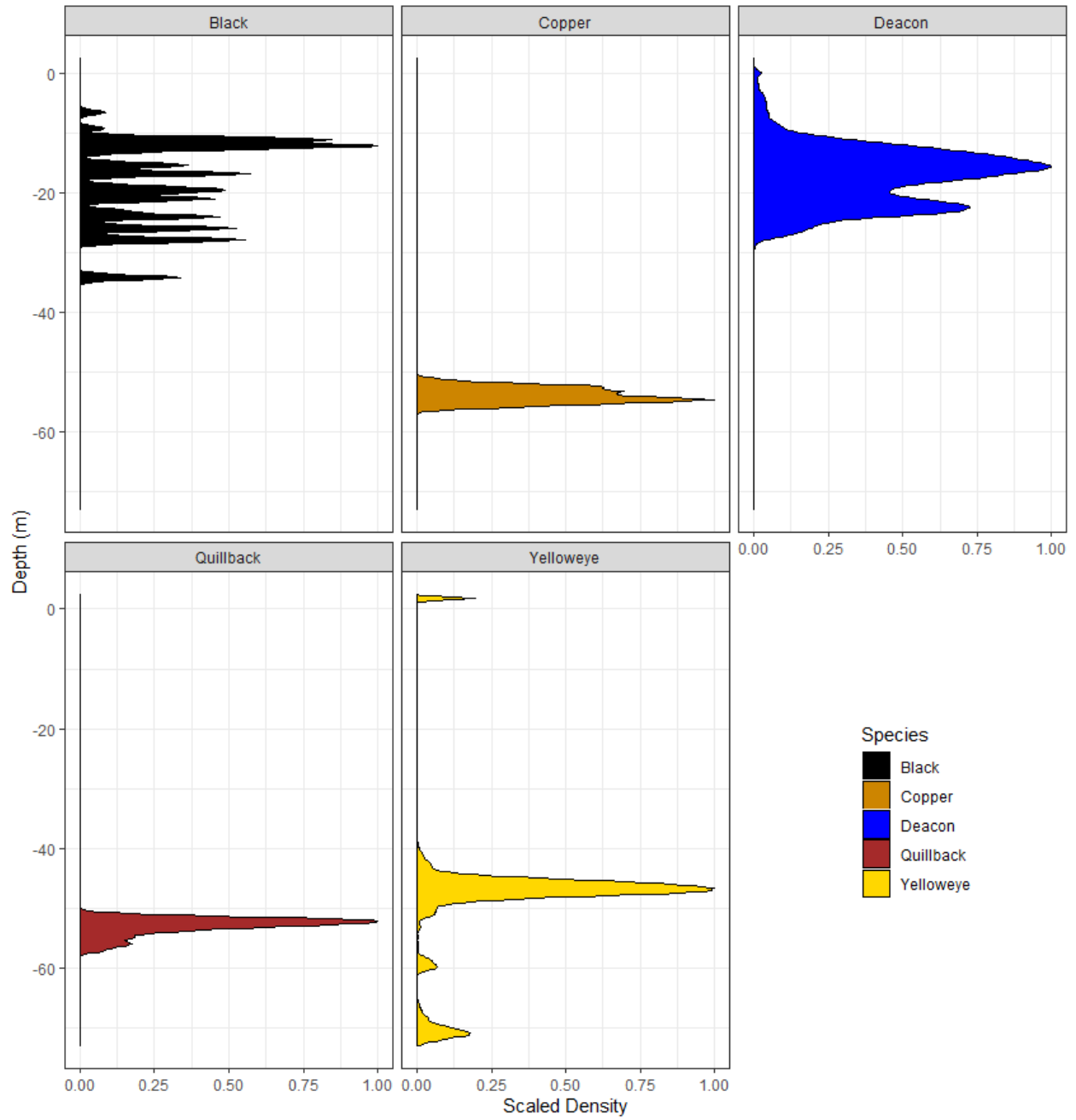


Fig 6. Scaled density plots of depth utilization for each of the five focal species.

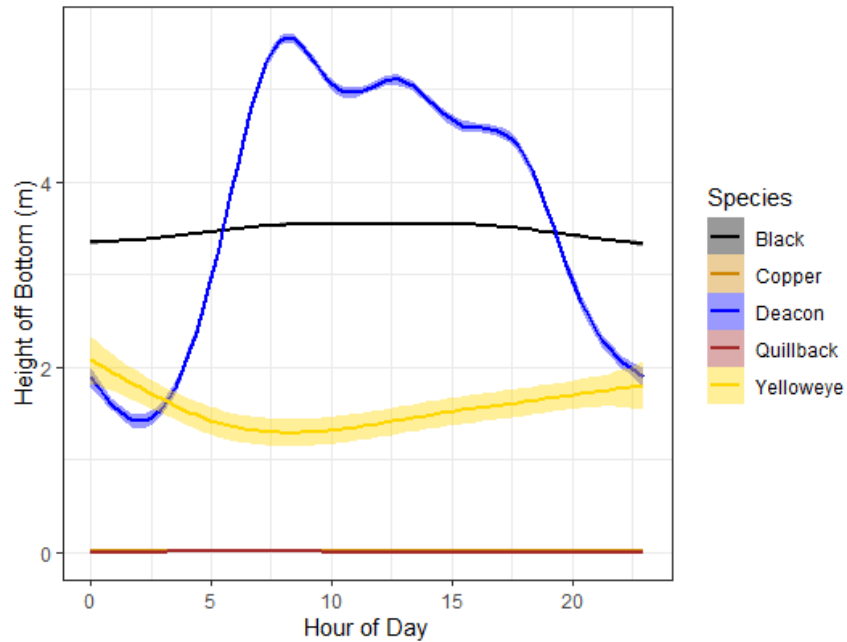


Fig. 7. Average height off bottom throughout a 24-hour period for each of the five focal species. Data from Copper and Quillback Rockfish are both near bottom and make it difficult to see the two different color schemes.

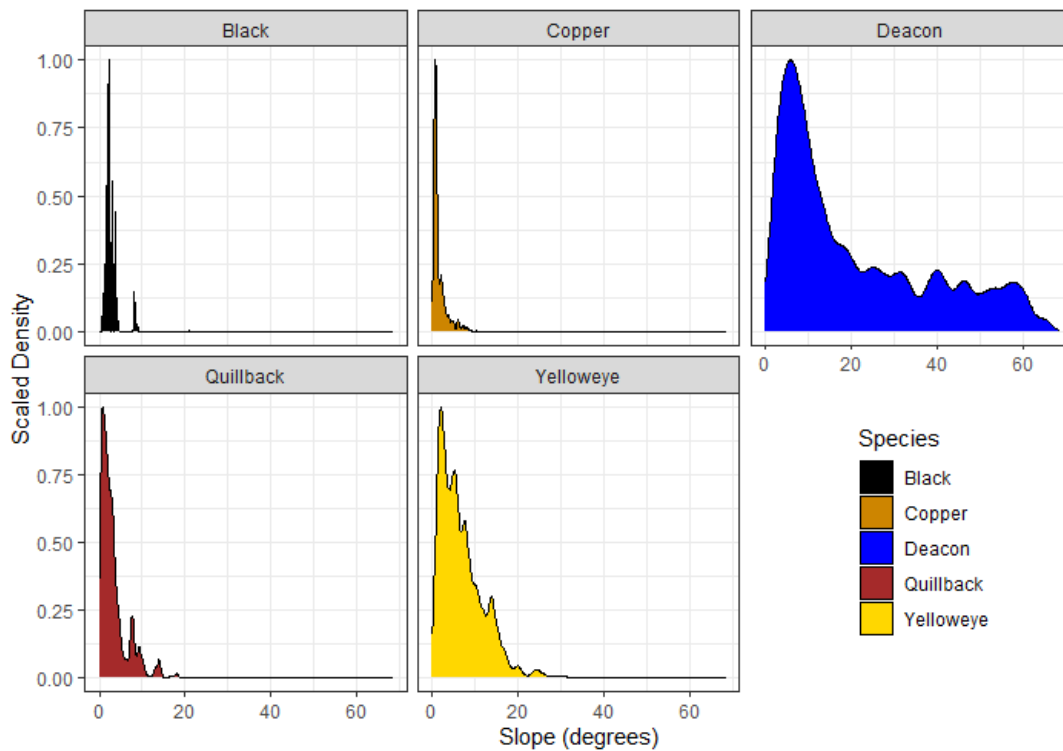


Fig 8. Scaled density plots of the slope of the habitat utilized by each of the five focal species.

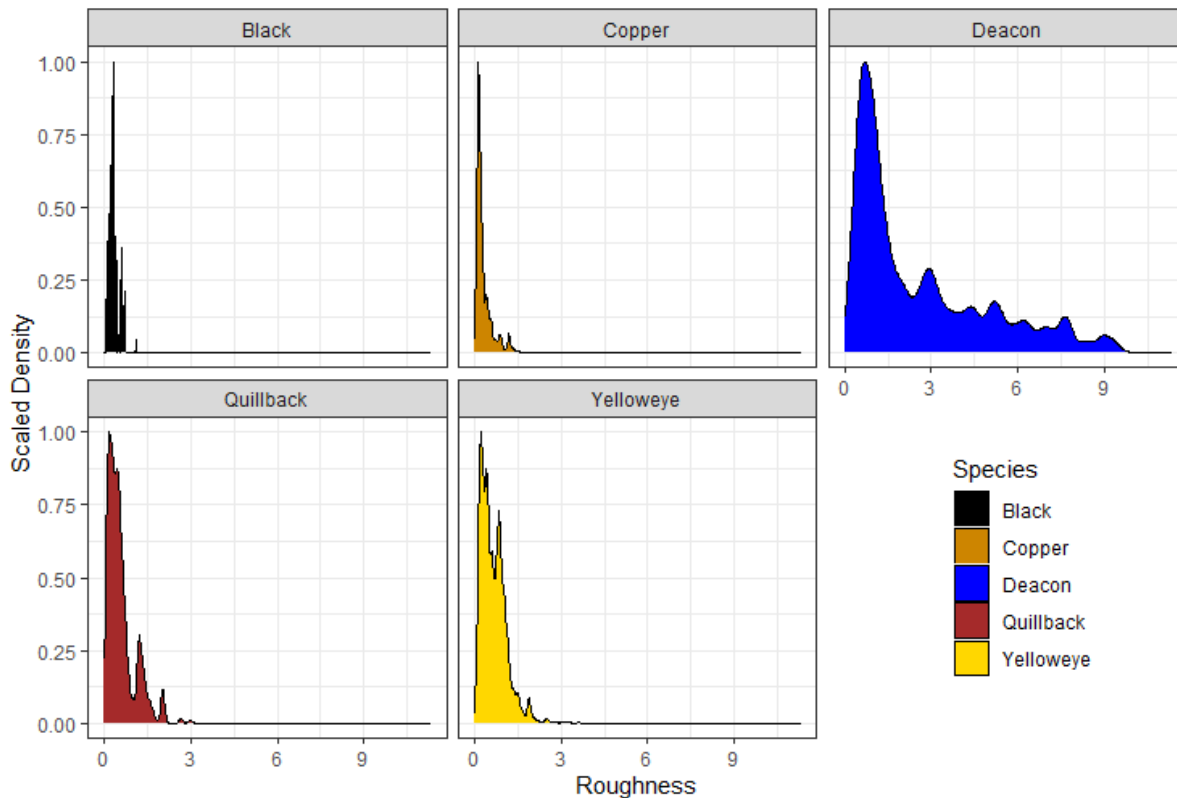


Fig 9. Scaled density plots of the roughness of the habitat utilized by each of the five focal species.

DISCUSSION

These analyses clearly demonstrate that the behavior of rockfish differs dramatically between species. Although, the studies we reanalyze here arrive at similar findings, they often focus their discussion on the variability in individual behaviors of the fish. While individuality occurs and is ecologically important, when designing a survey we survey the population, not the individual (Gunderson, Donald R. 1993). Thus, the understanding of what a species does on average, as provided in this paper, is useful in informing fishery independent population surveys.

Although the current re-analysis provides a temporally robust data set for each of the five species, each species was only studied at one reef and the studies were not always at the same reef. As such, the interpretations should be considered experimental until other studies can be repeated at additional sites within Oregon. Ideally, all of these species should be studied at a single reef to allow for a better intra-reef comparison of behavior and habitat usage.

Based on the findings of our height off bottom analysis, Black, Deacon and Yelloweye Rockfish, should be available to hydroacoustic survey methods. While both Black and Deacon Rockfish live off-bottom, they occupied parts of the reef with different vertical relief and exhibited distinctly different habitat preferences. This may be influenced by the vastly different dietary preferences between the two species (Hobson and Chess 1976; McClure 1982; Doran 2020). Yelloweye Rockfish used somewhat rugose habitat, a trend well established in the literature (Johnson et al. 2003; Mumm 2015).

The discovery that Black and Deacon Rockfish are available to hydroacoustics is not surprising. Both fish are known to school off bottom and Black Rockfish have been surveyed using hydroacoustic methods in Washington and Alaska (Boettner and Burton 1990; Tschersich 2015). However, the telemetry study that generated the data in this paper questioned the utility of hydroacoustics for Black Rockfish based on the presence of individual behaviors that may make those individuals unavailable to traditional acoustic methods (Parker et al. 2008). This demonstrates the importance of assessing the behavior of fish at the species level when considering development of a survey. Deacon Rockfish were also available to hydroacoustics but displayed a distinct diel change in height off bottom (Rasmuson In Press). This suggests that any acoustic operations should be conducted during daytime hours. The relief and slope of the habitat utilized by Deacon's also suggest that trawls would be highly ineffective at providing an accurate estimation of population size.

The finding that Yelloweye Rockfish are available to hydroacoustics is somewhat surprising. Yelloweye Rockfish are characteristically considered a near bottom fish. While the data suggests an acoustic method may be effective for Yelloweye, we propose more research is needed. What is likely more important from our findings is that, surveys of other semi-pelagic continental shelf rockfish (e.g. Widow (*Sebastes entomelas*), Yellowtail (*Sebastes flavidus*) or Pacific Ocean Perch (*Sebastes alutus*), should consider potential presence of Yelloweye Rockfish (Stanley 1999, 2000). Further, it is worth noting that the Yelloweye study occurred on the continental shelf and at greater depths than the other studies. It is unknown if Yelloweye in the nearshore or on the continental slope exhibit these same behaviors and therefore we are unsure how representative our data are of the species as a whole. Finally, as described in Rankin (2019), tagging Yelloweye Rockfish is difficult, with only some fish remaining in the survey array, while others leave the array for long periods of time. In the future, satellite tags may be an effective way to assess where these wandering individuals go, and what their behavior is (Rodgveller et al. 2017). What is not surprising is that based on the habitat use of Yelloweye, a bottom trawl is unlikely to be an effective survey tool (Jagiello et al. 2003; Hannah and Blume 2012, 2014).

Only acoustic survey methods that are resistant to the near bottom acoustic deadzone (e.g. broadband methods or near bottom towed bodies) would be able to differentiate fish echoes from those of the bottom (Kloser 1996), and would be useful for Quillback and Copper Rockfish which remain close to the bottom. Contrary to previous publications, these species did use lower relief habitat than Yelloweye and Deacon Rockfish (Richards 1987). This suggests that on average, their bottom tending behavior, combined with their utilization of relatively low relief habitat, should make them available to traditional bottom trawl surveys. Cape Perpetua, where the Copper and Quillback Rockfish were tagged, is relatively low relief compared to the rest of the state's reefs. As such, these species especially would benefit from additional research at a larger higher relief reef. Further, horizontal diel and tidally influenced movements of both of these species have been reported in the literature, and by averaging our data across the entire study diel and tidal behaviors may have been obscured (Tolimieri et al. 2009). Finally, although trawls may be effective, deployment of bottom trawls in nearshore environments comes with concerns about the ecological and social perception concerns suggesting other survey technologies may be better equipped to quantify these species (Watson and Huntington 2016; Huntington and Watson 2017).

Acoustic telemetry data provide deep insight into the availability of rockfish to acoustics and bottom trawl. However, there are some shortcomings of these types of data. First, high resolution acoustic telemetry studies are often only able to tag a relatively small number of individuals. As such, it is possible that the low sample size hides larger trends. Secondly, to provide these high-resolution data, the receiver arrays can only cover a relatively small geographic area. Thus, for species or individuals that move great distances (e.g. some Yelloweye Rockfish), the telemetry data only describes the behavior of those individuals with relatively small home ranges.

Although the data used in this study were collected over a long time period, recent work has shown that fishing pressure can influence individual fishes schooling behavior (Guerra et al. 2020), and that size selective harvesting influences the behavior of the population as a whole (Sbragaglia et al. 2019). Further, the removal of predators by fishing has been demonstrated to increase the boldness of fishes (Rhoades et al. 2019). Thus, these studies and analyses would benefit from re-analysis in the future. Despite our position that we should focus more on the population than the individual for the purpose of surveying fish, we want to acknowledge the importance of the individual. Specifically, the concept of behavioral syndromes should be considered as a potentially important contribution to the effect on fish behavior on fisheries independent surveys being applied to the stock assessment process (Bell and Sih 2007).

In conclusion, our work demonstrates that summarizing high resolution acoustic telemetry data is an effective way to understand how the behavior of different fish species would influence its

availability to different survey tools. While in this document we focused on the availability of the different species to hydroacoustics and bottom trawls, these interpretations can easily be extended to other sampling tools like hook and line and underwater video. While highlighting the variability of species behavior has implications for life-history parameters that may contribute to a stock assessment, it is also very informative to the survey development process and helps insure the most appropriate survey tools and methods are being applied.

ACKNOWLEDGMENTS

I thank all of the authors and scientists who conducted all of the hard field work and data analysis outlined in the original manuscripts. Obviously, this work would not have been possible without their hard work. I also thank Kelly Lawrence, David Fox, Katie Pierson, and Scott Malvitch for reviewing this manuscript for me.

REFERENCES

- Arreguin-Sanchez, F. 1996. Catchability: a key parameter for fish stock assessment. *Reviews in Fish Biology and Fisheries* 6(2).
- Baker, M. R., W. Palsson, M. Zimmermann, and C. N. Rooper. 2019. Model of trawlable area using benthic terrain and oceanographic variables—Informing survey design and habitat maps in the Gulf of Alaska. *Fisheries Oceanography* 28(6):629–657.
- Bell, A. M., and A. Sih. 2007. Exposure to predation generates personality in threespined sticklebacks (*Gasterosteus aculeatus*). *Ecology Letters* 10(9):828–834.
- Boettner, J., and S. Burton. 1990. Hydroacoustic stock assessment study of Washington coastal black rockfish of Washington state. Washington Department of Fish and Wildlife Technical Report 108.
- Cope, J. M., D. Sampson, A. Stephens, M. Key, P. P. Mirick, M. Stachura, S. Tsou, P. Weyland, A. Berger, T. Buell, E. Councill, E. J. Dick, K. H. Fenske, M. Monk, and B. T. Rodomsky. 2015. Assessments of California, Oregon and Washington Stocks of Black Rockfish (*Sebastes melanops*) in 2015:402.
- Dennis, D., É. Plagányi, I. Van Putten, T. Hutton, and S. Pascoe. 2015. Cost benefit of fishery-independent surveys: Are they worth the money? *Marine Policy* 58:108–115.
- Dick, E. J., A. M. Berger, J. Bizarro, K. Bosley, J. Cope, J. Field, L. Gilbert-Horvath, N. Grunloh, M. Ivens-Duran, R. Miller, K. Privitera-Johnson, and B. T. Rodomsky. 2017. The combined status of Blue and Deacon Rockfishes in U.S. waters off California and Oregon in 2017. Pacific Fishery Management Council.
- Doran, R. 2020. Diet analysis of Black Rockfish (*Sebastes melanops*) from stomach contents off the coast of Newport, Oregon. Honors, Oregon State University.

- DuFour, M. R., C. M. Mayer, S. S. Qian, C. S. Vandergoot, R. T. Kraus, P. M. Kocovsky, and D. M. Warner. 2018. Inferred fish behavior its implications for hydroacoustic surveys in nearshore habitats. *Fisheries Research* 199:63–75.
- Gertseva, V., and J. M. Cope. 2017. Stock assessment of the yelloweye rockfish (*Sebastes ruberrimus*) in state and Federal waters off California, Oregon and Washington:293.
- Goldfinger, C., S. Henkel, C. Romsos, and B. Havron. 2014. Benthic habitat characterization offshore the Pacific Northwest volume 1: evaluation of continental shelf geology. U.S. Department of the Interior, Bureau of Ocean Energy Management, Pacific Outer Continental Shelf Region, OCS Study BOEM 2014-662, Camarillo, California.
- Guerra, A. S., A. B. Kao, D. J. McCauley, and A. M. Berdahl. 2020. Fisheries-induced selection against schooling behaviour in marine fishes. *Proceedings of the Royal Society B: Biological Sciences* 287(1935):20201752.
- Gunderson, Donald R. 1993. *Surveys of fisheries resources*. John Wiley & Sons.
- Hannah, R. W., and M. T. O. Blume. 2012. Tests of an experimental unbaited video lander as a marine fish survey tool for high-relief deepwater rocky reefs. *Journal of Experimental Marine Biology and Ecology* 430–431:1–9.
- Hannah, R. W., and M. T. O. Blume. 2014. The Influence of Bait and Stereo Video on the Performance of a Video Lander as a Survey Tool for Marine Demersal Reef Fishes in Oregon Waters. *Marine and Coastal Fisheries* 6(1):181–189.
- Hijmans, R. J. 2020. raster: Geographic analysis and modeling with raster data.
- Hobson, E. S., and J. R. Chess. 1976. Trophic interactions among fishes and zooplankters near shore at Santa Catalina Island, California. *Fish. Bull* 74(3):567–598.
- Huntington, B. E., and J. L. Watson. 2017. Tailoring Ecological Monitoring to Individual Marine Reserves: Comparing Longline to Hook-and-Line Gear to Monitor Fish Species. *Marine and Coastal Fisheries* 9(1):432–440.
- Jagiello, T., A. Hoffmann, J. Tagart, and M. Zimmermann. 2003. Demersal groundfish densities in trawlable and untrawlable habitats off Washington: implications for the estimation of habitat bias in trawl surveys. *Fishery Bulletin* 101(3):545–565.
- Johnson, S. W., M. L. Murphy, and D. J. Csepp. 2003. Distribution, Habitat, and Behavior of Rockfishes, *Sebastes* spp., in Nearshore Waters of Southeastern Alaska: Observations From a Remotely Operated Vehicle. *Environmental Biology of Fishes* 66(3):259–270.
- Kloser, R. 1996. Improved precision of acoustic surveys of benthopelagic fish by means of a deep-towed transducer. *ICES Journal of Marine Science* 53(2):407–413.
- Kotwicki, S., J. K. Horne, A. E. Punt, and J. N. Ianelli. 2015. Factors affecting the availability of walleye pollock to acoustic and bottom trawl survey gear. *ICES Journal of Marine Science* 72(5):1425–1439.
- Love, M. S. 2006. Gimme shelter The importance of crevices to some fish species inhabiting a deeper-water rocky outcrop in Southern California. *CalCOFI Rep*.

- Love, M. S., M. M. Yoklavich, and L. Thorsteinson. 2002. The rockfishes of the Northeast Pacific. University of California Press.
- McClure, R. 1982. Neritic reef fishes of central Oregon: Aspects of life histories and the recreational fishery. Oregon State University.
- Meyer-Gutbrod, E., C. H. Greene, A. Packer, H. Dorn, and J. Griffith. 2012. Long term autonomous fisheries survey utilizing active acoustics. Pages 1–5 2012 Oceans. IEEE, Hampton Roads, VA.
- Mumm, J. D. 2015. Master of Science in Environmental Science. Masters Thesis, Alaska Pacific University.
- Parker, S., J. Olson, P. Rankin, and J. Malvitch. 2008. Patterns in vertical movements of black rockfish *Sebastes melanops*. *Aquatic Biology* 2:57–65.
- R Core Team. 2020. R: A language and environment for statistical computing. R Foundation for statistical computing Vienna, Austria. URL <https://www.R-project.org>.
- Rasmuson, L., M.T.O. Blume, P.S. Rankin. 2021. Habitat use and activity patterns of female Deacon Rockfish (*Sebastes diaconus*) at seasonal scales and in response to episodic hypoxia. *Env Biol of Fishes*. In Press
- Rankin, P., R. Hannah, and M. Blume. 2013. Effect of hypoxia on rockfish movements: implications for understanding the roles of temperature, toxins and site fidelity. *Marine Ecology Progress Series* 492:223–234.
- Rankin, P. S. 2019. Summary of Yelloweye Rockfish (*Sebastes ruberrimus*) acoustic telemetry conducted at Stonewall Bank from 2005-2013.
- Research Group, LLC. 2015. Oregon marine recreational fisheries economic contributions in 2013 and 2014. Prepared for Oregon Department of Fish and Wildlife and Oregon Coastal Zone Management Association, Corvallis, Oregon. September 2015.
- Rhoades, O. K., S. I. Lonhart, and J. J. Stachowicz. 2019. Human-induced reductions in fish predator boldness decrease their predation rates in kelp forests. *Proceedings of the Royal Society B: Biological Sciences* 286(1900):20182745.
- Richards, L. J. 1987. Copper rockfish (*Sebastes caurinus*) and quillback rockfish (*Sebastes maliger*) habitat in the Strait of Georgia, British Columbia. *Can J Zoology* 65:12.
- Rodgveller, C. J., C. A. Tribuzio, P. W. Malecha, and C. R. Lunsford. 2017. Feasibility of using pop-up satellite archival tags (PSATs) to monitor vertical movement of a *Sebastes* : A case study. *Fisheries Research* 187:96–102.
- Rodomsky, B. T., T. Calavan, and K. M. Matteson. 2020. The Oregon Commercial Nearshore Fishery Data Update. Page 55. ODFW Fishery Update.
- Rooper, C. 2010. Assessing habitat utilization and rockfish (*Sebastes* spp.) biomass on an isolated rocky ridge using acoustics. *Can J Fish Aquat Sci*.

- Rotherham, D., A. J. Underwood, M. G. Chapman, and C. A. Gray. 2007. A strategy for developing scientific sampling tools for fishery-independent surveys of estuarine fish in New South Wales, Australia. *ICES Journal of Marine Science* 64(8):1512–1516.
- Sbragaglia, V., J. Alós, K. Fromm, C. T. Monk, C. Díaz-Gil, S. Uusi-Heikkilä, A. E. Honsey, A. D. M. Wilson, and R. Arlinghaus. 2019. Experimental Size-Selective Harvesting Affects Behavioral Types of a Social Fish. *Transactions of the American Fisheries Society* 148(3):552–568.
- Stanley, R. 2000. Estimation of a widow rockfish (*Sebastes entomelas*) shoal off British Columbia, Canada as a joint exercise between stock assessment staff and the fishing industry. *ICES Journal of Marine Science* 57(4):1035–1049.
- Stanley, R. D. 1999. Diel vertical migration by yellowtail rockfish, *Sebastes flavidus*, and its impact on acoustic biomass estimation. *Fish Bull.*
- Stoner, A. W., C. H. Ryer, S. J. Parker, P. J. Auster, and W. W. Wakefield. 2008. Evaluating the role of fish behavior in surveys conducted with underwater vehicles. *Canadian Journal of Fisheries and Aquatic Sciences* 65(6):1230–1243.
- Tolimieri, N., K. Andrews, G. Williams, S. Katz, and P. Levin. 2009. Home range size and patterns of space use by lingcod, copper rockfish and quillback rockfish in relation to diel and tidal cycles. *Marine Ecology Progress Series* 380:229–243.
- Trenkel, V. M., R. C. Francis, P. Lorange, S. Mahévas, M.-J. Rochet, and D. M. Tracey. 2004. Availability of deep-water fish to trawling and visual observation from a remotely operated vehicle (ROV). *Marine Ecology Progress Series* 284:293–303.
- Tschersich, P. 2015. Hydroacoustic survey of Black Rockfish abundance and distribution operational plan for the Afognak and Northeast districts of the Kodiak management area, 2015. Alaska Department of Fish and Game, Division of Sport Fish, Research and Technical Services, Alaska Department of Fish and Game, Division of Commercial Fisheries, Regional Operational Plan ROP. CF. 4K.2015.18, Kodiak.
- Watson, J. L., and B. E. Huntington. 2016. Assessing the performance of a cost-effective video lander for estimating relative abundance and diversity of nearshore fish assemblages. *Journal of Experimental Marine Biology and Ecology* 483:104–111.
- Wilson, M. F. J., B. O’Connell, C. Brown, J. C. Guinan, and A. J. Grehan. 2007. Multiscale Terrain Analysis of Multibeam Bathymetry Data for Habitat Mapping on the Continental Slope. *Marine Geodesy* 30(1–2):3–35.
- Wood, S. 2006. Generalized additive models: An introduction with R. CRC Press, Boca Raton, FL.
- Wood, S. 2011. Fast stable REML and ML estimation of semiparametric GLMs. *J Roy Stat Soc B Met* 73:3–36.
- Zimmermann, M. 2003. Calculation of untrawlable areas within the boundaries of a bottom trawl survey. *Canadian Journal of Fisheries and Aquatic Sciences* 60(6):657–669.

7: COMBINED VIDEO-HYDROACOUSTIC SURVEY OF NEARSHORE SEMI-PELAGIC ROCKFISH IN UNTRAWLABLE HABITATS.

LEIF K. RASMUSON^{1*}, STEPHANIE A. FIELDS¹, MATTHEW T.O. BLUME¹, KELLY A. LAWRENCE¹,
POLLY S. RANKIN¹

This paper was published in ICES Journal of Marine Science (<https://academic.oup.com/icesjms/article/79/1/100/6470671>). It is recreated here for simplicity.

ABSTRACT

New survey technologies are needed to survey untrawlable habitats in a cost effective and nonlethal manner with minimal impacts on habitat and nontarget species. Here we test the efficacy of integrating data from a suspended underwater camera with acoustic data to generate population estimates for nearshore Black (*Sebastes melanops*), Blue (*Sebastes mystinus*) and Deacon Rockfish (*Sebastes diaconus*). We surveyed Seal Rock Reef near Newport, Oregon, and compared our results to population estimates derived from a mark-recapture study conducted at the same reef. We compared fish density estimates from video deployments to those calculated from applying published target strength to length regression models to our acoustics data. Densities derived from the acoustics, using a generalized physoclist target strength to length model, were significantly different from densities derived from video; conversely, a rockfish-specific target strength to length model generated densities that were not statistically different from video densities. To assess whether, and how, fish behaviour was influenced by the presence of an underwater camera, we deployed our camera under the acoustic transducer. No statistical difference was observed in the acoustic density of fish before, during, or after camera deployment. Our work suggests that combining acoustic and stereo video data provided a similar population estimate to historic survey results, but an accurate acoustic density estimate was dependent on using the proper acoustic target-strength model. We contend that combining camera data with hydroacoustic data is effective for surveying rockfish in untrawlable habitats.

1. INTRODUCTION

Fisheries independent surveys provide an important unbiased data input into fisheries stock assessments (Hilborn and Walters, 1992). Fisheries independent surveys are often time consuming and costly, making their implementation difficult for all but the most economically important fisheries. Bottom trawls are currently the most commonly used fishery independent survey tool for groundfish (Gunderson, Donald R., 1993); however, research continues to demonstrate that trawls may not be effective in rugose habitats, which may significantly impact

the survey data products as well as the tool being a relatively destructive way to sample (Zimmermann, 2003; Pirtle *et al.*, 2015). Alternatively, other methodologies and technologies are being considered to survey “untrawlable habitats” (Tolimieri *et al.*, 2008; Williams *et al.*, 2010). Technologies, such as hydroacoustic and underwater video, are being examined as potentially more efficient and cost-effective than traditional survey methods.

In Oregon’s nearshore waters, Black Rockfish (*Sebastes melanops* Girard 1856), Blue Rockfish (*Sebastes mystinus* Jordan & Gilbert 1881) and Deacon Rockfish (*Sebastes diaconus* Frable *et al.*, 2015) are the primary target of the recreational bottomfish fishing fleet (Cope *et al.*, 2015). These species are known to occur off the bottom in schools, as well as near the bottom and are often deemed semi-pelagic. These species also represent an important component of commercial nearshore hook and line, and longline fisheries. Despite their economic importance, there are currently no fishery independent surveys conducted in Oregon’s waters that target nearshore rockfish. Historically, a mark-recapture passive integrated transponder (PIT) tagging study for Black Rockfish was conducted at a single reef on the central Oregon coast (Krutzikowsky *et al.*, 2019). However, this study only provided a population estimate of one reef, making the data difficult to use as a stock assessment model input because it is not representative of the entire stock, which is distributed across multiple reefs.

An accurate estimation of stock size is an integral component of sustainable fisheries management (Maunder and Punt, 2013), and this estimation has been hindered by a lack of fishery independent data (Cope *et al.*, 2015; Dick *et al.*, 2017). Hydroacoustic population estimates are attractive to stock assessors because they provide numerical estimates of fish abundance rather than a relative abundance index which can better inform the size of the stock. However, for hydroacoustics to be effective, the fish must be detectable by the acoustics (Ona and Mitson, 1996; Kotwicki *et al.*, 2015) and a proper target-strength to length model needs to be available (Love, 1971; Foote, 1987). Detectability, for semi-pelagic fishes, requires the fish to be high enough off the seafloor to allow their acoustic signature to be differentiated from the seafloor (Mello and Rose, 2009; Rasmuson, 2021). Fish whose backscattering signature cannot be differentiated from the seafloor are said to be located within the near bottom acoustic dead zone. While the presence of the acoustic dead zone makes population estimates of benthic rockfish species difficult, previous studies have shown hydroacoustic surveys to be well suited for semi-pelagic rockfish (Parker *et al.*, 2008). Previous studies on the congeneric Widow (*Sebastes entomelas* Jordan and Gilbert 1880) and Yellowtail Rockfish (*Sebastes flavidus* Ayres 1862), off the coast of Oregon and British Columbia, suggested that hydroacoustic surveys are a viable method for these species (Stanley, 1999, 2000). Hydroacoustic surveys of Black Rockfish in Alaska and Washington also provided accurate and repeatable population estimates (Boettner and Burton, 1990; Tschersich, 2015). This suggests

hydroacoustic surveys may be an effective survey method for Oregon's semi-pelagic nearshore rockfish.

In order to convert the acoustic backscattering data into fish densities, hydroacoustic data is paired with species composition and length data (McClatchie *et al.*, 2000). Traditionally, this data comes from midwater trawls (Williams *et al.*, 2010; Jones *et al.*, 2019); however, midwater trawls are difficult to operate in highly rugose areas, and lethally sample fish. In environments where trawling is difficult, and lethal sampling is not desirable, alternative sampling tools are necessary. Underwater video tools are becoming an increasingly common non-lethal alternative for producing both species composition and length data (Rooper, 2010; Bacheler *et al.*, 2017). The advent of stereo camera technology allows scientists to measure lengths of fish observed by the camera (Langlois *et al.*, 2012; Hannah and Blume, 2016). Combining species composition and length data from stereo video with hydroacoustic data has been shown to be an effective survey combination, producing accurate fish densities (Starr *et al.*, 1996; Jones *et al.*, 2012; Boldt *et al.*, 2018). To date, combining species composition and length data with hydroacoustic data has never been done for Black Rockfish. In the case of Tschersich (2015), species composition data were obtained from a single camera and no lengths were obtained. In the case of Boettner and Burton (1990), a midwater trawl was used. Advancements in how species composition and length data can be obtained from, and combined with, acoustic surveys of Black Rockfish are necessary. Further, when selecting the sampling tool, it is essential to account for the fact that all sampling tools have some form of sampling bias error associated with them. The effect of sampling error associated with each tool and how those assumptions influence both length and species composition data and the effect of this error must be considered.

Here, we tested the efficacy of combining hydroacoustic data and underwater stereo video data (length and species composition data) to generate a population estimate of three of Oregon's nearshore rockfish species (Black, Blue and Deacon Rockfish). We created a novel camera system that is uniquely designed for semi-pelagic rockfish species found in rocky reef habitat. This system was designed to be paired with hydroacoustic data. One concern with all survey tools, is the catchability of a species by the tools (Koslow *et al.*, 1995; Stoner *et al.*, 2008; Somerton *et al.*, 2017). For acoustic surveys, catchability is the ability of the acoustics, as well as the ability of the trawl (or in our case, video sampling tool), to detect fish. For video and acoustic survey tools, where fish are not actually caught, catchability is known as detectability. In this manuscript we use detectability to refer to the ability of acoustic and video sampling tools to accurately provide a representative sample of the focal population(s) (Arreguin-Sanchez, 1996). Hydroacoustic detectability may be reduced due to the near bottom dead zone, and video detectability may be reduced due to fish avoidance of the video tool, as well as poor underwater visibility. We address detectability of the hydroacoustic and video tools by

examining the potential impact the acoustic dead zone and camera deployment may have on the abundance estimate.

2. METHODS

2.1 FIELD WORK

We conducted a pilot survey to test the integration of hydroacoustic data with suspended stereo camera data to generate a population estimate of midwater rockfishes. The survey was conducted from September 25-29, 2017 at Seal Rock Reef, just south of Newport, Oregon (**Fig. 1**). This reef was chosen due to the presence of historic data from this location, and its nearness to research facilities. The goal of this study was not intended to provide a regional population estimate, but to assess the utility of the survey method. All surveys were conducted from a 15.25 m long charter passenger fishing vessel operating at an average speed of 9.25 kph. Thirty-eight parallel transects were established and spaced 0.5 km apart (in the North/South direction). Transects began 500 m offshore of known hard bottom habitat and extended 500 m inshore of the hard bottom, or to a water depth of 5 m, whichever occurred first. To minimize the effect of ocean swell, acoustic data were collected while the vessel traveled from offshore to inshore,

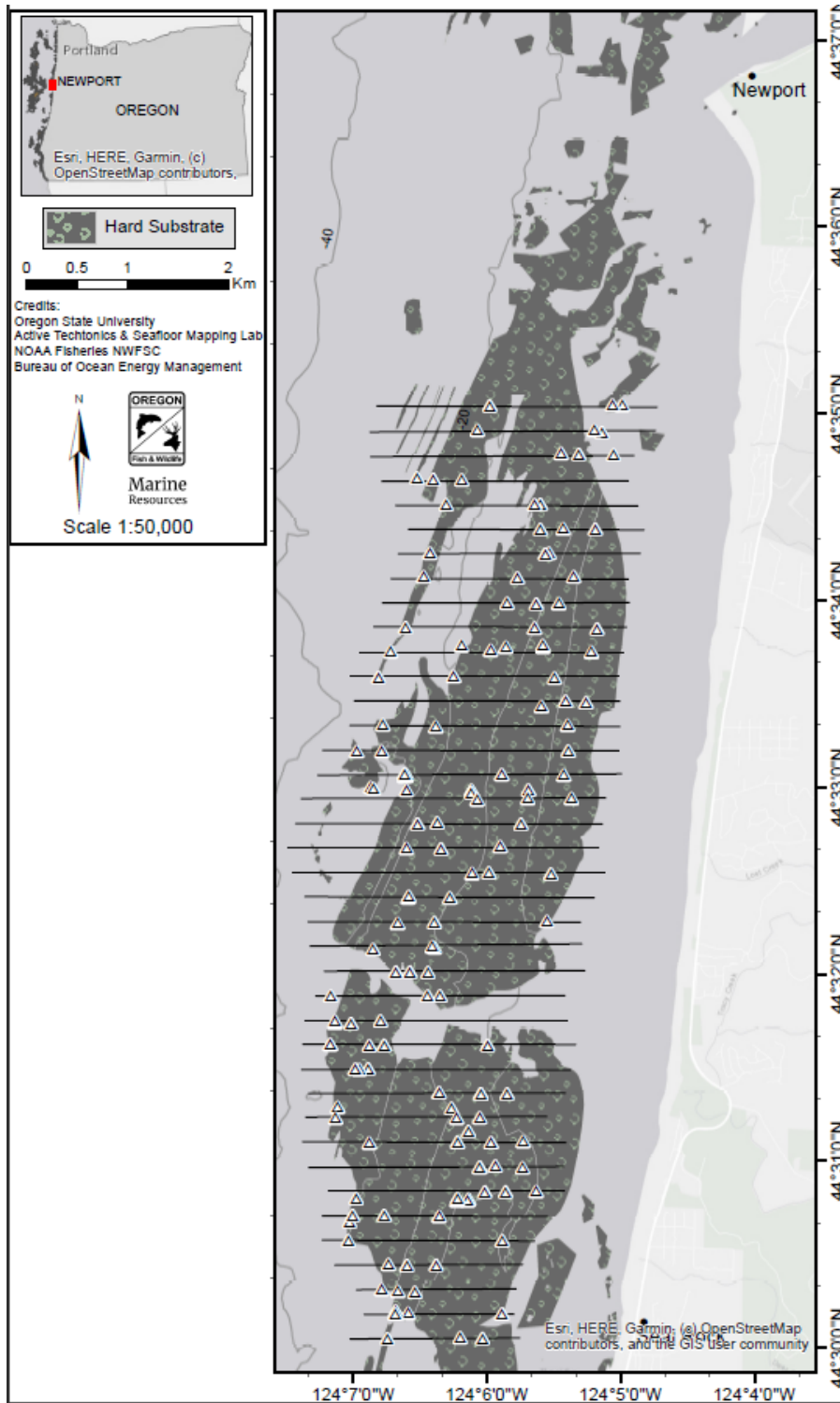


Fig. 1 Map of survey transects (black lines) overlaid on the known hard substrate. Triangles denote deployment locations of the BASSCam. Transect lines extended 500 m offshore and shoreward of the known hard bottom substrate.

using a 201 kHz BioSonics DT-X transducer. The transducer was calibrated 6 months prior to the survey and immediately following the survey at the BioSonics factory. The transducer was pole mounted in a downward facing orientation on the starboard side of the vessel. The beam width of the transducer was 6.5° and the unit transmitted 0.3 ms pulses at a ping rate of 5.0 pings per second.

On each transect, while collecting the acoustic data, three fish schools were identified from the acoustics and marked on a GPS for later sampling with a suspended camera system. Previous work demonstrated rockfish schools remain at relatively the same locations on the reef for days to weeks, making it possible to return to schools to deploy the camera after the acoustic data was collected for the entire transect (Rasmuson unpublished data). Video sampling of each school occurred within one hour of the transect being ensonified. At each transect, three fish schools were selected for video deployments. If less than three schools were observed, the camera system was deployed on high relief rocky habitat, identified in the acoustics, for a total of three video deployments per transect. If more than three fish schools were observed, schools were selected haphazardly for video sampling.

The suspended camera data was collected with our Benthically Anchored Suspended Stereo Camera system (hereafter BASSCam). The BASSCam was equipped with a pair of forward-looking GoPro Hero4 Black Edition cameras in a calibrated stereo configuration, with illumination from two Big Blue VL7500P LED lights. The cameras were calibrated using a 3-dimensional calibration cube, developed by SeaGIS, and calibration coefficients were generated using the SeaGIS CAL software. In addition to the forward-looking stereo cameras, the platform also had one GoPro Hero4 Black Edition camera looking downward from the forward plane at an angle of 22 degrees, illuminated by two Big Blue VL2800P LED lights. Based on height of the camera system off bottom, and the angle of the downward facing camera, we know that 78% of the volume viewed by the downward camera is within 1 m of the bottom (what we define as the near bottom acoustic dead zone in this paper). The platform was equipped with a Star-Oddi DST tilt sensor that recorded the 3-dimensional orientation of the camera system as well as depth and temperature. The BASSCam was designed to remain upright and orient into the current (**Fig. 2**). A 2 m tether was attached to the bottom of the camera with an 18 kg piece of scrap iron as an anchor, which was designed to break-away if caught on the rocky bottom habitat.

Prior to each deployment, the video system was turned on while onboard, and a synchronizing video frame was generated using a video clapper board. The captain then positioned the vessel over (or near) the fish school and the camera deployed so it drifted into the target fish school. The camera system was tended at the surface while tethered by an armored umbilical (2.57 mm). One camera (left) was connected to the umbilical and sent live video signal to the vessel for real-time viewing. The live camera was used to determine if the fish school was successfully

sampled, if it was not, to the camera was re-deployed. The camera was retrieved using an electric motor and spool after a minimum of two minutes from the time the camera's anchor reached the bottom. Bottom time was determined with a stopwatch. Two minutes of bottom time was shown to be enough time to provide accurate size and length data (Rasmuson unpublished data).

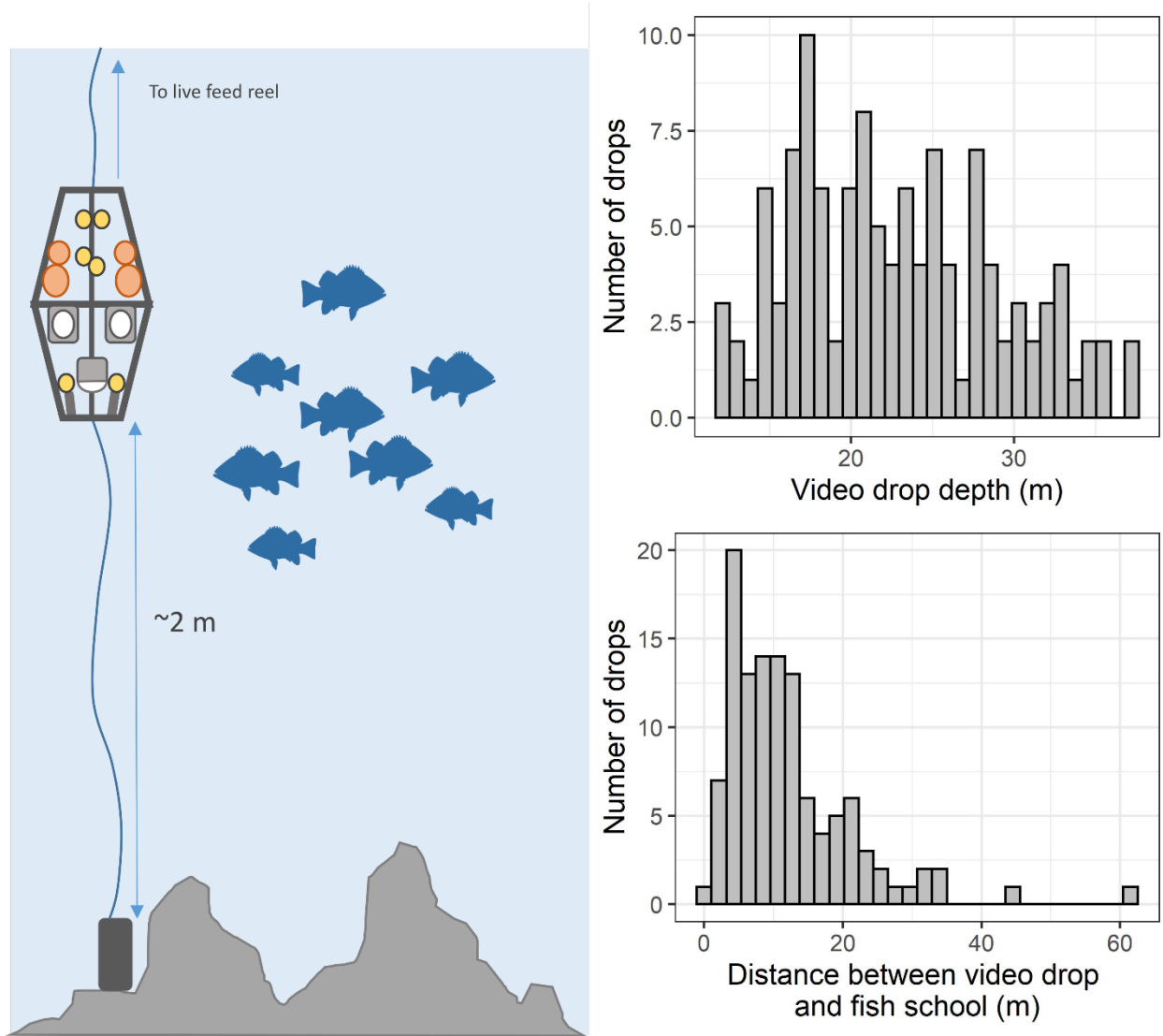


Fig. 2 Schematic of BASSCam deployed in a school of fish (left) and number of BASSCam deployments by water depth (upper right) and the distance from the BASSCam deployment location to the fish school identified by the hydroacoustics (lower right). On the left, the white and grey boxes denote the location of the three video cameras, the orange circles denote non-compressible trawl floats used to provide buoyancy and the yellow circles denote the locations of the underwater lights.

2.2 ANALYSIS

All statistical analyses were conducted using R version 3.6.3 Holding Windsock (R Core Team, 2020). Distances from the targeted fish schools to the BASSCam deployment locations were calculated using the Geosphere package. Our analysis required us to combine acoustic and video data in multiple ways to answer the hypotheses we generated; to aid the reader, a flow chart is included to assist in understanding which data were used to answer each question (**Fig. 3**).

2.2.1 VIDEO ANALYSIS

Videos were reviewed using the EventMeasure software developed by SeaGIS. Only the first two minutes of video, after the camera reached the bottom, were reviewed. All species were identified to the lowest taxonomic unit possible. Blue and Deacon Rockfish were scored as a single species complex because they are routinely difficult to differentiate due to poor water visibility. There is considerable debate in the literature about the best way to review stationary underwater video. Therefore we reviewed videos from the BASSCam's forward cameras using both a MaxN and a MeanCount approach (Schobernd *et al.*, 2014). The results of this analysis are available in the online supplement.

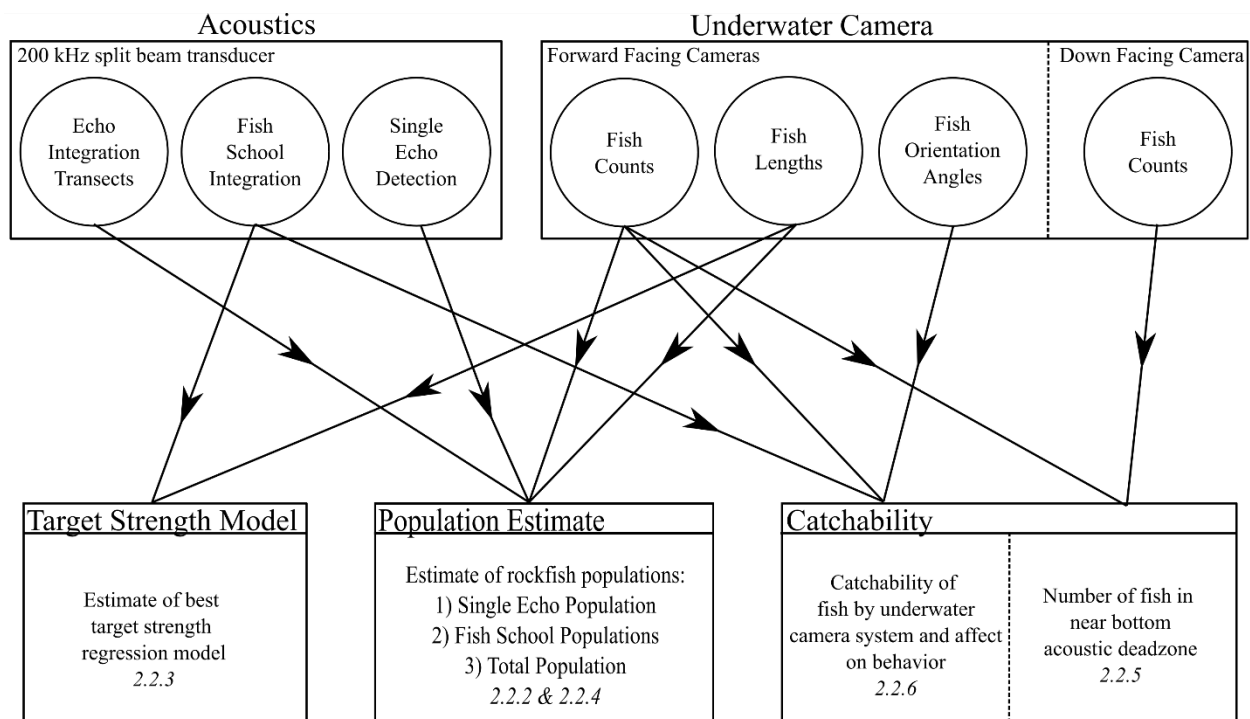


Fig. 3 Flow chart depicting the relationship of acoustic and video inputs for each component of the analysis process.

We found the MeanCount method to be the most statistically robust and efficient way to review video. MeanCount was conducted by enumerating all fish in each of the five randomly selected frames from the two-minute bottom time. Fish were counted in the left forward-facing stereo camera only. No attempts were made to ascertain whether fish being counted in each of the five frames were the same fish. In the downward facing camera, fish were counted in the same frames that we counted in the forward camera. Of the fish counted in the left camera, we attempted to measure each fish, which is only possible if the fish's head and tail are observed in both forward-facing cameras. To do this, reviewers tracked each fish both forwards and backwards in the video to find a frame where they were best able to identify and measure the fish. Due to the rarity of some species, we aggregated non-focal species into functional groups. Black Rockfish were kept as a single species group and Blue and Deacon Rockfish were kept as a congeneric cryptic species group. Yellowtail Rockfish, Widow Rockfish and Canary Rockfish (*Sebastes pinniger* Gill 1864) were all categorized as non-focal semi-pelagic rockfish, and all remaining rockfish were categorized as demersal rockfish. Black and Blue/Deacon Rockfish < 20 cm in length (as measured using EventMeasure stereo software) were classified as juvenile Black/Blue/Deacon Rockfish. This cut off was based on genetic identification of hook and line caught fish, which suggested fish < 20 cm in length are difficult to positively identify visually, even when in-hand (Rasmuson *et al.*, 2021b).

To generate a volumetric density of fish (number of fish per m³) for each video deployment, we followed the methods of Williams *et al.* (2018) to convert the viewable area into a volume. We then used the average number of each species identified in all 5 frames to generate an average density of rockfish for each video deployment conducted.

Acoustic data were processed in Echoview v9.0 using a combination of echo counting and echo integration methods. We defined the near bottom acoustic dead zone from 0-1 m off bottom, and the nearfield dead zone from 2.5-0 m from the transducer face; both areas were excluded from all analyses (Ona and Mitson, 1996). Our acoustic data had a large amount of noise from zooplankton and other acoustic scatterers, so masking procedures were used to reduce noise (Fig. 4).

2.2.2 ACOUSTIC ANALYSIS

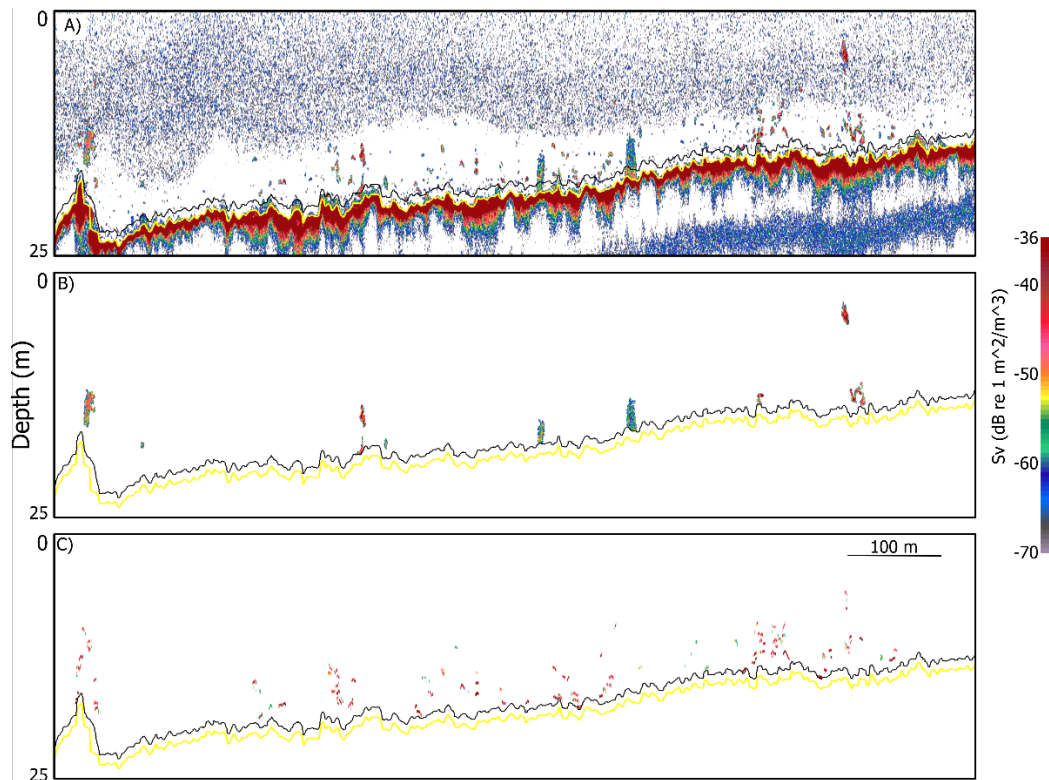


Fig. 4 A) Uncorrected echogram with the bottom detection line (yellow line), and the near bottom acoustic dead zone exclusion line (black line), B) Echogram displaying only the fish schools identified by the school detection algorithm; all other data have been masked, C) Single targets identified in the echogram that were used in conjunction with the fish tracking algorithm; all other data have been masked. In panels B and C, data from the near bottom acoustic dead zone were masked by the processing algorithms.

2.2.2.1 ECHO INTEGRATION

Regions for echo integration were identified using the Sawada index as well as the ratio of multiple echoes (Sawada *et al.*, 1993). Regions where the Sawada index values were < 0.04 , and the ratio of multiple echoes value was < 0.7 , were used for single target analysis. Both methods allow the research to identify areas where the density of fish is too large to count individuals. In regions where densities of fish were too large, data were analyzed using echo integration. Schools were identified on echograms, smoothed with a 3x3 median filter, and defined using the school detection algorithm described by Barnage (1994), Haralabous (1996), and Nero and Magnuson (1989). The algorithm used a series of thresholds and criteria to define regions as a school of rockfish, which were then edited by the reviewer (**Table 1**). The unfiltered backscattering data were then masked to only display the regions defined as schools by the

school detection algorithm. The raw total backscatter (NASC) was exported for each transect as a whole, to be used for population estimations, as well as exported for individual schools, to be used in the selection of a target strength model. Backscattering cross-section data were calculated in 1 cm bins, and scaled for relative abundance of each species, or species group, following methods of Robertis et al. (2014). Backscattering cross-section data (σ_{bs}) were calculated using the standard target strength to length equation given as:

$$TS=20\log_{10}(L)-b_{20} \quad E.1$$

where TS is the fish target strength, L is the fish length in cm, and b_{20} is a species-specific constant. See section 2.2.3 below for how b_{20} was determined for this study. Length data were obtained from a survey-wide distribution of stereo measurements from the BASSCam. Mean back scattering cross-section was calculated as

$$\overline{\sigma_{bs}} = \sum_{i,g} (P_{i,g} * \sigma_{bs,i}) \quad E.2$$

Where $\overline{\sigma_{bs}}$ is the mean back scattering coefficient, $P_{i,g}$ is the proportion of a group of rockfish (g) at length i and $\sigma_{bs,i}$ is the back scattering cross-section at length i . The proportion of each species group by length was calculated as

$$P_{i,g} = \frac{NCamFish_{i,g}}{\sum NCamFish_i} \quad E.3$$

Where $NCamFish_{i,g}$ is the number of fish in a length bin (i) for a given species group (g) observed in by the BASSCam, and $\sum NCamFish_i$ is the sum of all rockfish groups in a length bin i observed by the BASSCam. Mean back scattering cross-section was converted to number of fish using

$$Eldens_{i,g,t} = \left(\left(\frac{NASC_t}{4\pi\sigma_{bs}} \right) * P_{i,g} \right) * \left(\frac{1}{3.43 * 10^6} \right) \quad E.4$$

Where $Eldens_{i,g,t}$ is the density of fish in a length bin i for each species group (g) in number of fish per meter square on given transect t . $NASC_t$ is the nautical areal scattering coefficient provided as an output from the acoustic software for transect t .

Table 1. Parameter settings for school detection, single target detection and fish tracking in Echoview acoustic software. Note: dB values in this table are dB re. 1 m²/m³.

School Detection

<i>Parameter</i>	<i>Value</i>
Minimum school length	5.00 m
Minimum school height	2.00 m
Minimum candidate length	3.00 m
Maximum vertical linking distance	5.00 m
Maximum horizontal linking distance	2.00 m

Single Target Detection

<i>Parameter</i>	<i>Value</i>
Compensates target strength threshold	-60.00 dB
Pulse length determination level	6.00 dB
Minimum normalized pulse length	0.30
Maximum normalized pulse length	2.00
Maximum beam compensation	12.00 dB
Maximum standard deviation exclusion of minor axis angles	4.00 degrees
Maximum standard deviation exclusion of major axis angles	4.00 degrees

Fish Tracking (collected for 4d data)

<i>Parameter</i>	<i>Value</i>
Alpha major axis	0.800
Alpha minor axis	0.800
Alpha range	0.800
Beta major axis	0.100
Beta minor axis	0.100
Beta range	0.100
Target gate major axis exclusion distance	1.00 m
Target gate minor axis exclusion distance	1.00 m
Target gate range exclusion distance	0.20 m
Target gate major axis missed ping expansion	50.00 %
Target gate minor axis missed ping expansion	50.00 %
Target gate range missed ping expansion	100.00 %

2.2.2.2 ECHO COUNTING

For regions analyzed by echo counting, we follow the protocol outlined in Tschersich (2015) for identifying single targets. Echoes within these regions were identified using the Echoview single target identification algorithm described by (Soule, 1997; Ona, 1999) which differentiates single fish signals from multiple fish signals. However, multiple detections are often made of the same fish so a fish tracking algorithm (Balk and Lindem, 2000; ICES, 2000), was then applied to identify where groups of single targets were in fact a single fish (**Table 1**). Following (Tschersich, 2015) fish density was computed from individual fish tracks using:

$$ECdens_t = \frac{1}{l_t} \sum_{f=1}^{f_n} \left(\frac{1}{2 \tan(\theta) * z_n} \right) \quad E.5$$

ECdens is the summed density contributions (number of fish per m²) of all single fish tracks on a specific transect (denoted by *t*), *l* is the length of the transect in meters, ϑ is half of the full angle beam width of the transducer (3.25° in this case), and *z* is the depth, in meters, of each individual fish track (denoted by *f*) from the face of the transducer.

2.2.2.3 TARGET STRENGTH MODEL- USED FOR ECHO INTEGRATION

Echo integration requires a target strength to length relationship (E.1). In previous acoustic studies of rockfish in the Northeast Pacific Ocean, the generalized regression model for physoclist fish ($b_{20} = -67.4$, reported by Foote (1987)) has been used to convert backscattering data to abundance estimates (Stanley, 2000; Rooper, 2010; Jones *et al.*, 2012). However, recent work in the Northwest Pacific has provided target strength regression models for the congeneric Korean Rockfish (*Sebastes schlegeli* Hilgendorf 1880) ($b_{20} = -70.93$), and Dark-banded Rockfish (*Sebastes inermis* Cuvier 1829) ($b_{20} = -72.8$) (Kang and Hwang, 2003; Hwang, 2015). In an attempt to confirm our selection of a target strength model, we converted backscatter values into a volumetric density of fish for each school identified in the acoustics using each of the three existing target strength regression models (Foote, 1987; Kang and Hwang, 2003; Hwang, 2015). Based on morphological examination of Korean and Dark-banded Rockfish, we hypothesized that a model “in-between” these two species may be more representative of Black, Blue and Deacon Rockfish. We took the arithmetic mean of the b_{20} values from these two target strength regression models, providing an average *Sebastes spp.* Model ($b_{20} = -71.9$). Backscattering data for individual schools was converted into densities using the length distribution derived from video deployments conducted within 10 m of an ensoufied fish school. We then used a one-way Analysis of Variance (ANOVA) with a Tukey-HSD post hoc test

to compare the volumetric fish densities from the acoustics; to the volumetric densities of fish from the camera deployments.

2.2.2.4 POPULATION ESTIMATE

No attempts were made to use a modeling or geostatistical approach to generate a population estimate. Further, no attempts were made to estimate or correct for the component of the population that resided within the near bottom acoustic dead zone. Only a very simple design-based approach was used. BASSCam data from all video deployments were combined to determine the ratio of each species abundance relative to total fish abundance as well as to generate a distribution of lengths for each species. Species specific ratios by size (1 cm bins) from the BASSCam were used to convert the hydroacoustic data into a survey level density estimate of Black Rockfish and of Blue/Deacon Rockfish. Densities were generated independently for the echo counting and echo integration data. Average echo integration density of each group of rockfish for Seal Rock was calculated as the total density for each group at each transect averaged by the total number of transects sampled:

$$\overline{EIdens}_g = \frac{\sum_t(\sum_i EIdens_{g,t})}{n_t} \quad E.6$$

$$EIstddev_g = \sqrt{\frac{\sum(EIdens_{g,t} - \overline{EIdens}_g)^2}{n_t}} \quad E.7$$

Where \overline{EIdens}_g is the average echo integration density in number of fish per m² of each group of rockfish (*g*) for the entire reef, and n_t is the total number of transects ($n = 38$). $EIstddev_g$ is the standard deviation of average echo integration density for each group of rockfish. Average echo counting density and standard deviation was calculated as:

$$\overline{ECdens}_g = \frac{\sum ECdens_t}{n_t} \quad E.8$$

$$ECstddev_g = \sqrt{\frac{\sum(ECdens_t - \overline{ECdens}_g)^2}{n_t}} \quad E.9$$

Where \overline{ECdens}_g is the average echo counting density for each rockfish group (*g*) in number of fish per m², $ECstddev_g$ is the standard deviation of echo counting density, and n_t is the total number of transects ($n = 38$). These densities and standard deviations were then multiplied by the total survey area (m²) to generate an average abundance and standard deviation of rockfish at Seal Rock. Survey area (m²) was calculated by drawing a polygon around the outer edges of all transects. Abundance estimates from the single target and echo integration methods were summed to generate a total abundance.

2.2.2.5 NEAR BOTTOM FISH POPULATION

While it would be ideal to know exactly how many fish were located only within 1 m of the bottom (the near bottom acoustic dead zone), our downward camera includes fish counts from both the near bottom dead zone (78% of volume viewed) and those above the near bottom dead zone (22% of volume viewed). To determine if our focal species are located above the bottom 1 meter of the water column, we examined the ratio of fish counted in downward facing camera to the total number of fish counted in both the forward and downward facing cameras for Black, Blue/Deacon Rockfish and juvenile Black/Blue/Deacon Rockfish using the following formula;

$$\text{BottomCameraRatio} = \frac{n_{fish_d}}{n_{fish_d} + n_{fish_f}} \quad E. 10$$

Where BottomCameraRatio is the ratio of fish counted in the down camera (n_{fish_d}) relative to the number counted in the forward (n_{fish_f}) and down combined.

2.2.2.6 FISH ORIENTATION AND BEHAVIOR

Orientation of a fish's swim bladder, and consequently the fish's overall orientation, has the potential to influence acoustic backscattering cross-section values, and therefore alter the final abundance estimate. Underwater stereo cameras provide us with the ability to study the three-dimensional underwater orientation of our focal species. For each camera deployment, we determined the average orientation of the camera system relative to a flat horizontal plane with data from a tilt sensor. Using the three-dimensional coordinates of the head and tail of each measured fish, obtained during the measurement process in EventMeasure, we applied trigonometric functions to determine the orientation of the fish relative to a plane parallel with a hypothetical horizontal seafloor. These data were not used in this study to correct the acoustics due to the lack of tilt corrected target strength models for *Sebastes spp.* Future work hopes to incorporate orientation data into population estimates.

To assess how deploying the BASSCam influences the behavior of a fish school, we compared the acoustic backscattering values of three schools of fish. Deployments occurred in approximately 30 m of water depth, where the area sampled by the acoustic beam had an approximate sample area of 33 m². Each school was observed: before the camera was deployed, while the camera was deployed in the school, and after the camera was removed. To do this, the camera was deployed (to the seafloor) directly below the acoustic transducer while a fish school was ensonified. The buoys on the camera provide an acoustic signal that was visible during the deployment, the only deployments used were those where the camera was visible under the transducer for the entire test period. For the duration of the two-minute deployment, the captain positioned the vessel over the top of the camera and school, using both of the vessel propellers. The captain then kept the vessel over the school while the camera

was retrieved, and for an additional two minutes after the camera was removed. Upon review of this data, the estimated backscattering value attributable to the camera was subtracted from the school. Corrected backscattering values of the fish school for each time-period were compared using an ANOVA.

3. RESULTS

Thirty-eight acoustic transects were completed for a total sampled distance of ~120 km which encompassed 24.1 km² of reef (**Fig. 1**). From the acoustics, the school identification algorithm identified 1,018 schools of fish presumed to be Black, Blue or Deacon Rockfish. The echo counting algorithms identified 2,077 fish tracks presumed to be Black, Blue and Deacon Rockfish (**Fig. 5**).

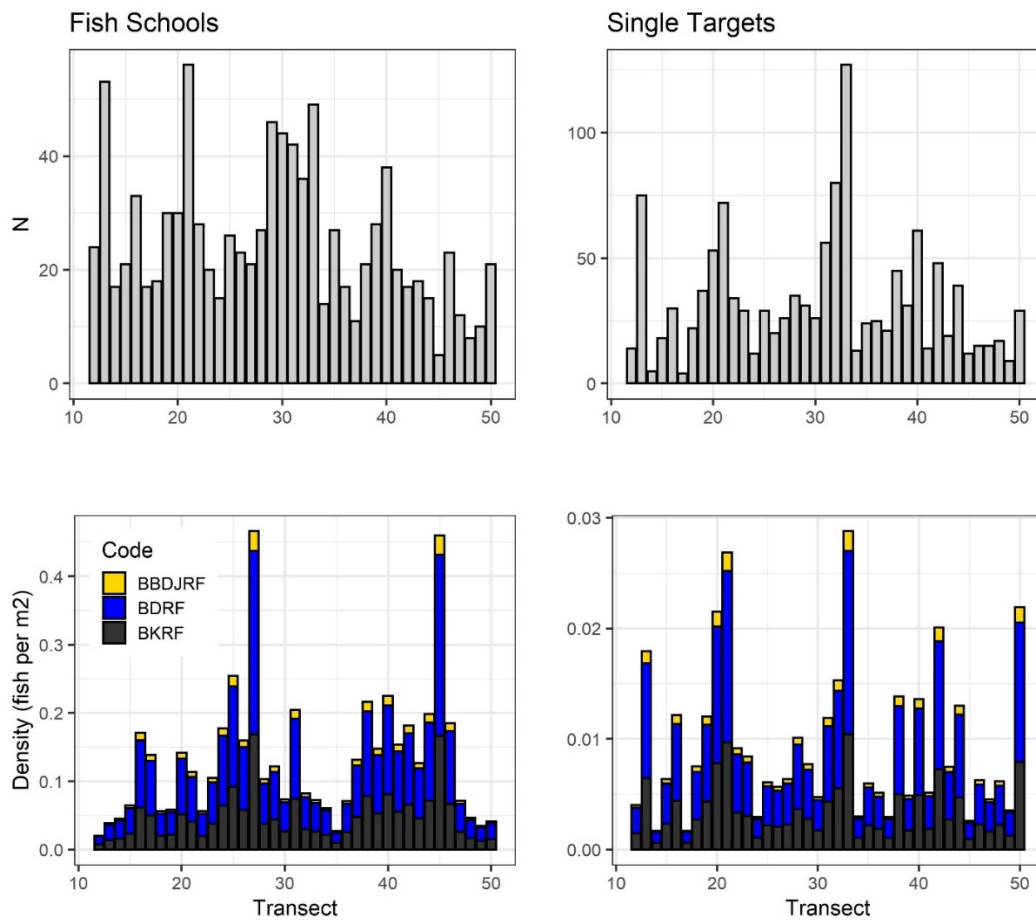


Fig. 5 Number of schools (top left) and their conversion to density (no. fish/m²) for the three focal species groups (bottom left). Number of single echoes (top right) and their conversion to density (no. fish/m²) for the three focal species groups (lower right). BBDJRF are juvenile Black/Blue/Deacon Rockfish, BDRF are Blue/Deacon Rockfish, and BKRF are Black Rockfish.

One hundred twenty video deployments were conducted at depths ranging from 12 to 38 m (**Fig. 6**). Most deployments occurred within 15 m of the target fish school identified during the acoustic transect. Of the 120 video deployments, fish were observed on 81 deployments. Blue/Deacon Rockfish were the most frequently observed species followed by Black Rockfish. Of the 3,383 fish identified from video, 2,514 were observed by the forward cameras, and 869 in the downward camera (**Table 2**). The majority of Black and Blue/Deacon Rockfish were observed in the forward cameras rather than in the downward facing camera. Of the rockfish observed in the downward facing camera, 17% of the total observed were Blue/Deacon Rockfish, 36% Black Rockfish, and 42% juvenile Black/Blue/Deacon Rockfish.

Table 2. Number of each species or species group counted in the forward or downward facing cameras on the suspended BASSCam.

	Forward Facing Camera	Downward Facing Camera	Total Number of Fish Counted
Juvenile Black/Blue/Deacon Rockfish	155	114	269
Blue/Deacon Rockfish	1,429	283	1,712
Black Rockfish	899	452	1,351
Fish Without a Swim Bladder	6	12	18
Fish With a Swim Bladder	21	3	24
Unidentified Rockfish	4	5	9
Total Number of Fish Counted	2,514	869	3,383

Of the 25 deployments where Blue/Deacons were observed, in only one instance were they solely present in the downward facing camera (**Fig. 6**). Of the 36 deployments where Black Rockfish were observed, in only three instances were they solely present in the downward facing camera. Of the 15 deployments where juvenile Black/Blue/Deacon Rockfish were observed, in only four instances were they solely present in the downward facing camera (**Fig. 6**). Further, in 23 of 25 deployments (92%), >50% of Blue/Deacon Rockfish were observed in the forward cameras, and in 29 of 36 deployments (80.5%), >50% of the Black Rockfish were observed in the forward cameras. In 9 of 15 deployments (60%) >50% of juvenile Black/Blue/Deacon Rockfish were observed in the forward cameras.

Black Rockfish were observed at a slightly closer distance to the BASSCam than Blue/Deacon Rockfish (**Fig. 7**) and juvenile Black/Blue/Deacon Rockfish were the closest. On average, all species and size classes were observed at distances ranging from 0.5 m to approximately 2.5 m

from the BASSCam. On average, Blue/Deacon Rockfish (mean: 267 ± 41 mm) were smaller than Black Rockfish (mean: 349 ± 50 mm, **Fig. 8**). Length data of juvenile Black/Blue/Deacon Rockfish were bimodal with an average length of 161 ± 30 mm.

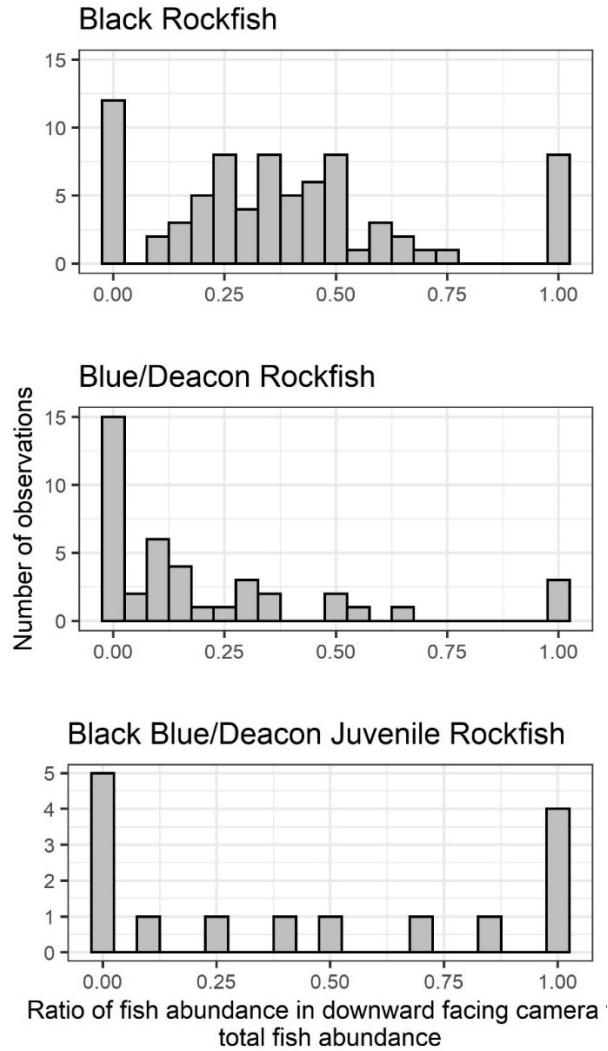
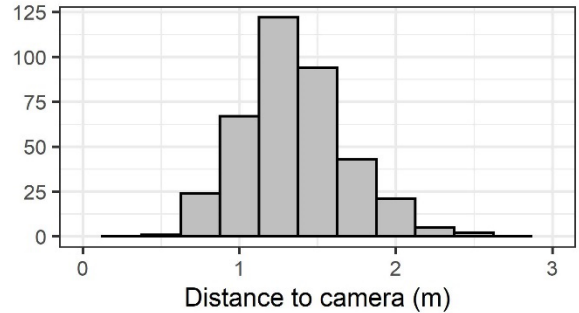
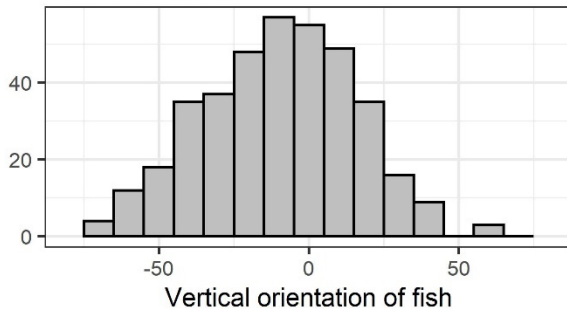
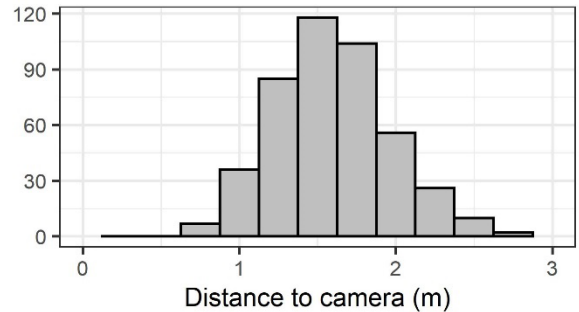
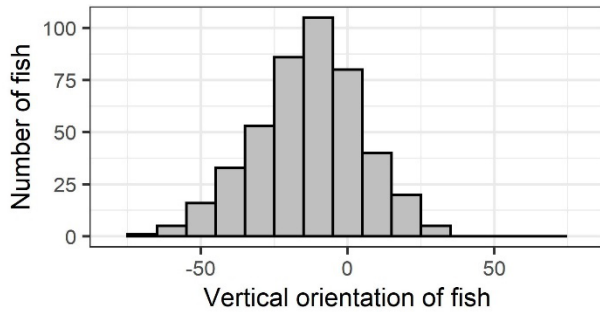


Fig. 6 Histogram displaying the ratio of Black, Blue/Deacon, and juvenile Black/Blue/Deacon Rockfish abundance in the downward facing camera relative to the total abundance of fish (forward + downward). A value of 1 denotes fish observed only in the downward facing camera, a value of 0 denotes fish were only observed in the forward camera, and .5 indicates 50% of the fish were in the forward camera and 50% were in the downward facing camera.

Black Rockfish



Blue/Deacon Rockfish



Black Blue/Deacon Juvenile Rockfish

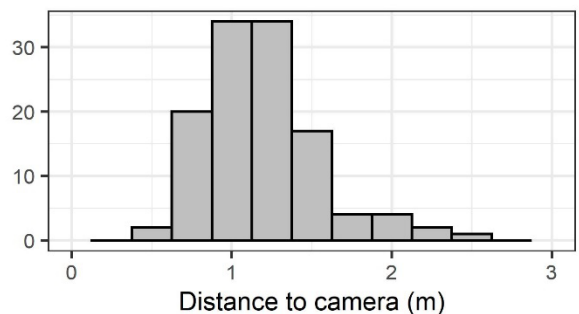
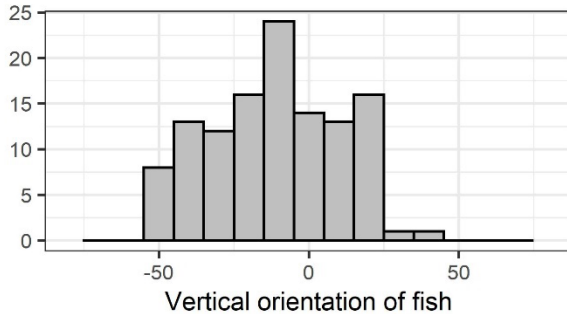


Fig. 7 The measured distance of Black, Blue/Deacon, and juvenile Black/Blue/Deacon Rockfish to the BASSCam (Left) and vertical orientation of Black, Blue/Deacon and juvenile Black/Blue/Deacon Rockfish relative to a hypothetical horizontal plane extending out from the stereo cameras (Right). Left- Only fish that were measured contributed to the distance data. Right- Positive values denote the fish's head was tilted upwards towards the water surface, and negative values denote the fish's head was tilted down towards the seafloor. All vertical fish orientations were corrected for tilt of the BASSCam.

A comparison of Black Rockfish lengths from our video to lengths of fish caught and retained in the recreational fishery (mean: 386 ± 40 mm), and by the fishery independent PIT tagging project (mean: 372 ± 38 mm), show similar size distributions, although the camera system observes a larger number of smaller fishes than those captured by fishing. For Blue/Deacon

Rockfish, the camera system observed much smaller fish than those retained by the recreational fleet (mean: 321 ± 38 mm). For all species, the largest size classes captured by the recreational fleet were also observed by the camera system, though the relative abundance of these larger fishes was reduced in the video data due to the high abundance of smaller fish.

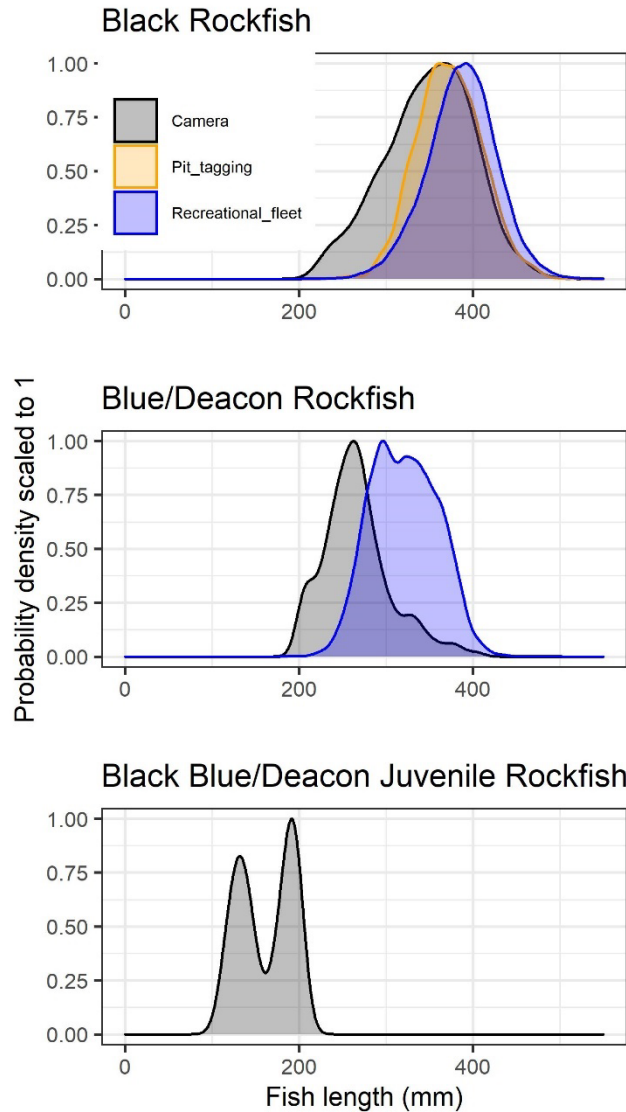


Fig. 8 Scaled size distributions of Black, Blue/Deacon, and juvenile Black/Blue/Deacon Rockfish, observed by the BASSCam (gray area), caught by the recreational fleet (blue area), and caught as part of a fisheries independent PIT tagging project (gold area).

Blue/Deacon Rockfish heads were oriented below a horizontal plane located at the location of camera deployment at 13.5 ± 18.0 degrees, on average. Black Rockfish were also oriented downwards at 9.6 ± 25.3 degrees (**Fig. 8**). Juvenile Black/Blue/Deacon Rockfish heads were oriented upwards at 5.2 ± 21.5 degrees. The distribution of Blue/Deacon Rockfish orientations

was much narrower than for Black Rockfish, while juvenile Rockfish distribution has more uniform shape than that of adult Black and Blue/Deacon Rockfish.

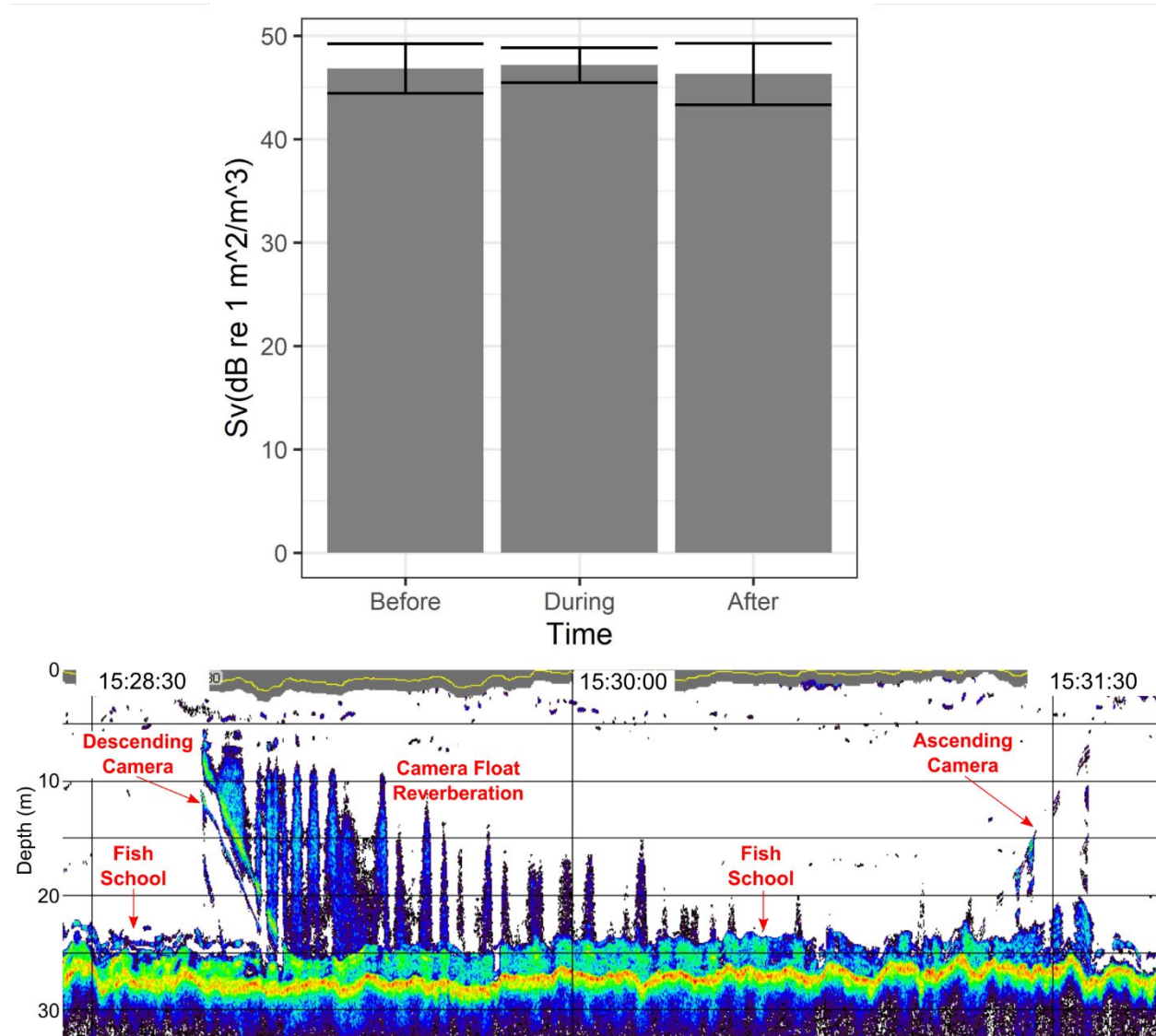


Fig. 9 Changes in average backscattering values before, during, and after the deployment of the BASSCam into a school of fish (upper), and an example echogram of the camera deployment into a school of fish, during observations of the school, and retrieved from a school of fish (lower).

For the three test deployments of the BASSCam below the transducer used to test for fish behavioral response to the camera (a measure of the tool's detectability), there was no significant change in the backscattering values of the school before, during, or after deployment of the BASSCam ($F(2,6)=0.052$, $p=0.95$; **Fig. 9**).

Forty-three camera deployments were conducted within 10 m of an ensonified school of fish. Average volumetric density of individuals schools of rockfish calculated from the video data was 0.47 rockfish per m³ (**Fig. 10**). The density estimates from the video data differed significantly from the acoustic density estimates generated using the Foote model, but did not differ significantly from the other three models (**Fig. 10**; $F(4,210)=6.142$, $p<0.001$). Although all acoustic densities generated with rockfish-specific target strength models did not statistically differ from camera derived densities; our b_{20} averaged model provided fish densities (0.46 fish per m³)

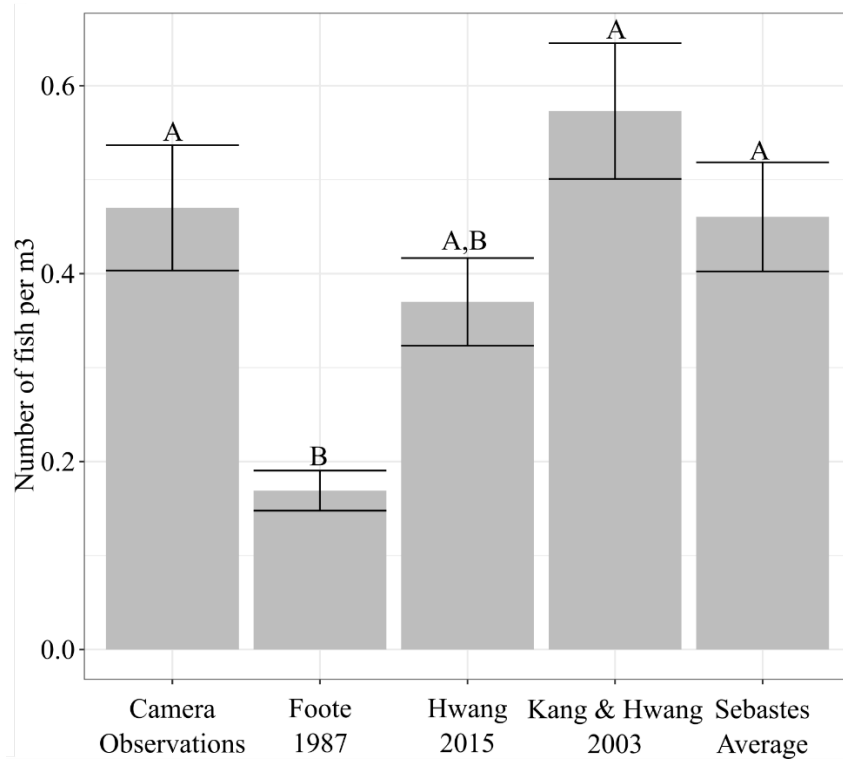


Fig. 10 Volumetric densities (no. fish/m³) generated from our camera system observations and fish schools identified in the acoustics. Acoustics were converted from backscattering values to densities using length data from the closest video deployment to that school. Only camera deployments occurring within 10 m of fish schools are reported here. Letters over bars denote significant statistical differences between datasets, as identified with a Tukey HSD test.

most similar to video derived densities. Therefore, going forward, all echo integrations were conducted using the b_{20} value of -71.9 dB re. m^2/m^3 .

On average, there were 25.4 ± 12.4 (mean \pm standard deviation) schools of fish and 33.4 ± 24.7 single target echoes identified per acoustic transect (**Fig. 5**). The following estimates are generated from combining the acoustic data with species composition and length data from the stereo video. For Black Rockfish, the average density of schooling individuals was 0.04 ± 0.03

fish per m² and for single echoes the average density was 0.003 ± 0.003 fish per m². For Blue/Deacon Rockfish, the average density of schooling individuals was 0.08 ± 0.06 fish per m², and 0.005 ± 0.004 fish per m² for single echoes. For juvenile Black/Blue/Deacon Rockfish, the average density of schooling individuals was 0.008 ± 0.006 fish per m², and 0.0005 ± 0.0004 fish per m² for single echoes. Extrapolated to the reef area, this results in a total population of 1,188,222 ± 601,249 Black Rockfish; 1,888,731 ± 955,712 Blue/Deacon Rockfish; and 204,866 ± 103,663 juvenile Black/Blue/Deacon Rockfish (**Table 3**). Our coefficient of variation for these estimates was 50.6%.

Table 3. Design-based estimate of fish abundance at Seal Rock. Values are number of fish plus and minus the standard deviation.

	Single Targets	Fish Schools- Echo Integration	Combined
Black	80,161 ± 58,610	1,108,061 ± 848,272	1,188,222 ± 601,249
Blue/Deacon	127,420 ± 93,164	1,761,312 ± 1,348,366	1,888,731 ± 955,712
Juvenile Black/Blue/Deacon Rockfish	13,821 ± 10,105	191,045 ± 146,254	204,866 ± 103,663
Combined	221,402 ± 161,879	3,060,417 ± 2,342,891	3,281,819 ± 1,660,624

4. DISCUSSION

The benefit of this survey method is not only the ability of the tool to work in untrawlable habitat during rougher ocean conditions than most other survey techniques, but to also work on chartered vessels, of a variety of sizes, with a small scientific crew. These methods could easily be implemented with a crew of three. In a separate study, these same tools were also operated off a 7.5 m trailer-able boat, which allowed for application in shallow waters near wash rocks and shorelines, areas known to be important habitat for nearshore rockfish (Love *et al.*, 2002). The versatility and cost-effective nature of this survey method is in contrast with other common methods of nearshore rockfish methods such as PIT tagging and hook and line sampling, which require a captain, deckhands, and multiple anglers; often resulting in a crew of 10 + individuals. Oregon’s ocean is notoriously rough and difficult to work on, so developing tools and methods that require relatively few days at sea are ideal. The biggest drawback of this survey method is the extensive post processing required for both the video and acoustic data. However, the use of pre-developed workflows in both the acoustic software and the video processing software significantly decreased processing time.

For survey data to be incorporated into a stock assessment or used to produce an independent abundance estimate, the “catchability” coefficient, must be estimated or measured (Arreguin-Sanchez, 1996; Kotwicki *et al.*, 2018). Catchability for a survey tools that don’t actually catch fish is deemed detectability. Detectability of fish by an acoustic transducer is more influenced by the general behavior of the fish rather than the fish’s response to the tool (Lawson and Rose, 1999; Stanley, 1999). In the case of Black Rockfish, high resolution telemetry work suggests that as long as operations are conducted during daylight hours, fish should be detectable by the

acoustics (Parker *et al.*, 2008). Using similar telemetry data, we have shown that Deacon Rockfish have a distinct diel cycle (Rasmuson *et al.*, 2021a). Telemetry data demonstrated Black and Deacon Rockfish lie directly on the substrate at night making them undiscernible from the acoustic return from the bottom. Combining these data with other high resolution acoustic telemetry data for nearshore rockfish, we demonstrated that Deacon and Black Rockfish should be available to hydroacoustics during daylight hours (Rasmuson, 2021). In a previous exploratory study, we routinely collected acoustic data, during daylight hours, on four transects at Seal Rock over the course of two months, and found that regardless of time of day, sea state, and tidal cycle, fish schools were always present, and frequently observed at the same locations along the transect (Rasmuson unpublished data). Similarly, detectability of rockfish with video tools is affected by time of day (Rooper *et al.*, 2020), indicating video operations should be conducted during daylight hours as well.

The detectability of fish by cameras has received a lot of attention in the last decade (Stoner *et al.*, 2008). Our survey vessel consistently deployed the BASSCam very close to the intended target, and fish were observed in a majority of deployments. Further, when the camera was deployed directly below the transducer there was little, or no avoidance or attraction behavior observed. Fish can either be attracted to, or repelled by the camera, due to sounds, lights, or simply the presence of the camera on the seafloor (Koslow *et al.*, 1995; Somerton *et al.*, 2017). In this study, we saw no change in the acoustic signature of the school of fish throughout camera deployment, and we found no trend in the number of fishes, of either species, observed for the duration of the video. Overall, our suspended camera design and deployment method does not seem to repel or attract fish. While we cannot fully discount detectability issues in our survey method, we hypothesize that the effects are minimal.

The remaining component of the detectability discussion is the effect of fish inhabiting the near bottom acoustic dead zone, temporarily or permanently. While there have been many advances in methods to correct for, or estimate, fish abundances in the acoustic dead zone (Ona and Mitson, 1996; Mello and Rose, 2009), exclusion of data from the near bottom region, as we have done in the present study, remains the most common methodology. Other work on *Sebastes spp.* suggests a general pattern of the fish moving out of the dead zone during the day and into the dead zone at night (Stanley, 1999; Rooper, 2010). In our survey, the use of the downward facing camera allowed us to estimate the ratio of our focal species in the near the bottom region. Our finding of a similar ratio of Black Rockfish located 0-1 m above the seafloor to those located <1 m above the seafloor, and fewer Blue/Deacon Rockfish in 0-1 m than in <1 m, suggests our focal species are located above the near bottom dead zone, and are therefore available to the acoustic signal during daylight sampling. At our deepest survey depth of 36 m, the dead zone was calculated to be 0.33 m thick (following Ona and Mitson 1996), therefore excluding data within 1 m of the bottom from our data analysis is extremely conservative. Such

a conservative approach was taken because there is considerable debate about how large of a contribution to a population estimate fish within 1 m represent. Despite this conservative exclusion, our population estimate for Black Rockfish was similar to population estimates generated by the PIT tagging project, further supporting our hypothesis that most semi-pelagic fishes are located above the near bottom acoustic dead zone during daytime sampling. The combined effects of the dead zone on survey design and survey results are currently being studied by pairing a larger scale hydroacoustic/video survey with data from a remotely operated vehicle (ROV) (Rasmuson In Preparation). Although not done in the present study, data from the downward facing camera could be used to provide measured correction indices to estimate the abundance of fish in the near bottom dead zone. Modeling population estimates within the near bottom dead zone will be possible in future studies when the survey is implemented at a statewide level resulting in a larger dataset. Nevertheless, based on the results of this pilot study, we confidently conclude that a combined acoustic and suspended camera survey method is an effective sampling methodology for Oregon's nearshore rockfish and can be used conservatively by excluding data in the near bottom dead zone, or less conservatively by expanding the population estimate into the near bottom dead zone. In future studies we suggest the exclusion zone can and should be reduced from 0-1 m off bottom to 0-0.5 m .

Studies continue to show that fishery independent surveys are critical to effective fisheries management (Hilborn, 2007; Dennis *et al.*, 2015) and, as mentioned, trawls are currently the primary survey tool used throughout the world's oceans. However, while rockfish assemblages differ widely between trawlable and untrawlable areas, trawls are inoperable in rugose habitats (Matthews and Richards, 1991; Zimmermann, 2003). Further, trawls lethally sample fish which can potentially create social concerns and impact benthic habitats. The use of cameras and acoustics are an attractive alternative or complement to trawl surveys because of their ability to operate in these regions, and because they have been proven to be effective for a variety of rockfish species (Williams *et al.*, 2010; Jones *et al.*, 2012). Jones *et al.* (2012) demonstrated that density estimates from trawl and acoustic surveys differed by as much as 5-60 times, signaling potential for a significant underestimation of population size when applying trawl data to untrawlable habitats. As both acoustics and cameras provide volumetric densities of fish, there is an ability to relate the data from the two tools. A point which we illustrate here by using our video-derived volumetric densities to help inform which target strength to length regression model to use.

Another unique benefit of using a stereo camera system is the ability to generate fish orientation data, a variable which can strongly influence a population estimate derived from acoustics (Huse, 1996; McClatchie, 1996). While it is worth noting that a video reviewer only measures a fish when the fish is oriented close to parallel with the camera faces, the

orientation of the fish, relative to a horizontal plane extending from the cameras (i.e., head tilted towards the surface or bottom), does not influence the reviewer's choice to measure a fish. Therefore, bias in our fish orientation data based on our method for measuring fish is assumed to be minimal. The use of cameras to provide tilt data has proven effective for krill and mackerel (Kubilius *et al.*, 2015; Fernandes *et al.*, 2016). Kang and Hwang (2003) demonstrated that for *Sebastes schlegeli*, the tilt of the fish changed the target strength of the fish by as much as 30 dB re. m^2/m^3 . In the current study, we have not applied any orientation corrections to our data because target strength models have not been developed for our focal fish species (Frouzova *et al.*, 2005). We are in the process of developing models of the swim bladders for future use. These new swim bladder models, used in combination with the orientation of the fish, will increase the precision of the population estimates generated by the combination of underwater video and acoustics data.

Our stereo camera system targets semi-pelagic rockfish more completely than other survey tools. It provides a more complete representation of the length distributions of our focal species than survey gear such as trawls and hook and line. Hook and line suffers from hook selectivity and trawls suffer from mesh size dependent selectivity as well as net avoidance (Campbell *et al.*, 2014; Kuriyama *et al.*, 2019). While behavioral avoidance is common with underwater camera systems, our work demonstrated no change in school size with the deployment of our camera system, which suggests minimal behavioral impacts. The greater density of small fishes in our length distributions also suggests we are sampling across the size distribution of nearshore rockfish. Especially in acoustics, where length data are directly used to calculate biomass, this strongly demonstrates the benefit of using a benthically anchored buoyant camera system in combination with hydroacoustics. Overall, the novelty of our camera system, over other tools used in conjunction with acoustics, is the addition of both the downward facing camera and the tilt sensor. Both tools make the camera system uniquely well adapted to working with rockfish in highly turbid and productive waters because they provide the opportunity to apply corrections to the population estimate. Here, we did not apply tilt corrections or near bottom dead zone corrections from the downward facing camera due to several limitations that will be addressed in subsequent studies.

The combined methodology of our study produces comparable population estimates to previous survey results. The resulting population estimate from our combined video and acoustic survey suggest a population of ~ 1.2 million $\pm 600,000$ (mean ± 1 SD) Black Rockfish within the survey area. An eleven-year-long PIT tagging study that encompassed our study area, and a few additional small reefs, reported an abundance of 1-2 million Black Rockfish (Krutzikowksy *et al.*, 2019). The similarity between the two studies, suggests that the combination of acoustics and underwater cameras can provide an accurate population estimate. We offer that when used in combination, hydroacoustic data and data from our

suspended stereo camera system, create a robust survey method for nearshore rockfish. In the future, combining this methodology with hook and line sampling to provide age and maturity samples should create a robust nearshore fisheries-independent survey. In the short-term, this would provide stock assessors with an estimate of biomass for this particular year, which could be used in the assessment to inform absolute stock size (i.e., help to reduce uncertainty in the estimation of population scale). Population size is the most uncertain parameter in Black Rockfish, and most other nearshore species stock assessments, which creates extremely high levels of uncertainty associated with quotas and has implications for sustainable fisheries management. This method could be used iteratively over time to create an index of abundance for Black Rockfish which fills a critical need for west coast nearshore species, as identified by regional management councils.

Overall, we propose the survey method outlined here is an efficient and effective way to survey Oregon's nearshore rockfish. To be effective this survey should be extended throughout Oregon's nearshore waters so as to provide a complete estimate of nearshore rockfish abundance. Increasing the habitat coverage of fishery independent surveys is a necessary addition to the stock assessment process, and the method described here may serve as a relatively low-cost, high return survey for the rugose and untrawlable nearshore environment. The acknowledged drawback of video and acoustic tools is the amount of post-processing required for the data collected. However, we have demonstrated that development of a standardized analysis process can reduce processing time significantly. Further, as automated approaches continue to advance, the requirement for human hours to process these data will decline (Richards *et al.*, 2019). Another flaw of this survey method was the coefficient of variation was quite high (~50%). Going forward, a stratified survey design (adjusting effort allocations based on bottom hardness) combined with a geostatistical or model-based abundance estimation may allow for a reduction in variance. A preliminary attempt to model the population size of these same data using a geostatistical approach resulted in a coefficient of variation of ~19% and very little change in the population estimate, further supporting the theory that a larger, more robust survey design, combined with species specific target strength models, will allow generation of accurate population estimates for Oregon's economically and ecologically important nearshore rockfish.

DATA AVAILABILITY

The data underlying this article will be shared on reasonable request to the corresponding author.

ACKNOWLEDGMENTS

The authors thank the Saltonstall-Kennedy grant program NA17NMF4270223 for funding the staff time and fieldwork. We thank David Fox, Greg Krutzikowsky, Scott Marion and Alison Whitman for developing the grant. We thank Captain Dave DeBelloy and crew of the CPFV Enterprise. We thank Maggie Sommer, and David Fox from ODFW and Dr. Chris Rooper from Fisheries and Oceans Canada for providing early reviews of the manuscript. Drs. Dezhong Chu, Sandy Parker-Stetter and Kresimir Williams provided valuable advice on the data processing.

LITERATURE CITED

- Arreguin-Sanchez, F. 1996. Catchability: a key parameter for fish stock assessment. *Reviews in Fish Biology and Fisheries*, 6. <http://link.springer.com/10.1007/BF00182344> (Accessed 9 September 2020).
- Bacheler, N., Geraldi, N., Burton, M., Muñoz, R., and Kellison, G. 2017. Comparing relative abundance, lengths, and habitat of temperate reef fishes using simultaneous underwater visual census, video, and trap sampling. *Marine Ecology Progress Series*, 574: 141–155.
- Balk, H., and Lindem, T. 2000. Improved fish detection in data from split-beam sonar. *Aquat Living Resour*, 13: 297–303.
- Barange, M. 1994. Acoustic identification, classification and structure of biological patchiness on the edge of the Agulhas Bank and its relation to frontal features. *S Afr J Mar Sci*, 14: 333–347.
- Beamish R.J., and D.A. Fournier. 1981. A method for comparing the precision of a set of age determinations. *Canadian Journal of Fisheries and Aquatic Sciences* 38: 982–983.
- Boettner, J., and Burton, S. 1990. Hydroacoustic stock assessment study of Washington coastal black rockfish of Washington state. Washington Department of Fish and Wildlife Technical Report, 108.
- Boldt, J. L., Williams, K., Rooper, C. N., Towler, R. H., and Gauthier, S. 2018. Development of stereo camera methodologies to improve pelagic fish biomass estimates and inform ecosystem management in marine waters. *Fisheries Research*, 198: 66–77.
- Campbell, M. D., Pollack, A. G., Driggers, W. B., and Hoffmayer, E. R. 2014. Estimation of Hook Selectivity of Red Snapper and Vermilion Snapper from Fishery-Independent Surveys of Natural Reefs in the Northern Gulf of Mexico. *Marine and Coastal Fisheries*, 6: 260–273.
- CARE (Committee of Age Reading Experts). 2006. Manual on generalized age determination procedures for groundfish. Prepared for the Technical Subcommittee of The Canada/U.S. Groundfish Committee. 52 p.
- Cope, J. M., Sampson, D., Stephens, A., Key, M., Mirick, P. P., Stachura, M., Tsou, S., *et al.* 2015. Assessments of California, Oregon and Washington Stocks of Black Rockfish (*Sebastes melanops*) in 2015: 402.

- Dennis, D., Plagányi, É., Van Putten, I., Hutton, T., and Pascoe, S. 2015. Cost benefit of fishery-independent surveys: Are they worth the money? *Marine Policy*, 58: 108–115.
- Dick, E. J., Berger, A. M., Bizzarro, J., Bosley, K., Cope, J., Field, J., Gilbert-Horvath, L., *et al.* 2017. The combined status of Blue and Deacon Rockfishes in U.S. waters off California and Oregon in 2017. Pacific Fishery Management Council.
- Fernandes, P. G., Copland, P., Garcia, R., Nicosevici, T., and Scouling, B. 2016. Additional evidence for fisheries acoustics: small cameras and angling gear provide tilt angle distributions and other relevant data for mackerel surveys. *ICES Journal of Marine Science: Journal du Conseil*, 73: 2009–2019.
- Foote, K. G. 1987. Fish target strengths for use in echo integrator surveys. *The Journal of the Acoustical Society of America*, 82: 981–987.
- Frouzova, J., Kubecka, J., Balk, H., and Frouz, J. 2005. Target strength of some European fish species and its dependence on fish body parameters. *Fisheries Research*, 75: 86–96.
- Gunderson, Donald R. 1993. *Surveys of fisheries resources*. John Wiley & Sons.
- Hannah, R. W., and Blume, M. T. O. 2016. Variation in the Effective Range of a Stereo-Video Lander in Relation to Near-Seafloor Water Clarity, Ambient Light and Fish Length. *Marine and Coastal Fisheries*, 8: 62–69.
- Haralabous, J. 1996. Artificial neural networks as a tool for species identification of fish schools. *ICES Journal of Marine Science*, 53: 173–180.
- Hilborn, R., and Walters, C. J. 1992. *Quantitative fisheries stock assessment: choice, dynamics and uncertainty*. Chapman and Hall, New York.
- Hilborn, R. 2007. Moving to sustainability by learning from successful fisheries. *AMBIO: A Journal of the Human Environment*, 36: 296–303.
- Huse, I. 1996. Tilt angle distribution and swimming speed of overwintering Norwegian spring spawning herring. *ICES Journal of Marine Science*, 53: 863–873.
- Hwang, B. 2015. Morphological Properties and Target Strength Characteristics for dark banded rockfish (*Sebastes inermis*). *Journal of the Korean Society of Fisheries Technology*, 51: 120–127.
- ICES. 2000. Report on Echo Trace Classification. ICES. [http://www.ices.dk/sites/pub/Publication Reports/Forms/DispForm.aspx?ID=35681](http://www.ices.dk/sites/pub/Publication%20Reports/Forms/DispForm.aspx?ID=35681) (Accessed 9 September 2020).
- Jones, D., Lauffenburger, N. E., Williams, K., and De Robertis, A. 2019. Results of the acoustic trawl survey of walleye pollock (*Gadus chalcogrammus*) in the Gulf of Alaska, June August 2017 (DY2017-06). AFSC Processed Rep. 2019-08.
- Jones, D. T., Wilson, C. D., De Robertis, A., Rooper, C. N., Weber, T. C., and Butler, J. L. 2012. Evaluation of rockfish abundance in untrawlable habitat: combining acoustic and complementary sampling tools. *Fishery Bulletin*, 110: 332–343.
- Kang, D., and Hwang, D. 2003. Ex situ target strength of rockfish (*Sebastes schlegeli*) and red sea bream (*Pagrus major*) in the Northwest Pacific. *ICES Journal of Marine Science*, 60: 538–543.

- Kang, D. 2003. Ex situ target strength of rockfish (*Sebastes schlegeli*) and red sea bream (*Pagrus major*) in the Northwest Pacific. *ICES Journal of Marine Science*, 60: 538–543.
- Koslow, J. A., Kloser, R., and Stanley, C. A. 1995. Avoidance of a camera system by a deepwater fish, the orange roughy (*Hoplostethus atlanticus*). *Deep Sea Research Part I: Oceanographic Research Papers*, 42: 233–244.
- Kotwicki, S., Horne, J. K., Punt, A. E., and Ianelli, J. N. 2015. Factors affecting the availability of walleye pollock to acoustic and bottom trawl survey gear. *ICES Journal of Marine Science*, 72: 1425–1439.
- Kotwicki, S., Ressler, P. H., Ianelli, J. N., Punt, A. E., and Horne, J. K. 2018. Combining data from bottom-trawl and acoustic-trawl surveys to estimate an index of abundance for semipelagic species. *Canadian Journal of Fisheries and Aquatic Sciences*, 75: 60–71.
- Krutzikowsky, G., Wagman, D. W., and Davis, R. 2019. Population status of Black rockfish in Oregon Coastal waters. F-186-R-10.
- Kubilius, R., Ona, E., and Calise, L. 2015. Measuring *in situ* krill tilt orientation by stereo photogrammetry: examples for *Euphausia superba* and *Meganyctiphanes norvegica*. *ICES Journal of Marine Science: Journal du Conseil*, 72: 2494–2505.
- Kuriyama, P. T., Branch, T. A., Hicks, A. C., Harms, J. H., and Hamel, O. S. 2019. Investigating three sources of bias in hook-and-line surveys: survey design, gear saturation, and multispecies interactions. *Canadian Journal of Fisheries and Aquatic Sciences*, 76: 192–207.
- Langlois, T. J., Fitzpatrick, B. R., Fairclough, D. V., Wakefield, C. B., Hesp, S. A., McLean, D. L., Harvey, E. S., *et al.* 2012. Similarities between Line Fishing and Baited Stereo-Video Estimations of Length-Frequency: Novel Application of Kernel Density Estimates. *PLoS ONE*, 7: e45973.
- Lawson, G. L., and Rose, G. A. 1999. The importance of detectability to acoustic surveys of semi-demersal fish. *ICES Journal of Marine Science*, 56: 370–380.
- Love, M. S., Yoklavich, M. M., and Thorsteinson, L. 2002. *The rockfishes of the Northeast Pacific*. University of California Press. 405 pp.
- Love, R. H. 1971. Measurements of fish target strength: A review. *Fish Bull.*
- Matthews, K. R., and Richards, L. J. 1991. Rockfish (*Scorpaenidae*) Assemblages of Trawlable and Untrawlable Habitats off Vancouver Island, British Columbia. *North American Journal of Fisheries Management*, 11: 312–318.
- Maunder, M. N., and Punt, A. E. 2013. A review of integrated analysis in fisheries stock assessment. *Fisheries Research*, 142: 61–74.
- MacLellan, S.E. 1997. How to age rockfish (*Sebastes*) using *S. alutus* as an example—the otolith burnt section technique. *Canadian Technical Report of Fisheries and Aquatic Sciences* 2146: 39 p.
- McClatchie, S. 1996. A re-evaluation of relationships between fish size, acoustic frequency, and target strength. *ICES Journal of Marine Science*, 53: 780–791.

- McClatchie, S., Thorne, R. E., Grimes, P., and Hanchet, S. 2000. Ground truth and target identification for fisheries acoustics. *Fisheries Research*, 47: 173–191.
- Mello, L. G. S., and Rose, G. A. 2009. The acoustic dead zone: theoretical vs. empirical estimates, and its effect on density measurements of semi-demersal fish. *ICES Journal of Marine Science*, 66: 1364–1369.
- Nero, R. W., and Magnuson, J. J. 1989. Characterization of Patches Along Transects Using High-Resolution 70-kHz Integrated Acoustic Data. *Canadian Journal of Fisheries and Aquatic Sciences*, 46: 2056–2064.
- Ona, E., and Mitson, R. B. 1996. Acoustic sampling and signal processing near the seabed: the deadzone revisited. *ICES Journal of Marine Science*, 53: 677–690.
- Ona, E. 1999. Methodology for target strength measurements. ICES Cooperative research report, 235: 59.
- Parker, S., Olson, J., Rankin, P., and Malvitch, J. 2008. Patterns in vertical movements of black rockfish *Sebastes melanops*. *Aquatic Biology*, 2: 57–65.
- Pirtle, J. L., Weber, T. C., Wilson, C. D., and Rooper, C. N. 2015. Assessment of trawlable and untrawlable seafloor using multibeam-derived metrics. *Methods in Oceanography*, 12: 18–35.
- R Core Team. 2020. R: A language and environment for statistical computing. R Foundation for statistical computing, Vienna, Austria. URL <https://www.R-project.org>.
- Rasmuson, L. 2021. Susceptibility of five species of rockfish (*Sebastes* spp.) to different survey gears inferred from high resolution behavioral data. *Science Bulletin*, 2021–05. Oregon Department of Fish and Wildlife, Salem.
- Rasmuson, L. K., Blume, M. T. O., and Rankin, P. S. 2021a. Habitat use and activity patterns of female Deacon Rockfish (*Sebastes diaconus*) at seasonal scales and in response to episodic hypoxia. *Environmental Biology of Fishes*, 104: 535–553.
- Rasmuson, L. K., Rankin, P. S., Kautzi, L. A., Berger, A., Blume, M. T. O., Lawrence, K. A., and Bosley, K. 2021b. Cross-Shelf Variability of Deacon Rockfish *Sebastes diaconus* Age, Growth, and Maturity in Oregon Waters and Their Effect on Stock Status. *Marine and Coastal Fisheries*, 13: 379–395.
- Richards, B. L., Beijbom, O., Campbell, M. D., Clarke, M. E., Cutter, G., Dawkins, M., Edington, D., *et al.* 2019. Automated Analysis of Underwater Imagery: Accomplishments, Products, and Vision. NOAA Technical Memorandum, NMFS-PIFSC-83. Pacific Islands Fisheries Science Center (U.S.). <https://repository.library.noaa.gov/view/noaa/20234> (Accessed 28 September 2021).
- Robertis, A. D., McKelvey, D., Taylor, K., and Honkalehto, T. 2014. Development of Acoustic-Trawl Survey Methods to Estimate the Abundance of age-0 Walleye Pollock in the Eastern Bering Sea Shelf During the BeringArctic Subarctic Integrated Survey (BASIS): 55.

- Rooper, C. 2010. Assessing habitat utilization and rockfish (*Sebastes* spp.) biomass on an isolated rocky ridge using acoustics. *Can J Fish Aquat Sci*.
- Rooper, C. N., Williams, K., Towler, R. H., Wilborn, R., and Goddard, P. 2020. Estimating habitat-specific abundance and behavior of several groundfishes using stationary stereo still cameras in the southern California Bight. *Fisheries Research*, 224: 105443.
- Sawada, K., Furusawa, M., and Williamson, N. J. 1993. Conditions for the precise measurement of fish target strength in situ. *The Journal of the Marine Acoustics Society of Japan*, 20: 73–79.
- Schobernd, Z. H., Bacheler, N. M., Conn, P. B., and Trenkel, V. 2014. Examining the utility of alternative video monitoring metrics for indexing reef fish abundance. *Canadian Journal of Fisheries and Aquatic Sciences*, 71: 464–471.
- Somerton, D. A., Williams, K., and Campbell, M. D. 2017. Quantifying the behavior of fish in response to a moving camera vehicle by using benthic stereo cameras and target tracking. *Fishery Bulletin*, 115: 343–354.
- Soule, M. 1997. Performance of a new phase algorithm for discriminating between single and overlapping echoes in a split-beam echosounder. *ICES Journal of Marine Science*, 54: 934–938.
- Stanley, R. 2000. Estimation of a widow rockfish (*Sebastes entomelas*) shoal off British Columbia, Canada as a joint exercise between stock assessment staff and the fishing industry. *ICES Journal of Marine Science*, 57: 1035–1049.
- Stanley, R. D. 1999. Diel vertical migration by yellowtail rockfish, *Sebastes flavidus*, and its impact on acoustic biomass estimation. *Fish Bull*.
- Starr, R. M., Fox, D. S., Hixon, M. A., Tissot, B. N., Johnson, G., and Barss, W. H. 1996. Comparison of submersible-survey and hydroacoustic-survey estimates of fish density on a rocky bank. *Fish Bull*, 94: 113–123.
- Stoner, A. W., Ryer, C. H., Parker, S. J., Auster, P. J., and Wakefield, W. W. 2008. Evaluating the role of fish behavior in surveys conducted with underwater vehicles. *Canadian Journal of Fisheries and Aquatic Sciences*, 65: 1230–1243.
- Tolimieri, N., Clarke, M., Singh, H., and Goldfinger, C. 2008. Evaluating the SeaBED AUV for Monitoring Groundfish in Untrawlable Habitat. *In* *Marine Habitat Mapping Technology for Alaska*, pp. 129–142. Ed. by J. Reynolds and H. Greene. Alaska Sea Grant, University of Alaska Fairbanks. <http://www.alaskaseagrant.org/bookstore/pubs/AK-SG-08-03.html> (Accessed 4 September 2020).
- Tschersich, P. 2015. Hydroacoustic survey of Black Rockfish abundance and distribution operational plan for the Afognak and Northeast districts of the Kodiak management area, 2015. Alaska Department of Fish and Game, Division of Commercial Fisheries, Regional Operational Plan ROP. CF. 4K.2015.18, Kodiak. Alaska Department of Fish and Game, Division of Sport Fish, Research and Technical Services.

https://wc.adfg.state.ak.us/static/regulations/regprocess/fisheriesboard/pdfs/2012-2013/ayk/fms12_07.pdf (Accessed 21 July 2017).

Williams, K., Rooper, C. N., and Towler, R. 2010. Use of stereo camera systems for assessment of rockfish abundance in untrawlable areas and for recording pollock behavior during midwater trawls. *Fishery Bulletin*, 108: 352–362.

Williams, K., Rooper, C. N., De Robertis, A., Levine, M., and Towler, R. 2018. A method for computing volumetric fish density using stereo cameras. *Journal of Experimental Marine Biology and Ecology*, 508: 21–26.

Zimmermann, M. 2003. Calculation of untrawlable areas within the boundaries of a bottom trawl survey. *Canadian Journal of Fisheries and Aquatic Sciences*, 60: 657–669.

SUPPLEMENT

Videos were reviewed using both the MeanCount approach and the MaxN approach. We then examined these data to assess 1) how size frequency of focal species differed between the methods, 2) how the ratio of individual species abundance relative to total abundance differed between the two methods, and 3) which method was the most efficient. Size and species ratio data are used in echo integration to convert acoustic data into number of fish.

1) SIZE FREQUENCY OF TARGET SPECIES:

For each species/species group we compared the size distributions between the two video review methods using a Kolmogorov-Smirnov test. The size distributions were not statistically different between the MaxN and MeanCount video processing methods (Fig S1, Black Rockfish: $D=0.05$, $p=0.98$; Blue Deacon Rockfish: $D=0.08$, $p=0.43$; Black Blue Deacon Juvenile Rockfish $D=0.25$, $p=0.22$). Based on these results, either video review method will generate similar distributions.

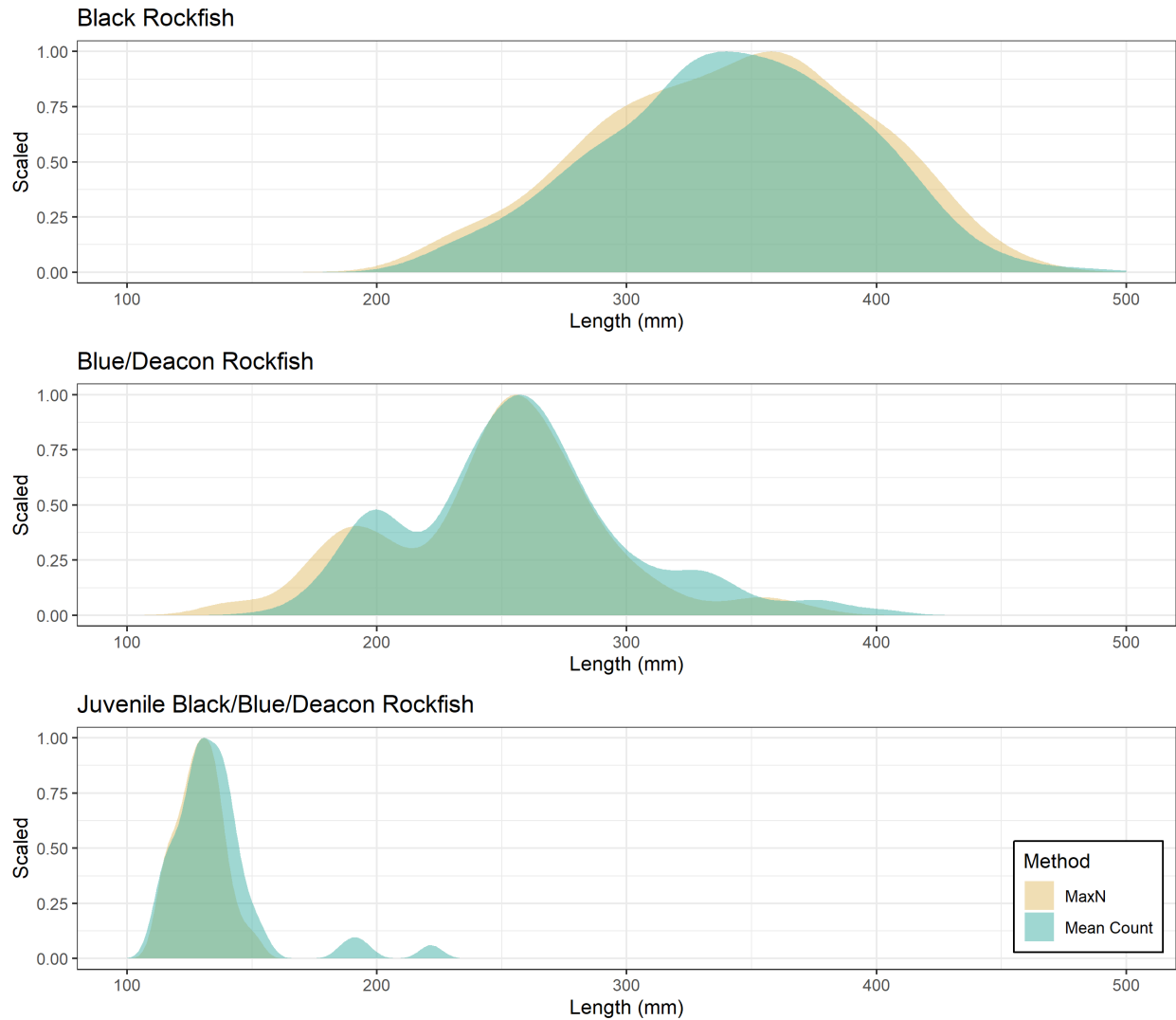


Fig. S1. Scaled size distribution of Black (top), Blue/Deacon (middle) and Juvenile Black/Blue/Deacon Rockfish (bottom) using the MaxN and MeanCount approach to video review.

2) RATIOS OF TARGET SPECIES:

To determine if the ratio of Black to Blue/Deacon Rockfish differed between the two methods we used a generalized linear model with binomial distribution to compare species proportions. The proportions of Black and Blue/Deacon Rockfish did not differ significantly between the MaxN and MeanCount methodologies (Fig S2, Table S1). Based on these results, either video review method will generate similar species proportions.

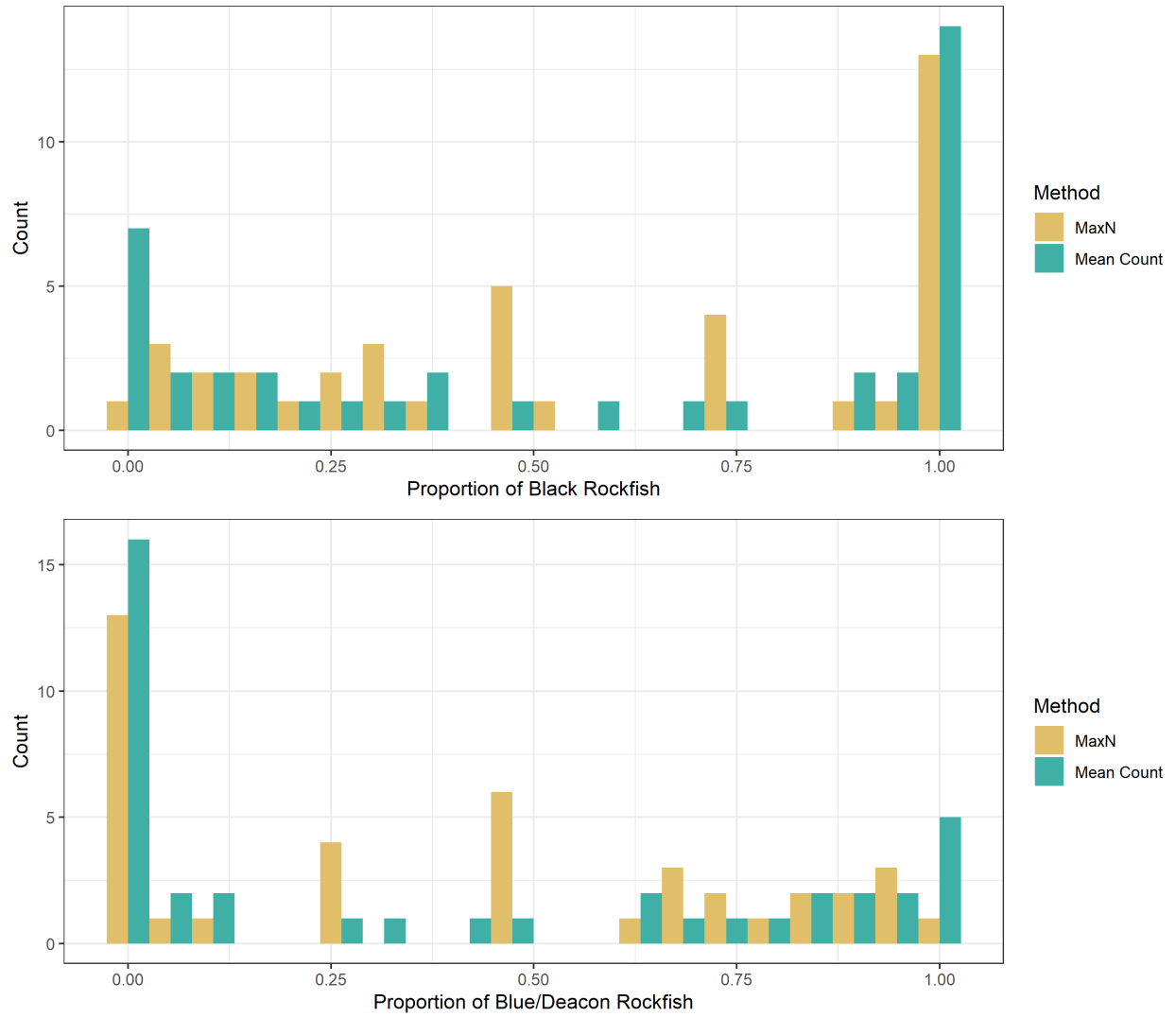


Fig. S2. Summary of number of video drops with proportions of Black versus Blue/Deacon Rockfish for each of the two video review methods.

Table S1: Results of binomial generalized linear model comparing species proportions between the methods for Black and Blue/Deacon Rockfish.

Black Rockfish Proportions

	Est.	S.E.	z val.	p
(Intercept)	-0.37	0.32	-1.14	0.25
MeanCount	-0.13	0.45	-0.29	0.77

Blue/Deacon Proportions

	Est.	S.E.	z val.	p
(Intercept)	-0.37	0.32	-1.14	0.25
MeanCount	-0.07	0.46	-0.16	0.87

3) EFFICIENCIES OF THE MAXN VS. MEANCOUNT VIDEO PROCESSING:

Given that the above evidence suggests there is no difference in the resultant size and species proportion data with either review method, we examined the review efficiencies using simulations. We first examined the distribution of sampling times to process the videos using each method. These data were best described by a gamma distribution. We then simulated 1,000 video drops using the rgamma function in R. We repeated this 2,000 times to see how long it would take to process all 1,000 videos on average. The MeanCount video methodology proved to be a more time efficient method (Fig. S3). This finding combined with the evidence of no statistical differences in species proportions or sizes is the reason we elected to conduct our video review using the MeanCount approach.

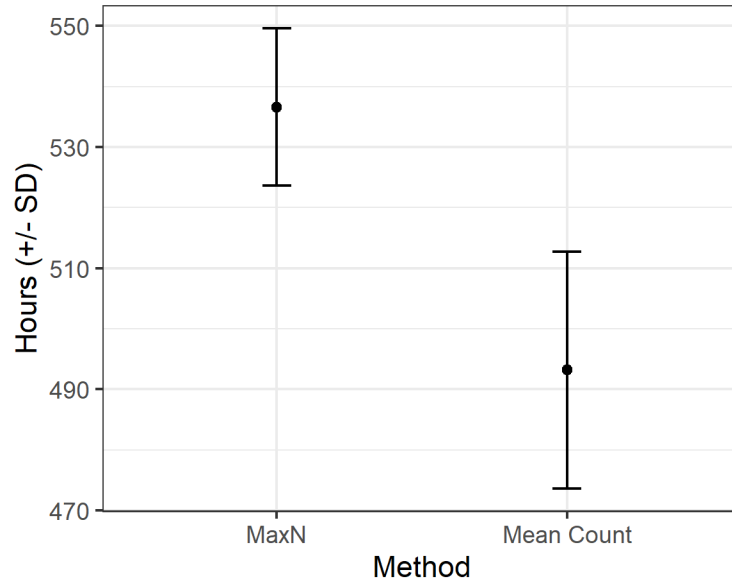


Fig. S3 Average number of hours required to review 1,000 video drops using the MaxN and MeanCount video review methods.

8: INFLUENCE OF NEAR BOTTOM FISH DISTRIBUTION ON THE EFFICACY OF A COMBINED HYDROACOUSTIC VIDEO SURVEY.

LEIF K. RASMUSON^{1*}, SCOTT R. MARION¹, STEPHANIE A. FIELDS¹, MATTHEW T.O. BLUME¹,
KELLY A. LAWRENCE¹, POLLY S. RANKIN¹

This paper is in press at ICES Journal of Marine Science. It is recreated here for simplicity.

ABSTRACT

Combining hydroacoustics and underwater video is an effective tool for generating fish population estimates. However, hydroacoustics cannot be used to differentiate fish from the seafloor within an area known as the acoustic dead zone. A common way to address this is to exclude data near the bottom. The effect of this exclusion zone on population estimates of nearshore semi-pelagic rockfish is unknown. This study explores the effect of a near bottom (0-1 m) exclusion zone by comparing ROV video data to data from a combined hydroacoustic and video method. Higher densities of semi-pelagic species (Black and Blue/Deacon Rockfish) were observed in the combined acoustic and video method, suggesting that most of the population resides above the exclusion zone. Demersal rockfish observed by the ROV did not contaminate acoustic data of semi-pelagic species, since they remained within the exclusion zone. Results demonstrate that extrapolation of school data into the exclusion zone provided a realistic correction to the acoustic data for Black Rockfish. Our work demonstrates that excluding the data within 1 m of the bottom does not negatively affect the ability of the combined video hydroacoustic method to sample semi-pelagic rockfish.

INTRODUCTION

Effective fishery management benefits from rigorous and systematic fisheries independent surveys to provide fish abundance estimates (Hilborn and Walters, 1992). Fisheries independent surveys can take many forms including hook and line, trawl, video, and acoustic sampling techniques. Acoustic surveys are cost effective because large areas can be surveyed relatively quickly with minimal staff, but often need to be paired with another tool to provide species and length composition data (Misund, 1997; McClatchie *et al.*, 2000). These methods have proven effective for many pelagic and semi-pelagic stocks, as well as for stocks that occupy deep (depths greater than 100 m) high relief environments such as: Acadian Redfish (*Sebastes fasciatus*) and Orange Roughy (*Hoplostethus atlanticus*) (Kloser *et al.*, 2002; Gauthier and Rose, 2005). Although acoustic methods are well developed for species occupying deeper habitats, there has been limited research on the utilization of acoustics in shallow (less than 50 m depth) high relief environments. For semi-pelagic species that spend some component of their time on or very near the bottom, differentiation of a fish's echo from that of the bottom is a difficulty for many acoustic systems (Ona and Mitson, 1996; Rasmuson, 2021).

Hydroacoustic surveys often refer to the area directly above the bottom as the acoustic dead zone, hereafter referred to as the dead zone (Ona and Mitson, 1996; Totland *et al.*, 2009; Kotwicki *et al.*, 2018). The dead zone is a region in which acoustic returns of fish overlap with returns from the seafloor. The thickness of this region is influenced by echosounder settings, water depth, and bottom relief. Unintended integration of the bottom signal into the fish signal, even if relatively small, can inflate a population estimate (Mello and Rose, 2009; Tušer *et al.*, 2013; Kotwicki *et al.*, 2018). Therefore, it is common to either extrapolate the above dead zone acoustic returns into the dead zone or exclude acoustic data near the bottom all together. The former assumes homogeneity in fish density and distribution, while the latter may result in underestimating the population, however, both require calculating the thickness of the dead zone to ensure these data are probably addressed (Mcquinn *et al.*, 2005). In shallow water, the mathematically calculated dead zone is thin relative to the depth of the water column (Ona and Mitson, 1996). Even so, for semi-pelagic fish occupying the region directly above the bottom, exclusion of near bottom fish could reduce the population estimate (Mcquinn *et al.*, 2005). Thus, in order to provide a corrected population estimate that includes the dead zone, some surveys have combined multiple survey tools that sample different regions of the water column to determine the fish density both above and within the dead zone (Kloser, 1996; Jones *et al.*, 2012; Kotwicki *et al.*, 2018).

Population estimates derived from acoustics require assigning acoustic observations to species, a process which is susceptible to error due to vertical segregation of both different species and different sizes of individuals within species (Stanley, 1999; McClatchie *et al.*, 2000; Gauthier and Rose, 2005). The potential for incorrect assignment of species is higher when vertical segregation occurs near the dead zone boundary. Therefore, employing sampling techniques both above and within the dead zone is necessary in order to assign inter- and intra-species vertical segregation (Jones *et al.*, 2012; Kotwicki *et al.*, 2018). In low-relief habitats, combining bottom and midwater trawls is an effective, albeit potentially destructive, way to sample both above and within the dead zone. However, for semi-pelagic species that occupy high relief habitats, use of trawls is not feasible. Underwater cameras are proposed as an alternative tool to sample high relief areas (Jones *et al.*, 2012), and by utilizing stereo camera technology, are also able to provide fish lengths (Denney *et al.*, 2017).

Due in part to the large diversity and geographic range of the genus *Sebastes*, rockfish have been a pivotal species group to the development of combined video and hydroacoustic sampling methods. Early work showed acoustic sampling was effective for the continental shelf stocks of Yellowtail (*Sebastes flavidus*) and Widow Rockfish (*Sebastes entomelas*) (Stanley, 2000). In these studies, length and species composition data came from midwater trawls. Examining deep water demersal rockfish, Jones *et al.* (2012) demonstrated that deep untrawlable rocky reefs are important rockfish habitats that need to be surveyed and included

in population estimates. Jones et al. (2012) compared the utility of using a stereo drop camera to estimate the population size of rockfish in the dead zone, to the extrapolation method of Ona and Mitson (1996). They demonstrated that the dead zone contained many of their focal species. Nearshore semi-pelagic rockfish are under-surveyed, even though species like Black Rockfish (*Sebastes melanops*) are the primary catch of the recreational and commercial nearshore fleets in Oregon. Tschersich (2015) and Boettner and Burton (1990) demonstrated that acoustics are a viable tool for Black Rockfish surveys. However, Tschersich (2015) utilized only echo counting (not echo-integration, as is necessary for large dense schools) and therefore did not require length composition. Boettner and Burton (1990) obtained length samples using a midwater trawl which, while effective, is not suitable in high-relief nearshore habitat. Thus, Rasmuson et al. (2021) combined a suspended stereo camera system with hydroacoustics to estimate nearshore semi-pelagic rockfish densities. They suggested that this combination is an effective and efficient way to survey semi-pelagic rockfish densities in shallow, high-relief areas. However, near-bottom was excluded when analyzing the acoustic data and the effect of that procedure was not fully examined, further the relative contribution of other rockfish species to the signal in the acoustic data was not considered.

In the present study, our goal was to estimate the influence of near bottom fish on the combined acoustic-visual survey designed to provide a population estimate for three semi-pelagic species – Black, Blue (*Sebastes mystinus*), and Deacon Rockfish (*Sebastes diaconus*). Specifically, we determined what portion of the population of these three species occurred within the area of the water column directly above the bottom that is not captured by our acoustic system, an area we refer to as the exclusion zone, as well as whether or not demersal rockfish affected population estimates of the three target semi-pelagic species. To answer these questions, we compared acoustic swath data and point estimates from our suspended camera with co-located benthic-oriented video data from remotely operated vehicle (ROV) belt transects conducted immediately following the acoustic sampling. We assessed whether the survey tool observations were associated by testing if 1) the ROV and suspended camera generate similar size distribution estimates and 2) the acoustic-visual sampling followed by ROV sampling was successful in detecting spatially consistent concentrations of fish across the reef. Assuming associations between tools were found, we examined how these data could be used to provide density corrections to the exclusion zone. Finally, for each species/species group, we compared total density estimates from each tool as a proxy for how much of each population was above (available to acoustics) versus within (available to ROV) the exclusion zone.

MATERIALS AND METHODS

FIELD WORK

Acoustic and visual surveys of shallow, nearshore rocky reefs were conducted in the spring and fall of 2018 (Fig. 1). Surveys were conducted on five reefs spread over 250 km along the

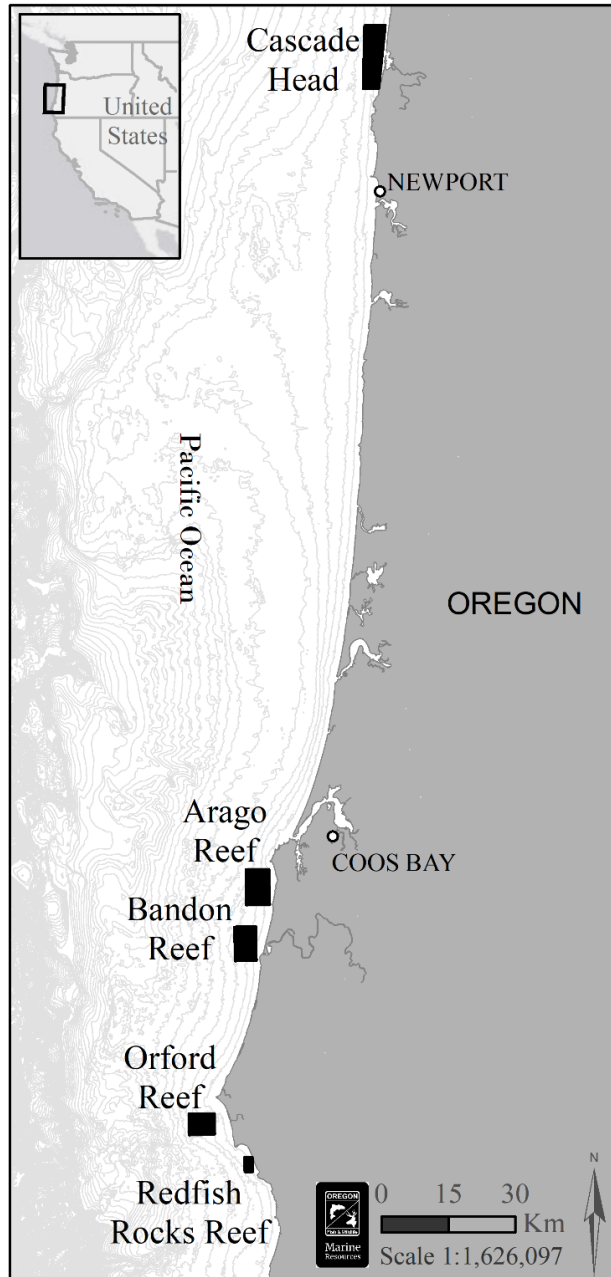


Fig. 1. Map of study areas along Oregon Coast. Black boxes denote the approximate locations of each reef. Cascade Head was sampled in May of 2018 whereas all other reefs were sampled in September 2018.

south/central Oregon coast: Cascade Head (44.88° N, 124.09° W), Cape Arago (43.28° N, 124.46° W), Bandon (43.17° N, 124.48° W), Orford Reef (42.77° N, 124.60° W) and Redfish Rocks (42.70° N, 124.48° W). At each reef, transects were randomly placed within the known area of rocky reef, defined as mapped areas having cobble or larger substrates, between 20 m and 50 m depth. These survey boundaries reflected the shallow end of the ROV's safe working range and the deep end of the expected distribution of Black Rockfish (Love *et al.*, 2002). All transects were oriented in a NW-SE direction, anticipating the likely direction of predominant winds and waves. Transects conducted in the spring were 300 m in length and in the fall transects were lengthened to 500 m. Transects were conducted from one hour after sunrise to one hour before sunset, as previous work has shown that species are sufficiently above the bottom to be available to acoustics during this time (Rasmuson 2021).

ACOUSTICS AND BASSCAM

Except for Cascade Head, surveys were conducted aboard a 15.3 m charter passenger fishing vessel. At Cascade Head surveys were conducted 7.6 m aluminum vessel. Operations and acoustic settings were the same on both vessels. Transects were first ensonified using a BioSonics 201 kHz split beam DT-X transducer with a beam width of 6.9 degrees. Acoustic data were collected using a ping rate of 5 pings per second and a pulse duration of 0.3 ms. The transducer was calibrated at the BioSonics factory before and after the survey. The three largest fish schools identified while ensonifying the transect were sampled with the camera system following the transect completion. In the event no schools were identified from the acoustics; rugose habitat regions were targeted for camera deployments. Camera drops occurred within one hour of completion of the transect, though most occurred within 20 min.

Camera deployments were conducted using the benthically anchored suspended stereo camera (BASSCam) described by Rasmuson *et al.* (2021). Briefly, the system floats 2 m off bottom and consists of a stereo pair of forward-facing GoPro Hero4 Black cameras and a single GoPro Hero4 Black camera facing downward at an angle of 22 degrees below horizontal (see Figure S4 in the online supplement for a diagram of the viewed areas by the forward and downward facing cameras). The forward-facing cameras were spaced 39.4 cm apart from one another and angled inwards at 8°. The three cameras were illuminated by Big Blue LED dive lights, four 9000 lumen lights looking forward and two 7500 lumen lights looking down. Unlike in previous work, there was no live video feed to the surface. Two-minute deployments were conducted; previous work showed a 2 min deployment was sufficient to provide accurate length and count data (Rasmuson unpublished), and that the BASSCam has little to no effect on the behavior of schooling fish (Rasmuson *et al.* 2021).

ROV

ROV surveys were conducted using a Deep Ocean Engineering Phantom HD2+2 ROV. The primary fish abundance data were gathered using a high-definition video camera (Blackmagic Micro Cinema with an 8 mm wide-angle lens) at an angle of 30 degrees below horizontal, with parallel red lasers providing a 10 cm scale reference. Two Nuytco 200-watt H.M.I. lights provided illumination for the forward-looking camera. Altitude above the seafloor was recorded with two ranging altimeters, one mounted on the forward-looking camera housing and one mounted vertically. A second Blackmagic camera, paired with a pair of 10 cm scaling lasers, was pointed straight down in front of the ROV for navigation purposes, but these data were not used in the present study. Two down-facing SeaLite Matrix LED lights illuminated the substrate for the downward facing camera. A calibrated forward-facing stereo video system provided sub-centimeter accurate measurements of fish length and fish height off bottom. Two GoPro Hero4 Black cameras were mounted in custom flat-port housings (Sexton Corporation) on the front of the ROV spaced 47 cm apart from one another and angled inwards at 6°.

The ROV was navigated using an acoustic tracking system (ORE Offshore Trackpoint III), with raw ROV positions determined at 4 s intervals and subsequently smoothed to minimize any positional artifacts. This equipment and processing typically yield a positional accuracy of ± 4 m. ROV transects were conducted between 0.5 and 1.5 m above the bottom at a target speed of 0.5-1 knot, resulting in a typical transect width of 2 - 5 m. ROV sampling occurred within approximately one hour of the acoustic transect for half of all transects, and within 2 hours for 90% of all transects.

DATA PROCESSING

BASSCAM

BASSCam video was reviewed using EventMeasure software by SeaGIS followed methods described by Rasmuson et al. (2021). In each video, five randomly selected frames were chosen and all fish in each frame were identified to the lowest taxonomic level possible. Fish were counted and the observation coded as occurring in either the forward or downward facing camera. Fish in the forward cameras were measured only if they were oriented approximately perpendicular to the cameras.

The focus of this study was nearshore semi-pelagic rockfish (Black, Blue and Deacon Rockfish). Blue Rockfish and Deacon Rockfish can be difficult to distinguish from one another in video so were considered as a single species group. All other observed semi-pelagic species (Yellowtail, Widow, Puget Sound (*Sebastes emphaeus*) and Canary Rockfish (*Sebastes pinniger*)) were aggregated into a functional group called non-focal semi-pelagic rockfish. Remaining rockfish species observed were classified into a functional group called demersal rockfish (Table 1).

Juvenile rockfish were excluded from analysis because of discrepancies in how the two video tools identified juvenile rockfish. Differences were associated with if juveniles were coded by species or as unidentified and if they unidentified were specific to juveniles or all age groups together. All other observed species and functional groups were excluded from additional analysis.

ACOUSTICS

Processing of the acoustic data, including algorithm settings, followed the methods outlined by Rasmuson et al. (2021). Additionally, an example echogram and a description of the acoustic review process are presented in Rasmuson et al. (2021). In the present study, to exclude the near bottom dead zone, sub tidal aquatic vegetation and to allow for comparison with the ROV, acoustic data within 1 m of the bottom was excluded. All analyses were conducted in Echoview version 11. Acoustic data were analyzed using both echo integration and echo counting. Portions of echograms were assigned to each analytical method using the Sawada index and the ratio of multiple echoes (Sawada *et al.*, 1993). Both indices independently identify regions of the echogram where fish densities are so high that they cannot be analyzed using echo counting and are therefore analyzed using echo integration. In regions analyzed with echo integration, the school detection algorithm identified schools that had been smoothed with a median 3x3 filter. The school detection algorithm applies user defined thresholds and algorithms to identify fish schools in the echogram (Nero and Magnuson, 1989; Barange, 1994; Haralabous, 1996). The regions defined as schools were then visually checked for accuracy and edited as needed. To convert the acoustic backscattering data from fish schools into densities, the *Sebastes* average target strength to length relationship described by Rasmuson et al. (2021) was used. The same methods were used to derive fish densities. Length data were provided by the BASSCam in 1 cm length bins and scaled by species/species groups.

After school detections were complete, the echogram was examined visually to define regions for echo counting. In these regions, Echoview's single target algorithm was applied to identify individual fish echoes. Considering it is common for multiple acoustic targets to represent a single observed fish, we then used Echoview's fish tracking algorithm (Balk and Lindem, 2000; ICES, 2000) to identify instances where multiple echoes were attributable to only a single fish and convert them into a single fish observation (known as a fish track). Individual fish echoes were converted to density by taking into account its depth in the water column and the area surveyed by the acoustic beam at that depth (Tschersich, 2015). Densities of fish echoes were summed to generate a total density per transect.

ROV

Digital video files from the main forward-oblique camera were reviewed by a highly trained technician, and time-stamped fish observations were geolocated by merging with time-stamped ROV navigation records.

A trapezoidal screen overlay extending from the full width at the bottom of the screen, tapering to 80% of screen width at 80% of screen height, was used to exclude areas too distant or marginal to allow reliable fish identification. Sections of video were excluded if the reviewer estimated that a 20 cm fish could be obscured in more than 20% of the review frame (for example due to poor visibility, terrain obstructions, or ROV maneuvering), or if the ROV was not making relatively linear forward progress. For the remaining valid portions of transects, subsequently referred to as “non-gap” data, fish were identified to species, where possible, for 24 target species and otherwise were recorded in higher-level taxonomic groupings.

Using the scaling laser contact points with the seafloor and predetermined camera calibrations, transect width was derived at 30 s intervals then interpolated for each 1 s interval. Surveyed area for each 1 s interval was calculated by multiplying the transect width by the along-transect distance. Fish densities were generated from fish counts by dividing non-gap fish counts by the non-gap surveyed area.

ROV derived stereo imagery was reviewed using EventMeasure. Total length was measured for each appropriately positioned and oriented fish. Fish height off bottom was measured by estimating and measuring to the nearest visible rock, when both a distinguishable feature on the bottom and a fish were visible in a stereo image. Fish visibly resting on the seafloor were assigned a height of zero.

Table 1. Fish species and counts observed by the ROV and BASSCam. BASSCam counts are from one randomly selected observation frame per deployment.

Common Name	Scientific Name	Species/Species Group	ROV	BASS
Black Rockfish	<i>Sebastes melanops</i>	Black	1,770	1,111
Blue Rockfish	<i>Sebastes mystinus</i>	Blue/Deacon	25	NA
Blue/Deacon Rockfish	<i>Sebastes mystinus/diaconus</i>	Blue/Deacon	3,022	2,325
Canary Rockfish	<i>Sebastes pinniger</i>	Non-Focal Semi-pelagic	689	95
China Rockfish	<i>Sebastes nebulosus</i>	Demersal	211	8
Copper Rockfish	<i>Sebastes carnatus</i>	Demersal	44	8
Deacon Rockfish	<i>Sebastes diaconus</i>	Blue/Deacon	2,980	NA
Puget Sound Rockfish	<i>Sebastes emphaeus</i>	Demersal	54	0
Quillback Rockfish	<i>Sebastes maliger</i>	Demersal	338	9
Rosethorn Rockfish	<i>Sebastes helvomaculatus</i>	Demersal	25	0
Tiger Rockfish	<i>Sebastes nigrocinctus</i>	Demersal	14	0
Vermilion Rockfish	<i>Sebastes miniatus</i>	Demersal	81	11
Widow Rockfish	<i>Sebastes entomelas</i>	Non-Focal Semi-pelagic	88	6
Yelloweye Rockfish	<i>Sebastes ruberrimus</i>	Demersal	142	17
Yellowtail Rockfish	<i>Sebastes flavidus</i>	Non-Focal Semi-pelagic	183	38

STATISTICAL ANALYSIS

All statistical analyses were conducted using R version 4.1.2 Bird Hippie (R Core Team, 2020).

LENGTH DATA COMPARISON

To determine if the ROV and BASSCam observed fish of similar lengths, we compared the length distributions of Black and Blue/Deacon Rockfish between the two tools at each reef. Plots were developed using scaled densities and statistically compared using a Kolmogorov-Smirnoff test.

We also used the selectivity ratio defined by Kotwicky et al. (2017) to determine if either tool observed a greater proportion of Black or Blue/Deacon Rockfish of a certain size class. The selectivity ratio was calculated using the SCMM approach and the *mgcv* package in R (Wood, 2006, 2011). Lengths were aggregated into 2 cm bins and a two-stage resampling method with 1000 bootstrap resamples was applied.

SPATIAL CORRESPONDENCE AMONG TOOLS

To assess the validity of the assumption that the two sampling tools were sampling a similar spatial distribution of fish along the reef (i.e., that schools did not move substantially between observation by the acoustics and observation by the ROV, and that the proximity of the ROV transect to the acoustic transect was sufficient), we spatially compared the fish densities observed by the acoustics with those observed by the ROV along each transect. Transects were divided into segments, approximately 50 m in length. To avoid splitting schools at segment boundaries, we adjusted segment split points by examining local acoustically-estimated fish density and moving split points to a local minimum. Resultant segments had variable lengths, with 90% of segments falling between 42 m and 63 m. Data were excluded where the ROV and acoustic transects were separated by more than 10 m, and entire segments were excluded if the total remaining area sampled by ROV was less than 25 m². This resulted in a data reduction of ~10%.

To examine the spatial agreement in the presence and absence of fish between the ROV and acoustics, we generated a confusion matrix (Visa *et al.*, 2011). The confusion matrices were generated for the Black, Blue/Deacon, non-focal semi-pelagic and demersal rockfish categories separately. Data from Cascade Head were excluded from this analysis due to the extreme low numbers of fish observed by both tools. Using these confusion matrices, we derived two indices to assess the agreement between our tools. Accuracy, an index of relative agreement between the tools (Allouche *et al.*, 2006), was calculated as:

$$\text{Accuracy} = \frac{RA+N}{RA+N+R+A} \quad (1)$$

Where *R* denotes only the ROV detected fish, *A* only the acoustics detected fish, *RA* both tools detected fish, and *N* neither tool detected fish. Sensitivity of the was calculated as:

$$Sensitivity = \frac{RA}{RA+A} \quad (2)$$

Where RA and A are defined as above.

In addition to assessing the correspondence between the acoustics and ROV in segment-scale presence/absence, we also calculated the Pearson's correlation coefficient between the segment-scale densities from the two tools.

EXCLUSION ZONE DENSITIES WITHIN FISH SCHOOLS

The goal of this analytical component was to determine if the BASSCam's downward facing camera accurately accounted for fish in the exclusion zone in the acoustics. Determining how proportions of fish differed above and below the exclusion zone informed whether there is a need for a numerical density correction above the exclusion zone when multiplying data downwards into the exclusion zone. Analyses were conducted on BASSCam and ROV data, no acoustics were included in this analysis. BASSCam drops were excluded if there was no ROV data collected within 20 m of the deployment. This resulted in no demersal rockfish observations for the BASSCam. We modeled the proportion of fish above the exclusion zone (thereby standardizing differences in viewed areas between tools), using the explanatory variables: tool, functional species/species group, and reef. Data from Cascade Head were excluded from this analysis due to the extremely low numbers of fish observed by both tools.

ROV count data within 20 m of the BASSCam drop were summed to provide total counts above and within the exclusion zone for each transect. The distance of fish off bottom measured in the ROV video was determined using the forward-facing stereo cameras. Proportion of fish located above the exclusion zone was then calculated as the number above 1 m divided by the total number measured.

BASSCam volume was calculated from the area viewed by the forward cameras using a fixed maximum range across all transects. The fixed maximum range was the average of each transects maximum range (i.e., the distance to the furthest fish viewed in the three BASSCam drops). Maximum range did not differ greatly (2.8 ± 0.4 m), so a single value was used for all transects. In all instances, the downward camera's maximum viewed distance was the bottom, so the volume for the downward facing camera was calculated using the known height of the camera off bottom and assuming a flat bottom. The volume of water viewed by the downward-facing camera was 88% of the volume viewed by the forward camera. Therefore, fish counts from the downward-facing camera were first divided by 0.88 to standardize counts between the two volumes. Then, as the goal was to determine how many fish were in the exclusion zone, we also determined that 78% of the observed volume observed by the downward facing camera occurred within the exclusion zone (from 0–1 m off bottom). Therefore, a correction was applied to the standardized counts from the downward facing camera by multiplying them

by 0.78 to represent only what was counted within the exclusion zone. All fish viewed in the forward camera were considered above the exclusion zone. We made this assumption since, in most instances, only the area above 1 m was viewed due to poor visibility. The proportion of fish above the exclusion zone was generated for the BASSCam by dividing the number of fish in the forward camera by the number in the forward plus the corrected number from downward-facing camera.

We modeled the proportion of fish above the exclusion zone using a binomial distribution. Modeling required summing counts across the three BASSCam deployments per transect, and analyzing proportions, instead of raw counts. Models were fit using the *glm* function in the base *stats* package, using the potential covariates: Species/species group/functional group, Reef, and Camera. All possible model iterations were fit, and a best fit model was selected using the Akaike Information Criterion (AIC). Relative strength of model selection was assessed using both Akaike weights and log likelihood.

FISH DENSITIES OUTSIDE SCHOOLS

In a hypothetical survey utilizing only acoustics and BASSCam, data on fish abundance and composition in the exclusion zone would come only from BASSCam drops, which, in the current study only targeted schools. Therefore, data regarding fish in the exclusion zone but away from schools are missing from the BASSCam and acoustics. To assess whether this away-from-schools near-bottom data was influential to overall conclusions about semi-pelagic fish abundance, background fish density (defined here as the density of fish outside fish schools in the exclusion zone) was calculated from ROV data. First, the location of fish schools and school edges were defined from the acoustic data. Fish densities of each species/species group in the ROV data were then calculated in concentric 5 m increments from the school edge to a distance of 50 m.

To determine at what distance from a school background fish densities were observed, we used generalized additive models. Each species/species group was modeled independently. Response data were fish counts per 5 m distance bin. Explanatory variables were distance from school and reef. Fish count was modeled with a negative binomial distribution. Viewed area per increment was provided as a model offset. The best fit models were selected from all possible model formulations that included variables reef and distance, using AIC and relative strength of model selection, assessed using Akaike weights and log likelihood. The resulting GAM plots were used to visually identify the distance at which background density occurred. We calculated the mean (“background”) density in the exclusion zone from all ROV data at distances from schools greater than the selected threshold distance.

DENSITY ESTIMATE

Density estimates from acoustic data were generated from the echo integration and echo counting data (see section 2.2.2) and were created for each species/species group separately. Densities from both methods were summed for each transect and mean transect density calculated for each species/species group at each reef.

ROV fish count data from the main camera were used to generate mean densities per species/species group per reef. For each transect, each species/species group's density was calculated as the total fish count within non-gap portions of the transect divided by the non-gap surveyed area. The reef-level mean density was calculated as the weighted mean +/- weighted standard deviation of the transect densities, using the non-usable survey area for each transect as the weight.

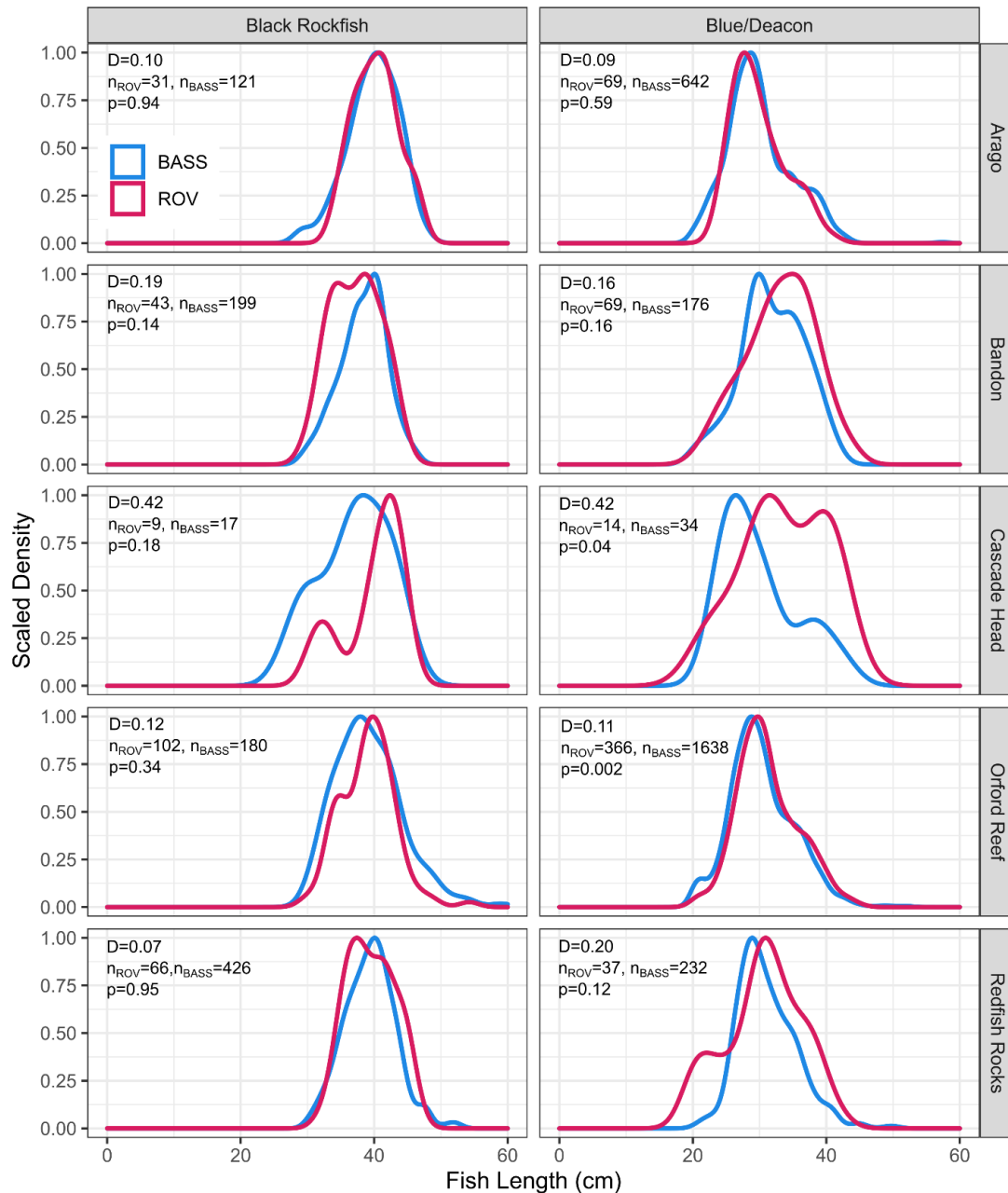


Fig. 2 Scaled density plots of length distributions for the three target species/species groups at each reef. Values in the plot represent the results of a statistical comparison of the two densities using a Kolmogorov-Smirnov test. D is the Kolmogorov-Smirnov test statistic.

RESULTS

A total of 157 transects were sampled with both the ROV and the acoustics/BASSCam survey methods (see online supplement for maps of each reefs transects). The two video tools

observed thirty-seven species or species groups, and 38,656 fish were counted; of these, 13,294 individual fish from 16 species or species groups were used in additional analyses (Table 1). The ROV, with a far greater area surveyed, observed more species and individuals than the BASSCam. In the acoustic data, 340 schools of fish and 1,403 fish tracks were identified.

LENGTH DATA COMPARISON

Length distributions between the two tools at each reef were similar (Fig. 2). Exceptions were Blue/Deacon Rockfish at Cascade Head and Orford Reef. Although there were some statistical differences among these species and locations, their overall distributions were visually quite similar.

Length selectivity analysis for Black and Blue/Deacon Rockfish demonstrated the BASSCam observed slightly more fish with lengths of 12-30 cm than the ROV, and the ROV observed more fish at lengths > 30 cm (Fig. 3). However, the selectivity ratio was very small (average of 1.07), suggesting that although evidence of selectivity in length existed, the magnitude of the effect was very small.

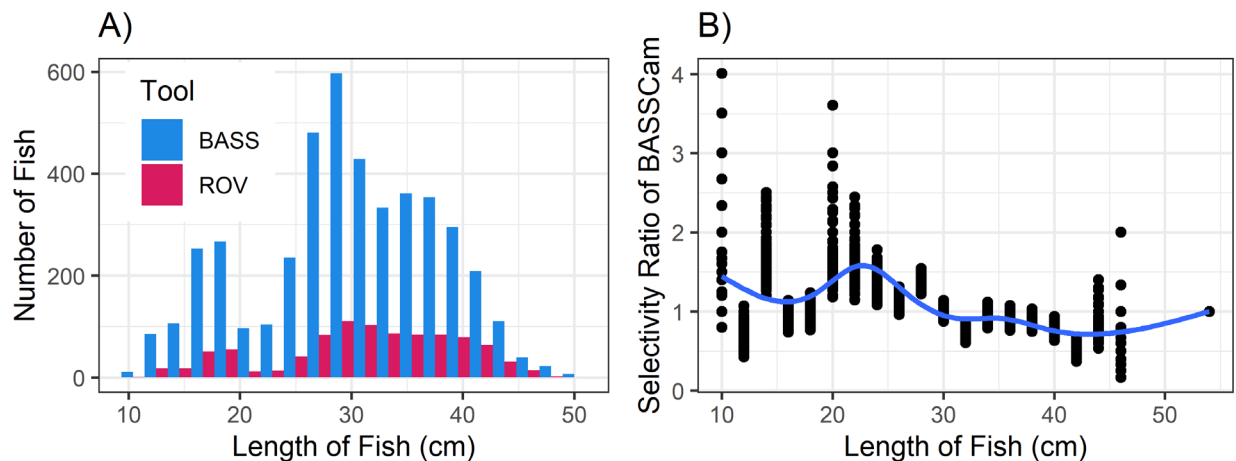


Fig. 3 Number of fish measured by length (A) and selectivity of the BASSCam relative to the ROV for Black and Blue/Deacon Rockfish (B). For selectivity, values above 1 indicate greater selection by the BASSCam and values less than 1 indicate greater selection by the ROV. Black dots denote each estimate of selectivity from 1000 sampling iterations and the blue line denotes the estimate of selectivity from a generalized additive model of selectivity vs. length.

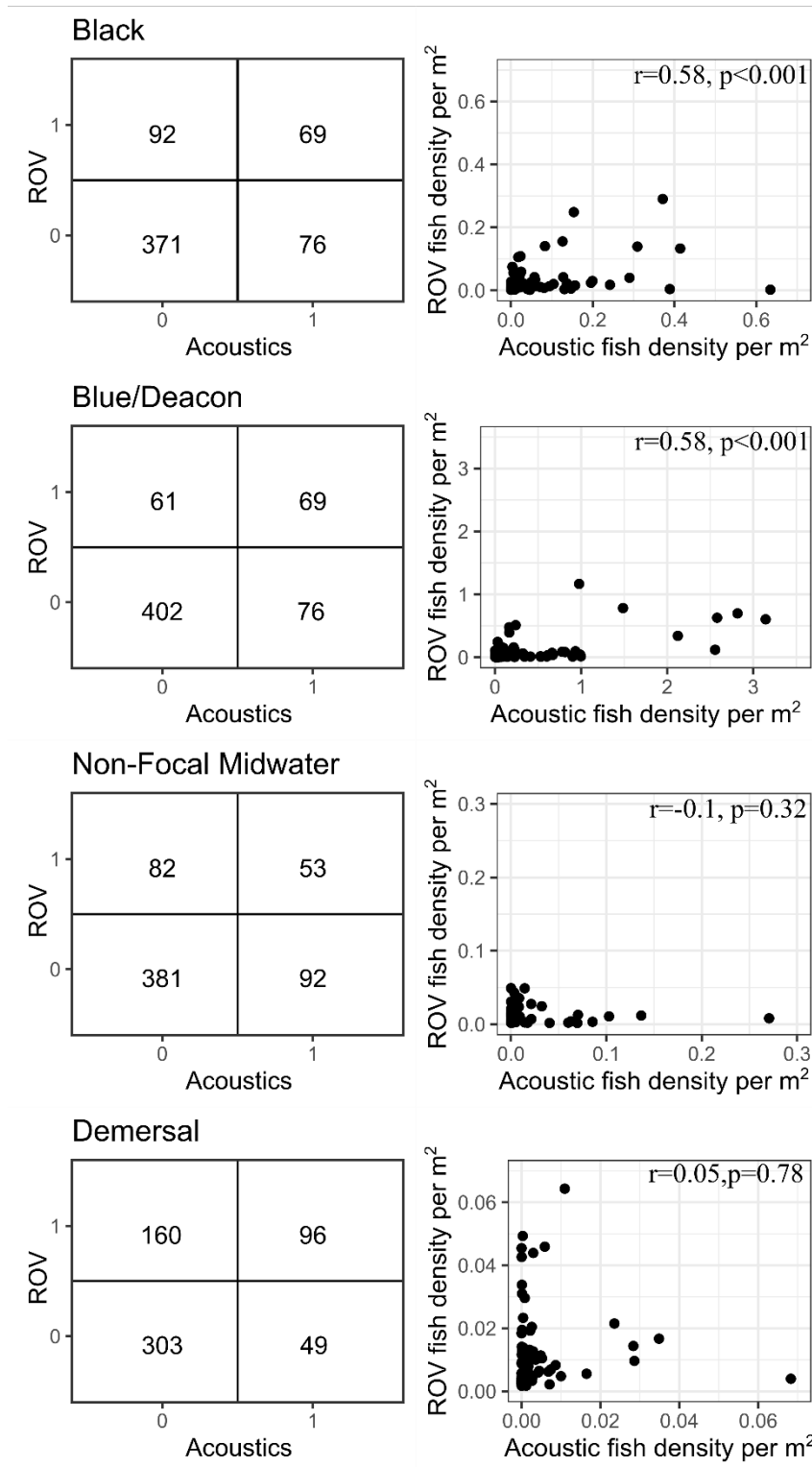


Fig. 4 Confusion matrices of fish presence/absence by transect segment (left) and correlation of segment fish densities (right, with Pearson's correlation statistics) among tools (Acoustics vs. ROV) for each species group. In the confusion matrices 1 denotes fish were observed and 0 denotes no fish were observed.

SPATIAL CORRESPONDENCE AMONG TOOLS

In general, there was spatial overlap in where the ROV and the acoustics/BASSCam observed fish. The accuracy calculated from the presence/absence confusion matrix was 72% for Black Rockfish, 77% for Blue/Deacon Rockfish, 71% for non-focal semi-pelagic rockfish, and 65% for demersal rockfish. The sensitivity was 42% for Black Rockfish, 53% for Blue/Deacon Rockfish, 39% for non-focal semi-pelagic rockfish, and 37% for demersal rockfish. Density estimates for Black Rockfish and Blue/Deacon Rockfish were moderately well correlated between tools ($r = 0.58$, $p < 0.001$ for both groups, Fig. 4). For the non-focal semi-pelagic and demersal rockfish, density correlations were non-significant, and poor, respectively (Fig. 4).

Table 2. Relative model fit variables and model selection criteria (Delta AIC, Log Likelihood and Akaike Weight) for every model formulation used to compare the proportion of fish in the exclusion zone among tools. Delta AIC, Log Likelihood and Akaike weight are used to assess the quality of model fits. A Delta AIC of 0 denotes the best fit model. A log likelihood and Akaike weight of 1 denotes a model with strong support. Reef: Study reef; Camera: ROV vs BASSCam; Species: species/species group (Table 1). The response variable was the proportion of fish within the exclusion zone out of the total number counted and was modeled using GLMs with a binomial distribution.

Formula	Delta AIC	Log Likelihood	Akaike Weight
Camera*Species*Reef	26.09	0	0
Species*Reef	29.74	0	0
Camera*Reef	41.86	0	0
Camera*Species	0	1.00	1.00
Species	16.22	0	0
Reef	80.72	0	0
Camera	34.31	0	0
1	79.67	0	0

EXCLUSION ZONE DENSITIES WITHIN FISH SCHOOLS

Our best fit model included an interaction between species/species group and video tool (Table 2, see online supplement Table S1 for summary of best fit model). The next best fit models had AIC values ~ 15 units higher than the best fit model, suggesting strong consensus in model selection. This was corroborated by Akaike weight and log likelihood values of 1. The BASSCam observed a higher proportion of fish above the exclusion zone than the ROV for all semi-pelagic functional groups (Fig. 5). The ROV observed few demersal rockfish above the exclusion zone. Blue/Deacon Rockfish were seen primarily above the exclusion zone in both tools.

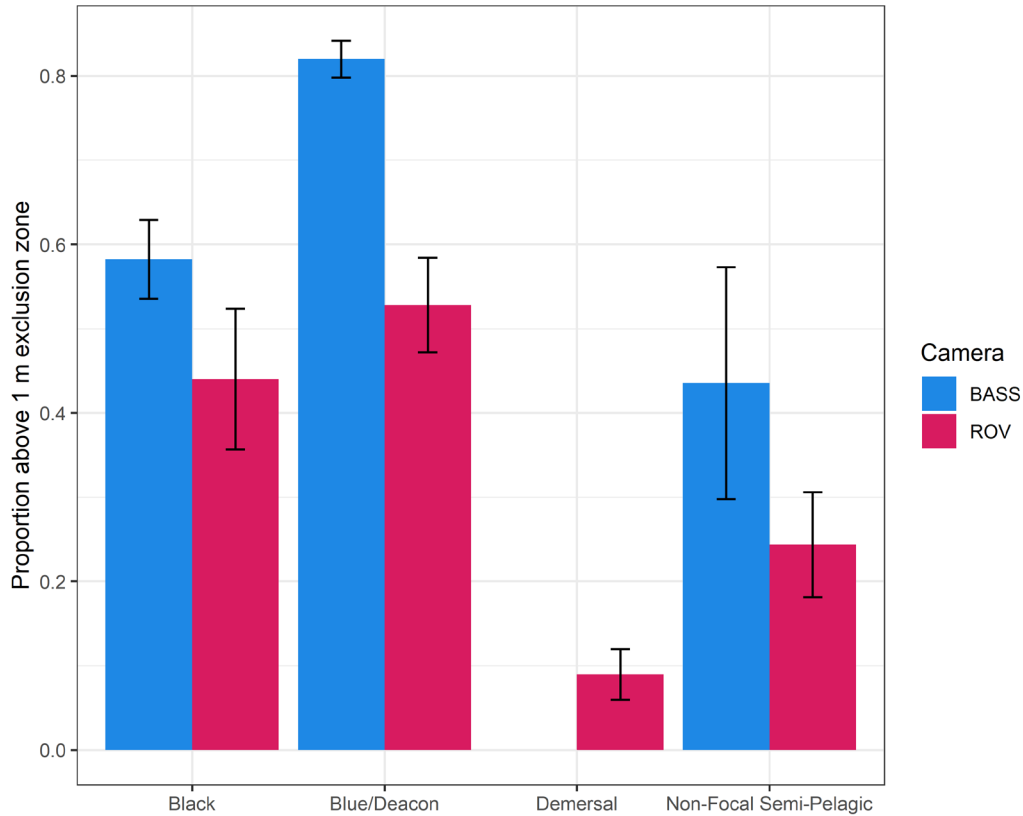


Fig. 5 Average proportion (\pm standard deviation) of fish observed above the exclusion zone (0-1 m) across all reefs by each tool, for each of the four species/species groups. No demersal fish were observed by the BASSCam in locations with collocated ROV data. Model selection suggested there was no effect of reef (see Table 2).

FISH DENSITIES OUTSIDE SCHOOLS

Our best fit model of fish density in relation to distance from school included an interaction between reef and distance, with reef as an independent factor (Table 3, see online supplement for summary of best fit models and plots of raw data). The best fit model for each species/species group, except demersals, was well supported (high Akaike weights). Unsurprisingly, models of demersals had relatively poor fits, as trends in demersal rockfish density were not expected to be influenced by the locations of schooling fish. Examination of the GAM smooths suggested that excluding the area within 35 m of fish schools would result in a reasonably conservative estimate of background (non-school) fish density (i.e., likely to exclude all influence of schools), for Black and Blue/Deacon rockfish (Fig. 6). Background densities were calculated for each species/species group using all data from the region greater than 35 m from school edges (Table 4).

Table 3. Delta AIC, Log Likelihood and Akaike Weight values for every potential model formulation assessing the relationship between ROV-derived density and distance from the edge of each acoustically-detected school. Delta AIC, Log Likelihood and Akaike weight are used to assess the quality of model fits. A Delta AIC of 0 denotes the best fit model. A log likelihood and Akaike weight of 1 denotes a model with strong support. Distance: Distance from the edge of each fish school; Reef: Study reef.

<u>Black</u>			
Formula	Delta AIC	Log Likelihood	Akaike Weight
Distance*Reef+Reef	0	1.00	0.92
Distance*Reef	4.84	0.09	0.08
Distance+Reef	13.99	0	0
Distance	38.29	0	0
Reef	42.48	0	0
~1	71.71	0	0

<u>Blue/Deacon</u>			
Formula	Delta AIC	Log Likelihood	Akaike Weight
Distance*Reef+Reef	0	1.00	1.00
Distance*Reef	44.96	0	0
Distance+Reef	10.83	0	0
Distance	43.26	0	0
Reef	26.85	0	0
~1	53.23	0	0

<u>Demersal</u>			
Formula	Delta AIC	Log Likelihood	Akaike Weight
Distance*Reef+Reef	0	1.00	0.47
Distance*Reef	1.62	0.44	0.21
Distance+Reef	3.65	0.16	0.08
Distance	2.08	0.35	0.17
Reef	5.97	0.05	0.02
~1	4.53	0.10	0.05

<u>Non-Focal Semi-pelagic</u>			
Formula	Delta AIC	Log Likelihood	Akaike Weight
Distance*Reef+Reef	0	1.00	1.00
Distance*Reef	10.96	0	0
Distance+Reef	14.49	0	0
Distance	18.63	0	0
Reef	21.89	0	0
~1	26.74	0	0

Table 4. Background ROV density (individuals per 100 m²) and standard deviation at each reef for each species/functional group. Background densities were calculated for the entire region >35 m from the outside edge of schools observed in the acoustic sampling. Raw density: the mean transect density assessed by the ROV main camera; SD: the standard deviation of the raw density among transects; Adjusted density in exclusion zone: Raw density multiplied by the proportion of fish in the 0-1 m exclusion zone in the ROV's stereo cameras, out of the total fish within 2 m of the bottom; N: number of transects.

Species	Reef	Raw density	SD	Adjusted density in exclusion zone	Adjusted SD	N
Black	Bandon	0.193	0.317	0.141	0.233	17
Black	Arago	0.449	0.866	0.324	0.624	13
Black	Orford Reef	0.193	0.331	0.130	0.223	18
Black	Redfish					
Black	Rocks	0.311	0.357	0.120	0.138	17
Black	All Reefs	0.275	0.487	0.170	0.301	65
Blue/Deacon	Bandon	0.123	0.362	0.070	0.207	17
Blue/Deacon	Arago	0.380	0.630	0.191	0.317	13
Blue/Deacon	Orford Reef	0.981	1.357	0.476	0.658	18
Blue/Deacon	Redfish					
Blue/Deacon	Rocks	0.108	0.266	0.037	0.091	17
Blue/Deacon	All Reefs	0.408	0.867	0.197	0.418	65
Demersal	Bandon	0.289	0.299	0.278	0.288	17
Demersal	Arago	0.530	0.555	0.505	0.528	13
Demersal	Orford Reef	0.324	0.243	0.304	0.228	18
Demersal	Redfish					
Demersal	Rocks	0.174	0.168	0.165	0.159	17
Demersal	All Reefs	0.317	0.343	0.300	0.325	65
Non-Focal Semi-pelagic	Bandon	0.550	1.832	0.523	1.742	17
Non-Focal Semi-pelagic	Arago	0.263	0.389	0.222	0.328	13
Non-Focal Semi-pelagic	Orford Reef	0.186	0.218	0.136	0.160	18
Non-Focal Semi-pelagic	Redfish					
Non-Focal Semi-pelagic	Rocks	0.143	0.247	0.108	0.186	17
Non-Focal Semi-pelagic	All Reefs	0.285	0.961	0.228	0.766	65

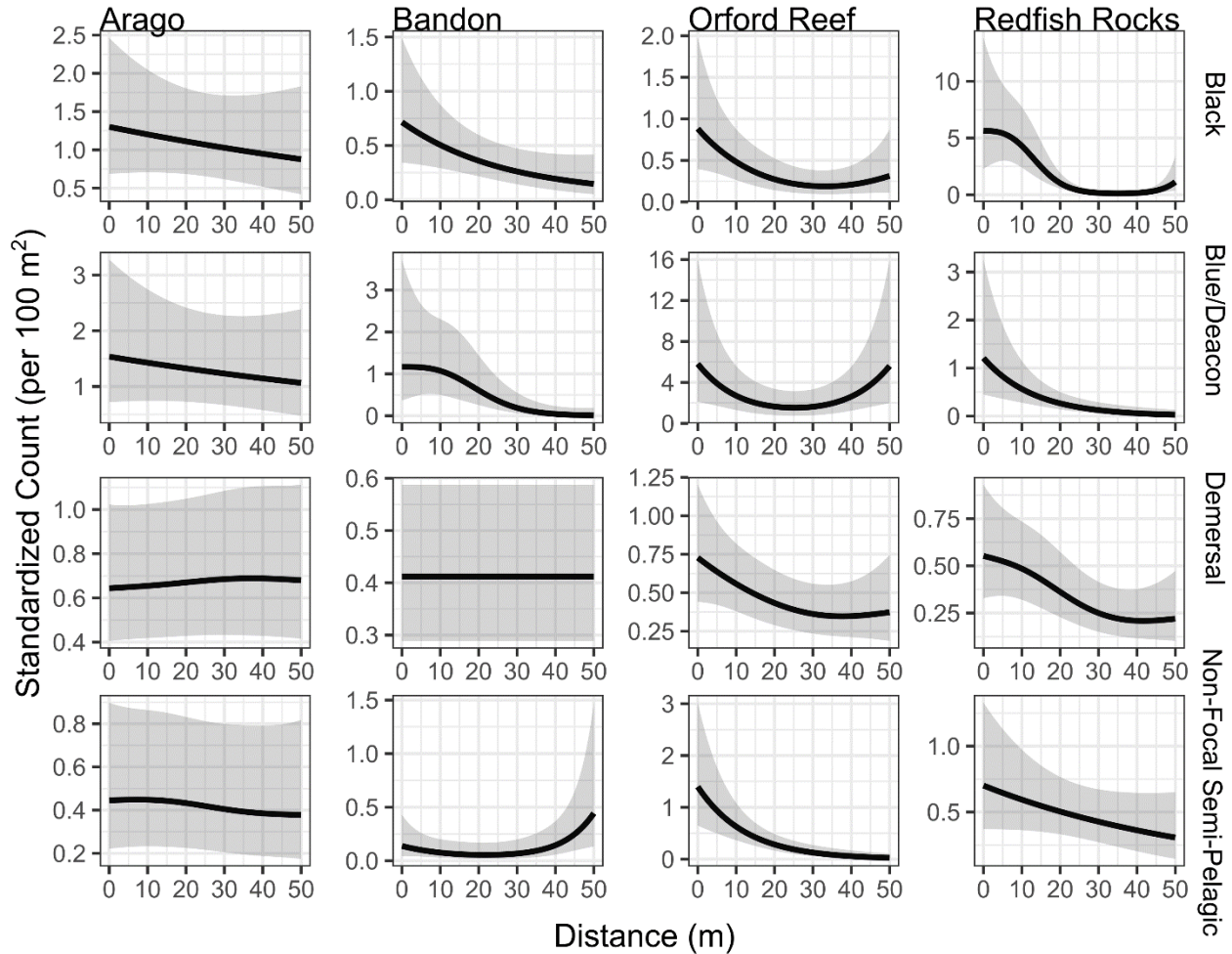


Fig.6 Generalized additive models relating the number of fish counted by the ROV to the distance from the edge of schools (as identified by acoustics). The analysis extended to 50 m from the school edge. 0 m represents counts within the school. See Table 3 for model selection. Note that y-axis scaling differs among plots.

DENSITY ESTIMATE

The total reef density estimates of Black and Blue/Deacon Rockfish were higher when derived from the acoustics/BASSCam than from the ROV (Fig. 7), which was expected, due to the ROV only viewing the bottom component of the vertical distribution of the schooling species. Black Rockfish were 5.7 times more prevalent in the video-hydroacoustic data than in the ROV data and Blue/Deacon Rockfish were 9.7 times more prevalent in the video-hydroacoustics than in the ROV data. However, an extremely high density of Blue/Deacon Rockfish was observed in the video-hydroacoustics at Cape Arago and if these data are excluded, Blue/Deacons were only 2.9 times more prevalent in the video-hydroacoustics than the ROV data. Conversely, demersal rockfish were 16.5 times more prevalent in the ROV data than the video-hydroacoustics, again consistent with the on-bottom distribution of these solitary species. Non-focal semi-pelagic

rockfishes were 1.6 times more prevalent in the video-hydroacoustics than ROV, but it is worth noting the densities of this species group were extremely low and variable compared to the other species groups. The coefficient of variation was quite high for both tools (Table 5).

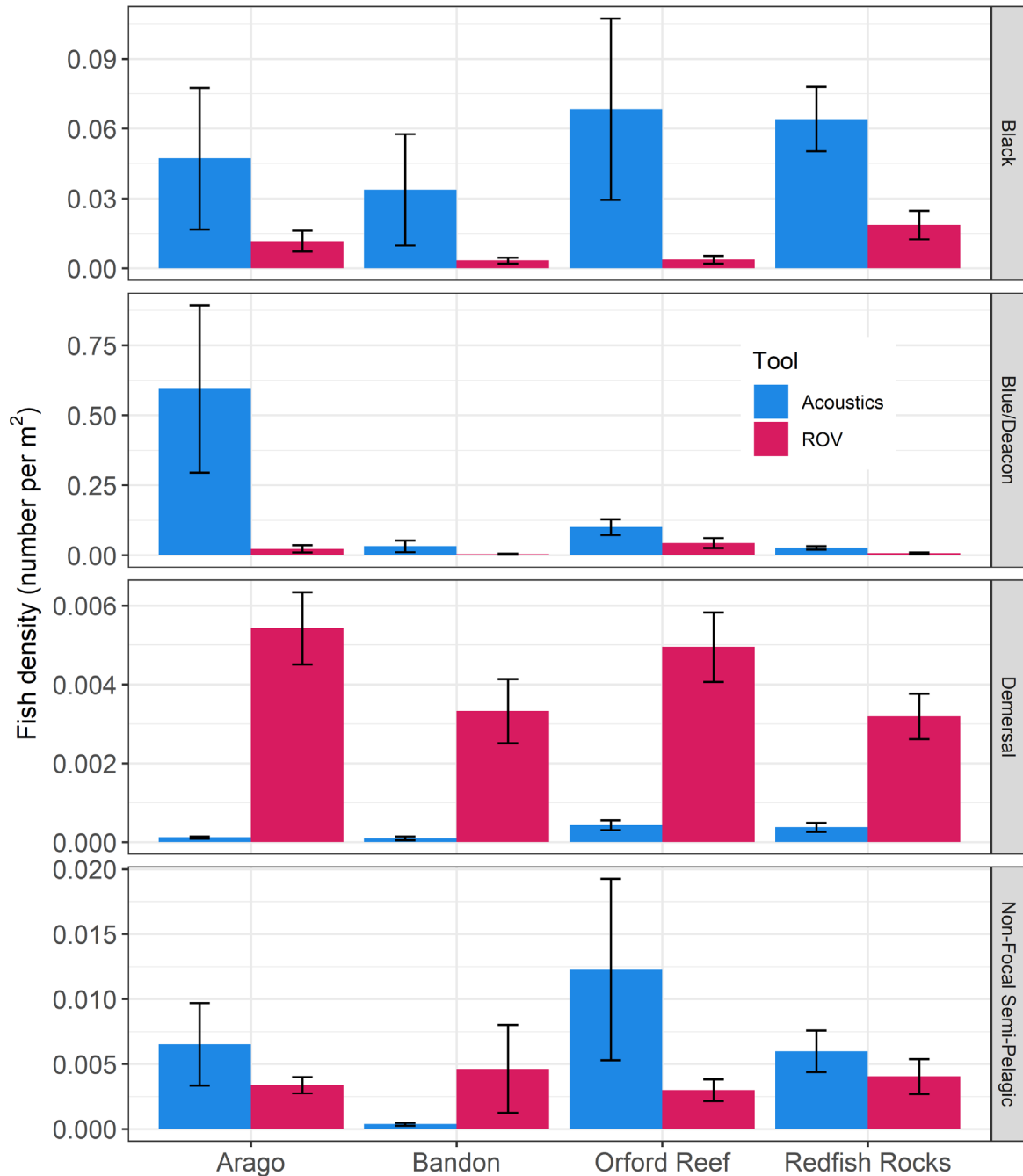


Fig. 7 Mean reef-level density estimates from each of the two sampling tools for each reef and species group. Error bars denote standard deviation. Acoustics- denotes densities generated from video-hydroacoustic combined sampling.

DISCUSSION

In this study we set out to assess the relative effect of applying a near-bottom exclusion zone (area above the bottom excluded to account for the near bottom dead zone) to an acoustic survey of Oregon’s nearshore semi-pelagic rockfish. We paired a combined hydroacoustic and underwater video sampling method (BASSCam) with ROV video sampling to determine the relative contribution of the exclusion zone to the overall abundance estimate. However, we first had to assess whether the observations from each tool were similar to one another. We found that the length distributions of our target species/species groups differed minimally between the tools and there was little evidence of size selectivity between tools (Kotwicki *et al.*, 2017). Further, there was good spatial coherence in the observations between our two tools, and the densities of observed fish were well correlated for the schooling semi-pelagic fish species targeted by this study. Based on these findings, we conclude that by comparing these two survey methods we were able to accurately assess the relative importance of fish in the exclusion zone in an acoustic-based abundance estimate for semi-pelagic rockfish. We found that overall, a relatively small proportion of our focal semi-pelagic rockfish were within the exclusion zone, suggesting the combined hydroacoustic suspended camera survey is able to accurately observe most of our focal species. The findings reported in this study suggest the BASSCam approach could correct for fish within the exclusion zone that are missed by the acoustics and support further investigation into the use of a combined hydroacoustic video methodology in future, large-scale surveys. However, our results also show that longer acoustic transects are necessary in order to reduce the variability in density estimates.

Table 5. Coefficient of variation for the density estimates for each of the species/species groups for each tool at each reef, and for all reefs on average.

Reef	Black		Blue/Deacon		Non-Focal Semi-pelagic		Demersal	
	<u>Acoustics</u>	<u>ROV</u>	<u>Acoustics</u>	<u>ROV</u>	<u>Acoustics</u>	<u>ROV</u>	<u>Acoustics</u>	<u>ROV</u>
Arago	0.43	0.72	0.54	0.48	0.56	1.50	1.25	1.64
Bandon	0.39	0.74	0.42	0.63	1.06	0.37	0.62	1.13
Orford Reef	0.45	0.59	0.95	0.66	0.46	0.95	1.03	1.50
Redfish Rocks	1.28	0.84	1.37	0.65	1.12	0.83	0.99	1.53
Average	0.63	0.72	0.82	0.61	0.80	0.91	0.97	1.45

Different video sampling tools, especially moving platforms, inherently have the potential to affect fish behavior. In this study, the ROV may elicit behavioral responses due to movement, noise, and artificial light of the tool. The BASSCam may elicit behavioral responses due to lights, structure in the water column, and bottom disturbance at the time of deployment. A quantitative assessment of how our two video sampling devices affected fish behavior was not possible within the scope of this study. Previous work has shown that there is little effect of the

BASSCam on fish behavior (Rasmuson *et al.*, 2021). Further, during the review of many hours of video no systematic behavioral response to either camera platform was observed. Specifically, none of the species entered the field of view of the ROV in a manner that suggested either approach toward or flight from the device. Fish also did not appreciably change their height off bottom in response to the device.

Quantitative assessments of behavioral interaction of reef fish with sampling platforms can be exceedingly complex (Somerton *et al.*, 2017; Garner *et al.*, 2022) and species-specific behaviors (gear approach and gear avoidance) should be anticipated (Stoner *et al.*, 2008). Thus, extrapolating results from other species in different regions is not advised. Studying the *Sebastes* genus, Ryer *et al.* (2009) assessed simulated underwater vehicle lighting on behavior of Black and Blue Rockfish. They found fish avoided approaching light, but that response was drastically reduced in high ambient light conditions. Our study was conducted in shallow water (< 50 m) during daylight, suggesting high ambient light and a potentially lower risk of artificial light avoidance. Laidig *et al.* (2013) assessed movement of rockfish in California in response to an approaching ROV, but their study was much deeper (70-400 m), so the ambient lighting was much less than in our study and neither Black Rockfish nor Deacon Rockfish were assessed. As such, although some studies have been conducted on the species of interest to this paper, further work is necessary to fully quantify behavioral responses to survey tools.

The dead zone has the potential to greatly influence the population estimates of species surveyed with hydroacoustics (Ona and Mitson, 1996). A common way to correct acoustic data is to extrapolate the acoustic backscattering data from above the exclusion zone into the exclusion zone (Kloser, 1996). While this method is often applied without validating the assumption of consistent density, here we tested that assumption by comparing proportions of fish observed above and within the exclusion zone and were able to confidently state that a linear extrapolation into the exclusion zone would provide a realistic correction to the acoustic data for Black Rockfish. The two video tools (ROV and BASSCam) found the proportion of Black Rockfish was only minimally different above and within the exclusion zone. In contrast, Blue/Deacon Rockfish were much more prevalent just above the exclusion zone than within it, so simple extrapolation of above-exclusion-zone densities from video would erroneously inflate a density estimate (and therefore the corresponding total abundance estimate) for this species. Our data suggest that either 1:1 extrapolation of acoustic data from above the exclusion zone into the exclusion zone or an inclusion of a density estimate from the BASSCam could be used for Black Rockfish. However, for Blue/Deacon Rockfish an acoustic extrapolation would need to be reduced to account for the greater abundance above the exclusion zone suggesting a density estimate from the BASSCam may be more suitable.

Although our data suggest the BASSCam's downward facing camera provides adequate data for correcting fish schools by multiplying their acoustic signature from above the exclusion zone

into the exclusion zone, there is still potential that non-schooling fish located within the exclusion zone are being missed. Because the BASSCam is only deployed in schools identified by the acoustics, and if no acoustically identified school above the exclusion zone exists, the acoustics cannot be extrapolated downwards to correct for these missed fish. In this study, the addition of ROV belt transects allowed us to estimate background density, the density of fish within the exclusion zone that are not associated with fish schools. Since we observed little difference in the background densities of our target species/species groups between reefs we suggest a single background density correction could be considered for all survey areas. In future studies, utilizing either BASSCam or ROV derived background density data would allow for a full population estimate that corrects for these missed fish. As a co-occurring ROV survey and large-scale acoustic-visual survey is not feasible, it is possible that a fixed correction could be generated by ROV surveys conducted outside of the time frame of the acoustic-visual survey or that the BASSCam could be deployed haphazardly along the transect and counts from the downward facing camera used to generate a background density. A cheaper solution is to apply the background density data from this study, but would need to be done in association with the caveat that the potential for time varying densities is being ignored.

An important consideration with genera like *Sebastes* is the allocation of acoustic data to different species. Opportunely, our finding that demersal rockfish remained within 1 m of the bottom implies that despite the great diversity of rockfish in Oregon's nearshore, many of these species occur outside of the observational scope of the acoustics and therefore do not contribute to our acoustic estimates or the resulting population estimate. As such, potential contamination to our population estimate is only from 3 species (Canary (*Sebastes pinniger*), Widow and Yellowtail Rockfish). The challenge of species differentiation is further simplified by the ease of detection of these species with the BASSCam. These non-focal semi-pelagic species have been shown to be good candidates for acoustic surveys (Stanley, 1999, 2000) and the methods we describe here could easily be adapted to continental shelf stocks.

A potential concern in using the BASSCam to provide species and length composition data to apportion backscattering data into density is that it creates point estimates from a limited number of fish schools on each transect, as opposed to species and length data from the entire length of the transect. As the ROV conducted belt transects, we were able to assess whether our point estimates missed species and/or size classes of fish. There were few species only observed by one video tool and not the other. Where species were only observed by one tool, it was often the ROV observing non-rockfish species or demersal rockfish. The first were excluded from analyses based on the school detection algorithm because it is adjusted to look for schools known to be rockfish. The latter were excluded since, as discussed above, they are almost exclusively located in the exclusion zone. Therefore, we suggest point estimates from the

BASSCam can provide valid assessments of species and length composition of acoustically-available species for a reef.

It is worth noting that the total number of fish counted by the ROV is much higher than the total for the BASSCam; however, since the conversion of acoustic backscattering data into density only requires the relative proportions of the species (where total abundance is not important), this has little effect. The length distribution observed by the ROV and BASSCam did not differ in most instances. Because the ROVs length data were taken from the entirety of the transect and the BASSCam from schools, this suggests that there is no size fractionation between schools and individuals not located within schools. Overall, these data suggest that point estimates taken within schools, by the BASSCam, provide accurate species and length composition data.

Density estimates for schooling target species/species groups derived from our video-hydroacoustics were much greater than those derived from ROV data. This result was expected based on the semi-pelagic position of many of these fish. Rasmuson et al. (2021) demonstrated there was strong coherence between the population estimate from a previous passively integrated transponder (PIT) tagging study and combined video-hydroacoustic survey. Our work further confirms that this combined survey method is well designed for the target species/species groups in this study. Similar to the findings of Rooper et al. (2020), the choice of which video sampling tool is used depends on habitat and species. In our case we find that the suspended stereo system is better designed to sample nearshore semi-pelagic fish than bottom oriented tools like benthic video landers and ROVs. Although some individuals of our focal species are present within the exclusion zone, most are located above it and therefore are readily observed by the acoustics and the BASSCam, as is shown by the much higher density of fish estimated by the acoustic-visual survey tool. Regardless, fish within the exclusion zone not observed by the acoustics (both schools and background densities), potentially could be corrected for using the downward facing camera on the BASSCam. Advantageously, most of the non-focal species are located almost exclusively within the exclusion zone, so they do not contribute to the acoustic estimate. Regardless of the utility of the tools, it is important to note that the coefficient of variation values for both survey tools were high. This is likely because the transects were very short (300-500 m). which greatly contributed to increased variability in the data. Application of a combined hydroacoustic video survey to a full, regional-scale, population survey would require longer (multiple kilometers) transects, which would likely reduce the variance in the density estimate seen in the present study. Further, this study demonstrated strong spatial and temporal variability within and between reefs, suggesting that for both the ROV and acoustics, modeling-based approaches to population estimates are likely the best way forward.

While these methods are specifically designed for nearshore species, they can easily be adapted to work with semi-pelagic shelf rockfish stocks. Our work demonstrates that the exclusion zone does not negatively affect the ability of the tool to sample our target species/species groups. Using our conservative exclusion zone (all areas within 1 m of the bottom) enhances the utility of the tool by reducing the number of species we observe. Ultimately this ensures the acoustic density estimate primarily reflects target semi-pelagic rockfish and is not contaminated by demersal rockfish. Furthermore, targeting fish schools with an easily deployable stereo video system provides an accurate estimate of species composition and length data. In an area where the visibility is characteristically bad, the ability to first identify large schools with hydroacoustic equipment and then deploy cameras directly into these schools greatly increases the chance of collecting data. In short, we find that the combination of acoustics and suspended stereo cameras is an effective survey tool for semi-pelagic rockfish.

ACKNOWLEDGMENTS

We thank captain Dave DeBelloy of the CPFV Enterprise and captain Bob Pedro of the RV Miss Linda for their assistance in this project. We thank Alison Whitman, Greg Krutzikowsky and David Fox for their assistance in obtaining the grant funding, and Bill Miller and Steve Kupillas for survey implementation and video review. Funding for this project was made available from the NOAA Saltonstall-Kennedy grant program grant number NA17NMF4270223.

REFERENCES

- Allouche, O., Tsoar, A., and Kadmon, R. 2006. Assessing the accuracy of species distribution models: prevalence, kappa and the true skill statistic (TSS): Assessing the accuracy of distribution models. *Journal of Applied Ecology*, 43: 1223–1232.
- Balk, H., and Lindem, T. 2000. Improved fish detection in data from split-beam sonar. *Aquat Living Resour*, 13: 297–303.
- Barange, M. 1994. Acoustic identification, classification and structure of biological patchiness on the edge of the Agulhas Bank and its relation to frontal features. *S Afr J Mar Sci*, 14: 333–347.
- Denney, C., Fields, R., Gleason, M., and Starr, R. 2017. Development of New Methods for Quantifying Fish Density Using Underwater Stereo-video Tools. *Journal of Visualized Experiments*. <https://www.jove.com/video/56635/development-new-methods-for-quantifying-fish-density-using-underwater> (Accessed 14 August 2018).
- Garner, S. B., Ahrens, R., Boswell, K. M., Campbell, M. D., Correa, D., Tarnecki, J. H., and Patterson, W. F. 2022. A multidisciplinary approach to estimating red snapper, *Lutjanus campechanus*, behavioral response to mobile camera and sonar sampling gears. *Fisheries Research*, 246: 106155.

- Gauthier, S., and Rose, G. 2005. Diel vertical migration and shoaling heterogeneity in Atlantic redfish: effects on acoustic and bottom-trawl surveys. *ICES Journal of Marine Science*, 62: 75–85.
- Haralabous, J. 1996. Artificial neural networks as a tool for species identification of fish schools. *ICES Journal of Marine Science*, 53: 173–180.
- Hilborn, R., and Walters, C. J. 1992. *Quantitative fisheries stock assessment: choice, dynamics and uncertainty*. Chapman and Hall, New York.
- ICES. 2000. Report on Echo Trace Classification. ICES. [http://www.ices.dk/sites/pub/Publication Reports/Forms/DispForm.aspx?ID=35681](http://www.ices.dk/sites/pub/Publication%20Reports/Forms/DispForm.aspx?ID=35681) (Accessed 9 September 2020).
- Jones, D. T., Wilson, C. D., De Robertis, A., Rooper, C. N., Weber, T. C., and Butler, J. L. 2012. Evaluation of rockfish abundance in untrawlable habitat: combining acoustic and complementary sampling tools. *Fishery Bulletin*, 110: 332–343.
- Kloser, R. 1996. Improved precision of acoustic surveys of benthopelagic fish by means of a deep-towed transducer. *ICES Journal of Marine Science*, 53: 407–413.
- Kloser, R. J., Fisheries Research & Development Corporation (Australia), CSIRO (Australia), and Marine Research. 2002. Development and application of a combined industry/scientific acoustic survey of orange roughy in the eastern zone. Fisheries Research and Development Corp. : CSIRO Marine Research, Hobart, Tas.
- Kotwicki, S., Lauth, R. R., Williams, K., and Goodman, S. E. 2017. Selectivity ratio: A useful tool for comparing size selectivity of multiple survey gears. *Fisheries Research*, 191: 76–86.
- Kotwicki, S., Ressler, P. H., Ianelli, J. N., Punt, A. E., and Horne, J. K. 2018. Combining data from bottom-trawl and acoustic-trawl surveys to estimate an index of abundance for semipelagic species. *Canadian Journal of Fisheries and Aquatic Sciences*, 75: 60–71.
- Laidig, T. E., Krigsman, L. M., and Yoklavich, M. M. 2013. Reactions of fishes to two underwater survey tools, a manned submersible and a remotely operated vehicle. *Fishery Bulletin*, 111. <http://fisherybulletin.nmfs.noaa.gov/1111/laidig.pdf> (Accessed 19 April 2018).
- Love, M. S., Yoklavich, M. M., and Thorsteinson, L. 2002. *The rockfishes of the Northeast Pacific*. University of California Press. 405 pp.
- McClatchie, S., Thorne, R. E., Grimes, P., and Hanchet, S. 2000. Ground truth and target identification for fisheries acoustics. *Fisheries Research*, 47: 173–191.
- McQuinn, I., Simard, Y., Stroud, T., Beaulieu, J., and Walsh, S. 2005. An adaptive, integrated ‘acoustic-trawl’ survey design for Atlantic cod (*Gadus morhua*) with estimation of the acoustic and trawl dead zones. *ICES Journal of Marine Science*, 62: 93–106.
- Mello, L. G. S., and Rose, G. A. 2009. The acoustic dead zone: theoretical vs. empirical estimates, and its effect on density measurements of semi-demersal fish. *ICES Journal of Marine Science*, 66: 1364–1369.
- Misund, O. A. 1997. Underwater acoustics in marine fisheries and fisheries research. *Reviews in Fish Biology and Fisheries*, 7: 1–34.

- Nero, R. W., and Magnuson, J. J. 1989. Characterization of Patches Along Transects Using High-Resolution 70-kHz Integrated Acoustic Data. *Canadian Journal of Fisheries and Aquatic Sciences*, 46: 2056–2064.
- Ona, E., and Mitson, R. B. 1996. Acoustic sampling and signal processing near the seabed: the deadzone revisited. *ICES Journal of Marine Science*, 53: 677–690.
- R Core Team. 2020. R: A language and environment for statistical computing. R Foundation for statistical computing, Vienna, Austria. URL <https://www.R-project.org>.
- Rasmuson, L. 2021. Susceptibility of five species of rockfish (*Sebastes* spp.) to different survey gears inferred from high resolution behavioral data. *Science Bulletin*, 2021–05. Oregon Department of Fish and Wildlife, Salem.
- Rasmuson, L. K., Fields, S. A., Blume, M. T. O., Lawrence, K. A., and Rankin, P. S. 2021. Combined video–hydroacoustic survey of nearshore semi-pelagic rockfish in untrawlable habitats. *ICES Journal of Marine Science*: fsab245.
- Rooper, C. N., Williams, K., Towler, R. H., Wilborn, R., and Goddard, P. 2020. Estimating habitat-specific abundance and behavior of several groundfishes using stationary stereo still cameras in the southern California Bight. *Fisheries Research*, 224: 105443.
- Ryer, C., Stoner, A., Iseri, P., and Spencer, M. 2009. Effects of simulated underwater vehicle lighting on fish behavior. *Marine Ecology Progress Series*, 391: 97–106.
- Sawada, K., Furusawa, M., and Williamson, N. J. 1993. Conditions for the precise measurement of fish target strength in situ. *The Journal of the Marine Acoustics Society of Japan*, 20: 73–79.
- Somerton, D. A., Williams, K., and Campbell, M. D. 2017. Quantifying the behavior of fish in response to a moving camera vehicle by using benthic stereo cameras and target tracking. *Fishery Bulletin*, 115: 343–354.
- Stanley, R. 2000. Estimation of a widow rockfish (*Sebastes entomelas*) shoal off British Columbia, Canada as a joint exercise between stock assessment staff and the fishing industry. *ICES Journal of Marine Science*, 57: 1035–1049.
- Stanley, R. D. 1999. Diel vertical migration by yellowtail rockfish, *Sebastes flavidus*, and its impact on acoustic biomass estimation. *Fish Bull.*
- Stoner, A. W., Ryer, C. H., Parker, S. J., Auster, P. J., and Wakefield, W. W. 2008. Evaluating the role of fish behavior in surveys conducted with underwater vehicles. *Canadian Journal of Fisheries and Aquatic Sciences*, 65: 1230–1243.
- Totland, A., Johansen, G. O., Godø, O. R., Ona, E., and Torkelsen, T. 2009. Quantifying and reducing the surface blind zone and the seabed dead zone using new technology. *ICES Journal of Marine Science*, 66: 1370–1376.
- Tschersich, P. 2015. Hydroacoustic survey of Black Rockfish abundance and distribution operational plan for the Afognak and Northeast districts of the Kodiak management area, 2015. Alaska Department of Fish and Game, Division of Commercial Fisheries, Regional Operational Plan ROP. CF. 4K.2015.18, Kodiak. Alaska Department of Fish and

- Game, Division of Sport Fish, Research and Technical Services. https://wc.adfg.state.ak.us/static/regulations/regprocess/fisheriesboard/pdfs/2012-2013/ayk/fms12_07.pdf (Accessed 21 July 2017).
- Tušer, M., Prchalová, M., Mrkvička, T., Frouzová, J., Čech, M., Peterka, J., Jůza, T., *et al.* 2013. A simple method to correct the results of acoustic surveys for fish hidden in the dead zone. *Journal of Applied Ichthyology*, 29: 358–363.
- Visa, S., Ramsay, B., Ralescu, A., and Van Der Knapp, E. 2011. Confusion matrix-based feature selection. *In* MAICS, pp. 120–127.
- Wood, S. 2006. *Generalized additive models: An introduction with R*. CRC Press, Boca Raton, FL.
- Wood, S. 2011. Fast stable REML and ML estimation of semiparametric GLMs. *J Roy Stat Soc B Met*, 73: 3–36.

SUPPLEMENT

The following maps show the individual transects sampled at each reef overlaid on the best available multibeam bathymetry.

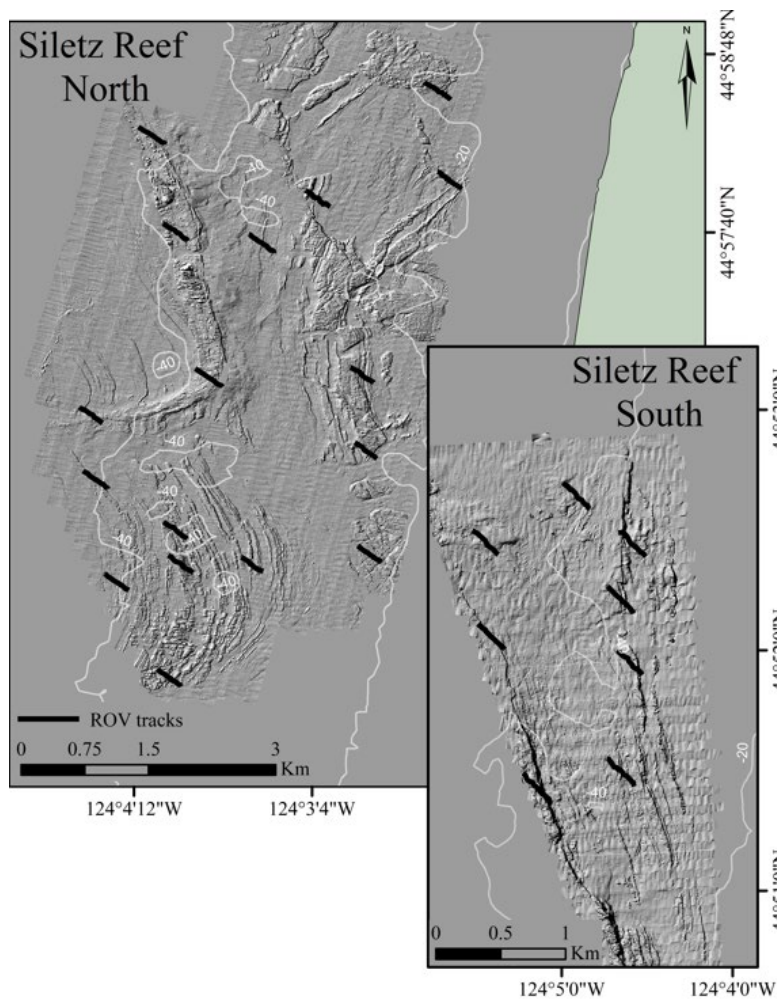


Fig. S1 Cascade Head (Siletz Reef) survey areas. Black lines are the transects sampled by the ROV and acoustics. On each transect three BASSCam drops were conducted (not depicted here due to figure resolution).

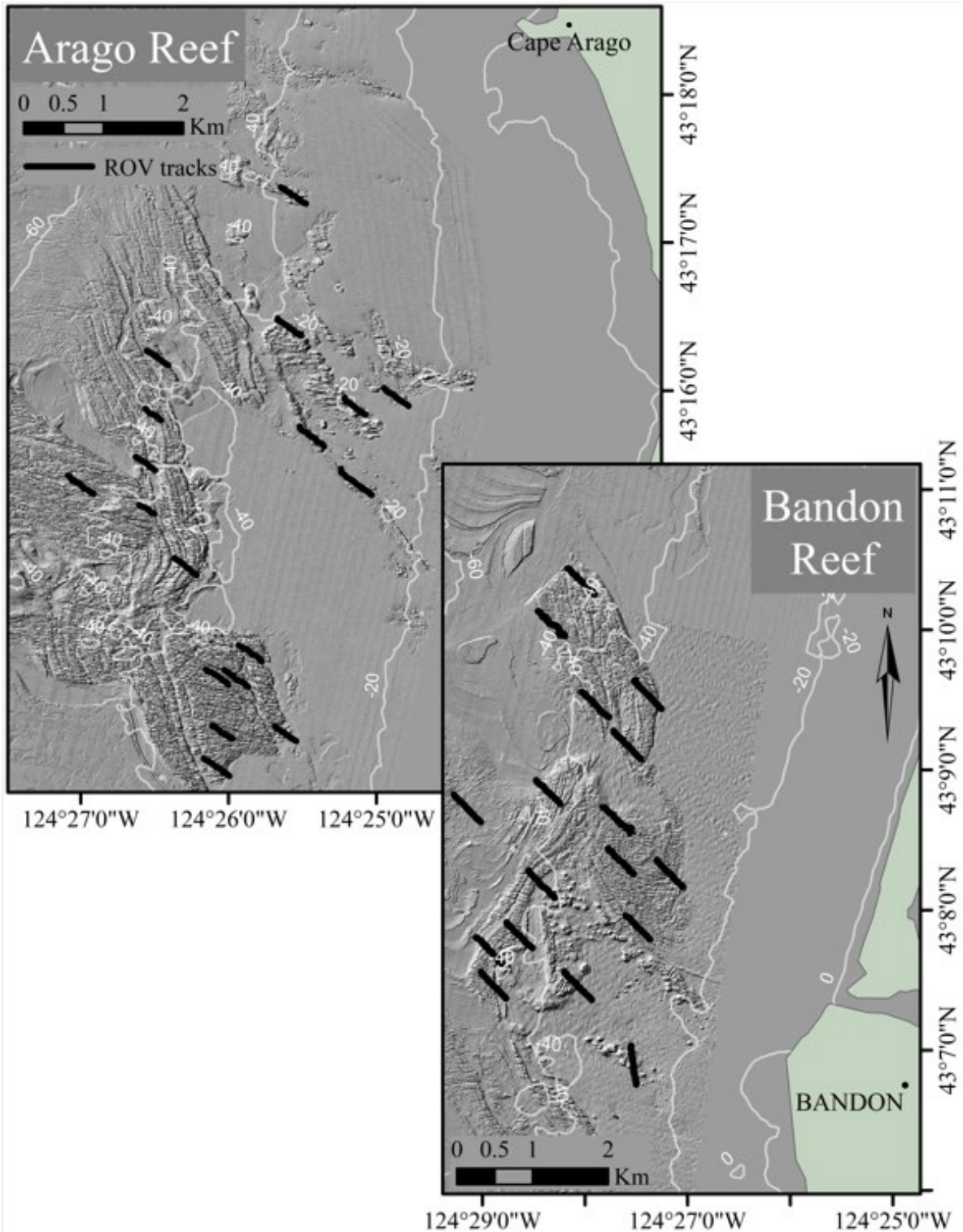


Fig. S2 Arago and Bandon survey areas. Black lines are the transects sampled by the ROV and acoustics. On each transect three BASSCam drops were conducted (not depicted here due to figure resolution).

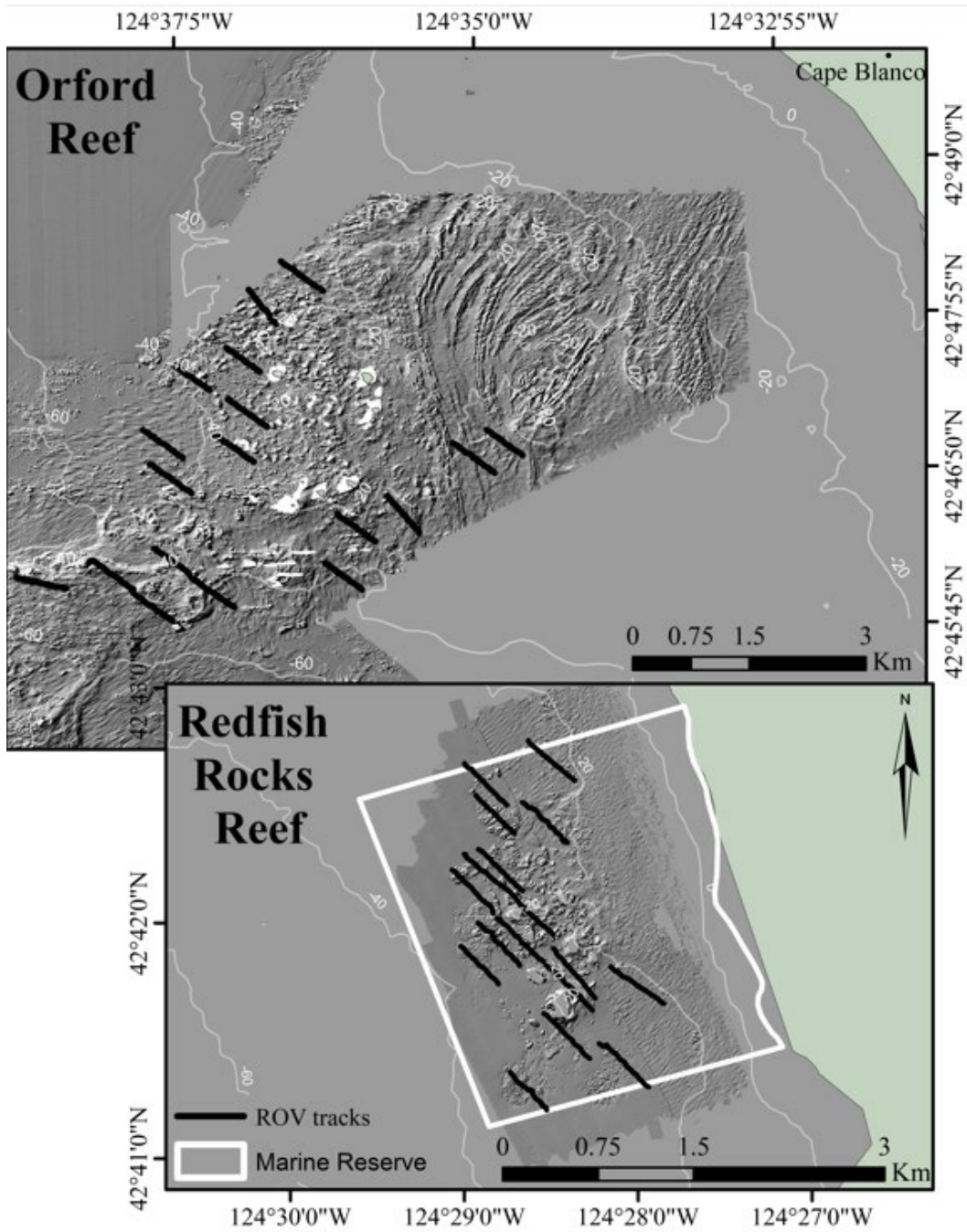
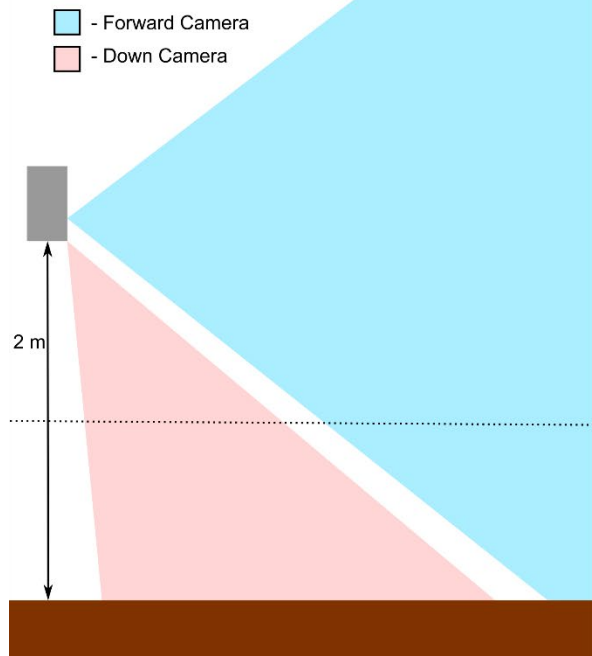


Fig. S3 Orford and Redfish Rocks survey areas. Black lines are the transects sampled by the ROV and acoustics. On each transect three BASSCam drops were conducted (not depicted here due to figure resolution).

A) BASSCam View Diagram



B) BASSCam Example

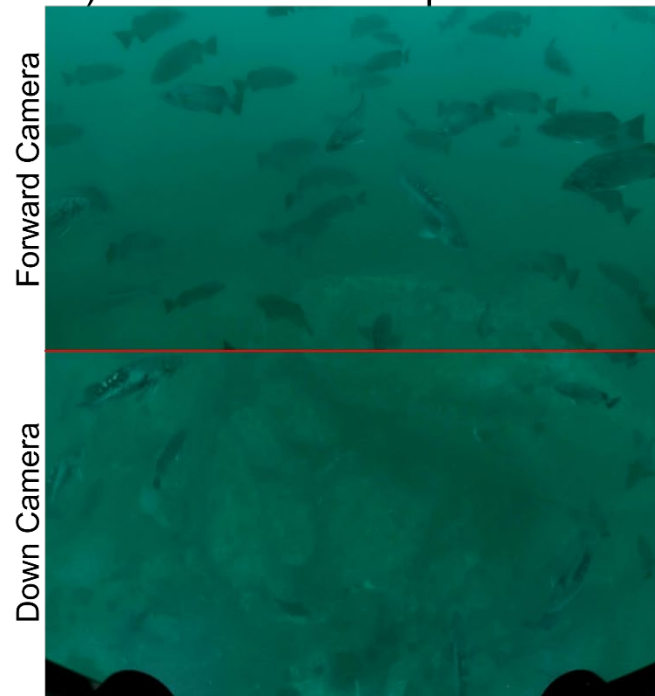


Fig. S4 Diagram of viewed areas by the forward and down cameras on the BASSCam (A) and an example of a fish school being viewed by the BASSCam (B). Note the diagram (A) is not to scale.

Table S1 Model summary output for the best-fit GAM to examine the effect of Camera, Reef and Species on proportion of fish in the dead zone (section 2.3.3 and 3.3 in the primary manuscript).

glm(formula = Proportion Fish ~ Camera * Species, family = binomial)

Deviance Residuals:

Min	1Q	Median	3Q	Max
-1.3212	-0.4334	-0.1655	0.3748	2.1964

	Estimate	Std. Error	z value	Pr(> z)
(Intercept)	0.3318	0.4323	0.767	0.44281
Camera=ROV	-0.5718	0.5856	-0.976	0.32888
Species=Blue/Deacon	1.1837	0.6213	1.905	0.05676
Species=Demersal	-2.0782	0.6642	-3.129	0.00175
Species=Non-Focal Semi-pelagic	-0.5917	0.8764	-0.675	0.49955
Camera = ROV & Species=Blue/Deacon	-0.8313	0.8031	-1.035	0.30061
Camera = ROV & Species=Demersal	NA	NA	NA	NA
Camera = ROV & Species=Non-Focal Semi-pelagic	-0.3015	1.0643	-0.283	0.77696

Null deviance: 147.957 on 196 degrees of freedom

Residual deviance: 94.042 on 190 degrees of freedom

Number of Fisher Scoring iterations: 5

Table S2. Model summary tables for the best-fit GAMs to examine the effect of distance on fish abundance (section 2.3.4 and 3.4 in the primary manuscript). Each species was modeled independently.

Black Rockfish

Family: Negative Binomial(0.28)

Link function: log

Formula: Number Fish ~ s(Distance, by = Reef, k = 4) + Reef

Parametric coefficients:

	Estimate	Std. Error	z value	Pr(> z)
Bandon	-5.76366	0.26278	-21.933	< 2e-16
Cape Arago	1.22560	0.36210	3.385	0.000712
Orford Reef	0.02068	0.35588	0.058	0.953661
Redfish Rocks	1.00997	0.34177	2.955	0.003125

Approximate significance of smooth terms:

	edf	Ref.df	Chi.sq	p-value
Distance * Bandon Reef	0.9043	3	4.981	0.0154
Distance * Cape Arago	0.4201	3	0.631	0.2202
Distance * Orford Reef	1.5574	3	6.785	0.0123
Distance * Redfish Rocks	2.6900	3	42.482	<2e-16

R-sq.(adj) = 0.518

-REML = 494.9

Deviance explained = 29.6%

Scale est. = 1

n = 520

Blue/Deacon Rockfish

Family: Negative Binomial(0.133)

Link function: log

Formula: Number Fish ~ s(Distance, by = Reef, k = 4) + Reef

Parametric coefficients:

	Estimate	Std. Error	z value	Pr(> z)
Bandon	-6.1411	0.4440	-13.831	< 2e-16
Cape Arago	1.7823	0.5388	3.308	0.00094
Orford Reef	2.5274	0.5136	4.921	8.61e-07
Redfish Rocks	-0.1681	0.5748	-0.292	0.76995

Approximate significance of smooth terms:

	edf	Ref.df	Chi.sq	p-value
Distance * Bandon Reef	1.7230	3	11.109	0.001351
Distance * Cape Arago	0.2957	3	0.504	0.191436
Distance * Orford Reef	1.5484	3	4.748	0.047082
Distance * Redfish Rocks	0.9258	3	11.376	0.000455

R-sq.(adj) = 0.421

Deviance explained = 27.9%

-REML = 499.97

Scale est. = 1

n = 520

Demersal Rockfish

Family: Negative Binomial(0.802)

Link function: log

Formula: Number Fish ~ s(Distance, by = Reef, k = 4) + Reef

Parametric coefficients:

	Estimate	Std. Error	z value	Pr(> z)
Bandon	-5.49192	0.18122	-30.305	<2e-16
Cape Arago	0.48794	0.28703	1.700	0.0891
Orford Reef	0.07113	0.24605	0.289	0.7725
Redfish Rocks	-0.25444	0.25706	-0.990	0.3223

Approximate significance of smooth terms:

	edf	Ref.df	Chi.sq	p-value
Distance * Bandon Reef	0.000198	3	0.000	0.8403
Distance * Cape Arago	0.130716	3	0.156	0.2886
Distance * Orford Reef	1.238448	3	4.232	0.0343
Distance * Redfish Rocks	1.359661	3	5.985	0.0130

R-sq.(adj) = 0.646

Deviance explained = 5.04%

-REML = 433.61

Scale est. = 1

n = 520

Non-Focal Semi-Pelagic Rockfish

Family: Negative Binomial(0.271)

Link function: log

Formula: Number Fish ~ s(Distance, by = Reef, k = 4) + Reef

Parametric coefficients:

	Estimate	Std. Error	z value	Pr(> z)
Bandon	-6.8524	0.3599	-19.038	< 2e-16
Cape Arago	1.3682	0.4800	2.851	0.004362
Orford Reef	0.5957	0.4824	1.235	0.216886
Redfish Rocks	1.4794	0.4197	3.525	0.000423

Approximate significance of smooth terms:

	edf	Ref.df	Chi.sq	p-value
Distance * Bandon Reef	1.7168	3	5.594	0.0345
Distance * Cape Arago	0.2503	3	0.256	0.3425
Distance * Orford Reef	0.9487	3	16.733	2.73e-05
Distance * Redfish Rocks	0.6976	3	2.137	0.0800

R-sq.(adj) = -0.926

Deviance explained = 17.4%

-REML = 336.69

Scale est. = 1

n = 520

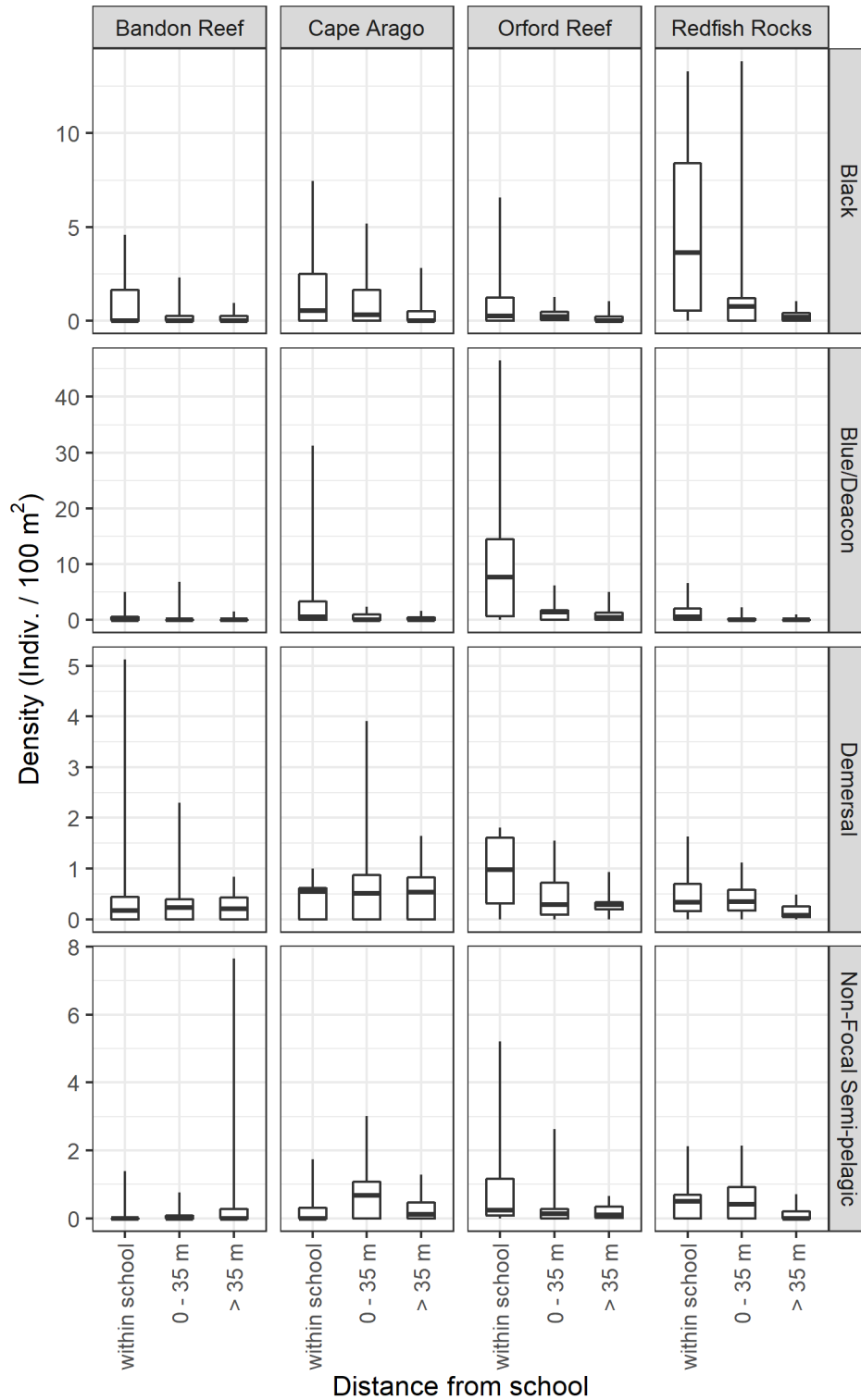


Fig. S5. Boxplots of fish densities within fish schools, in the transition zone (0-35 m from the school) and at distances >35 m from the school.

9: SURVEY DESIGN SIMULATIONS

Video Data

The video count data for both the Black and Blue/Deacon Rockfish were simulated using a negative binomial distributions. We tested how the number of video drops we conducted affected the CV of the number of fish counted. Previous work on efficiencies suggests 1,000 video drops is the reasonable number of video drops that could be scored in a season so simulations were conducted testing a range of hypothetical video drops from 1 to 1,000. Using these data, we also examined how many fish were likely to be counted given a different numbers of video drops. Further, the mock survey demonstrated that only 38% of fish that can be counted in the video, can be measured. Therefore, we scaled the number of counted fish by 38% to assess how many fish were likely to be measured given a set number of video drops. We also simulated hypothetical length data using a normal distribution assuming we measured up to 1,000 fish.

In general, we found that counting relatively few fish resulted in extremely high CVs (Fig. 13) but at ~100 fish counted the CV leveled off. For the fish lengths, CVs were much lower with values leveling off at ~125 fish measured (Figure 1 & 2).

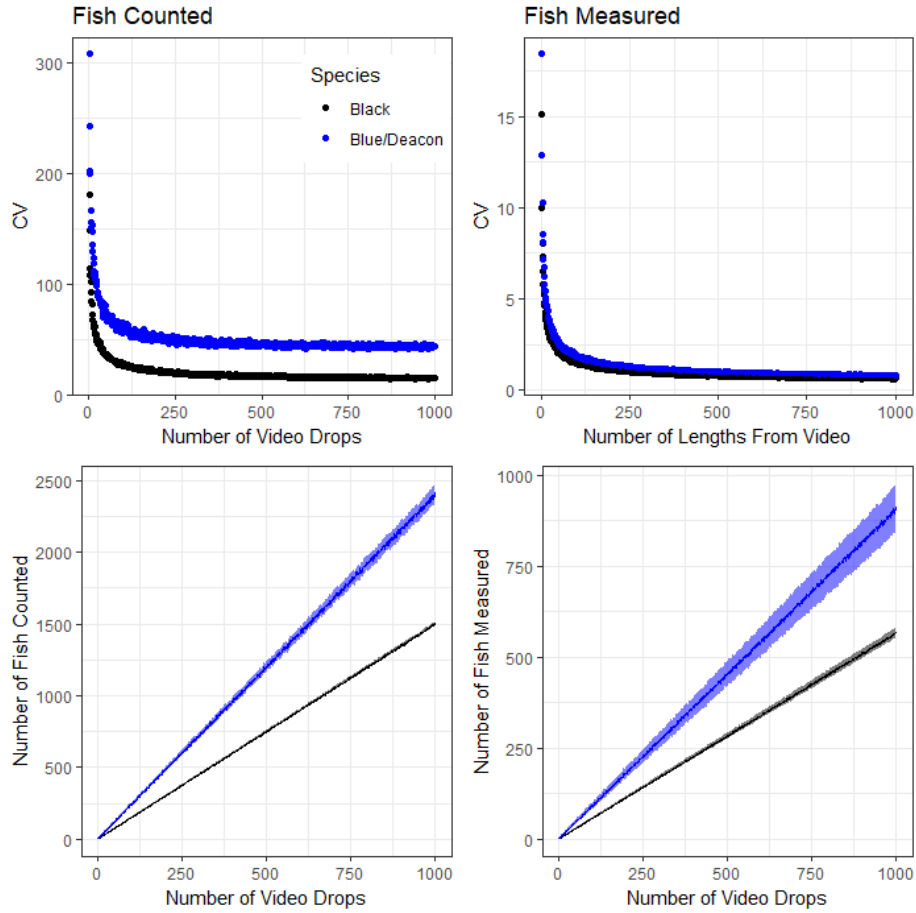


Fig. 1. CV of Black and Blue/Deacon Rockfish counted and measured with the underwater camera system and the number of video drops needed to measure or count a certain number of fish.

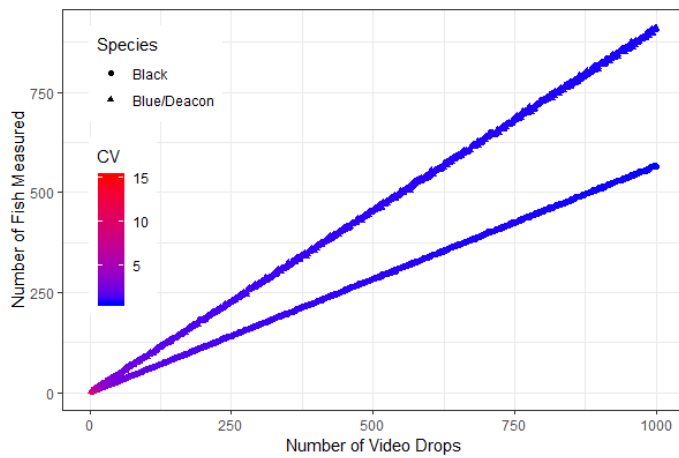


Fig. 2. Relationship between the number of video drops and how many fish are measured and the associated CV of the data.

Age Reading Data

For our hook and line sampling simulations we used data from our 2016-17 Deacon Rockfish school study (Vaux et al. in review & Rasmuson et al. in review). Using the von Bertalanffy growth curve fits from this study we simulated von Bertalanffy growth data using the LHMIXR package. We then examined how the CV of the age (for each year) and length (for each 5 cm bin) changed with increasing the number of fish sampled. Further, previous work has demonstrated that for Black Rockfish the male to female ratio is highly skewed from 50/50 (Fig. 15). Therefore we calculated how the total number of fish that need to be caught in order provide a specific sample size of the least common sex. We calculated this sex ratios ranging from 90/10 to 50/50 in 10 percent increments. We found that CV declined precipitously from a sample size of 0 to 50 and then began to level off (Fig. 16). Further, larger disparities in sex ratios demonstrated that very large sample sizes were required to obtain

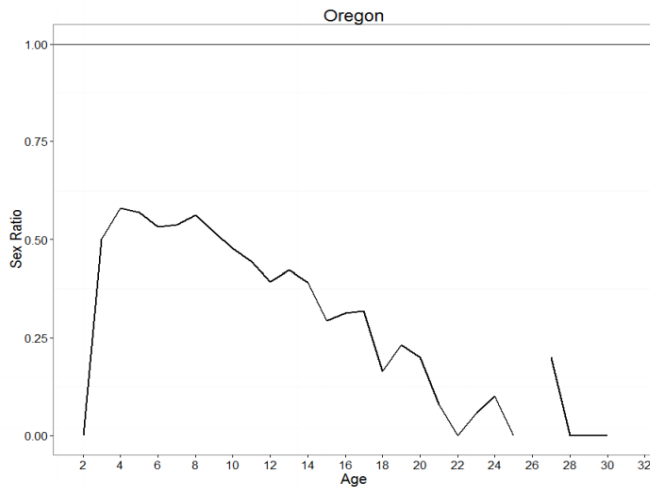


Fig. 3. Proportion of the Black Rockfish population that is female for a given age. Borrowed from the most recent Black Rockfish stock assessment.

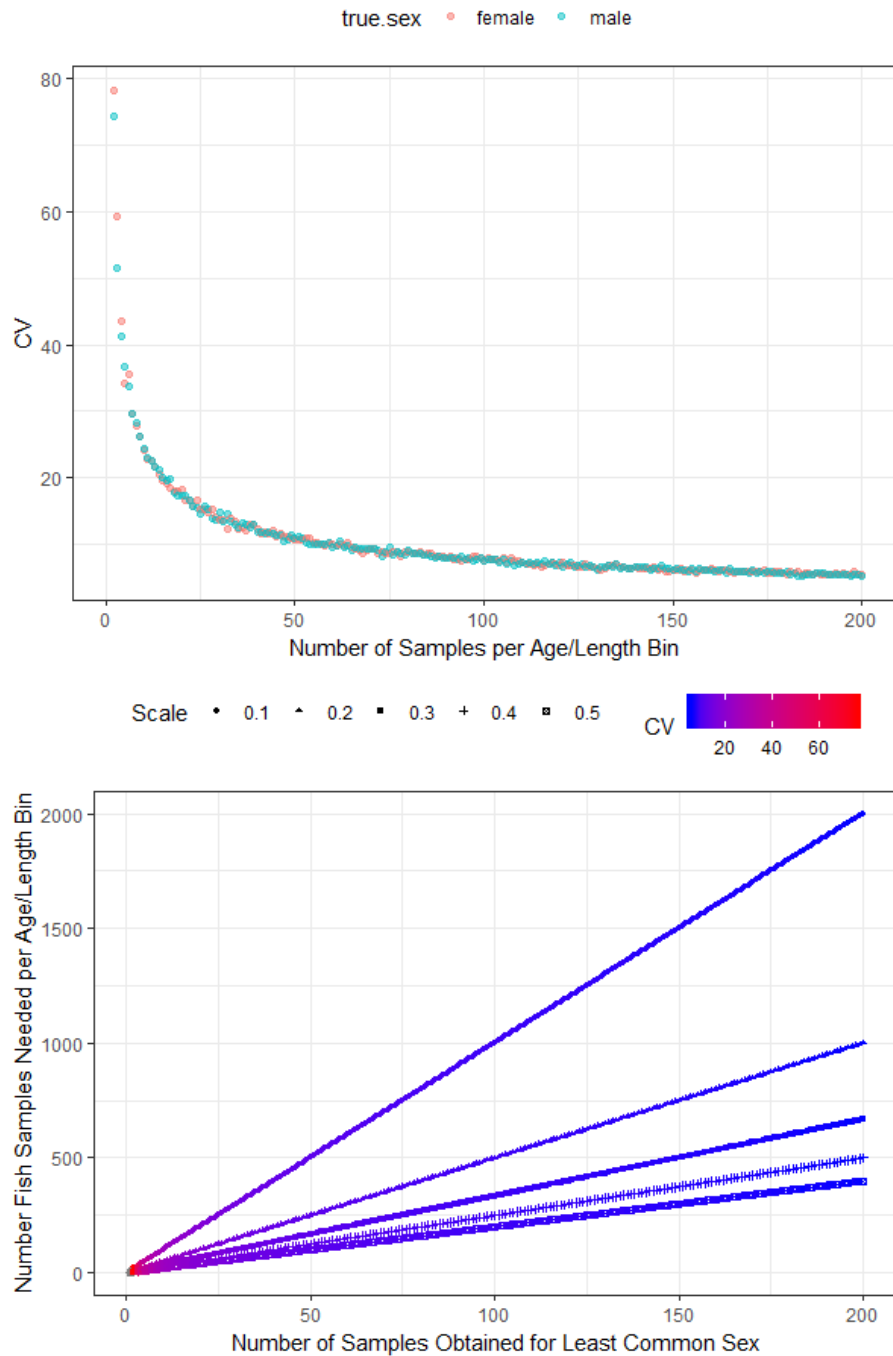


Fig. 4. Effect of sample size per age or length bin on the CV of the von Bertalanffy growth fit (upper) and the number of samples required to be caught in order to obtain a specific number of the rarer sex colored by the CV of the age length CV estimates.

4) Survey Design Discussion

Given the higher importance of the video data over the hook and line data I propose 75% of the station time be dedicated to video collection and 25% of the time dedicated to hook and line sampling with some extra time allocated to adaptive video samples.

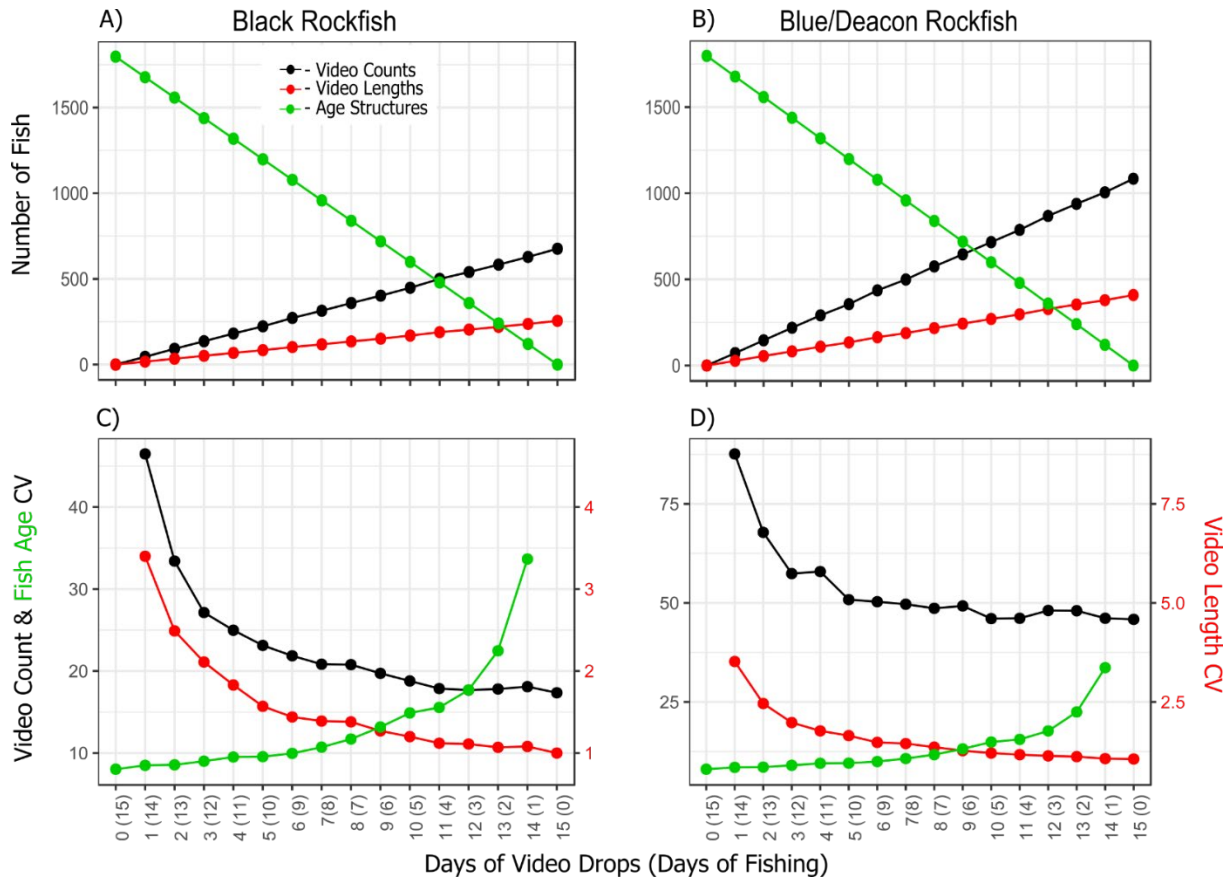


Fig. 5. Number of samples for video or age data (upper) for Black and Blue/Deacon Rockfish and their effect on CV (lower) with the number of video drops increasing from left to right and the number of age samples increasing from right to left.



Marine Fisheries Research Project
Marine Resources Program, Oregon Department of Fish and Wildlife
2040 SE Marine Science Dr.
Newport OR, 97365

